

Topics in Current Chemistry Collections

Arkaitz Correa *Editor*

# Ni- and Fe-Based Cross-Coupling Reactions

 Springer

# Topics in Current Chemistry Collections

## Journal Editors

Massimo Olivucci, Siena, Italy and Bowling Green, USA  
Wai-Yeung Wong, Hong Kong

## Series Editors

Hagan Bayley, Oxford, UK  
Kendall N. Houk, Los Angeles, USA  
Greg Hughes, Codexis Inc, USA  
Christopher A. Hunter, Cambridge, UK  
Kazuaki Ishihara, Nagoya, Japan  
Michael J. Krische, Austin, Texas  
Jean-Marie Lehn, Strasbourg, France  
Rafael Luque, Córdoba, Spain  
Jay S. Siegel, Tianjin, China  
Joachim Thiem, Hamburg, Germany  
Margherita Venturi, Bologna, Italy  
Chi-Huey Wong, Taipei, Taiwan  
Henry N.C. Wong, Hong Kong  
Vivian Wing-Wah Yam, Hong Kong  
Chunhua Yan, Beijing, China  
Shu-Li You, Shanghai, China

## **Aims and Scope**

The series Topics in Current Chemistry Collections presents critical reviews from the journal Topics in Current Chemistry organized in topical volumes. The scope of coverage is all areas of chemical science including the interfaces with related disciplines such as biology, medicine and materials science.

The goal of each thematic volume is to give the non-specialist reader, whether in academia or industry, a comprehensive insight into an area where new research is emerging which is of interest to a larger scientific audience.

Each review within the volume critically surveys one aspect of that topic and places it within the context of the volume as a whole. The most significant developments of the last 5 to 10 years are presented using selected examples to illustrate the principles discussed. The coverage is not intended to be an exhaustive summary of the field or include large quantities of data, but should rather be conceptual, concentrating on the methodological thinking that will allow the non-specialist reader to understand the information presented.

Contributions also offer an outlook on potential future developments in the field.

More information about this series at <http://www.springer.com/series/14181>

Arkaitz Correa

Editor

# Ni- and Fe-Based Cross-Coupling Reactions

*With contributions from*

Lutz Ackermann • Livia N. Cavalcanti • Gianpiero Cera  
Naoto Chatani • Arkaitz Correa • Janine Cossy • Yijing Dai  
Morgane Gaydou • Hegui Gong • Amandine Guérinot  
Kenichiro Itami • Takanori Iwasaki • Francisco Juliá-Hernández  
Nobuaki Kambe • Zhiping Li • Leiyang Lv • Ruben Martin  
Gary A. Molander • Kei Muto • Eloisa Serrano • Mamoru Tobisu  
Manuel van Gemmeren • Xuan Wang • Junichiro Yamaguchi

 Springer



*Editor*

Arkaitz Correa

Universidad del País Vasco-Euskal Herriko Unibertsitatea (UPV/EHU)

Donostia-San Sebastián

Spain

Originally published in *Top Curr Chem (Z)* Volume 374 (2016),

© Springer International Publishing Switzerland 2016

ISSN 2367-4067

ISSN 2367-4075 (electronic)

Topics in Current Chemistry Collections

ISBN 978-3-319-49783-9

ISBN 978-3-319-49784-6 (eBook)

DOI 10.1007/978-3-319-49784-6

Library of Congress Control Number: 2016959994

© Springer International Publishing AG 2017

This work is subject to copyright. All rights are reserved by the Publisher, whether the whole or part of the material is concerned, specifically the rights of translation, reprinting, reuse of illustrations, recitation, broadcasting, reproduction on microfilms or in any other physical way, and transmission or information storage and retrieval, electronic adaptation, computer software, or by similar or dissimilar methodology now known or hereafter developed.

The use of general descriptive names, registered names, trademarks, service marks, etc. in this publication does not imply, even in the absence of a specific statement, that such names are exempt from the relevant protective laws and regulations and therefore free for general use.

The publisher, the authors and the editors are safe to assume that the advice and information in this book are believed to be true and accurate at the date of publication. Neither the publisher nor the authors or the editors give a warranty, express or implied, with respect to the material contained herein or for any errors or omissions that may have been made.

Printed on acid-free paper

This Springer imprint is published by Springer Nature

The registered company is Springer International Publishing AG

The registered company address is: Gewerbestrasse 11, 6330 Cham, Switzerland

## Contents

|   |     |
|---|-----|
| <b>Editorial</b> .....  | vii |
| Arkaitz Correa  |     |
| <b>Ni-Catalyzed C–C Couplings Using Alkyl Electrophiles</b> .....   | 1   |
| Takanori Iwasaki, Nobuaki Kambe   |     |
| <b>Photoredox Catalysis in Nickel-Catalyzed Cross-Coupling</b> .....  | 37  |
| Livia N. Cavalcanti, Gary A. Molander   |     |
| <b>Nickel-Catalyzed Reductive Couplings</b> .....   | 61  |
| Xuan Wang, Yijing Dai, Hegui Gong   |     |
| <b>Ni- and Fe-catalyzed Carboxylation of Unsaturated Hydrocarbons with CO<sub>2</sub></b> .....                     | 91  |
| Francisco Juliá-Hernández, Morgane Gaydou, Eloisa Serrano, Manuel van Gemmeren, Ruben Martin                        |     |
| <b>Nickel-Catalyzed Cross-Coupling Reactions of Unreactive Phenolic Electrophiles via C–O Bond Activation</b> ..... | 129 |
| Mamoru Tobisu, Naoto Chatani  |     |
| <b>Nickel-Catalyzed Aromatic C–H Functionalization</b> .....  | 157 |
| Junichiro Yamaguchi, Kei Muto, Kenichiro Itami  |     |
| <b>Iron-Catalyzed C–H Functionalization Processes</b> .....   | 191 |
| Gianpiero Cera, Lutz Ackermann  |     |
| <b>Fe-Catalyzed Cross-Dehydrogenative Coupling Reactions</b> .....  | 225 |
| Leiyang Lv, Zhiping Li  |     |
| <b>Iron-Catalyzed C–C Cross-Couplings Using Organometallics</b> .....   | 265 |
| Amandine Guérinot, Janine Cossy   |     |

## Editorial

Arkaitz Correa<sup>1</sup>

© Springer International Publishing Switzerland 2016

The genesis of cross-coupling reactions is often traced back to Ni-catalyzed reactions of Grignard reagents with aryl or vinyl halides reported in the 1970s. However, earlier reports by Kharasch in the 1940s already demonstrated the ability of simple iron salts to act as catalysts in couplings involving Grignard reagents. Unfortunately, these Fe and Ni-catalyzed processes were overshadowed by the meteoric development of palladium chemistry discovered shortly thereafter. Despite the undeniable maturity of Pd-based processes, the recent years have witnessed a renaissance in Fe and Ni-catalyzed reactions providing new dogmas for achieving practical and unconventional bond disconnections that were beyond reach using classical Pd regimes. Consequently, cross-coupling reactions have impressively evolved from standard laboratory procedures into indispensable and routine techniques in chemical industry. As an illustrative example of the high value and tremendous impact of these chemical processes, the Nobel Prize in Chemistry 2010 was awarded jointly to Richard F. Heck, Ei-ichi Negishi and Akira Suzuki for their important discoveries in palladium-catalyzed cross-coupling reactions.

Unlike palladium, iron and nickel can adopt a broad spectrum of oxidation states, thus allowing different modes of reactivity and radical mechanisms. Likewise, the low cost of nickel and environmentally friendly character of iron make them privileged catalysts from the standpoints of economics and sustainability. This topical collection aims to cover recent developments in nickel and iron-based cross-couplings and illustrate how the intrinsic and unique properties of those first-row metals have enabled their use as convenient and highly versatile catalysts for a myriad of unprecedented, yet intriguing, chemical transformations. Accordingly, insightful contributions from several leading

---

This article is part of the Topical Collection “Ni- and Fe-Based Cross-Coupling Reactions”; edited by Arkaitz Correa.

---

✉ Arkaitz Correa  
[arkaitz.correa@ehu.es](mailto:arkaitz.correa@ehu.es)

<sup>1</sup> Universidad del País Vasco-Euskal Herriko Unibertsitatea (UPV/EHU), Joxe Mari Korta R&D Center, Av. Tolosa 72, 20018 Donostia-San Sebastián, Spain

experts in this cutting-edge research field are collected, with particular emphasis on relevant recent progress and highlighting the utmost potential of both iron and nickel catalysis as broadly applicable synthetic tools in the realm of organic chemistry.

This topical collection begins with a set of contributions on Ni-catalyzed C–C couplings. Within this broad theme, N. Kambe focuses on reactions between alkyl electrophiles and organometallic reagents by means of Ni catalysis. G. Molander covers insightful discussion of photoredox/nickel dual catalysis using alkyl electrophiles. H. Gong describes Ni-catalyzed reductive coupling reactions between two distinct electrophiles. R. Martin comprehensively reviews the development of carboxylation events of unsaturated hydrocarbons with carbon dioxide. M. Tobisu and N. Chatani summarize key aspects on the use of phenol derivatives as versatile electrophiles via Ni-catalyzed C–O bond activation. The discussion on nickel catalysis is closed by a contribution of J. Yamaguchi and K. Itami on aromatic C–H functionalization processes including selected examples of natural product synthesis. This topical collection then shifts direction to discuss the use of environmentally friendly and cost-efficient iron catalysis: L. Ackermann introduces the most important results in Fe-catalyzed C–H functionalization processes, Z. Li gives a comprehensive understanding of cross-dehydrogenative couplings via iron catalysis, and J. Cossy closes the topical collection by covering Fe-catalyzed C–C coupling processes involving organometallic reagents. All in all, the reviews assembled herein provide an excellent overview of this burgeoning research area and will clearly open up new synthetic opportunities of paramount chemical significance. At present, however, limited knowledge has been gathered regarding the mechanism of some of the nickel and iron-catalyzed events disclosed herein, which sometimes are merely speculative and based on indirect experimental evidence. In this respect, mechanistic understanding of the underlying key elemental steps through isolation of putative reaction intermediates will certainly fuel wider applications in the near future at the forefront of organonickel and organiron chemistry.

I am grateful to Ruben Martin for kindly encouraging me to take on this task and deeply indebted to all distinguished colleagues who have contributed with their expert knowledge to make this comprehensive compilation on contemporary nickel and iron chemistry possible. Likewise, I would like to acknowledge the assistance of all the reviewers.

UPV/EHU, July 2016



Arkaitz Correa

# Ni-Catalyzed C–C Couplings Using Alkyl Electrophiles

Takanori Iwasaki<sup>1</sup> · Nobuaki Kambe<sup>1</sup>

Received: 27 June 2016 / Accepted: 18 August 2016  
© Springer International Publishing Switzerland 2016

**Abstract** Much effort has been devoted to developing new methods using Ni catalysts for the cross-coupling reaction of alkyl electrophiles with organometallic reagents, and significant achievements in this area have emerged during the past two decades. Nickel catalysts have enabled the coupling reaction of not only primary alkyl electrophiles, but also sterically hindered secondary and tertiary alkyl electrophiles possessing  $\beta$ -hydrogens with various organometallic reagents to construct carbon skeletons. In addition, Ni catalysts opened a new era of asymmetric cross-coupling reaction using alkyl halides. Recent progress in nickel-catalyzed cross-coupling reaction of alkyl electrophiles with  $sp^3$ -,  $sp^2$ -, and  $sp$ -hybridized organometallic reagents including asymmetric variants as well as mechanistic insights of nickel catalysis are reviewed in this chapter.

**Keywords** Cross-coupling · Homogeneous catalysis · Nickel · Alkyl halides · Organometallic reagents

## 1 Introduction

Transition metal-catalyzed cross-coupling reactions of alkyl electrophiles such as alkyl halides and pseudohalides with organometallic reagents are among the most useful methods to construct saturated hydrocarbon frameworks [1]. Since the epoch-making discoveries of reductive elimination reaction of diorganonickel complexes

---

This article is part of the Topical Collection “Ni- and Fe-Based Cross-Coupling Reactions”; edited by Arkaitz Correa.

---

✉ Nobuaki Kambe  
[kambe@chem.eng.osaka-u.ac.jp](mailto:kambe@chem.eng.osaka-u.ac.jp)

<sup>1</sup> Department of Applied Chemistry, Graduate School of Engineering, Osaka University, Suita, Osaka 565-0871, Japan

Published online: 31 August 2016

Reprinted from the journal

by Yamamoto [2] and Ni-catalyzed cross-coupling reaction by Kumada and Tamao [3] and Corriu [4], nickel has been employed as one of the most promising catalysts for carbon–carbon bond forming reactions. However, because of troublesome side reactions often encountered using alkyl electrophiles as a coupling partner, the cross-coupling reaction of alkyl electrophiles with organometallic reagents was relatively less developed compared to the reaction of unsaturated electrophiles such as haloarenes, haloalkenes, and haloalkynes until the beginning of this century. During the past two decades, much effort has been devoted to the development of new transition metal catalysts for the cross-coupling reaction of alkyl electrophiles, as well as alkyl nucleophiles [5]. For such transformations, Pd catalysts were often employed with a combined use of bulky trialkylphosphines [6] or *N*-heterocyclic carbenes [7] as the ligands [8, 9]. Nickel has also received considerable attention as promising catalyst for the cross-coupling reaction of alkyl halides and pseudo-halides (for representative reviews: [10–20]). A big difference between these two metals from a mechanistic view point is that various nickel complexes with a wide range of oxidation states from 0 to 4 can participate in catalytic cycles to facilitate the coupling reactions [8, 9] (for representative reviews: [10–20]). In particular, carbon-(pseudo)halogen bond cleavage may involve oxidative addition to either Ni(0), Ni(I), or Ni(II) intermediates via ionic or radical mechanisms. In addition, Ni complexes at a high oxidation state, Ni(IV) or Ni(III), as well as Ni(II), facilitate reductive elimination to form carbon–carbon bonds. These mechanistic flexibilities of nickel catalysts allow the use of various alkyl (pseudo)halides including less reactive alkyl halides as coupling partners to provide convenient synthetic tools to construct saturated hydrocarbon frameworks. For these Ni catalysts, electron-deficient olefins, dienes, and nitrogen-based bi- or tridentate ligands are frequently employed. This is in sharp contrast to the cases of Pd catalysts, which often prefer phosphine or carbene ligands.

This chapter summarizes recent progresses in nickel-catalyzed cross-coupling reaction of alkyl electrophiles with  $sp^3$ -,  $sp^2$ -, and  $sp$ -hybridized organometallic reagents. Asymmetric coupling reactions as well as mechanistic insights of nickel catalysis are also discussed. Applications of these cross-coupling reactions to synthesize natural products and biologically active compounds are briefly overviewed.

Cross-coupling reactions by reverse combinations of reagents, such as aryl or vinyl (pseudo)halides with alkyl metal reagents [3], have long been known as straightforward methods for introducing alkyl groups into organic molecules and are not covered in this chapter [21]. Various useful procedures for this transformation have been reported and employed in synthetic reactions using Ni and other transition metals as the catalyst [21], although unwanted side-reactions such as isomerization of alkyl groups and reduction of organohalides are occasionally encountered [22, 23] (for recent progresses: [24, 25]) (for a representative mechanistic study: [26]). Therefore, the coupling reaction using alkyl electrophiles overviewed herein is a good alternative to construct carbon frameworks containing a saturated carbon chain.

Catalytic C–H bond alkylation using alkyl electrophiles [27] and reductive coupling reaction of alkyl halides with organohalides [28] are documented in this topical collection.

## 2 Reaction of Alkyl Electrophiles

### 2.1 C(sp<sup>3</sup>)-C(sp<sup>3</sup>) Coupling Reaction

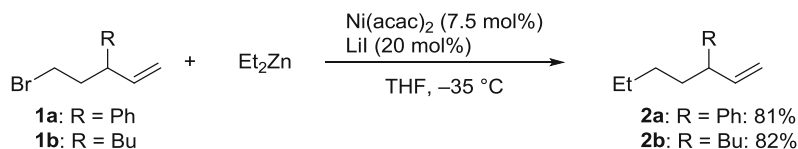
In 1995, Knochel disclosed that intramolecular coordination of an olefin [29] or keto group [30] to Ni facilitated cross-coupling reaction of alkyl iodides and bromides with dialkylzinc reagents in the presence of a catalytic amount of Ni(acac)<sub>2</sub>. For instance, alkyl bromides **1** bearing a double bond unit underwent the coupling reaction to give **2** in good yields (Scheme 1). In contrast, halogen-zinc exchange reaction took place exclusively, when the analogs **3** carrying no olefinic moiety were employed to the reaction (Scheme 2).

It was also revealed that the Negishi type alkyl-alkyl cross-coupling reaction catalyzed by Ni proceeded efficiently by using acetophenone or styrene derivatives as the additive. For example, the reaction of an alkyl iodide **5** with dipentylzinc reagent in the presence of 10 mol% of Ni(acac)<sub>2</sub> afforded only 20 % yield of the coupling product **6**, whereas the addition of one equivalent of acetophenone improved the yield to 71 % yield (Scheme 3) [30–32].

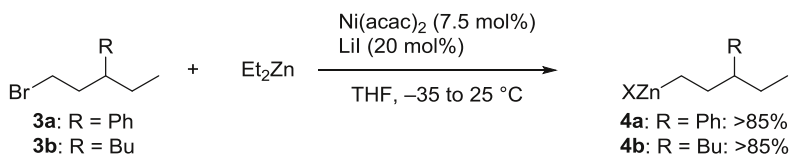
In 2002, Kambe demonstrated that 1,3-butadiene plays crucial roles in achieving Ni-catalyzed cross-coupling reaction of alkyl halides with alkyl Grignard reagents. When 1-bromodecane (*n*-Dec-Br) was treated with *n*-BuMgCl and a catalytic amount of NiCl<sub>2</sub>, significant amounts of decane and decenes were yielded by the reduction and the dehydrobromination, respectively. The use of 1,3-butadiene as an additive drastically improved the selectivity yielding the cross-coupling product exclusively (Scheme 4) [33].

The role of 1,3-butadiene is not the case of the simple coordination toward nickel intermediates, but the formation of bis(π-allyl)nickel intermediate as a catalytic active species by oxidative dimerization is the key (for representative reviews: [12]). Since the present Ni-catalyzed cross-coupling reaction proceeds under mild conditions, at 0 °C or below, polar functional groups including amide, ester, and ketone remained intact [34]. When Ni containing perovskite, LaFe<sub>0.8</sub>Ni<sub>0.2</sub>O<sub>3</sub>, was used as a heterogeneous Ni precursor in the presence of 1,3-butadiene additive, the coupling reaction of alkyl halides with alkyl Grignard reagents smoothly proceeded to give coupling products. It was proposed that this reaction was catalyzed by a trace amount of Ni in the liquid phase with a quite high TON in the order of 10<sup>7</sup> [35].

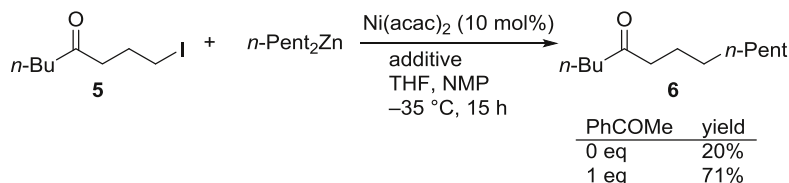
The use of tetraenes, such as **7**, as the ligand precursor instead of 1,3-butadiene enabled the cross-coupling with alkyl fluorides via cleavage of the C–F bond. For instance, the reaction of 1-fluorononane (*n*-Non-F) with *n*-PrMgBr



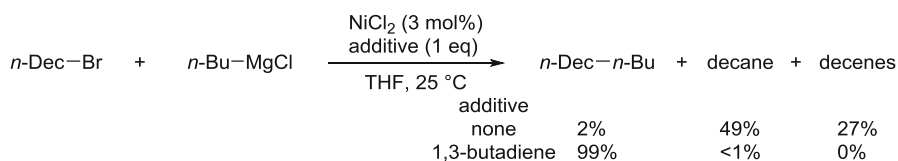
**Scheme 1** Cross-coupling of alkyl bromides bearing an alkene moiety with Et<sub>2</sub>Zn



**Scheme 2** Halogen–zinc exchange reaction of alkyl bromides



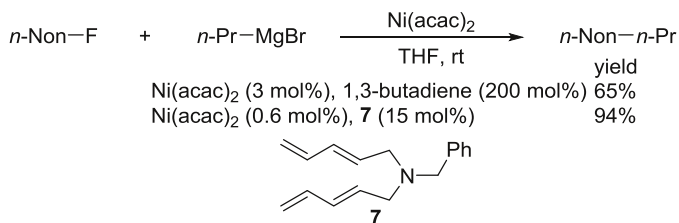
**Scheme 3** Cross-coupling of an alkyl iodide with an alkylzinc reagent using acetophenone as an additive



**Scheme 4** Cross-coupling using 1,3-butadiene as an additive

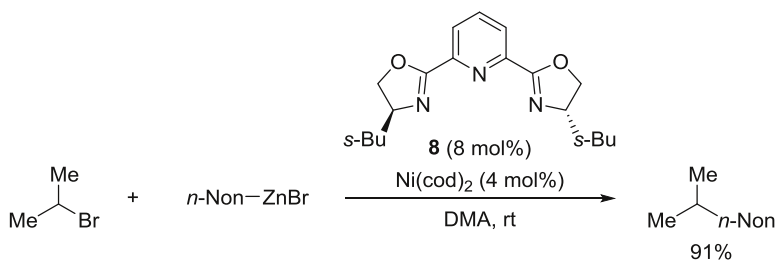
proceeded in the presence of only 0.6 mol% of Ni catalyst and 15 mol% of the ligand precursor **7** to give dodecane in 94 % yield (**Scheme 5**) [36]. In addition, such tetraene ligand precursors were found to be more effective than 1,3-butadiene in Negishi-coupling reaction of alkyl halides with alkylzinc reagents [37].

These Ni-catalyzed reactions of alkyl halides proceed via ionic mechanisms. It seems difficult to use sterically congested electrophiles in these systems, and no successful result was reported for secondary alkyl halides [29–37]. Similarly, Pd-catalyzed cross-coupling reaction of alkyl halides suffers from much slower oxidative addition process of secondary alkyl halides than that of primary alkyl halides [8, 9]. A breakthrough to overcome this difficulty arising from usage of secondary alkyl electrophiles was made by Fu in 2003, (for representative reviews:

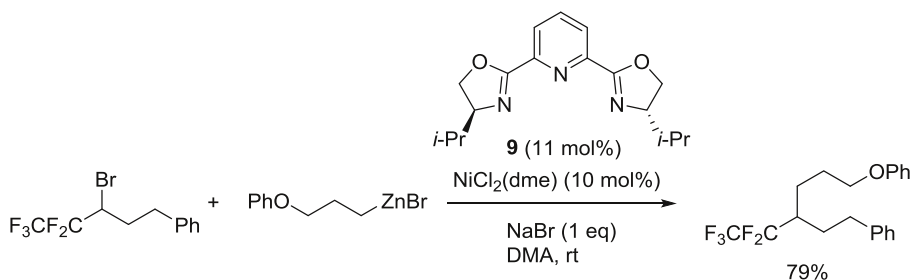


**Scheme 5** Cross-coupling of an alkyl fluoride with *n*-PrMgBr using a tetraene



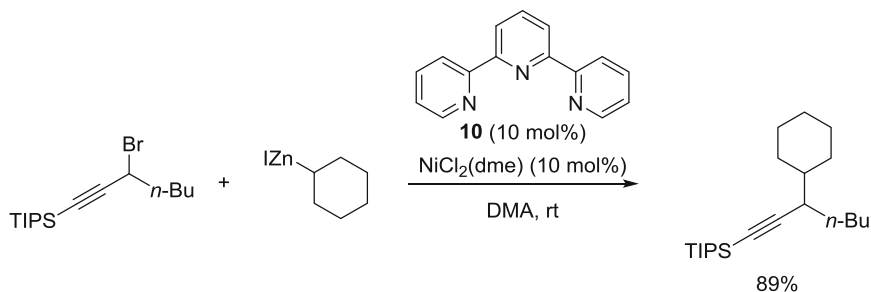


**Scheme 6** Cross-coupling of *i*-PrBr with an alkylzinc reagent

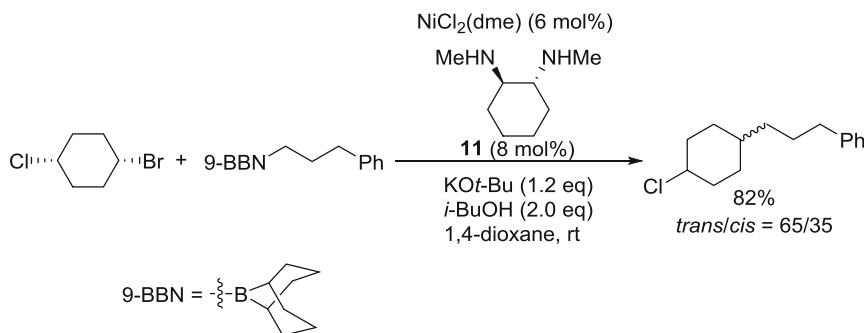


**Scheme 7** Cross-coupling of a fluorinated secondary alkyl bromide

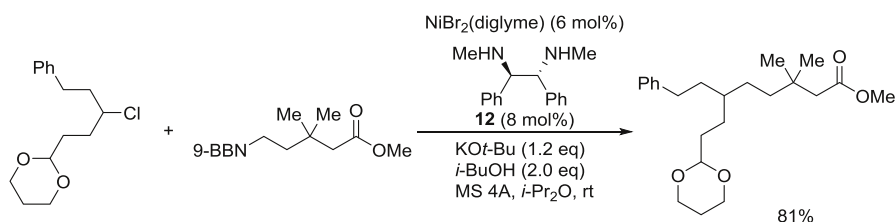
[14]) where they demonstrated that the combined use of Ni and an NNN tridentate ligand, pybox **8**, efficiently catalyzed cross-coupling reaction of nonactivated secondary alkyl bromides and iodides with primary alkylzinc reagents (Scheme 6) [38]. This catalytic system is also effective for the secondary alkyl halides having perfluoroalkyl groups at the  $\alpha$ -position (Scheme 7) [39]. In these reactions,  $\beta$ -hydrogen and  $\beta$ -fluorine elimination were suppressed by pybox ligand. When propargylic secondary bromides and chlorides were used as the electrophiles, secondary alkylzinc reagents could be used to achieve cross-coupling reaction between two secondary carbon centers by using terpyridine (tpy) **10** as the ligand (Scheme 8) [40].



**Scheme 8** Cross-coupling of a secondary alkyl bromide with a secondary alkylzinc reagent



**Scheme 9** Suzuki–Miyaura coupling of a secondary alkyl bromide with an alkylboron reagent



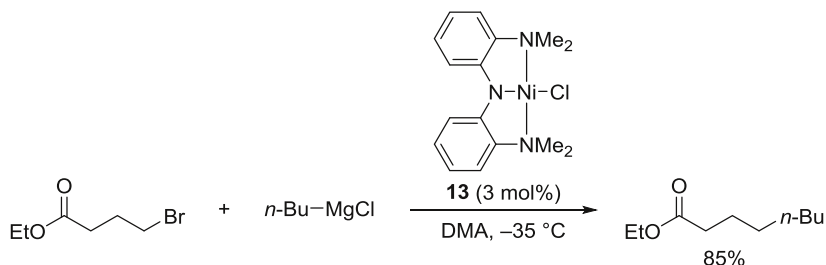
**Scheme 10** Cross-coupling reaction of a secondary alkyl chloride with an alkylboron reagent

Vicic also reported Ni-terpyridine catalyzed cross-coupling reaction of unactivated alkyl halides with alkylzinc reagents by use of terpyridine ligands [41, 42].

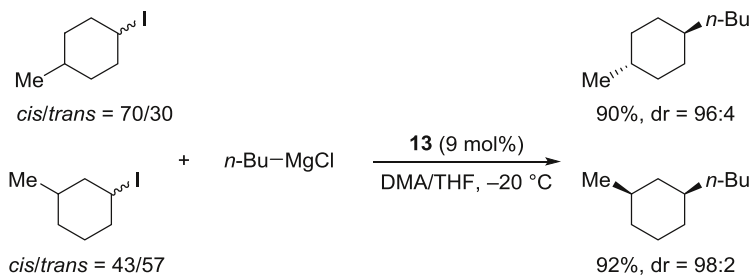
In 2007, Fu disclosed Ni-catalyzed Suzuki–Miyaura coupling reaction of secondary alkyl halides with primary alkylboron reagents using *trans*-*N,N'*-dimethyl-1,2-cyclohexanediamine **11** as the ligand (Scheme 9). Although the use of 1,2-cyclohexanediamine gave the coupling product in 53 % yield, a similar diamine *N,N,N',N'*-tetramethyl-1,2-cyclohexanediamine showed no additive effect [43]. When *cis*-1-bromo-4-chlorocyclohexane was employed, a mixture of *cis*- and *trans*-coupling products was formed (Scheme 9), suggesting the formation of the alkyl radical intermediates in the catalytic cycle. A modified catalytic system using *N,N'*-dimethyl-1,2-diphenylethylenediamine **12** as the ligand enabled the use of secondary alkyl chlorides as coupling partners (Scheme 10) [44]. Due to the high functional group tolerance of organoboron reagents, alkylboron reagents having polar functionalities could be employed.

A monoanionic NNN tridentate ligand in complex **13** was employed as an effective ligand for Ni-catalyzed Kumada–Tamao–Corriu cross-coupling reaction of primary and secondary alkyl halides [45, 46]. When nickel complex **13** was used, the cross-coupling reaction proceeded even at  $-35\text{ }^\circ\text{C}$  with high tolerance to various functional groups (Scheme 11).

The Ni complex **13** also exhibited catalytic activity toward Suzuki–Miyaura cross-coupling of primary alkyl bromides and iodides giving the products in moderate to good yields at  $80\text{ }^\circ\text{C}$  or higher [47].



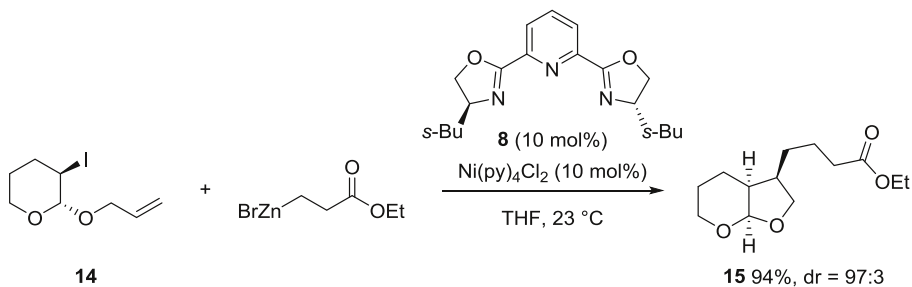
**Scheme 11** Kumada-Tamao-Corriu coupling using Ni complex **13**



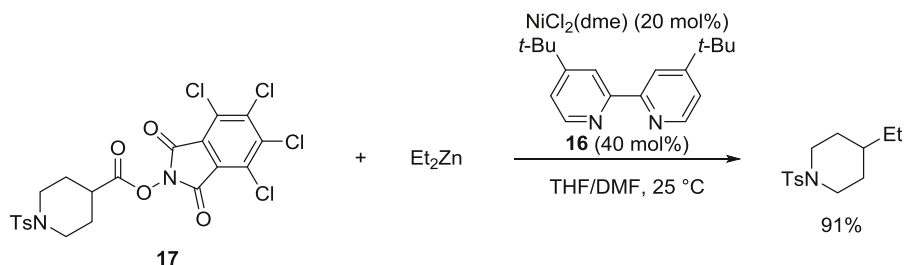
**Scheme 12** Diastereoselective alkylation of cyclohexyl iodides

Since the reaction using **13** involves alkyl radical intermediates, excellent diastereoselectivities were attained in the cross-coupling reaction of 3- or 4-substituted cyclohexyl halides via relatively more stable diequatorial cyclohexyl-nickel intermediates formed by recombination of a Ni species with the alkyl radicals in the oxidative addition step (Scheme 12) [48].

Another profitable example involving alkyl radical intermediates is a cyclization/cross-coupling cascade [49, 50]. It is well known that alkyl radicals possessing an alkene moiety at the 5-position quickly undergo 5-*exo* radical cyclization to form a new alkyl radical with a 5-membered ring. Cárdenas designed alkyl halides bearing an alkene moiety and employed them to Ni/pybox **8** catalytic system. As expected, cyclization/cross-coupling cascade took place to give the product **15** with excellent diastereoselectivity from **14** and an alkylzinc reagent (Scheme 13) [49]. Alkyl



**Scheme 13** Cyclization/cross-coupling cascade



**Scheme 14** Decarboxylative cross-coupling of carboxylic esters

Grignard reagents could be also employed to afford cyclization/cross-coupling products even in the presence of polar functional groups [50].

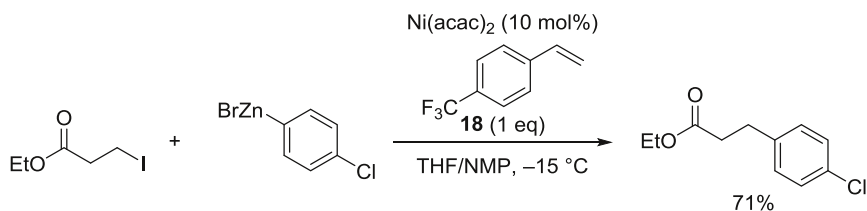
Most recently, Baran et al. demonstrated that carboxylic esters of *N*-hydroxytetrachlorophthalimide **17** coupled with alkylzinc reagents through decarboxylation by the aid of a Ni catalyst (**Scheme 14**) [51]. This method would provide a useful addition to the conventional cross-coupling reactions employing alkyl (pseudo)halides due to the ubiquity of carboxylic acids as the source of the coupling partners. The coupling products were obtained in good to excellent yields from secondary alkyl carboxylic acid derivatives and in moderate yields from primary and tertiary ones.

## 2.2 $\text{C}(\text{sp}^3)\text{--}\text{C}(\text{sp}^2)$ Coupling Reaction

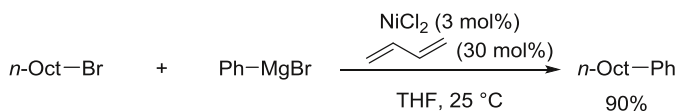
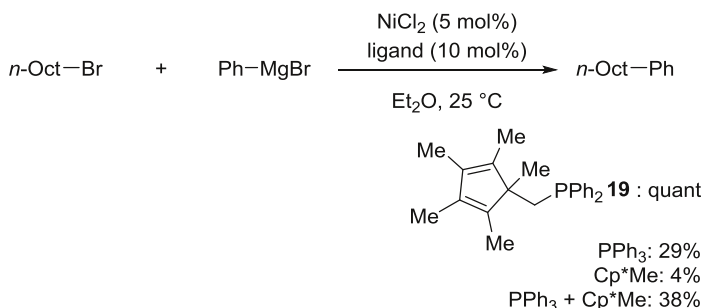
Early examples of Ni-catalyzed cross-coupling reaction of alkyl halides with aryl metal reagents were reported by Scott employing  $\text{NiCl}_2(\text{dppf})$  as the catalyst. The reaction of alkyl iodides with arylmagnesium and zinc reagents proceeded efficiently when alkyl iodides carrying no  $\beta$ -hydrogen were employed [52, 53]. As a more general catalytic system, Knochel demonstrated that an electron deficient styrene **18** showed an excellent additive effect for the coupling reaction of primary alkyl iodides with arylzinc reagents (**Scheme 15**) [54].

Nickel/1,3-butadiene catalytic system promoted the coupling reaction of alkyl bromides and tosylates with aryl Grignard reagents (**Scheme 16**) [33]. In contrast, vinylic Grignard reagents did not give the corresponding coupling product under similar conditions.

Yorimitsu and Oshima demonstrated Ni-catalyzed Kumada–Tamao–Corriu type cross-coupling reaction of primary and secondary alkyl bromides by the aid of a



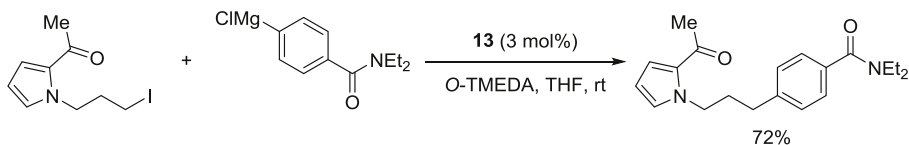
**Scheme 15** Negishi coupling of an alkyl iodide with  $\text{PhZnBr}$

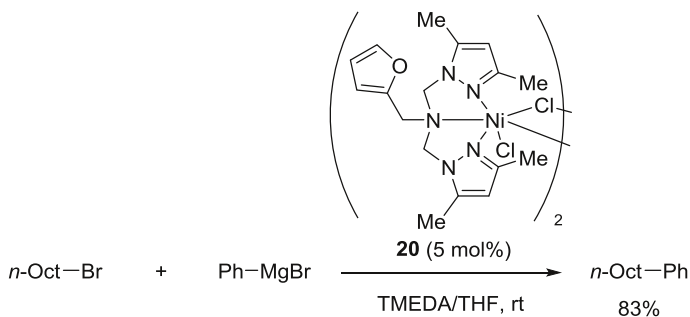
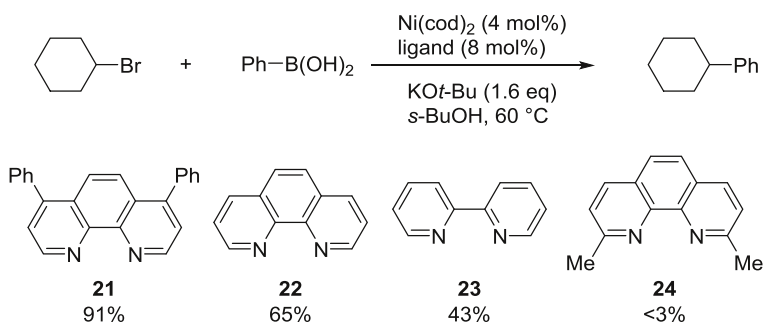
**Scheme 16** Cross-coupling of *n*-OctBr with PhMgBr by the Ni/1,3-butadiene system**Scheme 17** Cross-coupling using phosphine ligand **19**

newly designed phosphine ligand **19** bearing a pentamethylcyclopentadiene moiety with a methylene tether unit [55]. A systematic comparison of the phosphine ligand **19** with other monophosphines and diene ligands demonstrated superiority of this ligand. Use of PPh<sub>3</sub> and/or Cp\*Me resulted in low yields of the coupling product (Scheme 17). The high efficiency of **19** was explained by that the pentamethylcyclopentadiene moiety occupies vacant coordination sites to suppress unwanted  $\beta$ -hydrogen elimination of alkylnickel intermediates. Involvement of alkyl radical intermediates was confirmed by ring-opening of a cyclopropylmethyl bromide and ring-closure of an alkene-containing alkyl iodide.

Hu demonstrated high functional group tolerance in Ni-catalyzed Kumada–Tamao–Corriu coupling using the complex **13**. For instance, an alkyl iodide possessing an *N*-heterocycle and a carbonyl group successfully coupled with an amide containing aryl Grignard reagent, generated by Knochel's method [56], to give the corresponding coupling product in 72 % yield (Scheme 18) [57].

Dinuclear Ni complex **20** having an amine-bis(pyrazolyl) ligand also catalyzed cross-coupling reaction of primary and secondary alkyl bromides with aryl Grignard reagents. Interestingly, the furan moiety in complex **20** is needed to achieve high performance (Scheme 19). When the furan moiety was replaced with thiophene, the yield dropped to 21 % [58].

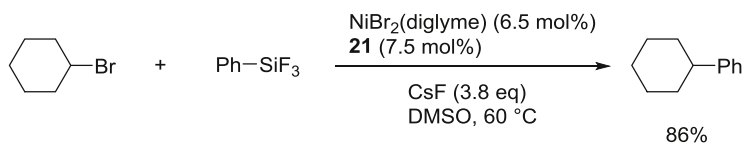
**Scheme 18** Functional group tolerance of Kumada–Tamao–Corriu coupling

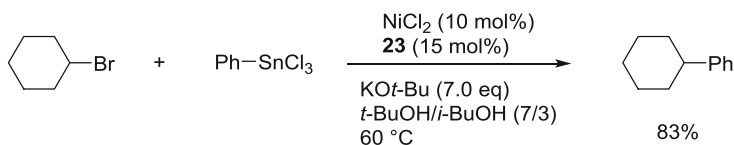
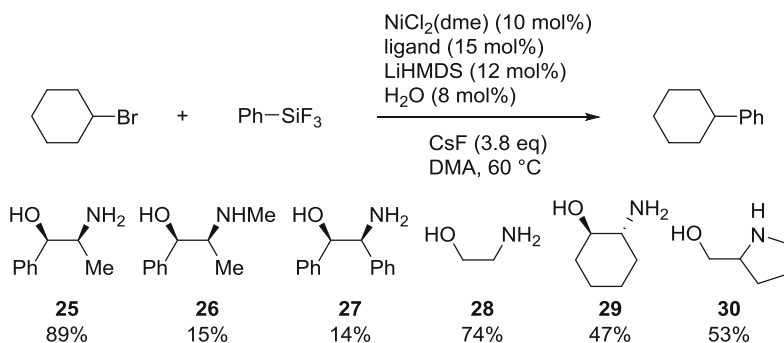
**Scheme 19** Cross-coupling using complex **20****Scheme 20** Reaction of CyBr with PhB(OH)<sub>2</sub> using bipyridine-type ligands

Systematic studies on the ligands for the Ni-catalyzed cross-coupling reaction of cyclohexyl bromide with phenylboronic acid were performed and revealed that *N,N*-bidentate ligands showed positive ligand effects but almost no reaction took place with phosphine ligands and tridentate nitrogen based ligands. Among bidentate ligands tested, bathophenanthroline **21** gave the best result, yielding the cross-coupling products from various primary and secondary alkyl halides with arylboronic acids (Scheme 20) [59].

This catalytic system is also applicable to Hiyama [60] and Stille [61] coupling reactions of primary and secondary alkyl halides with aryl trifluorosilane and trichlorostannane reagents with simple modifications (Schemes 21 and 22).

The ligand effects of aminoalcohols **25**–**30** were also examined for the Hiyama coupling reaction of cyclohexyl bromide with PhSiF<sub>3</sub> with the combination of Ni salt and LiHMDS as a base. Among aminoalcohols tested, norephedrine **25** showed an excellent ligand effect giving the better yield than methylated analog **26**, more

**Scheme 21** Hiyama coupling of a secondary alkyl bromide

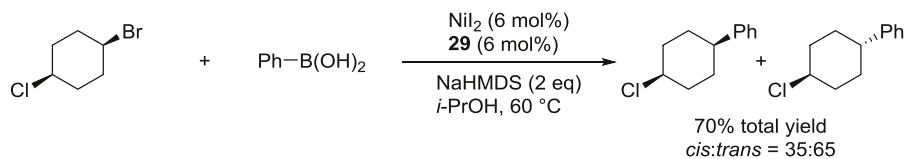
**Scheme 22** Stille coupling of a secondary alkyl bromide**Scheme 23** Hiyama coupling of a secondary alkyl bromide using aminoalcohols as ligand

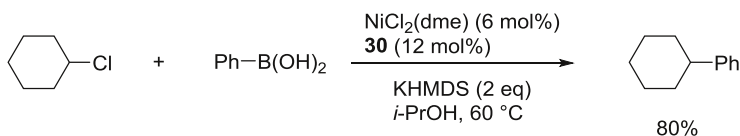
bulky 1,2-diphenylethanolamine **27** and cyclic aminoalcohols **29** and **30** (Scheme 23) [62].

It is obvious that the structure of the aminoalcohol ligands is crucial to achieve the coupling reaction efficiently and that the desired optimal electronic and steric properties for ligands vary largely depending on the substrates employed. In fact, *trans*-aminocyclohexanol **29** was found to be the best ligand in Suzuki–Miyaura coupling reaction of alkyl bromides and iodides (Scheme 24). On the other hand, the cross-coupling reaction of alkyl chlorides with arylboronic acids was successfully promoted by prolinol **30** as the ligand (Scheme 25) [63].

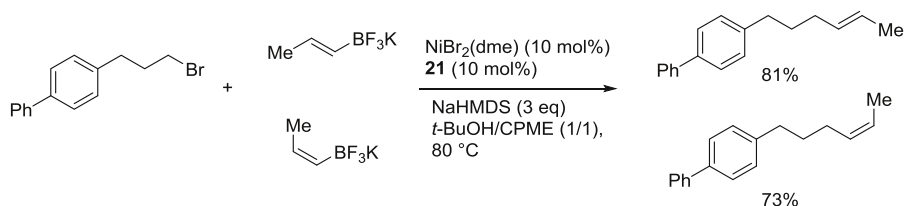
In the coupling reaction of alkyl bromides with alkenyltrifluoroborates in *t*-BuOH/cyclopentyl methyl ether (CPME) catalyzed by Ni/bathophenanthroline **21**, stereochemistry of the alkenyltrifluoroborates remained unchanged giving rise to the corresponding *E*- and *Z*-alkenes selectively (Scheme 26) [64].

Since alkenyl-9-BBNs are easily accessible from the corresponding alkyne and H-9-BBN, the direct use of alkenyl-9-BBN generated in situ for the coupling reaction makes a convenient procedure to produce internal alkenes via cross-coupling reaction.  $\beta$ -alkylstyrene was prepared by a one-pot operation via hydroboration/cross-coupling sequence using a Ni complex **13** (Scheme 27) [65].

**Scheme 24** Stereochemistry of arylation of a secondary alkyl bromide



**Scheme 25** Cross-coupling of a secondary alkyl chloride with  $\text{PhB(OH)}_2$

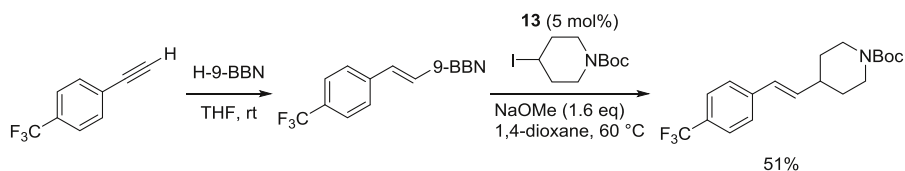


**Scheme 26** Stereoselective alkylation of alkenylborates

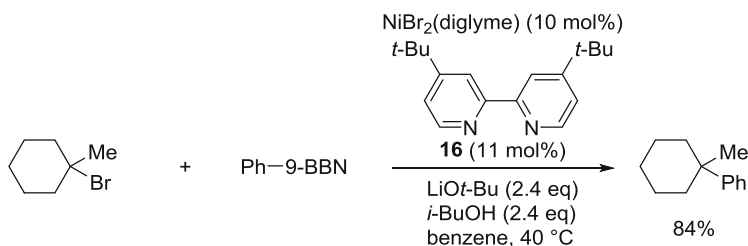
Although cross-coupling reaction to construct new quaternary carbon center is one of the most attractive transformations in this area, tertiary alkyl halides are the most difficult electrophiles to use in cross-coupling reaction. Interestingly, however, when an Ni salt and a bipyridine derivative **29** were employed, the cross-coupling reaction of a tertiary alkyl halide with  $\text{Ph-9-BBN}$  smoothly took place to give the corresponding coupling product in 84 % yield (Scheme 28) [66].

A similar catalytic system was applied to the cross-coupling reaction of a bicyclic iodocyclopropane derivative **31** with arylboronic acids. The reaction proceeded to give **32** in 83 % yield with complete retention of stereochemistry of **31** probably due to the steric rigidity of the fused cyclopropane ring (Scheme 29) [67].

As an alternative coupling partner of alkyl halides, various active esters have been tested in the coupling reaction with an arylzinc reagent in the presence of Ni

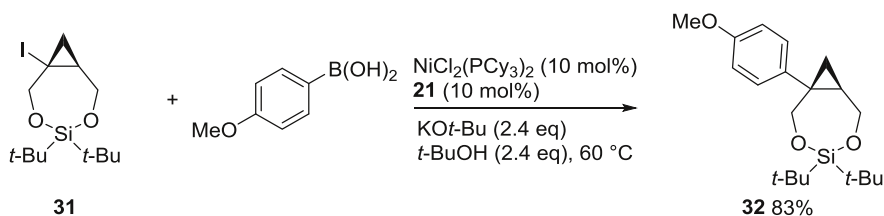
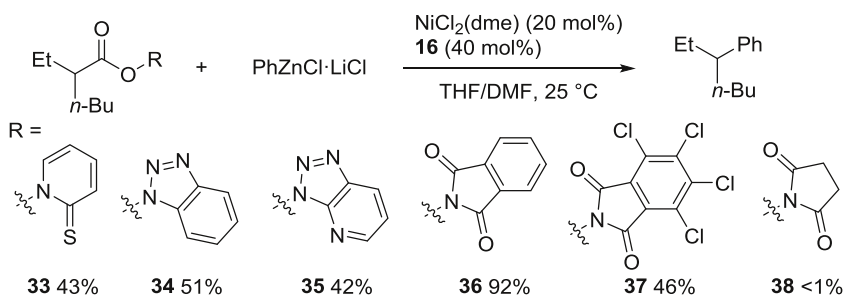


**Scheme 27** Olefin synthesis by alkylation of alkynes via hydroboration/cross-coupling sequence



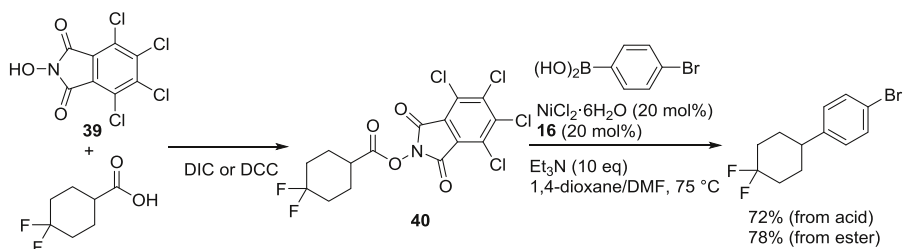
**Scheme 28** Cross-coupling reaction of a tertiary alkyl bromide



**Scheme 29** Cross-coupling of a bicyclic iodycyclopropane**Scheme 30** Decarboxylative cross-coupling of esters

catalyst (**Scheme 30**) [68]. The reaction of Barton ester **33** of 2-ethylhexanoic acid with  $\text{PhZnCl}\cdot\text{LiCl}$  in the presence of catalytic amounts of  $\text{NiCl}_2(\text{dme})$  and ligand **16** gave the corresponding coupling product in 43 % yield. The screening of esters revealed that HOAt (**34**) and HOBt (**35**) esters underwent the decarboxylative coupling reaction in moderate yields. *N*-Hydroxyphthalimide (NHPI) ester **36** improved the yield of the coupling product to 92 %. On the other hand, the corresponding tetrachlorinated NHPI ester **37** resulted in a lower yield and *N*-hydroxysuccinimide ester **38** did not give the coupling product.

Under similar conditions, esters of *N*-hydroxytetrachlorophthalimide coupled with arylboronic acids [69]. It is noteworthy that an ester **40** generated in situ by treating the corresponding carboxylic acid and hydroxytetrachlorophthalimide **39** with a condensation reagent could be used for the coupling reaction without purification and the desired coupling product was obtained without significant loss of yield compared to the reaction using isolated ester **40** (**Scheme 31**). These results

**Scheme 31** One-pot cross-coupling of a carboxylic acid via active ester **40**

imply that the coupling reaction provides a powerful tool to construct carbon frameworks from easily accessible carboxylic acids through a simple one-pot/two-operation process.

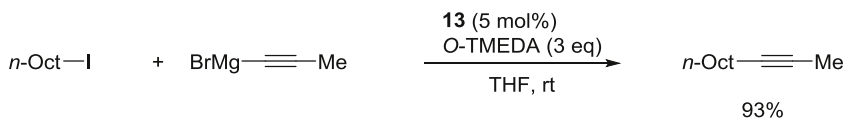
The evidence that cyclopropane ring opening was observed when a cyclopropylacetate was employed suggests the formation of alkyl radical intermediates in the decarboxylation step.

### 2.3 C(sp<sup>3</sup>)-C(sp) Coupling Reaction

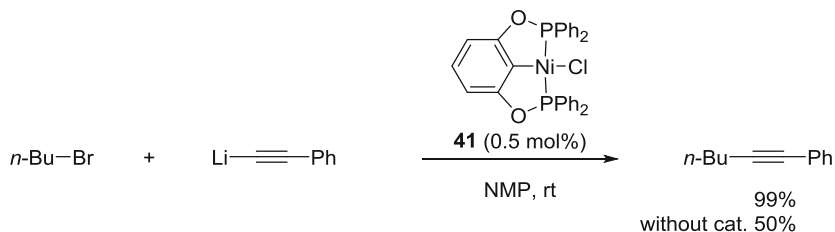
Cross-coupling reaction of alkyl halides with metal acetylides is a useful method to produce internal alkynes having an alkyl group, which are actually difficult to access by conventional methods such as Pd-catalyzed Sonogashira coupling reaction due to the unwanted side-reactions arising from  $\beta$ -hydrogen elimination. In 2011, Hu and Sun independently reported Ni-catalyzed cross-coupling reaction of unactivated alkyl halides with alkynylmagnesium and -lithium reagents, respectively. When the Ni complex **13** was employed as the catalyst in the presence of bis[2-(*N,N*-dimethylaminoethyl)]ether (*O*-TMEDA), *n*-OctI coupled with 1-propynylmagnesium bromide to give 2-undecyne in 93 % yield at rt (Scheme 32) [70].

Because of higher nucleophilicity of alkynyllithium reagents, a primary alkyl bromide coupled with alkynyllithium in *N*-methylpyrrolidone (NMP) without any catalysts in 50 % yield. The addition of Ni complex **41** carrying PCP pincer ligand improved the yield up to 99 % yield (Scheme 33) [71].

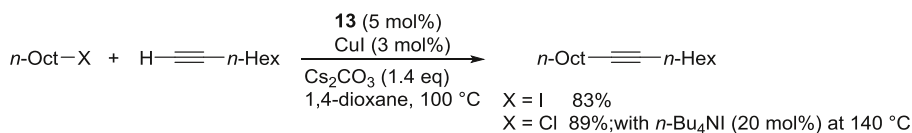
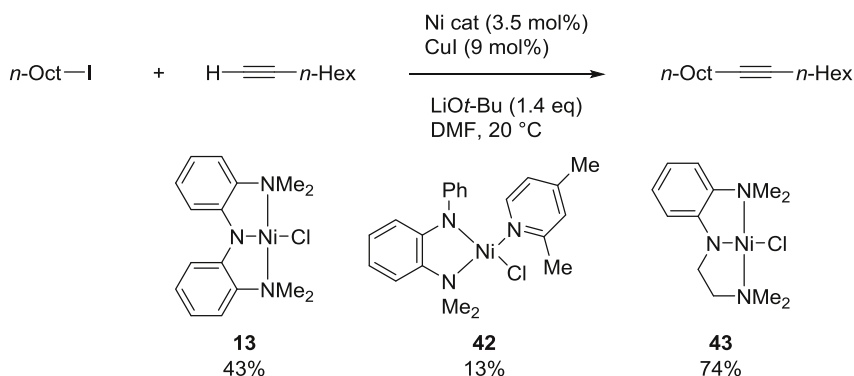
A more straightforward synthetic route toward internal alkynes is Sonogashira-type cross-coupling reaction of alkyl electrophiles with terminal alkynes, which are converted into the corresponding copper acetylides in situ without using strong bases. However, due to the difficulty in using alkyl halides as the coupling partner, over a period of three decades since its discovery in 1975 [72], no effective catalysts for Sonogashira reaction of alkyl halides had been reported. Fu and Glorius demonstrated that Pd-NHC catalytic systems promote Sonogashira coupling reaction of alkyl halides carrying  $\beta$ -hydrogen(s) [73, 74]. In 2009, Hu reported



**Scheme 32** Cross-coupling reaction of *n*-OctI with an alkynylmagnesium bromide



**Scheme 33** Cross-coupling reaction of *n*-BuBr with an alkynyllithium

**Scheme 34** Sonogashira-type coupling of alkyl halides with a terminal alkyne**Scheme 35** Cross-coupling of *n*-OctI with a terminal alkyne using tridentate amine ligands

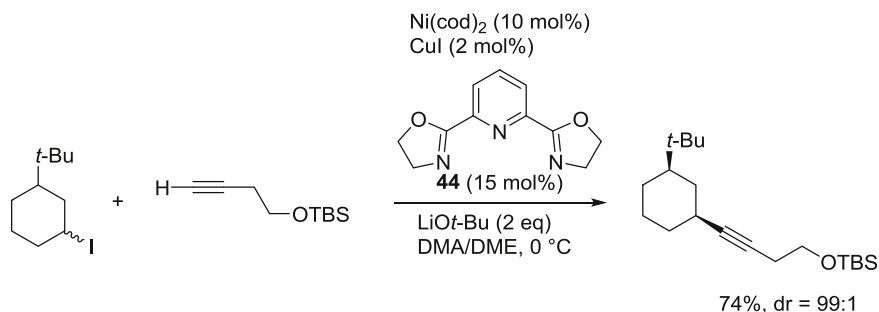
the first example of Ni-catalyzed Sonogashira coupling reaction of primary alkyl halides with various terminal alkynes by the combined use of complex **13** and CuI [75]. This catalytic system is applicable to not only alkyl iodides and bromides but also nonactivated alkyl chlorides albeit at high temperatures (Scheme 34).

When a suitable tridentate ligand was employed, the coupling reaction proceeded even at room temperature. For instance, the reaction of *n*-OctI with octyne at 20 °C resulted in only 43 and 13 % yields by use of Ni complexes **13** and **42**, respectively. On the other hand, Ni complex **43** efficiently catalyzed the coupling reaction to give the coupling product in 74 % yield (Scheme 35) [76]. The hemilabile nature of the dimethylaminoethyl ligand in complex **43** seems to be the key for this improved performance.

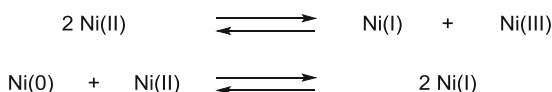
Liu screened various combinations of Ni salts with nitrogen based ligands and found that pybox **44** was the effective ligand for the coupling reaction of secondary alkyl halides with terminal alkynes. When substituted cyclohexyl iodides were employed as the coupling partner, the Sonogashira coupling reaction proceeded in highly diastereoselective manner through the formation of alkyl radical intermediates (Scheme 36) [77].

### 3 Mechanisms

As it is well established, Pd-catalyzed cross-coupling reaction of organohalides with organometallic reagents usually includes three elementary processes, that is (1) oxidative addition of organohalides to Pd(0), (2) transmetalation between R-Pd-X and organometallic reagents, and (3) reductive elimination of two organic groups on



**Scheme 36** Diastereoselective alkyne coupling of a substituted cyclohexyl iodide



**Scheme 37** Disproportionation/comproportionation equilibria of Ni species

Pd(II). These processes of Pd catalysis smoothly proceed when  $sp$ - and/or  $sp^2$ -hybridized coupling partners are employed; however, the reactions using alkyl halides may suffer from slow oxidative addition of alkyl halides as well as slow reductive elimination of alkylpalladium intermediates. As the result, various side-reactions such as  $\beta$ -hydrogen elimination from the alkylpalladium complexes often take place [8, 9].

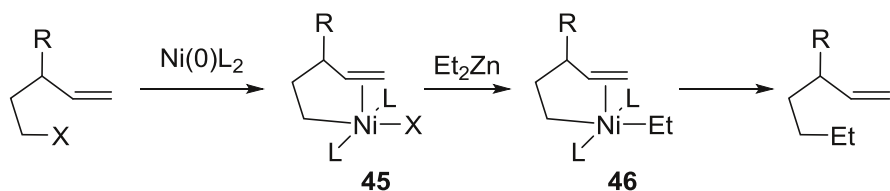
Principally, Ni behaves similarly as Pd does and catalyzes similar transformations. In some cases, however, Ni can catalyze the cross-coupling reaction of alkyl electrophiles in different mechanisms [15, 17]. While Pd usually catalyzes cross-coupling reaction via Pd(0)/Pd(II) catalytic cycle, Ni complexes having various oxidation states from Ni(0) to Ni(IV) can participate in the catalytic cycles that may include one-electron transfer from a Ni complex to the substrates employed and the facile disproportionation/comproportionation equilibria (Scheme 37) [20].

The formation of alkyl radicals from alkyl halides via single electron transfer (SET) usually results in unwanted side-reactions such as homocoupling, reduction, or dehydrohalogenation of alkyl halides; however, if thus formed alkyl radicals are recombined efficiently with Ni complexes in the reaction media, the corresponding alkylnickel complexes can play important roles as intermediates in cross-coupling reaction. Indeed, some of catalysts mentioned above involve the formal oxidative addition through the formation of alkyl radicals by SET from Ni intermediates.

In this section, reaction mechanisms proposed in some representative Ni catalytic systems are overviewed.

### 3.1 Ni/Electron Deficient $\pi$ -Ligand System

It is known that alkylmetal intermediates, generated by oxidative addition of alkyl halides to low valent metal catalysts, easily undergo  $\beta$ -hydrogen elimination to form the corresponding alkenes and metal hydrides, which can act as a reducing agent



**Scheme 38** Ni-catalyzed Negishi coupling assisted by intramolecular olefin coordination

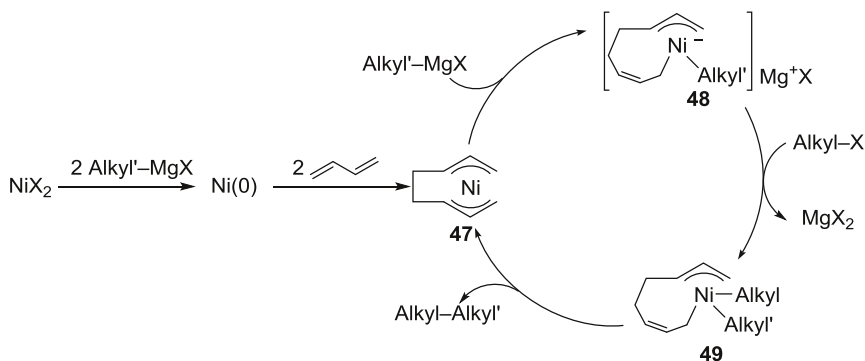
toward alkyl halides in some cases. Because  $\beta$ -hydrogen elimination from alkylnickel complexes is less favorable than the Pd case [78], the reduction and the dehydrohalogenation of alkyl halides can of course take place, but might be less serious in Ni-catalyzed reactions.

As shown in [Scheme 1](#), when alkyl iodides and bromides having a C–C double bond at 4- or 5-positions were employed, the Negishi cross-coupling reaction proceeded efficiently. In these cases, oxidative addition of alkyl halides toward Ni(0) species, generated in situ by reduction of the Ni(II) salt, proceeded efficiently without formation of the corresponding alkyl radicals. On the other hand, alkyl halides having no double bond unit underwent halogen–zinc exchange reaction, exclusively ([Scheme 2](#)). These results could be explained by assuming that the  $\pi$ -electrons of the double bond coordinate to diorganonickel intermediates **46**, generated by oxidative addition of Ni(0) with alkyl halides and following transmetalation of complex **45** with  $\text{Et}_2\text{Zn}$ , and accelerate reductive elimination ([Scheme 38](#)). Indeed, pioneering work by A. Yamamoto [2] and following studies by T. Yamamoto [79] revealed that the coordination of an electron deficient  $\pi$ -ligand toward square planer diorganonickel complexes enhances reductive elimination.

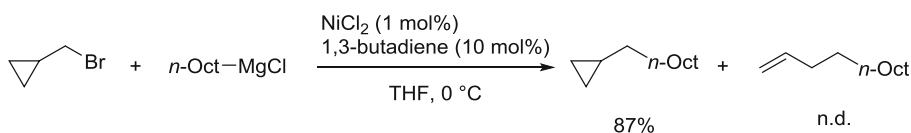
Indeed, the addition of styrene derivatives having an electron-withdrawing substituent or ketones is also effective to perform the coupling reaction efficiently. These additives coordinate to the Ni center to promote the reductive elimination selectively suppressing  $\beta$ -hydrogen elimination from the alkylnickel intermediates [29–32].

### 3.2 Ni/1,3-Butadiene Catalytic System

As shown in [Scheme 4](#), Ni represents high catalytic activity toward cross-coupling reaction of alkyl halides in the presence of 1,3-butadiene. The proposed catalytic cycle of the Ni/1,3-butadiene catalyzed cross-coupling of alkyl halides with alkyl Grignard reagents is depicted in [Scheme 39](#), where 1,3-butadiene acts as the ligand precursor. An in situ generated Ni(0) undergoes oxidative dimerization of 1,3-butadiene to form bis( $\pi$ -allyl)nickel complex **47**. The Ni center in the complex **47** has +2 oxidation state and is inert toward further oxidative addition of alkyl halides, but readily reacts with alkyl Grignard reagents to form anionic Ni complex **48** [80, 81]. In this complexation step, one of two allyl ligands changes its coordination mode from  $\pi$ -allyl to  $\sigma$ -allyl to maintain the 16e state at the Ni center and the other  $\pi$ -allyl ligand stabilizes the ate complex by withdrawing the anionic charge on Ni to



**Scheme 39** Ni/1,3-butadiene catalytic system with nickelate intermediates



**Scheme 40** Nonradical mechanism of Ni/1,3-butadiene catalytic system

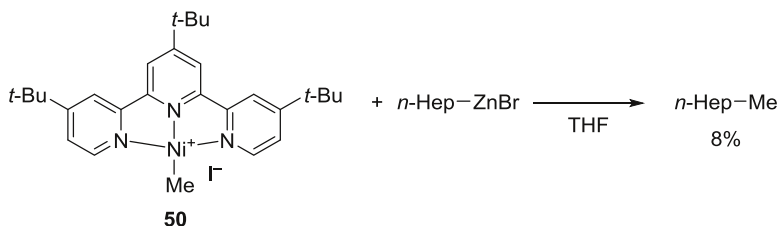
its LUMO orbital by the  $\pi$ -back donation. The anionic complex **48** possesses enhanced nucleophilicity and attacks alkyl halides to form Ni(IV) intermediates **49**, which then quickly undergo reductive elimination to give the cross-coupling products with regeneration of the bis( $\pi$ -allyl)Ni complex **47**. Alternatively, the alkyl group on anionic Ni may react directly with alkyl halides to yield coupling products. The reductive elimination from the Ni(IV) intermediates **49** at a high oxidation state should be a fast process and the reaction of alkyl halides with the anionic Ni complex **48** was found to be the rate-determining step in the catalytic cycle in the cases of alkyl bromides, iodides and tosylates [82]. Since all Ni intermediates **47–49** have the 16e structure with no open coordination site, the reaction can proceed smoothly with complete suppression of  $\beta$ -hydrogen elimination leading to the selective cross-coupling reaction. Computational studies on the catalytic cycle support these mechanisms [83, 84].

A reaction of cyclopropylmethyl bromide with an alkyl Grignard reagent gave the corresponding coupling product in 87 % yield without ring opening of the cyclopropane (**Scheme 40**), supporting this ionic pathway without alkyl radical intermediates that can possibly be generated from alkyl halides via an SET process [33].

The reaction of the anionic Ni complex **48** with alkyl halides is mainly controlled by enthalpy factors [82]. In sharp contrast, the oxidative addition of alkyl halides to a Pd(0)-trialkylphosphine complex is entropy controlled [85].

### 3.3 Ni/nitrogen Based Ligand System

In addition to the ionic pathways mentioned above, Ni-catalyzed cross-coupling proceeds by alternative pathways involving radical intermediates via homolytic



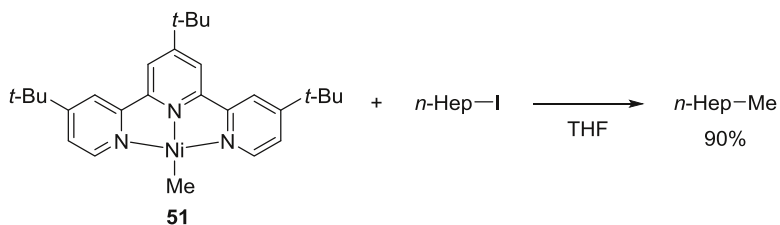
**Scheme 41** A control experiment of cationic Ni(II) complex **50** with an alkylzinc reagent

cleavage of the C–X bond of alkyl halides triggered by SET from a Ni complex in the presence of nitrogen based ligands, which can be classified into four types, that is, (1) neutral tridentate, (2) neutral bidentate, (3) anionic tridentate, and (4) anionic bidentate ligands.

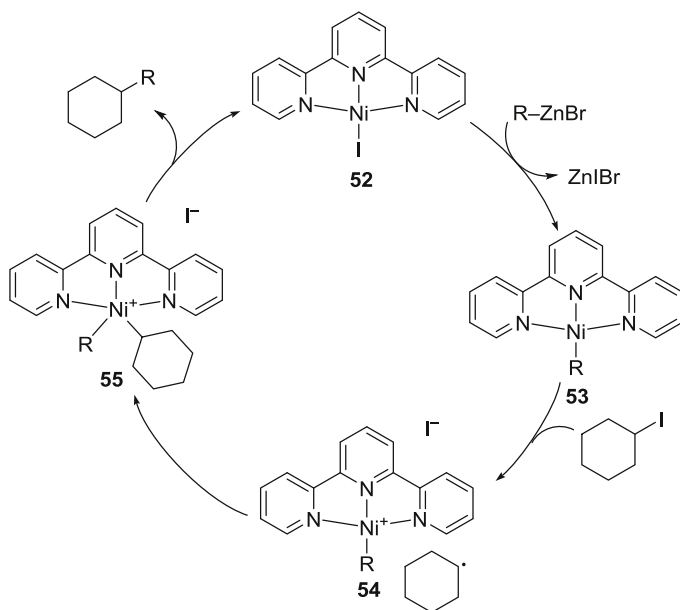
As the type 1 ligands, the reactivity of alkylnickel complexes bearing a terpyridine ligand and the catalytic reaction mechanisms were examined [41, 42, 86]. The reaction of Ni(0) with MeI in the presence of a terpyridine ligand provided a cationic methylnickel(II) complex **50** and the treatment of NiMe<sub>2</sub>(tmeda) with the same ligand gave a neutral methylnickel(I) complex **51**. The reaction of the cationic Ni(II) complex **50** with an alkylzinc reagent gave only 8 % yield of the coupling product (Scheme 41). On the other hand, the neutral methylnickel(I) complex **51** reacted with *n*-HepI to give the corresponding coupling product in 90 % yield (Scheme 42). These results suggest that the Ni/NNN tridentate catalytic system does not include a simple Ni(0)/Ni(II) mechanism comprising the oxidative addition of alkyl halides toward a Ni(0), transmetalation, and reductive elimination.

A plausible catalytic cycle for the Ni-terpyridine-catalyzed cross-coupling reaction of alkyl iodides with alkylzinc reagents is shown in Scheme 43. The in situ formed Ni(I) complex **52** undergoes transmetalation with organozinc reagents to give the corresponding organonickel species **53**. SET from the Ni complex **53** to alkyl iodides forms alkyl radicals and Ni(II) complex **54**. Recombination of these radicals gives Ni(III) species **55** as an intermediate of formal oxidative addition, which then undergoes reductive elimination to yield coupling products with regeneration of Ni(I) species **52** to complete the catalytic cycle.

As an example of type 1 ligands, Fu et al. reported mechanistic studies on Ni/pybox-catalyzed Negishi coupling reaction (Sect. 4) [87]. Phenylnickel(II) complex



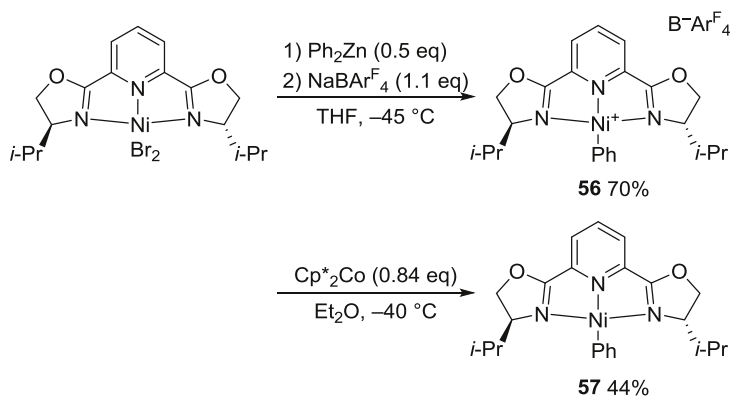
**Scheme 42** Intermediacy of neutral Ni(I) complex **51** with an alkyl iodide



**Scheme 43** Proposed catalytic cycle of Ni/terpyridine catalytic system

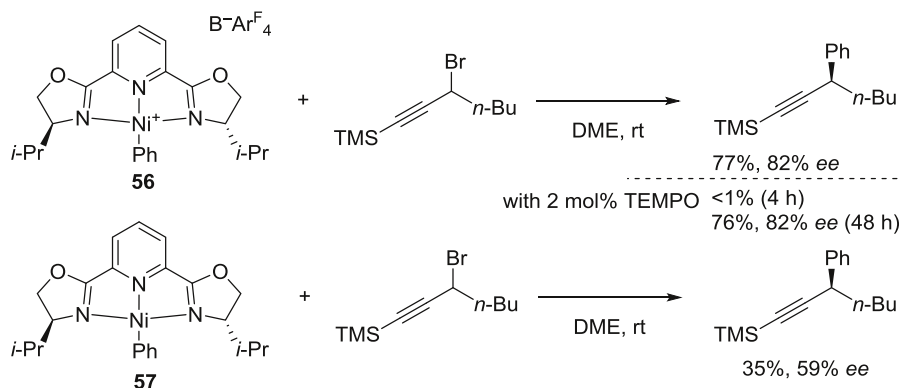
**56** and phenylnickel(I) complex **57** (Scheme 44) were synthesized and their molecular structures were determined by X-ray crystallography. Both of these complexes adopt a square planar geometry. The ESR spectrum of Ni(I) complex **57** showed a signal with coupling to a  $^{14}\text{N}$  atom, suggesting that the radical character located mainly in the pybox ligand.

When Ni(II) complex **56** was treated with a propargyl bromide, the corresponding coupling product was obtained with a comparable yield and enantioselectivity [88]. The stoichiometric reaction was largely affected by the addition of TEMPO, resulting in no reaction in 4 h. However, the reaction did proceed to give the



**Scheme 44** Synthesis of phenylnickel(I) and (II) complexes bearing pybox ligand

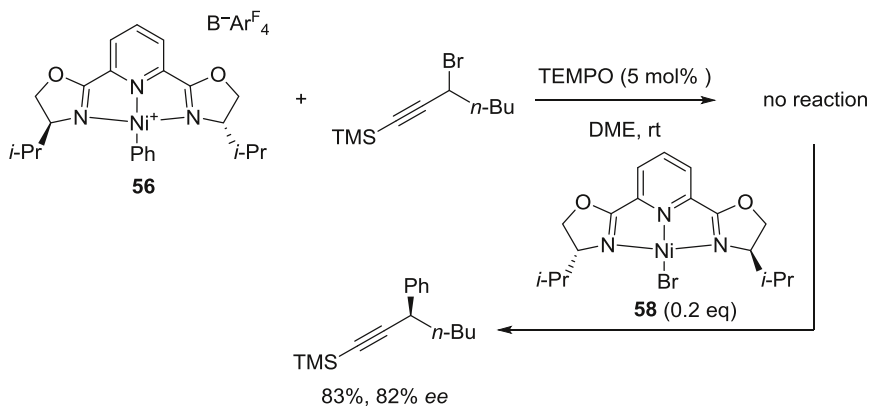




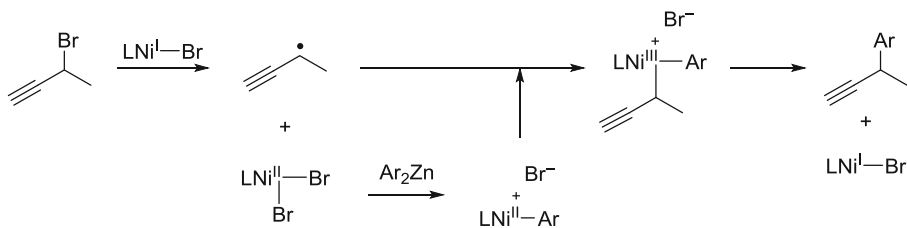
**Scheme 45** Reactivity of cationic Ni(II) and neutral Ni(I) complexes toward a secondary alkyl bromide

product in 76 % yield by prolonging the reaction time to 48 h, suggesting a TEMPO-induced induction period. In contrast, somewhat lower yield and enantioselectivity was observed when Ni(I) complex **57** was subjected to the same stoichiometric reaction (**Scheme 45**).

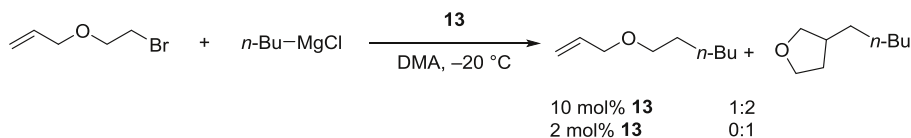
The stoichiometric reaction employing phenylnickel(II) complex **56** and Ni(I) complex **58** carrying the opposite enantiomer of the pybox ligand provided interesting information about the reaction pathway of this catalytic system (**Scheme 46**). When Ni(II) complex **56** was treated with a racemic propargyl bromide in the presence of 5 mol% of TEMPO, no reaction took place as shown above. The addition of Ni(I) complex **58** to the reaction mixture did promote the coupling reaction to give the corresponding coupling product with the same *ee* as in **Scheme 45**. This result indicates that propargyl radical selectively recombines with initially added Ni(II) complex **56** and Ni(I) complex **58** acts as an activator or a promoter. A proposed pathway is depicted in **Scheme 47**.



**Scheme 46** Reaction of phenylnickel complex **56** with a secondary alkyl bromide promoted by Ni(I) complex **58**

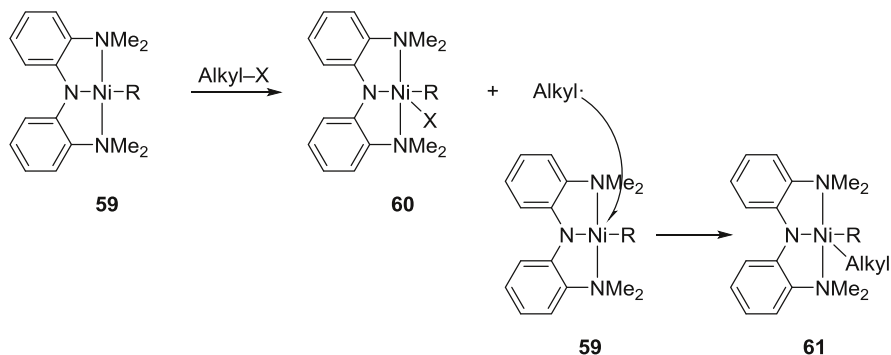


**Scheme 47** Proposed reaction pathway of Ni/pybox catalytic system

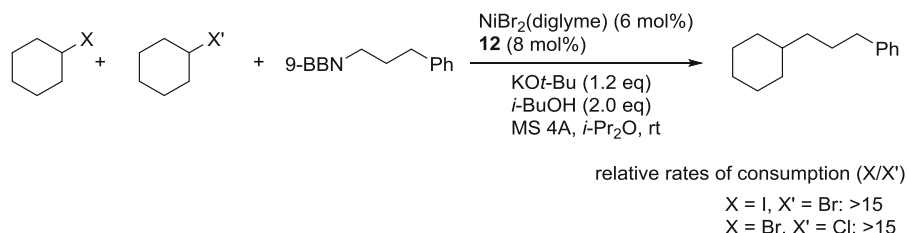


**Scheme 48** Direct cross-coupling vs. cyclization/cross-coupling

A modified catalytic cycle including carbon radical intermediates was proposed for the reactions using anionic tridentate *N*-based ligands where two Ni(II) complexes are involved in the catalytic cycle [89, 90]. In the coupling reaction of allyl bromoethyl ether with *n*-BuMgCl using the Ni complex **13** as the catalyst, the product ratio of the direct cross-coupling product and the cyclized product varied depending on the amount of the catalyst employed, i.e., the cyclized product predominated at low catalyst loading conditions (**Scheme 48**). This result and other evidences suggested a bimetallic oxidative addition pathway is operating (**Scheme 49**). The transmetalation of **13** with organometallic reagents forms an alkylnickel(II) complex **59**, which then reacts with alkyl halides to give alkyl radicals and a nickel(III) complex **60**. Thus formed alkyl radicals recombine with another alkylnickel(II) complex **59** to generate diorganonickel(III) **61** which undergoes reductive elimination giving rise to the coupling product and a Ni(I) complex. The successive comproportionation of thus formed Ni(I) species with the nickel(III) complex **60** regenerates the Ni(II) intermediates **13** and **59** to complete the catalytic cycle. This pathway is supported by kinetic studies.



**Scheme 49** Bimetallic mechanism of oxidative addition of alkyl halides toward Ni



**Scheme 50** Competitive reactions of alkyl halides

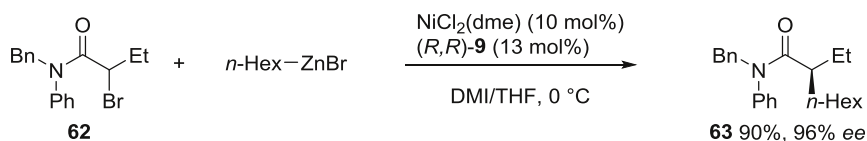
Catalytic reactions using bidentate ligands are also examined. When  $\alpha$ -bromo-sulfonamides and  $\alpha$ -sulfones with a C–C double bond at the 5-position were subjected to a cross-coupling with  $\text{ArZnX}$  in nickel/bis(oxazoline) system (type 2), the ratio of uncyclized/cyclized products changed depending on the concentration of the catalyst [91]. This result supports the formation of free carbon radicals and their trapping by a Ni intermediate.

Kinetic studies of Ni-catalyzed Suzuki–Miyaura coupling reaction using secondary alkyl halides and a type 4 ligand **12** was performed (Scheme 50) [44]. The rate law for the reaction of cyclohexyl bromide is first-order in the catalyst ( $\text{NiBr}_2$ -diglyme/ligand **12**), first-order in the alkylborane, and zeroth-order in the electrophile. These results suggest that the oxidative addition process is not the rate-determining step in the case of cyclohexyl bromide. In contrast, for cyclohexyl chloride, the rate of cross-coupling depends on the concentration of the electrophile.

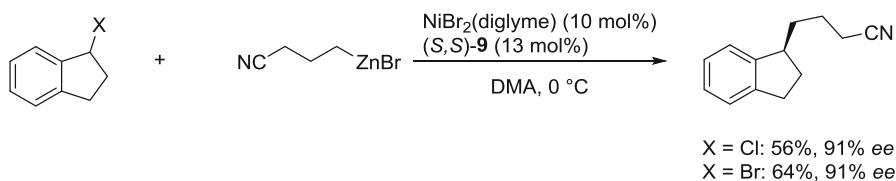
## 4 Asymmetric Coupling Reaction of Alkyl Electrophiles

When alkyl radical intermediates are involved in the cross-coupling reaction, the stereochemistry of the products can be controlled by chiral ligands regardless of the stereochemistry of the alkyl halides employed (for representative reviews :[13, 18, 19]). This section covers recent advances on Ni-catalyzed asymmetric cross-coupling reaction using alkyl electrophiles.

The pioneering studies on asymmetric cross-coupling were performed by Fu using activated alkyl halides [89, 92]. The reaction of racemic  $\alpha$ -bromoamide **62** with an alkylzinc reagent using pybox **9** as a chiral ligand gave the coupling product **63** in 90 % yield with 96 % *ee* (Scheme 51) [92]. The reaction was sensitive to the structure of the substrates and almost no reaction took place when an *N,N*-diethyl amide was used instead of **62**. The bromide was recovered as a racemic mixture after the reaction indicating no evidence of kinetic resolution. The result that the  $\alpha$ -bromoamide reacted selectively even in the presence of other simple primary and



**Scheme 51** Stereoconvergent Negishi coupling of an  $\alpha$ -bromoamide

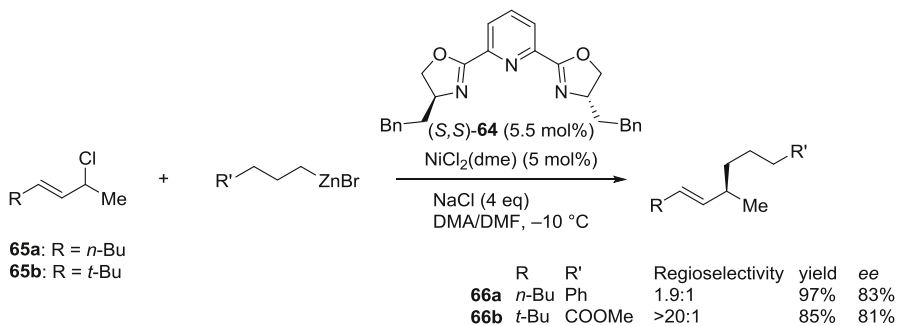


**Scheme 52** Stereoconvergent Negishi coupling of benzylic halides

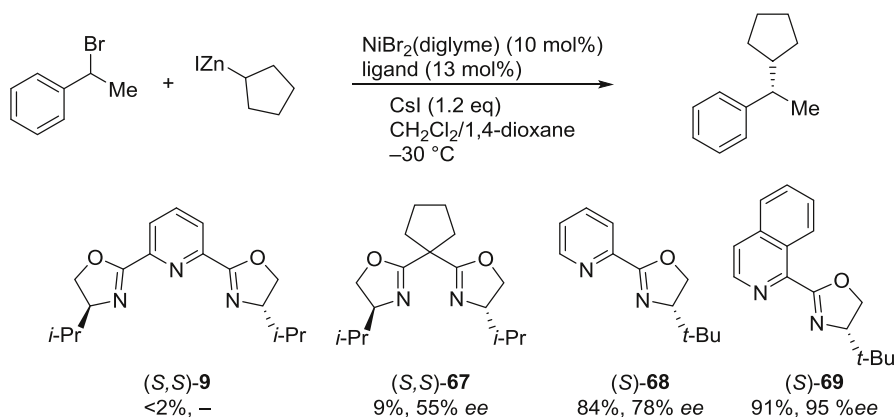
secondary alkyl bromides implies that the *N*-aryl amide moiety plays important roles in the C–X bond cleavage processes.

Benzylic and allylic secondary alkyl chlorides and bromides were found to be suitable alkyl electrophiles for the stereoconvergent Negishi coupling reaction. For instance, chloro- and bromoindane coupled with an alkylnickel reagent in the presence of NiBr<sub>2</sub>(diglyme) and chiral pybox ligand **9** to give the alkylated product in good yields with high enantioselectivities (Scheme 52). Substituted haloindane derivatives also coupled with alkylnickel reagents in excellent enantioselectivity higher than 91% *ee*, while 1-bromoethylbenzene resulted in somewhat lower enantioselectivity of 75% *ee* [93]. Allylic chlorides **65** coupled with alkylnickel halides under similar conditions. This reaction was accelerated by addition of 4 equiv. of NaCl, either by increasing the ionic strength of the reaction mixture and/or by activating the organozinc reagents, without affecting the enantioselectivities [94]. Symmetrical allylic chlorides gave the corresponding coupling products in good yields with high enantiomeric excesses. Unfortunately, reactions of unsymmetrical allylic chlorides **65** sometimes result in poor regioselectivities, although high enantioselectivities can be attained (Scheme 53).

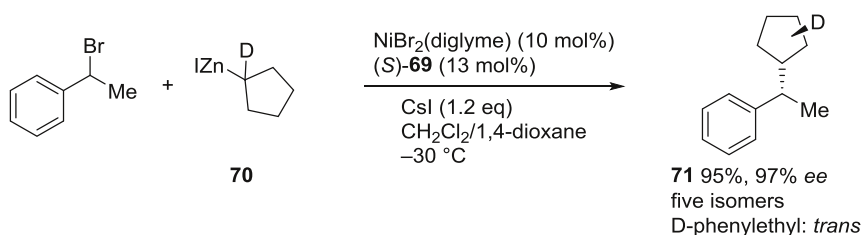
Superiority of bidentate ligands having only one chiral oxazoline moiety **68** and **69** in comparison with pybox **9** and box **67** was demonstrated for asymmetric Negishi coupling of acyclic secondary alkyl bromides with secondary alkylnickel reagents, which affords high yields and excellent enantioselectivities (Scheme 54) [95]. However, the use of these modified ligands sometimes suffers from unwanted isomerization of alkyl groups via β-hydrogen elimination. Actually, a mixture of coupling products having *i*-Pr and *n*-Pr groups was produced when *i*-PrZnI was used as a secondary alkylnickel reagent. Another evidence of this isomerization was



**Scheme 53** Stereoconvergent Negishi coupling of allylic chlorides



**Scheme 54** Ligand effect on cross-coupling of a secondary bromide with a secondary alkylzinc reagent using oxazoline-based ligands

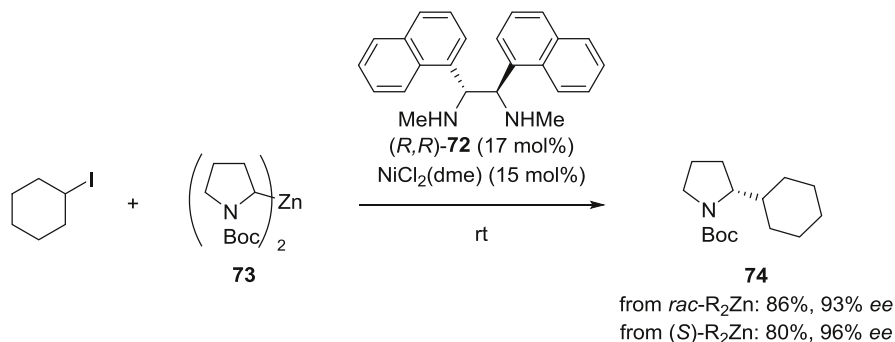


**Scheme 55** An evidence of isomerization of an alkyl group

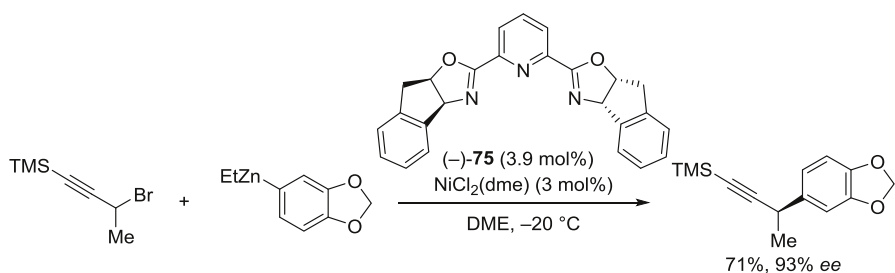
obtained by the use of a deuterated cyclopentylzinc reagent **70** which coupled with a secondary alkyl bromide to give a mixture of five isomers **71** having D at different positions (Scheme 55).

By using a chiral diamine **72**, Ni-catalyzed asymmetric cross-coupling of cyclic and acyclic secondary alkyl iodides with racemic *N*-Boc-pyrrolidinylzinc reagent **73** afforded excellent yields and *ee* (Scheme 56) [96]. Racemic products were obtained by the combination of a chiral zinc reagent **73** with an achiral catalyst. In addition, the use of either enantiomer of the stereochemically stable chiral alkylzinc reagent **73** gave the product having the same stereochemistry, which was controlled only by the chiral ligand **72**. No evidence of kinetic resolution of the alkylzinc reagent **73** and epimerization of the chiral center was observed. With these results, the stereochemistry might be determined by  $\beta$ -hydride elimination/ $\beta$ -migratory insertion pathway without dissociation of the olefin from Ni under the chiral environment created by the ligands.

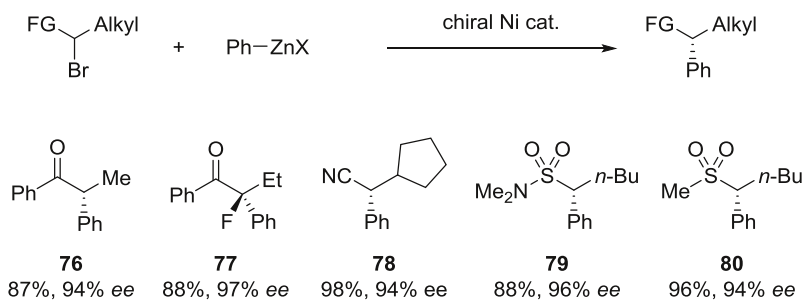
Asymmetric cross-coupling of arylzinc reagents with racemic propargyl halides was also achieved using Ni/pybox **75** catalytic system with high enantioselectivities (Scheme 57) [88]. Under the similar reaction conditions, the coupling reaction of propargyl carbonates with arylzinc reagents smoothly proceeded with good enantioselectivities [97].



**Scheme 56** Enantioselective alkylation of *N*-Boc-pyrrolidinylzinc reagent **73**

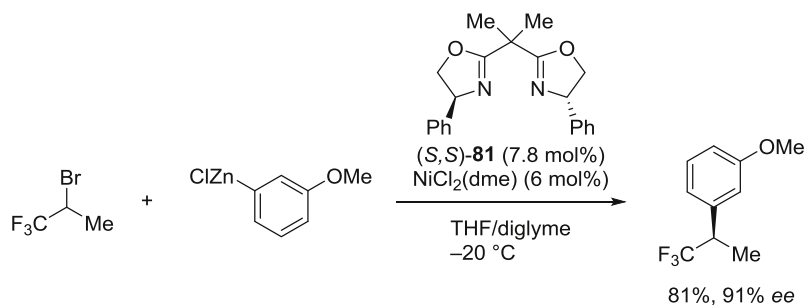


**Scheme 57** Asymmetric cross-coupling of a propargyl bromide with an arylzinc reagent



**Scheme 58** Scope of stereoconvergent Negishi coupling of activated secondary alkyl bromides

As shown in [Scheme 58](#), alkyl halides having various functional groups were subjected to enantioselective coupling reaction with arylzinc reagents using tridentate and bidentate *N*-based ligands. An  $\alpha$ -bromoacetophenone derivative coupled with phenylzinc reagent to give **76** in high yield and enantioselectivity [98]. Introduction of fluorine atom at the  $\alpha$ -position of ketones did not affect the reaction giving rise to enantiomerically enriched tertiary alkyl fluoride **77** [99]. In addition,  $\alpha$ -bromo cyanides [100], sulfonamides, and sulfones [91] underwent the asymmetric cross-coupling reaction to give the corresponding coupling products **78–80** with high *ee*.

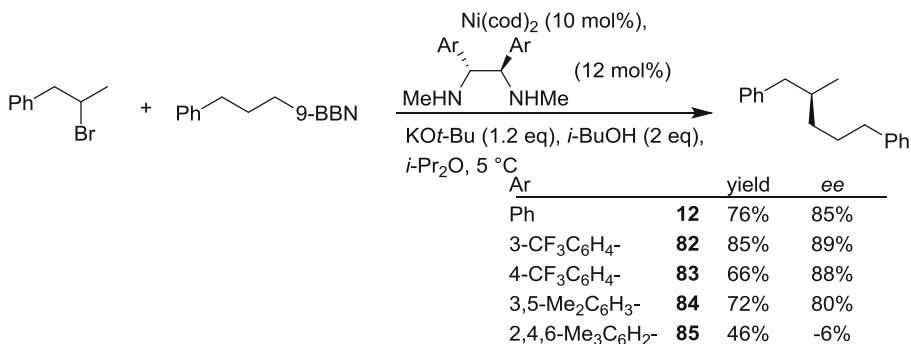


**Scheme 59** Enantioselective arylation of 2-bromo-1,1,1-trifluoropropane

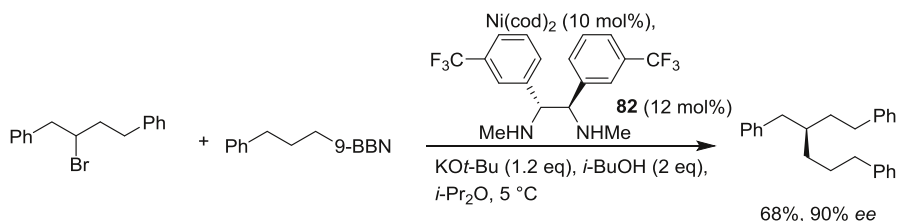
For the enantioselective cross-coupling reaction of  $\text{CF}_3$  substituted secondary alkyl halides with arylzinc reagents, chiral box ligand **81** afforded the best result. Surprisingly, the chiral Ni/box catalyst could discriminate between  $\text{CF}_3$  and  $\text{CH}_3$  to give the coupling product in 91 % *ee* (Scheme 59) [101].

Secondary alkyl bromides carrying C–O double bond of ketone, ester, or amide at the adjacent position underwent the asymmetric cross-coupling reaction with various alkenyl and aryl metal reagents involving organoboron [102], silicon [103], magnesium [104], and zirconium [105] reagents by the aid of appropriate chiral ligands and additives.

Fu et al. examined commercially available chiral diamine ligands for the Suzuki–Miyaura coupling and found that the reaction of a secondary homobenzylic bromide with an alkyl-9-BBN proceeded in enantioselective manner by the aid of chiral *N,N'*-dimethylethylenediamine type ligands [106]. The electron deficient diamines having trifluoromethylphenyl group **82** provided a good yield with a high enantiomeric excess. When a sterically congested diamine ligand **85** was used, both yield and *ee* decreased (Scheme 60). The electron deficient chiral ligand **82** afforded high enantioselectivities for various homobenzylic secondary alkyl bromides. This reaction is sensitive to the structures of the substrates. For example, the reactions of 2-bromo-1,2,3,4-tetrahydronaphthalene as a cyclic homobenzylic bromide and (3-bromobutyl)benzene as a  $\gamma$ -phenyl bromide resulted in poor *ee*.



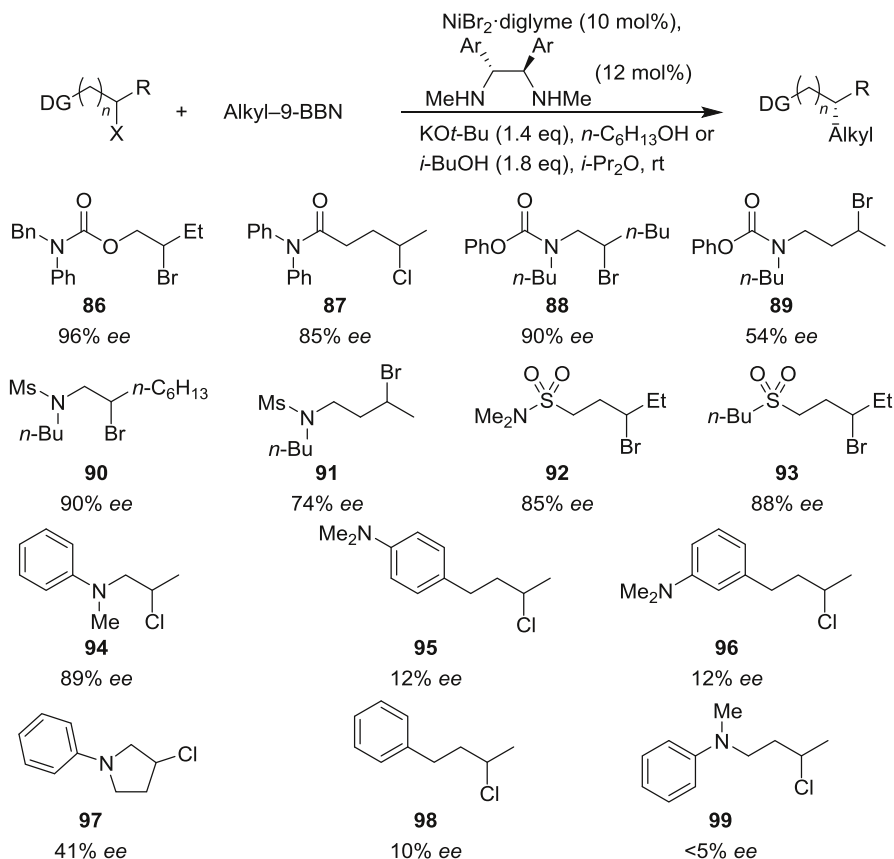
**Scheme 60** Enantioselective cross-coupling using chiral diamine ligands



**Scheme 61** Stereocontrol by phenyl groups at remote positions

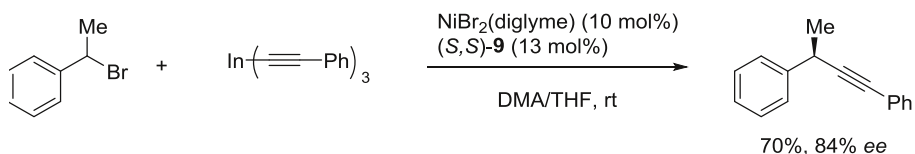
However, 2-bromo-1,4-diphenylbutane as a  $\beta,\gamma$ -diphenyl bromide afforded the corresponding alkylated product with 90 % enantioselectivity (**Scheme 61**) [106]. These results suggest that the interaction between  $\beta$ -aryl group and Ni center plays an important role in the stereoselection step of the catalytic cycle.

The effects of functionalities at remote positions on the stereoselectivities were examined using substrates bearing coordinating heteroatom functionalities, and the results are summarized in **Scheme 62**. Carbonyl group of an acylated halohydrin **86**



**Scheme 62** Scope and limitations of stereoconvergent Suzuki–Miyaura coupling





**Scheme 63** Asymmetric alkylation of a secondary bromide



**Scheme 64** Diastereoselective alkylation of halosaccharides

[107], a  $\gamma$ -haloamide **87** [108], and a carbamate-protected haloamine **88** [109] effectively controlled their enantioselectivities. Carbamate-protected  $\gamma$ -haloamine **89** afforded a lower *ee*, whereas sulfonamides **90–92** and sulfone **93** at the  $\gamma$ -position also act as the appropriate directing groups in the asymmetric Suzuki–Miyaura coupling reactions.

Tertiary amino groups also play important roles, but their positions are important to achieve high enantioselectivity, as shown in [Scheme 62](#) [110]. Dimethylamino group on the phenyl ring at *m*- or *p*-position in substrates **95** and **96** exhibited little effect on the *ee*. Cyclic analog **97** was not a suitable substrate for the asymmetric Suzuki–Miyaura coupling reaction. The evidence that **94** reacts faster than **98** but the ratio of the relative rates is only two suggests that the amino groups do not largely affect the reactivity of the Suzuki–Miyaura coupling but play important role in the stereo selection process.

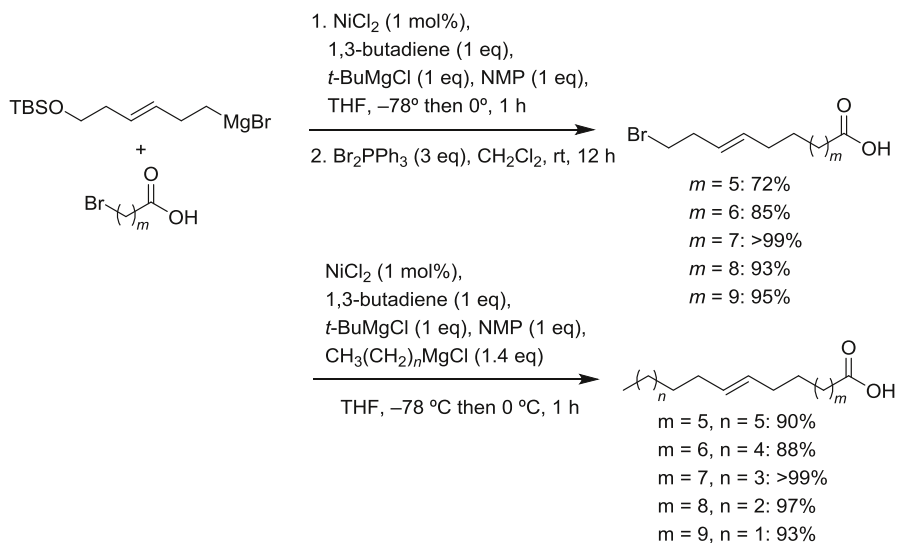
Asymmetric alkylation of benzylic secondary alkyl bromides with alkyne–indium has also been achieved using chiral Ni/pybox **9** complex ([Scheme 63](#)) [111].

Gagné demonstrated the Ni-catalyzed diastereoselective *C*-alkylation of halosaccharides with organozinc reagents. The diastereoselectivity largely depended on the structure of sugars and mannose derivative **100** showed excellent diastereoselectivity rather than glucose and galactose derivatives ([Scheme 64](#)) [112, 113].

## 5 Applications

In this section, applications of Ni-catalyzed cross-coupling reaction to the synthesis of natural products and their analogues are briefly overviewed.

The Ni-butadiene catalytic system was employed to construct long alkyl chains of fatty acids and related compounds by the cross-coupling of  $\omega$ -halocarboxylic acids. In order to avoid messy protection-deprotection processes of the carboxylic moieties, carboxylic acids were treated with *t*-BuMgCl to convert into their



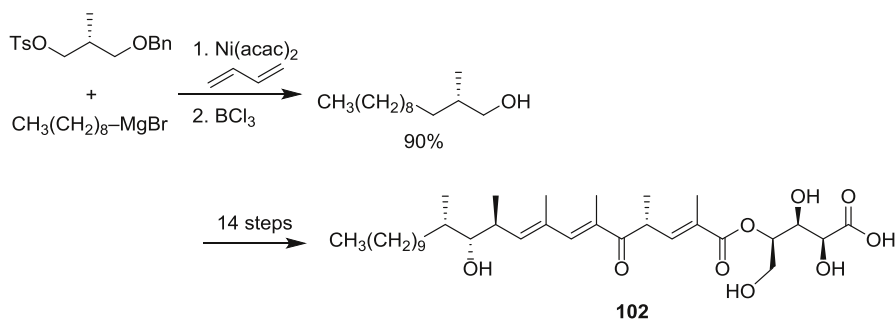
**Scheme 65** Synthesis of elaidic acid and its regioisomers by iterative coupling

magnesium salts [114] prior to the Ni-catalyzed cross-coupling. Iterative cross-coupling by a one-pot procedure provided elaidic acid, which has *trans*-olefin moiety at  $\omega$ -9 position, and its regioisomers in excellent yields (Scheme 65) [115].

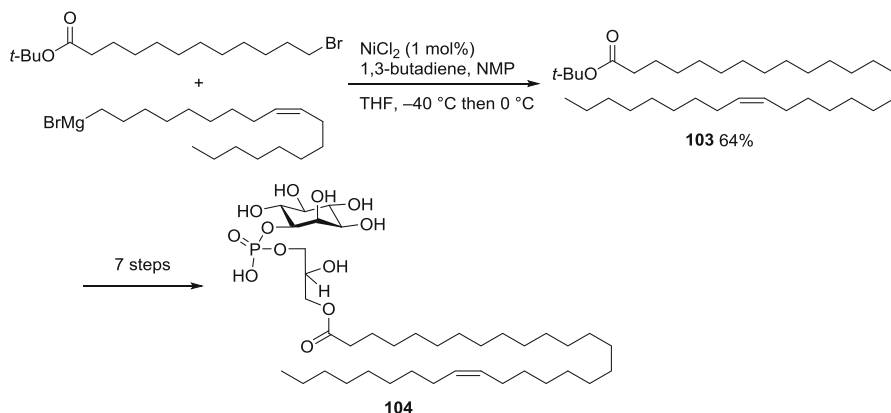
Kobayashi employed the cross-coupling reaction using Ni-butadiene catalytic system in the synthesis of the C7–C22 fragment of an antifungal agent, khafrefungin **102**, as a key step of the asymmetric total synthesis (Scheme 66) [116].

By the use of Ni/1,3-butadiene catalytic system, a long unsaturated fatty acid moiety **103** having 30 carbons of an inositol phospholipid **104** from *E. histolytica* was synthesized and used for the total synthesis of the natural product (Scheme 67) [117].

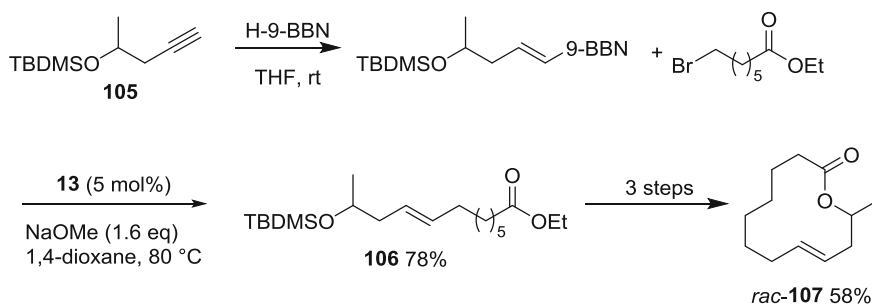
Hu et al. demonstrated the utility of their one-pot hydroboration/cross-coupling sequence by synthesizing a natural macrolide, recifeiolid **107**. Hydroboration of alkyne **105** and subsequent cross-coupling reaction with ethyl 7-bromoheptanoate by Ni complex **13** gave the corresponding cross-coupling product **106** in 78 % yield.



**Scheme 66** Total synthesis of khafrefungin **102**



**Scheme 67** Total synthesis of an inositol phospholipid **104**

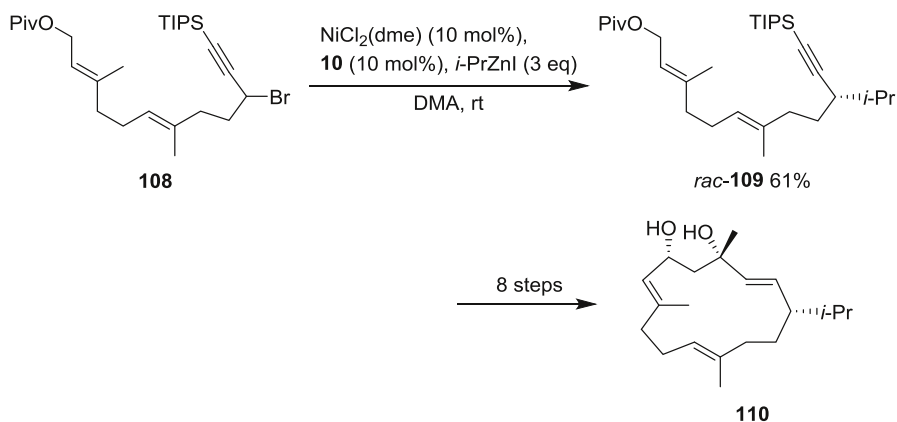


**Scheme 68** Total synthesis of recifeiolid **107**

Deprotection and macrolactonization of **106** afforded *rac*-**107** in good yield (**Scheme 68**) [65].

An antitumor active cembranoid diterpene, ( $\pm$ )- $\alpha$ -cembra-2,7,11-triene-4,6-diol **110**, has tertiary carbon centers with the 14-membered macrocycle skeleton. The adjacent tertiary carbon centers were successfully constructed by Ni-catalyzed secondary–secondary coupling of a propargyl bromide **108** with *i*-PrZnI to synthesize an intermediate **109**. (**Scheme 69**) [40].

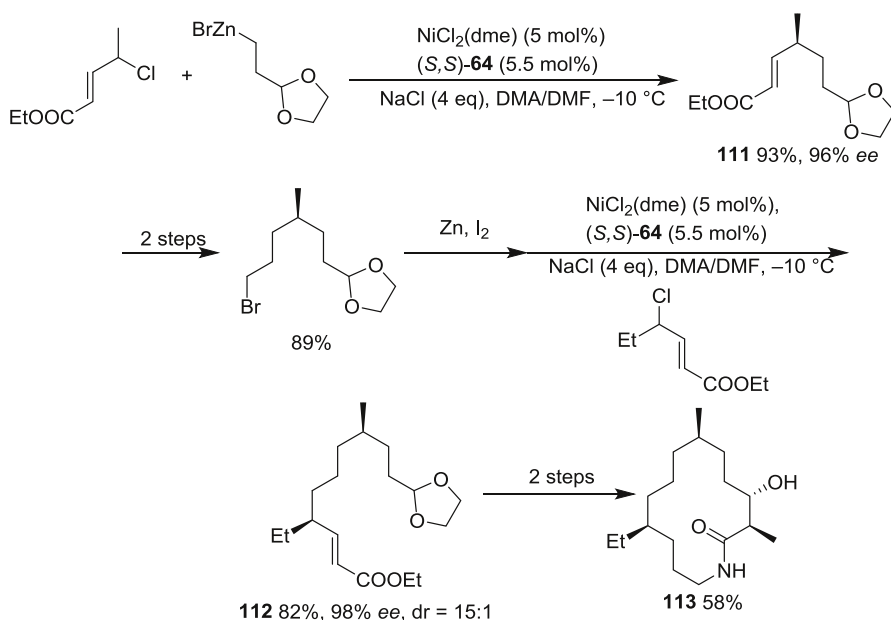
The asymmetric formal total synthesis of fourteen membered macrocycle, fluvirucinine  $A_1$  **113**, possessing two tertiary stereocenters has been achieved by asymmetric Negishi reaction using Ni/pybox **64**. The coupling reaction of an allylic chloride with an alkylzinc reagent gave the corresponding coupling product **111** in 93 % yield with 96 % *ee*. Subsequent asymmetric Negishi coupling of a racemic secondary allyl chloride with an alkylzinc reagent derived from **111** gave the coupling product **112** with excellent enantio- and diastereoselectivities. Fluvirucinine  $A_1$  **113** was successfully synthesized by the following two step operations (**Scheme 70**) [94]. Due to the difficulty of constructing isolated chiral centers based on diastereoselective strategies, the present method would be useful for the asymmetric total synthesis of a wide variety of natural products.



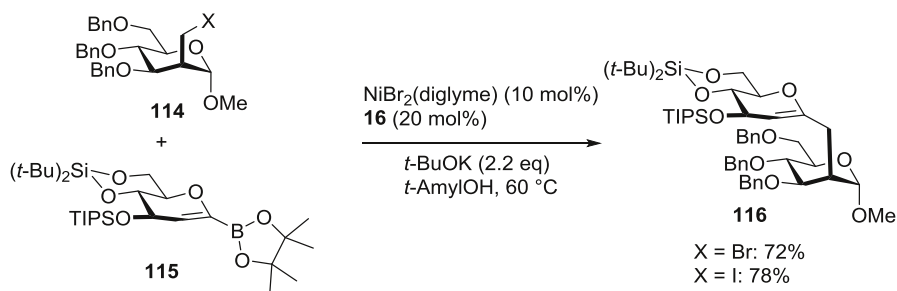
**Scheme 69** Total synthesis of (±)- $\alpha$ -cembra-2,7,11-triene-4,6-diol **110**

Although connecting two saccharide units by cross-coupling reaction is a highly challenging issue in organic synthesis due to the difficulties arising from their highly functionalized skeletons, Ni-catalyzed Suzuki–Miyaura cross-coupling provides a reliable synthetic tool to combine two saccharides by forming a C–C bond. For instance, 2-halomethylhexose derivative **114** was coupled with borylated D-glucal **115** in the Ni/**16** catalytic system giving **116** in good yields (Scheme 71) [118].

Total synthesis of a family of salmochelins, metabolites of the ferric-binding siderophores produced by *E. coli* and *S. enterica*, was achieved by Gagné and Gong et al. employing Ni-catalyzed cross-coupling reaction of a bromoglucose derivative

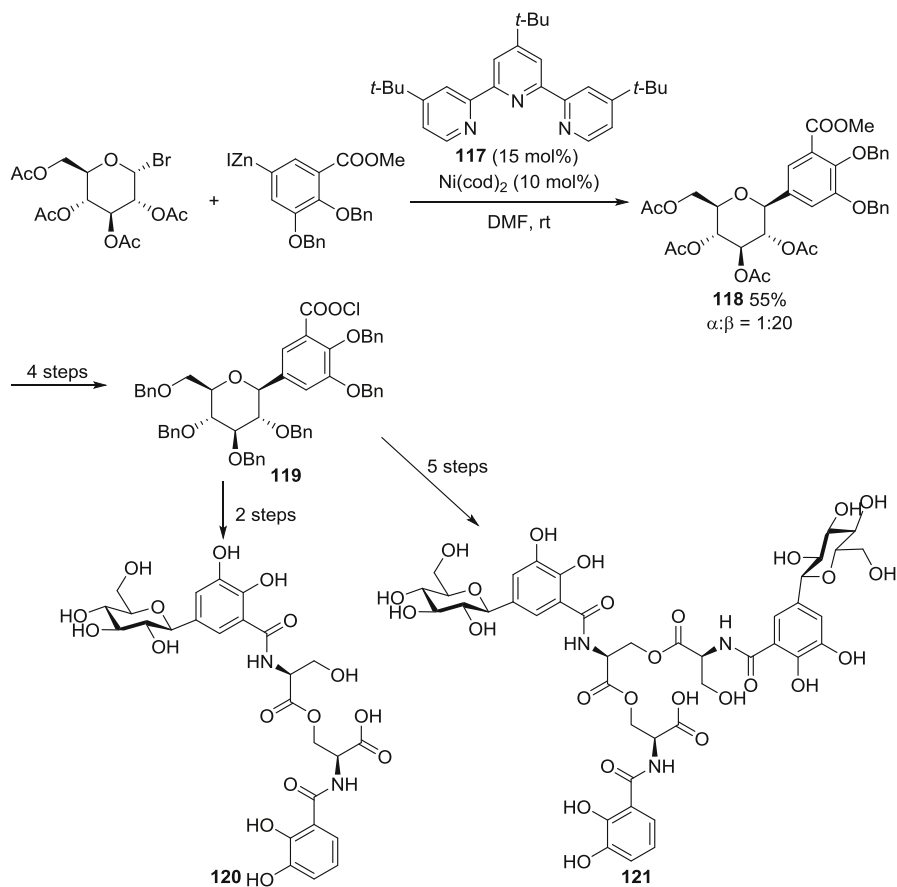


**Scheme 70** Asymmetric synthesis of fluvirucinine A1 **113**



Scheme 71 Cross-coupling between saccharide derivatives

with an arylzinc reagent using terpyridine ligand **117** [113]. The key coupling reaction proceeded with excellent diastereoselectivity in a good yield to give **118**. The *C*-aryl glycoside **118** was successfully converted into salmochelin S1 **120** and S2 **121** by subsequent condensation and deprotection processes (Scheme 72) [119].



Scheme 72 Total synthesis of salmochelins

## 6 Conclusion and Outlook

During the past two decades, a great deal of effort has been devoted to developing cross-coupling reaction using alkyl electrophiles. Among various transition metals that can catalyze such transformation, Ni exhibits promising and unique catalytic activities. The reaction proceeds efficiently under mild conditions with high tolerance to a wide range of functional groups even in the cross-coupling with Grignard reagents. Various alkyl halides including fluorides and pseudo halides such as tosylates and carbonates, as well as carboxylic acid esters via decarboxylation can be employed as the source of saturated carbon frameworks, which include not only primary and secondary alkyls, but also tertiary alkyls. The scope of coupling partners includes various organometallic compounds with any types of carbon skeletons such as *n*-, *sec*-, *tert*-alkyl, vinyl, aryl, and alkynyl groups carrying various metals such as B, Mg, Zn, Si, Zr, and In. An attractive feature of the Ni-catalyzed system is the stereoconvergent cross-coupling of racemic alkyl electrophiles using chiral ligands. This procedure will provide a new route to create stereogenic carbon centers. These interesting features of Ni-catalyzed cross-coupling are in part due to the properties of the nickel metal that can take various oxidation states from 0 to 4, i.e., oxidative addition of alkyl halides can be facilitated by an electron transfer mechanism which also enables stereoconvergent synthesis and formation of Ni complexes at high oxidation states accelerates reductive elimination. With these successful C–C bond formations on sp<sup>3</sup>-carbon centers, Ni-catalyzed cross-coupling reactions have been employed for the synthesis of various natural products and their analogues.

The cross-coupling reaction provides a powerful tool for recombination of single bonds as the metathesis reorganizes unsaturated bonds. It was thought for a long time that use of alkyl electrophiles in cross-coupling is not practical. Now, as mentioned above, such transformations emerged as a promising tool to construct saturated carbon frameworks and will open a new era in organic synthesis by means of providing new convenient routes for constructing organic molecules.

## References

1. de Meijere A, Bräse S, Oestreich M (2014) Metal-catalyzed cross-coupling reactions and more. Wiley-VCH, Weinheim
2. Yamamoto T, Yamamoto A, Ikeda S (1971) *J Am Chem Soc* 93:3350
3. Tamao K, Sumitani K, Kumada M (1972) *J Am Chem Soc* 94:4374
4. Corriu RJP, Masse JP (1972) *J C S Chem Commun* 144
5. Iwasaki T, Kambe N (2014) Coupling reactions between sp<sup>3</sup> carbon centers. In: Molander GA, Knochel P (eds) *Comprehensive organic synthesis*, vol 3, 2nd edn. Elsevier, Oxford, p 337
6. Netherton MR, Dai C, Neuschütz K, Fu GC (2001) *J Am Chem Soc* 123:10099
7. Hadei N, Kantchev EAB, O'Brien CJ, Organ MG (2005) *Org Lett* 7:3805
8. Netherton MR, Fu GC (2005) *Top Organomet Chem* 14:85
9. Kambe N, Iwasaki T, Terao J (2011) *Chem Soc Rev* 40:4937
10. Netherton MR, Fu GC (2004) *Adv Synth Catal* 346:1525
11. Terao J, Kambe N (2006) *Bull Chem Soc Jpn* 79:663
12. Terao J, Kambe N (2008) *Acc Chem Res* 41:1545
13. Glorius F (2008) *Angew Chem Int Ed* 47:8347
14. Rudolph A, Lautens M (2009) *Angew Chem Int Ed* 48:2656

15. Phapale VB, Cárdenas DJ (2009) *Chem Soc Rev* 38:1598
16. Lin S, Agapie T (2011) *Synlett* 1
17. Hu X (2011) *Chem Sci* 2:1867
18. Taylor BLH, Jarvo ER (2011) *Synlett* 2761
19. Swift EC, Jarvo ER (2013) *Tetrahedron* 69:579
20. Tasker SZ, Standley EA, Jamison TF (2014) *Nature* 509:299
21. Jana R, Pathak TP, Sigman MS (2011) *Chem Rev* 111:1417
22. Tamao K, Kiso Y, Sumitani K, Kumada M (1972) *J Am Chem Soc* 94:9268
23. Hayashi T, Konishi M, Yokota K-i, Kumada M (1980) *Chem Lett* 767
24. Lohre C, Dröge T, Wang C, Glorius F (2011) *Chem Eur J* 17:6052
25. Joshi-Pangu A, Wang C-Y, Biscoe MR (2011) *J Am Chem Soc* 133:8478
26. Phapale VB, Guisán-Ceinos M, Buñuel E, Cárdenas DJ (2009) *Chem Eur J* 15:12681
27. Yamaguchi J, Muto K, Itami, K (2016) *Top Curr Chem (Z)* 374:55
28. Wang X, Dai Y, Gong H (2016) *Top Curr Chem (Z)* 374:43
29. Devasagayaraj A, Stüdemann T, Knochel P (1995) *Angew Chem Int Ed* 34:2723
30. Giovannini R, Stüdemann T, Dussin G, Knochel P (1998) *Angew Chem Int Ed* 37:2387
31. Giovannini R, Stüdemann T, Devasagayaraj A, Dussin G, Knochel P (1999) *J Org Chem* 64:3544
32. Piber M, Jensen AE, Rottländer M, Knochel P (1999) *Org Lett* 1:1323
33. Terao J, Watanabe H, Ikumi A, Kuniyasu H, Kambe N (2002) *J Am Chem Soc* 124:4222
34. Singh SP, Terao J, Kambe N (2009) *Tetrahedron Lett* 50:5644
35. Singh SP, Iwasaki T, Terao J, Kambe N (2011) *Tetrahedron Lett* 52:774
36. Terao J, Todo H, Watabe H, Ikumi A, Shinohara Y, Kambe N (2008) *Pure Appl Chem* 80:941
37. Terao J, Todo H, Watanabe H, Ikumi A, Kambe N (2004) *Angew Chem Int Ed* 43:6180
38. Zhou J, Fu GC (2003) *J Am Chem Soc* 125:14726
39. Liang Y, Fu GC (2015) *Angew Chem Int Ed* 54:9047
40. Smith SW, Fu GC (2008) *Angew Chem Int Ed* 47:9334
41. Anderson TJ, Jones GD, Vivic DA (2004) *J Am Chem Soc* 126:8100
42. Jones GD, McFarland C, Anderson TJ, Vivic DA (2005) *Chem Commun* 4211
43. Saito B, Fu GC (2007) *J Am Chem Soc* 129:9602
44. Lu Z, Fu GC (2010) *Angew Chem Int Ed* 49:6676
45. Vechorkin O, Hu X (2009) *Angew Chem Int Ed* 48:2937
46. Vechorkin O, Csok Z, Scopelliti R, Hu X (2009) *Chem Eur J* 15:3889
47. Di Franco T, Boutin N, Hu X (2013) *Synthesis* 45:2949
48. Perez Garcia PM, Di Franco T, Orsino A, Ren P, Hu X (2012) *Org Lett* 14:4286
49. Phapale VB, Buñuel E, García-Iglesias M, Cárdenas DJ (2007) *Angew Chem Int Ed* 46:8790
50. Guisán-Ceinos M, Soler-Yanes R, Collado-Sanz D, Phapale VB, Buñuel E, Cárdenas DJ (2013) *Chem Eur J* 19:8405
51. Qin T, Cornella J, Li C, Malins LR, Edwards JT, Kawamura S, Maxwell BD, Eastgate MD, Baran PS (2016) *Science* 352:801
52. Yuan K, Scott WJ (1991) *Tetrahedron Lett* 32:189
53. Park K, Yuan K, Scott WJ (1993) *J Org Chem* 58:4866
54. Giovannini R, Knochel P (1998) *J Am Chem Soc* 120:11186
55. Uemura M, Yorimitsu H, Oshima K (2006) *Chem Commun* 4726
56. Knochel P, Krasovskiy A, Sapountzis I (2005) Polyfunctional magnesium organometallics for organic synthesis. In: Knochel P (ed) *Handbook of functionalized organometallics*, vol1. Wiley-VCH, Weinheim, p 109
57. Vechorkin O, Proust V, Hu X (2009) *J Am Chem Soc* 131:9756
58. Xue F, Zhao J, Hor TSA (2013) *Dalton Trans* 42:5150
59. Zhou J, Fu GC (2004) *J Am Chem Soc* 126:1340
60. Powell DA, Fu GC (2004) *J Am Chem Soc* 126:7788
61. Powell DA, Maki T, Fu GC (2005) *J Am Chem Soc* 127:510
62. Strotman NA, Sommer S, Fu GC (2007) *Angew Chem Int Ed* 46:3556
63. González-Bobes F, Fu GC (2006) *J Am Chem Soc* 128:5360
64. Molander GA, Argintaru OA (2014) *Org Lett* 16:1904
65. Di Franco T, Epenoy A, Hu X (2015) *Org Lett* 17:4910
66. Zultanski SL, Fu GC (2013) *J Am Chem Soc* 135:624
67. Yotsuji K, Hoshiya N, Kobayashi T, Fukuda H, Abe H, Arisawa M, Shuto S (2015) *Adv Synth Catal* 357:1022

68. Cornella J, Edwards JT, Qin T, Kawamura S, Wang J, Pan C-M, Gianatassio R, Schmidt M, Eastgate MD, Baran PS (2016) *J Am Chem Soc* 138:2174
69. Wang J, Qin T, Chen T-G, Wimmer L, Edwards JT, Cornella J, Vokits B, Shaw SA, Baran PS (2016) *Angew Chem Int Ed* 55:9676
70. Vechorkin O, Godinat A, Scopelliti R, Hu X (2011) *Angew Chem Int Ed* 50:11777
71. Xu G, Li X, Sun H (2011) *J Organomet Chem* 696:3011
72. Sonogashira K, Tohda Y, Hagihara N (1975) *Tetrahedron Lett* 4467
73. Eckhardt M, Fu GC (2003) *J Am Chem Soc* 125:13642
74. Altenhoff G, Würtz S, Glorius F (2006) *Tetrahedron Lett* 47:2925
75. Vechorkin O, Barmaz D, Proust V, Hu X (2009) *J Am Chem Soc* 131:12078
76. García PMP, Ren P, Scopelliti R, Hu X (2015) *ACS Catal* 5:1164
77. Yi J, Lu X, Sun YY, Xiao B, Liu L (2013) *Angew Chem Int Ed* 52:12409
78. Lin BL, Liu L, Fu Y, Luo SW, Chen Q, Guo QX (2004) *Organometallics* 23:2114
79. Yamamoto T, Abila M (1997) *J Organomet Chem* 535:209
80. Terao J, Naitoh Y, Kuniyasu H, Kambe N (2007) *Chem Commun* 825
81. Iwasaki T, Min X, Fukuoka A, Kuniyasu H, Kambe N (2016) *Angew Chem Int Ed* 55:5550
82. Iwasaki T, Tsumura A, Omori T, Kuniyasu H, Terao J, Kambe N (2011) *Chem Lett* 40:1024
83. Pratt LM, Voit S, Okeke FN, Kambe N (2011) *J Phys Chem A* 115:2281
84. Chass GA, Kantchev EAB, Fang DC (2010) *Chem Commun* 46:2727
85. Hills ID, Netherton MR, Fu GC (2003) *Angew Chem Int Ed* 42:5749
86. Jones GD, Martin JL, McFarland C, Allen OR, Hall RE, Haley AD, Brandon RJ, Konovalova T, Desrochers PJ, Pulay P, Vivic DA (2006) *J Am Chem Soc* 128:13175
87. Schley ND, Fu GC (2014) *J Am Chem Soc* 136:16588
88. Smith SW, Fu GC (2008) *J Am Chem Soc* 130:12645
89. Breitenfeld J, Ruiz J, Wodrich MD, Hu X (2013) *J Am Chem Soc* 135:12004
90. Breitenfeld J, Wodrich MD, Hu X (2014) *Organometallics* 33:5708
91. Choi J, Martín-Gago P, Fu GC (2014) *J Am Chem Soc* 136:12161
92. Fischer C, Fu GC (2005) *J Am Chem Soc* 127:4594
93. Arp FO, Fu GC (2005) *J Am Chem Soc* 127:10482
94. Son S, Fu GC (2008) *J Am Chem Soc* 130:2756
95. Binder JT, Cordier CJ, Fu GC (2012) *J Am Chem Soc* 134:17003
96. Cordier CJ, Lundgren RJ, Fu GC (2013) *J Am Chem Soc* 135:10946
97. Oelke AJ, Sun J, Fu GC (2012) *J Am Chem Soc* 134:2966
98. Lundin PM, Esquivias J, Fu GC (2009) *Angew Chem Int Ed* 48:154
99. Liang Y, Fu GC (2014) *J Am Chem Soc* 136:5520
100. Choi J, Fu GC (2012) *J Am Chem Soc* 134:9102
101. Liang Y, Fu GC (2015) *J Am Chem Soc* 137:9523
102. Lundin PM, Fu GC (2010) *J Am Chem Soc* 132:11027
103. Dai X, Strotman NA, Fu GC (2008) *J Am Chem Soc* 130:3302
104. Lou S, Fu GC (2010) *J Am Chem Soc* 132:1264
105. Lou S, Fu GC (2010) *J Am Chem Soc* 132:5010
106. Saito B, Fu GC (2008) *J Am Chem Soc* 130:6694
107. Owston NA, Fu GC (2010) *J Am Chem Soc* 132:11908
108. Zultanski SL, Fu GC (2011) *J Am Chem Soc* 133:15362
109. Wilsily A, Tramutola F, Owston NA, Fu GC (2012) *J Am Chem Soc* 134:5794
110. Lu Z, Wilsily A, Fu GC (2011) *J Am Chem Soc* 133:8154
111. Caeiro J, Pérez Sestelo J, Sarandeses LA (2008) *Chem Eur J* 14:741
112. Gong H, Sinisi R, Gagné MR (2007) *J Am Chem Soc* 129:1908
113. Gong H, Gagné MR (2008) *J Am Chem Soc* 130:12177
114. Baer TA, Carney RL (1976) *Tetrahedron Lett* 4697
115. Iwasaki T, Higashikawa K, Reddy VP, Ho WWS, Fujimoto Y, Fukase K, Terao J, Kuniyasu H, Kambe N (2013) *Chem Eur J* 19:2956
116. Shirokawa Si, Shinoyama M, Ooi I, Hosokawa S, Nakazaki A, Kobayashi S (2007) *Org Lett* 9:849
117. Aiba T, Sato M, Umegaki D, Iwasaki T, Kambe N, Fukase K, Fujimoto Y (2016) *Org Biomol Chem* 14:6672
118. Oroszova B, Choutka J, Pohl R, Parkan K (2015) *Chem Eur J* 21:7043
119. Yu X, Dai Y, Yang T, Gagné MR, Gong H (2011) *Tetrahedron* 67:144



# Photoredox Catalysis in Nickel-Catalyzed Cross-Coupling

Livia N. Cavalcanti<sup>1</sup> · Gary A. Molander<sup>2</sup>

Received: 31 March 2016 / Accepted: 17 May 2016 / Published online: 13 June 2016  
© Springer International Publishing Switzerland 2016

**Abstract** The traditional transition metal-catalyzed cross-coupling reaction, although well suited for C(sp<sup>2</sup>)–C(sp<sup>2</sup>) cross-coupling, has proven less amenable toward coupling of C(sp<sup>3</sup>)-hybridized centers, particularly using functional group tolerant reagents and reaction conditions. The development of photoredox/Ni dual catalytic methods for cross-coupling has opened new vistas for the construction of carbon–carbon bonds at C(sp<sup>3</sup>)-hybridized centers. In this chapter, a general outline of the features of such processes is detailed.

**Keywords** Photoredox catalysis · Cross-coupling · Alkyltrifluoroborates · Alkylsilicates

## 1 Introduction

Transition metal-catalyzed cross-couplings are among the most important classes of reaction for carbon–carbon bond formation [1], with the synthesis of many biologically relevant molecules being realized by using at least one cross-coupling step in their construction [2]. Through the years, the development of new catalysts, ligands, and substrates have greatly improved the scope of this transformation [3],

---

This article is part of the Topical Collection “Ni- and Fe-Based Cross-Coupling Reactions”; edited by “Arkaitz Correa”.

---

✉ Gary A. Molander  
[gmolandr@sas.upenn.edu](mailto:gmolandr@sas.upenn.edu)

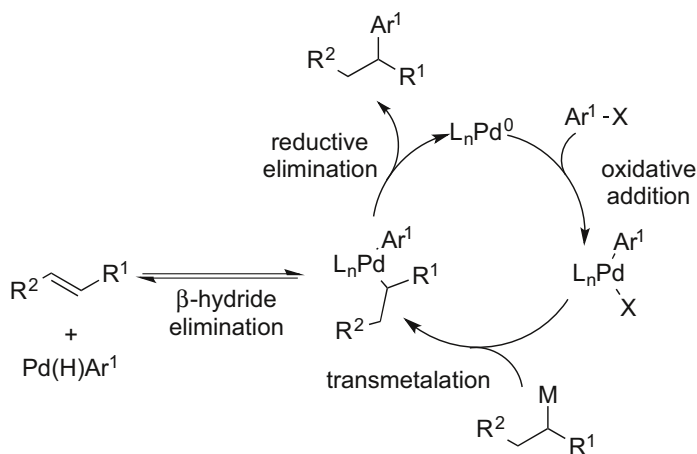
Livia N. Cavalcanti  
[liviacavalcanti81@gmail.com](mailto:liviacavalcanti81@gmail.com)

<sup>1</sup> Instituto de Química-Universidade Federal do Rio Grande do Norte, Natal, RN, Brazil

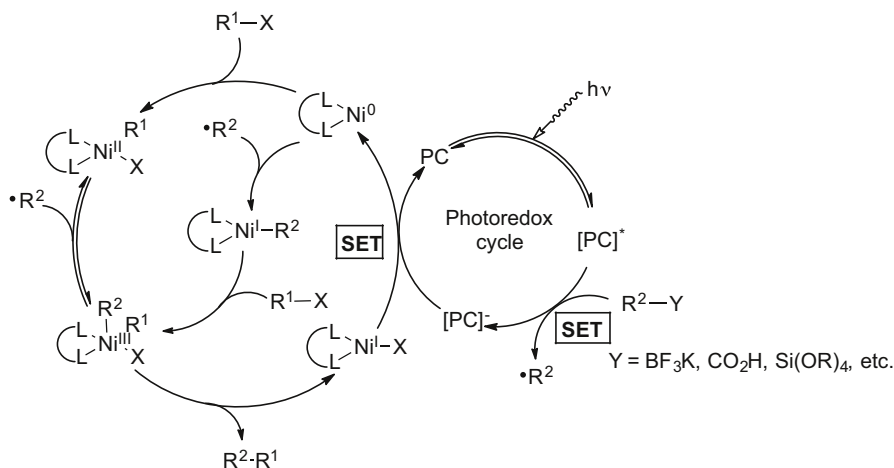
<sup>2</sup> Roy and Diana Vagelos Laboratories, Department of Chemistry, University of Pennsylvania, Philadelphia, PA 19104-6323, USA

making it efficient for a variety of electrophiles (organic halides and pseudohalides) and nucleophiles (organometallic compounds). Nonetheless, although very efficient for coupling of C(sp<sup>2</sup>)–C(sp<sup>2</sup>) centers, current methods often lack diversity when it comes to coupling of sp<sup>3</sup>-hybridized carbons. The major challenge arises from lower rates of transmetalation and subsequent competition with protodemetalation as well as undesired β-hydride elimination pathways observed using methods transpiring through the traditional two-electron catalytic cycle (Scheme 1). The development of new ligands and the use of other metal catalysts, such as nickel- and iron-based complexes, have expanded the scope of the electrophilic partner for this reaction to include unactivated and sterically hindered alkyl substrates by diminishing the formation of β-hydride elimination side products [4]. However, the incorporation of C(sp<sup>3</sup>)-hybridized nucleophilic components has remained a challenge, often requiring more highly reactive reagents (e.g., Grignard reagents [5] or organozinc reagents [6]) for successful coupling. Alternatively, harsh reaction conditions, such as excess base and high temperatures using superstoichiometric amounts of less reactive nucleophiles (i.e., organoboron reagents [7, 8]) to improve the rates of transmetalation can also be utilized. In either case, current protocols have become highly restrictive in terms of their tolerance of sensitive functional groups.

To overcome these limitations, a novel mechanistic paradigm has been developed. Thus, a combination of visible light photoredox/nickel dual catalysis has become a powerful tool for cross-couplings of C(sp<sup>3</sup>)-hybridized substrates, allowing new and improved reactivity patterns never achieved in a traditional cross-coupling cycle. The utility of this method comes from the capacity of the photocatalyst to “activate” the nucleophilic coupling partner by generating a high-energy radical intermediate via single-electron transfer (SET) chemistry, making C(sp<sup>3</sup>)-hybridized nucleophiles ideal substrates for this transformation. In essence, the interaction of the photocatalyst with visible light provides the energy of activation needed to overcome the often-prohibitive energy barrier associated with



**Scheme 1** Traditional Pd-catalyzed cycle for cross-couplings reaction



**Scheme 2** Proposed mechanism for photoredox/Ni dual catalytic cross-coupling

the transmetalation of minimally nucleophilic (but functional group tolerant) partners under two-electron mechanistic schemes.

A prototypical mechanistic scenario for photoredox/Ni dual catalytic cross-coupling is depicted in [Scheme 2](#) [9]. In the photoredox cycle, a C(sp<sup>3</sup>)-hybridized radical is generated from SET oxidation of a suitable precursor by an excited-state photocatalyst (PC) complex. This radical can enter the cross-coupling cycle in two different pathways: addition to an organonickel(II) species, formed after oxidative addition of an aryl halide to a Ni(0) catalyst, or direct radical addition to the Ni(0) catalyst followed by oxidative addition of the aryl halide. Both pathways provide a common Ni(III) intermediate that can rapidly dissociate the stabilized radical or more slowly undergo reductive elimination to afford the desired coupled product and a Ni(I) species. The latter can be reduced by the iridium complex to regenerate both the Ni(0) and the photocatalysts ([Scheme 2](#)).

This chapter provides an overview of the advances made in this newly established area, which includes cross-coupling with organotrifluoroborates, silicates, and carboxylates, among others, showcasing the utility of these methods for cross-coupling of C(sp<sup>3</sup>)-hybridized nucleophiles.

## 2 Cross-Coupling with Organotrifluoroborates

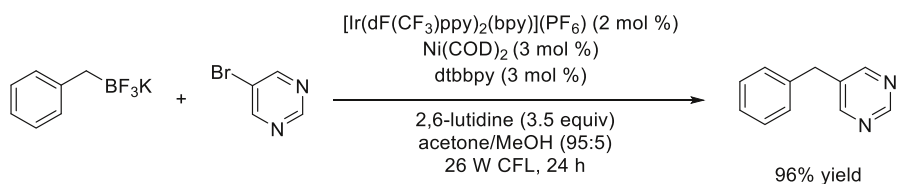
Organotrifluoroborates have been utilized through the years as robust nucleophilic partners in Suzuki–Miyaura cross-coupling reactions [10]. They are known for undergoing a variety of transformations while keeping the appended carbon–boron bond intact [11–13]. Consequently, molecular complexity can be built into various functionalized core reagents, providing more diversity by which targeted molecular platforms can be constructed. Moreover, when compared to other boron species,

such as boronic acids and boronate esters, organotrifluoroborates are more stable, allowing them to be stored for years without appreciable decomposition. Despite all these advantages and concerted efforts, examples of cross-coupling of C(sp<sup>3</sup>)-hybridized alkyltrifluoroborates have been limited [14–16], and successful protocols still require harsh conditions (excess base, high temperatures) to overcome a slow transmetalation.

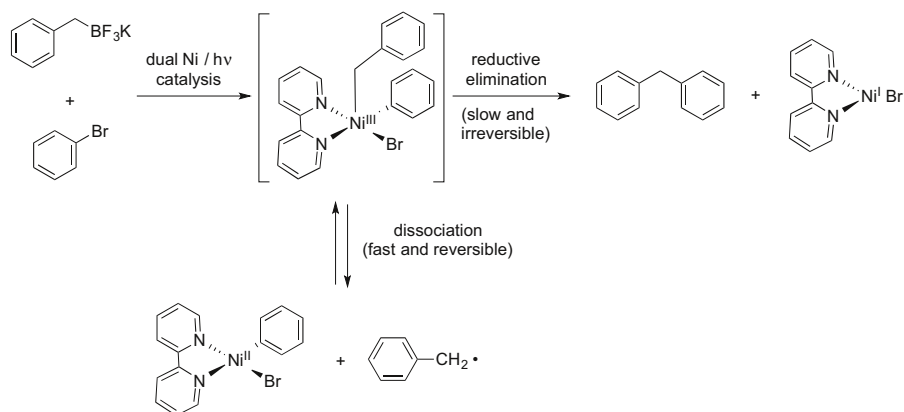
Given the enormous resources devoted by several groups to the development of suitable conditions for C(sp<sup>3</sup>)-hybridized cross-coupling using organoboron reagents, it became apparent that a new approach to the challenge was needed. The seminal breakthrough in cross-coupling of secondary alkyltrifluoroborates came with the development of an elegant and mild protocol combining visible light photoredox/nickel dual catalysis to allow cross-couplings reactions of these nucleophiles [17]. This approach takes advantage of the fact that the effective transmetalation step, in which the alkyl group on boron ends up on the nickel center through a net one-electron oxidation of the Ni (Scheme 2), is a virtually barrierless process [9]. This single electron pathway thus transforms the problematic, high-energy, two-electron transmetalation into a facile one-electron process.

The ease of SET oxidation associated with many alkyltrifluoroborates (making them suitable carbon radical precursors) along with favorable single-electron redox potentials of the nickel catalysts, were the perfect match to allow the cross-coupling of benzyl and alkoxyalkyltrifluoroborates with aryl- and heteroaryl bromides. Thus, employing [Ir(dF(CF<sub>3</sub>)ppy)<sub>2</sub>(bpy)](PF<sub>6</sub>) as a photocatalyst, Ni(COD)<sub>2</sub>/dtbbpy as the cross-coupling precatalyst, and irradiation from a 26-W compact fluorescent light bulb (CFL) at room temperature for 24 h, the desired coupled products were obtained in good to excellent yields (Scheme 3). In the SET oxidation of the alkyltrifluoroborates, BF<sub>3</sub> is released as a byproduct. This was found to inhibit the cross-coupling, and thus additives are needed to sequester this Lewis acid. In the initial report, 2,6-lutidine was used for this purpose. Other bases, including amines, inorganic bases, and metal fluorides, have subsequently found use in this role.

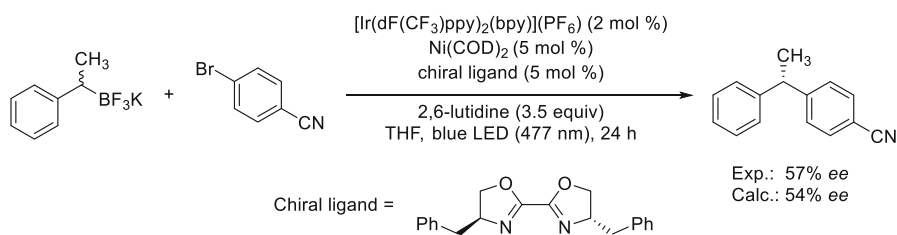
Once this unique paradigm of reactivity was established, a computational analysis of the process was conducted to gain insight into and confirm the intricacies of this novel class of reaction [9]. As outlined previously (Scheme 2), these studies revealed that the radical formed in the photoredox cycle can add to nickel either after or before oxidative addition, depending on the concentration of Ni(0) or Ni(II), with both pathways converging to a common Ni(III) intermediate. This diorganonickel(III) intermediate undergoes dissociation to form a Ni(II) species faster than the subsequent reductive elimination (Scheme 4). According to these calculations, the



**Scheme 3** Cross-coupling of benzyltrifluoroborate under dual photoredox/nickel catalysis



**Scheme 4** Computational study outcome of photoredox/Ni dual catalysis cross-coupling

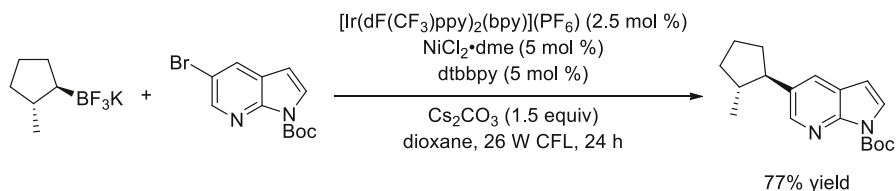


**Scheme 5** Comparison between experimental and calculated stereoinduction

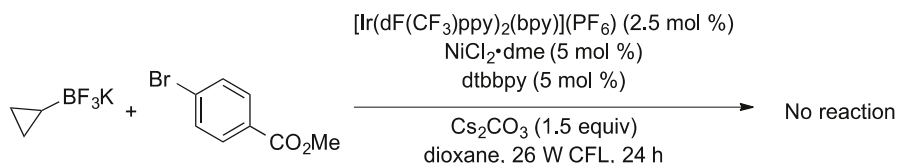
reactive Ni(II) and Ni(III) intermediates thus reside in a Curtin–Hammett regime, pointing to the reductive elimination step being responsible for the stereoselectivity of these processes via dynamic kinetic resolution (DKR) when a chiral nickel ligand is utilized.

The prediction made with the theoretical study was confirmed with experiments that tested this hypothesis (Scheme 5). The practical value of this new method derives from the fact that readily available, racemic alkyltrifluoroborates may be utilized in a stereoconvergent process to access enantio-enriched products simply by using chiral ligands for the nickel catalyst. Proof of principle was provided in the synthesis of an enantioenriched diarylmethane.

With a better understanding of the mechanism of these reactions, the method was further extended to a variety of organotrifluoroborate nucleophiles. The scope of secondary alkyltrifluoroborates was studied under similar conditions, changing the nickel catalyst to  $\text{NiCl}_2\text{-dme}$  and the base additive to  $\text{Cs}_2\text{CO}_3$  [18]. Alkyltrifluoroborates with different ring sizes and steric demands were efficiently coupled with aryl- and heteroaryl bromides. In contrast to previous results for similar transformations under traditional Pd-catalyzed conditions [13, 16], ( $\pm$ )-2-methylcycloalkyltrifluoroborates afforded the desired products without rearrangement, giving only the racemic, *trans*-diastereomer (Scheme 6). Importantly,



**Scheme 6** Photoredox/Ni dual catalytic cross-coupling of secondary alkyltrifluoroborate

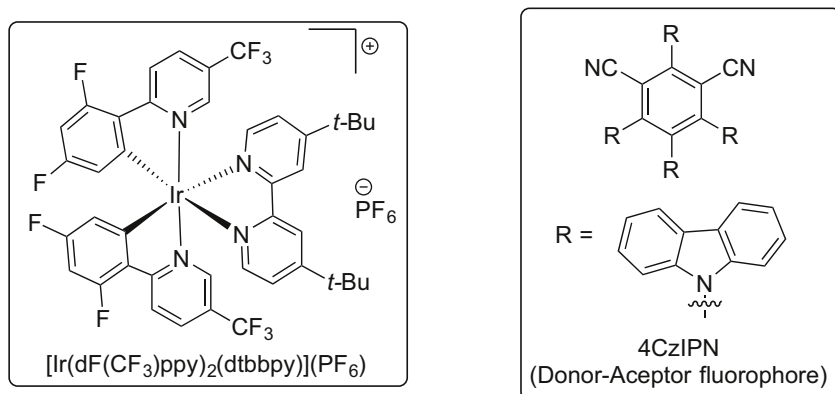


**Scheme 7** Photoredox/Ni dual catalytic cross-coupling of cyclopropyltrifluoroborate

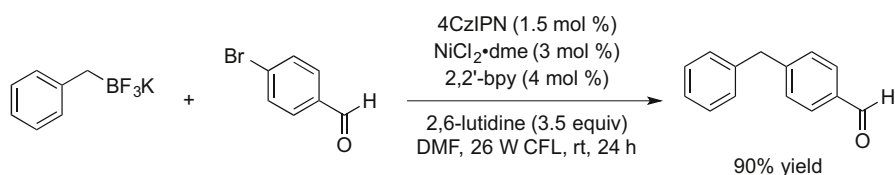
alkyltrifluoroborates in which the alkyl group possesses greater *s*-character have unfavorable redox potentials (because radicals generated from these species are less stable than those with less *s*-character), thus inhibiting radical formation. Consequently, the desired coupled product was not detected when cyclopropyltrifluoroborate was tested. This is not of particular concern because cyclopropyltrifluoroborates couple extremely well under normal Pd-catalyzed conditions [19, 20], but this result does serve to showcase one of the limitations of the process and also points to the complementary nature of the photoredox/Ni dual catalytic method relative to that of two-electron cross-coupling methods (Scheme 7).

The efficacy of the photoredox/Ni dual catalysis cross-coupling of benzyltrifluoroborates was tested using inexpensive, donor–acceptor fluorophores instead of the expensive Ir catalyst for the photoredox cycle (Scheme 8) [21]. After optimization, the alternative 4CzIPN photoredox catalyst was found efficient, affording the desired coupled products in yields comparable to those obtained using iridium photoredox catalysts. The use of this fluorophore catalyst allowed photoredox/Ni cross-coupling of benzylic trifluoroborates with aryl- and heteroaryl bromides bearing electron-poor and electron-rich substituents (Scheme 9). If this organic photocatalyst proves to be generally applicable to related applications, it would provide a way to carry out these transformations in a highly economical manner, with Ni as the only base transition metal catalyst.

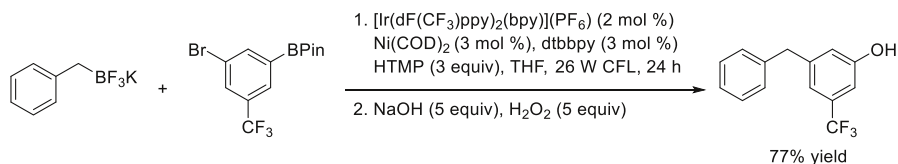
High selectivity was anticipated in the photoredox/Ni dual catalytic transformations of  $sp^3$ -hybridized alkyltrifluoroborate partners over  $sp^2$ -hybridized boronate esters. The former are more easily oxidized not only because the radical generated upon oxidation is more stable, but also because the boronate esters are isoelectronic with electron deficient carbocations, and thus highly resistant toward single electron oxidation. In the event, reaction of benzylic trifluoroborates with aryl bromides containing tricoordinate,  $sp^2$ -hybridized boron species was achieved under photoredox/Ni dual catalytic conditions (Scheme 10) [22]. The products obtained



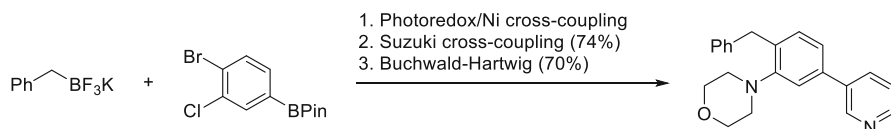
**Scheme 8** Traditional Ir-based photoredox catalyst and donor–acceptor fluorophore catalyst



**Scheme 9** Photoredox/Ni cross-coupling using donor–acceptor fluorophore 4CzIPN



**Scheme 10** Orthogonal photoredox/Ni dual cross-coupling



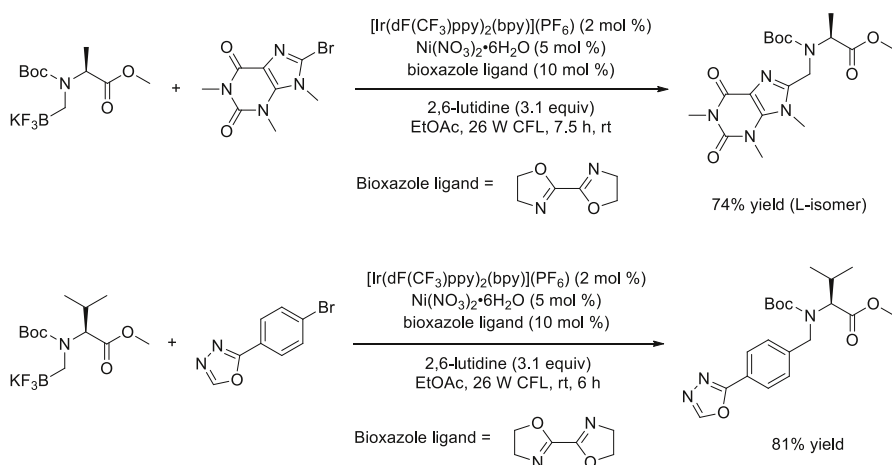
**Scheme 11** Photoredox/Ni orthogonal reactivity and further functionalization

were further reacted in known transformations to build molecular complexity in an efficient, modular manner, taking advantage of the highly selective cross-coupling of the benzyltrifluoroborate with aryl bromides (**Scheme 11**).

Chiral  $\alpha$ -aminomethyltrifluoroborates were also tested in the cross-coupling reaction with aryl- and heteroaryl bromides, using synergistic photoredox/Ni dual catalysis [23]. The best set of conditions was established using

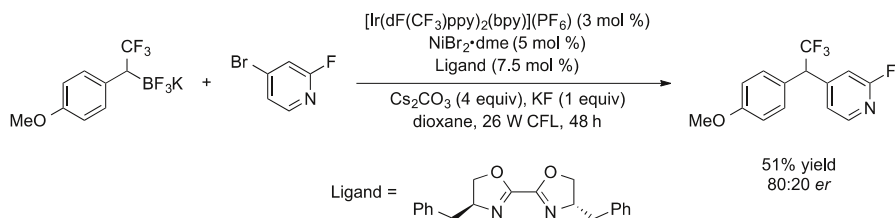
$[\text{Ir}(\text{dF}(\text{CF}_3)\text{ppy})_2(\text{bpy})](\text{PF}_6)$  as the photocatalyst,  $\text{Ni}(\text{NO}_3)_2 \cdot 6\text{H}_2\text{O}$ /bioxazole as the cross-coupling precatalyst, and 2,6-lutidine as an additive, with irradiation from a 26-W CFL at room temperature to promote the reaction (Scheme 12). This method allowed access to a variety of valuable *N*-benzylic amino acids, including those with a highly functionalized caffeine motif and pharmacologically relevant  $\text{SF}_5$ , thienyl sulfonamide, and boronic acid functional groups. Importantly, no epimerization of the stereogenic center was observed under the developed conditions, validating the mild reaction conditions of this protocol.

Fluorinated molecules are of great importance to the pharmaceutical and agrochemical industries [24]. The presence of one fluorine atom can enhance the bioavailability of a compound compared to non-fluorinated species. Hence, methods to access fluorine-containing structures are highly desirable and yet challenging because of the high electronegativity associated with this atom, which often conveys unexpected reactivity patterns. As an approach to introduce the  $\text{CF}_3$  group in a novel manner, the use of  $\alpha$ -trifluoromethylated alkylboron reagents in combination with photoredox/Ni catalytic cross-coupling became a valuable tool to synthesize new trifluoromethylated products. Thus, utilizing very similar reaction conditions to the previously developed photoredox/Ni cross-coupling of secondary alkyltrifluoroborates, the coupled products of  $\alpha$ -trifluoromethylated trifluoroborates with a variety of aryl- and heteroaryl bromides has been reported [25]. The substrate scope for this reaction included nitrile, ester and ketone functional groups in addition to a variety of aryl- and nitrogenated heteroaryl bromides. Importantly, after extensive screening using traditional Pd-catalyzed cross-coupling protocols, no conditions could be found that provided useful conversion to the desired target structures. Although the photoredox/Ni cross-coupling reactions were not optimized for high enantioselectivity, modest asymmetric induction could be achieved from racemic trifluoroborates in the transformations, induced by the chiral ligand in a stereoconvergent process (Scheme 13) [26]. Non-benzylic, trifluoromethylated

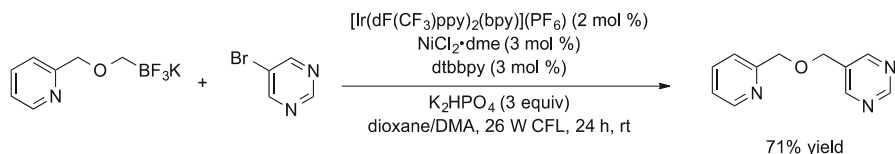


**Scheme 12** Photoredox/Ni dual catalytic cross-coupling of Boc-*N*-trifluoroboratomethyl amino acids





**Scheme 13** Cross-coupling of  $\alpha$ -trifluoromethylated trifluoroborates under dual photoredox/Ni catalysis

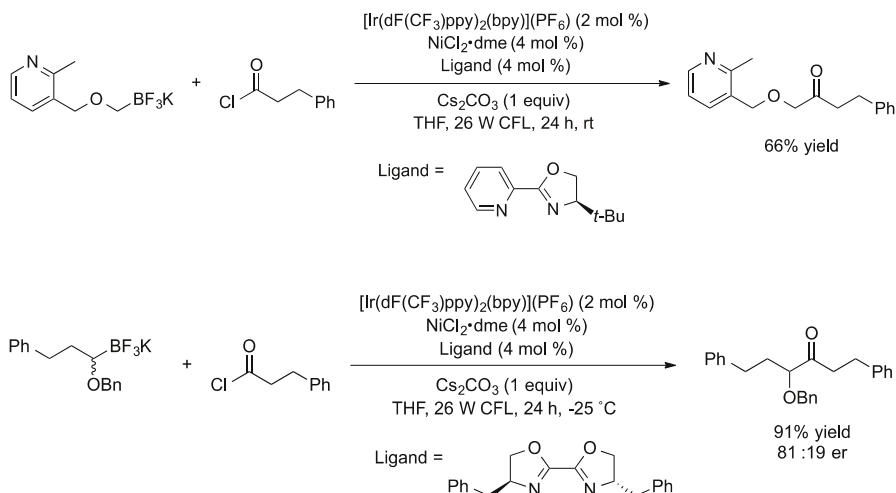


**Scheme 14** Photoredox/Ni cross-coupling of alkoxymethyltrifluoroborates with aryl bromides

trifluoroborates were ineffective using the developed protocol, probably due to the high oxidation potentials of the trifluoroborates. Poor or no conversions were observed for aryl chloride electrophiles.

Another important and unique class of organotrifluoroborate that has been utilized in the synergistic photoredox/Ni cross-coupling are alkoxymethyltrifluoroborates, which undergo cross-couplings with aryl- and heteroaryl bromides [27] as well as acyl chlorides [28], affording benzylic ethers and  $\alpha$ -alkoxy ketones, respectively. The scope of the reaction with aryl bromides included partners with aldehyde, ketone, nitrile, methoxy, fluoride, trifluoromethyl, and amide functional groups. Bromides embedded within heteroaryl substructures such as benzothio- phene, thiophene, benzofuran and a variety of nitrogen-containing heterocycles, such as pyridines, quinolines and pyrimidines, were also successfully coupled with the alkoxymethyltrifluoroborates (Scheme 14). This protocol allows a unique access to benzylic and pseudobenzylic ethers, which are normally prepared by Williamson ether-type syntheses. The novel carbon–carbon bond connect permits the introduction of much more structural diversity into such systems, because it incorporates readily available aryl- and heteroaryl halide partners as opposed to the more scarce benzylic derivatives required for carbon–oxygen bond formation.

Using acyl chlorides as the electrophiles, alkoxymethyltrifluoroborates contain- ing primary, secondary, and tertiary alkoxy groups were efficiently coupled under the developed protocol, and a broad range of acyl chlorides with aryl-, alkyl-, and heteroaryl substituents could be utilized as well (Scheme 15). As was the case with the benzyl ether syntheses outlined above, the  $\alpha$ -alkoxy ketone synthesis derives from a unique bond connection that complements every other approach to this class of molecules. Modest asymmetric induction could be achieved in a stereoconver- gent process starting with a racemic alkyltrifluoroborate partner in conjunction with a chiral ligand on the nickel cross-coupling catalyst.

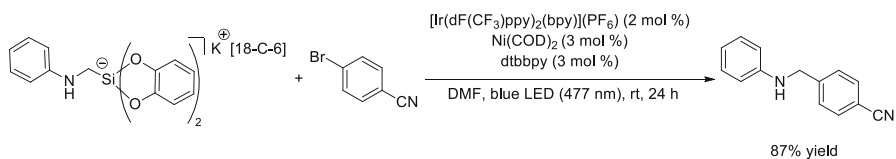


**Scheme 15** Photoredox/Ni cross coupling of alkoxymethyltrifluoroborates with acyl chlorides

### 3 Cross-Coupling with Silicates

Although the photoredox/Ni dual catalytic cross-coupling of alkyltrifluoroborates constitutes a remarkable breakthrough for couplings of C(sp<sup>3</sup>)-C(sp<sup>2</sup>) bonds, these methods are still limited by the high oxidation potential of these pro-nucleophiles. The implication of this is that only relatively stabilized radicals can be generated from the alkyltrifluoroborates (e.g., 2° alkyl,  $\alpha$ -alkoxy, and  $\alpha$ -amino), and additionally an expensive Ir photocatalyst is often used for partners that are more challenging to oxidize. Furthermore, these reactions require base additives to sequester the BF<sub>3</sub> generated, and high dilution is ideal owing to the poor solubility of potassium organotrifluoroborates in many solvents.

In response to these limitations, radical precursor reagents were sought that would resolve these issues, and attention was turned toward alkylammonium bis(catecholato)silicates. The reported ability of these reagents to serve as radical precursors in photoredox processes [29] made such substrates an attractive alternative to use as nucleophilic partners in the photoredox/Ni dual catalyzed cross-couplings. Their oxidation potentials were much more favorable than those of the alkyltrifluoroborates, they exhibited enhanced solubility in a variety of solvents, and moreover, the byproducts generated during the catalytic cycle (bis

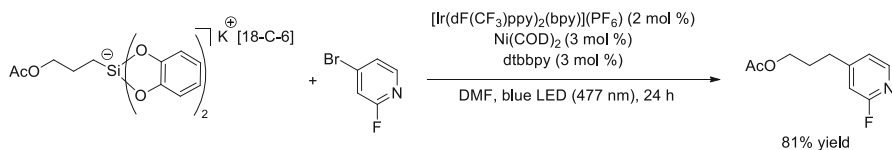


**Scheme 16** Photoredox/Ni dual catalysis cross-coupling of alkylsilicates

catecholsilane and alkylammonium bromide) are benign, thus avoiding the need for base additives. Preliminary work using this concept was reported for alkyl bis(catecholato) silicates with 4-bromobenzonitrile using  $[\text{Ir}(\text{dF}(\text{CF}_3)\text{ppy})(\text{bpy})_2](\text{PF}_6)_2$  as a photocatalyst, and  $\text{Ni}(\text{COD})_2/\text{dtbbpy}$  as the precatalyst, with irradiation from a blue LED at room temperature for 24 h [30]. Six different alkyl bis(catecholato) silicates ( $1^\circ$  and  $2^\circ$  alkyl as well as aminomethyl derivatives) were utilized, and the resulting products were obtained in very good yields (Scheme 16). A *tert*-butyl derivative provided none of the desired product under the developed conditions. Because potassium was the counterion of choice in these early studies, the addition of the expensive additive 18-crown-6 was necessary to aid in both the stability and solubility of the compounds.

Under the same set of conditions developed, the scope of this work was later expanded to a variety of aryl- and heteroaryl bromides containing electron-withdrawing and electron-donating groups, such as ketones, fluorides, hydroxyls, chlorides, and silyl and boronate esters, and the coupled products were obtained in moderate to good yields (Scheme 17) [31]. Benzylic, allylic, and primary alkylsilicates were also suitable partners for this transformation. The crown ether stabilizer was again utilized to improve solubility and yields.

Despite the proof of principle that alkylsilicates could be used as alternative nucleophilic partners in a combined photoredox/Ni cross-coupling, the reported method utilized similar conditions to those developed for organotrifluoroborates without exploiting the lower oxidation potential of primary alkylsilicates ( $E^0 = +0.75$  V vs. SCE) [32] when compared to primary alkyltrifluoroborates ( $E^0 > +1.50$  V vs. SCE) [33]. Furthermore, the use of the unstable  $\text{Ni}(\text{COD})_2$  as a precatalyst and the high cost of the 18-C-6 additive made these protocols wholly impractical. With these considerations in mind, concurrent studies were carried out in which the method was dramatically improved. First, alkylsilicates possessing inexpensive alkylammonium counterions were synthesized from alkyltrimethoxysilanes and two equivalents of catechol in the presence of various amines (e.g.,  $\text{Et}_3\text{N}$  or *i*- $\text{Pr}_2\text{NH}$ ). This protocol provided excellent yields of the desired bis(catecholato) silicates, which were easily isolated as indefinitely stable crystalline solids or free-flowing powders. Taking advantage of the more favorable redox potential of alkylsilicates relative to that of alkyltrifluoroborates, a base-free photoredox/Ni cross-coupling was developed using a less expensive ruthenium photocatalyst ( $E^0 = +0.77$  V vs. SCE) [34]. After optimization, suitable conditions were found using  $[\text{Ru}(\text{bpy})_3](\text{PF}_6)_2$  as the photocatalyst,  $\text{NiCl}_2 \cdot \text{dme}/\text{dtbbpy}$  as the cross-coupling precatalyst in DMF solvent with visible light. The scope of the silicate



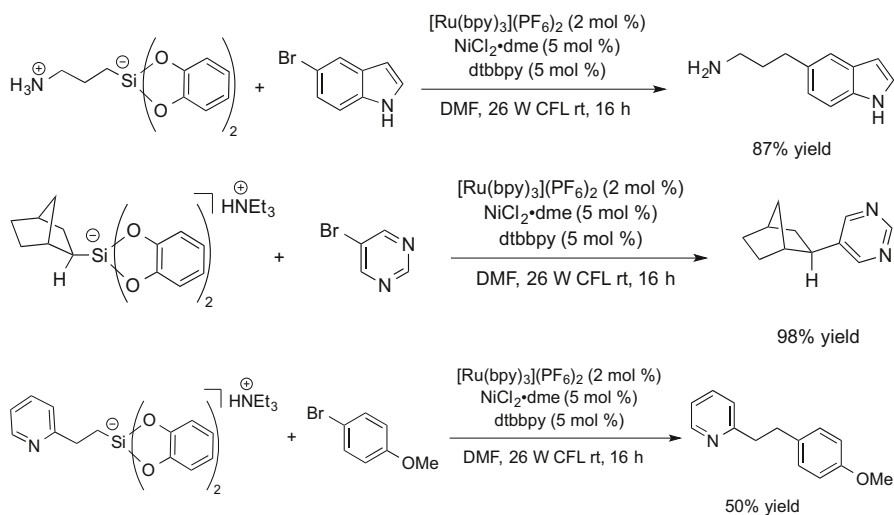
**Scheme 17** Photoredox/Ni dual catalysis cross-coupling of alkylsilicates with bromoarenes

partner was shown to include primary and secondary alkyl bis(catecholato)silicates containing pyridine, esters, lactams and most importantly, free primary amine functional groups (Scheme 18). Aryl- and heteroaryl bromides with electron-donating and electron-withdrawing groups were also successful under this set of conditions.

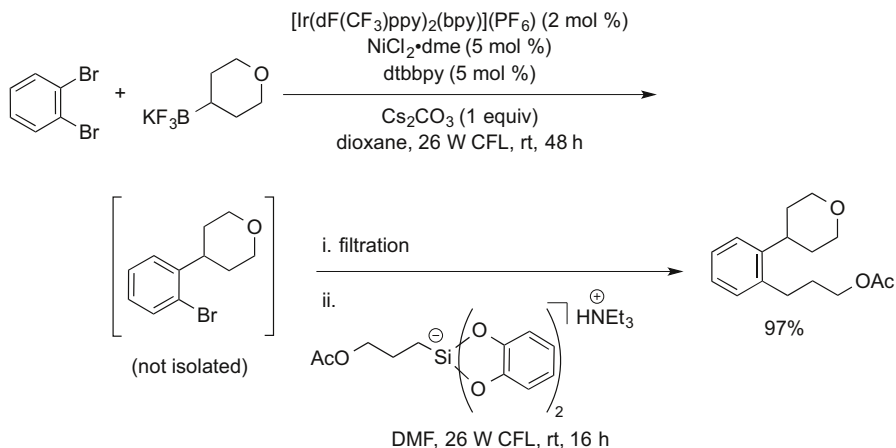
To showcase the complementary nature of this method with that of the corresponding alkyltrifluoroborate coupling, two consecutive photoredox/Ni dual catalytic cross-couplings were carried out using dibrominated arenes. The first cross-coupling was performed using an alkyltrifluoroborate under the previously reported Ir-based photoredox/Ni dual catalysis. The product of this reaction was not isolated, but only filtered and concentrated. Addition of a suitable solvent and a 1° alkylsilicate (coupling of which could not be accomplished with the analogous trifluoroborates) provided the second coupled product in very good yield over two steps (Scheme 19).

As an extension of this protocol, alkenyl halides were utilized as electrophiles in the cross-coupling [35]. Alkenyl iodides, -bromides and even unactivated alkenyl chlorides were all efficient in producing the desired coupled products in moderate to very good yields (Scheme 20). Of note, no isomerization of the double bond was observed under the developed set of conditions. The reaction with an alkenyl bromide containing a free hydroxyl group was not successful, with no desired product being detected. Both primary and secondary alkylsilicates underwent cross-coupling in moderate to excellent yields.

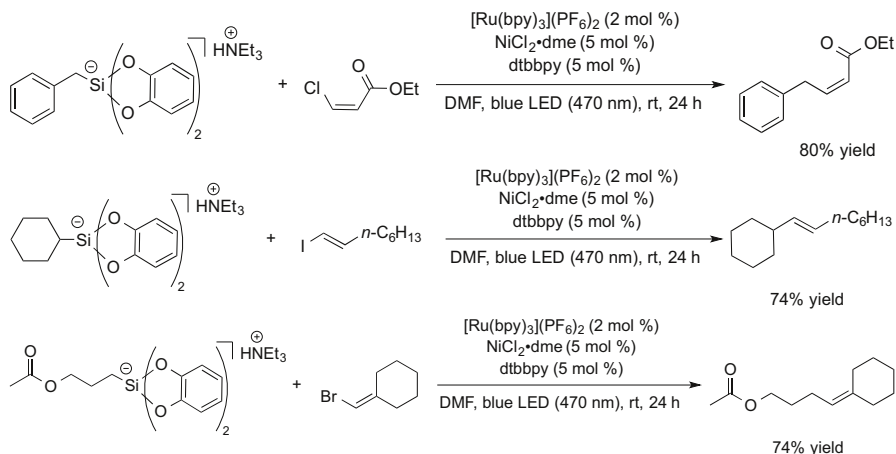
Interestingly, while attempting the cross-coupling of an alkylthiosilicate under the same set of conditions, a new thioesterification process was discovered [36]. This unanticipated transformation was proposed to derive from an intermediate thiyl radical, formed by a hydrogen-atom transfer (HAT) from the initially formed alkyl



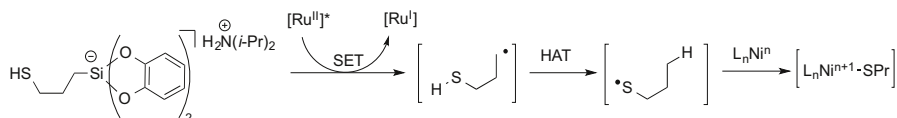
**Scheme 18** Photoredox/Ni dual cross-coupling of ammonium alkylsilicates and aryl bromides



**Scheme 19** Consecutive photoredox/Ni dual cross-couplings



**Scheme 20** Photoredox/Ni dual cross-coupling of ammonium alkylsilicates and alkenyl halides



**Scheme 21** Formation of the thiyl radical

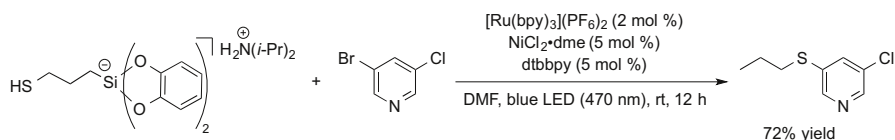
radical (**Scheme 21**). Once generated, it is the thiyl radical that engages with the nickel complex in a single electron oxidation process (**Scheme 2**), that eventually leads to reductive elimination to generate the thioether.

With this new reactivity pattern, the photoredox/Ni dual catalytic cross-coupling of thiosilicates with aryl and heteroaryl bromides was investigated. Aryl- and heteroaryl bromides containing electron-rich and electron-poor functional groups were well tolerated in this protocol, affording arylthioethers in good yields (Scheme 22). Notable exceptions were 4-bromophenol and 5-bromobenzofuran, which failed to give the product under this developed protocol.

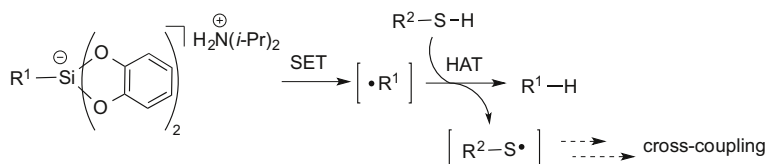
Because thiol-substituted trimethoxysilanes [used as precursors in the formation of the bis(catecholato)thiosilicates] have limited availability, a version of this transformation using thiols and a sacrificial alkylsilicate as a hydrogen atom abstractor was envisioned. The proposed mechanistic pathway would involve a HAT from thiol to the alkyl radical formed through SET oxidation of the silicate, yielding a thiyl radical that would be the species to enter the dual catalytic cycle (Scheme 23).

This protocol proved to be highly efficient, and a wide range of thiols were coupled with diverse aryl- and heteroaryl bromides (Scheme 24). The products were obtained in moderate to excellent yields for primary, secondary and tertiary thiols containing free hydroxyl groups, unprotected primary amines, cysteine, esters, and ketones. The method provides a useful route that is highly complementary to existing methods of synthesis of aryl alkyl thioethers. Such materials are normally prepared by  $S_NAr$  reactions of alkylthiolates onto activated aromatic systems, or  $S_N2$  reactions of aryl thiolates onto alkyl halides. Both of these routes have rather severe mechanistic/substrate restrictions, and thus the development of the photoredox/Ni cross-coupling approach provides a unique entry into this important subclass of molecules.

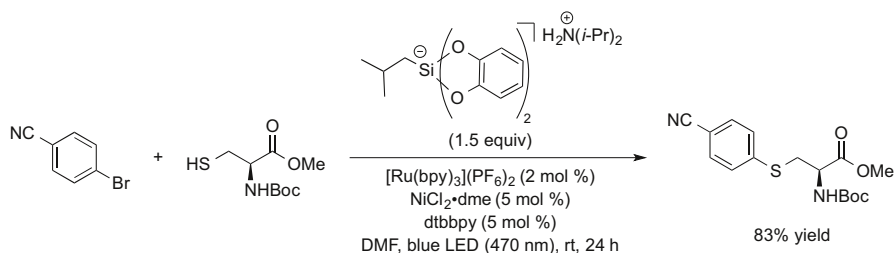
Borazaronaphthalenes are a unique and important class of heteroaromatic compounds. The B–N bond in these species exhibits isosterism with C = C bonds in aromatic congeners [37]. The introduction of the B–N bond into new molecular platforms is of great interest in medicinal chemistry, because it has the potential to



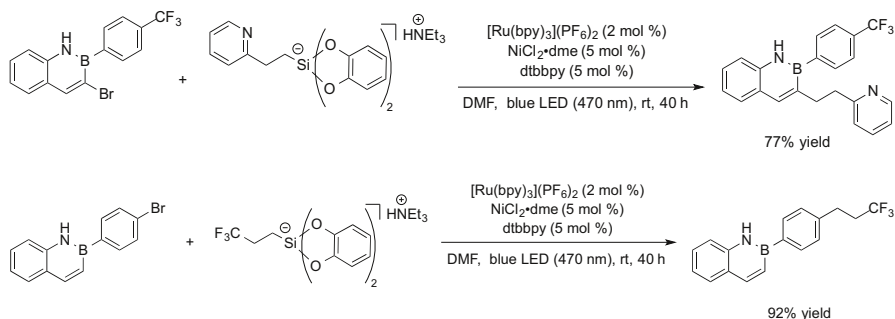
**Scheme 22** Photoredox/Ni dual catalysis thioetherification



**Scheme 23** Proposed hydrogen-atom transfer for thiyl radical formation



**Scheme 24** Photoredox/Ni thioetherification using silicates as H-atom abstractor



**Scheme 25** Photoredox/Ni dual catalyzed cross-coupling of brominated borazonaphthalenes

lead to new, biologically active drugs [38]. In this context, the use of borazonaphthalenes in the photoredox/Ni dual catalysis cross-coupling protocol is a highly attractive transformation to provide an increase in molecular diversity [39]. Thus, using the same set of conditions previously developed for bromoarene electrophiles, a variety of brominated borazonaphthalenes were successfully engaged in photoredox/Ni catalysis with ammonium alkylbis(catecholato)silicates (Scheme 25). The scope of the silicate partner was shown to include primary and secondary unprotected amines, amides, esters and heteroaryl functional groups.

## 4 Decarboxylative Cross-Coupling

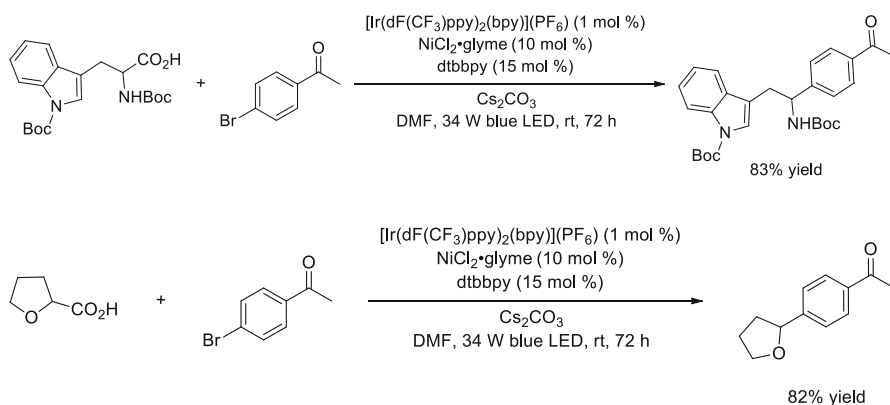
Concomitant with the development of the photoredox/Ni dual catalysis with organotrifluoroborates came the findings of decarboxylative cross-couplings using a similar mechanistic paradigm. Carboxylic acids have the advantage of being widely available, stable, and generally inexpensive precursor reagents. Their use as nucleophilic partners in decarboxylative cross-couplings with aryl halides to form  $\text{C}(\text{sp}^2)\text{--C}(\text{sp}^2)$  bonds has been well established, and many examples with benzoic acid derivatives as well as aryl and heteroaryl halides have been reported to date [40, 41]. Nonetheless, alkyl carboxylic acids are more challenging partners in cross-couplings reactions, often requiring activated substrates such as cyclohexadienyl [42] or  $\alpha$ -cyano acids [43]. The pioneering work of MacMillan/Doyle and

coworkers using the synergistic photoredox/nickel catalysis strategy for cross-coupling of  $\alpha$ -amino acids is a viable alternative to the reported methods [44]. The formation of carbon-centered radicals in the proposed catalytic cycle makes C(sp<sup>3</sup>) centers ideal nucleophilic partners for this transformation. Optimal conditions were found using  $[\text{Ir}(\text{dF}(\text{CF}_3)\text{ppy})_2(\text{bpy})](\text{PF}_6)$  as the photocatalyst,  $\text{NiCl}_2\cdot\text{glyme}/\text{dtbbpy}$  as the precatalyst, and  $\text{Cs}_2\text{CO}_3$  as an additive, with irradiation coming from a 34-W blue LED at room temperature. An array of aryl halides, including aryl iodides, -bromides, and -chlorides containing electron-donating and electron-withdrawing groups, as well as heteroaryl halides, were successfully cross-coupled with diverse  $\alpha$ -amino acids and an  $\alpha$ -oxycarboxylic acid (Scheme 26).

The proposed mechanism for this transformation involves the formation of a radical species from a single electron transfer oxidation/decarboxylation promoted by a photoexcited Ir(III) complex (Scheme 27), which can enter the nickel catalytic cycle to form the desired product.

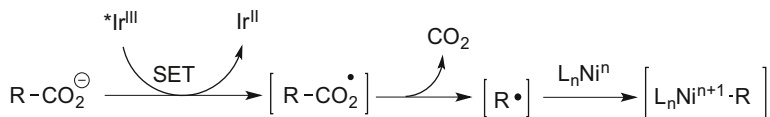
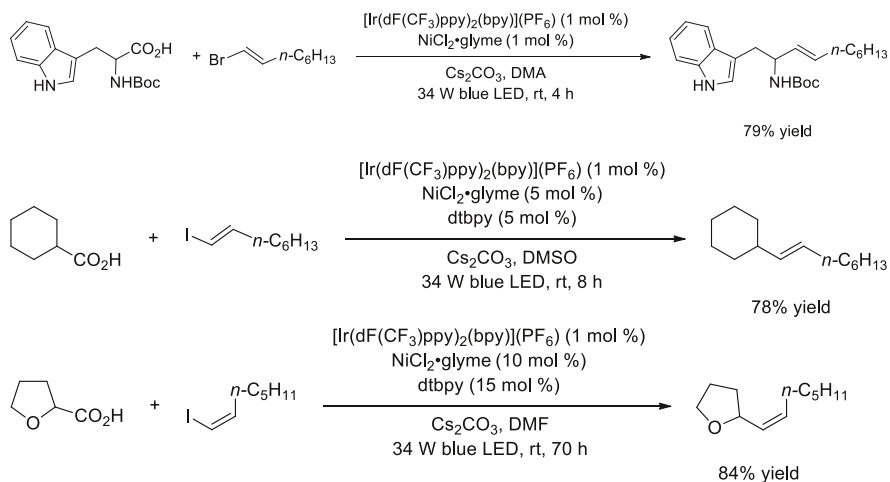
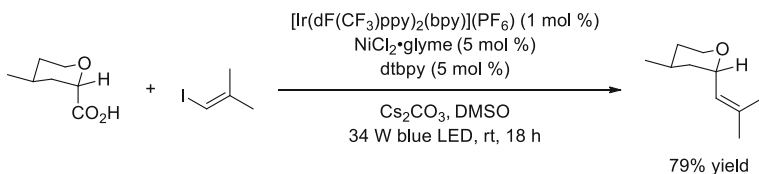
Merging photoredox and nickel catalysis in decarboxylative cross-coupling was further studied for a variety of carboxylic acid precursors with alkenyl halides [45]. Using a similar set of conditions as the one developed for aryl halides, the scope of the reaction was shown to include cyclopentenyl- and cyclohexenyl ring systems, ribose-derived cyclic  $\alpha$ -oxycarboxylic acids, acyclic primary and secondary  $\alpha$ -oxycarboxylic acids,  $\alpha$ -amino acids, as well as secondary alkyl and benzylic carboxylic acids (Scheme 28). In terms of the electrophiles, alkenyl iodides and -bromides containing aromatic rings, benzyl ethers and silane functional groups could be used. Importantly, when a (*Z*)-alkenyl iodide was utilized, no isomerization of the double bond was observed. Primary alkyl carboxylic acids afforded the desired coupled products, albeit in low yield (11 %), whereas tertiary alkyl carboxylic acids were not efficient partners in this method.

Finally, the synthesis of a natural product was realized utilizing the developed protocol. Hence, *trans*-rose oxide was obtained in 79 % yield from a combined photoredox/Ni catalytic cross-coupling of a *trans*-tetrahydropyran carboxylic acid and an alkenyl iodide (Scheme 29).

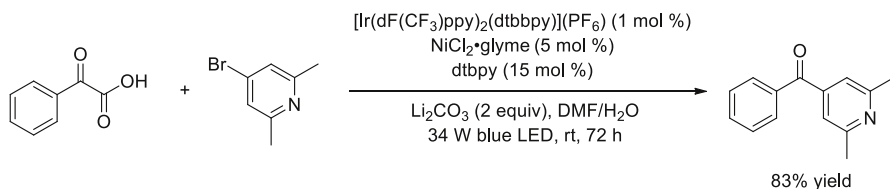


**Scheme 26** Decarboxylative cross-coupling of  $\alpha$ -amino acids under photoredox/Ni dual catalysis



**Scheme 27** Formation of an alkyl radical from decarboxylative SET oxidation**Scheme 28** Photoredox/Ni dual decarboxylative cross-coupling with alkenyl halides**Scheme 29** Photoredox/Ni decarboxylative cross-coupling in the synthesis of rose oxide

The synthesis of aryl ketones was also developed utilizing photoredox/Ni catalysis in the decarboxylative cross-couplings of  $\alpha$ -keto acids [46]. Reaction conditions were developed to carry out an efficient coupling of a variety of  $\alpha$ -keto

**Scheme 30** Photoredox/Ni decarboxylative cross-coupling of  $\alpha$ -keto acids

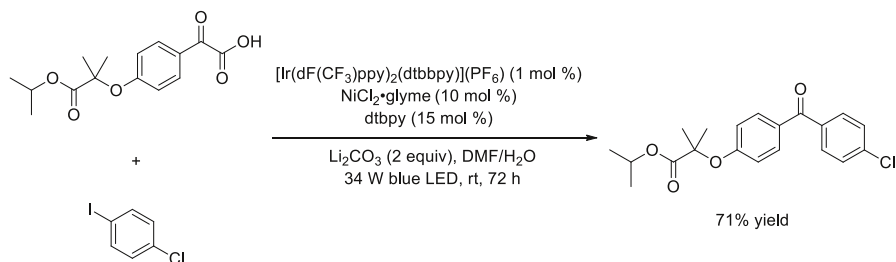
acids bearing aromatic and aliphatic substituents as well as for aryl-, heteroaryl-, alkenyl-, and secondary alkyl halides (Scheme 30).

This reaction protocol was also utilized in the synthesis of fenofibrate, a cholesterol-modulating drug, further highlighting its utility (Scheme 31).

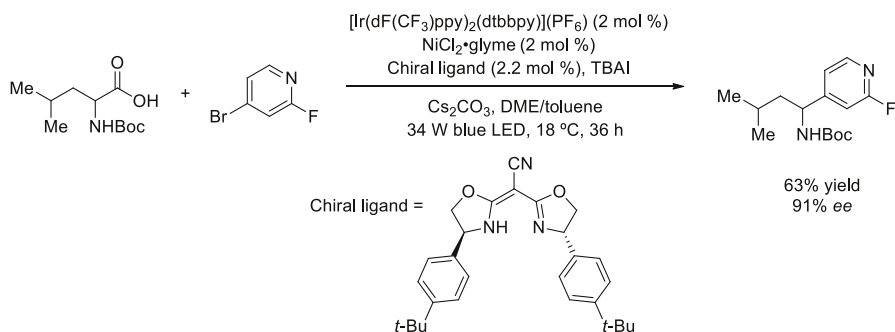
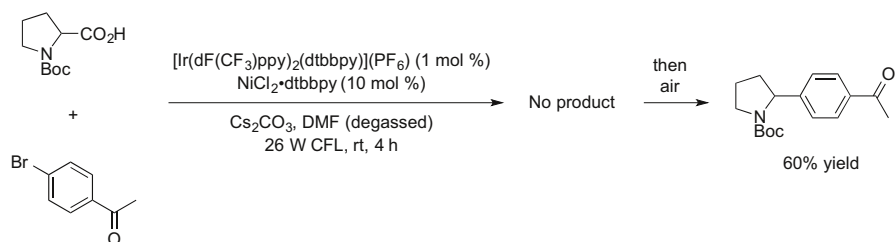
An enantioselective version of the dual photoredox/Ni catalyzed cross-coupling of commercially available  $\alpha$ -amino acids and aryl bromides was also sought [47]. Under conditions very similar to those developed for the achiral transformation but using a chiral ligand, it was possible to synthesize benzylic amines in good to excellent yields and *ees* up to 92 % (Scheme 32). The scope of the reaction was shown to allow electron-rich and electron-poor aryl bromides, and bromopyridines containing trifluoromethyl and fluorine functional groups. Substituents such as carbamate, ether, ester, indole, and thiophene were well tolerated in the Boc-protected  $\alpha$ -amino acid moiety. Changing the protecting group to N-Cbz still afforded the coupled product, albeit in lower yields.

Complementary studies on the decarboxylative cross-coupling of  $\alpha$ -amino acids to investigate the influence of oxygen, solvent, and light on these transformations were carried out [48]. The protocol reported by MacMillan and coworkers for photoredox/Ni dual catalytic cross-coupling of Boc-Pro-OH with 4-iodotoluene was utilized as a model for the study. Under rigorous exclusion of O<sub>2</sub> no coupled product was observed, showing the requirement of an O<sub>2</sub> atmosphere. When other ligands, solvents and Ni catalysts were tested, all showed the dependence of oxygen with lower yields or no conversions being observed in a degassed reaction mixture (Scheme 33).

As in the case of the alkyltrifluoroborates (Scheme 9), the use of donor–acceptor fluorophore catalysts was also investigated for the photoredox/Ni cross-coupling of carboxylic acid partners [21]. The alternative 4CzIPN photoredox catalyst was found efficient to afford the desired coupled products in yields comparable to those obtained using iridium complexes. The use of this fluorophore photocatalyst allowed photoredox/Ni decarboxylative cross-coupling of  $\alpha$ -amino acids and  $\alpha$ -oxy carboxylic acids with aryl- and heteroaryl halides (iodides, bromides, and chlorides) bearing electron-poor and electron-rich substituents (Scheme 34).

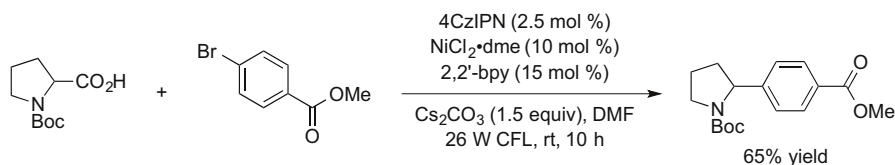


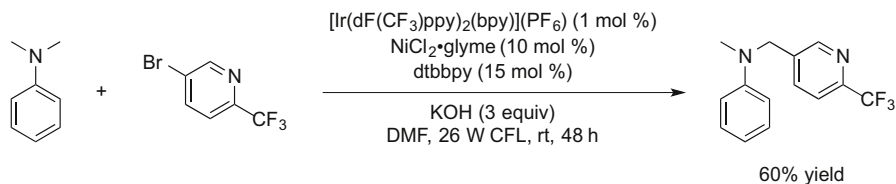
**Scheme 31** Photoredox/Ni decarboxylative cross-coupling in the synthesis of fenofibrate

**Scheme 32** Enantioselective dual photoredox/Ni decarboxylative cross-coupling**Scheme 33** Effects of  $\text{O}_2$  in decarboxylative photoredox/Ni catalyzed cross-coupling

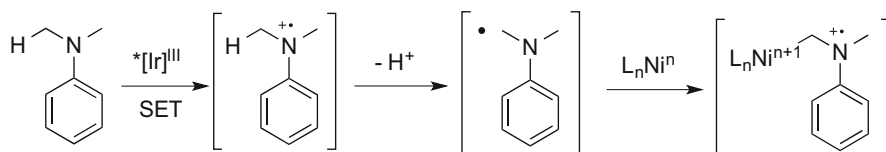
## 5 Miscellaneous

During the development of the decarboxylative cross-coupling under photoredox/Ni dual catalysis by MacMillan/Doyle, the direct functionalization of C(sp<sup>3</sup>)-H bonds using *N,N*-dimethylanilines was achieved, affording the products in moderate to good yields (Scheme 35) [44]. In this preliminary finding, three aryl iodides containing methyl-, chloro- and methoxy substituents, as well as one pyridine-based heteroaryl bromide, were found to be efficient in this transformation. The proposed mechanism for this reaction requires the formation of the nitrogen-stabilized alkyl radical of dimethylaniline from a SET oxidation promoted by an excited-state iridium complex (Scheme 36). This radical can enter the Ni cross-coupling cycle (Scheme 2) to complete this dual catalytic reaction.

**Scheme 34** Decarboxylative photoredox/Ni cross-coupling using donor-acceptor 4CzIPN



**Scheme 35** Direct C(sp<sup>3</sup>)-H cross-coupling using dual photoredox/Ni catalysis

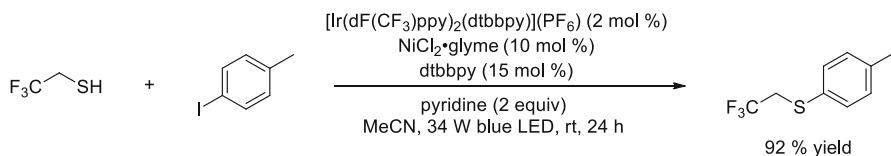
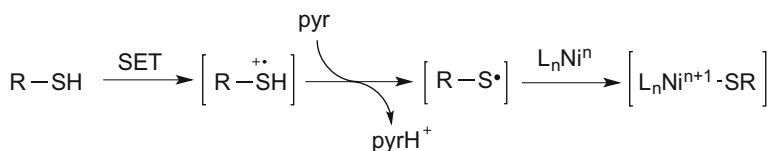


**Scheme 36** Radical formation by SET oxidation

Thioethers are important structures found in many drugs for treatment of diseases such as cancer, HIV, and Alzheimer's disease [49]. The traditional transition metal-catalyzed synthesis of thioethers often requires strong bases, high temperatures, specially designed ligands, and high catalyst loading, limiting functional group tolerance [50, 51]. Thiyl radicals are easily formed from thiols, making them useful substrates for radical reactions in organic synthesis [52]. Using this concept, thiols were utilized as nucleophilic partners in a photoredox/Ni dual catalytic cross-coupling in a method that complements that previously outlined in [Scheme 24](#) [53]. Optimal conditions were found utilizing  $[\text{Ir}(\text{dF}(\text{CF}_3)\text{ppy})_2(\text{dtbbpy})](\text{PF}_6)$  as the photocatalyst,  $\text{NiCl}_2\cdot\text{glyme}/\text{dtbbpy}$  as the cross-coupling precatalyst, pyridine as an additive, and irradiation with a 34-W blue LED at room temperature. A wide variety of aryl iodides containing electron-rich and electron-poor functional groups were tolerated, forming the thioethers in moderate to very good yields. The scope of the thiol nucleophile was found to include thiophenols, *N*-Boc-cysteine, as well as primary and secondary functionalized alkylthiols ([Scheme 37](#)).

The proposed mechanism for formation of the thiyl radical entering the photoredox/Ni dual catalytic cycle starts with a single-electron transfer oxidation of the thiol by the photoexcited Ir complex to produce a thiol radical cation, which undergoes deprotonation by pyridine to yield the desired thiyl radical ([Scheme 38](#)). The latter feeds into the Ni-catalyzed cross-coupling cycle.

Indolines are important scaffolds in total synthesis and medicinal chemistry. The synthesis of these compounds generally relies on Pd- or Rh-catalyzed cyclization of alkenes with aryl halides [54] or C–H activation [55]. However, because of the ease of  $\beta$ -hydride elimination (Heck-type reaction) for the alkyl intermediate formed after alkene insertion, these methods often require strongly deactivating alkenes or alkenes bearing no  $\beta$ -hydrogen, thus limiting the utility of this transformation. The use of photoredox/Ni dual catalytic cross-coupling for the synthesis of indolines allows the formation of the desired products because  $\beta$ -hydride elimination can be avoided [56]. Thus, reaction of 2-iodoacetanilide derivatives with various alkenes

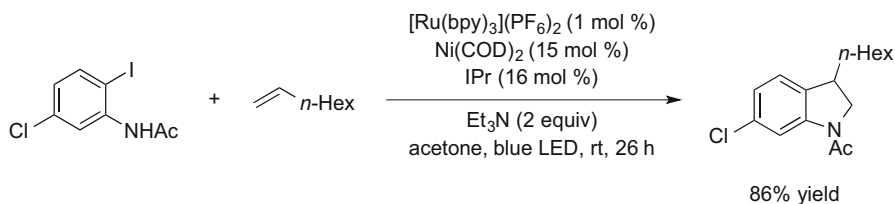
**Scheme 37** Photoredox/Ni dual catalytic cross-coupling of thiols**Scheme 38** Proposed mechanistic formation of thiyl radical under photoredox/Ni dual catalysis

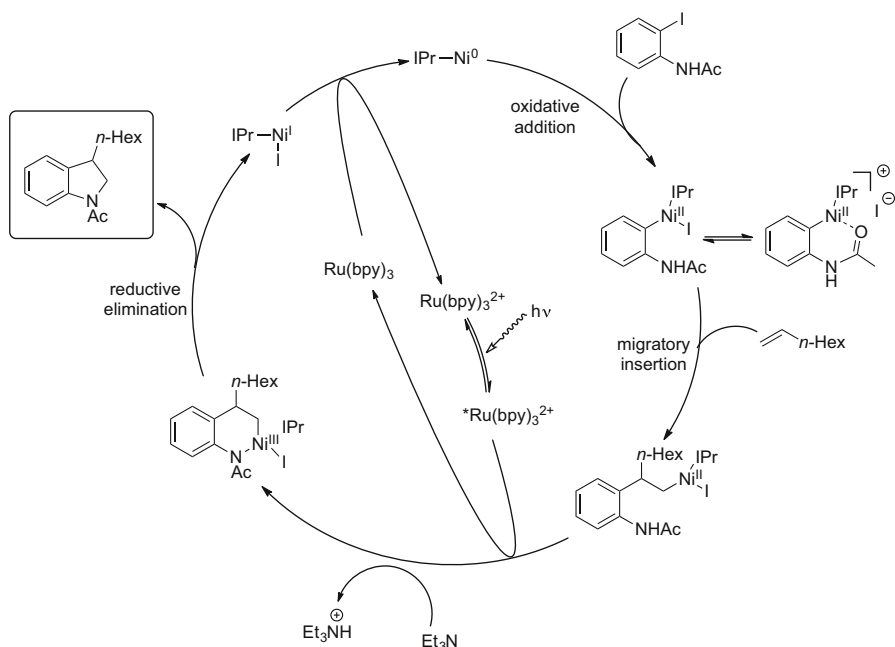
under optimized photoredox/Ni cross-coupling conditions provided a variety of functionalized indolines in low-to-good yields (**Scheme 39**). Within the alkene partner, a number of functional groups could be embedded, including alkylsilyl groups, silyl-protected alcohols, nitriles, chlorides, Boc-protected primary amines, esters, and arenes.

The proposed mechanism for this transformation differs from the established cycle for the photoredox/Ni dual catalysis cross-coupling, because in this case there is no radical formation. Instead, after oxidative addition of the aryl halide, the organonickel(II) species undergoes a migratory insertion with an alkene, forming a new organonickel(II) species. This intermediate, upon deprotonation and oxidation by an excited Ru complex, forms a Ni(III) complex that undergoes reductive elimination to provide the product and release Ni(I) halide, which is reduced to Ni(0) by the Ru photocatalyst (**Scheme 40**).

## 6 Conclusions and Outlook

The photoredox/Ni dual catalytic cross-coupling protocol has opened new vistas for carbon–carbon bond-forming reactions. Not only has it enabled transformations that were extremely challenging, if not impossible, under previous conditions, but these

**Scheme 39** Photoredox/Ni dual catalysis indoline synthesis



**Scheme 40** Proposed mechanism for indoline synthesis using photoredox/Ni dual catalysis

reactions can also be carried out in a highly sustainable manner using readily available starting materials at room temperature. Visible light is utilized to overcome the previously problematic high-energy transition state barriers associated with the transmetalation from non-nucleophilic organoboron and organosilicon coupling partners. New coupling partners (e.g., carboxylic acids) have been introduced, and all of these reactions take place using inexpensive, Ni-based catalysts. With the introduction of suitable organic photocatalysts, practitioners are now in a position to carry out unprecedented cross-coupling reactions in a highly effective and economical manner, while at the same time significantly expanding three-dimensional chemical space. With the promise of performing all of these reactions in a stereoconvergent manner from racemic precursors, photoredox/Ni cross-coupling represents an incredibly powerful new renaissance for this important class of carbon–carbon bond-forming transformations.

**Acknowledgments** The authors thank the National Institute of General Medical Sciences for a grant (R01 GM-113878) that has supported our research in this area. We are also grateful to Frontier Scientific and Evonik for supplying many of the materials used in our studies.

## References

1. Molander GA (2013) (ed) Science of synthesis cross-coupling and Heck-type reactions: C-C cross-coupling using organometallic partners. Thieme, Stuttgart
2. Nicolaou KC, Bulger PG, Sarlah D (2005) *Angew Chem Int Ed* 44:4442
3. Seechurn CCCJ, Kitching MO, Colacot TJ, Snieckus V (2012) *Angew Chem Int Ed* 51:5062

4. González-Bobes F, Fu GC (2006) *J Am Chem Soc* 128:5360
5. Krasovskiy AL, Haley S, Voigtritter K, Lipshutz BH (2014) *Org Lett* 16:4066
6. Yang Y, Niedermann K, Han C, Buchwald SL (2014) *Org Lett* 16:4638
7. Jiang X, Gandelman M (2015) *J Am Chem Soc* 137:2542
8. St. Denis JD, Scully CCG, Lee CF, Yudin AK (2014) *Org Lett* 16:1338
9. Gutierrez O, Tellis JC, Primer DN, Molander GA, Kozlowski MC (2015) *J Am Chem Soc* 137:4896
10. Lennox AJJ, Lloyd-Jones GC (2014) *Chem Soc Rev* 43:412
11. Molander GA, Ribagorda M (2003) *J Am Chem Soc* 125:11148
12. Molander GA, Figueroa R (2006) *Org Lett* 8:75
13. Molander GA, Petrillo DE (2006) *J Am Chem Soc* 128:9634
14. Dreher SD, Dormer PG, Sandrock DL, Molander GA (2008) *J Am Chem Soc* 130:9257
15. Dreher SD, Lim S-E, Sandrock DL, Molander GA (2009) *J Org Chem* 74:3626
16. Li L, Zhao S, Joshi-Pangu A, Diane M, Biscoe MR (2014) *J Am Chem Soc* 136:14027
17. Tellis JC, Primer DN, Molander GA (2014) *Science* 345:433
18. Primer DN, Karakaya I, Tellis JC, Molander GA (2015) *J Am Chem Soc* 137:2195
19. Molander GA, Gormisky PE (2008) *J Org Chem* 73:7481
20. Molander GA, Beaumard F, Niethamer TK (2011) *J Org Chem* 76:8126
21. Luo J, Zhang J (2016) *ACS Catalys* 6:873
22. Yamashita Y, Tellis JC, Molander GA (2015) *Proc Natl Acad Sci USA* 112:12026
23. Khatib ME, Serafim RAM, Molander GA (2016) *Angew Chem Int Ed* 55:254
24. Muller K, Faeh C, Diederich F (2007) *Science* 317:1881
25. Ryu D, Primer DN, Tellis JC, Molander GA (2016) *Chem Eur J* 22:120
26. Ryu, DaWeon PhD (2015) *Synthesis and applications of novel alkylboron compounds*. Thesis, University of Pennsylvania, Philadelphia, PA, USA
27. Karakaya I, Primer DN, Molander GA (2015) *Org Lett* 17:3294
28. Amani J, Sodagar E, Molander GA (2016) *Org Lett* 18:732
29. Matsuoka D, Nishigaichi Y (2015) *Chem Lett* 43:559
30. Corcé V, Chamoreau L-M, Derat E, Goddard J-P, Ollivier C, Fensterbank L (2015) *Angew Chem Int Ed* 54:11414
31. Levêque C, Chenneberg L, Corcé V, Goddard J-P, Ollivier C, Fensterbank L (2016) *Org Chem Front* 3:462
32. Yasu Y, Koike T, Akita M (2012) *Adv Synth Catal* 354:3414
33. Nishigaichi Y, Suzuki A, Takuwa A (2007) *Tetrahedron Lett* 48:211
34. Jouffroy M, Primer DN, Molander GA (2016) *J Am Chem Soc* 138:47
35. Patel NR, Kelly CB, Jouffroy M, Molander GA (2016) *Org Lett* 18:764
36. Jouffroy M, Kelly CB, Molander GA (2016) *Org Lett* 18:876
37. Zhou HB, Nettles KW, Bruning JB, Kim Y, Joachimiak A, Sharma S, Carlson KE, Stossi F, Katzenellenbogen BS, Greene GL, Katzenellenbogen JA (2007) *Chem Biol* 14:659
38. Baldock C, Rafferty JB, Sedelnikova SE, Baker PJ, Stuitje AR, Slabas AR, Hawkes TR, Rice DW (1996) *Science* 274:2107
39. Jouffroy M, Davies GHM, Molander GA (2016) *Org Lett* 18:1606
40. Li H, Miao T, Wang M, Li P, Wang L (2016) *Synlett*. doi:10.1055/s-0035-1561388
41. Rodríguez N, Goossen L (2011) *J Chem Soc Rev* 40:5030
42. Chou C-M, Chatterjee I, Studer A (2011) *Angew Chem Int Ed* 50:8614
43. Shang R, Ji D-S, Chu L, Fu Y, Liu L (2001) *Angew Chem Int Ed* 50:4470
44. Zao Z, Ahneman DT, Chu L, Terrett JA, Doyle AG, MacMillan DWC (2014) *Science* 345:437
45. Noble A, McCarver SJ, MacMillan DWC (2014) *J Am Chem Soc* 137:624
46. Chu LC, Lipshultz JM, MacMillan DWC (2015) *Angew Chem Int Ed* 54:7929
47. Zuo Z, Cong H, Li W, Choi J, Fu GC, MacMillan DWC (2016) *J Am Chem Soc* 138:1832
48. Oderinde MS, Varela-Alvarez A, Aquila B, Robbins DW, Johannes JW (2015) *J Org Chem* 80:7642
49. Sun ZY, Botros E, Su AD, Kim Y, Wang EJ, Baturay N, Kwon CH (2000) *J Med Chem* 43:4160
50. Beletskaya IP, Ananikov VP (2011) *Chem Rev* 111:1596
51. Hartwig JF (2008) *Acc Chem Res* 41:1534
52. Dénes F, Pichowicz M, Povie G, Renaud P (2014) *Chem Rev* 114:2587
53. Oderinde MS, Frenette M, Robbins DW, Aquila B, Johannes JW (2016) *J Am Chem Soc* 138:1760
54. Larock RC, Yum EK (1991) *J Am Chem Soc* 113:6689
55. Zhao D, Vásquez-Céspedes S, Glorius F (2015) *Angew Chem Int Ed* 54:1657
56. Tasker SZ, Jamison TF (2015) *J Am Chem Soc* 137:9531

# Nickel-Catalyzed Reductive Couplings

Xuan Wang<sup>1</sup> · Yijing Dai<sup>1</sup> · Hegui Gong<sup>1,2</sup>

Received: 29 March 2016 / Accepted: 30 May 2016 / Published online: 23 June 2016  
© Springer International Publishing Switzerland 2016

**Abstract** The Ni-catalyzed reductive coupling of alkyl/aryl with other electrophiles has evolved to be an important protocol for the construction of C–C bonds. This chapter first emphasizes the recent progress on the Ni-catalyzed alkylation, arylation/vinylation, and acylation of alkyl electrophiles. A brief overview of CO<sub>2</sub> fixation is also addressed. The chemoselectivity between the electrophiles and the reactivity of the alkyl substrates will be detailed on the basis of different Ni-catalyzed conditions and mechanistic perspective. The asymmetric formation of C(sp<sup>3</sup>)–C(sp<sup>2</sup>) bonds arising from activated alkyl halides is next depicted followed by allylic carbonylation. Finally, the coupling of aryl halides with other C(sp<sup>2</sup>)–electrophiles is detailed at the end of this chapter.

**Keywords** Reductive coupling · Nickel catalysis · Electrophiles · Selectivity

## 1 Introduction

In recent years, development of transition metal-catalyzed cross-coupling between two electrophiles has received considerable attention (for reviews, see [1–6]). These methods avoid the preparation of nucleophiles that are often converted from their

---

This article is part of the Topical Collection “Ni- and Fe-Based Cross-Coupling Reactions”; edited by “Arkaitz Correa”.

---

✉ Hegui Gong  
[hegui\\_gong@shu.edu.cn](mailto:hegui_gong@shu.edu.cn)

<sup>1</sup> Department of Chemistry, Center for Supramolecular Materials and Catalysis, Shanghai University, 99 Shang-Da Road, Shanghai 200444, China

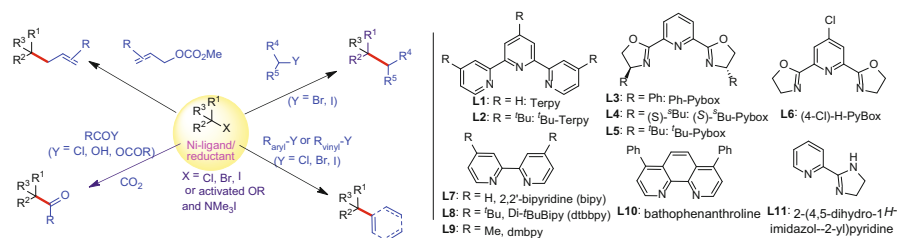
<sup>2</sup> Shanghai Key Lab of Chemical Assessment and Sustainability, Tongji University, 1239 Siping Road, Shanghai 200092, China



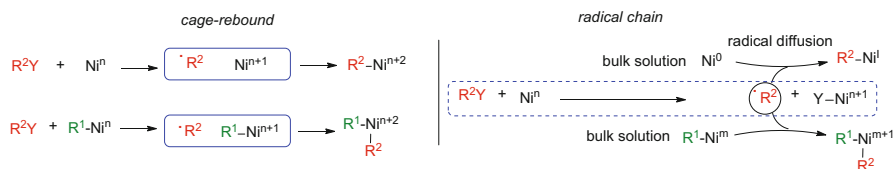
more stable and accessible electrophile precursors, which may become critically useful when entries to certain nucleophiles are exceedingly difficult [7, 8]. In particular, reductive coupling of alkyl electrophiles with other electrophiles has advanced to be an important strategy for the construction of C–C(sp<sup>3</sup>) bonds, wherein nickel, and in some cases cobalt, catalysts have proven to be exceptionally powerful (Scheme 1) (for reviews, see [1–6]). The electrophiles capable of coupling with alkyl halides and pseudo-halides include C(sp<sup>3</sup>)–(e.g., unactivated alkyl halides and allylic acetates) and C(sp<sup>2</sup>)–substrates (e.g., acyl and aryl/vinyl halides), as well as CO<sub>2</sub> and other carbonyl-type compounds. The asymmetric C(sp<sup>2</sup>)–C(sp<sup>3</sup>) bond formation has also been developed using activated halides (e.g., benzyl,  $\alpha$ -chloronitriles). Under these reductive coupling conditions, the nickel catalysts have shown remarkable efficiency in differentiating the two different electrophiles and manipulating the reactivity of alkyl substrates. The highly competitive homocoupling and the  $\beta$ -elimination issues can be well controlled by suitable choices of the catalytic conditions (for reviews on Ni-catalyzed conventional coupling chemistry, see [9–15]).

Although insightful understanding of the reaction mechanisms still requires tremendous studies, it is now well accepted that alkyl halides participate in the Ni-catalyzed reductive coupling reactions through a radical process [1–6]. The radical can diffuse to a bulk solution, and bind to an organonickel [e.g., C(sp<sup>2</sup>)–Ni<sup>II</sup>] intermediate via a radical-chain process (Scheme 2) (for other examples involving Ni-catalyzed radical-chain mechanism, see [16–20]). It may also bind to the catalytic species in a cage upon its generation via one-electron reduction or halide abstraction by low-valent Ni (cage-rebound, Scheme 2) [21–23]. While radical-chain mechanisms may operate for construction of C(sp<sup>3</sup>)–C(sp<sup>2</sup>) bonds, (for reviews on Ni-catalyzed conventional coupling chemistry, see [9–15]) formation of C(sp<sup>3</sup>)–C(sp<sup>3</sup>) bonds via a cage-rebound process is possible according to previous studies on the Ni-catalyzed Negishi chemistry (Scheme 2) [23]. The latter transformation, however, is much less understood [21].

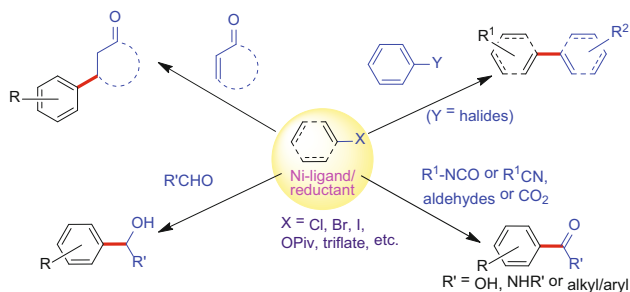
By comparison, transition metal-catalyzed reductive coupling of aryl or vinyl halides (or pseudo halides) with other C(sp<sup>2</sup>)–electrophiles is generally well explored. The Ni-catalyzed protocols in particular have enabled efficient cross-assembly of aryl/vinyl with aryl/vinyl, carbonyl groups as well as activated alkenes



**Scheme 1** Reductive coupling of alkyl halides with other electrophiles (left), and the representative ligands used for the transformations (right)



**Scheme 2** Illustration of the cage-rebound (left) and radical-chain (right) processes in the Ni-catalyzed reductive coupling chemistry



**Scheme 3** Reductive coupling of  $C(sp^2)$ -halides with other electrophiles

and alkynes (Scheme 3). Of special note is the moderate efficiency for cross-Ullmann reactions between two aryl electrophiles due to competitive homodimerization. A marked improvement of cross-selectivity was recently achieved between aryl halides and aryl triflates via a Pd/Ni-dual catalytic system (see Sect. 2.7), which may proceed through a  $Ni^0/Ni^{II}$  catalytic pathway rather than a  $Ni^I/Ni^{III}$  process often suggested in the reductive biaryl synthesis [24, 25].

In this review, we focus on the summary of important advances on the Ni-catalyzed reductive coupling of  $C(sp^3)$ - and  $C(sp^2)$ -halides and pseudo-halides. The origin of the selectivities and the reactivity of substrates is detailed, particularly from a mechanistic perspective. The three categories pertaining to alkyl electrophiles include alkylation, arylation and vinylation, and acylation (including  $CO_2$ , acid derivatives) of alkyl electrophiles. Following this, the asymmetric reductive arylation, vinylation, and carbonylation of activated alkyl electrophiles are illustrated. The last section of this chapter summarizes the coupling of  $C(sp^2)$ -halides with other  $C(sp^2)$ - and  $C(sp)$ -electrophiles. Due to the extensive reviews that have been published on reductive acylation (including  $CO_2$  fixation), arylation of alkyl electrophiles [1–6], electrochemical coupling, as well as Co-catalyzed reductive coupling methods [3], only recent progress will be highlighted for these chemistries.

## 2 Reductive Coupling of Two Electrophiles

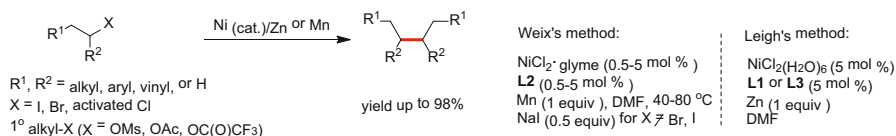
### 2.1 Cross-Coupling of Two C(sp<sup>3</sup>)–Electrophiles

#### 2.1.1 Ni-Catalyzed Coupling Between Unactivated C(sp<sup>3</sup>)– and C(sp<sup>3</sup>)–Electrophiles

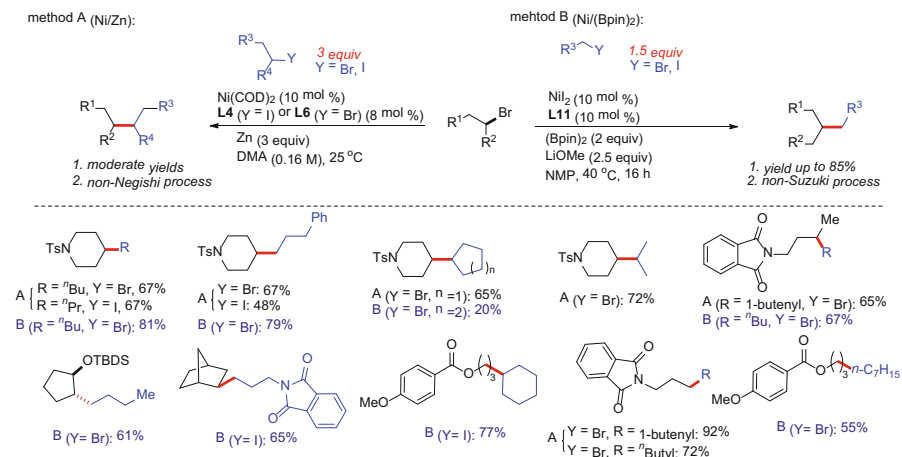
**1. Dimerization of alkyl halides** When the coupling takes place between two different alkyl electrophiles, the control of chemoselectivity becomes considerably challenging. The catalyst should effectively bias the subtle steric and electronic difference between the two alkyl partners, as the homocoupling of alkyl electrophiles under reductive coupling conditions may otherwise substantially impede the cross-coupling efficiency. Indeed, Ni<sup>II</sup>/Bu-Terpy (**L2**), Ph-Pybox (**L3**), Bipy (**L7**) (see [Scheme 1](#) for structures), ethyl acrylate or dppe (1,2-bis(diphenylphosphanyl)ethane)-catalyzed dimerization of alkyl halides has shown striking competence using Mn or Zn as the reductant ([Scheme 4](#)) [26–29]. The reaction is believed to proceed through a R<sub>alkyl</sub>–Ni<sup>III</sup>–R<sub>alkyl</sub> intermediate. Unfortunately, detection of the proposed Ni<sup>III</sup> species is not available (Vicic, Ni(III)) [30, 31].

**2. Cross-coupling using Ni/Zn conditions** In 2011, Gong et al. disclosed that Ni/Pybox catalytic conditions enabled the first catalytic cross-coupling of two different alkyl halides, wherein zinc powder served as the reductant ([Scheme 5](#)) [21]. This method efficiently generates C(sp<sup>3</sup>)–C(sp<sup>3</sup>) bonds in moderate-to-good yields, and features excellent functional group tolerance and broad substrate scope. However, the Ni/Zn reductive conditions only moderately bias the two alkyl coupling partners because one of the coupling halides needs threefold excess ([Scheme 5](#)). In addition to the formation of the cross-coupling products, the highly competitive homocoupling side reactions account for the mass balance of the excess alkyl halides.

**3. Cross-coupling using Ni(Bpin)<sub>2</sub> conditions** A significant improvement on chemoselectivity is observed when (Bpin)<sub>2</sub> (Bis(pinacolato)diboron) serves the reductant ([Scheme 5](#)) [22]. The reaction requires only 1.5 equiv of the second alkyl halides, which works effectively for the coupling of secondary as well as hindered primary halides with primary bromides. In most cases, the results were comparable to the conventional Ni-catalyzed Suzuki reactions. The formation of a possible Ni–Bpin complex may be responsible for differentiating the two alkyl halides in the oxidative addition step, by taking advantage of subtle electronic and steric differences of the two alkyl partners. This work represents the first efficient coupling of unactivated alkyl halides using boron as the terminal reductant. The preliminary



**Scheme 4** Ni-catalyzed dimerization of alkyl electrophiles

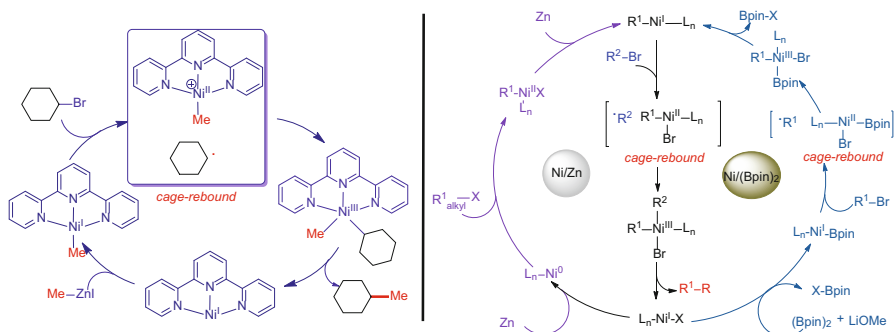


**Scheme 5** Ni-catalyzed cross-coupling of two different alkyl halides under Ni/Zn or Ni/(Bpin)<sub>2</sub> conditions [(Bpin)<sub>2</sub> = bis(pinacolato)diboron, DMA = *N,N*-dimethyl acetamide, NMP = *N*-methyl-2-pyrrolidone]

mechanistic investigation excludes the possibility of in situ organoboron/Suzuki process.

4. *Possible mechanism* On the basis of Vicic's proposal on the Ni-catalyzed Negishi coupling of alkyl halides, Terpy-Ni<sup>I</sup>-Me was suggested to be a key intermediate, which reacts with cyclohexyl bromide to give the coupling product (Scheme 6, left) [23]. The mechanism likely involves one-electron transfer or halide abstraction to generate R<sub>alkyl</sub> radical and Terpy-Ni<sup>II</sup>-Me. Rapid combination of the two species in a cage gives Terpy-Ni<sup>III</sup>(R<sub>alkyl</sub>)-Me species, which generates the product upon reductive elimination.

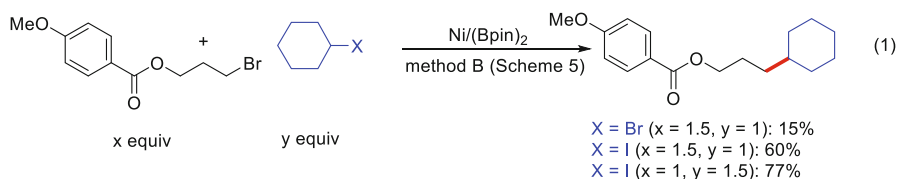
Both Ni/Zn and Ni/(Bpin)<sub>2</sub> systems likely comprise alkyl radical processes, which are evidenced by use of the radical clocks. The reaction mechanism for the Ni/Zn method is proposed to undergo two steps of oxidative addition of alkyl



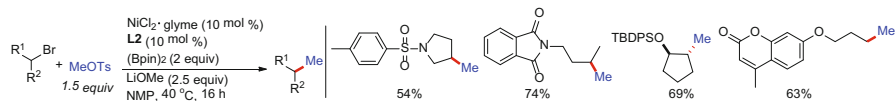
**Scheme 6** Mechanistic proposals for Ni-catalyzed Negishi process (left), and cross-coupling of two different alkyl halides under Ni/Zn or Ni/(Bpin)<sub>2</sub> conditions (right)

halides to low valent Ni species (Scheme 6, right). Namely, oxidative addition of the first alkyl halide to a low valent  $\text{Ni}^n(\text{L}_n)$  ( $n = 0$  or  $1$ ) results in  $\text{R}_{\text{alkyl}}^1 - \text{Ni}^{n+2}(\text{L}_n)$  complex, which is then reduced by Zn to give  $\text{R}_{\text{alkyl}}^1 - \text{Ni}^I(\text{L}_n)$ . A second oxidative addition of  $\text{R}_{\text{alkyl}}^2$  halide leads to  $\text{R}_{\text{alkyl}}^1 - \text{Ni}^{\text{III}}(\text{L}_n) - \text{R}_{\text{alkyl}}^2$  species, which releases the product upon reductive elimination. The origin of the selectivity relies on the formation of  $\text{R}_{\text{alkyl}}^1 - \text{Ni}^{n+2}(\text{L}_n)$  and  $\text{R}_{\text{alkyl}}^1 - \text{Ni}^{\text{III}}(\text{L}_n) - \text{R}_{\text{alkyl}}^2$  intermediates, wherein the  $\text{Ni}(\text{L}_n)$  may sterically and electronically differentiate the two alkyl groups. In the  $\text{Ni}/(\text{Bpin})_2$  conditions, generation of  $\text{R}_{\text{alkyl}}^1 - \text{Ni}^I$  may arise from oxidative addition of  $\text{R}_{\text{alkyl}}^1 - \text{X}$  to  $\text{Ni}^I(\text{L}_n) - \text{Bpin}$  followed by reductive elimination of  $\text{X} - \text{Bpin}$  (Scheme 6, right).

5. *Effect of leaving groups* Based on the proposed reaction mechanisms, one strategy to induce a different rate in the oxidative addition step is use of different leaving groups [21, 22]. Experimental studies have shown a general decreasing trend in reactivity of the alkyl halides: secondary iodide > primary iodide > secondary bromide > primary bromide. It is not clear whether the rates of oxidative addition of alkyl halides to Ni will precisely follow the reactivity sequence of the alkyl substrates. Steric effect should also be taken into account. However, the selection of halide sources is critical for the coupling events. In the  $\text{Ni}/\text{Zn}$  conditions, it was found that at least one of the alkyl substrates needs to be bromides, whereas the  $\text{Ni}/(\text{Bpin})_2$  conditions generally necessitate both coupling partners to be bromides. However, for those substrates not bearing functional groups (usually electron-withdrawing ones), use of their iodides seems to be critical to promote the reactivity so as to match that of the other coupling partners which are alkyl bromides (Eq. 1).

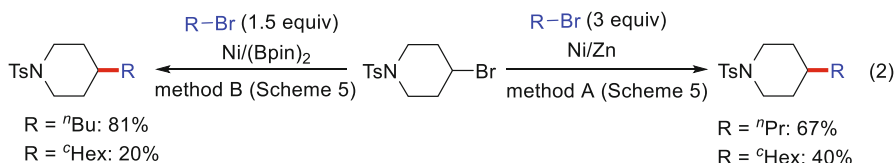


The effect of leaving groups is also found critical for methyl electrophiles [32]. While methyl iodide is not suitable for the reductive coupling with other alkyl electrophiles, methyl tosylate proves to be effective under modified  $\text{Ni}/(\text{Bpin})_2$  conditions (Scheme 7). The in situ generated methyl iodide or chloride at much lower concentration may account for the chemoselectivity between methyl and more hindered alkyl groups, wherein formation of ethane or  $\text{Me} - \text{ZnX}$  is not favored.

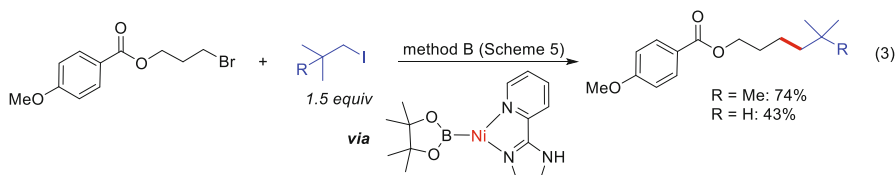


**Scheme 7** Ni-catalyzed methylation of alkyl halides under  $\text{Ni}/(\text{Bpin})_2$  conditions (glyme = dme = 1,2-dimethoxyethane)

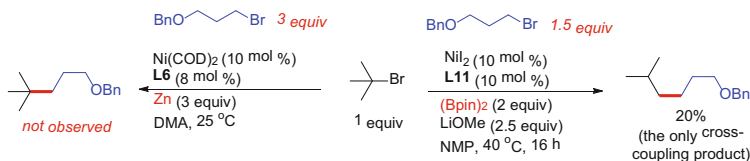
6. *Steric effect* The steric effect in the Ni/Zn reductive conditions is not as prominent as the Ni/(Bpin)<sub>2</sub> protocol [21]. The coupling of 1 equiv of secondary bromide with 3 equiv of *n*-propyl- and cyclohexyl bromides under Zn conditions gave the products in 67 and 40 % yields, respectively [22]. In contrast, the coupling of cyclohexyl bromide under the Ni/(Bpin)<sub>2</sub> conditions is much less effective (Eq. 2) [22].



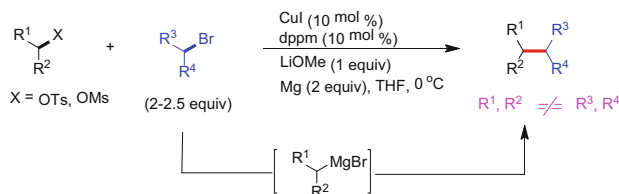
In the Ni/(Bpin)<sub>2</sub> conditions, the impact of steric hindrance can be attributed to the formation of a Ni–Bpin complex, which may preferentially react with sterically more reactive R<sup>1</sup>–alkyl halides (e.g., secondary bromides and more hindered primary iodides as opposed to primary bromides) [22]. The resultant R<sup>1</sup>–Ni<sup>I</sup> species selectively reacts with less hindered primary alkyl bromides. When 1-iodo-2,2-dimethylpropane is subjected to the coupling with benzyloxy appended propyl bromide, marked promotion for the coupling efficiency is observed (Eq. 3). In contrast, the less hindered 1-iodo-2-methylpropane is much less competent possible due to enhanced homocoupling side reaction. These results suggest that steric and electronic properties of the substrates together have a profound effect on the coupling outcomes [22]



The steric effect appears predominantly important for tertiary alkyl halides. When coupling of <sup>t</sup>Bu–Br with unactivated primary bromide, no products containing all carbon quaternary centers were observed under both Ni/Zn and Ni/(Bpin)<sub>2</sub> conditions. The only detectable cross-coupling product arose from isomerization of the tertiary alkyl groups under the Ni/(Bpin)<sub>2</sub> conditions (Scheme 8) [22, 33].



**Scheme 8** Reductive coupling of <sup>t</sup>Bu–Br with a primary alkyl bromide under Ni/Zn and Ni/(Bpin)<sub>2</sub> conditions



**Scheme 9** Cu-catalyzed alkyl/alkyl in situ Kumada coupling [dppm = bis(diphenylphosphanyl)methane]

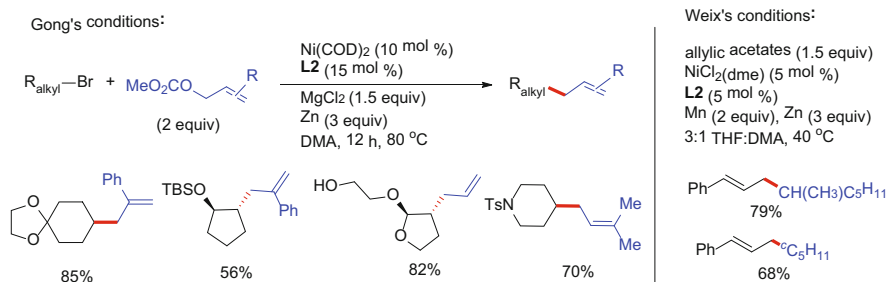
*Cu-catalyzed in situ Kumada method* In 2014, Liu reported that by meriting the different reactivity for alkyl tosylates and bromides in the formation of the organometallic reagents, in situ Cu-catalyzed Kumada coupling between two alkyl electrophiles could be achieved (Scheme 9) [34]. This protocol features a higher rate of Grignard formation from alkyl bromides than that of homocoupling or reduction, whereas alkyl tosylate remains inert to magnesium insertion.

### 2.1.2 Coupling with Activated Alkyl Electrophiles

The activated alkyl halides such as allyl, benzyl,  $\alpha$ -carbonyl, nitrile,  $\alpha$ -oxo and aza-electrophiles have been extensively studied. Of special interest is the competence of many of these substrates in the development of asymmetric coupling methods, which is discussed separately in Sect. 2.5. Homocoupling and reduction of the C–halide bonds of the activated substrates may become more problematic due to enhanced reactivity as compared to the unactivated counterparts [35]. While most transformations based on activated alkyl electrophiles emphasize C(sp<sup>3</sup>)–C(sp<sup>2</sup>) bond forming methods (see Sects. 2.2–2.5), the cross-coupling of allylic acetates (or carbonates) with unactivated alkyl halides represents the only example for the construction of hetero C(sp<sup>3</sup>)–C(sp<sup>3</sup>) bonds utilizing activated alkyl electrophiles [36–38].

Provided the double oxidative addition mechanistic model operates (Scheme 6), the chemoselectivity in the reductive coupling event may drastically alter when the two electrophiles exhibit pronounced rate difference in the oxidative addition steps. Allylic electrophiles, e.g., allyl carbonates can form  $\eta^1$ -,  $\eta^3$ - or  $\pi$ -Ni-allyl complexes via oxidative addition to Ni<sup>0</sup>, which is faster than that of unactivated alkyl halides. The second oxidative addition of allyl carbonate to the Ni-allyl species should be disfavored as opposed to unactivated alkyl halides.

The Ni-catalyzed reductive coupling protocol enables allylation of a wide set of alkyl halides (Scheme 10) [36–38]. The reactions display excellent regioselectivities wherein addition of alkyl groups to the less hindered allylic positions is adopted. Only *E*-olefins were detected even *cis*-alkenes were initially used. In Gong's method, the effect of substituents on unactivated alkyl halides is prominent on the coupling results. For instance, cyclohexyl bromide generally gives low-to-moderate yields as opposed to good results for the functionalized secondary alkyl substrates [36]. While Gong's conditions are more effective for secondary alkyl halides, Weix's method accommodates primary alkyl bromides when coupling with 1-aryl-decorated allylacetates [36, 37]. The reactivity of the alkyl halides is tunable



**Scheme 10** Ni-catalyzed allylation of alkyl halides with allyl carbonates and acetates (<sup>t</sup>Bu-Terpy = **L2**, Scheme 1)

with judicious choice of the catalysts. Sterically more demanding secondary and tertiary alkyl halides, as well as the more hindered 1,3-disubstituted allylic electrophiles remains unsatisfactory.

### 2.1.3 Cyclization of Dielectrophiles

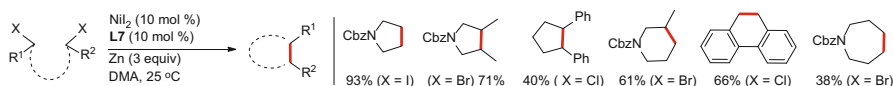
The reductive coupling strategies for  $\text{C}(\text{sp}^3)-\text{C}(\text{sp}^3)$  bond formation are applicable to intramolecular cyclization of alkyl dihalides [39]. The construction of five-membered rings is generally more efficient than six-membered ones, whereas the formation of seven-membered rings is the least effective (Scheme 11). The chemoselectivity issue may be deemphasized due to rapid intramolecular reactions. The formation of three- and four-membered rings is unsuccessful, possibly due to strained metallacyclobutane and pentane intermediates.

However, Jarvo discovered that formation of cyclopropane derivatives was highly effective via the intramolecular cyclization of benzylic ether-bearing chloroethyl groups under catalytic Ni/MeMgI reductive conditions (Scheme 12). The reactions are stereospecific, featuring retention of benzylic and inversion of C-Cl carbon centers. Both di- and tri-substituted chloroalkyl benzyl ethers are compatible with the reductive cyclization scenario [40].

## 2.2 Reductive Arylation and Vinylation of Alkyl Halides

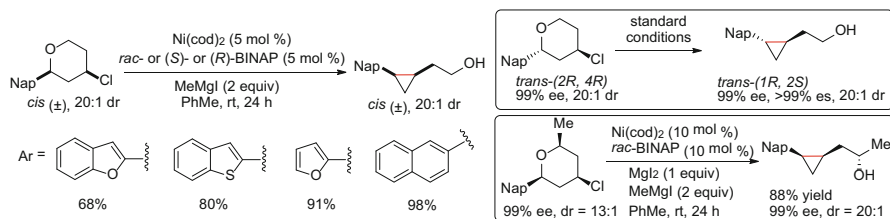
### 2.2.1 Ni-Catalyzed Reductive Arylation of Alkyl Halides

In 2009, Von Wangelin and Lipshultz independently published Fe- and Pd-catalyzed in situ Kumada and Negishi coupling of alkyl and aryl halides (Scheme 13) [41, 42]. Both methods merit faster formation of alkyl magnesium

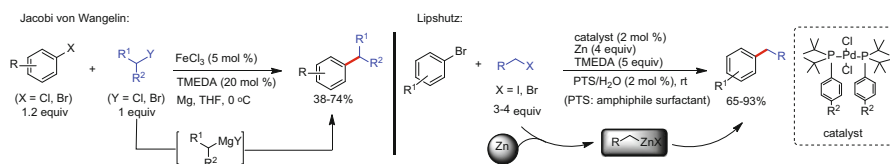


**Scheme 11** Ni-catalyzed reductive cyclization of alkyl dihalides





**Scheme 12** Ni-catalyzed reductive cyclization of dialkyl electrophiles bearing C(sp<sup>3</sup>)-Cl and benzyl ethers

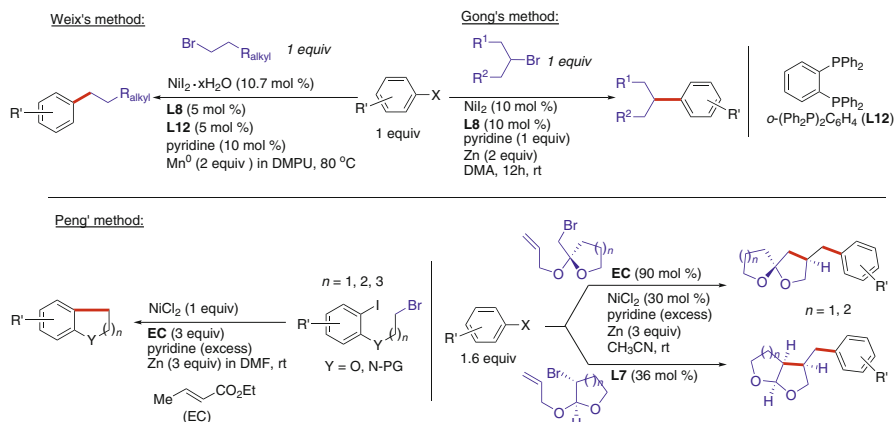


**Scheme 13** In situ Kumada (*left*) and Negishi (*right*) coupling of alkyl with aryl halides (TMEDA = *N,N',N'',N''*-tetramethylethane-1,2-diamine)

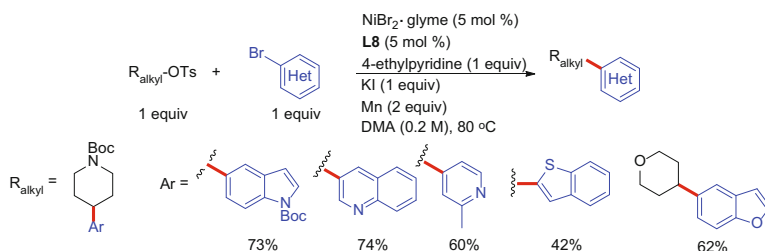
and zinc reagents than aryl ones when exposure to Mg or Zn. Unlike these in situ nucleophile/electrophile coupling processes, the recent Ni-catalyzed reductive arylation of alkyl electrophiles possesses distinctive mechanisms, which has sparked important novel dual catalytic arylation/vinylation modes.

*1 Ni-catalyzed arylation of primary and secondary alkyl halides* Weix first reported a Ni-catalyzed reductive coupling of alkyl and aryl halides in the presence of 10 mol% pyridine using Mn as the reductant, wherein in situ generation of organometallic reagents is not involved (Scheme 14, left) [43]. A wide range of alkyl and aryl halides are suitable under mild reaction conditions. A notable feature of this work is the remarkable chemoselectivity, wherein equimolar alkyl and aryl halides are used. The method is highly effective for primary alkyl halides. Only moderate-to-good yields were obtained for secondary halides. The initial use of phosphine ligand **L12** can be avoided under modified Ni/Mn conditions [44]. Concurrently, similar results using cobalt/phosphine catalytic systems were disclosed by Gosmini, which appears to limit to electron-deficient aryl bromides [45]. Improvement by Gong was later achieved using 1 equiv of pyridine as the additive and Zn as the reductant, which is significantly efficient for secondary alkyl halides, but not for primary ones (Scheme 14, right) [46]. Moreover, Peng has utilized acrylates as additives for intramolecular cyclization of primary alkyl-aryl halides [47, 48]. Liu and coauthors extended the Ni-catalyzed reductive coupling strategy to arylation of chiral iodoalanine with aryl halides, which provides convenient modification of amino acids [49].

Very recently, Molander demonstrated that alkyl tosylates could be incorporated into reductive arylation upon heating (Scheme 15) [50]. A set of heteroaryl bromides give the products in good yields. In addition, Zhang reported a Ni-



**Scheme 14** Ni-catalyzed reductive arylation of alkyl halides [DMPU = 1,3-dimethyl-3,4,4,5,6-tetrahydro-2(1H)-pyrimidinone]

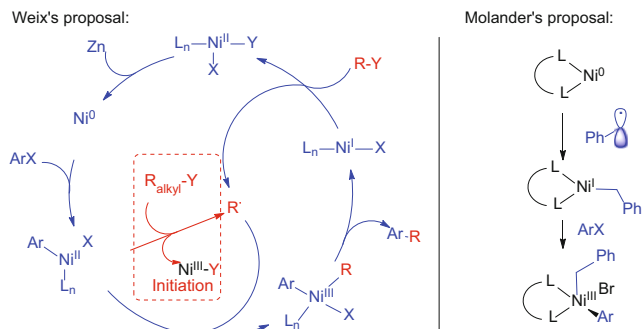


**Scheme 15** Ni-catalyzed reductive arylation of alkyl tosylates

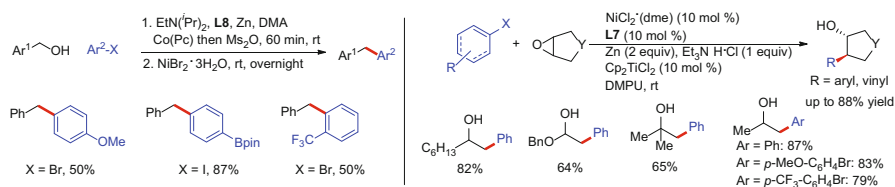
catalyzed reductive coupling protocol for arylation of fluorinated secondary alkyl bromides [51]. Addition of  $FeBr_2$  suppresses the hydrodebromination and  $\beta$ -fluorine elimination of fluorinated substrates.

**2. Possible mechanism** The origin of chemoselectivity is believed to stem from selective oxidative addition of aryl halides to low valent Ni (e.g.,  $Ni^0$ ) rather than from unactivated alkyl halides, which results in  $Ar-Ni^{II}$  intermediate. A radical chain process is proposed for the formation of the  $Ni^{III}$  species through addition of alkyl radical to  $Ar-Ni^{II}$  complex (Scheme 16, left) [16]. Alkyl radical can be generated via halide abstraction from the alkyl halides by  $Ni^I$ , which results from the reductive elimination of the  $Ar-Ni^{III}$ -alkyl intermediate. Meanwhile, the stoichiometric reaction of  $Ar-Ni^{II}L_n-X$  with alkyl halides delivers the coupling product in good yield, suggesting that radicals can be initiated by the  $Ar-Ni^{II}$  species.

On the other hand, Molander illustrates that under Ru-catalyzed photoredox/Ni-catalyzed conditions, the addition of benzyl radicals to  $Ni^0$  is likely favored according to the DFT studies [52]. The resultant  $Bn-Ni^I$  can further react with aryl halides to give  $Ar-Ni^{III}-Bn$  (Scheme 16, right). It should be noted that Peng



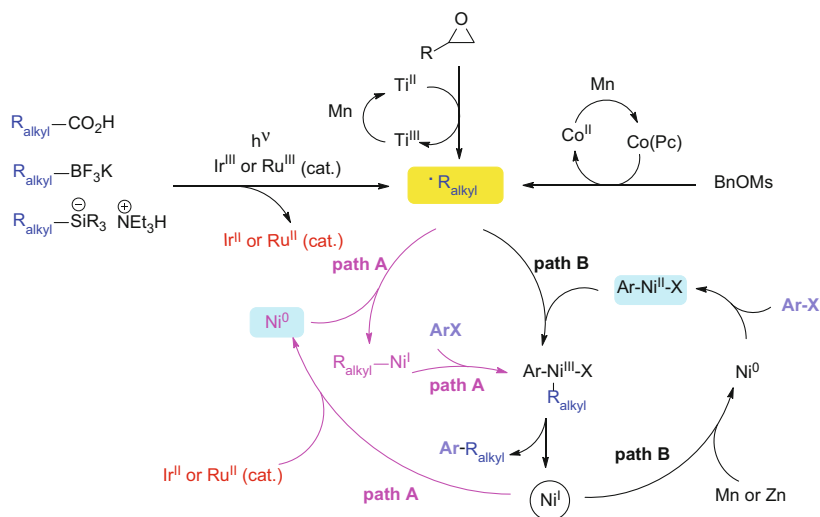
**Scheme 16** Mechanistic proposals for Ni-catalyzed reductive arylation of alkyl halides (*left*) and photo redox/Ni dual catalytic reactions (*right*)



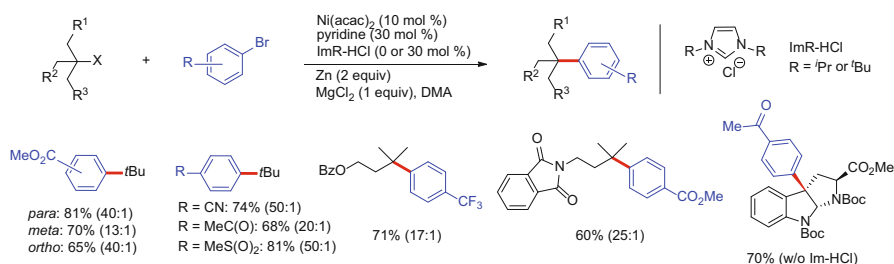
**Scheme 17** Dual catalytic conditions involving Ni-catalyzed reductive arylation of benzyl tosylates and epoxides [Pc = phthalocyanine, DMPU = 1,3-Dimethyl-3,4,5,6-tetrahydro-2(1H)-pyrimidinone]

proposed a mechanism involving oxidative addition of aryl iodides to unactivated alkyl-Ni<sup>I</sup> intermediate in their intramolecular cyclization work [48]. Whether this catalytic scenario is applicable to unactivated alkyl halides is not clear at this time. However, the small energy difference between Weix and Molander's proposals indicates that at least for benzyl type radicals, the addition of radicals to Ni<sup>0</sup> as opposed to Ni<sup>II</sup> is feasible, wherein oxidative addition of aryl halides to Ni<sup>0</sup> appears to be less facile.

**3. Development of dual-catalytic reactions** Based on the radical-chain mechanism, if radicals and organo-Ni species can be independently generated through dual catalysis, then development of new reaction modes is possible. Weix has disclosed a cobalt phthalocyanine (Co(Pc))/Ni co-catalytic system for the coupling of benzylic mesylates with aryl halides [53]. The cobalt catalyst is responsible for benzyl radical formation, which adds to Ar-Ni<sup>II</sup> to give Ar-Ni<sup>III</sup>-Bn. Reductive elimination gives the products and Ni<sup>I</sup>, which can be reduced by Zn to Ni<sup>0</sup>, and regenerate Ar-Ni<sup>II</sup> upon oxidative addition by ArX (Scheme 17, left). The same group also discovered a Ti and Ni co-catalyzed epoxide ring-opening/arylation process (Scheme 17, right) [54]. The epoxides can be utilized for generation of 2-hydroxyl alkyl radical in the presence of catalytic Ti<sup>III</sup>. The addition of alkyl radicals to Ar-Ni<sup>II</sup> proceeds in a similar manner to the radical-chain process, which delivers the product upon reductive elimination, except that the resultant Ti<sup>IV</sup> and



**Scheme 18** Possible radical-chain mechanisms for photo-redox/Ni (path A) and Ni/metal (path B) dual catalytic conditions



**Scheme 19** Ni-catalyzed arylation of tertiary alkyl halides

$\text{Ni}^{\text{I}}$  intermediates are individually reduced by Mn to  $\text{Ti}^{\text{III}}$  and  $\text{Ni}^{\text{0}}$  to allow the catalytic cycle to proceed (Scheme 17).

The recent development in Ir- or Ru-catalyzed photo-redox/Ni-catalyzed arylation of alkyl acids, borons, and silicates has led to successful arylation of a myriad of alkyl groups [18, 19, 55, 56]. A general catalytic scheme can be depicted using a radical chain process (Scheme 18), wherein the  $\text{Ir}^{\text{II}}$  or  $\text{Ru}^{\text{II}}$  serves as the reductants to reduce  $\text{Ni}^{\text{I}}$  to  $\text{Ni}^{\text{0}}$ .

**4. Reductive coupling with tertiary alkyl halides** For the coupling of sterically more demanding tertiary alkyl halides, the conditions used for both primary and secondary ones are not valid. When pyridine constitutes the sole additive or labile ligand combining with catalytic  $\text{Ni}(\text{acac})_2$ ,  $\text{MgCl}_2$ , and Zn in DMA, the reductive conditions enable effective construction of all carbon quaternary centers (Scheme 19) [57]. For  $t\text{Bu}-\text{Br}$ , the limiting reagents were set as aryl bromides. For the more hindered tertiary alkyl halides, two equivalents of aryl bromides

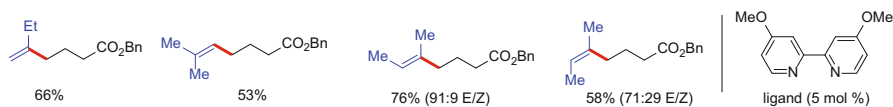
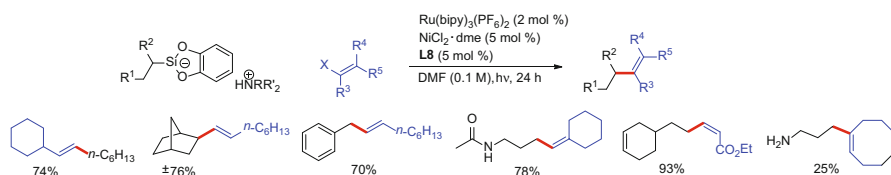


**Fig. 1** Examples from Weix's vinylation of alkyl halides using the arylation conditions



**Scheme 20** Molander's vinylation of alkyl silicates under photoredox dual catalytic conditions

necessitate the coupling process. Isomerization of the tertiary alkyl groups accounts for the major side reaction in the coupling event (ratio of quaternary to isomerization product shown in the parenthesis in [Scheme 19](#)). The addition of imidazolium salts promotes the reaction yields and inhibits the isomerization to minor degrees. The crucial requirement of pyridine as the labile ligand may be attributed to steric bulkiness of the tertiary alkyl groups, which balances the steric demand for Ni intermediates.

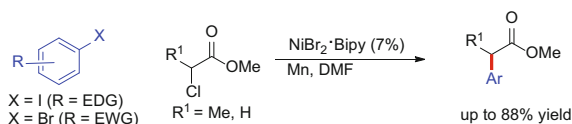
### 2.2.2 Vinylation of Unactivated Alkyl Halides

Weix's reductive arylation protocol also works moderately well for vinylation of primary alkyl halides, whereas secondary alkyl halides were not discussed ([Fig. 1](#)) [44]. Molander and McMillan independently discovered that the Ru and Ni co-catalyzed photoredox arylation conditions could be extended to efficient vinylation of alkyl silicates or alkyl acids [58, 59]. The reactions display excellent functional group tolerance. A broad range of  $\beta$ -vinyl halides bearing hydroxyl and amide is competent, so are a set of primary and secondary alkyl halides including *n*-hexyl and benzylic groups ([Scheme 20](#)).

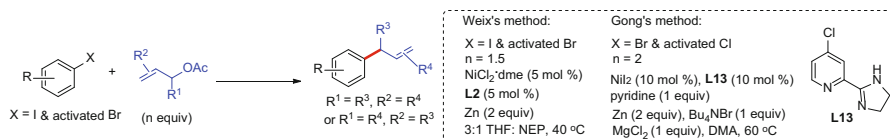
### 2.2.3 Coupling of Activated Alkyl Electrophiles

The selectivity arising from the coupling between  $C(sp^2)$ -electrophiles and the activated  $C(sp^3)$ -halides is nontrivial, since their preference in the oxidative addition to low valent Ni may become less distinctive. As discussed in Sect. 2.2.1, the photoredox/Ni-catalyzed arylation of benzyl chlorides may favor the formation of  $Bn-Ni^I$  by addition of benzyl radical to  $Ni^0$ . Therein, oxidative addition of  $ArX$  to  $Bn-Ni^I$  results in the key  $Ar-Ni^{III}(X)-Bn$  intermediate [52].

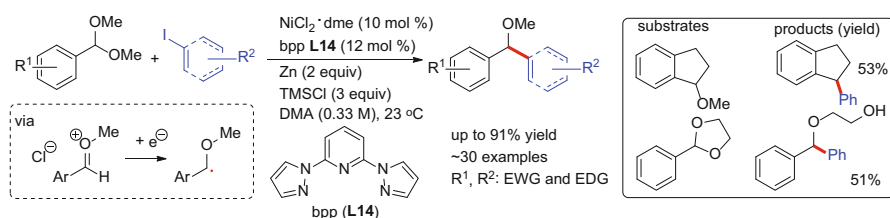
While electrochemical arylation and vinylation of  $\alpha$ -chloroketones and esters, as well as allyl acetates are well established [35], the equivalent chemical reduction methods have been documented for arylation of  $\alpha$ -chloroesters ([Scheme 21](#)) [60] and allylic acetates [37, 61]. The allylation of aryl halides is generally efficient for



**Scheme 21** Ni-catalyzed reductive arylation of  $\alpha$ -haloesters using Mn as the reductant (Bipy = **L7**, Scheme 1)



**Scheme 22** Ni-catalyzed reductive arylation of allylic acetates with aryl halides (<sup>t</sup>Bu-Terpy = **L2**, Scheme 1)

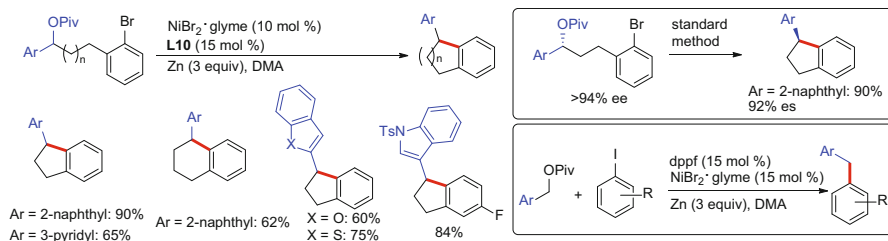


**Scheme 23** Ni-catalyzed reductive arylation of benzylic acetals with aryl iodides (dme = 1,2-dimethoxyethane)

both electron-deficient and -rich arenes, which display excellent regioselectivities by the addition of aryl groups to the less-hindered allylic terminals (Scheme 22) [37, 61]. The asymmetric vinylation and arylation of benzylic chlorides and  $\alpha$ -chloronitriles are detailed in Sect. 2.5.

Recently, Doyle disclosed that benzylic acetals could couple with aryl iodides under Ni-catalyzed reductive conditions, which produced dialyated ethers by replacement of one methoxy group with aryl (Scheme 23) [62]. The reaction mechanism was proposed involving the addition of benzyl radicals to ArNi<sup>II</sup>-X intermediate, analogous to Scheme 16. The generation of oxonium ion promoted by Lewis acid may account for the key precursor for reductive formation of the benzyl radical species (dash box, Scheme 23).

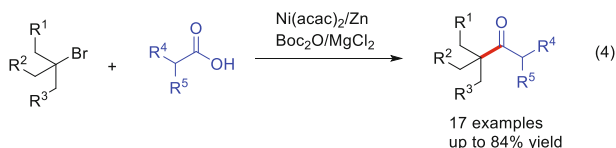
Activation of benzylic C–O bonds under Ni-catalyzed reductive conditions can be further manipulated for inter- and intramolecular coupling of benzyl pivalic acid esters with aryl halides, as demonstrated by Jarvo (Scheme 24) [63]. The employment of bathophenanthroline **L10** (Scheme 1) for cyclization and dppe for intermolecular process indicates that two sophisticated Ni catalytic processes are operative. Of note is the stereospecific feature for the cyclization of a chiral ester, which undergoes inversion of the benzyl centers.



**Scheme 24** Ni-catalyzed reductive arylation of benzylic esters with aryl halides [dppf = 1,1'-ferrocenediyl-bis(diphenylphosphine)]

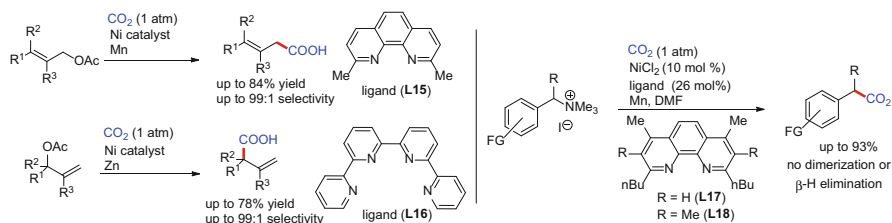
### 2.3 Ketone Synthesis

A summary of Ni-catalyzed reductive ketone formation has been detailed in recent reviews [1, 5]. The coupling protocols are suited for primary and secondary alkyl halides with acid derivatives, including acid chlorides, anhydrides, and in situ activated acids in the presence of Boc<sub>2</sub>O and MgCl<sub>2</sub> [63–68]. Although initial development was centered on primary and secondary alkyl iodides, finely tuning the reaction parameters satisfied alkyl bromides. It should be noted that *tertiary* alkyl halides are qualified for the coupling with alkyl acids but not with aryl acid derivatives (Eq. 4) [69]. Activated electrophiles competent for acylation comprise 1-bromo-sugar and benzyl chlorides [68, 69]. The reaction mechanism although needs more study; a radical-chain pathway similar to the arylation process in Sect. 2.2.1 appears to be more convincing. Noteworthy is that the photoredox/Ni dual catalysis has also been utilized to ketone synthesis under similar arylation conditions [70–72].

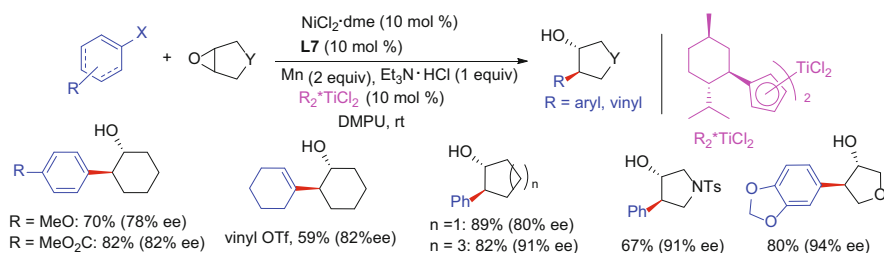


### 2.4 Carboxylation of Alkyl Halides with CO<sub>2</sub>

Significant progress on fixation of CO<sub>2</sub> has recently been achieved using Ni-catalyzed reductive coupling chemistry. A wide set of electrophiles including aryl halides and triflates, benzylic halides and ethers, allylic esters, as well as unactivated primary alkyl iodides are competent [73–77]. The use of CO<sub>2</sub> as the electrophiles expands the feedstock for the reductive coupling protocols. A comprehensive review has detailed this field; thus, only very recent examples are briefly discussed [5]. In particular, the regiodivergent synthesis of terminal and branched allylic acids was accomplished by regulation of ligands (Scheme 25, left) [76]. The use of benzylic ammonium iodide on the other hand provided the benzylic acids in high



**Scheme 25** Ni-catalyzed reductive formation of acids via coupling of allylic acetates (*left*) and benzyl ammonium salts (*right*) with CO<sub>2</sub>



**Scheme 26** Ni-/Ti-co-catalyzed asymmetric arylation of *meso*-epoxides

yields, in which a variety of alkyl-substituted benzyl groups were competent with no dimerization or  $\beta$ -H elimination side reactions that often occur in the reductive coupling of benzyl halides (Scheme 25, right) [77].

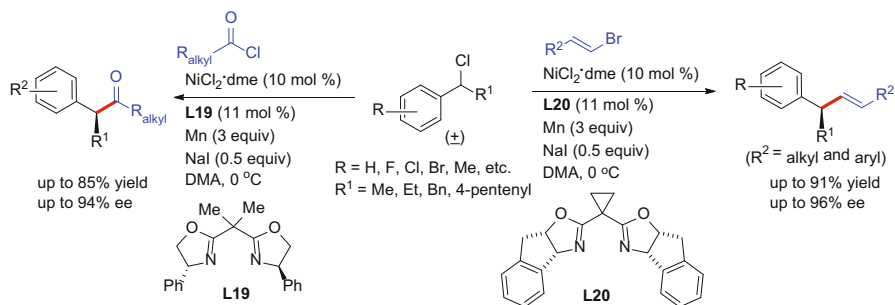
## 2.5 Enantioselective C(sp<sup>3</sup>)-C(sp<sup>2</sup>) Bond Formation

Control of enantioselectivity in reductive coupling chemistry is exceedingly sophisticated due to the radical nature of alkyl groups. Judicious use of a chiral Ti<sup>III</sup> catalyst in Weix's epoxide ring-opening/arylation method affords asymmetric arylation products in high ees under the Ni/Ti-co-catalyzed conditions (Scheme 26) [78]. The reactions tolerate a wide range of functional groups. The enantioselectivity arises from the formation of chiral Ti-O complexes that serve as the auxiliary in control of diastereoselectivity as well.

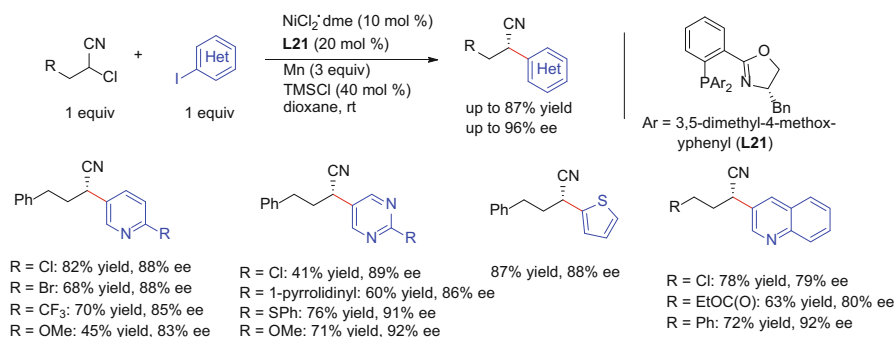
Reisman first discovered that under Ni-catalyzed reductive conditions, acylation of racemic benzylic chlorides with acid chlorides generated the ketones in high ees using a chiral box ligand (Scheme 27) [79]. With the Ni-catalyzed reductive coupling strategy, the same group also developed asymmetric vinylation of benzylic chlorides with vinyl bromides (Scheme 27). A box ligand was again found to be optimal [80]. The stable benzyl radicals may be key for the origin of high enantioselectivity, as unactivated alkyl halides appear to be incompetent in generation of enantioenriched products under a variety of Ni-catalyzed asymmetric reductive coupling conditions [21].

Likewise, Weix and Molander investigated the asymmetric arylation of benzylic chlorides using a chiral box ligand [52, 53]. A highest 65 % ee was disclosed, requiring further endeavors for this type of reaction [52].





**Scheme 27** Ni-catalyzed asymmetric acylation and vinylation of racemic benzyl chlorides



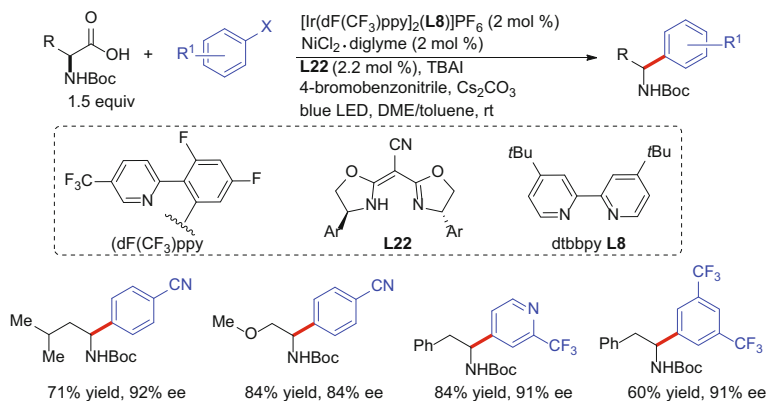
**Scheme 28** Ni-catalyzed asymmetric arylation of racemic  $\alpha$ -chloronitriles with heteroaryl iodides

The observation that activated alkyl halides are critical for high enantioselectivities is further evidenced in Reisman's recent success in the Ni-catalyzed asymmetric arylation of  $\alpha$ -chloronitriles (**Scheme 28**) [81]. A myriad of heteroaryl iodides are incorporated into the formation of  $\alpha$ -aryl nitriles in good yields and good-to-excellent ees. Understanding the insight into the origin of enantioselectivities will require significant investigation of the reaction mechanisms.

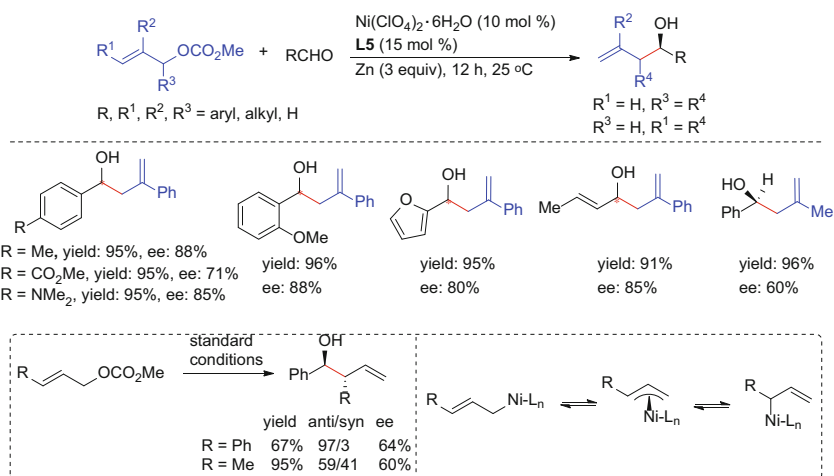
The asymmetric decarboxylative arylation of  $\alpha$ -amino acids under photoredox and nickel dual catalytic conditions has recently been developed by Macmillan and Fu (**Scheme 29**). A variety of naturally occurring amino acids can be readily transferred to chiral amines when coupling with aryl halides. The electron-deficient arenes appear to be more effective for high ees. The coupling with iodobenzene only produced 66 % ee and 64 % yield [82]. A mechanism illustrated in **Scheme 18** may operate.

## 2.6 Addition of Allyl and Benzyl Groups to Carbonyl Compounds

Gong reported the first asymmetric Ni-catalyzed reductive coupling of allylic carbonates with aldehydes utilizing zinc powder as the terminal reductant (**Scheme 30**) [83]. This method differs from the previous umpolung allylation methods, which exploit allylic halides or expensive transition metals. The homoallylic alcohols are generated in good-to-excellent yields and ees. The



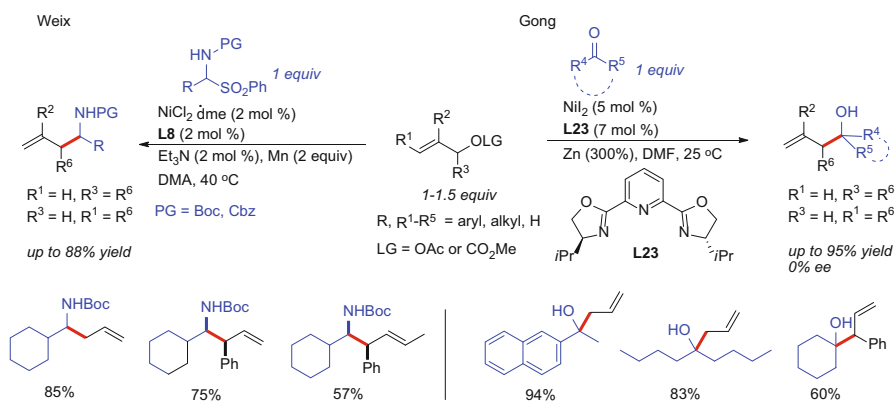
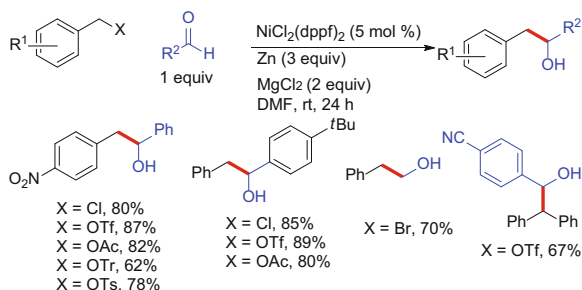
**Scheme 29** A photoredox and nickel dual catalytic protocol for decarboxylative arylation of  $\alpha$ -amino acids [diglyme = 1-methoxy-2-(2-methoxyethoxy)ethane]



**Scheme 30** Asymmetric allylic carbonylation under Ni/Pybox/Zn conditions

substitution patterns for both electron-withdrawing and -donating groups on the aryl aldehydes do not cause notable variations on the yields and enantioselectivities when coupling with 2-phenyl allyl carbonate. Furan-2-carbaldehyde and (*E*)-but-2-enal are competent. Substantial decrease of ee (60 %) was detected for 2-methyl allylic carbonate. A stoichiometric reaction of allyl carbonate, benzaldehyde and Ni<sup>0</sup>-L<sub>n</sub> in the absence of Zn was able to produce the product in a similar yield and ee to the catalytic conditions, suggesting allyl-Ni may be the key intermediate for the allylation event. This is distinctive from the Nozaki–Hiyama–Kishi reactions [84]. In addition, the 1- or 3-phenyl-substituted allyl carbonate gave the product in moderate yield and ee at −25 °C but with high anti/syn selectivities. The methyl-

**Scheme 31** Ni-catalyzed reductive benzylation of aldehydes [dppf = 1,1'-ferrocenediyl-bis(diphenylphosphine)]



**Scheme 32** Ni-catalyzed reductive allylation of in situ imines and ketones

substituted analogs, however, deliver poor anti/syn selectivities, which is possibly due to the rapid conversion of  $\eta$ -allyl-Ni from terminal to branched structures.

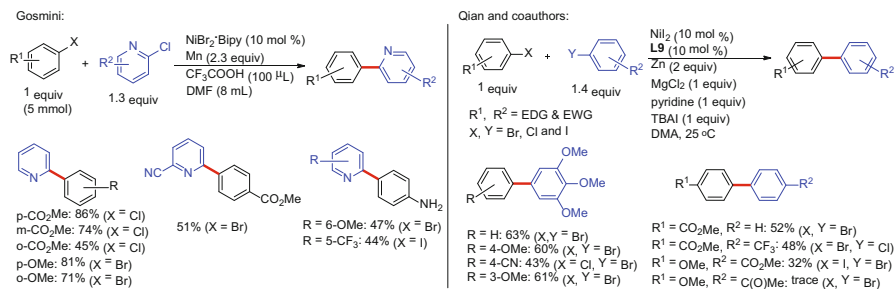
More recently, Iranpoor demonstrated that addition of benzyl halides and pseudo halides (OR) was viable using the Ni/dppf/Zn conditions, which generated alcohols in good-to-excellent yields. The excellent functional group tolerance is evidenced, wherein even nitro is compatible (Scheme 31) [85].

Extension of the same strategy to ketones and in situ generated imines has been achieved by Gong and Weix, respectively (Scheme 32) [86, 87]. The use of a chiral Pybox ligand and DMF solvent for the synthesis of quaternary homoallylic alcohols is pivotal, although no enantioselectivity was observed [86]. Similar regioselectivities to those in allylation of aldehydes were detected for 1- or 3-substituted allyl carbonates or acetates, wherein addition occurs on the more-hindered carbon centers [86, 87].

## 2.7 Reductive Coupling of Aryl Halides with Other $\text{C}(\text{sp}^2)$ -Electrophiles

### 2.7.1 Formation of Biaryl Compounds

In a 2008 report, Gosmini disclosed a cobalt-catalyzed unsymmetrical biaryl synthesis via direct assembly of two aryl electrophiles, using Mn as the reductant

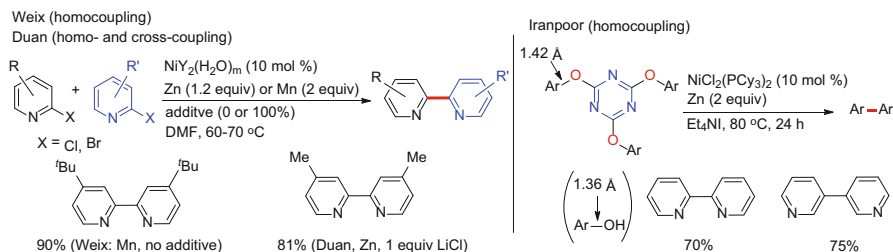


**Scheme 33** Ni-catalyzed reductive cross-coupling of pyridyl halides with aryl halides (left), and cross-coupling of two different aryl halides (Bipy = **L7** and dmbpy = **L9**, Scheme 1)

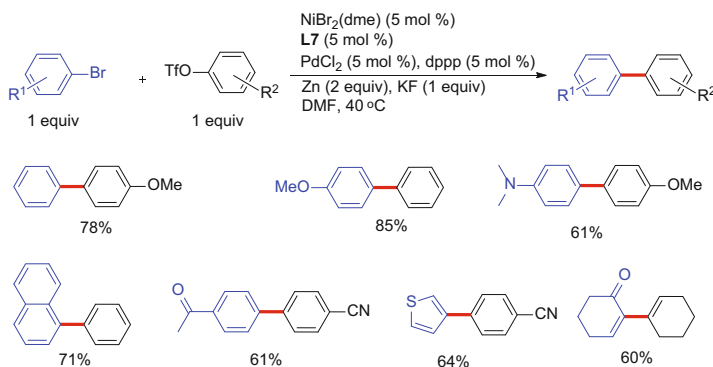
[88]. One of the aryl electrophiles was set as two equivalents in excess. By taking advantage of the reactivity gaps between the two aryl coupling partners, good-to-excellent yields are generally observed. The difference in reactivity can be resulted when the aryl electrophiles display notable differences in electron density and bear different leaving groups. Likewise, the same group has shown that the coupling of 6-halopyridine with a variety of aryl halides can be effectively carried out under Ni-catalyzed reaction conditions (Scheme 33, left) [89]. The initial use of 2-bromopyridine is highly competent for *para*- and *meta*-methoxycarbonyl phenyl bromides. However, a poor result was achieved for the *ortho*-analog. The coupling with 2-chloropyridine derivatives on the other hand allows a broad set of aryl halides to be compatible. Pyridines decorated with strong electron-withdrawing groups such as CN and CF<sub>3</sub>, and an electron-dense group such as MeO are suited, although the yields decrease for substituted pyridines. Qian et al. discovered that direct coupling of two substituted aryl halides can lead to the biaryl products in moderate-to-good yields [90]. When one of the aryl partners bear an electron-withdrawing group, low yield was observed. The chemoselectivity in these methods varies from poor to excellent, largely depending on the electron-density gap between the two aryl coupling partners. Although no details on the mechanism were addressed, a possible oxidative addition of Ar'X to Ar-Ni<sup>I</sup> is plausible according to previous stoichiometric studies [24, 25].

Application of Ni-catalyzed reductive biaryl synthesis to bipyridine derivatives was recently revealed by Weix, Duan, and Iranpoor (Scheme 34) [91–93]. The ligand-free conditions allow the construction of 2,2'-bipyridine in high yields. Duan also demonstrated cross-coupling between two different pyridyl halides by setting one of electrophiles in excess [92]. Iranpoor indicated that 1,3,5-triazine could be utilized for activation of aryl-O bonds [93]. By comparison, the bond length increases with respect to unactivated phenol. Use of Ni/PCy<sub>3</sub> catalyst enabled efficient homocoupling of the aryl moieties [93].

Perhaps the most remarkable breakthrough in achieving excellent chemoselectivities between two aryl electrophiles was found by Weix, which are controlled mainly by the catalysts rather than the substrates [94]. The utilization of both Ni and Pd co-catalysts enabled efficient coupling of equimolar aryl/vinyl bromides with aryl/vinyl triflates to generate unsymmetrical biaryls and dienes (Scheme 35). Although Gosmini has shown

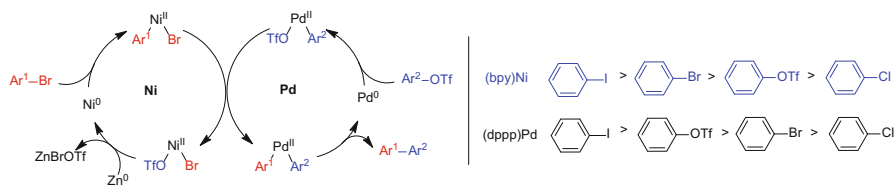


**Scheme 34** Ni-catalyzed reductive coupling of pyridyl halides (Cy<sub>3</sub>P = tricyclohexylphosphine)

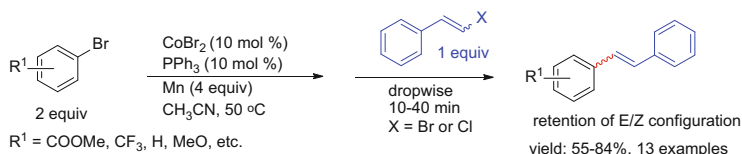


**Scheme 35** Pd/Ni-dual catalytic conditions for the coupling of equimolar aryl halides with triflates

that excellent yields can be obtained for the coupling of 2 equiv of 4-trifluoromethylsulfonyloxybenzoic acid ethyl ester with one equivalent of 4-bromoanisole, the intrinsic chemoselectivity does not seem to be governed by the cobalt/PPh<sub>3</sub> catalyst [88]. The origin of the high chemoselectivity in Weix's system is attributed to preferential reaction of Pd<sup>0</sup> to aryl triflates and Ni<sup>0</sup> to aryl bromides leading to Ar<sup>2</sup>-Pd<sup>II</sup>(dppp)-OTf and Ar<sup>1</sup>-Ni<sup>II</sup>(bpy)-Br, respectively (Scheme 36, left). The Pd<sup>II</sup> species is stable and persistent in solution, whereas the Ni<sup>II</sup> complex is highly reactive with the Pd<sup>II</sup> intermediate and itself. Subsequent transmetalation between the Ni<sup>II</sup> (low concentration) and Pd<sup>II</sup> (high concentration) intermediates affords Ar<sup>2</sup>-Pd<sup>II</sup>-Ar<sup>1</sup> and Br-Ni<sup>II</sup>-OTf species. This process is analogous to the persistent radical effect, where one radical is stable while the other is highly reactive and unselective. The following reductive elimination on the Pd center gives the products and regenerates Pd<sup>0</sup>, while Ni<sup>0</sup> can be produced by reduction of the Ni<sup>II</sup> salt with Zn. The use of KF as the additive is believed to suppress dimerization of aryl bromides. A comparison of the oxidative addition rates of aryl halides and triflates toward (bpy)Ni<sup>0</sup> and (dppp)Pd<sup>0</sup> is also outlined (Scheme 36, right) with iodides and chlorides being the most and least reactive in both cases. While bromobenzene is more vulnerable to (bpy)Ni than phenyltriflate, an inverted trend is found for (dppp)Pd [dppp = 1,3-bis(diphenylphosphanyl)propane].



**Scheme 36** Proposed mechanism for Pd/Ni-dual catalytic conditions (*left*), and reactivity of aryl electrophiles toward Ni and Pd catalysts



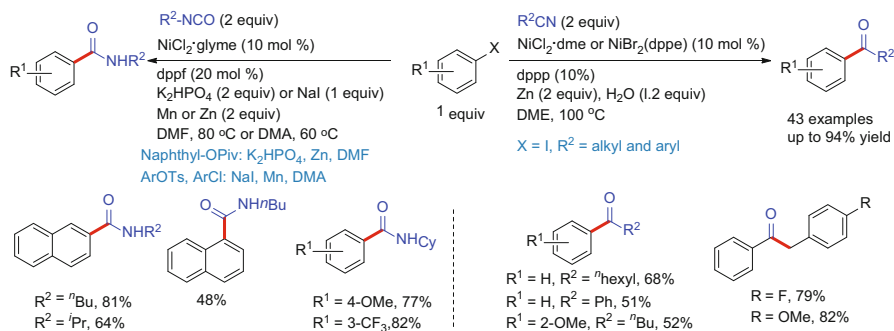
**Scheme 37** A two-step protocol for cobalt-catalyzed reductive vinylation of aryl halides

Although Ni-catalyzed reductive coupling of aryl with vinyl electrophiles has not been documented, the reactions under cobalt/PPh<sub>3</sub> catalytic conditions are known [95]. A variety of substituted aryl bromides can be effectively vinylated with undecorated β-bromo- or chlorostyrene using a two-step protocol (Scheme 37). Dropwise addition of bromostyrene to the pre-formed aryl-Co<sup>I</sup> intermediate appears to be key to avoiding severe homocoupling of the more reactive vinyl electrophile. Suitable selection of the halide source is pivotal for matching the reactivity of the two coupling partners. For instance, aryl iodides are generally less efficient due to rapid homocoupling.

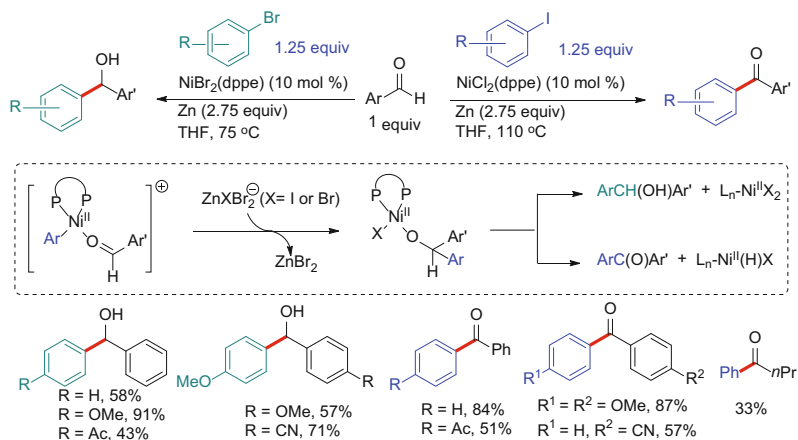
### 2.7.2 Coupling of Aryl Electrophiles with Carbonyl Compounds

Since a comprehensive review on the reactions of electrophiles with carbonyl compounds has been detailed in 2014 [5], this section only highlights the important features on Ni-catalyzed reductive coupling methods. Accordingly, the recent elegant development on CO<sub>2</sub> fixation with C(sp<sup>2</sup>)-electrophiles [e.g., C(sp<sup>2</sup>)-O and benzyl C(sp<sup>3</sup>)-O bond activation] and alkynes is not discussed [96, 97].

In 2014, Correa and Martin developed an efficient Ni-catalyzed reductive coupling method to amides by exposure of aryl electrophiles to isocyanates (Scheme 38) [98]. The competence of C(sp<sup>2</sup>)-O and C(sp<sup>3</sup>)-O electrophiles for amide synthesis significantly expands the source of electrophiles other than halides, since naphthyl and naphthalen-2-ylmethyl pivalates as well as aryl tosylates are suitable. Likewise, Cheng has shown that aryl iodides can be used for amide or imine synthesis under similar Ni/Zn reductive coupling conditions (Scheme 38) [99]. The same protocol is applicable to the reductive coupling of nitriles with aryl iodides affording ketones [100]. Both Martin and Cheng tentatively suggest Ni<sup>0</sup>/Ni<sup>II</sup> catalytic processes wherein the key step comprises addition of Ar to isocyanates or nitriles from a Ar-Ni<sup>II</sup> intermediate.



**Scheme 38** Ni-catalyzed reductive coupling of aryl halides with isocyanides and nitriles



**Scheme 39** Ni-catalyzed reductive coupling of aryl halides with aldehydes affording alcohols (*left*) and ketones (*right*)

Cheng has also investigated direct coupling of aryl halides with aldehydes under Ni/dppe reductive conditions [101, 102]. By careful selection of temperatures and halide source, the same reactions can lead to either ketones or Barbier-type alcohols using aryl bromides and iodides, respectively (**Scheme 39**) [101, 102]. The proposed reaction mechanism suggests that both reactions may involve  $L_n-Ni^{II}-Ar(Ar'CHO)$  complexes, wherein the coordination of carbonyl to Ni center is favored due to formation of a cationic  $Ni^{II}$  intermediate. Trapping the halide anion from  $Ar-Ni^{II}X$  with in situ formed  $ZnX_2$  salt is key for the formation of the cationic species. Subsequent addition of Ar to carbonyl results in a  $Ni^{II}$  alkoxide that undergoes hydrolysis to alcohol [101] or  $\beta$ -elimination to ketones, [102] relying on the temperatures. Excellent functional group tolerance is evidenced in both conditions (**Scheme 39**). The Ni-catalyzed reductive protocol can be extended to the formation of quaternary alcohols via intramolecular addition of vinyl and aryl chlorides to ketones, as demonstrated by Jia and Gao [103]. The use of bulky and electron-dense  $Cy_3P$  as the ligand is critical for activation of aryl chlorides.



**Scheme 40** Ni-catalyzed reductive coupling of unactivated alkenes with unactivated alkyl halides or aryl iodides

### 2.7.3 Coupling of Aryl Electrophiles with Michael Acceptors

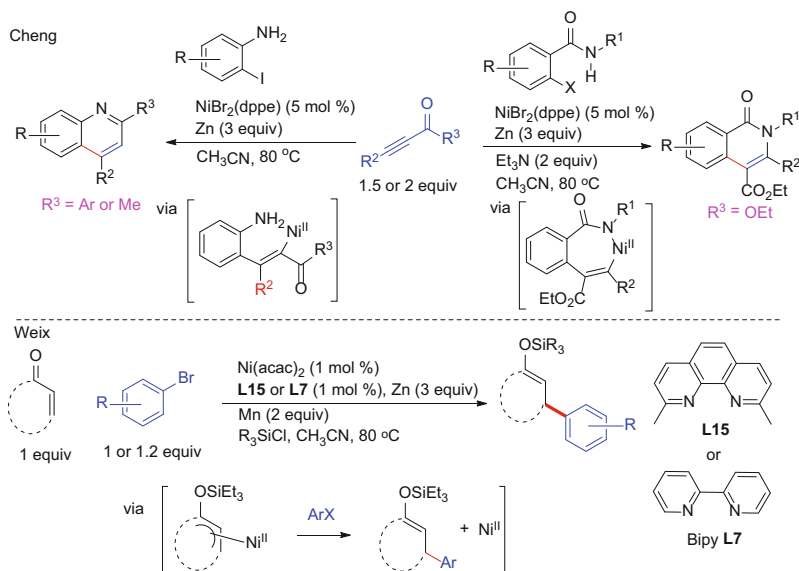
Trapping of alkyl halides with activated double bonds under Ni-catalyzed reductive conditions has been extensively summarized in an early review, which can lead to radical addition or Heck-type products [104]. Interestingly, a very recent work disclosed by Liu indicates that Ni catalyst enables the cross-coupling between unactivated olefins with unactivated alkyl or aryl halides in the presence of diethoxymethylsilane as the reductant [105]. Rather than generation of Heck products, direct hydroalkylation of unactivated olefins with a combination of 10 mol% of  $\text{NiBr}_2(\text{diglyme})$ , 15 mol% of dtbbpy (**L8**, Scheme 1), two equivalents of diethoxymethylsilane and  $\text{Na}_2\text{CO}_3$  in *N,N*-dimethyl acetamide (DMA) necessitates the addition of alkyl group to the terminal carbon of the alkenes (Scheme 40). The alkyl group is believed to proceed through a radical process.

On the other hand, the addition of aryl and vinyl halides with acrylates and styrenes in the presence of  $(\text{PPh}_3)_2\text{NiCl}_2$  (cat.)/Zn/pyridine effectively generates Heck-type products [106]. In 2010, Cheng expanded this strategy to the reductive condensation of aryl halides with conjugated alkynes in the presence of an ortho-amine or amide group (Scheme 41, top) [107, 108]. The enone intermediates can be trapped with amine or amide to give quinolone or isoquinolone derivatives. With a similar protocol, Weix disclosed that conjugate addition of aryl bromides to enones can lead to 1,4-addition product, and the resultant enolate can be trapped with trialkylchlorosilane reagent (Scheme 41, bottom) [109]. The reactions display excellent functional group tolerance. The authors also proposed a mechanism that differs from the conventional Heck-type mechanism involving insertion of  $\text{Ar-Ni}^{\text{II}}$  to alkenes. Instead, formation of allyl-Ni species followed by reaction with aryl halides was believed to be the key. The chemoselectivity between the two electrophiles arises from rapid reaction of Ni(0) with enone/trialkylchlorosilane, and steric effect of ligands that suppresses the dimerization of enones.

## 3 Conclusions

In summary, direct coupling of alkyl electrophiles with different electrophiles under reductive conditions has emerged as one of the very appealing research fields. The mild and easy-to-operate methods allow ready access to  $\text{C}(\text{sp}^3)\text{-C}(\text{sp}^3)$  and  $\text{C}(\text{sp}^3)\text{-}$





**Scheme 41** Reductive coupling of aryl halides with conjugated alkenes and alkynes

$\text{C}(\text{sp}^2)$  bonds without prepreparation of organometallic nucleophiles. The use of earth-abundant inexpensive transition metals such as Ni, Fe, Cu, and Co enables practical applications of these approaches in the construction of complex structures. The extensive studies on Ni-catalyzed reductive coupling methods in particular lead to successful control of the chemoselectivities between different electrophiles and manipulation of enantioselectivities for the activated alkyl halides. The reactivity of the electrophiles can be tuned by the catalysts. Understanding of the radical-chain mechanisms in the Ni-catalyzed  $\text{C}(\text{sp}^3)\text{--C}(\text{sp}^2)$  bond forming processes has inspired significant development of dual catalytic systems, which further diversifies the reaction types. The employment of other electrophiles such as  $\text{CO}_2$  has also broadened the scope of electrophiles and has led to useful protocols to acids. Finally, the more challenging tertiary alkyl halides have also proven to be competent for the reductive coupling strategies.

Likewise, the Ni-catalyzed reductive cross-coupling of two different  $\text{C}(\text{sp}^2)\text{--}$  electrophiles has achieved tremendous success, which provides ready access to aryl amides, ketones, and alcohols. The recent unsymmetrical biaryl synthesis using Pd/Ni dual catalytic conditions, in particular, opens the possibility for finely tuning the chemoselectivity between two aryl electrophiles.

Future work in this field may foresee incorporation of novel electrophiles and different transition metals that may result in new transformations and broaden the substrate scope for a wide range of electrophiles. More detailed mechanistic studies for the Ni-catalyzed reactions should be performed, which not only provide insight into the reaction process but may also inspire design of new reactions. Enrichment of the types of asymmetric coupling reactions, particularly the unactivated alkyl

substrates, is challenging, but important. Not only does this help in understanding the reaction mechanisms, but may also further enhance the practicality of the reductive coupling methods to the construction of complex molecules.

**Acknowledgments** Financial support was provided by the Chinese NSF (Nos. 21172140, 21372151, and 21572127), Shanghai Municipal Education Commission for the Programs for Professor of Special Appointment (Dongfang Scholarship), Shanghai Peak Discipline Construction (N.13-A302-15-L02), and Shanghai Science and Technology Commission (14DZ2261100).


## References

1. Gu J, Wang X, Xue W, Gong H (2015) *Org Chem Front* 2:1411
2. Everson DA, Weix DJ (2014) *J Org Chem* 79:4793
3. Knappe CE, Grupe S, Gärtner D, Corpet M, Gosmini C, von Jacobi Wangelin A (2014) *Chem Eur J* 20:6828
4. Weix DJ (2015) *Acc Chem Res* 48:1767
5. Moragas T, Correa A, Martin R (2014) *Chem Eur J* 20:8242
6. Nédélec J-Y, Périchon J, Troupel M (1997) *Top Curr Chem* 185:141
7. Jana R, Pathak TP, Sigman MS (2011) *Chem Rev* 111:1417
8. Thaler T, Haag B, Gavryushin A, Schober K, Hartmann E, Gschwind RM, Zipse H, Mayer P, Knochel P (2010) *Nat Chem* 2:125
9. Fu GC (2008) *Acc Chem Res* 41:1555
10. Netherton MR, Fu GC (2004) *Adv Synth Catal* 346:1525
11. Rudolph A, Lautens M (2009) *Angew Chem Int Ed* 48:2656
12. Frisch AC, Beller M (2005) *Angew Chem Int Ed* 44:674
13. Hu X (2011) *Chem Sci* 2:1867
14. Li Z, Liu L (2015) *Chin J Catal* 36:3
15. Tasker SZ, Standley EA, Jamison TF (2014) *Nature* 509:299
16. Biswas S, Weix DJ (2013) *J Am Chem Soc* 135:16192
17. Breitenfeld J, Ruiz J, Wodrich MD, Hu X (2013) *J Am Chem Soc* 135:12004
18. Tellis JC, Primer DN, Molander GA (2014) *Science* 345:433
19. Zuo Z, Ahneman DT, Chu L, Terrett JA, Doyle AG, MacMillan DW (2014) *Science* 345:437
20. Schley ND, Fu GC (2014) *J Am Chem Soc* 136:16588
21. Yu X, Yang T, Wang S, Xu H, Gong H (2011) *Org Lett* 13:2138
22. Xu H, Zhao C, Qian Q, Deng W, Gong H (2013) *Chem Sci* 4:4022
23. Jones GD, Martin JL, McFarland C, Allen OR, Hall RE, Haley AD, Brandon RJ, Konovalova T, Desrochers PJ, Pulay P, Vivic DA (2006) *J Am Chem Soc* 128:13175
24. Tsou TT, Kochi JK (1979) *J Am Chem Soc* 101:7547
25. Colon I, Kelsey DR (1986) *J Org Chem* 51:2627
26. Prinsell MR, Everson DA, Weix DJ (2010) *Chem Commun* 46:5743
27. Goldup SM, Leigh DA, McBurney RT, McGonigal PR, Plant A (2010) *Chem Sci* 1:383
28. Peng Y, Luo L, Yan C-S, Zhang J-J, Wang Y-W (2013) *J Org Chem* 78:10960
29. Wada M, Murata T, Oikawa H, Oguri H (2014) *Org Biomol Chem* 12:298
30. Zhang C-P, Wang H, Klein A, Biewer C, Stirnat K, Yamaguchi Y, Xu L, Gomez-Benitez V, Vivic DA (2013) *J Am Chem Soc* 135:8141
31. Yu S, Dudkina Y, Wang H, Kholin K, Kadirov M, Budnikova Y, Vivic D (2015) *Dalton Trans* 44:19443
32. Liang Z, Xue W, Lin K, Gong H (2014) *Org Lett* 16:5620
33. Unpublished results from the author's lab
34. Liu JH, Yang CT, Lu XY, Zhang ZQ, Xu L, Cui M, Lu X, Xiao B, Fu Y, Liu L (2014) *Chem Eur J* 20:15334
35. Durandetti M, Perichon J (2004) *Synthesis* 3079
36. Dai Y, Wu F, Zang Z, You H, Gong H (2012) *Chem Eur J* 18:808
37. Anka-Lufford LL, Prinsell MR, Weix DJ (2012) *J Org Chem* 77:9989
38. Qian X, Auffrant A, Felouat A, Gosmini C (2011) *Angew Chem Int Ed* 50:10402

39. Xue W, Xu H, Liang Z, Qian Q, Gong H (2014) *Org Lett* 16:4984
40. Tollefson EJ, Erickson LW, Jarvo ER (2015) *J Am Chem Soc* 137:9760–9763
41. Krasovskiy A, Duplais C, Lipshutz BH (2009) *J Am Chem Soc* 131:15592
42. Czaplik WM, Mayer M, von Jacobi Wangelin A (2009) *Angew Chem Int Ed* 48:607
43. Everson DA, Shrestha R, Weix DJ (2010) *J Am Chem Soc* 132:920
44. Everson DA, Jones BA, Weix DJ (2012) *J Am Chem Soc* 134:6146
45. Amatore M, Gosmini C (2010) *Chem Eur J* 16:5848
46. Wang S, Qian Q, Gong H (2012) *Org Lett* 14:3352
47. Yan CS, Peng Y, Xu XB, Wang YW (2012) *Chem Eur J* 18:6039
48. Peng Y, Xu XB, Xiao J, Wang Y-W (2014) *Chem Commun* 50:472
49. Lu X, Yi J, Zhang Z-Q, Dai J-J, Liu J-H, Xiao B, Fu Y, Liu L (2014) *Chem Eur J* 20:15339
50. Molander GA, Traister KM, O'Neill BT (2015) *J Org Chem* 80:2907
51. Li X, Feng Z, Jiang Z-X, Zhang X (2015) *Org Lett* 17:5570
52. Gutierrez O, Tellis JC, Primer DN, Molander GA, Kozlowski MC (2015) *J Am Chem Soc* 137:4896
53. Ackerman LK, Anka-Lufford LL, Naodovic M, Weix DJ (2015) *Chem Sci* 6:1115
54. Zhao Y, Weix DJ (2013) *J Am Chem Soc* 136:48
55. Yamashita Y, Tellis JC, Molander GA (2015) *Proc Natl Acad Sci USA* 112:12026
56. Jouffroy M, Primer DN, Molander GA (2015) *J Am Chem Soc* 138:475
57. Wang X, Wang S, Xue W, Gong H (2015) *J Am Chem Soc* 137:11562
58. Patel NR, Kelly CB, Jouffroy M, Molander GA (2016) *Org Lett* 18:764
59. Noble A, McCarver SJ, MacMillan DW (2015) *J Am Chem Soc* 137:624
60. Durandetti M, Gosmini C, Périchon J (2007) *Tetrahedron* 63:1146
61. Cui X, Wang S, Zhang Y, Deng W, Qian Q, Gong H (2013) *Org Biomol Chem* 11:3094
62. Arendt KM, Doyle AG (2015) *Angew Chem Int Ed* 54:9876
63. Konev MO, Hanna LE, Jarvo ER (2016) *Angew Chem Int Ed* 55: ASAP. doi:10.1002/anie.201601206
64. Wotal AC, Weix DJ (2012) *Org Lett* 14:1476
65. Wu F, Lu W, Qian Q, Ren Q, Gong H (2012) *Org Lett* 14:3044
66. Yin H, Zhao C, You H, Lin K, Gong H (2012) *Chem Commun* 48:7034
67. Lu W, Liang Z, Zhang Y, Wu F, Qian Q, Gong H (2013) *Synthesis* 45:2234
68. Jia X, Zhang X, Qian Q, Gong H (2015) *Chem Commun* 51:10302
69. Zhao C, Jia X, Wang X, Gong H (2014) *J Am Chem Soc* 136:17645
70. Le CC, MacMillan DW (2015) *J Am Chem Soc* 137:11938
71. Joe CL, Doyle AG (2016) *Angew Chem Int Ed* 55:4040
72. Amani J, Sodagar E, Molander GA (2016) *Org Lett* 18:732
73. León T, Correa A, Martin R (2013) *J Am Chem Soc* 135:1221
74. Moragas T, Cornella J, Martin R (2014) *J Am Chem Soc* 136:17702
75. Liu Y, Cornella J, Martin R (2014) *J Am Chem Soc* 136:11212
76. Wang X, Liu Y, Martin R (2015) *J Am Chem Soc* 137:6476
77. Moragas T, Gaydou M, Martin R (2016) *Angew Chem Int Ed* 55. doi:10.1002/anie.201600697
78. Zhao Y, Weix DJ (2015) *J Am Chem Soc* 137:3237
79. Cherney AH, Kadunce NT, Reisman SE (2013) *J Am Chem Soc* 135:7442
80. Cherney AH, Reisman SE *J Am Chem Soc* 136:14365
81. Kadunce NT, Reisman SE (2015) *J Am Chem Soc* 137:10480
82. Zuo Z, Cong H, Li W, Choi J, Fu GC, MacMillan DW (2016) *J Am Chem Soc* 138:1832
83. Tan Z, Wan X, Zang Z, Qian Q, Deng W, Gong H (2014) *Chem Commun* 50:3827
84. Liu X, Li X, Chen Y, Hu Y, Kishi Y (2012) *J Am Chem Soc* 134:6136
85. Panahi F, Bahmani M, Iranpoor N (2015) *Adv Synth Catal* 357:1211
86. Zhao C, Tan Z, Liang Z, Deng W, Gong H (2014) *Synthesis* 46:1901
87. Caputo JA, Naodovic M, Weix DJ (2015) *Synlett* 26:323–326
88. Amatore M, Gosmini C (2008) *Angew Chem Int Ed* 47:2089
89. Gosmini C, Bassene-Ernst C, Durandetti M (2009) *Tetrahedron* 65:6141
90. Qian Q, Zang Z, Chen Y, Lin K, Gong H (2013) *Synlett* 24:619
91. Iranpoor N, Panahi F (2015) *Org Lett* 17:214
92. Liao L-Y, Kong X-R, Duan X-F (2014) *J Org Chem* 79:777
93. Buonomo JA, Everson DA, Weix DJ (2013) *Synthesis* 45:3099
94. Ackerman LKG, Lovell MM, Weix DJ (2015) *Nature* 524:455
95. Moncombe A, Le Floch P, Lledos A, Gosmini C (2012) *J Org Chem* 77:5056

96. Correa A, León T, Martín R (2014) *J Am Chem Soc* 136:1062
97. Wang X, Nakajima M, Martín R (2015) *J Am Chem Soc* 137:8924
98. Correa A, Martín R (2014) *J Am Chem Soc* 136:7253
99. Hsieh J-H, Cheng C-H (2005) *Chem Commun* 4554
100. Hsieh J-C, Chen Y-C, Cheng A-Y, Tseng H-C (2012) *Org Lett* 14:1282
101. Majumdar KK, Cheng CH (2000) *Org Lett* 2:2295
102. Huang YC, Majumdar KK, Cheng CH (2002) *J Org Chem* 67:1682
103. Hu JX, Li CY, Sheng WJ, Jia YX, Gao JR (2011) *Chem Eur J* 17:5234
104. Qian Q, Zang Z, Chen Y, Tong W, Gong H (2013) *Mini Rev Med Chem* 13:802
105. Lu X, Xiao B, Zhang Z, Gong T, Su W, Yi J, Fu Y, Liu L (2016) *Nat Commun* 7:11129
106. Lebedev SA, Lopatina VS, Petrov ES, Beletskaya IP (1988) *J Organomet Chem* 344:253
107. Liu C-C, Parthasarathy K, Cheng C-H (2010) *Org Lett* 15:3518
108. Korivi RP, Cheng C-H (2006) *J Org Chem* 71:7079
109. Shrestha R, Dorn SCM, Weix DJ (2013) *J Am Chem Soc* 135:751

# Ni- and Fe-catalyzed Carboxylation of Unsaturated Hydrocarbons with CO<sub>2</sub>

Francisco Juliá-Hernández<sup>1</sup> · Morgane Gaydou<sup>1</sup> ·  
Eloisa Serrano<sup>1</sup> · Manuel van Gemmeren<sup>1</sup> ·  
Ruben Martin<sup>1,2</sup> 

Received: 11 May 2016 / Accepted: 11 June 2016 / Published online: 30 June 2016  
© Springer International Publishing Switzerland 2016

**Abstract** The sustainable utilization of available feedstock materials for preparing valuable compounds holds great promise to revolutionize approaches in organic synthesis. In this regard, the implementation of abundant and inexpensive carbon dioxide (CO<sub>2</sub>) as a C1 building block has recently attracted considerable attention. Among the different alternatives in CO<sub>2</sub> fixation, the preparation of carboxylic acids, relevant motifs in pharmaceuticals and agrochemicals, is particularly appealing, thus providing a rapid and unconventional entry to building blocks that are typically prepared via waste-producing protocols. While significant advances have been realized, the utilization of simple unsaturated hydrocarbons as coupling partners in carboxylation events is undoubtedly of utmost academic and industrial relevance, as two available feedstock materials can be combined in a catalytic fashion. This review article aims to describe the main achievements on the direct carboxylation of unsaturated hydrocarbons with CO<sub>2</sub> by using cheap and available Ni or Fe catalytic species.

**Keywords** Nickel · Iron · CO<sub>2</sub> · Carboxylation · Unsaturated hydrocarbons · Catalysis · Carboxylic acids · Cross-coupling

---

This article is part of the Topical Collection “Ni- and Fe-Based Cross-Coupling Reactions”; edited by “Arkaitz Correa”.

---

✉ Ruben Martin  
[rmartinromo@icmq.es](mailto:rmartinromo@icmq.es)

<sup>1</sup> Institute of Chemical Research of Catalonia (ICIQ), The Barcelona Institute of Science and Technology, Av. Països Catalans 16, 43007 Tarragona, Spain

<sup>2</sup> Catalan Institution for Research and Advanced Studies (ICREA), Passeig Lluís Companys, 23, 08010 Barcelona, Spain

## 1 Introduction

The atmospheric concentration of carbon dioxide (CO<sub>2</sub>) has been dramatically raised in the last decades as result of the industrial development of our society. The ever-growing concentration of CO<sub>2</sub> has led to discussions on how to alleviate the effects of the climatic change [1]. However, CO<sub>2</sub> is an abundant, inexpensive, and renewable feedstock that could be potentially used as a C1 building block for synthesis [2–4]. Although the implementation of CO<sub>2</sub> fixation in synthetic methods will certainly not reduce its concentration in the atmosphere, it could be transformed into high value-added fine chemicals. In fact, more than 110 megatons of CO<sub>2</sub> are used annually in industry for the synthesis of urea, salicylic acid, and carbonates [1, 5]. However, CO<sub>2</sub> is a highly oxidized and thermodynamically stable gas and, consequently, high activation energies are required for its functionalization [6–10].

Carboxylic acids rank amongst the most prevalent backbones in pharmaceuticals and agrochemicals. The main strategies for the synthesis of carboxylic acids are based on the oxidation of primary alcohols and aldehydes, and the hydrolysis of nitriles [11]. However, these methods suffer from the use of harsh conditions, strong oxidants, and/or high temperatures, inevitably resulting in a poor chemoselectivity profile. Alternatively, chemists have designed new routes for preparing carboxylic acids via direct carboxylation of well-defined organometallic species in which CO<sub>2</sub> inserts into a highly energetic metal–carbon bond that forms the corresponding carboxylic acid upon hydrolytic work-up [12]. While a significant step-forward, such a method is not particularly step-economical and requires handling with stoichiometric and, in many instances, air-sensitive organometallic species, thus reinforcing a change in strategy. Although the recent years have witnessed the discovery of a myriad of elegant catalytic reductive carboxylation techniques with organic (pseudo)halides [13–16], the utilization of unsaturated hydrocarbon counterparts constitutes an ideal platform in the carboxylation arena, as these motifs can be obtained in bulk from our petrochemical industry, thus representing a formidable and unique opportunity for converting raw materials into valuable products at the industrial level [17]. Additionally, such a scenario would allow for accessing carboxylic acids at a large scale while avoiding the utilization of toxic carbon monoxide [11].

The direct carboxylation of organic compounds has traditionally been associated with the utilization of Ni complexes, an observation that can be traced back to the seminal work of Aresta and coworkers by the isolation of the first CO<sub>2</sub> complex to a transition metal [Ni(η<sup>2</sup>-CO<sub>2</sub>)(PCy<sub>3</sub>)<sub>2</sub>] [18]. In the last three decades, CO<sub>2</sub> fixation into unsaturated hydrocarbons has garnered considerable attention from the scientific community, either using stoichiometric or catalytic amounts of transition metals, reaching remarkable levels of sophistication, efficiency, and applicability. Given the preparative potential of these transformations, we identified the need to review the most prominent advances in this field of expertise. Unlike other reviews for similar means, the purpose of this article is to focus on the most recent advances for preparing carboxylic acid derivatives from unsaturated hydrocarbon backbones using Ni as well as the cheaper and more abundant Fe species in a *homogeneous*

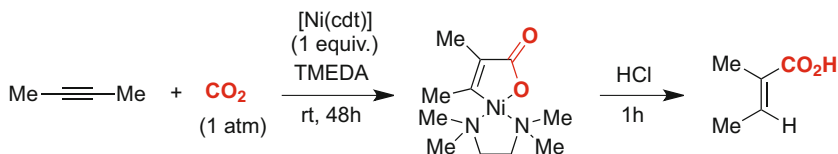
manner, including mechanistic considerations, when appropriate. Therefore, other catalytic CO<sub>2</sub> functionalization processes of paramount importance such as the area of cyclic carbonates [19–21], polymer formation, production of methanol or formic acid [22–24], electrochemical methods [25], co-catalyzed carboxylations [26], carbonylation methods [27], or reductive carboxylations of organic (pseudo)halides [14–16, 28, 29], among others, are beyond the scope of this review.

## 2 Carboxylation of Alkynes

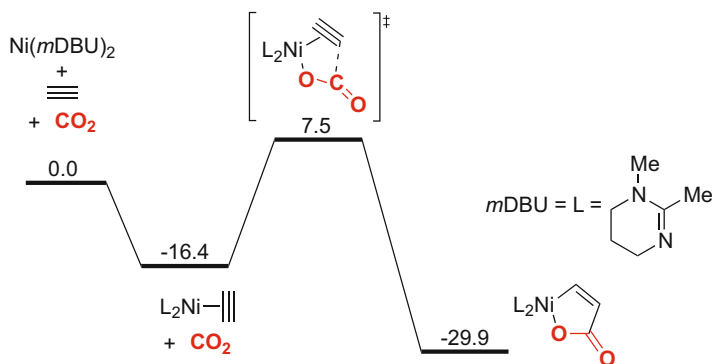
### 2.1 Stoichiometric Processes

Prompted by the seminal Ni-catalyzed oxidative cyclization work of Inoue for preparing 2-pyrones using CO<sub>2</sub> as coupling partner [30], Burkhart and Hoberg reported the isolation of an oxanickelacyclopentene (nickelalactone) from the coupling of 2-butyne and CO<sub>2</sub> with Ni(cdt) (cdt = 1,5,6-cyclododecatriene) and *N,N,N',N'*-tetramethylethylenediamine (TMEDA) [31]. The authors highlighted that the corresponding  $\alpha,\beta$ -unsaturated carboxylic acid can be easily within reach upon simple protonolysis (Scheme 1).

The intermediacy of nickelalactones was further corroborated by theoretical calculations [32–35]. Specifically, in 2008 Buntine and coworkers modeled the reaction with acetylene and CO<sub>2</sub> [34], selecting *m*DBU as a model ligand to mimic



**Scheme 1** Synthesis of acrylic acids via the intermediacy of nickelalactones [31]

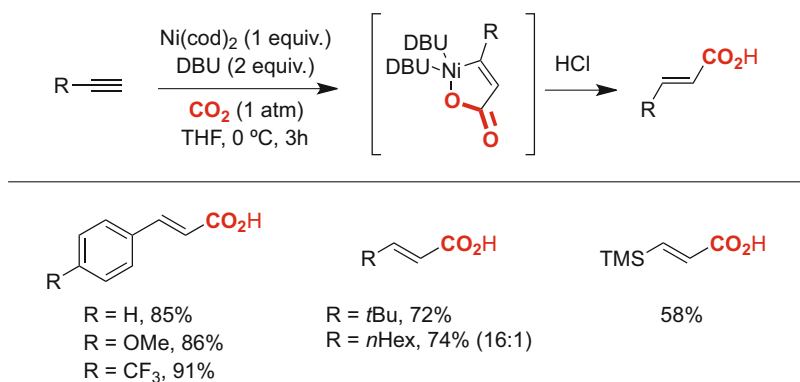


**Scheme 2** Gibbs free energies (kcal/mol) for the coupling of CO<sub>2</sub> with acetylene [34]

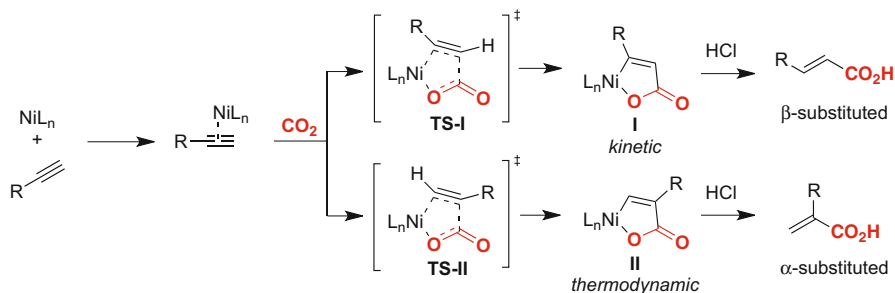
the behavior of DBU (DBU = diazabicyclo[5.4.0]undec-7-ene). The authors found that the reaction proceeds through an associative mechanism, first involving the  $\eta^2$ -coordination of the alkyne to the nickel(0) complex followed by a direct insertion of  $\text{CO}_2$  (Scheme 2). The reaction turned out to be thermodynamically favored, with an activation barrier of 23.9 kcal/mol for the key oxidative cyclization event without going through an Aresta-type complex.

Strikingly, it took more than 15 years until Yamamoto and Saito reported the preparation of nickelalactones with terminal alkynes [36]. In this work, the authors disclosed the stoichiometric carboxylation of terminal alkynes with in situ formed  $\text{Ni}(\text{DBU})_2$ , leading to the rapid formation of  $\beta$ -substituted carboxylic acids with high levels of chemo- and regioselectivity (Scheme 3). This reaction could be applied to differently substituted alkynes bearing aromatic, aliphatic or silyl groups with equal ease.

The regioselectivity observed in the oxidative cyclization of monosubstituted alkynes with  $\text{CO}_2$  was theoretically rationalized by Buntine (Scheme 4) [34]. The authors observed a markedly different energetic preference for the two possible transition states (TS-I and TS-II), with a lower energy barrier for TS-I leading to I, in which  $\text{CO}_2$  insertion takes place *distal* to the substituent on the alkyne motif.

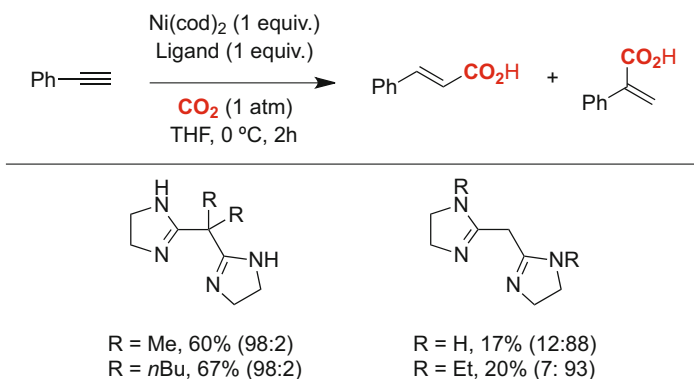


**Scheme 3** Nickel(0)-mediated carboxylation of terminal alkynes by Yamamoto and Saito [36]



**Scheme 4** Regioselectivity profile in the cycloaddition of terminal alkynes with  $\text{CO}_2$  [34]



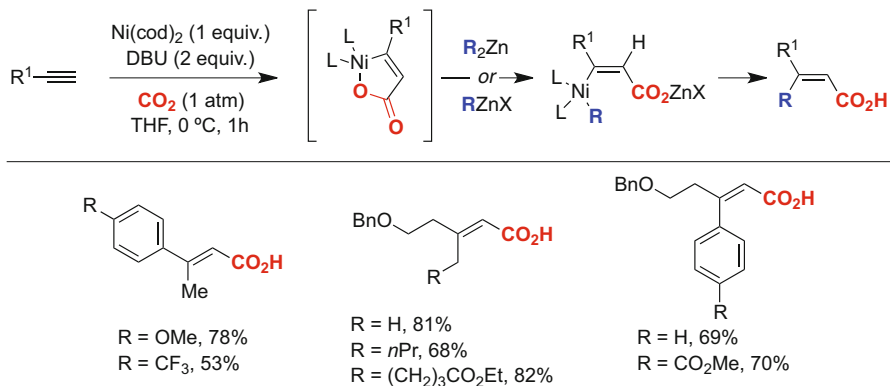


**Scheme 5** Bis(amidine)ligands in Ni-mediated synthesis of acrylic acids [37]

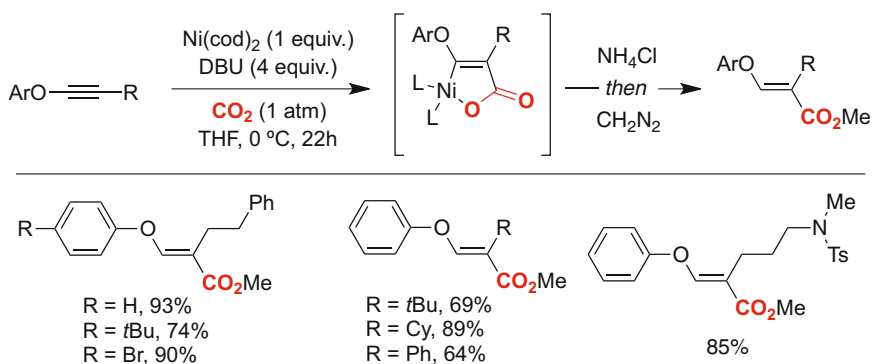
However, nickelalactone **II** turned out to be thermodynamically favored due to the avoidance of a steric clash of the substituent on the alkyne terminus with the Ni center. The effect of the ancillary ligand was also investigated, with DBU leading to lower activation energies when compared to 2,2'-bipyridine (bpy). It was particularly interesting to find out that polar solvents such as DMF lowered down all activation barriers due to the stabilizing effect of DMF on the transition states when compared with commonly employed tetrahydrofuran (THF).

In 2004, the group of Iwasawa reported a similar study for the stoichiometric carboxylation of terminal and unsymmetrical alkynes using a series of bis(amidine)ligands [37]. Interestingly, the nature of the ligand dictated the regioselectivity pattern; while ligands bearing substituents at the methylene carbon generated predominantly cinnamic acids in good yields, less substituted bis(amidine) ligands resulted in a switch of selectivity, leading preferentially to  $\alpha$ -substituted carboxylic acids, albeit in lower yields (Scheme 5). Although this transformation still required stoichiometric amounts of nickel, this work represented a formidable step forward for promoting a ligand-controlled regiodivergent carboxylation of alkynes.

Mori and coworkers significantly extended the application profile of the Ni-mediated carboxylation of alkynes with  $\text{CO}_2$  by using organozinc reagents as coupling partners, thus triggering a transmetalation with the in situ-generated nickelalactone, and giving rise to a formal alkylative or arylative carboxylation of terminal alkynes depending on the organozinc reagent utilized [38]. The reaction proceeded under mild conditions and a wide range of organozinc reagents could be used leading to  $\beta,\beta'$ -disubstituted unsaturated carboxylic acids with an excellent regioselectivity profile that goes in line with the hydrocarboxylation procedure reported by Yamamoto and Saito (Scheme 6) [36]. Notably, the authors found that heterocyclic structures were within reach by appropriately locating a tethered heteroatom on the side-chain, thus setting the stage for an intramolecular Michael addition [39, 40].



**Scheme 6** Ni(0)-mediated alkylative/arylate carboxylation of alkynes [38]

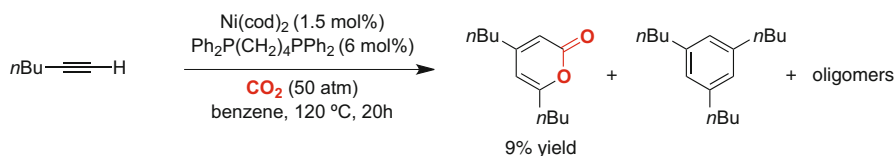


**Scheme 7** Ni(0)-promoted regioselective carboxylation of alkoxy acetylenes [41]

The nickel(0)-promoted carboxylation of alkoxy acetylenes has been recently developed by the group of Sato and Saito [41]. The authors predicted that the electron-donating properties of an ether substituent could dictate the regioselectivity profile when forming the intermediate nickelalactone, thus leading to a CO<sub>2</sub> insertion onto the most nucleophilic carbon. As shown in [Scheme 7](#), this turned out to be the case. Such an outcome is noteworthy as an opposite selectivity pattern was observed by Yamamoto and Saito, in which CO<sub>2</sub> insertion occurred at the less sterically congested carbon. The applicability of this transformation was further corroborated by a subsequent Rh-catalyzed asymmetric hydrogenation, affording enantioenriched β-aryloxypropionic acid derivatives.

## 2.2 Catalytic Carboxylation of Alkynes

The first metal-catalyzed carboxylation of alkynes with CO<sub>2</sub> was reported 3 years before the isolation of nickelalactones by Hoberg [31]. Specifically, in 1977 Inoue described the carboxylation of alkynes with CO<sub>2</sub> leading to the formation of



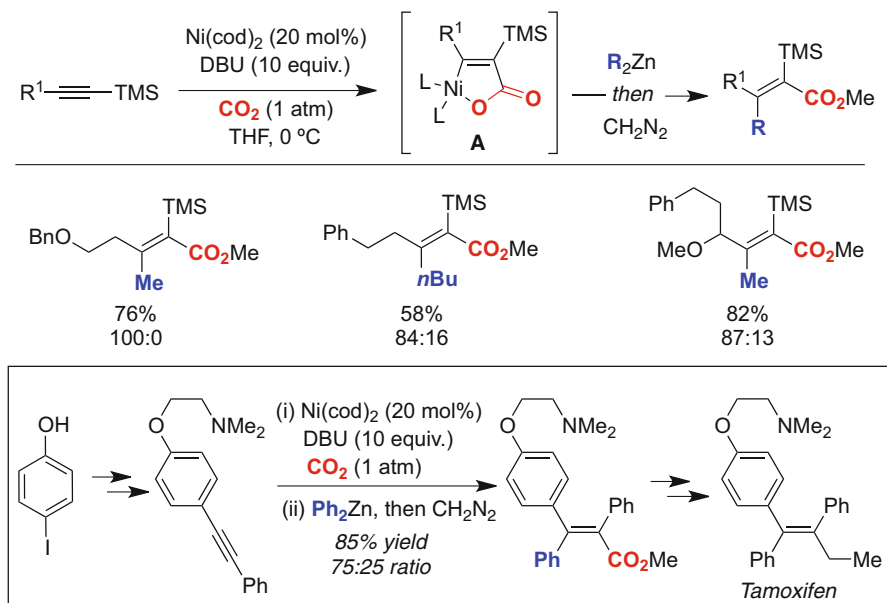
**Scheme 8** First Ni(0)-catalyzed cycloaddition of alkynes with CO<sub>2</sub> en route to 2-pyrones [30]

2-pyrones. The utilization of terminal acetylenes such as 1-hexyne in combination with a bidentate phosphine afforded the corresponding 2-pyrone in low yields, together with inevitable trimerization side products (Scheme 8) [30]. As expected, the parasitic trimerization could be avoided when using internal alkynes, affording high yields of the tetrasubstituted-2-pyrones [42, 43]. Further improvements in reactivity and selectivity were achieved by Walther [44] and Saegusa [45, 46], revealing a non-negligible effect on the nature of the ligand utilized in order to obtain the targeted 2-pyrones with high yields and selectivities.

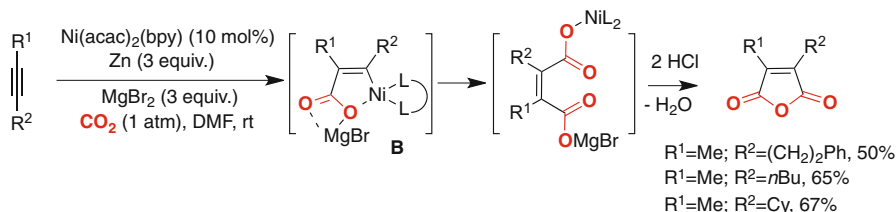
Inoue tentatively proposed a mechanism based on the intermediacy of a nickelacyclopentadiene formed via oxidative cyclization of two alkyne moieties. Subsequent CO<sub>2</sub> insertion into the Ni–C bond or an alternative [4 + 2] cycloaddition were proposed as conceivable pathways towards the corresponding 2-pyrones. Few years later, Hoberg's stoichiometric studies unambiguously revealed that this reaction proceeds via oxidative cyclization of an alkyne, CO<sub>2</sub> and Ni(0), thus forming the corresponding nickelalactone that would ultimately insert a second alkyne molecule to afford 2-pyrones upon final reductive elimination [45–47]. A comprehensive review on the use of the oxidative cyclization techniques starting from alkynes and CO<sub>2</sub> was nicely reported by Mori [48].

### 2.2.1 Reductive Carboxylation of Alkynes

Prompted by their previous work on the Ni-mediated carboxylation of disubstituted alkynes [38] (Scheme 6), Mori reported the Ni-catalyzed synthesis of  $\alpha$ -silyl- $\beta,\beta'$ -dialkyl  $\alpha,\beta$ -unsaturated carboxylic acids from silyl-substituted alkynes in presence of zinc reagents and an excess of DBU (Scheme 9). Although the reaction affords tetrasubstituted alkenes with a high regioselectivity and good yields, the methodology was unfortunately limited to Me<sub>2</sub>Zn, Bu<sub>2</sub>Zn, Ph<sub>2</sub>Zn or Bn<sub>2</sub>Zn as reagents [49, 50]. The regioselectivity was explained by the preferential formation of **A** in which the Ni center is located *distal* to the silyl group, an issue that can be interpreted on the basis of both electronic as well as steric effects [51]. Such a finding was further corroborated in subsequent theoretical calculations in which **A** was favored both from a kinetic and thermodynamic standpoint [34]. Not surprisingly, a selectivity switch was observed for alkynes not possessing a silyl group, such as *tert*-butyl or aromatic motifs. The synthetic utility of this methodology was showcased on a short total synthesis of tamoxifen, an antiestrogenic anticancer drug, in 36 % overall yield from *p*-iodophenol, using a



**Scheme 9** Ni-catalyzed carboxylation of silyl-substituted alkynes with  $R_2Zn$  [49, 50]



**Scheme 10** Nickel-catalyzed double carboxylation of alkynes [52]

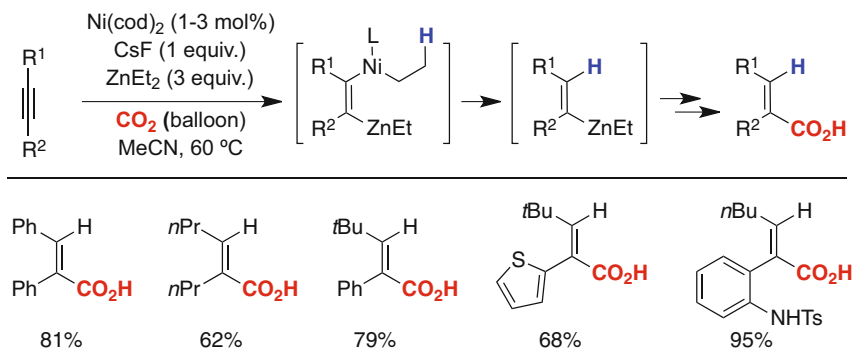
Ni-catalyzed carboxylation of a phenyl-substituted acetylene with  $CO_2$  and  $Ph_2Zn$  as the key step [50].

The double carboxylation of alkynes to afford maleic anhydrides using Ni precatalysts, Zn as reducing agent and  $MgBr_2$  as additive, has recently been developed by Tsuji and Fujihara (Scheme 10) [52]. Based on stoichiometric and DFT studies, the authors proposed a catalytic cycle consisting of the initial formation of Hoberg's nickelalactone, followed by one-electron reduction with Zn in the presence of  $MgBr_2$  to generate **B**. A second  $CO_2$  insertion into the Ni-C bond is mediated by the coordination of an  $MgBr^+$  fragment to both  $CO_2$  and the carboxylate moiety. Finally, one-electron reduction by Zn affords the dicarboxylated species that ultimately are converted into the corresponding maleic anhydride while recovering back the active propagating Ni(0) species.

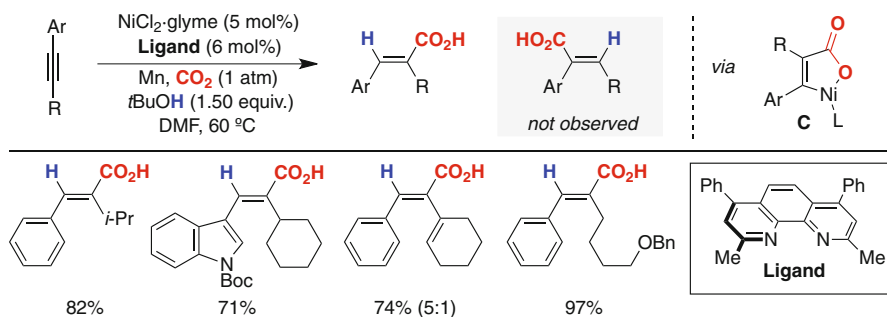
## 2.2.2 Catalytic Hydrocarboxylation of Alkynes

In 2011, the group of Ma described a nickel-catalyzed hydrocarboxylation of alkynes using  $\text{Ni}(\text{cod})_2$  and diethylzinc as reducing agent (Scheme 11) [53]. The reaction turned out to be highly regio- and stereoselective, thus accessing *syn*-hydrocarboxylated products at 1–3 mol % catalyst loadings. Although they employed stoichiometric amounts of cesium fluoride (CsF), no additional ligand was required, no doubt a formidable bonus when compared with other carboxylation techniques. While the mechanism remains speculative, the authors favored a transmetalation/ $\beta$ -hydride elimination pathway, resulting in an alkenyl zinc derivative that ultimately reacts with  $\text{CO}_2$  to deliver the targeted carboxylic acid. Notably,  $\text{CO}_2$  insertion typically occurs *adjacent* to the aromatic site in unsymmetrically substituted alkynes or in close proximity to a directing group such as *N*-tosyl motifs. It is worth noting that an otherwise related work was independently described by Tsuji using Cu catalysts in combination with organosilanes as reducing agents [54]. Later on, Ma and coworkers reported an otherwise related hydrocarboxylation and methyl-carboxylation technique of homopropargylic alcohols in which the pending alcohol directs the carboxylation en route to  $\alpha$ -alkylidene- $\gamma$ -butyrolactones [55, 56].

More recently, Martin and coworkers described a novel Ni-catalyzed regioselective hydrocarboxylation of alkynes that obviates the need for stoichiometric and air-sensitive organometallic species by using simple alcohols as proton sources (Scheme 12) [57]. Importantly, such a transformation was distinguished by an intriguing regioselectivity profile in which  $\text{CO}_2$  insertion took place exclusively *distal* to the aromatic site, regardless of whether a directing group was present or not, and independently on the substitution pattern on the alkyne terminus, an observation that demonstrates the complementarity of this method when compared with other protocols using metal hydrides [58]. The origin of the regioselectivity profile was attributed to the intermediacy of two nickelalactones that were in equilibrium upon  $\text{CO}_2$  extrusion followed by a preferential binding of the alcohol motif to the Ni(II) center in **C**, thus avoiding the clash with the bulkier aliphatic backbone. A subsequent two-electron reduction mediated by Mn recovers back the



**Scheme 11** Ni(0)-catalyzed *syn*-hydrocarboxylation of alkynes promoted by  $\text{Et}_2\text{Zn}$  [53]



**Scheme 12** Ni-catalyzed hydrocarboxylation of alkynes with alcohols as proton sources [57]

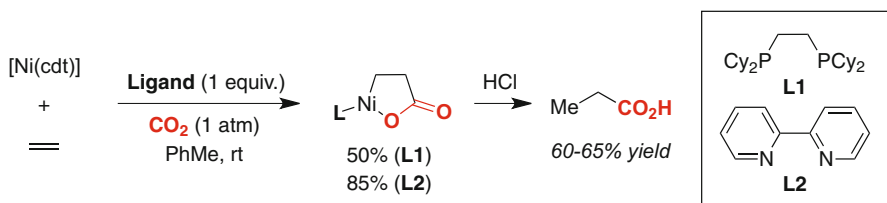
$\text{Ni}(0)\text{L}_n$  species while delivering a manganese carboxylate that upon hydrolytic workup results in the expected acrylic acid. Notably, the mild reaction conditions as well as the absence of highly nucleophilic organometallic reagents allowed for an excellent chemoselectivity profile, as functional groups such as nitriles, amides, aldehydes or alkenes, among others, were perfectly tolerated.

Although beyond the scope of this review, it is worth mentioning that a recent report by Fu has demonstrated that a Ni-catalyzed hydrocarboxylation of alkynes can be conducted using formic acid and a catalytic amount of anhydride via the in situ generation of carbon monoxide [59]. Likewise, a remarkable cocatalyzed carboxyzincation of alkynes has recently been reported by Tsuji and Fujihara, allowing for preparing highly functionalized acrylic acids, even in a multicomponent fashion, and under mild reaction conditions [26].

### 3 Carboxylation of Alkenes

#### 3.1 Stoichiometric Processes Involving Alkenes

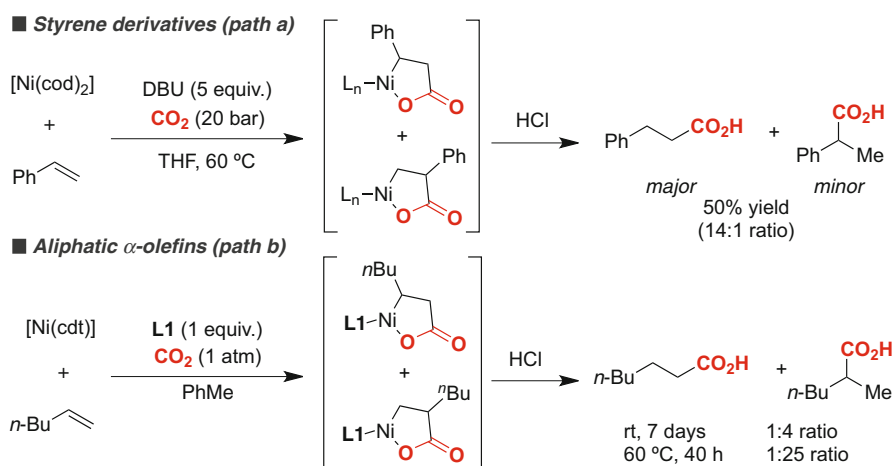
In 1982, pioneering studies by Hoberg et al. showed that electron-rich  $\text{Ni}(0)$  species were able to promote the oxidative cyclization of olefins and  $\text{CO}_2$  in an analogous manner to that shown previously for alkyne backbones [60, 61]. These processes gave rise to nickelalactones that were isolated and characterized with ethylene in the presence of bipyridine or bisphosphine ligands (**Scheme 13**) [61]. Protonolysis of



**Scheme 13** Ni-mediated oxidative cyclization of ethylene and  $\text{CO}_2$  en route to propionic acid [61]

these complexes led to the formation of the corresponding propionic acid in good yields, thus constituting a direct method to carboxylate alkenes in the presence of nickel complexes.

Prompted by this seminal work, efforts were subsequently focused on unraveling the fundamental features of the Ni-mediated oxidative cyclization of alkenes and CO<sub>2</sub> in terms of regioselectivity and reaction mechanism. The regioselectivity of the corresponding five-membered metallacycles depends on the nature of the ligand, alkene, and temperature. As shown in Scheme 13, both bipyridine and bisphosphine ligands can be equally used to prepare the corresponding nickelalactone. However, the formation of the five-membered metallacycle with mono- and 1,2-disubstituted alkenes is more efficient with electron-rich imines DBU [62] and **L1** [61]. Attempts to prepare a nickelalactone with aliphatic monosubstituted alkenes and Ni/**L2** systems resulted in the disproportionation of CO<sub>2</sub> while forming CO and [Ni(bpy)CO<sub>3</sub>] [61]. Interestingly, the electronic and steric nature of the alkene strongly determines product distribution in the cyclization process. Specifically, nickelalactones derived from styrene derivatives prefer to adopt a configuration in which the aryl substituent is located *adjacent* to the Ni center, due to a better stabilization of the Ni–C bond (Scheme 14, equation a). In this manner, the corresponding linear carboxylic acid is obtained as the major product after a final protonolysis event. In contrast, the regioselectivity with aliphatic  $\alpha$ -olefins (monosubstituted alkenes) is dictated by steric effects, and the most stable metallacycle contains the Ni center coordinated to a primary carbon atom (Scheme 14, equation b). Accordingly, the corresponding  $\alpha$ -branched carboxylic acid is formed predominantly after protonolysis. It is worth mentioning that the regioselectivity in the oxidative cyclization with olefins differs from that shown with alkyne counterparts (Scheme 3). Interestingly, the reaction temperature heavily influenced the product distribution in the presence of aliphatic substituents. While a 4:1 ratio favoring the  $\alpha$ -branched carboxylic acid was found at room temperature, a



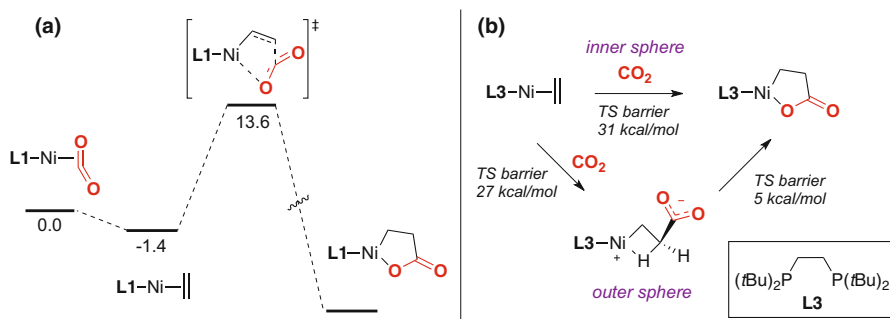
**Scheme 14** Regioselectivity in the oxidative cyclization of alkenes and CO<sub>2</sub> [61, 62]

negligible amount of linear carboxylic acid was observed at higher temperatures (25:1 ratio). This observation suggested that the two possible nickelalactones likely coexist in equilibrium upon CO<sub>2</sub> extrusion when using bidentate phosphine ligands, an observation that was univocally corroborated with further experimentation with olefin crossover experiments [47].

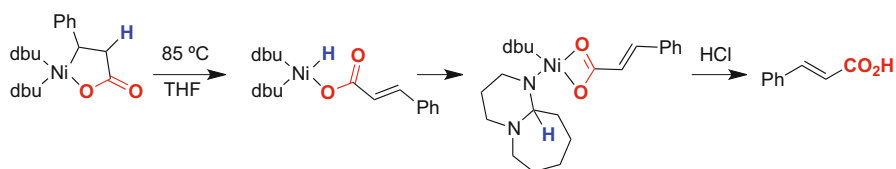
The design of new ligands led to a further improvement of the regioselectivity in the cyclization with aliphatic olefins. Particularly, pyridyl-phosphine ligands (P,N ligands) with different electronic and steric properties afforded a strict control of the position of the substituents in the nickelalactone [63, 64]. These ligands possess a push–pull character consisting of a mixture of electron-donating phosphine moieties with  $\pi$ -acidic pyridine fragments, which strongly stabilize the formation of the metallacycle, thus making the oxidative cyclization step irreversible. More recently, the formation of nickelalactones and subsequent protonolysis to give the corresponding saturated carboxylic acids could be achieved with activated trisubstituted olefins [65, 66]. In this case, methylenecyclopropanes led to the corresponding cyclopropanecarboxylic acids in the presence of stoichiometric amounts of Ni(0) species. The selectivity towards the formation of the carboxylic acid respect to the propene ring-opened product was dictated by the nature of ligand and solvent utilized.

Surprisingly, scarce mechanistic studies have been reported on the coupling of alkenes and CO<sub>2</sub> in the presence of Ni(0) species. Experimentally, a pathway consisting of an oxidative cyclization from an Aresta-type CO<sub>2</sub>-coordinated Ni(0) complex [18] and an external alkene was ruled out, as the substitution of CO<sub>2</sub> by the olefin was rapidly observed [67, 68]. This was also corroborated by the fact that nickelalactones decomposed at high temperatures to give the corresponding Ni(0)-olefin complexes by extrusion of CO<sub>2</sub> [47]. Interestingly, a more recent computational study shed light on the mode of operation of the oxidative cyclization reaction of ethylene and CO<sub>2</sub> with both Ni/L1 and Ni/L2 systems [69]. Two fundamental aspects were explored: (1) the possible intermediacy of a Ni(0)–CO<sub>2</sub> complex in the oxidative coupling process and (2) the nature of the transition state in the C–C bond forming step. At the given level of theory, the DFT model could validate the experimental observation that in the Aresta-type complex, the CO<sub>2</sub> ligand is substituted by ethylene in a process energetically favored by 1.4 kcal/mol with a negligible activation barrier. Therefore, an Aresta-type complex is not likely to be an intermediate in the oxidative coupling process. Additionally, Papai found that Hoberg's suggested 18-electron intermediate [Ni(L2)(C<sub>2</sub>H<sub>4</sub>)(CO<sub>2</sub>)] [47, 61] should be rather unstable as it would exothermically dissociate CO<sub>2</sub> with a negligible activation barrier of 0.8 kcal/mol. As in the case of alkynes, this indicates that the C–C bond forming step does not involve the simultaneous coordination of the unsaturated hydrocarbon and CO<sub>2</sub> to Ni(0). Furthermore, although the optimization of a transition state was not possible, calculations delivered a local maximum stationary point via the analysis of the intrinsic reaction coordinate (IRC). This revealed that the formation of the C–C bond would likely involve a single step in which the nickelalactone is formed from the ethylene-coordinated intermediate with an incoming molecule of CO<sub>2</sub> (Scheme 15, a). Therefore, it seems that the simultaneous coordination of both





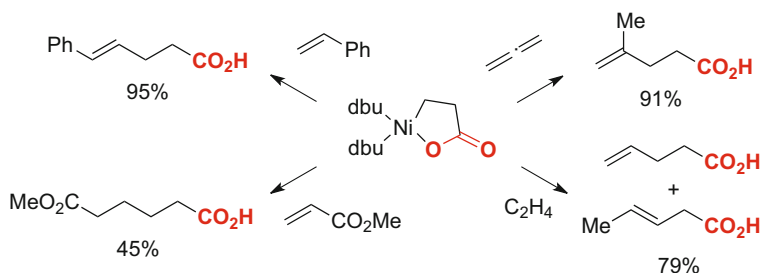
**Scheme 15** DFT calculations on the formation of nickelalactones derived from  $C_2H_4$  and  $CO_2$ . Energy levels are expressed in kcal/mol [69, 71]



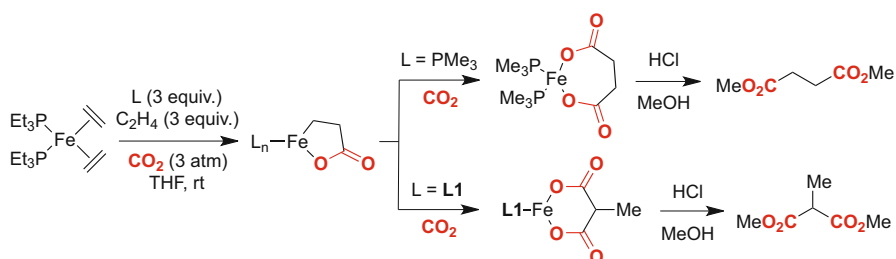
**Scheme 16** Cinnamic acid formation via  $\beta$ -hydride elimination [62]

$CO_2$  and  $C_2H_4$  is not indispensable for the formation of the nickelalactone. Calculations pointed towards a similar reaction pathway for **L1** and other modified bipyridines and bidentate phosphines, even though with different energetic profiles. Further theoretical studies were carried with other different ligands, leading to similar conclusions [70]. Interestingly, in 2014, Limbach et al. theoretically proposed two different modes of addition of  $CO_2$  into the Ni(0) ethylene intermediates with bidentate phosphine ligands, consisting of an inner sphere and outer sphere mechanism (Scheme 15, b) [71]. In the former, the insertion is believed to occur in a single concerted step, as previously reported by the group of Papai. However, the direct attack of  $CO_2$  to the coordinated ethylene without earlier interaction with the Ni center (outer sphere pathway) was suggested to be energetically more viable in polar solvents (THF) and with bulky ligands such as 1,2-bis(*di**tert*-butylphosphino)ethane (**L3**).

Although saturated aliphatic carboxylic acids were within reach from the corresponding nickelalactones, stoichiometric functionalizations of these metallacycles should in principle not be limited to protonolysis events. In 1986, Hoberg disclosed that the thermal decomposition of the DBU-containing nickelacycle derived from the oxidative coupling of styrene and  $CO_2$  led to the formation of cinnamic acid (Scheme 16) [62]. The rationale behind this result was interpreted on the basis of a  $\beta$ -hydride elimination from the corresponding nickelalactone, leading to a Ni(II)-hydride that adds into the C=N double bond of the DBU ligand, affording the corresponding unsaturated carboxylic acid after hydrolysis (Scheme 16). This



**Scheme 17** C–C bond-forming events with nickelalactones [72]



**Scheme 18** Ligand-controlled carboxylation of oxaferracyclopentanones [73]

singular discovery opened up new vistas for preparing industrially attractive acrylate derivatives from  $\text{CO}_2$  and simple olefins.

This rather intriguing reactivity could be turned into a strategic advantage by implementing tandem processes involving the insertion of unsaturated molecules prior to the  $\beta$ -hydride elimination step. In this manner, a variety of carboxylic acids of different nature were prepared in a stoichiometric manner (Scheme 17) [72].

While the cycloaddition of alkenes and  $\text{CO}_2$  has primarily been conducted with Ni(0) complexes, it is worth mentioning that similar reactivity has been observed with Fe(0) species, forming five-membered metallalactones in the presence of  $\text{CO}_2$  and ethylene [73]. However, the corresponding oxaferracyclopentanones are rather unstable and their isolation could not be unambiguously confirmed, certainly a serious limitation when compared with their Ni analogues (Scheme 18). In sharp contrast to their nickelalactone congeners, the oxaferracyclopentanones did not result in monocarboxylic acids upon simple protonolysis, but rather in structures bearing two carboxylic acids. Notably, the formation of linear or  $\alpha$ -branched products was strongly dependent on the bulkiness of the phosphine ligand utilized. For example, while linear bis-carboxylic acids were obtained when operating under a  $\text{PMe}_3$  regime, a protocol based upon **L1** resulted in a  $\beta$ -hydride elimination/migratory insertion scenario, leading to the branched product after a final  $\text{CO}_2$  insertion.

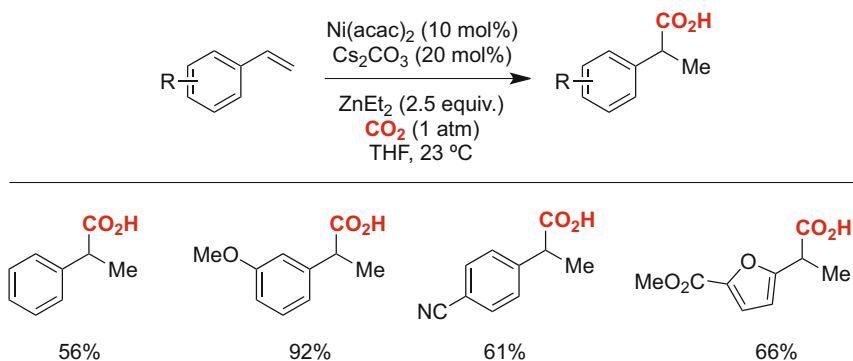
## 3.2 Catalytic Carboxylation of Olefins with CO<sub>2</sub>

Despite the elegant stoichiometric studies reported in the 80s and 90s, the catalytic preparation of carboxylic acids via the coupling of alkenes and CO<sub>2</sub> still remains challenging. This is likely attributed to the intrinsic inertness of CO<sub>2</sub>, making the reaction energetically endergonic and kinetically disfavored [74]. Although this issue has been partially overcome with the activation of both counterparts in oxidative cyclization pathways mediated by selected metals (Ni, Fe, Co), the corresponding metallacycles are remarkably stable, hence preventing the implementation of a catalytic process. Since the first report of nickelalactones, the vast majority of research has been conducted with the aim of enabling a catalytic carboxylation of olefinic counterparts. At present, two main strategies have been reported: (1) the preparation of saturated carboxylic acids via formal hydrocarboxylation of an olefin with CO<sub>2</sub>, and (2) the synthesis of acrylate derivatives via  $\beta$ -hydride elimination of in situ generated nickellelactone intermediates.

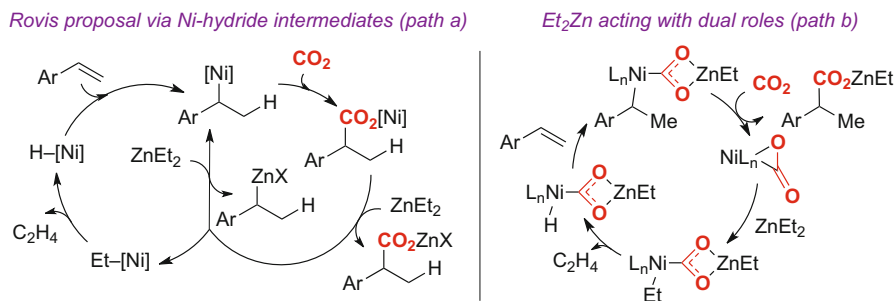
### 3.2.1 Catalytic Reductive Carboxylation of Alkenes with CO<sub>2</sub>

Although this review is focused on carboxylation processes involving Ni and Fe complexes, it is worth mentioning that the first report dealing with a catalytic hydrocarboxylation of alkenes was reported in 1978 by Lapidus et al. [75]. The reaction involved homogeneous and heterogeneous Rh and Pd catalysts, which were capable to carboxylate ethylene with CO<sub>2</sub> under high pressure and temperature (700 atm and 180 °C) in the presence of mineral acids. Under these conditions a 38 % yield of propionic acid could be obtained along with ethanol and ethyl propionate as main byproducts. Unfortunately, the authors did not explicitly indicate the catalyst loading utilized, thus leading to a reasonable ambiguity regarding the turnover numbers of this transformation. Apart from this isolated example, a rather limited number of methodologies have been shown to effectively carboxylate olefins with the direct participation of CO<sub>2</sub> in a reductive manner. In 2008, Rovis reported an elegant Ni-catalyzed direct hydrocarboxylation of styrenes to afford the corresponding  $\alpha$ -methyl arylacetic acids in a highly regioselective manner [76]. The reaction proceeded at room temperature in the presence of Ni(II) and Ni(0) precatalysts and using ZnEt<sub>2</sub> as a formal reducing agent (Scheme 19). A variety of electron-neutral and deficient styrenes with different substituent at the aryl moiety including ethers, ester, and ketones could be carboxylated in moderate to good yields. Under these conditions, electron-rich or  $\beta$ -substituted styrenes, as well as aliphatic  $\alpha$ -olefins showed to be almost completely unreactive, thus showing the inherent limitations of this protocol.

Taking into consideration the experimental results, the authors proposed a mechanistic scenario not consisting of the intermediacy of nickelalactones. Specifically, the authors proposed the participation of Ni(II) hydride species, which promote a rapid migratory insertion into the styrene backbone giving rise to a benzyl nickel intermediate. Direct carboxylation of the latter with CO<sub>2</sub> leads to the formation of the corresponding  $\alpha$ -branched carboxylate nickel complex (Scheme 20, path a). Catalytic turnover might be affected upon treatment with



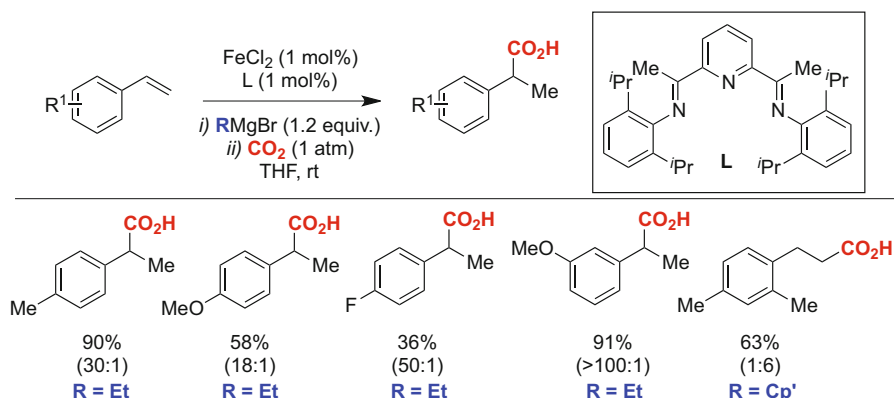
**Scheme 19** Ni-catalyzed hydrocarboxylation of styrenes with  $\text{Et}_2\text{Zn}$  [76]



**Scheme 20** Mechanism of the Ni-catalyzed hydrocarboxylation of styrenes [76, 77]

$\text{Et}_2\text{Zn}$  via  $\beta$ -hydride elimination or via transmetalation of the benzyl nickel species with  $\text{Et}_2\text{Zn}$ . This possibility was supported by deuterium incorporation at the benzylic position on the reduced product when quenching the reaction with  $\text{D}_2\text{O}$  at short reaction times.

Recently, the mechanism of this transformation has been studied in detail from a theoretical standpoint. Lin and Yuan compared the energetic profile of the carboxylation reaction via nickelalactone formation and Rovis' suggested nickel hydride intermediates (Scheme 20, path b) [77]. The *in silico* study revealed that the generation of a nickelalactone intermediate correlated to a thermodynamic sink, avoiding catalytic turnover. The involvement of nickel hydride species was slightly more favorable energetically, with a significantly lower energetic difference for electron-rich substrates, an observation that could explain their lack of reactivity. As for the nickel hydride pathway, theoretical calculations revealed that  $\text{ZnEt}_2$  act with dual roles, both as a hydride donor by forming ethyl-Ni(II) intermediate that evolves into the catalytically active nickel hydrides upon  $\beta$ -hydride elimination, as well as a Lewis acid for activating  $\text{CO}_2$  and therefore facilitating its coordination to the Ni center. In contrast to Rovis' proposal, theoretical calculations point at the formation of the corresponding carboxylic acid via reductive elimination of a  $\text{CO}_2$ -



**Scheme 21** Fe-catalyzed hydrocarboxylation of styrenes [79]

coordinated carboxylate benzyl nickel(II) species. Interestingly, the regioselectivity in the hydrometalation step was studied, revealing that the formation of nickel benzyl species is favored by 4 kcal/mol when compared to the corresponding phenylethyl derivatives.

Prompted by the seminal work of Rovis on the Ni-carboxylation of styrenes [76] as well as by the work of Hayashi and Shirakawa on the Fe- and Cu-catalyzed hydromagnesiation of terminal alkenes [78], Thomas reported the preparation of  $\alpha$ -methyl arylacetic acids in the presence of cheap and bench-stable iron/bis(imino)pyridine catalyst and Grignard reagents at room temperature (Scheme 21). [79] Unlike the Rovis protocol, this reaction turned out to be particularly efficient for styrene derivatives bearing electron-donating groups. However, the reactivity achieved did not seem to be exclusively dictated by electronic mesomeric factors, as 3-methoxystyrene (electron-poor substrate according to its known  $-I$  inductive effect of methoxy groups at the meta position:  $\sigma_{\text{meta}} = +0.12$ ) smoothly afforded the corresponding phenyl acetic acid. Unfortunately, the highly reactive nature of Grignard reagents made this methodology incompatible with the use of ketones, esters and other sensitive functional groups. Additionally, non-negligible amounts of the corresponding linear carboxylic acids were observed in certain cases, resulting in a selectivity switch when using cyclopentylmagnesium bromide ( $\text{Cp}'\text{MgBr}$ ) as reducing agent and *ortho*-substituted styrenes as substrates. Unfortunately, and in line with Rovis' protocol [76], substitution at the  $\alpha$  or  $\beta$  positions of the styrene backbone was not tolerated.

Quenching experiments with deuterated solvents revealed deuterium incorporation at the benzylic position, thus pointing towards the formation of iron hydride intermediates that trigger an initial migratory insertion into the styrene motif followed by transmetalation with the Grignard reagent. The corresponding in situ generated benzylmagnesium bromide derivatives would then react rapidly with  $\text{CO}_2$  to afford a magnesium carboxylate that upon acidic workup would generate the targeted phenyl acetic acid. In order to unravel the origin of the branched/linear selectivity, the authors tested the reactivity of phenylethylmagnesium bromide

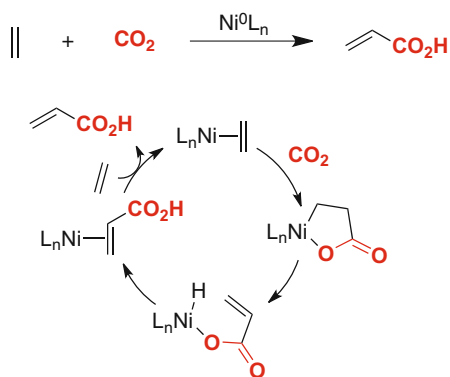
under the reaction conditions. In the presence of the iron catalyst, the linear acid was predominantly formed, suggesting that the  $\beta$ -hydride elimination/hydrometalation sequence is faster than the isomerization of the iron intermediate to produce the  $\alpha$ -branched product.

Although beyond the scope of this review, it is worth mentioning that a number of elegant hydroxycarbonylation processes have been reported in which  $\text{CO}_2$  conveniently serves as a surrogate of toxic carbon monoxide (CO) [80]. These processes make use of the so-called water–gas shift reaction (WGSR) using  $\text{CO}/\text{H}_2\text{O}$  and  $\text{CO}_2/\text{H}_2$  pairs [81]. A few number of reductive carboxylation of olefins following a reverse water–gas shift reaction ( $r$ WGSR) principle has been achieved, especially in the presence of Rh [82]. Recently, the hydroxycarbonylation of styrenes and aliphatic olefins has been addressed by in situ generation of CO from  $\text{CO}_2$  and MeOH, using Ni [83] and Ru catalysts [84]. However, these techniques still suffer from the use of harsh conditions, high temperatures, and pressures, as well as moderate branched/linear selectivities with aliphatic monosubstituted alkenes.

### 3.2.2 Carboxylation of Ethylene with $\text{CO}_2$ En Route to Acrylate Derivatives

The direct conversion of alkenes and  $\text{CO}_2$  into the corresponding  $\alpha,\beta$ -unsaturated carboxylic acids has been a major research topic in both academic and industrial laboratories [85]. Such interest is primarily associated to the possibility of transforming cheap and abundant chemical feedstocks such as ethylene and  $\text{CO}_2$  into acrylate derivatives, which rank amongst one of the most versatile building blocks used in chemical industry. After more than 30 years of intense research, however, this transformation is still considered one of the main challenges in modern synthetic chemistry [86].

Prompted by the observation that nickelalactones can readily be formed from ethylene and  $\text{CO}_2$  in the presence of a  $\text{Ni}(0)\text{L}_n$  complex, a reasonable pathway for the catalytic production of acrylates consists of a subsequent  $\beta$ -hydride elimination leading to carboxylate nickel hydride species that would deliver the corresponding acrylic acid after reductive elimination and ligand exchange with ethylene

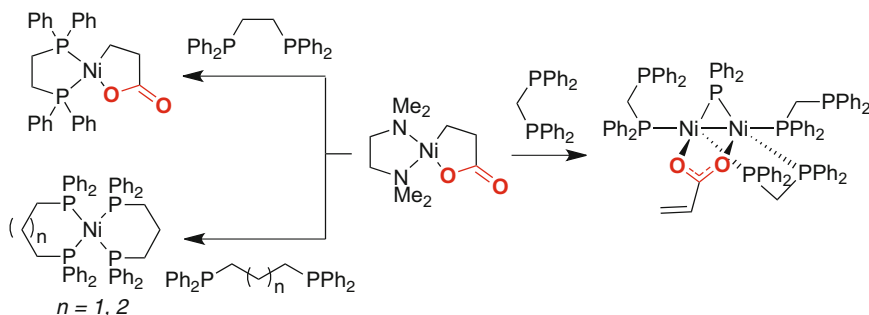


**Scheme 22** Hypothetical catalytic cycle for the formation of acrylates

(Scheme 22). Although a seemingly trivial transformation, there are a number of daunting challenges associated to this approach: (1) the direct transformation of ethylene and CO<sub>2</sub> into acrylic acid is endergonic by more than 20 kcal/mol, therefore making the reaction thermodynamically uphill [74]; (2) the activation barrier for  $\beta$ -hydride elimination step is energetically very costly (ca. 40 kcal/mol), resulting in a non-favorable kinetic profile [87] and (3) only a few number of ligands with specific features are able to efficiently promote the oxidative cyclization step en route to the key nickelalactone intermediates. Not surprisingly, the vast majority of efforts conducted in this field of expertise have been focused on adjusting the kinetics of the  $\beta$ -hydride elimination step.

Walther systematically studied the behavior of a number of bidentate phosphine ligands in the formation of acrylate derivatives from five-membered nickelalactone intermediates [88]. Specifically, bisdiphenylphosphine ligands with aliphatic bridges of different lengths were found to be particularly efficient for promoting the targeted reaction (Scheme 23). While the reaction of the TMEDA-containing nickelalactone with 1,2-bis(diphenylphosphino)ethane (dppe) cleanly gave rise to the corresponding nickelalactone, an intriguing reductive decomposition efficiently occurred with 1,3-bis(diphenylphosphino)propane (dppp) and 1,4-bis(diphenylphosphino)butane (dppb), thus forming the corresponding 18-electron Ni(0)L<sub>2</sub> complex. Interestingly, the utilization of a more labile ligand such as bis(diphenylphosphino)methane (dppm) resulted in the formation of a stable Ni(I)-Ni(I) dimer containing an acrylate ligand, thus demonstrating the viability for performing a  $\beta$ -hydride elimination.

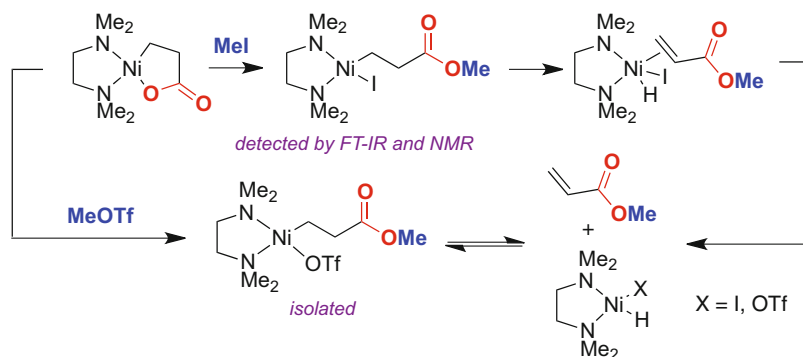
Encouraged by these results, DFT calculations were performed to study the viability of a catalytic preparation of acrylates from ethylene and CO<sub>2</sub>, revealing a rate-determining  $\beta$ -hydride elimination pathway [87]. Interestingly, a distortion-interaction analysis showed a tremendous energetic cost associated with the difficulty of the system to adopt a conformation that could allow a Ni-H agostic interaction, which is crucial for the success of the  $\beta$ -hydride elimination step. Therefore, a Ni-O bond elongation in the nickelalactone intermediate was predicted to facilitate this step by considerably reducing the ring strain. This crucial information was taken by Rieger, who based their strategy on breaking the Ni-O bond in the nickelalactone intermediate to promote the  $\beta$ -hydride elimination



**Scheme 23** Bisdiphenylphosphine ligands in the production of acrylates [88]

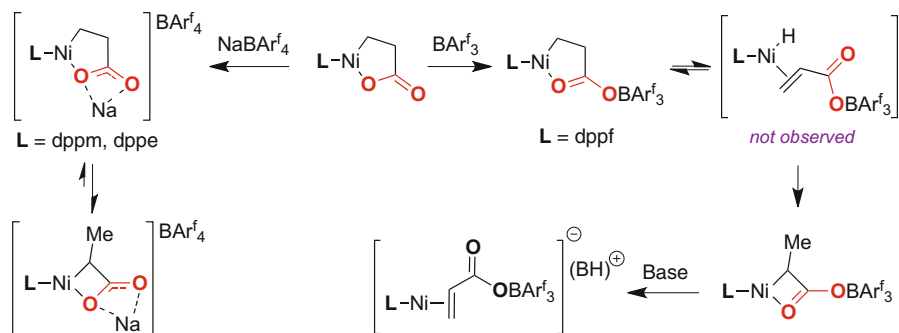
process via in situ alkylation of the carboxylate moiety [89]. When treating the corresponding dppp-nickelalactone with methyl iodide, a 33 % yield of the methyl acrylate could be detected. IR and NMR monitoring experiments showed the cleavage of the Ni–O bond during the reaction and the formation of methyl acrylate. This was further corroborated by the detection of methyl acrylate after the reaction of methyl 3-iodopropionate with the Ni/dppp system, which gives rise to the same intermediate. Based on these results, Kühn anticipated that the reaction with methyl iodide should be ligand-dependent [90]; as expected, this turned out to be the case and the ligand utilized exerted a tremendous influence on the formation of methyl acrylate. Among these, TMEDA proved to be superior than dppp and dppe; interestingly, no reaction was observed when exposing nickelalactones bearing dppb or pyridine-containing ligands. Although the corresponding alkyl Ni(II) iodide intermediate formed upon treatment with MeI could be detected by both FT-IR or NMR spectroscopy, its isolation proved to be particularly recalcitrant (Scheme 24). Importantly, DFT calculations revealed that the rate-determining step corresponded to the addition of methyl iodide. In line with this notion, the authors found that the inclusion of methyl triflate (MeOTf) significantly enhanced the rate of the reaction [91]. Unlike the use of methyl iodide, the reaction of MeOTf turned out to be particularly efficient with dppe, dppp, or even dppb, whereas the employment of TMEDA failed to provide the targeted methyl acrylate. While counterintuitive, this observation could be turned into a strategic advantage, as the corresponding alkyl Ni(II) triflate intermediate could be isolated and characterized.

Limbach and Hofmann reported a comprehensive theoretical study on the mechanism of the nickel-mediated synthesis of methyl acrylate from ethylene, CO<sub>2</sub> and methyl iodide [92]. DFT calculations revealed an S<sub>N</sub>2-type mechanism for the alkylation of the carboxylate ligand, which explain the experimental observations gathered by the groups of Rieger and Kühn. Subsequently, Bernskoetter described the ring-opening of the nickelalactone intermediates by coordination of the carboxylate fragment with Lewis acids [93]. Thus, the reaction of the dppf [bis(diphenylphosphino)ferrocene] nickelalactone with BAr<sub>3</sub><sup>f</sup> [Tris(pentafluorophenyl)borane] led to the formation of an activated five-membered nickelacycle



**Scheme 24** Nickelalactone ring opening triggered by methyl electrophiles [90, 91]



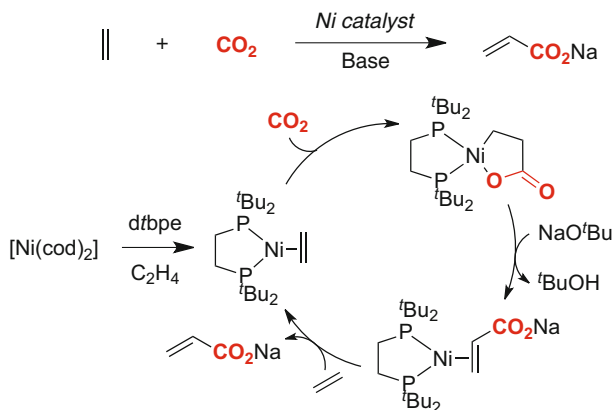


**Scheme 25** Ring opening of nickelalactones triggered by Lewis acids [93, 95]

( $\gamma$ -nickelalactone), in which the Lewis acid is coordinated to the carboxylate fragment, ultimately leading to a four-membered nickelacycle via  $\beta$ -hydride elimination and subsequent migratory insertion (Scheme 25). The latter species underwent formation of acrylate Ni(0)  $\pi$ -complexes upon addition of a base such as BTPP [*tert*-butyliminotri(pyrrolidino)phosphorane] or DBU. The enhanced selectivity towards the  $\beta$ -hydride elimination against unproductive pathways in the presence of a base was also studied from a theoretical standpoint [92, 94]. Later, the same group demonstrated that the  $\gamma$ -to- $\beta$  isomerization of nickelalactones could be also achieved with NaBARf<sub>4</sub>, [95] in which the Na<sup>+</sup> cations were able to lower down the barrier for  $\beta$ -hydride elimination as well as the energy of other putative reaction intermediates.

With all the knowledge acquired from the stoichiometric experiments, Limbach et al. attempted the development of a catalytic carboxylation of ethylene with CO<sub>2</sub> using *dtbpe* [1,2-bis(ditertbutylphosphino)ethane] as the ligand [96]. The authors showed that exposure of *dtbpe* nickelalactone to either sodium *tert*-butoxide (Na<sup>t</sup>OBu) or sodium hexamethyldisilazide (NaHMDS) resulted in the formation of the acrylate Ni(0) complex via  $\beta$ -hydride elimination (90 and 87 % yield, respectively). Interestingly, while ligand exchange of the acrylate Ni(0) complex with ethylene occurred effectively at high pressure of ethylene (8–30 bar), thus releasing sodium acrylate, no ligand exchange was observed with acrylic acid. These experiments demonstrated the feasibility of preparing acrylate derivatives from ethylene and CO<sub>2</sub> (Scheme 26).

Although Limbach demonstrated the feasibility of all elementary steps within the catalytic cycle, the implementation of a fully integrated catalytic process was far from trivial. Indeed, while nickelalactone formation had to be prepared under a high pressure of CO<sub>2</sub>, the  $\beta$ -hydride elimination and ligand exchange needed to be conducted in the absence of CO<sub>2</sub> to avoid the formation of carbonic acid half-esters. Still, the authors developed an iterative regime at high and low pressure of CO<sub>2</sub> that allowed reaching ten catalytic turnovers, thus constituting the first catalytic reaction of CO<sub>2</sub> and ethylene to prepare acrylate derivatives. Recently, Schaub et al. discovered that formation of carbonic acid half-esters could be avoided by increasing the temperature up to 145 °C, successfully obtaining catalytic turnover

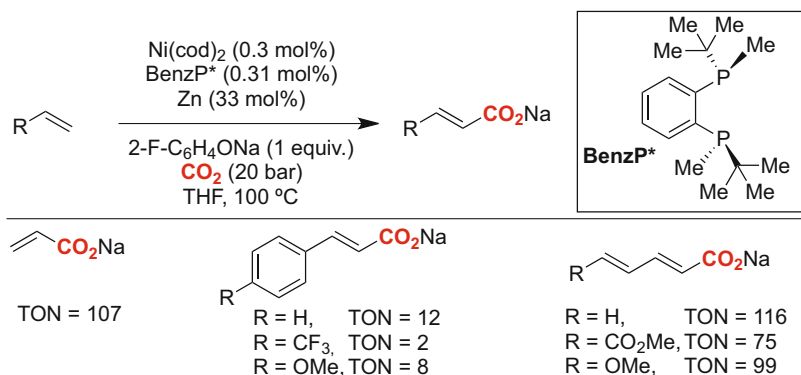


**Scheme 26** Catalytic carboxylation of ethylene and CO<sub>2</sub> to produce sodium acrylate [96]

for the non-iterative carboxylation process [97]. In 2014, Pidko exhaustively studied this catalytic transformation in the presence of different bidentate phosphine ligands using DFT calculations [70]. Although this study confirmed the important role of the ligand on nickelalactone formation, there was a marginal electronic, geometric, or steric effect of the ligand on the catalytic activity. In line with the experiments performed by Limbach, it was found that the energy barrier for  $\beta$ -hydride elimination was particularly low when employing NaOMe, due to a fast deprotonation and an increased stabilization of the putative intermediates by the presence of Na<sup>+</sup>.

Undoubtedly, the need for an iterative technique at high and low pressure of CO<sub>2</sub>, together with the requirement for strong nucleophilic bases, represented an important drawback to be overcome when designing a catalytic production of sodium acrylate from ethylene. The authors found a subtle balance of nucleophilicity and basicity when dealing with sodium 2-fluorophenoxide as the base, efficiently promoting the formation of the acrylate Ni(0) complex via deprotonation of the corresponding nickelalactone in the presence of CO<sub>2</sub> [98]. This result enabled the design of a one-pot catalytic carboxylation of ethylene, styrenes and 1,3-dienes with electron-rich bidentate phosphine ligands. Fine-tuning of the reaction conditions (ligand, Ni catalyst, and additives) led to the development of a highly active catalytic procedure, able to promote the carboxylation of ethylene to more than 100 turnover numbers (TON) (Scheme 27). Notably, styrene displayed moderate reactivity (12 TONs) whereas the inclusion of electron-withdrawing or electron-donating groups resulted in lower TONs. Interestingly, (E)-configured acrylic acids were obtained in all cases analyzed.

Recently, Schaub has experimentally investigated the mechanism of this transformation and expanded the scope of this reaction to 1,3-dienes [99]. Simultaneously, Vogt reported a different strategy to achieve the catalytic formation of acrylate derivatives from CO<sub>2</sub> and ethylene. The authors tackled the critical ring opening of nickelalactone derivatives with the utilization of a hard Lewis acid that



**Scheme 27** Catalytic synthesis of acrylates in the presence of sodium 2-fluorophenoxide [98]

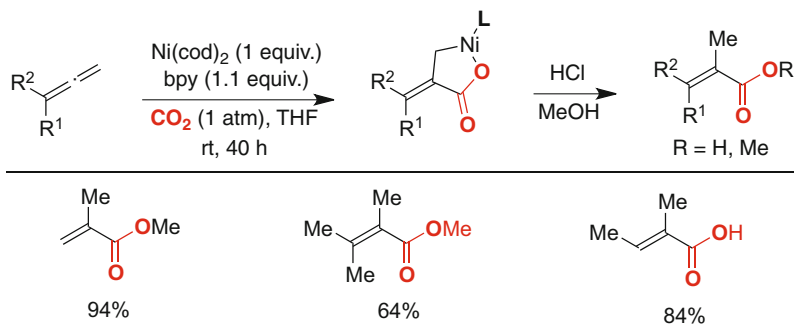
could compete with the Ni center for binding the carboxylate moiety. Specifically, the authors could enable the  $\beta$ -hydride elimination event by adding lithium iodide and triethylamine as base [100]. Furthermore, DFT calculations predicted an improved behavior of  $\text{Li}^+$  compared to  $\text{Na}^+$  when promoting the ring opening of the nickelalactone followed by  $\beta$ -hydride elimination. A series of experiments led to the optimal conditions for the carboxylation of ethylene using a regime based on  $\text{Ni(cod)}_2$ , dcpp [1,3-bis(dicyclohexylphosphino)propane] as ligand, LiI, triethylamine, and Zn, forming lithium acrylate in chlorobenzene at 50 °C with a *TON* of 21. The presence of overstoichiometric amounts of Zn was indispensable to avoid catalyst deactivation by converting  $[\text{Ni(dcpp)I}_2]$  to the corresponding propagating active Ni(0) species. More recently, Schaub has further improved the catalytic preparation of acrylates avoiding the use of stoichiometric Zn [101], thus univocally demonstrating that this technology is still at its infancy for producing industrially relevant acrylic acid from ethylene and  $\text{CO}_2$  [102].

## 4 Carboxylation of Multiple Unsaturated Systems

### 4.1 Allenes

#### 4.1.1 Stoichiometric Reactions Using Allenes

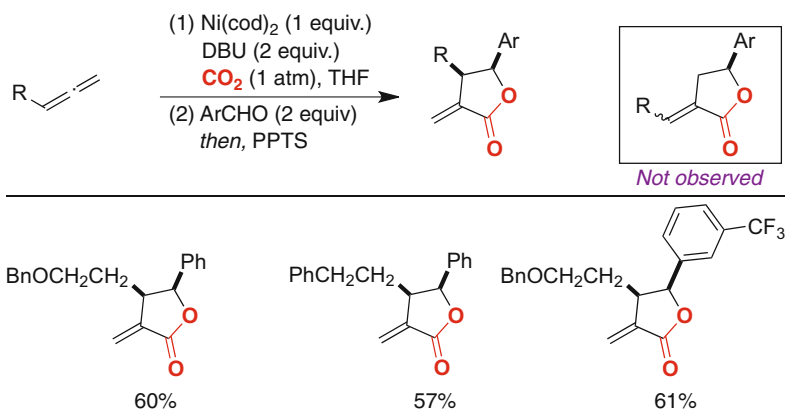
In 1984, Hoberg reported the first Ni(0)-mediated carboxylation of allenes with  $\text{CO}_2$  (Scheme 28) [103]. Interestingly, the reaction turned out to be highly regio- and stereoselective, as illustrated by the fact that a wide variety of compounds were obtained as single products. Specifically, it was found that the reaction proceeds via the formation of the less-hindered nickelalactone and that the corresponding *E*-isomer was formed preferentially. Subsequently, Mori reported that DBU could efficiently be used for an otherwise identical transformation [104]. Interestingly, the utilization of 1-silyl-3-alkyl-substituted allenes turned out to be highly advantageous, obtaining high yields of the targeted products and with an excellent regioselectivity profile



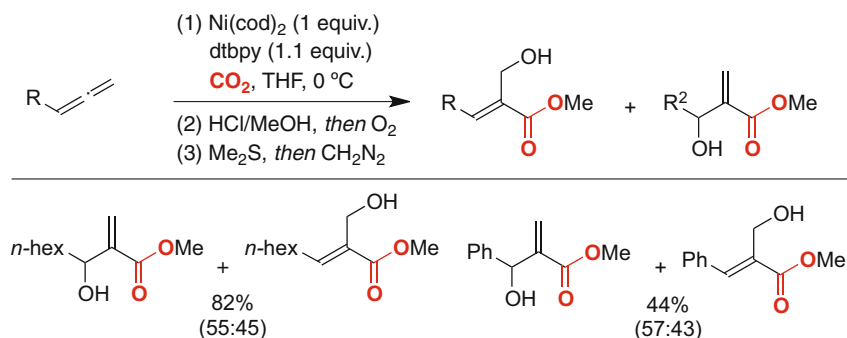
**Scheme 28** Ni(0)-mediated carboxylation of allenes reported by Hoberg [103]

[105]. In 2004, the Iwasawa group disclosed the use of bidentate bis-amidine ligands in the Ni-mediated carboxylation of allenes, obtaining regioisomeric mixtures of the targeted carboxylic acids, an issue that can be tentatively attributed to the in situ formation of two regioisomeric nickelalactones [37].

The Mori group demonstrated the viability of trapping the intermediate nickelalactone deriving from an allene, Ni(0) and CO<sub>2</sub> with electrophiles other than a proton source. Specifically, it was found that lactones possessing an exocyclic double bond are within reach upon treatment with aldehydes and a final acidic workup with pyridinium *p*-toluenesulfonate (PPTS) (**Scheme 29**) [104]. Interestingly, the regioselectivity observed differs from that shown in the absence of ArCHO upon simple acidic workup, suggesting that the selectivity switch depends predominantly on the electrophile utilized. With all the experimental results in hand, the authors proposed that the observed regioselectivity could be dictated by two alternate pathways dealing with the intermediacy of  $\pi$ -allyl Ni intermediate or the formation of a single nickelalactone intermediate that would evolve to the targeted product via *ipso* substitution. Recently, the Sato group demonstrated the possibility



**Scheme 29** Ni(0)-mediated lactone formation from allenes and CO<sub>2</sub> [104]



**Scheme 30** Oxidative cleavage of allene-derived nickelalactones using O<sub>2</sub> [107]

of conducting an otherwise related transformation, but in an intramolecular fashion [106].

In 2007, Iwasawa reported an interesting oxidative cleavage of the nickelalactone intermediates utilizing oxygen as oxidizing agent (Scheme 30) [107]. Unlike previous carboxylation of allene intermediates, the reaction resulted in regioisomeric mixtures of allylic alcohols, with a slight preference for the corresponding secondary alcohol. The authors rationalized these results via the involvement of a  $\pi$ -allyl Ni(II)-intermediate, although it was not possible to rule out an alternative based on the formation of regioisomeric  $\sigma$ -complexes.

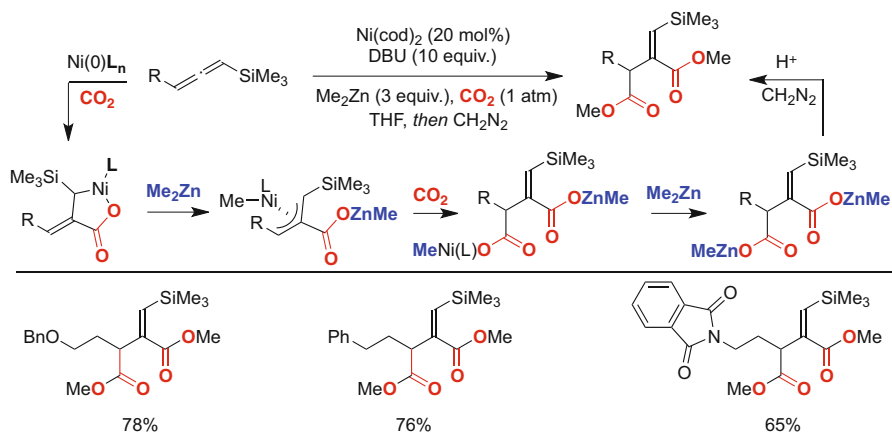
#### 4.1.2 Catalytic Processes Involving Allenes as Substrates

Unlike the wealth of literature data on stoichiometric reactions of allenes with CO<sub>2</sub>, a limited number of Ni-catalyzed protocols have been reported. Prompted by the seminal electrochemical method reported by Duñach [108], Mori and Sato described a Ni-catalyzed carboxylation of 1-silyl-3-alkyl-substituted allenes using Me<sub>2</sub>Zn (Scheme 31) [109]. Interestingly, the transformation occurred with a neat incorporation of two molecules of CO<sub>2</sub> into the allene backbone, producing a single regioisomer and with high yields. The observed regioselectivity was in agreement with the initial stoichiometric studies reported by Mori when dealing with silanes [105] and carbonyl-type electrophiles [104], via the intermediacy of  $\pi$ -allyl intermediates. It was believed that the inclusion of Me<sub>2</sub>Zn triggered a transmetalation event of in situ generated nickelalactone, thus forming a nucleophilic allyl Ni(II)-methyl species that trigger a subsequent carboxylation event instead of a reductive elimination event.

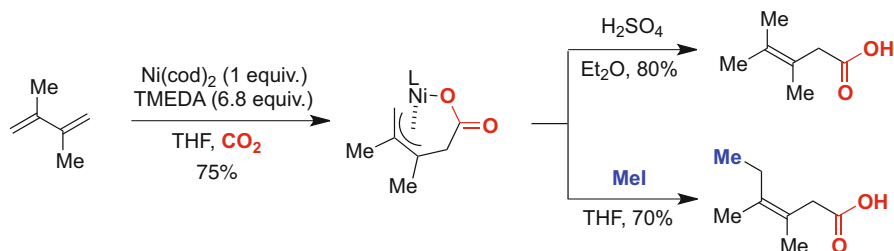
## 4.2 Dienes and Related Unsaturated Systems

### 4.2.1 Stoichiometric Studies

In 1982, Walther disclosed a stoichiometric carboxylation of 2,3-dimethyl butadiene using Ni(0) with TMEDA as ligand (Scheme 32) [110, 111]. The authors isolated



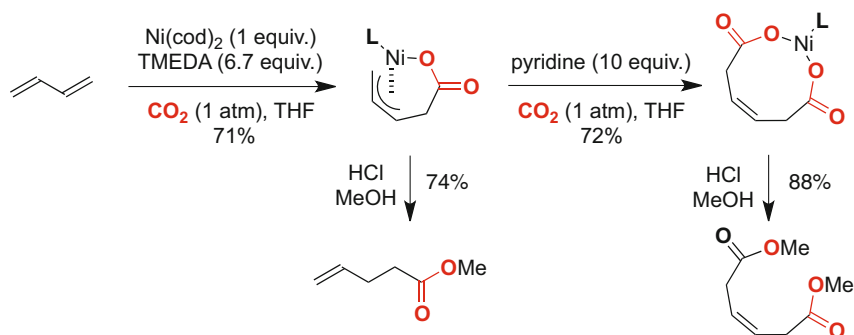
**Scheme 31** Ni-catalyzed double carboxylation of allenes [109]



**Scheme 32** Walther's studies on the Ni-mediated carboxylation of 2,3-dimethyl butadiene [110, 111]

and fully characterized by X-ray crystallography a  $\pi$ -allyl complex that formally consisted of a 1:1:1 adduct of a butadiene derivative, Ni-TMEDA, and  $\text{CO}_2$ . Stoichiometric studies revealed that these species could be converted into the targeted carboxylic acids by either treatment with aqueous  $\text{H}_2\text{SO}_4$  or MeI. In the latter case, a formal homologation of the 1,3-diene backbone was achieved, an observation that is consistent with a nucleophilic attack of the more basic C-Ni bond to MeI.

In parallel to these investigations, Hoberg studied a very similar process using butadiene as model substrate (Scheme 33) [112, 113]. In this case, however, the corresponding  $\pi$ -allyl Ni(II) intermediate could not be isolated in its pure form. Indirect evidence for such intermediate, however, was revealed upon quenching with aqueous HCl and subsequent MeOH treatment, as the corresponding methyl ester possessing a terminal double bond on the side-chain was exclusively observed. Unlike the Walther method, this protocol ended up in the corresponding terminal alkenes, an observation that is tentatively ascribed to the substitution pattern present on the diene backbone. More interestingly, (*Z*)-dimethyl-3-hexenedioate was found to be within reach via a subsequent  $\text{CO}_2$  from the nickelalactone intermediate [113, 114].

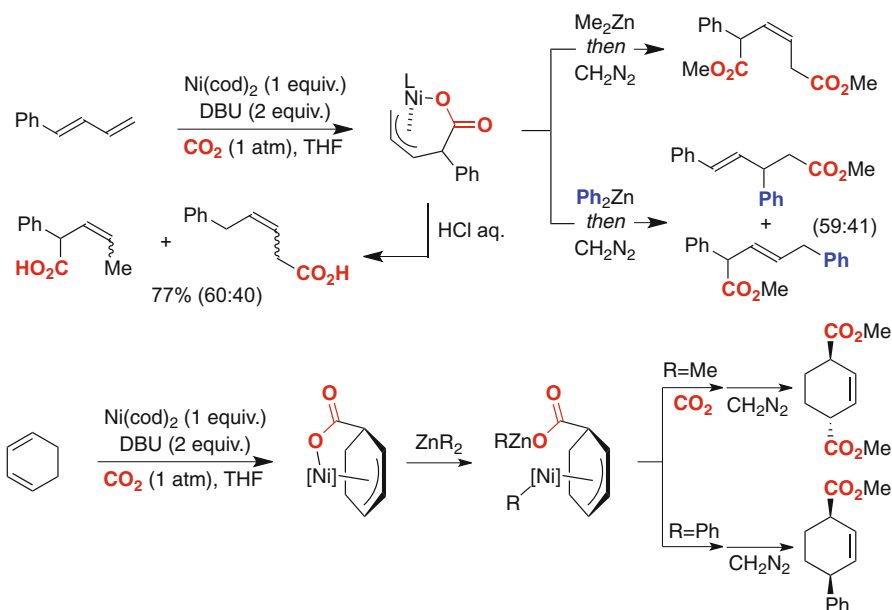


**Scheme 33** Hoberg's studies on the Ni-mediated mono- and bis-carboxylation of butadiene [112, 113]

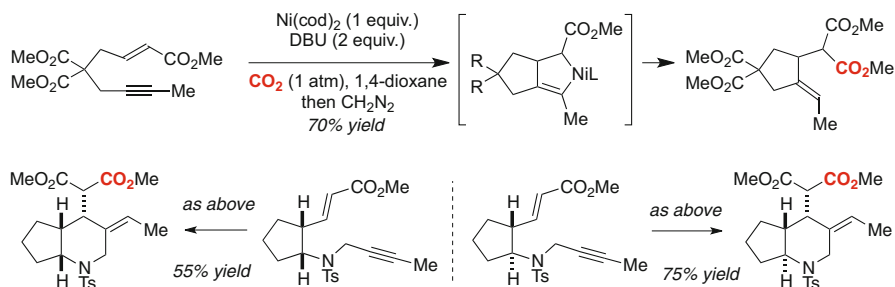
Behr and Kanne studied the behavior of trienes bearing both an isolated olefin and a conjugated 1,3-diene moiety under similar conditions, demonstrating that the carboxylation event is selective for 1,3-dienes and that the isolated olefin does not affect the outcome of the reaction [115]. Hoberg showed that an otherwise identical mono- and bis-carboxylation could also be achieved using Fe-complexes [116]. Kinetic studies by Geyer and Schindler using isoprene as model compound highlighted the importance of the ligands employed, suggesting that future catalytic variants should be focused on ligand design [117]. Furthermore, Saito, Yamamoto and coworkers showed that mono-carboxylation of 1,3-unsaturated backbones can be accomplished using enynes and diynes, in which CO<sub>2</sub> insertion occurred at the alkyne terminus and at the less-hindered site [36].

In 2001, a significant step-forward the development of a catalytic methodology was reported by Takimoto and Mori (Scheme 34) [118]. In this work, the authors described that DBU significantly increased the efficiency of the initial  $\pi$ -allyl Ni(II) complex. Simple protonolysis of such adduct resulted in a mixture of regioisomers, with slight preference for the carboxylation at the benzylic position. Interestingly, while a *cis*-configured double carboxylation product was obtained upon treatment with CO<sub>2</sub> in the presence of Me<sub>2</sub>Zn, the inclusion of Ph<sub>2</sub>Zn delivered a mixture of *trans*-configured monocarboxylation products. The rationale behind these results was attributed to a change in mechanism; while the second carboxylation event occurs by a CO<sub>2</sub> insertion into the allyl C(sp<sup>3</sup>)-Ni bond, the presence of Ph<sub>2</sub>Zn triggers a fast transmetalation followed by reductive elimination. Such hypothesis could be corroborated by conducting a reaction with cyclohexadiene as substrate, observing that the double carboxylation with Me<sub>2</sub>Zn gave rise to the *trans*-product whereas a *cis*-isomer was obtained upon treatment with Ph<sub>2</sub>Zn.

In 2005, Sato and Mori described the viability of performing a carboxylation of 1,6- and 1,7-enynes mediated by Ni(cod)<sub>2</sub> and DBU (Scheme 35) [119, 120]. Unlike the previous method reported by Mori [118], conjugation of the two  $\pi$ -components was not required; unfortunately, however, the method was limited to a rather specific class of substrates with a Thorpe-Ingold effect for building up five- and six-membered rings, in all cases requiring the presence of electron-withdrawing substituents at the olefin backbone. Still, excellent diastereoselectivities were



**Scheme 34** Reactivity of 1,3-diene:CO<sub>2</sub>:Ni adducts [118]



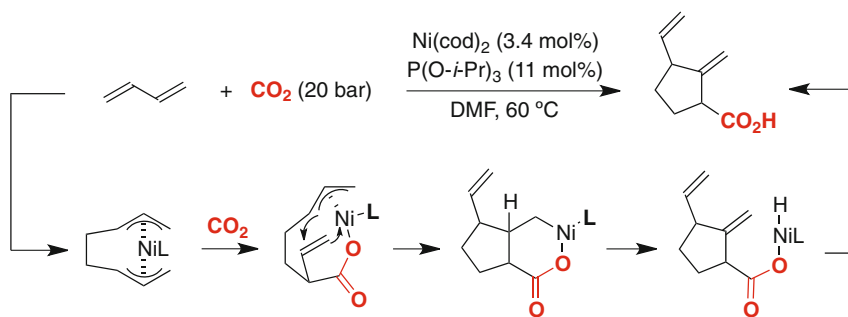
**Scheme 35** Ni-mediated cyclization/carboxylation reaction of 1,6-enynes [119, 120]

observed in all cases analyzed, thus setting the stage for the application of this protocol for natural product synthesis as well as for the design of a catalytic process [121].

#### 4.2.2 Catalytic Carboxylation of 1,3-dienes

In 1987, Hoberg pioneered the development of a catalytic carboxylation of butadiene using CO<sub>2</sub> at high pressures, resulting in cyclopentane carboxylic acids deriving from a dimerization/carboxylation event (**Scheme 36**) [122]. Although low turnover numbers were obtained, the molecular complexity achieved in this carboxylation event is certainly noteworthy. The postulated catalytic cycle consisted



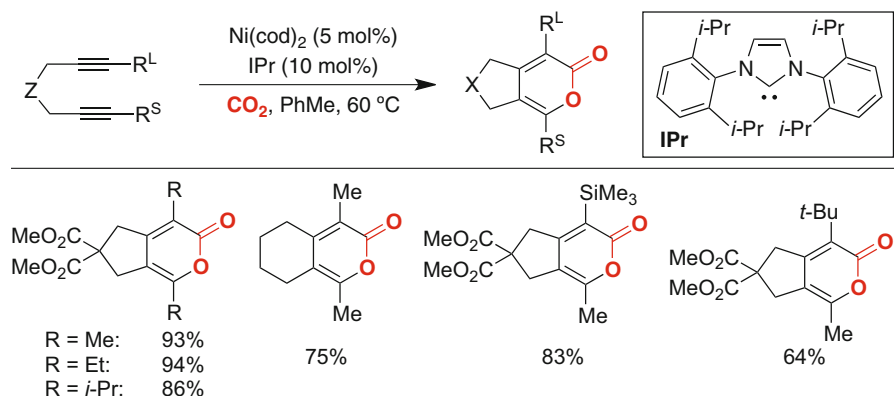


**Scheme 36** Ni-catalyzed butadiene dimerization/carboxylation at high pressure CO<sub>2</sub> [122]

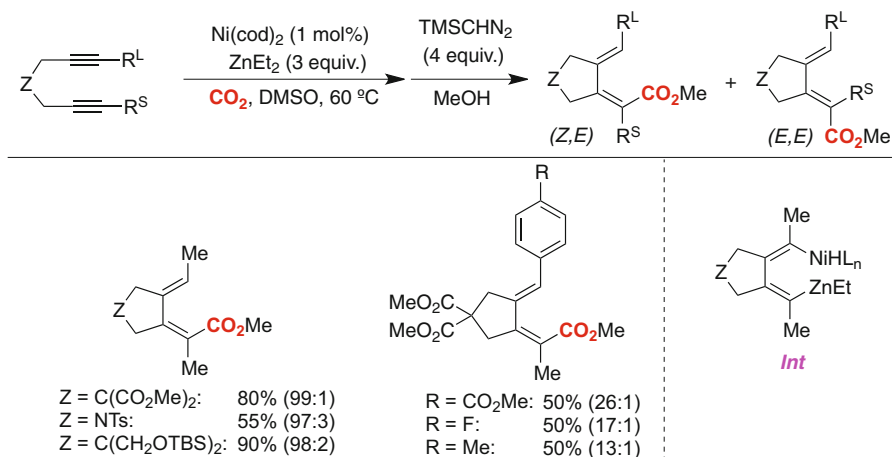
of an initial dimerization of butadiene followed by CO<sub>2</sub> insertion into the C–Ni bond. The resulting  $\pi$ -allyl Ni(II) species triggered an intramolecular carbometallation en route to a six-membered nickelacycle that likely evolves via  $\beta$ -hydride elimination and a final reductive elimination while recovering back the propagating Ni(0) species. Unfortunately, no details were indicated regarding the stereochemistry of the final carboxylated product.

Shortly after, the group of Tsuda and Saegusa reported their studies on the Ni-catalyzed carboxylative cyclization of 1,6- and 1,7-diyne using phosphine ligands at high pressure CO<sub>2</sub> (50 bar) [123, 124]. Unlike the dimerization protocol described by Hoberg, this reaction was proposed to proceed through an initial nickelalactone formation with one of the alkyne terminus followed by carbometallation with the pending alkyne, leading to a seven-membered intermediate that ultimately gives rise to a bicyclic  $\alpha$ -pyrone while regenerating the active Ni(0) catalyst. While the mechanistic rationale invoked that CO<sub>2</sub> insertion occurred at the less hindered alkyne, Louie revealed in a subsequent study that the regiochemistry was misassigned and that CO<sub>2</sub> insertion occurs adjacent to the most sterically hindered site, consistent with the preferential formation of a nickelalactone with the most sterically hindered alkyne (Scheme 37) [125, 126]. In contrast to the protocol described by Tsuda and Saegusa, Louie employed *N*-heterocyclic carbene ligands (NHC), enabling to operate at atmospheric pressure of CO<sub>2</sub> under exceptional mild conditions. In all cases analyzed, good yields and excellent regioselectivities of the corresponding bicyclic  $\alpha$ -pyrones were obtained for unsymmetrical diynes, regardless of whether substituents at the tether were present or not. This observation was further corroborated by X-ray crystallographic analysis.

Very recently, the group of Ma has reported the hydrocarboxylation of similar 1,6- or 1,7-diyne compounds giving rise to the corresponding methyl 2,4-alkadienoate esters after treatment with CH<sub>2</sub>N<sub>2</sub> (Scheme 38) [127]. The reaction is remarkably regioselective in the case of diynes containing aliphatic substituents, providing the corresponding (Z,E)-carboxylic acids in high yields. However, mixtures of the two possible (Z,E) and (E,E) isomers were found when using aryl substituents, especially bearing electron-withdrawing groups, with preferential formation of the (Z,E)-product. After gathering some mechanistic insights, the



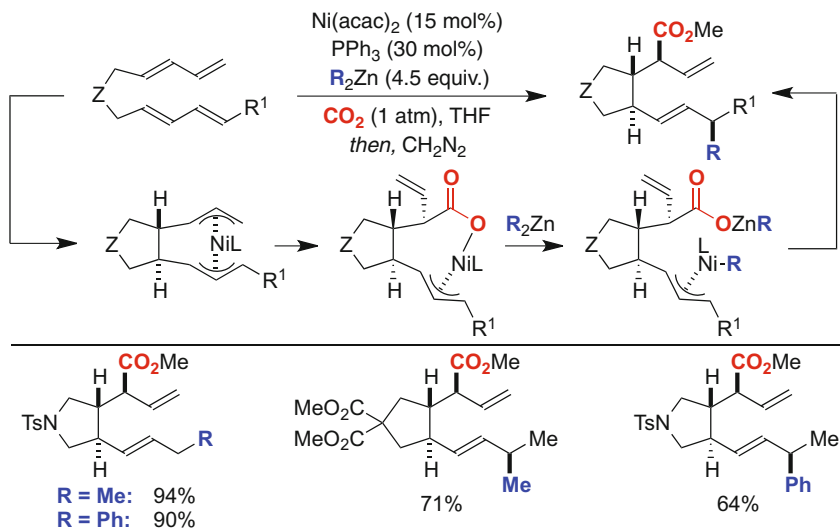
**Scheme 37** Ni-catalyzed carboxylative cyclization of 1,6 and 1,7-diyne [125, 126]



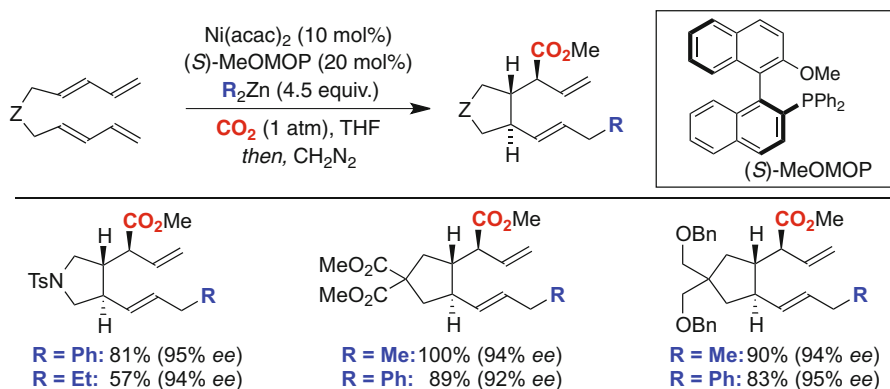
**Scheme 38** Ni-catalyzed regioselective hydrocarboxylation of 1,6 and 1,7-diyne [127]

authors explained the formation of the products via an alkyne-directed hydrocarboxylation pathway. First, the Ni(0) active species oxidatively inserts into the more electron-rich alkyne followed by a transmetalation with  $\text{ZnEt}_2$ . After  $\beta$ -hydride elimination, the in situ generated Ni–H intermediate inserts into the second alkyne leading to **Int** (Scheme 38). Finally, C–H bond-forming reductive elimination followed by carboxylation of the organozinc species ultimately affords the corresponding products.

Following up on their previous stoichiometric work, Takimoto and Mori disclosed a Ni-catalyzed carboxylative cyclization of bis(1,3-dienes) possessing substituents at the tether with  $\text{CO}_2$  and organozinc reagents (Scheme 39) [128]. The reaction was proposed to proceed via initial intramolecular dimerization of two diene moieties, leading to a bis- $\pi$ -allyl Ni(II) intermediate that rapidly reacts with  $\text{CO}_2$ , resulting in a



Scheme 39 Ni-catalyzed cyclization/carboxylation of bis(1,3-dienes) [128]



Scheme 40 Enantioselective Ni-catalyzed cyclization/carboxylation of bis(1,3-dienes) [129]

$\pi$ -allyl carboxylate Ni(II) that was inherently disposed to a transmetalation with organozinc species. A final reductive elimination delivers the zinc carboxylate that ultimately is treated with  $\text{CH}_2\text{N}_2$  to afford the final ester motifs. The high diastereoselectivity observed is inevitably linked to the initial cyclization step that is facilitated by the presence of substituents at the tether. Furthermore, the utilization of unsymmetric bis(1,3-dienes) resulted in a  $\text{CO}_2$  insertion at the less hindered site. Interestingly, the nature of the organozinc derivative exerted a profound influence on the reaction outcome; while  $\text{Me}_2\text{Zn}$  and  $\text{Ar}_2\text{Zn}$  invariably provided good results, competitive  $\beta$ -hydride elimination was found when employing  $\text{Et}_2\text{Zn}$ .

In 2004, Mori and coworkers expanded the synthetic utility of the carboxylation of bis(1,3-dienes) by designing an enantioselective variant based on a MeO-MOP regime (Scheme 40) [129]. In all cases analyzed, excellent yields and enantioselectivities were

obtained for a wide range of substrates. Unlike the corresponding racemic version based on  $\text{PPh}_3$  (Scheme 39), the authors found that the chiral ligand utilized largely suppressed the parasitic  $\beta$ -hydride elimination when utilizing  $\text{Et}_2\text{Zn}$ . Interestingly, the reduced product was formed with an otherwise identical degree of enantioinduction, an observation that is in good agreement with the mechanistic rationale highlighted in Scheme 39, thus implying that the pathways leading to both product and reduced species only diverge after the enantiodetermining step has already occurred.

## 5 Conclusions and Future Perspective

The seminal stoichiometric studies reported by Hoberg in the early 1980s revealed the unique features of nickelalactones, compounds that derive from an oxidative cyclization of olefins and  $\text{CO}_2$ . This seemingly trivial discovery triggered unimaginable consequences in the field of organic synthesis, allowing for designing unconventional carboxylation techniques using  $\text{CO}_2$  as coupling partner. Indeed, the recent years have witnessed a meteoric development of Ni- and Fe-catalyzed carboxylation protocols, providing new dogmas for promoting  $\text{CO}_2$  insertion into unsaturated hydrocarbons, building blocks of utmost synthetic and industrial relevance. Despite the impressive preparative advances realized, there are ample opportunities in this vibrant research field as daunting challenges still need to be addressed in this area of expertise: (1) the regioselectivity of the corresponding carboxylation event is typically problematic when dealing with intermolecular techniques; (2) the vast majority of catalytic carboxylation events of unsaturated hydrocarbons remain confined to the utilization of well-defined, and air-sensitive stoichiometric organometallic species; (3) catalytic carboxylation techniques of alkenes are still rather substrate-specific, and a general solution to accommodate either styrenes or less activated  $\alpha$ -olefins remains rather elusive; (4) the preparation of industrially relevant acrylic acid derivatives from ethylene requires the design of an optimal catalytic protocol capable of operating at high turnover numbers under mild reaction conditions; (5) catalytic enantioselective carboxylation events are scarce. Taking into consideration the impressive knowledge acquired in catalytic endeavors, we are certainly optimistic that many of these challenges will be addressed in the near future, allowing for the implementation of green, efficient, and practical catalytic carboxylation methods that will create new paradigms in retrosynthetic analysis to be utilized in both industrial and academic laboratories. A long-term goal will obviously deal with the opportunity of mimicking nature by designing artificial catalytic photosynthesis in which  $\text{CO}_2$  is incorporated into organic matter with visible light.

**Acknowledgments** We thank ICIQ, European Research Council (ERC-277883), MINECO (CTQ2015-65496-R & Severo Ochoa Excellence Accreditation 2014-2018, SEV-2013-0319) and Cellex Foundation for support. E. Serrano, M. van Gemmeren and F. Juliá-Hernández thank MINECO, Alexander von Humboldt Foundation and COFUND for predoctoral and postdoctoral fellowships, respectively.

## References

1. Aresta M (1999) Recovery and utilisation of carbon dioxide. RUCADI, EU Report
2. von der Assen N, Voll P, Peters M, Bardow A (2014) Life cycle assessment of CO<sub>2</sub> capture and utilization: a tutorial review. *Chem Soc Rev* 43:7982–7994
3. Aresta M, Dibenedetto A, Angelini A (2014) Catalysis for the valorization of exhaust carbon: from CO<sub>2</sub> to chemicals, materials, and fuels. technological use of CO<sub>2</sub>. *Chem Rev* 114:1709–1742
4. Assen N, Muller LJ, Steingrube A, Voll P, Bardow A (2016) Selecting CO<sub>2</sub> sources for CO<sub>2</sub> utilization by environmental-merit-order Curves. *Environ Sci Technol* 50:1093–1101
5. Meylan FD, Moreau V, Erkman S (2015) CO<sub>2</sub> utilization in the perspective of industrial ecology, an overview. *J CO<sub>2</sub> Util* 12:101–108
6. Mikkelsen M, Jørgensen M, Krebs FC (2010) The teraton challenge. A review of fixation and transformation of carbon dioxide. *Energy Environ Sci* 3:43–81
7. Wang S, Du G, Xi C (2016) Copper-catalyzed carboxylation reactions using carbon dioxide. *Org Biomol Chem* 14:3666–3676
8. Sekine K, Yamada T (2016) Silver-catalyzed carboxylation. *Chem Soc Rev*. doi:10.1039/c5cs00895f
9. Yu D, Teong SP, Zhang Y (2015) Transition metal complex catalyzed carboxylation reactions with CO<sub>2</sub>. *Coord Chem Rev* 293–294:279–291
10. Guo C-X, Yu B, Ma R, He L-N (2015) Metal-promoted carboxylation of alkynes/allenes with carbon dioxide. *Curr Green Chem* 2:14–25
11. Industrial-scale preparation of low molecular weight acids is mainly carried out by carbonylation and/or oxidation of the corresponding alcohols and light olefins. See for instance: Samel U-R, Kohler W, Gamer A O, Keuser U, Yang S-T, Jin Y, Lin M, Wang Z (2014) Propionic acid and derivatives. *Ullmann's Encyclopedia of Industrial Chemistry* 1–20
12. Correa A, Martin R (2009) Metal-catalyzed carboxylation of organometallic reagents with carbon dioxide. *Angew Chem Int Ed* 48:6201–6204
13. Brill M, Lazreg F, Cazin CSJ, Nolan SP (2016) Transition metal-catalyzed carboxylation of organic substrates with carbon dioxide. *Top Organomet Chem* 53:225–278
14. Correa A, Leon T, Martin R (2014) Ni-catalyzed carboxylation of C(sp<sup>2</sup>)- and C(sp<sup>3</sup>)-O bonds with CO<sub>2</sub>. *J Am Chem Soc* 136:1062–1069
15. Moragas T, Gaydou M, Martin R (2016) Ni-catalyzed carboxylation of benzylic C–N bonds with CO<sub>2</sub>. *Angew Chem Int Ed* 55:5053–5057
16. Wang X, Liu Y, Martin R (2015) Ni-catalyzed divergent cyclization/carboxylation of unactivated primary and secondary alkyl halides with CO<sub>2</sub>. *J Am Chem Soc* 137:6476–6479
17. Aresta M, Dibenedetto A, Quaranta E (2016) Interaction of CO<sub>2</sub> with C–C multiple bonds. Reaction mechanisms in carbon dioxide conversion: doi:10.1007/978-3-662-46831-9\_5
18. Aresta M, Nobile CF, Albano VG, Forni E, Manassero M (1975) New nickel–carbon dioxide complex: synthesis, properties, and crystallographic characterization of (carbon dioxide)-bis(tricyclohexylphosphine)nickel. *J Chem Soc Chem Commun*. doi:10.1039/c39750000636
19. Rintjema J, Peña Carrodeguas L, Laserna V, Sopena S, Kleij AW (2015) Metal complexes catalyzed cyclization with CO<sub>2</sub>. *Top Organomet Chem* 53:39–71
20. Coates GW, Moore DR (2004) Discrete metal-based catalysts for the copolymerization of CO<sub>2</sub> and epoxides: discovery, reactivity, optimization, and mechanism. *Angew Chem Int Ed* 43:6618–6639
21. Sa-A G, Sivaram S (1996) Organic carbonates. *Chem Rev* 96:951–976
22. Federsel C, Jackstell R, Beller M (2010) State-of-the-art catalysts for hydrogenation of carbon dioxide. *Angew Chem Int Ed* 49:6254–6257
23. Wang W, Wang S, Ma X, Gong J (2011) Recent advances in catalytic hydrogenation of carbon dioxide. *Chem Soc Rev* 40:3703–3727
24. Goepfert A, Czaun M, Jones JP, Surya Prakash GK, Olah GA (2014) Recycling of carbon dioxide to methanol and derived products—closing the loop. *Chem Soc Rev* 43:7995–8048
25. Matthesen R, Fransær J, Binnemans K, De Vos DE (2014) Electrocarboxylation: towards sustainable and efficient synthesis of valuable carboxylic acids. *Beilstein J Org Chem* 10:2484–2500
26. Nogi K, Fujihara T, Terao J, Tsuji Y (2016) Carboxyzincation employing carbon dioxide and zinc powder: cobalt-catalyzed multicomponent coupling reactions with alkynes. *J Am Chem Soc* 138:5547–5550
27. Beller M, Gu X-F (2013) Transition metal catalyzed carbonylation reactions. Springer, New York

28. Fujihara T, Nogi K, Xu T, Terao J, Tsuji Y (2012) Nickel-catalyzed carboxylation of aryl and vinyl chlorides employing carbon dioxide. *J Am Chem Soc* 134:9106–9109
29. Liu Y, Cornella J, Martin R (2014) Ni-catalyzed carboxylation of unactivated primary alkyl bromides and sulfonates with CO<sub>2</sub>. *J Am Chem Soc* 136:11212–11215
30. Inoue Y, Itoh Y, Hashimoto H (1977) Incorporation of carbon dioxide in alkyne oligomerization catalyzed by nickel(0) complexes. Formation of substituted 2-pyrones. *Chem Lett* 6:855–856
31. Burkhart G, Hoberg H (1982) Oxanickelacyclopentene derivatives from Nickel(0), carbon dioxide, and alkynes. *Angew Chem Int Ed* 21:76
32. Sakaki S, Mine K, Taguchi D, Arai T (1993) Formation of the oxanickelacyclopentene complex from nickel(0), carbon dioxide, and alkyne. An ab initio MO/SD-CI study. *Bull Chem Soc Jpn* 66:3289–3299
33. Sakaki S, Mine K, Hamada T, Arai T (1995) Formation of the oxanickelacyclopentene complex from nickel(0), carbon dioxide, and alkyne. An ab initio MO/SD-CI Study. Part II. Reactivity and regioselectivity of hydroxyacetylene. *Bull Chem Soc Jpn* 68:1873–1882
34. Graham DC, Bruce MI, Metha GF, Bowie JH, Buntine MA (2008) Regioselective control of the nickel-mediated coupling of acetylene and carbon dioxide—a DFT study. *J Organomet Chem* 693:2703–2710
35. Li J, Jia G, Lin Z (2008) Theoretical studies on coupling reactions of carbon dioxide with alkynes mediated by Nickel(0) complexes. *Organometallics* 27:3892–3900
36. Saito S, Nakagawa S, Koizumi T, Hirayama K, Yamamoto Y (1999) Nickel-mediated regio- and chemoselective carboxylation of alkynes in the presence of carbon dioxide. *J Org Chem* 64:3975–3978
37. Aoki M, Kaneko M, Izumi S, Ukai K, Iwasawa N (2004) Bidentate amidine ligands for nickel(0)-mediated coupling of carbon dioxide with unsaturated hydrocarbons. *Chem Commun* 36(22):2568–2569
38. Takimoto M, Shimizu K, Mori M (2001) Nickel-promoted alkylative or arylative carboxylation of alkynes. *Org Lett* 3:3345–3347
39. Shimizu K, Takimoto M, Mori M (2003) Novel synthesis of heterocycles having a functionalized carbon center via Nickel-mediated carboxylation: total synthesis of Erythrocarine. *Org Lett* 5:2323–2325
40. Shimizu K, Takimoto M, Sato Y, Mori M (2006) Total synthesis of (±)-erythrocarine using diene-yne metathesis. *J Organomet Chem* 691:5466–5475
41. Saito N, Sun Z, Sato Y (2015) Nickel-promoted highly regioselective carboxylation of aryl ynol ether and its application to the synthesis of chiral beta-aryloxypropionic acid derivatives. *Chem Asian J* 10:1170–1176
42. Inoue Y, Itoh Y, Hashimoto H (1978) Oligomerization of 3-hexyne by nickel(0) complexes under CO<sub>2</sub>. Incorporation of CO<sub>2</sub> and novel cyclotrimerization. *Chem Lett* 7:633–634
43. Inoue Y, Itoh Y, Kazama H, Hashimoto H (1980) Reaction of dialkyl-substituted alkynes with carbon dioxide catalyzed by nickel(0) complexes. Incorporation of carbon dioxide in alkyne dimers and novel cyclotrimerization of the alkynes. *Bull Chem Soc Jpn* 53:3329–3333
44. Walther D, Schönberg H, Dinjus E (1987) Aktivierung von Kohlendioxid an Übergangsmetallzentren: selektive Cooligomerisation mit Hexin durch das Katalysatorsystem Acetonitril/trialkylphosphan/nickel(0) und Struktur eines Nickel(0)-Komplexes mit side-on gebundenem Acetonitril. *J Org Chem* 334:377–388
45. Tsuda T, Kunisada K, Nagahama N, Morikawa S, Saegusa T (1989) Nickel(0)-catalyzed cycloaddition of ethoxyethyne with carbon dioxide to 4,5-diethoxy- $\alpha$ -pyrone. *Synth Commun* 19:1575–1581
46. Tsuda T, Hasegawa N, Saegusa T (1990) Nickel(0)-catalyzed novel co-oligomerization of ethoxy(trimethylsilyl)ethyne with carbon dioxide to 4,6-diethoxy-3-[1-ethoxy-2,2-bis(trimethylsilyl)vinyl]-5-(trimethylsilyl)-2-pyrone. *J Chem Soc, Chem Commun* 945–947
47. Hoberg H, Schaefer D, Burkhart G, Krüger C, Romao MJ (1984) Nickel(0)-induzierte C-C-Verknüpfung zwischen Kohlendioxid und Alkinen sowie Alkenen. *J Organomet Chem* 266:203–224
48. Mori M (2007) Regio- and stereoselective synthesis of tri- and tetrasubstituted alkenes by introduction of CO<sub>2</sub> and alkylzinc reagents into alkynes. *Eur J Org Chem* 2007:4981–4993
49. Shimizu K, Takimoto M, Sato Y, Mori M (2005) Nickel-catalyzed regioselective synthesis of tetrasubstituted alkene using alkylative carboxylation of disubstituted alkyne. *Org Lett* 7:195–197
50. Sato Y, Mori M, Shimizu K, Takimoto M (2006) Effective synthesis of tamoxifen using nickel-catalyzed arylative carboxylation. *Synlett* 2006:3182–3184

51. Buchwald SL, Nielsen RB (1989) Selective, zirconium-mediated cross-coupling of alkynes: synthesis of isomerically pure 1,3-dienes and 1,4-diene 1,3-dienes. *J Am Chem Soc* 111:2870–2874
52. Fujihara T, Horimoto Y, Mizoe T, Sayyed FB, Tani Y, Terao J, Sakaki S, Tsuji Y (2014) Nickel-catalyzed double carboxylation of alkynes employing carbon dioxide. *Org Lett* 16:4960–4963
53. Li S, Yuan W, Ma S (2011) Highly regio- and stereoselective three-component nickel-catalyzed syn-hydrocarboxylation of alkynes with diethyl zinc and carbon dioxide. *Angew Chem Int Ed* 50:2578–2582
54. Fujihara T, Xu T, Semba K, Terao J, Tsuji Y (2011) Copper-catalyzed hydrocarboxylation of alkynes using carbon dioxide and hydrosilanes. *Angew Chem Int Ed* 50:523–527
55. Li S, Ma S (2011) Highly selective nickel-catalyzed methyl-carboxylation of homopropargylic alcohols for  $\alpha$ -alkylidene- $\gamma$ -butyrolactones. *Org Lett* 13:6046–6049
56. Li S, Ma S (2012) CO<sub>2</sub>-activation for gamma-butyrolactones and its application in the total synthesis of (±)-heteroplexisolide E. *Chem Asian J* 7:2411–2418
57. Wang X, Nakajima M, Martin R (2015) Ni-catalyzed regioselective hydrocarboxylation of alkynes with CO<sub>2</sub> by using simple alcohols as proton sources. *J Am Chem Soc* 137:8924–8927
58. Trost BM, Ball ZT (2005) Addition of metalloid hydrides to alkynes: hydrometallation with Boron, Silicon, and Tin. *Synthesis* 6:853–887
59. Fu M-C, Shang R, Cheng W-M, Fu Y (2016) Nickel-catalyzed regio- and stereoselective hydrocarboxylation of alkynes with formic acid through catalytic CO recycling. *ACS Catal* 6:2501–2505
60. Hoberg H, Schaefer D (1982) Nickel(0)-induzierte C-C Verknüpfung zwischen alkenen und kohlendioxid. *J Organomet Chem* 236:C28–C30
61. Hoberg H, Schaefer D (1983) Nickel(0)-induzierte C-C Verknüpfung zwischen kohlendioxid und etylen sowie mono- oder di-substituierten alkenen. *J Organomet Chem* 1983:C51–C53
62. Hoberg H, Peres Y, Milchereit A (1986) C-C Verknüpfung von alkenen mit CO<sub>2</sub> an Nickel(0); Herstellung von zimtsaure aus styrol. *J Organomet Chem* 307:C38–C40
63. Hoberg H, Ballesteros A, Sigan A, Jegat C, Barhausen D, Milchereit A (1991) Ligandgesteuerte ringkontraktion von Nickela-funfin vierringkomplexe-neuartige startsysteme für die preparative Chemie. *J Organomet Chem* 407:C23–C29
64. Greenburg ZR, Jin D, Williard PG, Bernskoetter WH (2014) Nickel promoted functionalization of CO<sub>2</sub> to anhydrides and ketoacids. *Dalton Trans* 43:15990–15996
65. Murakami M, Ishida N, Miura T (2006) Solvent and ligand partition reaction pathways in nickel-mediated carboxylation of methylenecyclopropanes. *Chem Comm* 14(6):643–645
66. Guo C-H, Tian L-C, Jia J, Wu H-S (2014) Theoretical study on the nickel(0)-mediated coupling of carbon dioxide and benzylidencyclopropane: mechanism and selectivity. *Comput Theor Chem* 1044:44–54
67. Aresta M, Quaranta E, Tommasi I (1988) Reduction of coordinated carbon dioxide to carbon monoxide via protonation by thiols and other Bronsted acids by Ni-systems: a contribution to the understanding of the mode of action of the enzyme carbon monoxide dehydrogenase. *J Chem Soc, Chem Commun.* doi:10.1039/c39880000450
68. Aresta M, Gobetto R, Quaranta E, Tommasi I (1992) A bonding-reactivity relationship of Ni(PCy<sub>3</sub>)<sub>2</sub>(CO)<sub>2</sub>: a comparative solid-state-solution nuclear magnetic resonance study (31P, 13C) as a diagnostic tool to determine the mode of bonding of CO<sub>2</sub> to a metal center. *Inorg Chem* 31:4286–4290
69. Papai I, Schubert G, Mayer I, Besenyei G, Aresta M (2004) Mechanistic details of Nickel(0)-assisted oxidative coupling of CO<sub>2</sub> with C<sub>2</sub>H<sub>4</sub>. *Organometallics* 23:5252–5259
70. Yang G, Schäffner B, Blug M, Hensen EJM, Pidko EA (2014) A mechanistic study of Ni-catalyzed carbon dioxide coupling with ethylene towards the manufacture of acrylic acid. *Chem Cat Chem* 6:800–807
71. Plessow PN, Schäfer A, Limbach M, Hofmann P (2014) Acrylate formation from CO<sub>2</sub> and ethylene mediated by Nickel complexes: a theoretical study. *Organometallics* 33:3657–3668
72. Hoberg H, Peres Y, Kruger C, Tsay Y-H (1987) A 1-oxa-2-nickela-5-cyclopentanone from ethene and carbon dioxide: preparation, structure, and reactivity. *Angew Chem Int Ed* 26:771–773
73. Hoberg H, Jenni K, Angermund K, Kruger C (1987) C-C-Linkages of ethene with CO<sub>2</sub> on an Iron(0) complex - Synthesis and crystal structure analysis of [(PEt<sub>3</sub>)<sub>2</sub>Fe(C<sub>2</sub>H<sub>4</sub>)<sub>2</sub>]. *Angew Chem Int Ed* 26:153–155
74. Kirillov E, Carpentier JF, Bunel E (2015) Carboxylic acid derivatives via catalytic carboxylation of unsaturated hydrocarbons: whether the nature of a reductant may determine the mechanism of CO<sub>2</sub> incorporation? *Dalton Trans* 44:16212–16223



75. Lapidus AL, Pirozhkov SD, Koryakin AA (1978) Catalytic synthesis of propionic acid by carboxylation of ethylene with carbon dioxide. *Izvestiya Akademii Nauk SSSR, Seriya Khimicheskaya* 12:2814–2816
76. Williams CM, Johnson JB, Rovis T (2008) Nickel-catalyzed reductive carboxylation of styrenes using CO<sub>2</sub>. *J Am Chem Soc* 130:14936–14937
77. Yuan R, Lin Z (2014) Computational insight into the mechanism of Nickel-catalyzed reductive carboxylation of styrenes using CO<sub>2</sub>. *Organometallics* 33:7147–7156
78. Shirakawa E, Ikeda D, Masui S, Yoshida M, Hayashi T (2012) Iron-copper cooperative catalysis in the reactions of alkyl Grignard reagents: exchange reaction with alkenes and carbometalation of alkynes. *J Am Chem Soc* 134:272–279
79. Greenhalgh MD, Thomas SP (2012) Iron-catalyzed, highly regioselective synthesis of alpha-aryl carboxylic acids from styrene derivatives and CO<sub>2</sub>. *J Am Chem Soc* 134:11900–11903
80. Rio I, Claver C, van Leeuwen PWNM (2001) On the mechanism of the hydroxycarbonylation of styrene with palladium systems. *Eur J Inorg Chem* 2001:2719–2738
81. Smith BRJ, Loganathan M, Shantha MS (2010) A review of the water gas shift reaction kinetics. *Int J Chem React Eng* 8:1542
82. Ostapowicz TG, Schmitz M, Krystof M, Klankermayer J, Leitner W (2013) Carbon dioxide as a C(1) building block for the formation of carboxylic acids by formal catalytic hydrocarboxylation. *Angew Chem Int Ed* 52:12119–12123
83. González-Sebastián L, Flores-Alamo M, García JJ (2012) Nickel-catalyzed reductive hydroesterification of styrenes using CO<sub>2</sub> and MeOH. *Organometallics* 31:8200–8207
84. Wu L, Liu Q, Fleischer I, Jackstell R, Beller M (2014) Ruthenium-catalysed alkoxycarbonylation of alkenes with carbon dioxide. *Nat Commun* 5:3091
85. Yu B, Diao Z-F, Guo C-X, He L-N (2013) Carboxylation of olefins/alkynes with CO<sub>2</sub> to industrially relevant acrylic acid derivatives. *J CO<sub>2</sub> Util* 1:60–68
86. Limbach M (2015) Acrylates from alkenes and CO<sub>2</sub>, the stuff that dreams are made of. *Adv Organomet Chem* 63:175–202
87. Graham DC, Mitchell C, Bruce MI, Metha GF, Bowie JH, Buntine MA (2007) Production of acrylic acid through Nickel-mediated coupling of ethylene and carbon dioxide—a DFT Study. *Organometallics* 26:6784–6792
88. Fischer R, Langer J, Malassa A, Walther D, Gørls H, Vaughan G (2006) A key step in the formation of acrylic acid from CO<sub>2</sub> and ethylene: the transformation of a nickelalactone into a nickel-acrylate complex. *Chem Comm* 2510–2512
89. Bruckmeier C, Lehenmeier MW, Reichardt R, Vagin S, Rieger B (2010) Formation of methyl acrylate from CO<sub>2</sub> and ethylene via methylation of nickelalactones. *Organometallics* 29:2199–2202
90. Lee SY, Cokoja M, Drees M, Li Y, Mink J, Herrmann WA, Kuhn FE (2011) Transformation of nickelalactones to methyl acrylate: on the way to a catalytic conversion of carbon dioxide. *Chem Sus Chem* 4:1275–1279
91. Lee SYT, Ghani AA, D'Elia V, Cokoja M, Herrmann WA, Basset J-M, Kühn FE (2013) Liberation of methyl acrylate from metallalactone complexes via M–O ring opening (M=Ni, Pd) with methylation agents. *New J Chem* 37:3512
92. Plessow PN, Weigel L, Lindner R, Schäfer A, Rominger F, Limbach M, Hofmann P (2013) Mechanistic details of the Nickel-mediated formation of acrylates from CO<sub>2</sub>, ethylene and methyl iodide. *Organometallics* 32:3327–3338
93. Jin D, Schmeier TJ, Williard PG, Hazari N, Bernskoetter WH (2013) Lewis acid induced  $\beta$ -elimination from a nickelalactone: efforts toward acrylate production from CO<sub>2</sub> and ethylene. *Organometallics* 32:2152–2159
94. Guo W, Michel C, Schwiedernoch R, Wischert R, Xu X, Sautet P (2014) Formation of acrylates from ethylene and CO<sub>2</sub> on Ni complexes: a mechanistic viewpoint from a hybrid DFT approach. *Organometallics* 33:6369–6380
95. Jin D, Williard PG, Hazari N, Bernskoetter WH (2014) Effect of sodium cation on metallacyclobeta-hydride elimination in CO<sub>2</sub>-ethylene coupling to acrylates. *Chem Eur J* 20:3205–3211
96. Lejkowski ML, Lindner R, Kageyama T, Bodizs GE, Plessow PN, Müller IB, Schäfer A, Rominger F, Hofmann P, Futter C, Schunk SA, Limbach M (2012) The first catalytic synthesis of an acrylate from CO<sub>2</sub> and an alkene—a rational approach. *Chem Eur J* 18:14017–14025
97. Manzini S, Huguet N, Trapp O, Paciello RA, Schaub T (2016) Synthesis of acrylates from olefins and CO<sub>2</sub> using sodium alkoxides as bases. *Catal Today*. doi:10.1016/j.cattod.2016.03.025



98. Huguet N, Jevtovikj I, Gordillo A, Lejkowski ML, Lindner R, Bru M, Khalimon AY, Rominger F, Schunk SA, Hofmann P, Limbach M (2014) Nickel-catalyzed direct carboxylation of olefins with CO<sub>2</sub>: one-pot synthesis of alpha, beta-unsaturated carboxylic acid salts. *Chem Eur J* 20:16858–16862
99. Jevtovikj I, Manzini S, Hanauer M, Rominger F, Schaub T (2015) Investigations on the catalytic carboxylation of olefins with CO<sub>2</sub> towards alpha, beta-unsaturated carboxylic acid salts: characterization of intermediates and ligands as well as substrate effects. *Dalton Trans* 44:11083–11094
100. Hendriksen C, Pidko EA, Yang G, Schaffner B, Vogt D (2014) Catalytic formation of acrylate from carbon dioxide and ethene. *Chem Eur J* 20:12037–12040
101. Manzini S, Huguet N, Trapp O, Schaub T (2015) Palladium- and Nickel-catalyzed synthesis of sodium acrylate from ethylene, CO<sub>2</sub>, and phenolate bases: optimization of the catalytic system for a potential process. *Eur J Org Chem* 2015:7122–7130
102. Goossen LJ, Goossen K (2008) Nachhaltigkeit durch atomökonomische Synthesen. Aktuelle Wochenschau der GDCh:18
103. Hoberg H, Oster BW (1984) Nickel(0)-induzierte C–C-verknüpfung zwischen 1,2-dienen und kohlendioxid. *J Organomet Chem* 266:321–326
104. Takimoto M, Kawamura M, Mori M (2003) Nickel(0)-mediated sequential addition of carbon dioxide and aryl aldehydes into terminal allenes. *Org Lett* 5:2599–2601
105. Takimoto M, Kawamura M, Mori M (2004) Nickel-mediated regio- and stereoselective carboxylation of trimethylsilyllallene under an atmosphere of carbon dioxide. *Synthesis* 2004:791–795
106. Takimoto M, Kawamura M, Mori M, Sato Y (2011) Nickel-promoted carboxylation/cyclization cascade of allenyl aldehyde under an atmosphere of CO<sub>2</sub>. *Synlett* 2011:1423–1426
107. Aoki M, Izumi S, Kaneko M, Ukai K, Takaya J, Iwasawa N (2007) Ni(0)-promoted hydroxycarboxylation of 1,2-dienes by reaction with CO<sub>2</sub> and O<sub>2</sub>. *Org Lett* 9:1251–1253
108. Déryen S, Clinet J-C, Duñach E, Périchon J (1990) Coupling of allenes and carbon dioxide catalyzed by electrogenerated nickel complexes. *Synlett* 2:361–364
109. Takimoto M, Kawamura M, Mori M, Sato Y (2005) Nickel-catalyzed regio- and stereoselective double carboxylation of trimethylsilyllallene under an atmosphere of carbon dioxide and its application to the synthesis of Chaetomelic acid A anhydride. *Synlett* 2005:2019–2022
110. Walther D, Dinjus E (1982) Aktivierung von Kohlendioxid an Übergangsmetallzentren; Die Metallringeschlußreaktion zwischen Kohlendioxid und 1,3-Dienen am elektronenreichen Nickel(0)-Komplexrumpf. *Zeitschrift für Chemie* 22:228–229
111. Walther D, Dinjus E, Seiler J, Thanh NN, Schade W, Leban I (1983) Aktivierung von CO<sub>2</sub> an Übergangsmetallzentren: struktur und reaktivität eines C–C-kopplungsproduktes von CO<sub>2</sub> und 2,3-dimethylbutadien am elektronenreichen Nickel(0). *Z Naturforsch B* 38:835–840
112. Hoberg H, Apotecher B (1984)  $\alpha$ ,  $\omega$ -Disäuren aus butadien und kohlendioxid an nickel(0). *J Organomet Chem* 270:c15–c17
113. Hoberg H, Schaefer D, Oster BW (1984) Dien-carbonsäuren aus 1,3-dienen und CO<sub>2</sub> durch C–C-verknüpfung an nickel(0). *J Organomet Chem* 266:313–320
114. Hoberg H, Schaefer D (1983) Sorbinsäure aus piperylen und CO<sub>2</sub> durch C–C-Verknüpfung an nickel(0). *J Organomet Chem* 255:C15–C17
115. Behr A, Kanne U (1986) Nickel complex induced C–C-linkage of carbon dioxide with trienes. *J Organomet Chem* 317:C41–C44
116. Hoberg H, Jenni K, Krüger C, Raabe E (1986) C–C-Kupplung von CO<sub>2</sub> und Butadien an Eisen(o)-Komplexen—ein neuer Weg zu  $\alpha$ ,  $\omega$ -Dicarbonsäuren. *Angew Chem* 98:819–820
117. Geyer C, Schindler S (1998) Kinetic analysis of the reaction of isoprene with carbon dioxide and a Nickel(0) complex. *Organometallics* 17:4400–4405
118. Takimoto M, Mori M (2001) Cross-coupling reaction of oxo-allylnickel complex generated from 1,3-diene under an atmosphere of carbon dioxide. *J Am Chem Soc* 123:2895–2896
119. Takimoto M, Mizuno T, Sato Y, Mori M (2005) Nickel-mediated carboxylative cyclization of enynes. *Tetrahedron Lett* 46:5173–5176
120. Takimoto M, Mizuno T, Mori M, Sato Y (2006) Nickel-mediated cyclization of enynes under an atmosphere of carbon dioxide. *Tetrahedron* 62:7589–7597
121. Mizuno T, Oonishi Y, Takimoto M, Sato Y (2011) Total synthesis of (–)-Corynantheidine by Nickel-catalyzed carboxylative cyclization of enynes. *Eur J Org Chem* 2011:2606–2609
122. Hoberg H, Gross S, Milchereit A (1987) Nickel(0)-catalyzed production of a functionalized cyclopentanecarboxylic acid from 1,3-Butadiene and CO<sub>2</sub>. *Angew Chem Int Ed* 26:571–572

123. Tsuda T, Morikawa S, Sumiya R, Saegusa T (1988) Nickel(0)-catalyzed cycloaddition of diynes and carbon dioxide to give bicyclic  $\alpha$ -pyrones. *J Org Chem* 53:3140–3145
124. Tsuda T, Morikawa S, Hasegawa N, Saegusa T (1990) Nickel(0)-catalyzed cycloaddition of silyl diynes with carbon dioxide to silyl bicyclic  $\alpha$ -pyrones. *J Org Chem* 55:2978–2981
125. Tekavec TN, Arif AM, Louie J (2004) Regioselectivity in nickel(0) catalyzed cycloadditions of carbon dioxide with diynes. *Tetrahedron* 60:7431–7437
126. Louie J, Gibby JE, Farnworth MV, Tekavec TN (2002) Efficient Nickel-catalyzed [2+2+2] cycloaddition of CO<sub>2</sub> and diynes. *J Am Chem Soc* 124:15188–15189
127. Cao T, Ma S (2016) Highly stereo- and regioselective hydrocarboxylation of diynes with carbon dioxide. *Org Lett* 18:1510–1513
128. Takimoto M, Mori M (2002) Novel catalytic CO<sub>2</sub> incorporation reaction: nickel-catalyzed regio- and stereoselective ring-closing carboxylation of bis-1,3-dienes. *J Am Chem Soc* 124:10008–10009
129. Takimoto M, Nakamura Y, Kimura K, Mori M (2004) Highly enantioselective catalytic carbon dioxide incorporation reaction: nickel-catalyzed asymmetric carboxylative cyclization of bis-1,3-dienes. *J Am Chem Soc* 126:5956–5957

# Nickel-Catalyzed Cross-Coupling Reactions of Unreactive Phenolic Electrophiles via C–O Bond Activation

Mamoru Tobisu<sup>1</sup> · Naoto Chatani<sup>2</sup>

Received: 19 April 2016 / Accepted: 30 May 2016 / Published online: 13 June 2016  
© Springer International Publishing Switzerland 2016

**Abstract** Nickel-catalyzed cross-coupling reactions of aryl esters, carbamates, carbonates, ethers and arenols are reviewed. Carbon–oxygen bonds in these phenol derivatives cannot be activated by palladium, a typical cross-coupling catalyst, but a low valent nickel species in conjunction with a strong  $\sigma$ -donor ligand is uniquely effective for achieving this. The review is organized primarily by substrate class and secondarily by coupling partners, encompassing organometallics, heteroatom nucleophiles, C–H bonds and many others. Although the reactions in this category are covered thoroughly, each reaction is described only briefly, so that it is possible to quickly overview the spectrum of nickel-catalyzed cross-coupling reactions of inert phenol derivatives. The robustness of inert phenol derivatives under typically used catalytic conditions as well as their utility as a directing group allow unique synthetic applications of these new C–O cross-coupling reactions, which is also included in cases where appropriate. Mechanistic aspects of C–O bond activation by nickel are also summarized, highlighting their diversity compared with the C–X bond activation involved in conventional cross-coupling processes.

**Keywords** Nickel catalyst · Cross-coupling · C–O bond activation · Phenol · Aryl ether

---

This article is part of the Topical Collection “Ni- and Fe-Based Cross-Coupling Reactions,” edited by “Arkaitz Correa.”

---

✉ Mamoru Tobisu  
[tobisu@chem.eng.osaka-u.ac.jp](mailto:tobisu@chem.eng.osaka-u.ac.jp)

✉ Naoto Chatani  
[chatani@chem.eng.osaka-u.ac.jp](mailto:chatani@chem.eng.osaka-u.ac.jp)

<sup>1</sup> Center for Atomic and Molecular Technologies, Graduate School of Engineering, Osaka University, Suita, Osaka 565-0871, Japan

<sup>2</sup> Faculty of Engineering, Osaka University, Suita, Osaka 565-0871, Japan

## 1 Introduction

Transition metal-catalyzed cross-coupling reactions of aryl electrophiles with organic and organometallic reagents have become indispensable tools for the synthesis of a wide range of aromatic compounds via carbon–carbon and carbon–heteroatom bond formation [1, 2]. In these reactions, the most frequently used aryl electrophile is an aryl halide. If aryl halides in such cross-coupling reactions could be replaced with phenol or phenol derivatives, it would be advantageous because the potential toxicity associated with halides could be avoided, and phenols are more abundant feedstock than aryl halides (some are naturally occurring) [3, 4]. In fact, phenols can participate in cross-coupling reactions when the phenolic hydroxyl group is converted into a better leaving group, such as a triflate, and the synthetic utility of such activated aryl sulfonates has been well appreciated. However, it would be more favorable if more readily accessible aryl esters, ethers or phenol itself could be coupled with nucleophiles. Despite the clear merit of using simpler phenolic electrophiles, the inertness of the C(aryl)–O bond in these compounds makes their cross-coupling processes difficult to realize, in particular with classical palladium catalyst systems (Fig. 1).

Nickel is one of the metal centers that was used in the pioneering studies of cross-coupling reactions. The use of low valent nickel complexes to activate strong  $\sigma$ -bonds [5] has attracted renewed interest, and significant advancements have been made in recent years. Particularly important among these advances are nickel-catalyzed cross-coupling reactions using inert phenolic electrophiles, which have become a subject of intense research. The focus of this review is on nickel-catalyzed cross-coupling reactions of readily available aryl esters (including carbamates), ethers and phenols, covering the literature through March 2016. Reactions are classified by the substrate involved (i.e., aryl esters, aryl ethers and arenoles) and subcategorized by the coupling partner. Cross-coupling reactions of inert phenol derivatives by other transition metal catalysts, such as Ru [6–10], Fe [11, 12], Co [13], Rh [14, 15] and Cr [16], are beyond the scope of this review. Catalytic transformations via alkenyl [17–28] and benzylic C–O bond [29, 30] activation are not covered. In addition, readers are encouraged to consult previous reviews on catalytic C–O bond activation reactions [31–38].

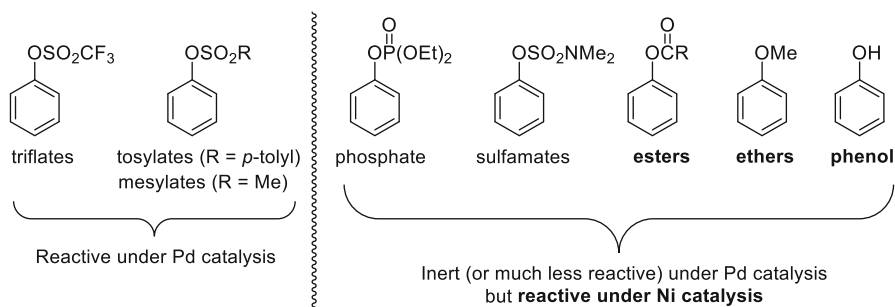


**Fig. 1** Phenolic electrophiles used in cross-coupling reactions

## 2 Cross-Coupling Reactions of Aryl Esters and Carbamates

### 2.1 Kumada-Tamao-Corriu Type Reactions

In 1992, the nickel-catalyzed cross-coupling of aryl carbamates with Grignard reagents was reported by Snieckus (Eq. 1) [39].  $\text{PhMgX}$  and  $\text{Me}_3\text{SiCH}_2\text{MgX}$  were reported to be coupled with aryl carbamates in the presence of a  $\text{Ni}(\text{acac})_2$  (acac = acetyl acetonate) catalyst without a need for an added ligand. A carbamoyl group can be substituted by a hydrogen when  $^i\text{PrMgX}$  is used. This protocol was successfully used for the synthesis of polysubstituted arenes via a carbamoyl-directed ortho functionalization followed by the removal of the directing group (Eq. 2).

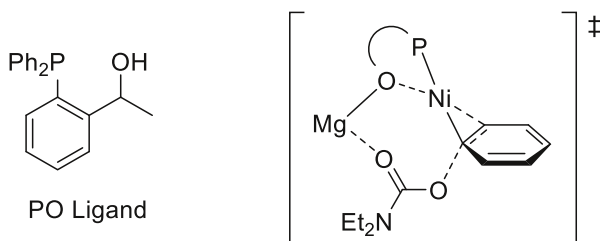
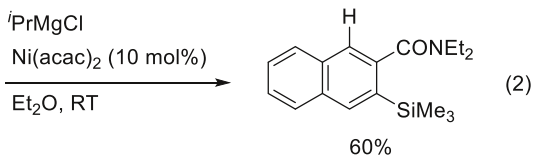
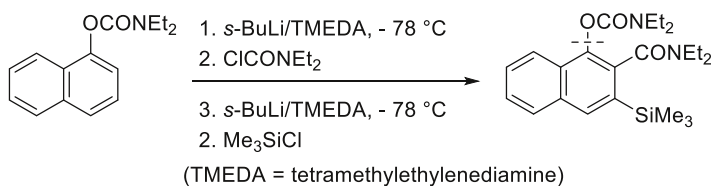
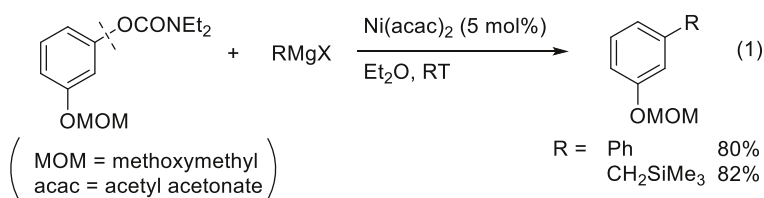
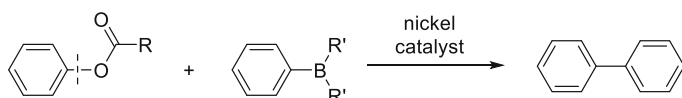


**Fig. 2** The PO ligand used for Kumada-Tamao-Corriu type cross-coupling and transition state model for C–O bond cleavage

Nakamura devised a new ligand for the Kumada-Tamao-Corriu type cross-coupling of aryl carbamates (Fig. 2) [40]. The ligand has a triphenylphosphine-based structure bearing a hydroxyl group, which was designed to assist the oxidative addition of a C–O bond by forming a magnesium salt in situ. The magnesium center functions as a Lewis acid to activate the carbamoyl group to facilitate the cleavage of the C–O bond by nickel.

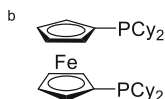
It should also be noted that cross-coupling reactions of aryl esters and carbamates with a wider range of Grignard reagents have also been achieved using iron catalysts, although they are beyond the scope of this chapter [11, 12].

**Table 1** Nickel-catalyzed Suzuki-Miyaura type cross-coupling of aryl esters, carbamates and carbonates



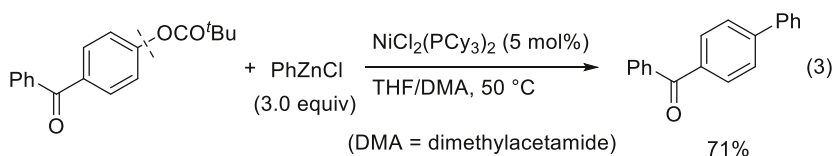
| Year | Author   | Phenolic substrate                               | Boron source  | Catalyst system  | Reference |
|------|----------|--|---|--|-----------|
| 2008 | Garg     | Ar-O-CO <sup>t</sup> Bu                          | Ar'B(OH) <sub>2</sub>                               | NiCl <sub>2</sub> (PCy <sub>3</sub> ) <sub>2</sub><br>K <sub>3</sub> PO <sub>4</sub>                                       | 42        |
| 2008 | Shi      | Ar-OCOR<br>(R = Me, <sup>t</sup> Bu, Ph)         | (Ar'BO) <sub>3</sub><br>+ 0.88 H <sub>2</sub> O     | NiCl <sub>2</sub> (PCy <sub>3</sub> ) <sub>2</sub><br>K <sub>3</sub> PO <sub>4</sub>                                       | 43        |
| 2009 | Garg     | Ar-OCONEt <sub>2</sub><br>Ar-OCO <sup>t</sup> Bu | Ar'B(OH) <sub>2</sub>                               | NiCl <sub>2</sub> (PCy <sub>3</sub> ) <sub>2</sub><br>K <sub>3</sub> PO <sub>4</sub>                                       | 44        |
| 2009 | Snieckus | Ar-OCONEt <sub>2</sub>                           | Ar'B(OH) <sub>2</sub><br>+ 0.1 (Ar'BO) <sub>3</sub> | NiCl <sub>2</sub> (PCy <sub>3</sub> ) <sub>2</sub><br>PCy <sub>3</sub> ·HBF <sub>4</sub><br>K <sub>3</sub> PO <sub>4</sub> | 46        |
| 2010 | Shi      | Ar-OCOMe <sub>2</sub>                            | (Ar'BO) <sub>3</sub><br>+ 1.0 H <sub>2</sub> O      | NiCl <sub>2</sub> (PCy <sub>3</sub> ) <sub>2</sub><br>PCy <sub>3</sub><br>K <sub>2</sub> CO <sub>3</sub>                   | 45        |
| 2010 | Molander | Ar-OCO <sup>t</sup> Bu<br>Ar-OCONEt <sub>2</sub> | ArBF <sub>3</sub> K<br>+ H <sub>2</sub> O           | Ni(cod) <sub>2</sub> <sup>a</sup><br>PCy <sub>3</sub> ·HBF <sub>4</sub><br>K <sub>3</sub> PO <sub>4</sub>                  | 49        |
| 2011 | Kuwano   | Ar-OCO <sub>2</sub> Me                           | Ar'B(OH) <sub>2</sub>                               | Ni(cod) <sub>2</sub><br>DCyPF <sup>b</sup><br>K <sub>2</sub> CO <sub>3</sub>   | 51        |

<sup>a</sup> cod = 1,5-cyclooctadiene



## 2.2 Negishi Type Reactions

The cross-coupling of aryl esters with organozinc reagents was reported by Shi (Eq. 3) [41]. Similar to the reactions described in the following sections,  $\text{PCy}_3$  serves as an effective ligand. The use of a pivaloyl group as the acyl moiety in the substrate is essential for an efficient reaction, presumably to avoid undesired cleavage of the  $\text{C}(\text{acyl})\text{--O}$  bond. Although polyaromatic substrates, such as naphthyl pivalates, successfully participate in this cross-coupling, the corresponding phenyl pivalates are much less reactive except those that contain an electron-withdrawing group. This is a general trend in the nickel-catalyzed cross-coupling of inert phenol derivatives with less reactive nucleophiles [38].



## 2.3 Suzuki-Miyaura Type Reactions

Among the nucleophiles used for cross-coupling reactions of aryl halides, organoboron reagents have been recognized as being particularly useful because of their stability to air and moisture, the fact that they tolerate a wide range of functional groups and are readily available. Therefore, development of a catalyst system that can allow organoboron cross-coupling for inert phenolic derivatives has been intensively studied to date (Table 1). The first Suzuki-Miyaura type cross-coupling of aryl esters was independently reported by two research groups in 2008. Garg reported that aryl pivalates can be coupled with arylboronic acids in the presence of a  $\text{NiCl}_2(\text{PCy}_3)_2$  catalyst [42], while Shi employed arylboroxines as nucleophiles in the presence of 0.88 equivalents of water, allowing for the cross-coupling of aryl acetates, pivalates and benzoates [43]. Both groups also extended their nickel-catalyzed protocols to the Suzuki-Miyaura type reactions of aryl carbamates [44, 45]. Snieckus simultaneously reported on the nickel-catalyzed cross-coupling of aryl carbamates using a 10:1 mixture of an aryl carbamate and an arylboroxine [46, 47]. A close inspection of the reactions conditions developed for Suzuki-Miyaura cross-couplings for aryl esters and carbamates indicates that the presence of a suitable amount of water is crucial for achieving an efficient catalysis. Indeed, Percec reported that these cross-coupling reactions do not proceed smoothly when arylboronic esters are used as nucleophiles, presumably because there is no water present in the system [48]. Molander demonstrated that potassium trifluoroborate salts can also serve as

effective coupling partners for the nickel-catalyzed cross-coupling of aryl pivalates and carbamates [49]. A nickel complex having a pincer-type ligand was shown to be a viable catalyst precursor, when used in conjunction with  $\text{PCy}_3$ , for the Suzuki-Miyaura type cross-coupling of hindered 9-anthracenyl pivalates [50]. Aryl carbonates have also been reported to undergo cross-coupling with organoboron compounds in the presence of  $\text{NiCl}_2(\text{PCy}_3)_2$  [44] or  $\text{Ni}(\text{cod})_2/\text{PCy}_3$  catalysts ( $\text{cod} = 1,5\text{-cyclooctadiene}$ ) [49]. Interestingly, Kuwano reported that a bidentate ligand DCyPF [1,1-bis(di-cyclohexylphosphino)ferrocene] can also serve as an effective ligand for the nickel-catalyzed cross-coupling of aryl carbonates with arylboronic acids [51].

The development of these cross-coupling processes using esters, carbamates and carbonates as leaving groups allows them to be used as convertible directing groups in arene functionalization reactions. For example, the directed ortho-metalation of dicarbamate **1**, followed by the reaction with an enal, gives the 2*H*-chromene derivative **2** (Fig. 3). The carbamate group in **2** can then be functionalized by nickel-catalyzed cross-coupling [46].

## 2.4 Cross-Coupling with C–H Bonds

The use of C–H bonds as coupling partners for cross-coupling reactions has emerged as some of the more powerful and greener alternatives to the classical cross-coupling reactions in which stoichiometric organometallic reagents are used [52–56]. A number of methods for coupling aryl halides with C–H bonds in various compounds, often called direct arylation, have been developed to date [57]. Naturally, it would become a widely applied method if inert phenol derivatives could be made to undergo direct arylation reactions. This class of reaction was first accomplished by Itami in the direct arylation of C–H bonds in azoles (Eq. 4) [58]. Naphthyl pivalates, carbamates and carbonates can be activated by  $\text{Ni}(\text{cod})_2/\text{dcype}$  [ $\text{dcype} = 1,2\text{-bis}(\text{dicyclohexylphosphino})\text{ethane}$ ] to participate in the cross-

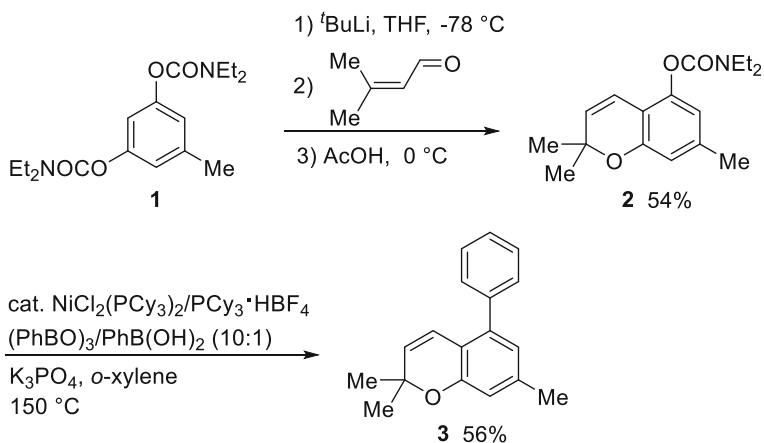
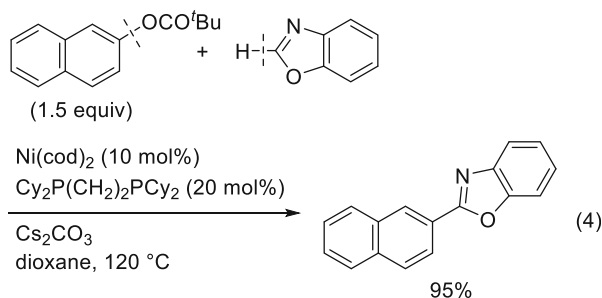


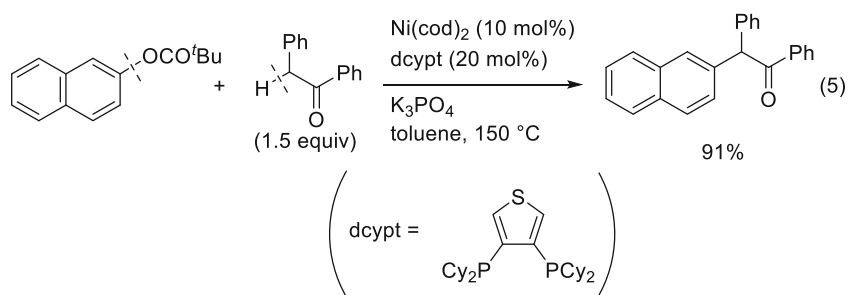
**Fig. 3** Synthetic application of the Suzuki-Miyaura type cross-coupling of aryl carbamates



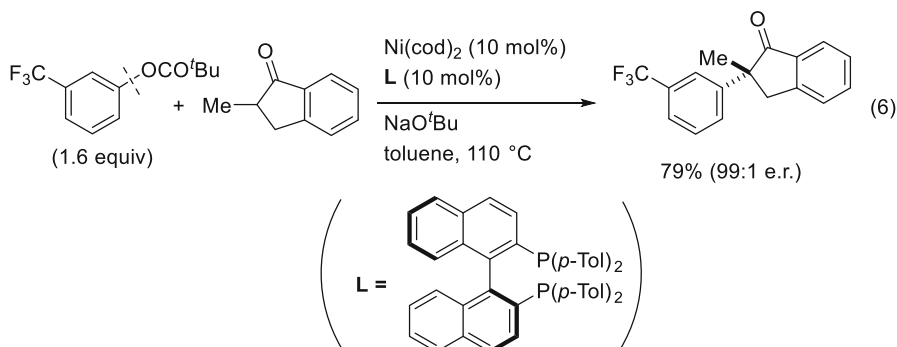
coupling with C–H bonds of oxazole and thiazole derivatives. The use of this electron-rich, bulky bisphosphine ligand is essential. The method was later extended to the direct arylation of imidazoles by slightly modifying the reaction conditions, which also permitted the scope of aryl carbamates to be extended to non-fused aromatics [59].



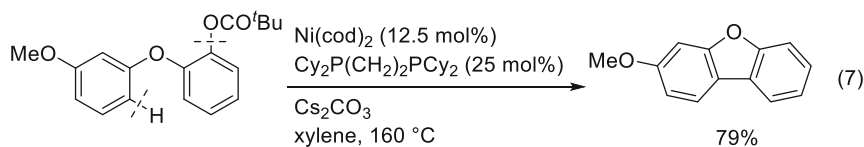
Itami's group also demonstrated that the nickel/bisphosphine system can be used to mediate the arylation of C–H bonds  $\alpha$  to a carbonyl group. A range of aryl pivalates can be used for the arylation of ketones (Eq. 5) [60]. An optimal ligand for this  $\alpha$ -arylation is the thiophene-based bisphosphine ligand dcypt [dcypt = 3,4-bis(dicyclohexylphosphino)thiophene], which has a relatively rigid backbone structure compared with dcyp. This catalyst system was further applied to the  $\alpha$ -arylation of esters and amides, in which aryl carbamates are particularly effective aryl sources [61].



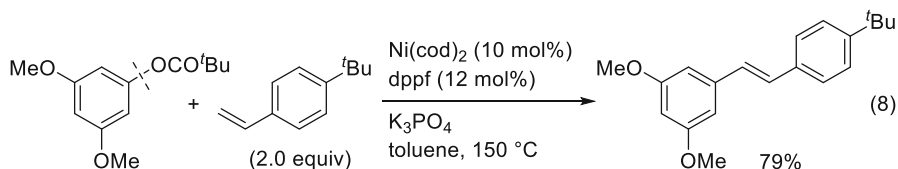
Martin reported that the  $\alpha$ -arylation reaction can proceed in an enantioselective manner when conducted with a chiral ligand. Thus, the reaction of aryl pivalates with a 2-substituted 1-indanone in the presence of a nickel catalyst and a BINAP-based ligand [BINAP = 2,2'-bis(diphenylphosphino)-1,1'-binaphthyl] generated the  $\alpha$ -arylated product with an excellent level of enantioselectivity at their quaternary stereogenic centers (Eq. 6) [62].



The nickel-catalyzed cross-coupling of inert phenol derivatives with aromatic C–H bonds has been limited to C–H bonds with a relatively high acidity, as in azoles. Although the direct arylation of benzene C–H bonds using an inert phenol-based aryl source awaits future studies, the viability of such a process was demonstrated in an intramolecular setting. Kalyani reported on a  $\text{Ni}(\text{cod})_2/\text{dcype}$ -catalyzed intramolecular arylation that proceeded via the cleavage of C–H and C–OCO<sup>t</sup>Bu bonds (Eq. 7) [63]. This reaction represents one of the rare examples of the C–H activation of benzene C–H bonds by a nickel catalyst [52]. Based on the finding of an intramolecular kinetic isotope effect of 2.8, C–H bond cleavage was proposed to proceed via a concerted metalation deprotonation pathway. On a related cobalt-catalyzed reaction that deserves to be noted: aryl carbamates can be coupled with C–H bonds of arenes intermolecularly when the arene contains an ortho-directing group such as a 2-pyridyl group [13].

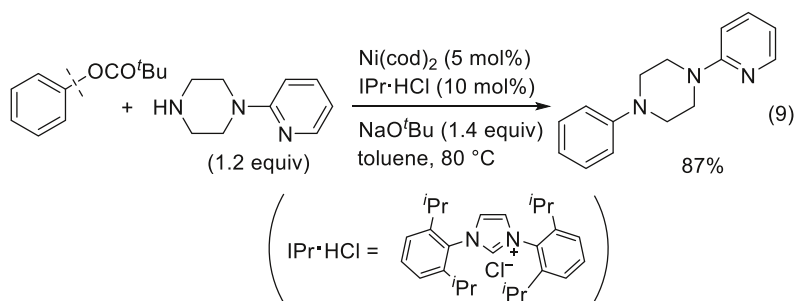


The cross-coupling of aryl halides with alkenes to form arylated alkenes, known as the Mizoroki–Heck reaction, represents another class of C–H functionalization reactions. Unlike cross-coupling with organometallic reagents, the Mizoroki–Heck type reaction follows a mechanistically distinct process, i.e., insertion of the alkenes and  $\beta$ -hydrogen elimination, after the oxidative addition of the aryl halide occurs. Watson reported on the first Mizoroki–Heck type reaction using inert phenol derivatives [64]. A range of styrenes could be arylated with aryl pivalates in the presence of  $\text{Ni}(\text{cod})_2/\text{dppf}$  catalyst [dppf = 1,1'-bis(diphenylphosphino)ferrocene] to form *trans*-stilbene derivatives (Eq. 8).

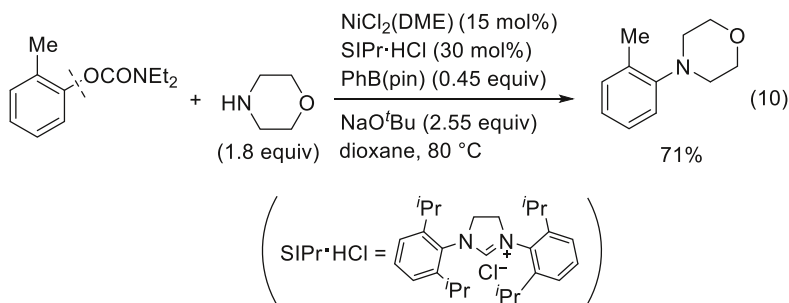


## 2.5 Carbon–Heteroatom Bond-Forming Reactions

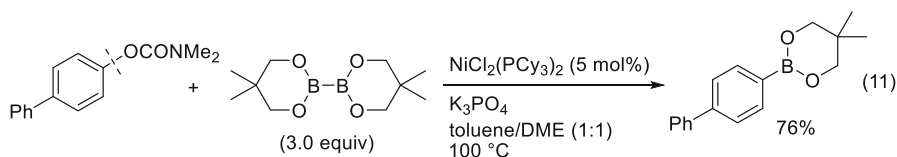
Recent progress in transition metal-catalyzed cross-coupling technology has reached the stage where aryl halides can be coupled with not only carbon nucleophiles, but also heteroatom-based nucleophiles, including amines, alcohols and related derivatives [65, 66]. Such carbon–heteroatom bond-forming reactions are also possible with aryl ester and carbamate substrates when a suitable nickel catalyst is used. For example, Tobisu and Chatani reported that amination of aryl pivalates occurs effectively in the presence of a Ni(cod)<sub>2</sub>/IPr catalyst [IPr = 1,3-bis(2,6-diisopropylphenyl)imidazol-2-ylidene] (Eq. 9) [67]. The use of pivalates as a leaving group is crucial to prevent undesired acyl-oxygen bond cleavage, which becomes a major pathway when aryl acetates and benzoates are used.



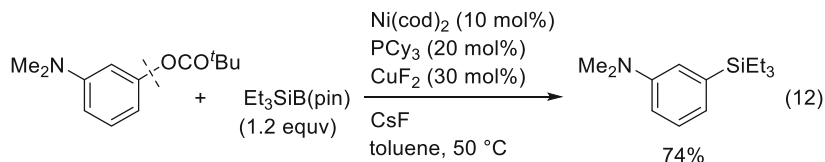
Garg's group reported on a similar amination reaction of aryl carbamates [68]. Several ortho substituents in aryl carbamates were found to be tolerated, thus allowing a carbamate-directed ortho C–H functionalization followed by aminative removal of the directing group. In addition, an air-stable nickel(II) precatalyst can be used when PhB(pin) (pin = pinacolate) is employed as a mild reducing agent for the generation of the active nickel(0) species in situ (Eq. 10) [69].



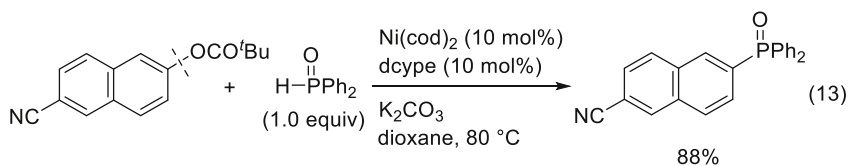
The nickel-catalyzed borylation of aryl carbamates was developed by Shi using a diboron reagent (Eq. 11) [70]. The suitable choice of solvent (toluene:DME = 1:1) and a base ( $\text{K}_3\text{PO}_4$ ) is important for an efficient reaction.



The carbon–silicon bond-forming cross-coupling of aryl pivalates was also developed by Martin by using  $\text{Et}_3\text{SiB}(\text{pin})$  as a silylating agent. The yield of the silylated product could be significantly increased when  $\text{CuF}_2$  was used as a cocatalyst, which allows C–O bond activation to occur at temperatures as low as  $50^\circ\text{C}$  (Eq. 12) [71]. The reaction is proposed to proceed by dual Ni/Cu catalysis, in which the  $\text{Et}_3\text{SiCu}$  species acts as a transmetalating agent.

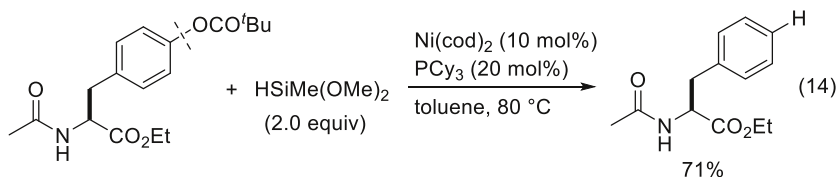


Phosphorus-based nucleophiles are among the most challenging because their strong coordinating ability can inhibit the nickel–ligand interaction that is required for C–O bond activation. Chen and Han addressed this issue by employing a nickel catalyst in conjunction with a chelating dcype ligand; these are sufficiently robust to promote the cross-coupling of aryl pivalates with phosphorus reagents including  $\text{Ph}_2\text{P}(\text{O})\text{H}$  ( $\text{EtO}$ ) $_2\text{P}(\text{O})\text{H}$  and  $\text{Ph}_2\text{PH}$  (Eq. 13) [72].



## 2.6 Miscellaneous

The catalytic deoxygenation of phenol derivatives into the parent arenes has widespread utility in organic synthesis, since it allows the electron-donating ability of the phenolic oxygen to be temporarily used in arene functionalization reactions. Tobisu and Chatani reported on the use of a hydrosilane reagent in the Ni(cod)<sub>2</sub>/PCy<sub>3</sub>-catalyzed reductive cleavage of aryl pivalates (Eq. 14) [73]. A range of functional groups, including amines, esters, amides and internal alkenes, are well tolerated.



Garg reported that a carbamoyl group can also be removed under similar nickel-catalyzed conditions using hydrosilane, which allows the carbamate group to be used as a removable ortho-directing group [74]. Using this protocol, both ipso and cine substitution strategies are possible (Fig. 4).

In 2012, Tsuji's group reported on the reaction of aryl halides with CO<sub>2</sub> to form aryl carboxylic acids in the presence of a nickel catalyst and a stoichiometric amount of powdered Mn [75]. They showed that an arylnickel(II) halide [ArNi(II)X] intermediate, generated by the oxidative addition of the aryl halide to Ni(0), is in situ reduced by the added Mn powder to produce an ArNi(I) species,

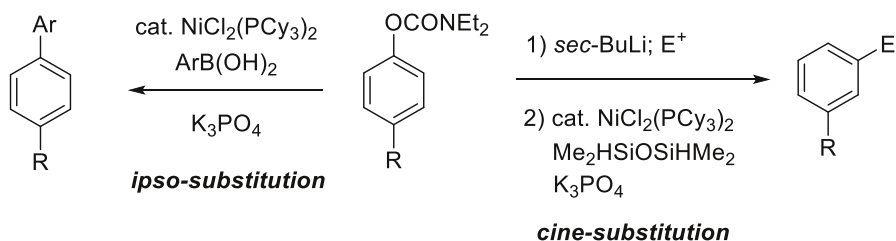
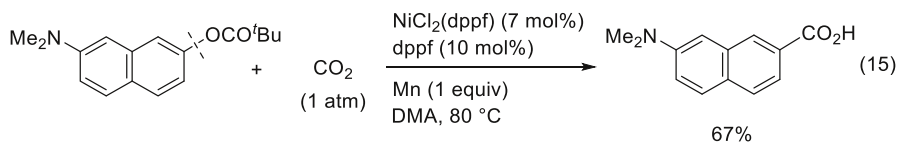
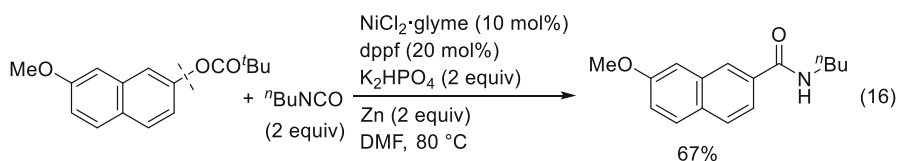


**Fig. 4** Ipso and cine substitution via nickel-catalyzed C–O bond functionalization

which is sufficiently reactive to capture  $\text{CO}_2$ . Martin successfully extended this reductive carboxylation strategy to aryl pivalate substrates (Eq. 15) [76]. This protocol is applicable to various  $\pi$ -extended aryl and heteroaryl pivalates, which have functional groups such as amines, ethers, amides and  $\text{NO}_2$ .



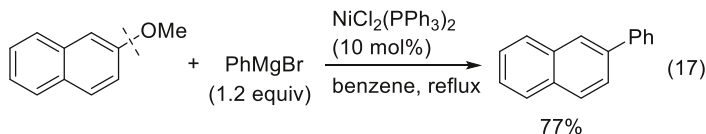
Isoelectronic isocyanates can also be arylated with the nickel catalyst system to form the corresponding carboxamides (Eq. 16) [77]. A range of aliphatic isocyanates were found to undergo reductive coupling with naphthyl pivalates.



### 3 Cross-Coupling Reactions of Aryl Ethers

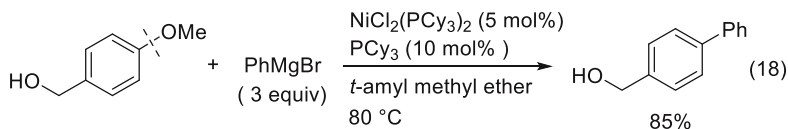
#### 3.1 Kumada-Tamao-Corriu Type Reactions

In 1979, Wenkert reported that methoxyarenes undergo cross-coupling with  $\text{PhMgBr}$  with the aid of a nickel catalyst (Eq. 17) [17, 18]. This reaction is the first example that demonstrates the feasibility of using aryl ethers as electrophilic coupling partners in cross-coupling reactions. The Wenkert reaction did not attract significant attention at this stage because only a limited range of aryl ethers (i.e., methoxynaphthalenes) exhibited sufficient reactivity, which renders more reactive aryl triflates the phenol derivatives of choice in cross-coupling reactions.

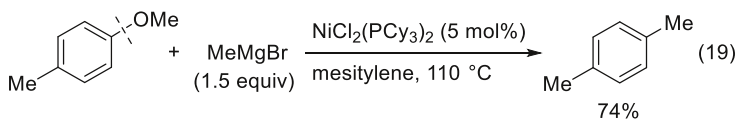


In the 25 years after Wenkert's report, Dankwardt revisited the methoxyarene cross-coupling reaction and found that switching the ligand to  $\text{PCy}_3$  significantly expanded the scope of the aryl ether substrates to include diverse anisole derivatives as well as heteroaryl ethers (Eq. 18) [78]. Shi reported that the  $\text{Ni}(0)/\text{PCy}_3$  system can also catalyze the cross-coupling of aryl silyl ethers with  $\text{ArMgX}$  [79]. Several

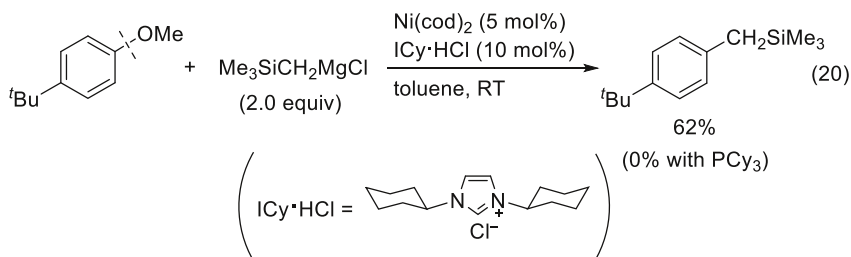
other ligands including modified PCy<sub>3</sub> [80] and NHC [81, 82] were also used in the Kumada-Tamao-Corriu type arylation of anisole derivatives.



In contrast to arylation reactions, methodology for the alkylation of aryl ethers remains underdeveloped. Shi reported that aryl ethers can also be methylated by using MeMgX in the presence of a NiCl<sub>2</sub>(PCy<sub>3</sub>)<sub>2</sub> catalyst (Eq. 19) [83]. However, no other alkyl Grignard reagents were found to undergo coupling under these conditions.

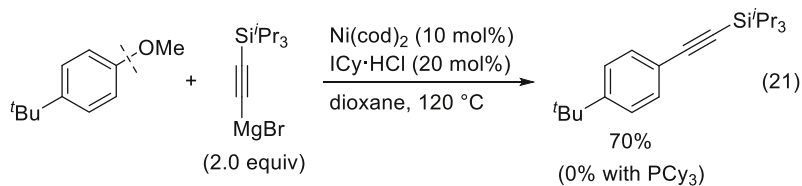


Tobisu and Chatani reported that other alkyl Grignard reagents that lack  $\beta$ -hydrogens such as benzyl and trimethylsilylmethylmagnesium halides can be successfully cross-coupled with anisole derivatives when 1,3-dicyclohexylimidazol-2-ylidene (ICy) is used as a ligand (Eq. 20) [84]. It is noteworthy that PCy<sub>3</sub>, the most frequently used ligand for aryl ether cross-coupling, is completely inactive for this reaction. Strained alkyl groups, including 1- and 2-adamantyl and cyclopropyl groups, can also be introduced, even in the presence of  $\beta$ -hydrogens, which represents the only examples of aryl ether cross-coupling reactions, in which secondary and tertiary alkyl groups are incorporated.



Despite the widespread utility of the Sonogashira reaction, the alkylation of aryl halides, the corresponding alkylation of inert phenol derivatives has not been developed, except for the following example. Tobisu and Chatani reported that ethynylmagnesium bromide bearing a triisopropylsilyl (TIPS) group at the terminal is a viable nucleophile for aryl ether cross-coupling to introduce an alkynyl group (Eq. 21) [85]. Protection with a TIPS group is essential for this reaction, probably to prevent the undesired interaction of an alkyne with the nickel catalyst. This alkylation protocol can be applied to a range of relatively

complex aryl ethers, including natural product derivatives bearing a methoxy group.



The nickel-catalyzed cross-coupling of aryl ethers promises to be a powerful method for late-stage functionalization because of the robustness of the methoxy group. For example, Nishihara exploited this feature of the nickel-catalyzed alkylation of methoxyarenes in the synthesis of  $\pi$ -conjugated compounds of interest in the field of organic semiconductors (Fig. 5) [86]. The key to the success of this synthesis is the stability of the methoxy group under repetitive palladium-catalyzed cross-coupling conditions.

### 3.2 Negishi Type Reactions

Wang and Uchiyama reported on the cross-coupling of aryl ethers with an organozinc reagent by a Ni(0)/PCy<sub>3</sub> catalyst [87]. Although common organozinc reagents such as PhZnX and Ph<sub>2</sub>Zn as well as monoanionic PhZnMe<sub>2</sub>Li failed to participate in the cross-coupling process, the use of dianionic PhZnMe<sub>3</sub>Li<sub>2</sub> resulted in the successful production of the product (Eq. 22).

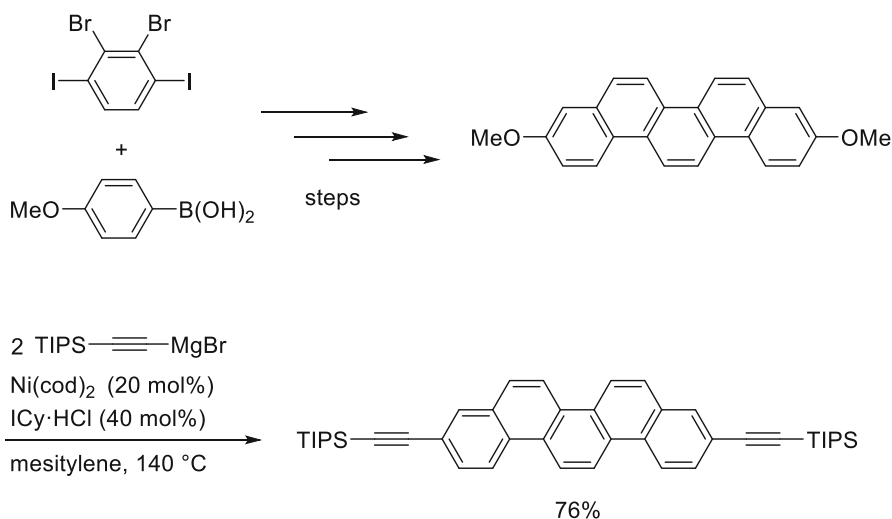
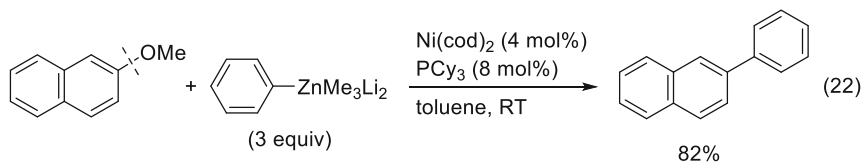


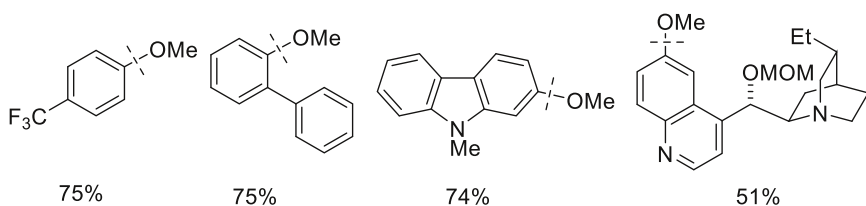
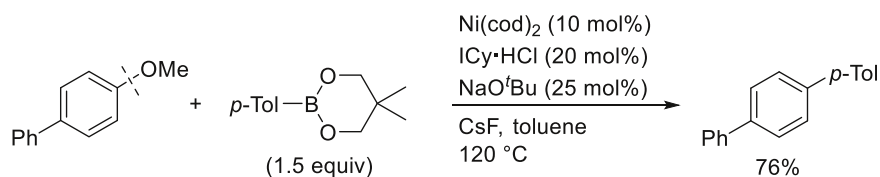
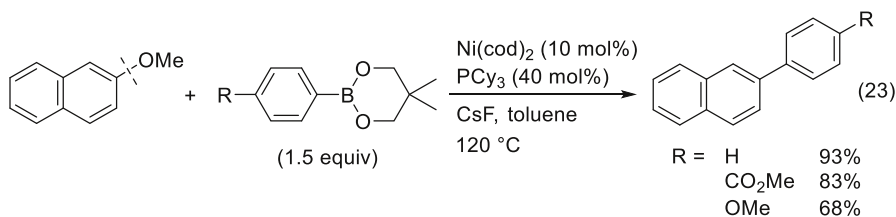
**Fig. 5** Nickel-catalyzed cross-coupling of aryl ethers for late-stage functionalization





### 3.3 Suzuki-Miyaura Type Reactions

Since the first report by Wenkert in 1979 (Eq. 17), until 2008, the intriguing ability of a nickel catalyst to activate a C–O bond in an aryl ether had been used only within the realm of Kumada-Tamao-Corriu type reactions using Grignard reagents (Sect. 3.1). Tobisu and Chatani developed the first Suzuki-Miyaura type cross-coupling of aryl ethers using  $\text{Ni}(\text{cod})_2/\text{PCy}_3$  catalyst (Eq. 23) [88]. Unlike cross-coupling reactions using Grignard reagents, ketones and esters were also found to be compatible. The scope of the aryl ethers is limited to polyaromatic substrates such as methoxynaphthalene, which, in turn, allowed for the regioselective arylation of compounds bearing two different methoxy groups (the last example in Eq. 23).



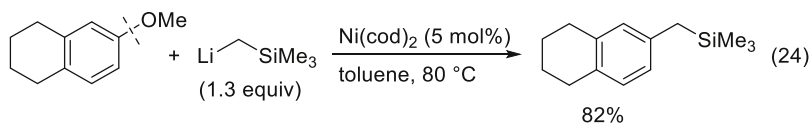
All the substrates shown in this scheme fail to react with  $\text{Ni}(0)/\text{PCy}_3$ .

**Fig. 6** The second-generation catalyst for the Suzuki-Miyaura type reaction of aryl ethers

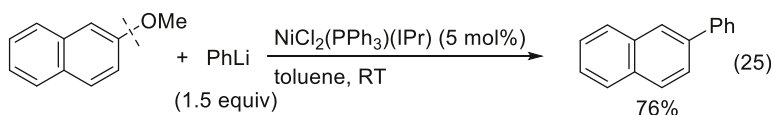
The same research group developed a second-generation catalyst consisting of  $\text{Ni}(\text{cod})_2/\text{ICy}$ , which allows the cross-coupling of anisole derivatives without a fused aromatic ring and heteroaryl substrates that were unreactive when the  $\text{Ni}(0)/\text{PCy}_3$  system was used (Fig. 6) [89].

### 3.4 Cross-Coupling with Other Organometallic Reagents

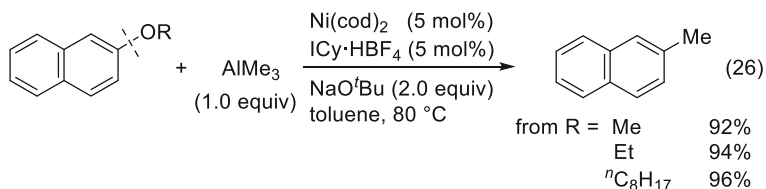
Organolithium reagents are also suitable nucleophiles for the cross-coupling of aryl ethers. Rueping reported on the coupling of methoxyarenes with  $\text{Me}_3\text{SiCH}_2\text{Li}$  in the presence of  $\text{Ni}(\text{cod})_2$  (Eq. 24) [90]. Considering the pivotal role of a strong  $\sigma$ -donor ligand in C–O activation in a series of aryl ether cross-couplings, it is surprising that no added ligand is required for this organolithium cross-coupling.



During the course of a study dealing with the nickel-catalyzed cross-coupling of aryl halides with  $\text{PhLi}$ , Hornillos and Feringa reported that methoxyarenes can also be arylated, although only three substrates were examined in their study (Eq. 25) [91].



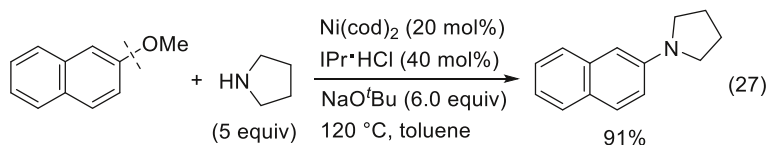
Tobisu and Chatani disclosed that  $\text{AlMe}_3$  can serve as a methylating agent for a range of aryl alkyl ethers (Eq. 26) [92]. Again,  $\text{ICy}$  performs much more effectively as the ligand than  $\text{PCy}_3$ .



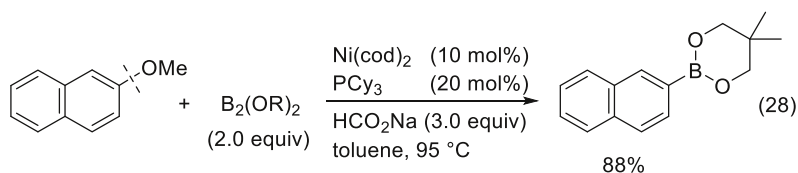
### 3.5 Carbon-Heteroatom Bond-Forming Reactions

Although a number of heteroatom-based nucleophiles can be used for aryl halides, they cannot easily be employed in the cross-coupling of inert phenol derivatives, in

particular aryl ethers. Indeed, only two types of heteroatom nucleophiles have been reported to have been successfully used for the cross-coupling of aryl ethers. One, which was developed by Tobisu and Chatani, is a carbon–nitrogen-forming reaction in which an amine is used as a nucleophile (Eq. 27) [93, 94]. Several methoxyarenes and heteroarenes have been reported to be aminated with secondary amines under conditions in which a Ni(0)/IPr catalyst is used.

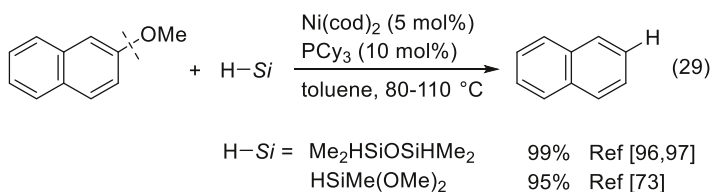


A second class of heteroatom nucleophile is a diboron reagent, which allows a synthetically useful boryl group to be added at the ipso position of methoxyarenes (Eq. 28) [95]. Martin reported that the addition of a weak base  $\text{HCO}_2\text{Na}$  improved the yield of the borylated product. Anisole derivatives without a fused aromatic ring can also be used when ester, amide and  $\text{CF}_3$  groups are present at the ortho position of the methoxy group.



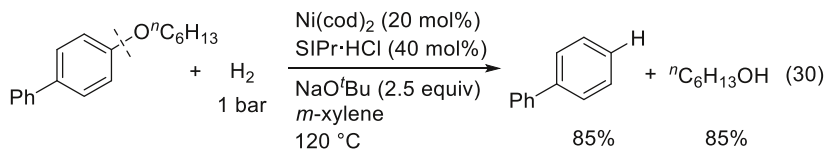
### 3.6 Miscellaneous

The reductive cleavage of a C(aryl)–O bond in aryl ethers was independently reported by two research groups. Martin's group employed tetramethyldisiloxane as a reducing agent [96, 97], while Tobisu and Chatani's protocol used  $\text{HSiMe(OMe)}_2$  and Chatani's protocol used  $\text{HSiMe(OMe)}_2$  and Chatani's protocol used  $\text{HSiMe(OMe)}_2$  [73] (Eq. 29). Both groups use the same Ni(0)/ $\text{PCy}_3$  catalyst, which promotes the dealkoxylation of  $\pi$ -extended aryl ethers. A methoxy group of an anisole derivative can also be removed when a coordinating group, such as a 2-pyridyl or ester, is located at the ortho position.



Hartwig reported that aryl ethers can be reductively cleaved using hydrogen as the reducing agent (Eq. 30) [98]. The addition of an excess amount of  $\text{NaOtBu}$  was

found to be effective for promoting the synthesis of various aryl ethers, including diaryl ethers, the hydrogenolysis of which would eventually lead to the realization of a catalytic depolymerization of lignin to produce low-molecular-weight aromatic compounds. They also reported that a similar hydrogenolysis can also be performed using a heterogeneous nickel system [99, 100].



The reductive cleavage of a C(aryl)–O bond in an aryl ether can occur, even in the absence of an external reducing agent. Tobisu and Chatani found that aryl ethers can be converted to the parent arenes when heated with a catalytic amount of Ni(cod)<sub>2</sub> and a newly developed NHC ligand bearing 2-adamantyl groups, I(2-Ad) (Fig. 7) [101]. Because no reducing agent such as hydrosilane and hydrogen is needed, this method allows unusual chemoselectivity: the alkoxy group is exclusively reduced without affecting the normally more reducible alkene and ketone moieties. Moreover, this reaction provides an experimental basis showing that oxidative addition is indeed a viable mechanism for C–O bond cleavage by a nickel catalyst (see Sect. 5 for more discussion).

Since the discovery of the Ullmann reaction in 1901 [102], the transition metal-mediated homocoupling of aryl electrophiles has served as a powerful tool for the synthesis of symmetrical biaryls. However, applicable substrates were limited to

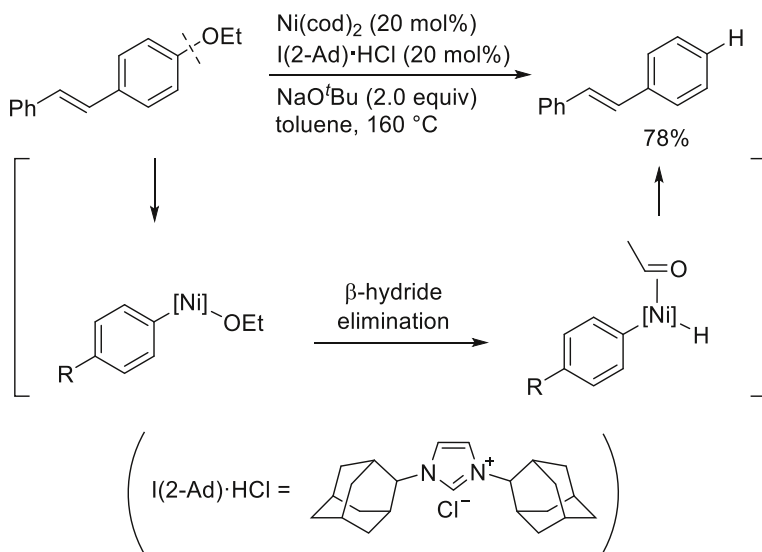


**Fig. 7** Nickel-catalyzed reductive cleavage of aryl ethers in the absence of an external reducing agent

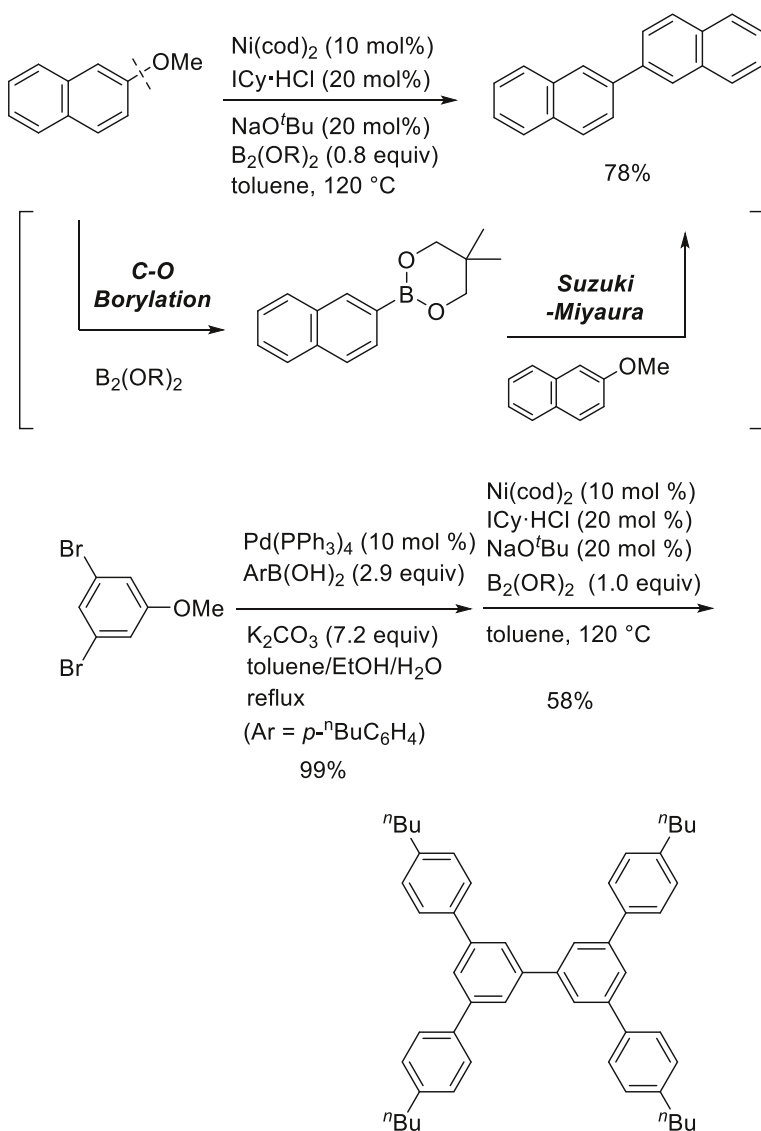


**Fig. 8** Nickel-catalyzed homocoupling of aryl ethers with the aid of a diboron reagent

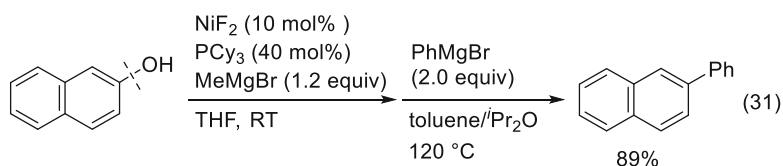
activated aryl electrophiles such as aryl halides or sulfonates. Tobisu and Chatani developed a protocol that allows the homocoupling of methoxyarenes to proceed [103]. The nickel-catalyzed reaction of methoxyarenes with 0.8 equivalents of a diboron reagent led to the selective formation of a biaryl product via C–O bond borylation [95], followed by Suzuki-Miyaura-type cross-coupling (Fig. 8, top) [88, 89]. The use of an ICy ligand is crucial for this homocoupling, and the major product is a borylated derivative when PCy<sub>3</sub> is used. The robustness of a methoxy

group allows a sequential cross-coupling/homocoupling process, enabling the rapid synthesis of  $\pi$ -extended arenes (Fig. 8, bottom).

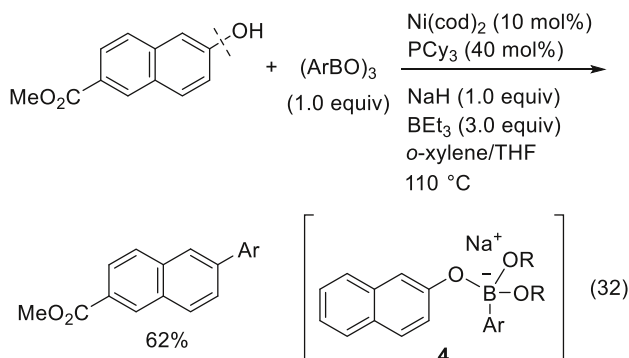
#### 4 Cross-Coupling Reactions of Arenols

A method for directly cross-coupling arenols with nucleophiles would be of the utmost utility in terms of substrate availability, atom efficiency and cost. Such a process could be possible by the in situ conversion of arenols into activated forms such as sulfonates or phosphonium [104, 105] through the addition of stoichiometric amounts of activating reagents. Because of space limitations, this section only deals with the nickel-catalyzed direct transformation of arenols using non-classical stoichiometric activating reagents.

Shi reported that naphthols can be cross-coupled with  $\text{ArMgX}$  in the presence of  $\text{NiF}_2/\text{PCy}_3$  (Eq. 31) [106]. The preformation of a magnesium salt of naphthol is essential for the success of this cross-coupling, indicating that the Lewis acidic  $\text{Mg}^{2+}$  likely assists the C–O bond activation by nickel.

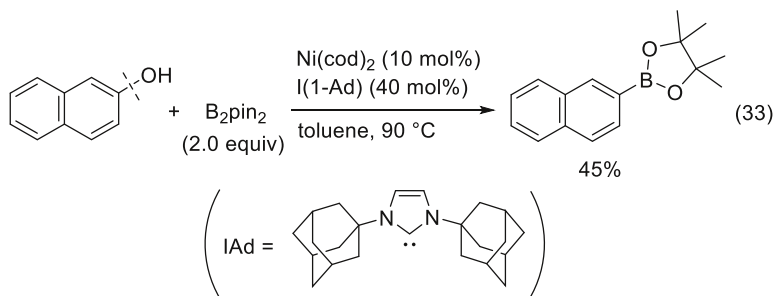


The same group also demonstrated that organoboron nucleophiles can also be used in the nickel-catalyzed naphthol cross-coupling reactions (Eq. 32) [107]. In this reaction, sodium functions as an optimal counter cation, and the addition of excess  $\text{BEt}_3$  was found to significantly enhance product yield. The borate salt **4** was proposed as a key intermediate, in which the C(aryl)–O bond is predicted to be more reactive toward a nickel species than a naphthol C–O bond.

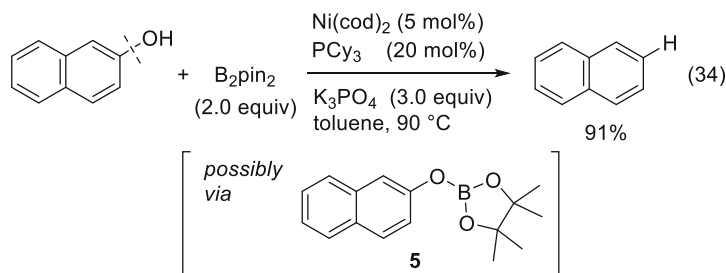


Shi's group also reported one interesting example in their study of the palladium-catalyzed borylation of benzyl alcohols. The nickel-catalyzed reaction of 2-naphthol

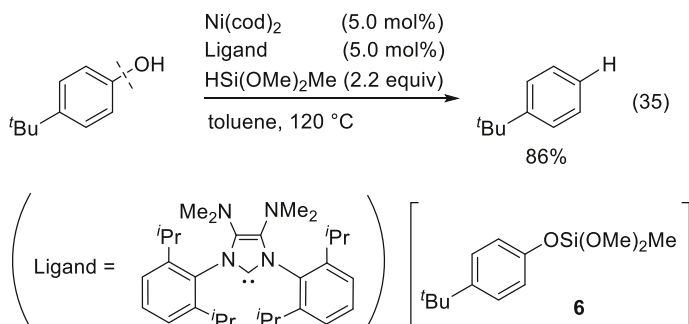
with a diboron reagent resulted in the formation of a borylated product (Eq. 33) [108].



Shi's group subsequently reported that the same set of reactants resulted in the formation of a deoxygenated product when the reaction conditions were modified slightly (Eq. 34) [109]. Labeling studies revealed that both residual water and toluene, as the solvent, can serve as a source of hydrogen atoms. The C(aryl)–O bond cleavage was proposed to occur via the naphthoxyborane intermediate **5**.



Nakao developed the nickel-catalyzed deoxygenation of arenols using hydrosilane as a reducing agent (Eq. 35) [110]. The use of a highly electron-donating NHC ligand allows the deoxygenation of a range of phenol derivatives. The reaction is proposed to proceed via a silyl ether intermediate **6**, which is more reactive than anisole under these reductive cleavage conditions.



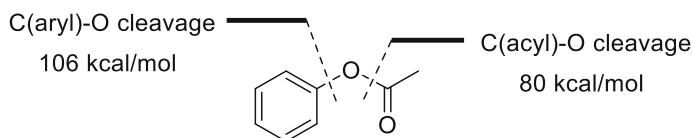


**Fig. 9** C(aryl)-O cleavage vs. C(acyl)-O cleavage

## 5 Mechanistic Aspects of the C–O Bond Activation of Inert Phenol Derivatives by Nickel Catalysts

### 5.1 Activation of Aryl Esters and Carbamates

The difficulty associated with the activation of C(aryl)-O bonds of aryl esters arises not merely from its higher bond dissociation energy (BDE) compared to aryl halides or triflates, but also from the selectivity relative to the undesired C(acyl)-O bond activation. The C(acyl)-O cleavage of aryl esters would be expected to occur more readily compared to the C(aryl)-O bond cleavage in terms of BDE (Fig. 9). Nevertheless, the nickel-catalyzed cross-coupling of aryl esters proceeds exclusively via C(aryl)-O cleavage, as discussed in Sect. 2.

Several theoretical studies of the nickel-catalyzed cross-coupling of aryl esters have been carried out in attempts to elucidate the mechanism of C–O activation reactions as well as C(aryl)-O/C(acyl)-O selectivity [47, 111–114]. Liu reported a theoretical study of the Ni(0)/PCy<sub>3</sub>-catalyzed Suzuki-Miyaura type cross-coupling of aryl acetates [111]. According to their calculation, the oxidative addition of a C(acyl)-O bond can occur reversibly with a relatively low barrier, but the subsequent transmetalation with phenylboronic acid is energetically much less favored (Fig. 10). In contrast, the oxidative addition of C(aryl)-O bonds can proceed irreversibly, and the subsequent transmetalation readily follows, which is in good agreement with the experimental outcome.

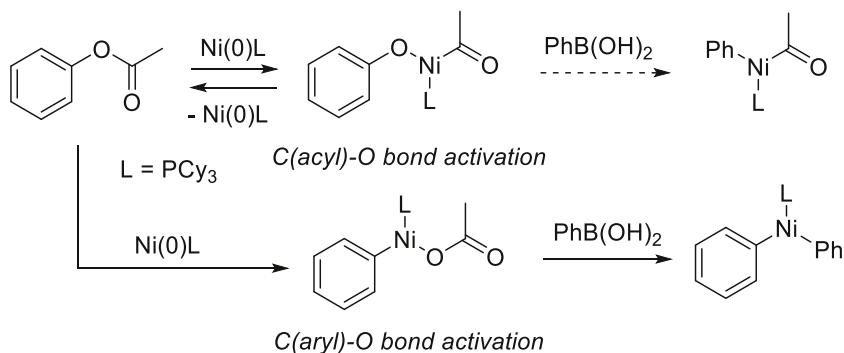


**Fig. 10** Rationale for the selectivity of C(aryl)-O and C(acyl)-O bond cleavage



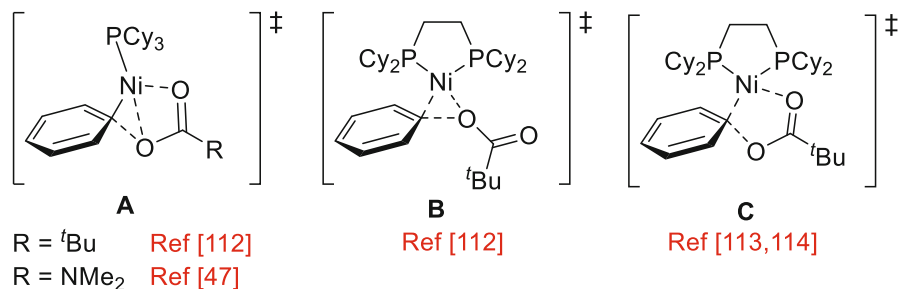
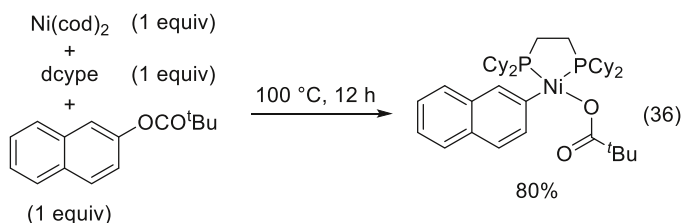


**Fig. 11** Calculated transition states for the oxidative addition of aryl esters and carbamates

A detailed mechanism for the oxidative addition of C(aryl)–O bond of aryl esters has been proposed based on the theoretical studies. In the case where  $\text{PCy}_3$  is used as the ligand, oxidative addition to the nickel monophosphine species is favored, since its vacant coordination site allows an additional Ni–O interaction, which lowers the activation barrier for this process (**A** in Fig. 11) [47, 112]. When a bidentate dcype ligand is involved, both the standard three-centered structure **B** [112] and five-centered structure **C** [113, 114] were identified as viable transition states, depending on the calculation method used.

The oxidative addition of a C(aryl)–O bond of aryl pivalates to a Ni(0)/dcype species has been unambiguously proved by the isolation of the oxidative addition complex from the stoichiometric reaction of  $\text{Ni}(\text{cod})_2$ , dcype and 2-naphthyl pivalate (Eq. 36) [115].



## 5.2 Activation of Aryl Ethers

Several but still a limited number of theoretical studies on the nickel-catalyzed transformation of aryl ethers have been reported to date. Those studies suggest that the mechanism responsible for the cleavage of C(aryl)–O bonds of aryl ethers can vary drastically, depending on the nature of the nucleophile. This aspect is in sharp contrast to cross-couplings of aryl halides or esters, in which the mode of C–X or C–O activation is consistently an oxidative addition, irrespective of the nucleophile employed.

Wang and Uchiyama reported on a theoretical study of the Ni(0)/ $\text{PCy}_3$ -catalyzed cross-coupling of anisole with phenyl magnesium bromide [116]. Their calculation

revealed that C(aryl)–O bond cleavage can occur with a lower activation barrier when an anionic nickelate complex **D**, which is generated by the reaction of Ni(0) with PhMgBr, is involved (Fig. 12). C–O bond cleavage via the five-membered transition state **E** is favored over the classical three-centered oxidative addition.

Gómez-Bengoa and Martin proposed a unique silylnickel(I)-mediated mechanism for the reductive cleavage of methoxynaphthalene using a hydrosilane reagent based on spectroscopic, kinetic and computational studies [97]. A silylnickel(I) species **F**, generated by the comproportionation of an initially formed (silyl)Ni(II)H species, adds across naphthalene to form intermediate **G**, which gives a reduced product via the concerted  $\alpha$ -elimination of silyl methoxide (Fig. 13). Interestingly, Martin's group also disproved the involvement of the classical oxidative addition mechanism for C(aryl)–OMe bond cleavage when PCy<sub>3</sub> is used as the ligand, based on the observation of a facile  $\beta$ -hydrogen elimination process [117] from ArNi(OMe) species [97].

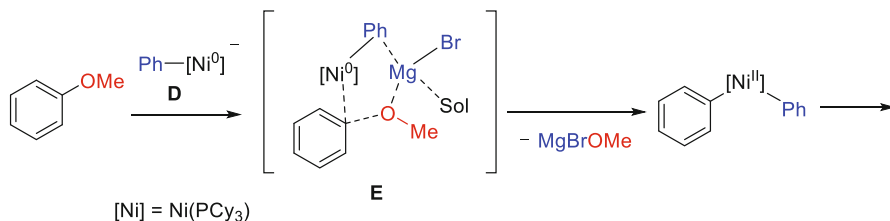


**Fig. 12** Calculated mechanism for C–O bond cleavage in nickel-catalyzed Kumada-Tamao-Corriu type cross-coupling of aryl ethers

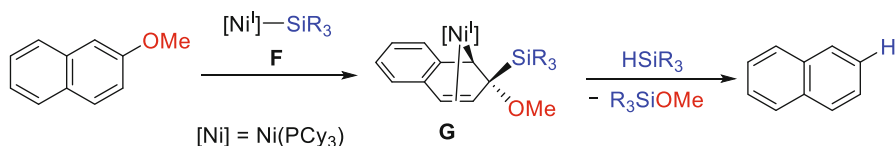


**Fig. 13** Calculated mechanism for C–O bond cleavage in the nickel-catalyzed reductive cleavage of aryl ethers using hydrosilane

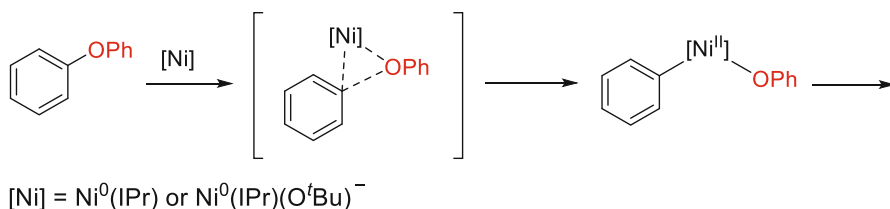


**Fig. 14** Calculated mechanism for C–O bond cleavage in the nickel-catalyzed hydrogenolysis of aryl ethers

Oxidative addition via the classical three-centered transition state can come into play under certain circumstances. For example, the above-mentioned mechanisms would not be operative in nickel-catalyzed reductive cleavage reactions in the absence of an external reducing agent (Fig. 7), and C–O cleavage via oxidative addition would be most likely. Surawatanawong [118, 119] as well as Chung [120] reported that the classical oxidative addition pathway is also viable for the Ni(0)/NHC-catalyzed hydrogenolysis of aryl ethers (Fig. 14).

## 6 Conclusions

Despite the seminal finding by Wenkert in 1979 on the nickel-catalyzed cross-coupling of methoxyarenes with Grignard reagents, the field of cross-coupling reactions has largely focused on the palladium-catalyzed transformation of activated aryl electrophiles. It has only been during the last decade that chemists have re-investigated the unique ability of low valent nickel complexes for activating C(aryl)–O bonds of inert phenol derivatives for use in their catalytic transformation. Although our knowledge and general understanding of cross-coupling chemistry have been accumulating, this knowledge has not readily translated into the nickel-catalyzed cross-coupling of inert phenol derivatives, due, in part, to the fact that completely different mechanisms are operating. Indeed, compared to the palladium-catalyzed cross-coupling of aryl halides, the scope and efficiency of these new C–O cross-coupling reactions currently remain limited, leaving numerous opportunities for the development of new C–O transformations. With respect to the mechanism responsible for C–O bond activation, there are also a number of opportunities to expand our knowledge base, in particular from an experimental standpoint such as the isolation of key intermediates [7, 121]. Continued efforts promise to definitely improve this infant but promising method (after the submission of this manuscript, two methods for the alkylation of anisole substrates have appeared [122, 123]).

## References

1. Miyaura N (ed) (2001) *Top Cur Chem* 219
2. de Meijere A, Diederich F (2004) *Metal-catalyzed cross-coupling reactions*, 2nd edn. Wiley, Weinheim
3. Tyman JHP (1996) *Synthetic and natural phenols*. Elsevier, Amsterdam
4. Rappoport Z (ed) (2003) *The chemistry of phenols*. Wiley, Chichester
5. Tasker SZ, Standley EA, Jamison TF (2014) *Nature* 509:299–309
6. Kakiuchi F, Usui M, Ueno S, Chatani N, Murai S (2004) *J Am Chem Soc* 126:2706–2707
7. Ueno S, Mizushima E, Chatani N, Kakiuchi F (2006) *J Am Chem Soc* 128:16516–16517
8. Kondo H, Akiba N, Kochi T, Kakiuchi F (2015) *Angew Chem Int Ed* 54:9293–9297
9. Zhao Y, Snieckus V (2014) *J Am Chem Soc* 136:11224–11227
10. Zhao Y, Snieckus V (2015) *Org Lett* 17:4674–4677
11. Li B-J, Xu L, Wu Z-H, Guan B-T, Sun C-L, Wang B-Q, Shi Z-J (2009) *J Am Chem Soc* 131:14656–14657
12. Silberstein AL, Ramgren SD, Garg NK (2012) *Org Lett* 14:3796–3799
13. Song W, Ackermann L (2012) *Angew Chem Int Ed* 51:8251–8254

14. Nakamura K, Yasui K, Tobisu M, Chatani N (2015) *Tetrahedron* 71:4484–4489
15. Kinuta H, Hasegawa J, Tobisu M, Chatani N (2015) *Chem Lett* 44:366–368
16. Cong X, Tang H, Zeng X (2015) *J Am Chem Soc* 137:14367–14372
17. Wenkert E, Michelotti EL, Swindell CS (1979) *J Am Chem Soc* 101:2246–2247
18. Wenkert E, Michelotti EL, Swindell CS, Tingoli M (1984) *J Org Chem* 49:4894–4899
19. Hayashi T, Katsuro Y, Kumada M (1980) *Tetrahedron Lett* 21:3915–3918
20. Shimasaki T, Konno Y, Tobisu M, Chatani N (2009) *Org Lett* 11:4890–4892
21. Sun C-L, Wang Y, Zhou X, Wu Z-H, Li B-J, Guan B-T, Shi Z-J (2010) *Chem Eur J* 16:5844–5847
22. Cornella J, Martin R (2013) *Org Lett* 15:6298–6301
23. Yu J-Y, Kuwano R (2009) *Angew Chem Int Ed* 48:7217–7220
24. Yu J-Y, Shimizu R, Kuwano R (2010) *Angew Chem Int Ed* 49:6396–6399
25. Lee HW, Kwong FY (2009) *Synlett* 19:3151–3154
26. Matsuura Y, Tamura M, Kochi T, Sato M, Chatani N, Kakiuchi F (2007) *J Am Chem Soc* 129:9858–9859
27. Iwasaki T, Miyata Y, Akimoto R, Fujii Y, Kuniyasu H, Kambe N (2014) *J Am Chem Soc* 136:9260–9263
28. Gärtner D, Stein AL, Grupe S, Arp J, Jacobi von Wangelin A (2015) *Angew Chem Int Ed* 54:10545–10549
29. Tollefson EJ, Hanna LE, Jarvo ER (2015) *Acc Chem Res* 48:2344–2353
30. Cherney AH, Kadunce NT, Reisman SE (2015) *Chem Rev* 115:9587–9652
31. Yu D-G, Li B-J, Shi Z-J (2010) *Acc Chem Res* 43:1486–1495
32. Li B-J, Yu D-G, Sun C-L, Shi Z-J (2011) *Chem Eur J* 17:1728–1759
33. Rosen BM, Quasdorf KW, Wilson DA, Zhang N, Resmerita A-M, Garg NK, Percec V (2011) *Chem Rev* 111:1346–1416
34. Mesganaw T, Garg NK (2013) *Org Process Res Dev* 17:29–39
35. Tobisu M, Chatani N (2013) *Top Organomet Chem* 44:35–53
36. Yamaguchi J, Muto K, Itami K (2013) *Eur J Org Chem* 2013:19–30
37. Cornella J, Zarate C, Martin R (2014) *Chem Soc Rev* 43:8081–8097
38. Tobisu M, Chatani N (2015) *Acc Chem Res* 48:1717–1726
39. Sengupta S, Leite M, Raslan DS, Quesnelle C, Snieckus V (1992) *J Org Chem* 57:4066–4068
40. Yoshikai N, Matsuda H, Nakamura E (2009) *J Am Chem Soc* 131:9590–9599
41. Li B-J, Li Y-Z, Lu X-Y, Liu J, Guan B-T, Shi Z-J (2008) *Angew Chem Int Ed* 47:10124–10127
42. Quasdorf KW, Tian X, Garg NK (2008) *J Am Chem Soc* 130:14422–14423
43. Guan B-T, Wang Y, Li B-J, Yu D-G, Shi Z-J (2008) *J Am Chem Soc* 130:14468–14470
44. Quasdorf KW, Riener M, Petrova KV, Garg NK (2009) *J Am Chem Soc* 131:17748–17749
45. Xu L, Li B-J, Wu Z-H, Lu X-Y, Guan B-T, Wang B-Q, Zhao K-Q, Shi Z-J (2010) *Org Lett* 12:884–887
46. Antoft-Finch A, Blackburn T, Snieckus V (2009) *J Am Chem Soc* 131:17750–17752
47. Quasdorf KW, Antoft-Finch A, Liu P, Silberstein AL, Komaromi A, Blackburn T, Ramgren SD, Houk KN, Snieckus V, Garg NK (2011) *J Am Chem Soc* 133:6352–6363
48. Leowanawat P, Zhang N, Percec V (2012) *J Org Chem* 77:1018–1025
49. Molander GA, Beaumard F (2010) *Org Lett* 12:4022–4025
50. Xu M, Li X, Sun Z, Tu T (2013) *Chem Commun* 49:11539–11541
51. Kuwano R, Shimizu R (2011) *Chem Lett* 40:913–915
52. Castro LCM, Chatani N (2015) *Chem Lett* 44:410–421
53. Wencel-Delord J, Glorius F (2013) *Nat Chem* 5:369–375
54. Yamaguchi J, Yamaguchi AD, Itami K (2012) *Angew Chem Int Ed* 51:8960–9009
55. Lyons TW, Sanford MS (2010) *Chem Rev* 110:1147–1169
56. Chen X, Engle KM, Wang D-H, Yu J-Q (2009) *Angew Chem Int Ed* 48:5094–5115
57. Miura M, Satoh T, Hirano K (2014) *Bull Chem Soc Jpn* 87:751–764
58. Muto K, Yamaguchi J, Itami K (2012) *J Am Chem Soc* 134:169–172
59. Muto K, Hatakeyama T, Yamaguchi J, Itami K (2015) *Chem Sci* 6:6792–6798
60. Takise R, Muto K, Yamaguchi J, Itami K (2014) *Angew Chem Int Ed* 53:6791–6794
61. Koch E, Takise R, Studer A, Yamaguchi J, Itami K (2015) *Chem Commun* 51:855–857
62. Cornella J, Jackson EP, Martin R (2015) *Angew Chem Int Ed* 54:4075–4078
63. Wang J, Ferguson DM, Kalyani D (2013) *Tetrahedron* 69:5780–5790
64. Ehle AR, Zhou Q, Watson MP (2012) *Org Lett* 14:1202–1205
65. Surry DS, Buchwald SL (2008) *Angew Chem Int Ed* 47:6338–6361

66. Hartwig JF (2008) *Acc Chem Res* 41:1534–1544
67. Shimasaki T, Tobisu M, Chatani N (2010) *Angew Chem Int Ed* 49:2929–2932
68. Mesganaw T, Silberstein AL, Ramgren SD, Nathel NFF, Hong X, Liu P, Garg NK (2011) *Chem Sci* 2:1766–1771
69. Hie L, Ramgren SD, Mesganaw T, Garg NK (2012) *Org Lett* 14:4182–4185
70. Huang K, Yu D-G, Zheng S-F, Wu Z-H, Shi Z-J (2011) *Chem Eur J* 17:786–791
71. Zarate C, Martin R (2014) *J Am Chem Soc* 136:2236–2239
72. Yang J, Chen T, Han L-B (2015) *J Am Chem Soc* 137:1782–1785
73. Tobisu M, Yamakawa K, Shimasaki T, Chatani N (2011) *Chem Commun* 47:2946–2948
74. Mesganaw T, Fine Nathel NF, Garg NK (2012) *Org Lett* 14:2918–2921
75. Fujihara T, Nogi K, Xu T, Terao J, Tsuji Y (2012) *J Am Chem Soc* 134:9106–9109
76. Correa A, León T, Martin R (2014) *J Am Chem Soc* 136:1062–1069
77. Correa A, Martin R (2014) *J Am Chem Soc* 136:7253–7256
78. Dankwardt JW (2004) *Angew Chem Int Ed* 43:2428–2432
79. Zhao F, Yu D-G, Zhu R-Y, Xi Z, Shi Z-J (2011) *Chem Lett* 40:1001–1003
80. Xie L-G, Wang Z-X (2011) *Chem-Eur J* 17:4972–4975
81. Iglesias MJ, Prieto A, Nicasio MC (2012) *Org Lett* 14:4318–4321
82. Zhang J, Xu J, Xu Y, Sun H, Shen Q, Zhang Y (2015) *Organometallics* 34:5792–5800
83. Guan B-T, Xiang S-K, Wu T, Sun Z-P, Wang B-Q, Zhao K-Q, Shi Z-J (2008) *Chem Commun* 44:1437–1439
84. Tobisu M, Takahira T, Chatani N (2015) *Org Lett* 17:4352–4355
85. Tobisu M, Takahira T, Ohtsuki A, Chatani N (2015) *Org Lett* 17:680–683
86. Chen X-C, Nishinaga S, Okuda Y, Zhao J-J, Xu J, Mori H, Nishihara Y (2015) *Org Chem Front* 2:536–541
87. Wang C, Ozaki T, Takita R, Uchiyama M (2012) *Chem Eur J* 18:3482–3485
88. Tobisu M, Shimasaki T, Chatani N (2008) *Angew Chem Int Ed* 47:4866–4869
89. Tobisu M, Yasutome A, Kinuta H, Nakamura K, Chatani N (2014) *Org Lett* 16:5572–5575
90. Leiendecker M, Hsiao C-C, Guo L, Alandini N, Rueping M (2014) *Angew Chem Int Ed* 53:12912–12915
91. Heijnen D, Gualtierotti J-B, Hornillos V, Feringa BL (2016) *Chem Eur J* 22:3991–3995
92. Morioka T, Nishizawa A, Nakamura K, Tobisu M, Chatani N (2015) *Chem Lett* 44:1729–1731
93. Tobisu M, Shimasaki T, Chatani N (2009) *Chem Lett* 38:710–711
94. Tobisu M, Yasutome A, Yamakawa K, Shimasaki T, Chatani N (2012) *Tetrahedron* 68:5157–5161
95. Zarate C, Manzano R, Martin R (2015) *J Am Chem Soc* 137:6754–6757
96. Álvarez-Bercedo P, Martin R (2010) *J Am Chem Soc* 132:17352–17353
97. Cornella J, Gómez-Bengoa E, Martin R (2013) *J Am Chem Soc* 135:1997–2009
98. Sergeev AG, Hartwig JF (2011) *Science* 332:439–443
99. Sergeev AG, Webb JD, Hartwig JF (2012) *J Am Chem Soc* 134:20226–20229
100. Gao F, Webb JD, Hartwig JF (2016) *Angew Chem Int Ed* 55:1474–1478
101. Tobisu M, Morioka T, Ohtsuki A, Chatani N (2015) *Chem Sci* 6:3410–3414
102. Ullmann F, Bielecki J (1901) *Chem Ber* 34:2174–2185
103. Nakamura K, Tobisu M, Chatani N (2015) *Org Lett* 17:6142–6145
104. Chen G-J, Huang J, Gao L-X, Han F-S (2011) *Chem Eur J* 17:4038–4042
105. Zhao Y-L, Wu G-J, Han F-S (2012) *Chem Commun* 48:5868–5870
106. Yu D-G, Li B-J, Zheng S-F, Guan B-T, Wang B-Q, Shi Z-J (2010) *Angew Chem Int Ed* 49:4566–4570
107. Yu D-G, Shi Z-J (2011) *Angew Chem Int Ed* 50:7097–7100
108. Cao Z-C, Luo F-X, Shi W-J, Shi Z-J (2015) *Org Chem Front* 2:1505–1510
109. Shi W-J, Li X-L, Li Z-W, Shi Z-J (2016) *Org Chem Front* 3:375–379
110. Ohgi A, Nakao Y (2016) *Chem Lett* 45:45–47
111. Li Z, Zhang S-L, Fu Y, Guo Q-X, Liu L (2009) *J Am Chem Soc* 131:8815–8823
112. Hong X, Liang Y, Houk KN (2014) *J Am Chem Soc* 136:2017–2025
113. Lu Q, Yu H, Fu Y (2014) *J Am Chem Soc* 136:8252–8260
114. Xu H, Muto K, Yamaguchi J, Zhao C, Itami K, Musaev DG (2014) *J Am Chem Soc* 136:14834–14844
115. Muto K, Yamaguchi J, Lei A, Itami K (2013) *J Am Chem Soc* 135:16384–16387
116. Ogawa H, Minami H, Ozaki T, Komagawa S, Wang C, Uchiyama M (2015) *Chem Eur J* 21:13904–13908

117. Kelley P, Lin S, Edouard G, Day MW, Agapie T (2012) *J Am Chem Soc* 134:5480–5483
118. Sawatlon B, Wititsuwannakul T, Tantirungrotechai Y, Surawatanawong P (2014) *Dalton Trans* 43:18123–18133
119. Wititsuwannakul T, Tantirungrotechai Y, Surawatanawong P (2016) *ACS Catal* 6:1477–1486
120. Xu L, Chung LW, Wu Y-D (2016) *ACS Catal* 6:483–493
121. Radkov V, Roisnel T, Trifonov A, Carpentier J-F, Kirillov E (2016) *J Am Chem Soc* 138:4350–4353
122. Liu X, Hsiao C-C, Kalvet I, Leiendecker M, Guo L, Schoenebeck F, Rueping M (2016) *Angew Chem Int Ed* 55:6093–6098
123. Tobisu M, Takahira T, Morioka T, Chatani N (2016) *J Am Chem Soc*. doi:10.1021/jacs.6b03253 (**in press**)

# Nickel-Catalyzed Aromatic C–H Functionalization

Junichiro Yamaguchi<sup>1</sup> · Kei Muto<sup>1</sup> · Kenichiro Itami<sup>2,3</sup>

Received: 13 May 2016 / Accepted: 11 July 2016 / Published online: 1 August 2016  
© Springer International Publishing Switzerland 2016

**Abstract** Catalytic C–H functionalization using transition metals has received significant interest from organic chemists because it provides a new strategy to construct carbon–carbon bonds and carbon–heteroatom bonds in highly functionalized, complex molecules without pre-functionalization. Recently, inexpensive catalysts based on transition metals such as copper, iron, cobalt, and nickel have seen more use in the laboratory. This review describes recent progress in nickel-catalyzed aromatic C–H functionalization reactions classified by reaction types and reaction partners. Furthermore, some reaction mechanisms are described and cutting-edge syntheses of natural products and pharmaceuticals using nickel-catalyzed aromatic C–H functionalization are presented.

**Keywords** C–H functionalization · C–H activation · Nickel · Heteroarenes · Arenes · Catalyst

---

This article is part of the Topical Collection “Ni- and Fe-Based Cross-Coupling Reactions”, edited by Arkaitz Correa.

---

✉ Junichiro Yamaguchi  
[junyamaguchi@waseda.jp](mailto:junyamaguchi@waseda.jp)

✉ Kenichiro Itami  
[itami@chem.nagoya-u.ac.jp](mailto:itami@chem.nagoya-u.ac.jp)

<sup>1</sup> Department of Applied Chemistry, Waseda University, Tokyo 169-8555, Japan

<sup>2</sup> Institute of Transformative Bio-Molecules (WPI-ITbM) and Graduate School of Science, Nagoya University, Chikusa, Nagoya 464-8602, Japan

<sup>3</sup> JST-ERATO, Itami Molecular Nanocarbon Project, Nagoya University, Chikusa, Nagoya 464-8602, Japan

## 1 Introduction

C–H functionalization using nickel catalysts has recently received significant attention from the field of organic chemistry because nickel catalysts are less expensive than noble transition metal catalysts and less toxic than commonly used metal catalysts such as palladium catalysts [1–7]. Important contributions to C–H activation of aromatic compounds by nickel were made as early as the 1960s. In 1963, Dubeck and coworkers prepared an oxidative adduct of a C–H bond on an aromatic ring onto a nickel complex (Scheme 1) [8]. When azobenzene (**1**) was mixed with nickelocene (**2**) at 135 °C, C–H nickelation at the *ortho* C–H bond of **1** occurred to give nickel complex **3** by using the diazo moiety as a directing group (chelation-assisted group). Thereafter, there were no reports describing the C–H nickelation of aromatic C–H bonds for more than 50 years. In 2006, Liang and coworkers reported that pincer nickel complex **4** could react with benzene (**5**) to furnish complex **6**, which likely occurred via the oxidative addition of the C–H bond of benzene without any directing group [9].

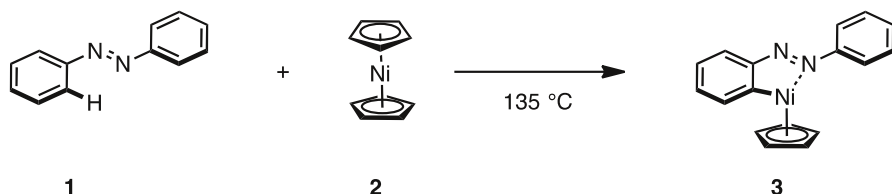
This review focuses on nickel-catalyzed C–H functionalization, particularly on aromatic rings (aromatic C–H functionalization), and showcases recent examples classified by reaction types and reaction partners. Furthermore, some reaction mechanisms are described and cutting-edge syntheses of natural products and pharmaceuticals using nickel-catalyzed aromatic C–H functionalization are presented.

## 2 Redox-Neutral Aromatic C–H Functionalization with Organohalides

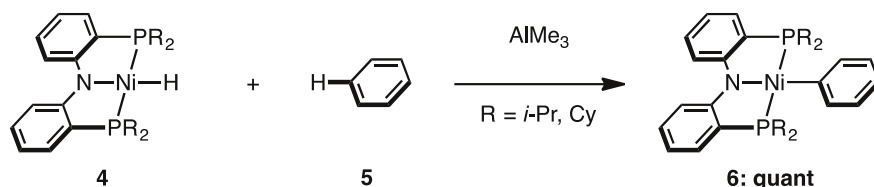
### 2.1 Aromatic C–H Arylation

Heterobiaryl frameworks such as 2-aryl-1,3-azoles represent privileged structural motifs often found or used in bioactive molecules. In 2009, the groups of Itami and

Dubeck (1963)



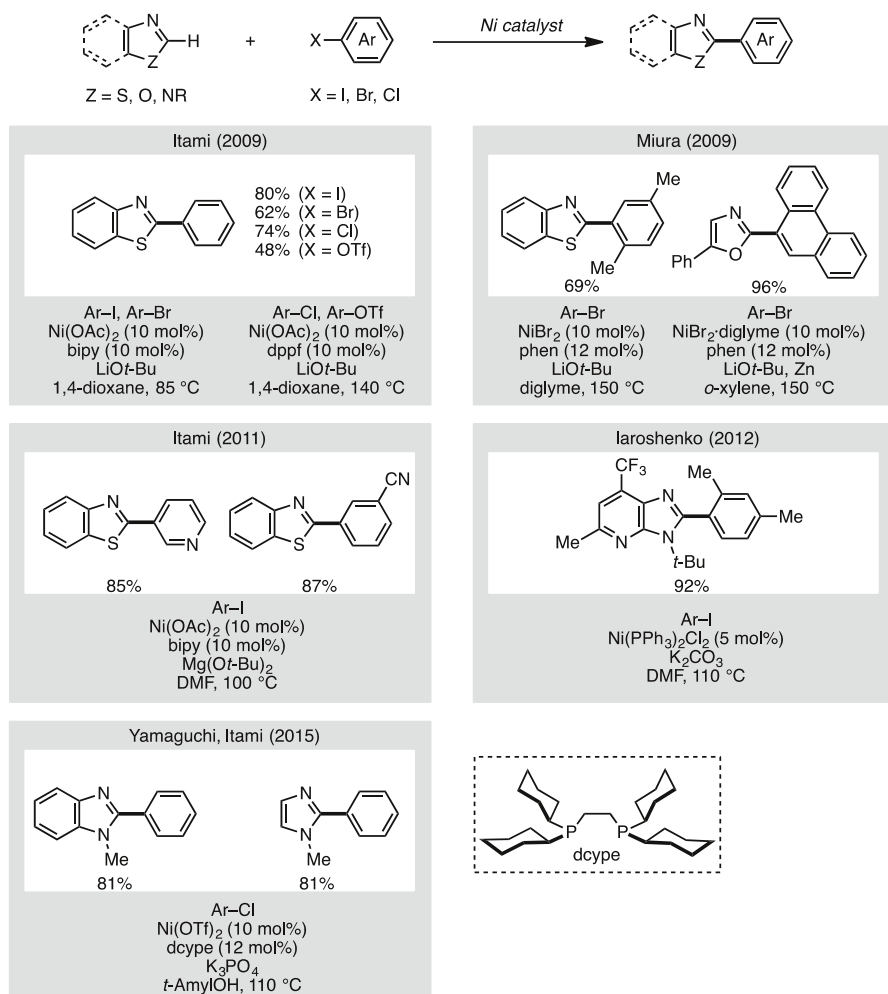
Liang (2006)



**Scheme 1** Pioneering work for C–H activation using nickel complexes



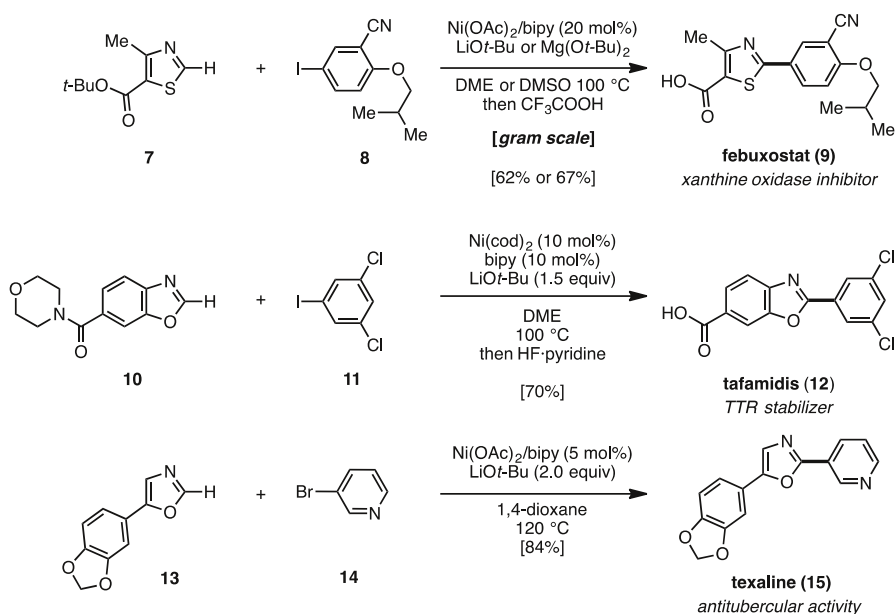
Miura independently reported the first example of nickel-catalyzed C–H arylation of 1,3-azoles with aryl halides to synthesize 2-aryl-1,3-azoles (Scheme 2) [10, 11]. Itami and coworkers developed a  $[\text{Ni}(\text{OAc})_2/2,2'$ -bipyridyl (bipy)/ $\text{LiOt-Bu}$ ] catalyst system for the C–H arylation of 1,3-azoles with aryl halides, while Miura simultaneously reported similar conditions  $[\text{NiBr}_2/1,10$ -phenanthroline (phen)/ $\text{LiOt-Bu}$ ] for the C–H arylation between 1,3-(benzo)azoles and aryl bromides. In both of these reaction conditions, it was essential to use  $\text{LiOt-Bu}$  as the base. Thereafter, a new protocol for  $\text{Ni}(\text{OAc})_2/\text{bipy}$ -catalyzed C–H arylation using  $\text{Mg}(\text{Ot-Bu})_2$  as a milder and less expensive alternative to  $\text{LiOt-Bu}$  was developed in 2011 by Itami and coworkers [12]. Compared with the protocol that uses  $\text{LiOt-Bu}$ , the newly developed  $\text{Mg}(\text{Ot-Bu})_2$ -based method is more effective for reactions involving



**Scheme 2** C–H arylation of 1,3-azoles with aryl halides

electron-deficient haloarenes. Then, in 2012, the Iaroshenko group reported that imidazo[4,5-*b*]pyridines can be reacted with aryl iodides or aryl bromides in the presence of  $\text{Ni}(\text{PPh}_3)_2\text{Cl}_2$  as the catalyst and  $\text{K}_2\text{CO}_3$  in DMF to give the corresponding coupling products [13]. Although these reactions can be performed with palladium catalysts, yields using the nickel catalyst were superior. In general, benzimidazoles and imidazoles had not been viable substrates in nickel-catalyzed C–H arylation. Additionally, aryl chlorides had not been commonly used for the nickel-catalyzed C–H arylation of 1,3-azoles. However, in 2015, Itami, Yamaguchi, and coworkers discovered optimal conditions for the C–H arylation of benzimidazoles and imidazoles with aryl chlorides [14]. The key to achieving the C–H arylation of imidazoles is to use *t*-AmylOH as the solvent with a Ni/1,2-bis(dicyclohexylphosphino)ethane (dcype) catalyst (for reactions involving other aryl sources under the same catalytic conditions, see Sect. 4.1).

These methods for the nickel-catalyzed C–H arylation of 1,3-azoles can be applied to the synthesis of biologically active molecules (Scheme 3) [10, 12]. Under the influence of a  $\text{Ni}(\text{OAc})_2/\text{bipy}$  catalyst and  $\text{LiOt-Bu}$ , thiazole **7** and aryl iodide **8** underwent coupling in dimethoxyethane (DME) at 100 °C to furnish the corresponding coupling product. A  $\text{Mg}(\text{Ot-Bu})_2/\text{dimethylsulfoxide}$  (DMSO) system was equally effective for the coupling. Subsequent treatment with  $\text{CF}_3\text{CO}_2\text{H}$  afforded febuxostat (**9**) [15], a xanthine oxidase inhibitor, in 62–67 % overall yield. Following the present synthetic route, only three steps are required (in 43–46 % overall yield) to accomplish the synthesis of **9**. Additionally, this reaction was applicable for the synthesis of tafamidis (**12**), a transthyretin (TTR) stabilizer [16].



**Scheme 3** Syntheses of febuxostat (**9**), tafamidis (**12**), and texaline (**15**) by Ni-catalyzed arylation of azoles

Carboxamide-substituted benzoxazole **10** was coupled with 1,3-dichloro-5-iodobenzene (**11**) to furnish the corresponding product. Subsequent hydrolysis of the amide using HF-pyridine provided **12** in 70 % overall yield. Additionally, it was found that texaline (**15**) [17], an antimycobacterial alkaloid, could be obtained in 84 % yield by coupling oxazole **13** with aryl bromide **14** by the action of the Ni(OAc)<sub>2</sub>/bipy/LiOt-Bu catalytic system in 1,4-dioxane at 120 °C. The efficient and rapid syntheses of febuxostat (**9**), tafamidis (**12**), and texaline (**15**) highlight the potential of the present nickel catalysis in a range of synthetic applications.

Concomitantly with the above C–H arylation of 1,3-azoles, Yamakawa and coworkers reported the direct arylation of simple benzene, naphthalene, and pyridine with aryl bromides using a Cp<sub>2</sub>Ni/BEt<sub>3</sub> (or PPh<sub>3</sub>)/KOt-Bu catalyst system (Scheme 4) [18]. It was presumed that the cross-coupling reaction proceeds through a radical-type pathway, because regioisomers were produced by this nickel-catalyzed system.

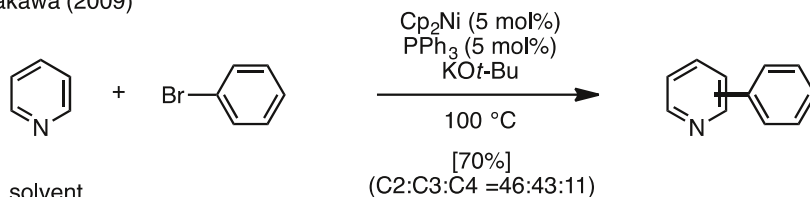
These nickel-catalyzed transformations work not only for heteroarenes, but also for arenes (benzene derivatives). In 2014, Chatani and coworkers reported a nickel-catalyzed C–H arylation of benzamides with aryl iodides (Scheme 5) [19]. For example, benzamide **16** bearing a quinoline moiety as a chelation-assisted group was coupled with iodobenzene (**17**) in the presence of catalytic Ni(OTf)<sub>2</sub> to afford the corresponding coupling product **18** in 92 % yield with exclusive *ortho*-selectivity.

## 2.2 Aromatic C–H Alkynylation

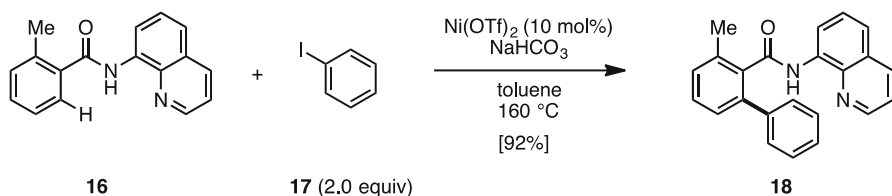
The first example of C–H alkynylation of heteroarenes was reported by Miura and coworkers (Scheme 6) [20]. For example, aryloxazole **19** was reacted with bromophenylethyne (**20**) using a nickel catalyst [Ni(cod)<sub>2</sub>/1,2-bis(diphenylphosphino)benzene (dppbz)] and LiOt-Bu as base to afford the corresponding alkynyl adduct **21** in 91 % yield.

In 2015, several examples of C–H alkynylation of six-membered (hetero)arenes with alkynyl bromides were published using chelation-assisted groups (Scheme 7) [21–23]. The groups of Shi (aromatic amides containing 2-pyridyldimethylamine), Li (aromatic amides containing 8-aminoquinoline), and Balaraman (aromatic amides containing 8-aminoquinoline) independently accomplished nickel-catalyzed C–H alkynylations of pyridylamide and benzamide derivatives with bromoethynes to give the corresponding *ortho*-substituted products in excellent yields.

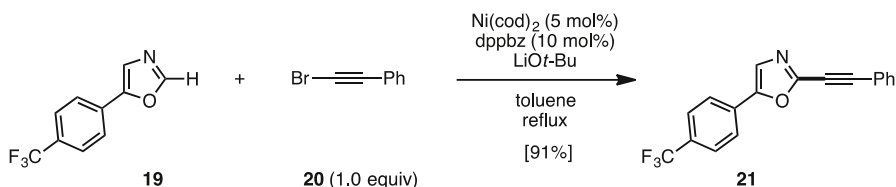
Yamakawa (2009)



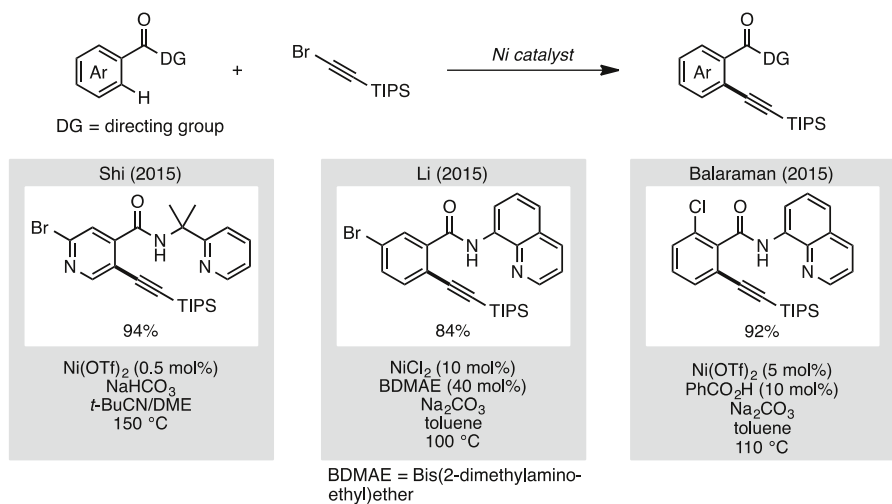
**Scheme 4** C–H arylation of pyridine with aryl halides



**Scheme 5** Chelation-assisted C–H arylation of benzamides

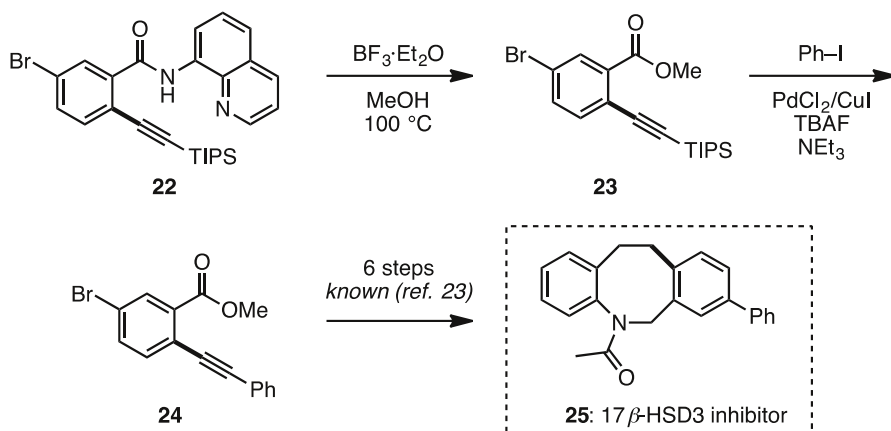


**Scheme 6** C–H alkylation of azoles with alkynyl bromides

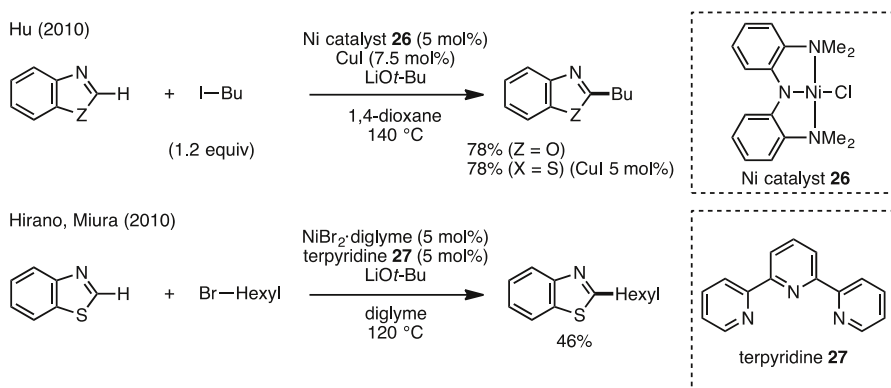


**Scheme 7** Aromatic C–H alkylation with alkynyl halides

The Li group also applied their method to synthesize an intermediate of a 17 $\beta$ -hydroxysteroid dehydrogenase type-3 (17 $\beta$ -HSD3) inhibitor, which was considered to be a clinical candidate for the treatment of prostate cancer (Scheme 8) [22]. The obtained alkynyl product **22** was treated with  $\text{BF}_3 \cdot \text{OEt}_2$  to give ester **23**, followed by sila-Sonogashira coupling with iodobenzene to give diarylethyne **24**, which was an intermediate toward 17  $\beta$ -HSD3 inhibitor **25** [24].



**Scheme 8** Synthesis of a 17β-HSD3 inhibitor



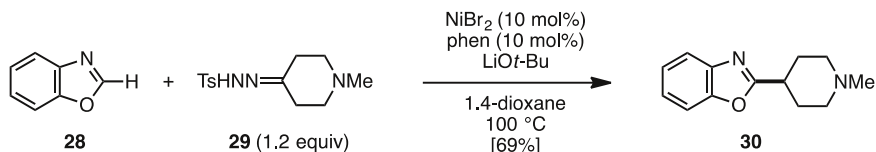
**Scheme 9** C–H alkylation of 1,3-azoles and alkyl halides

### 2.3 Aromatic C–H Alkylation

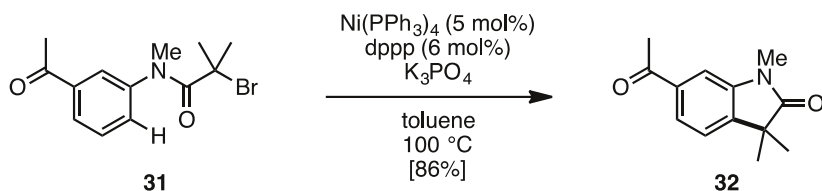
In 2010, C–H alkylations of 1,3-azoles with alkyl halides were reported independently by the groups of Hu and Miura (Scheme 9) [25, 26]. C–H activation using alkyl reactants is relatively rare compared with using unsaturated reactants because of the difficulty in suppressing the β-hydrogen elimination of alkylmetal reagents. To suppress β-hydrogen elimination, Hu's group used a pincer-type nickel catalyst **26** in the presence of CuI as a co-catalyst. Meanwhile, the Hirano and Miura group utilized terpyridine **27** as the ligand.

Although technically the reaction does not involve alkyl halides, the Miura group developed a C–H alkylation of 1,3-azoles with alkyl hydrazones as the alkylating agent in 2012 (Scheme 10) [27]. *N*-Tosylhydrazone **29** was converted to the diazo species in situ that reacted with benzoxazole (**28**) in the presence of a NiBr<sub>2</sub>/phen/LiOt-Bu catalytic system to afford the secondary alkylated product **30** in moderate

Hirano, Miura (2012)

**Scheme 10** Aromatic C–H alkylation using alkyl hydrazones

Lei (2013)

**Scheme 11** Intramolecular aromatic C–H alkylation

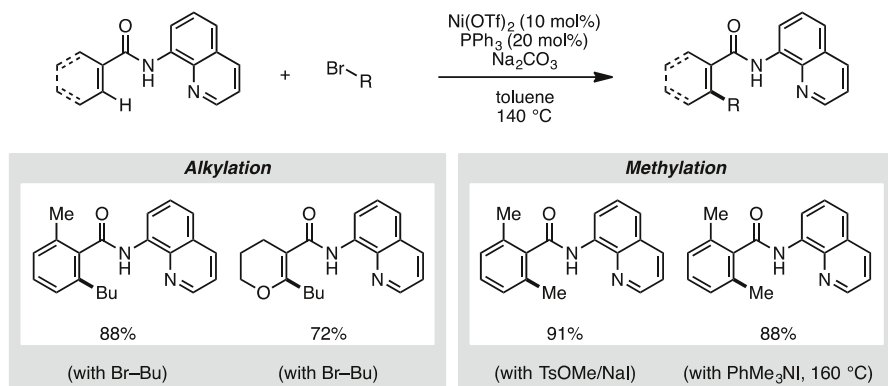
yields. It is of note that this reaction also proceeded when a cobalt catalyst was used. This C–H alkylation method shows the potential utility of alternative methods for alkylated 1,3-azoles.

Furthermore, the Lei group reported an intramolecular C–H alkylation of arenes in 2013 (**Scheme 11**) [28]. When  $\alpha$ -bromoamide **31** was reacted with catalytic Ni(PPh<sub>3</sub>)<sub>4</sub>/1,3-bis(diphenylphosphino)propane (dppp) and K<sub>3</sub>PO<sub>4</sub> in toluene at 100 °C, cyclization product **32** was formed in 86 % yield. It was assumed that this reaction proceeds through a radical pathway because the reaction was quenched when 2,2,6,6-tetramethylpiperidine 1-oxyl (TEMPO) was added as a radical scavenger. Additionally, this reaction worked well under visible light in the presence of a tris(2-phenylpyridinato)iridium [Ir(ppy)<sub>3</sub>] photocatalyst.

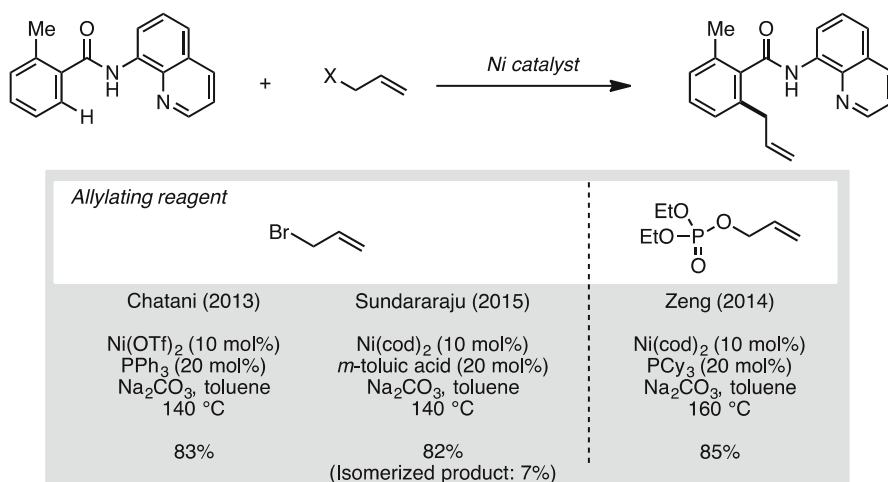
Intermolecular C–H alkylation of arenes through nickel catalysis was achieved by using a chelation-assisted group by Chatani and coworkers (**Scheme 12**) [29–31]. Arylamides containing 8-aminoquinoline reacted with various alkyl bromides in the presence of a Ni(OTf)<sub>2</sub>/PPh<sub>3</sub> catalyst to give C–H alkylation products in good yields. These reaction conditions can also be applied to methylation when using TsOMe/NaI or PhMe<sub>3</sub>NI as the methylating reagent.

In 2013, Chatani's group also demonstrated a C–H allylation of arylamides using allyl bromides (**Scheme 13**) [29]. Thereafter, Sundararaju and coworkers reported a similar result using *m*-toluic acid as an effective additive [32]. Furthermore, in 2014, the group of Zeng obtained the same products by using allyl phosphates as allylating reagents instead of allyl bromides [33].

This chelation-assisted group, the 8-aminoquinoline moiety, enabled the use of not only primary alkyl and allyl halides but also secondary alkyl halides (**Scheme 14**) [34]. The group of Ackermann found that bis(2-dimethylaminoethyl)ether (BDMAE) was an effective ligand for the nickel-catalyzed C–



**Scheme 12** C–H alkylation of benzamides with alkyl halides

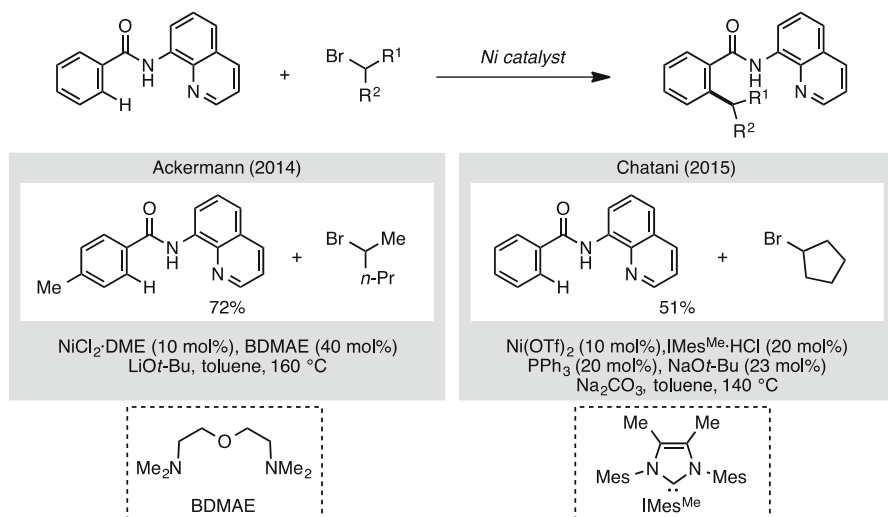


**Scheme 13** C–H allylation of benzamides

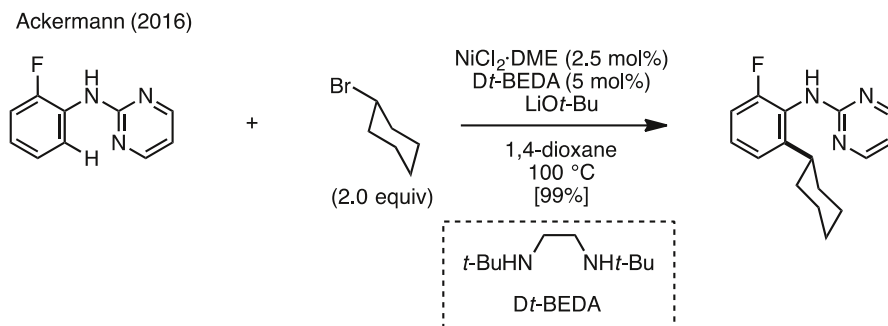
H alkylation of benzamides with secondary alkyl bromides. Although only one example was shown, Chatani and coworkers also reported a nickel-catalyzed C–H alkylation of benzamides with cyclopropyl bromide using  $\text{IMe}^{\text{Me}}$  as the ligand [30].

Very recently, Ackermann and coworkers reported a nickel-catalyzed C–H alkylation of anilines with secondary alkyl halides (Scheme 15) [35]. Use of *N,N'*-di-*tert*-butylethane-1,2-diamine (Dt-BEDA), a vicinal diamine, as a ligand, allowed anilines that bear a monodentate *N*-pyrimidyl substituent to be alkylated under nickel catalysis in excellent yield.

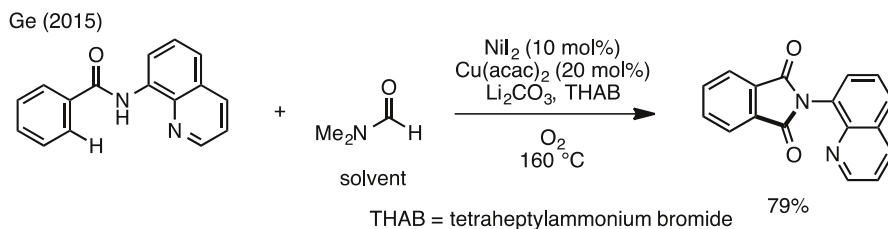
In 2014, a catalytic C–H carbonylation of arylamides was developed by Ge and coworkers (Scheme 16) [36]. Although similar types of carboxylation are known



**Scheme 14** C–H alkylations of benzamides with secondary alkyl halides



**Scheme 15** C–H alkylations of anilines with secondary alkyl halides



**Scheme 16** C–H acylation of benzamides

with palladium, ruthenium, rhodium, and cobalt catalysts, this was the first example involving nickel/copper catalysis. Additionally, these modified conditions can be applied to aliphatic amides.



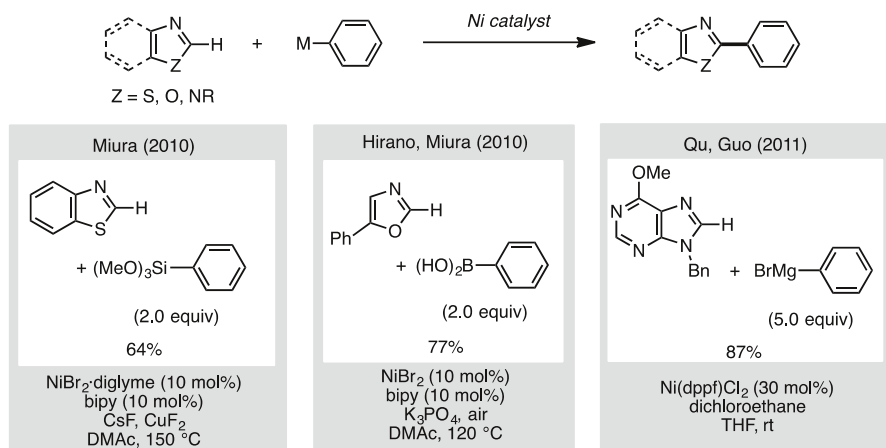
## 3 Oxidative Aromatic C–H Functionalization

### 3.1 Oxidative C–H Arylation and Alkenylation

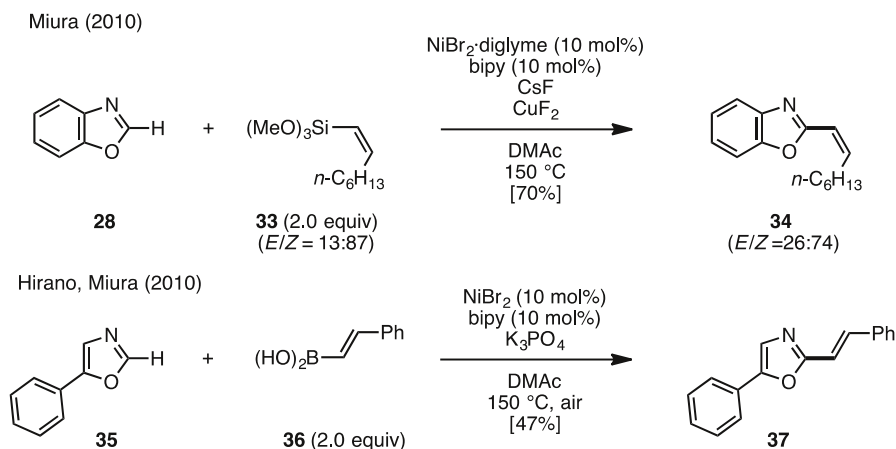
Nickel-catalyzed oxidative C–H arylations using arylmetal species as the aryl source have also been reported in recent years (Scheme 17). The first nickel-catalyzed oxidative direct arylation was disclosed by Miura and coworkers in 2010; they developed a direct arylation of 1,3-azoles with arylsilanes in the presence of Cu salts as oxidants [37]. This report can be regarded as an important finding not only because this is the first nickel-catalyzed oxidative C–H arylation but also because oxidative C–H arylation with arylsilanes is rare even with other transition metal catalysts. A nickel-catalyzed oxidative C–H arylation of (benz)oxazoles with arylboronic acids employing air as the oxidant was also developed by the group of Miura in the same year [38]. An oxidative direct arylation using aryl Grignard reagents through a nickel catalyst system was reported by Qu, Guo, and coworkers [39].

Miura's conditions can be used for the C–H alkenylation of 1,3-azoles with alkenylsilanes and alkenylboronic acids, and two examples are shown in Scheme 18 [35]. Benzoxazole (**28**) was reacted with alkenylsilane **33** under nickel catalysis to afford alkenylbenzoxazole **34** in 70 % yield. When alkenylboronic acid **36** was used as the alkenyl source, 5-phenyloxazole (**35**) could be alkenylated in the presence of a nickel catalyst to give the corresponding coupling product **37** in 47 % yield.

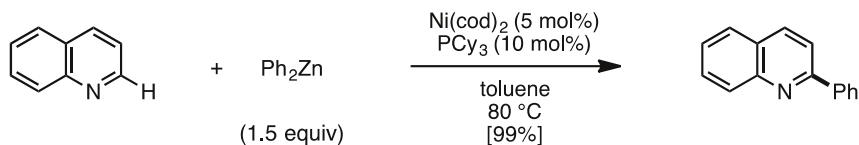
In 2009, Chatani, Tobisu, and coworkers reported a nickel-catalyzed C–H arylation of azines with an arylzinc species (Scheme 19) [40]. By using diarylzinc as an aryl nucleophile and Ni(cod)<sub>2</sub>/PCy<sub>3</sub> as a catalyst, various azines such as pyridines, quinolines, phenanthridines, and pyrazines were arylated in good to excellent yields. This reaction provided C2-arylated azines regioselectively.



**Scheme 17** Ni-catalyzed direct C–H arylation and alkenylation of azoles with organosilicon, boron, and Grignard reagents

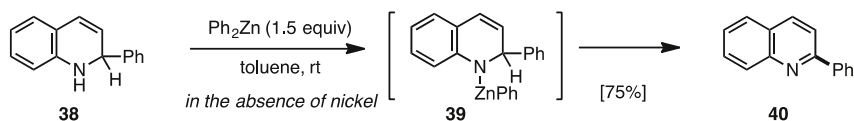


Tobisu, Chatani (2009)

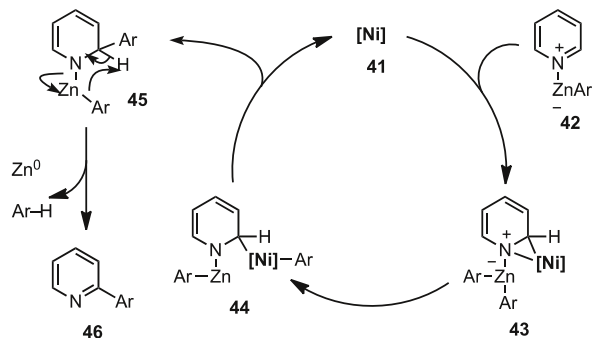


The mechanism of this coupling reaction is assumed to consist of addition of the aryl nucleophile under nickel catalysis, followed by in situ rearomatization to form the coupling product. To support this hypothesis, the rearomatization reaction was specifically studied by the group of Chatani [41]. Treatment of 2-phenyl-1,2-dihydroquinoline (**39**; prepared by nucleophilic addition of phenyllithium onto quinoline) with diphenylzinc at room temperature produced rearomatized product **40** without the nickel catalyst in 75 % yield (Scheme 20). According to this result, loss of the C2 hydrogen atom of **38** proceeds via the intermediacy of an organozinc species such as **39**. On the basis of this investigation, a reaction mechanism for the nickel-catalyzed C–H arylation of azines with diarylzinc was proposed. Nickel(0) species **41** initially reacts with diarylzinc–pyridine adduct **42** to form azanickelacyclopropane **43**. An intramolecular aryl transfer affords nickel species **44**, which subsequently liberates Ni<sup>0</sup> catalyst **41** along with zinc amide **45** by reductive elimination. The zinc amide species **45** then undergoes rapid oxidative rearomatization, leading to arylated product **46**.

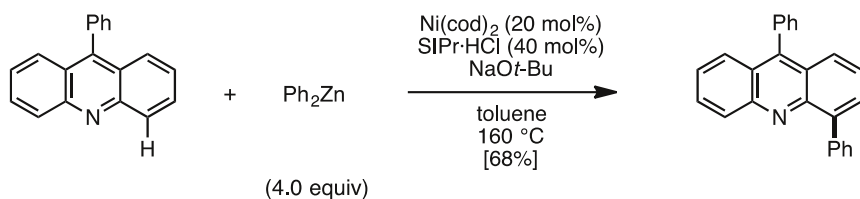
Similarly, a C–H arylation of acridine at its C4 position was also reported by the Chatani group using a Ni(cod)<sub>2</sub>/SIPr-HCl/NaOt-Bu catalytic system (Scheme 21) [42]. Under the influence of a catalytic amount of Ni(cod)<sub>2</sub>, 1,3-bis(2,6-diisopropylphenyl)imidazolium chloride (SIPr-HCl), and a stoichiometric amount



Possible reaction mechanism

**Scheme 20** Reaction mechanism for Ni-catalyzed C-H arylation of azines with arylzinc reagents

Tobisu, Chatani (2012)

**Scheme 21** C4-selective C-H arylation of acridine with arylzinc reagents

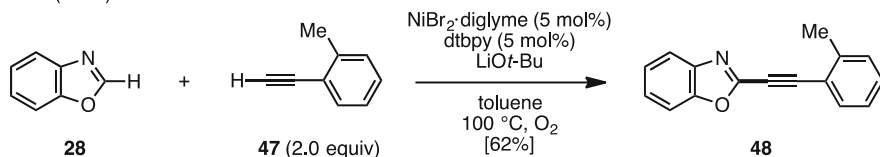
of  $\text{NaOt-Bu}$ , acridines were cross-coupled with excess amounts of diarylzinc reagents to afford C4-arylated products regioselectively.

### 3.2 Oxidative C-H Alkynylation

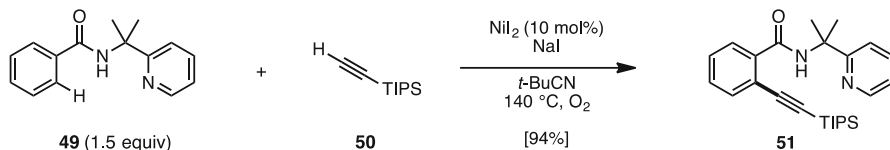
Nickel-catalyzed oxidative C-H alkynylation, which involves the use of alkynes directly without pre-functionalization, was also reported by the groups of Miura and Shi. For example, in the presence of catalytic  $\text{NiBr}_2/\text{di-}t\text{-butylbipyridyl}$  (dtbpy) and  $\text{LiOt-Bu}$  as a base in toluene under oxygen atmosphere, benzoxazole (**28**) was reacted with arylethyne **47** to afford coupling product **48** in 62 % yield (**Scheme 22**) [43].

In contrast, Shi and coworkers reported in 2015 that arylamides (**49**: containing a 2-pyridyldimethylamine moiety) can react with triisopropylsilyl acetylene **50** in the presence of catalytic  $\text{NiI}_2$  and  $\text{NaI}$  as an additive in  $t\text{-BuCN}$  (similar reaction conditions to **Scheme 7**) under an oxygen atmosphere to give C-H alkynylated product **51** in 94 % yield (**Scheme 23**) [44].

Miura (2010)

**Scheme 22** Oxidative C–H alkylation of azoles with acetylenes

Shi (2015)

**Scheme 23** Oxidative C–H alkylation of benzamides with silylacetylene

### 3.3 Oxidative C–H Alkylation

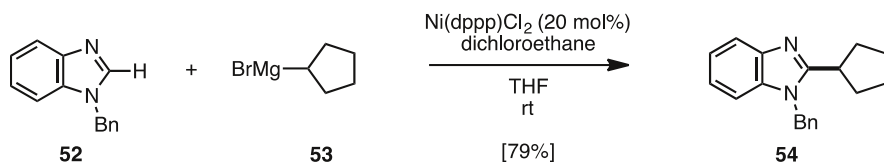
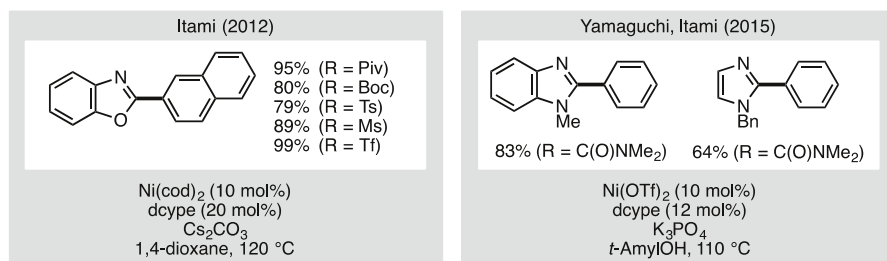
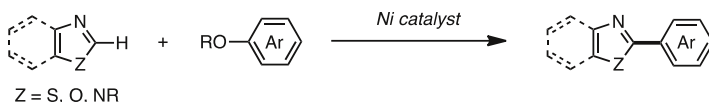
Nickel-catalyzed oxidative C–H alkylation was only recently reported by Qu, Guo, and coworkers in 2012 (**Scheme 24**) [45]. For example, benzimidazole **52** can be coupled with Grignard reagent **53** using 20 mol% of [1,3'-bis(diphenylphosphino)propane]nickel dichloride [ $\text{Ni}(\text{dppp})\text{Cl}_2$ ], and 1,2-dichloroethane as an oxidant in THF to afford the coupling product **54** in 79 % yield. When using these coupling partners, other metal catalysts such as palladium and iron were not effective and only trace amounts of product were obtained.

## 4 Aromatic C–H Functionalization with Unconventional Coupling Partners

### 4.1 Phenol and Alcohol Derivatives

In 2012, the first nickel-catalyzed C–H/C–O coupling of 1,3-azoles and phenol derivatives was reported by the Itami group (**Scheme 25**) [46]. In the presence of a  $\text{Ni}(\text{cod})_2/\text{dcype}$  catalyst and  $\text{Cs}_2\text{CO}_3$  as base in 1,4-dioxane, 1,3-azoles and phenol derivatives can be coupled to produce the corresponding 2-aryl-1,3-azoles. Intriguingly, this reaction displays dramatic ligand effects, as other ligands do not deliver coupling products. The  $\text{Ni}(\text{cod})_2/\text{dcype}$  catalyst is active for the coupling of other phenol derivatives such as carbamates, carbonates, sulfamates, triflates, tosylates, and mesylates. However, regarding the 1,3-azole coupling partner, it was limited in terms of substrate scope, as imidazoles did not react at all under these reaction conditions. More recently, Itami and Yamaguchi reported a new protocol for the C–H arylation of benzimidazoles and imidazoles with phenol derivatives

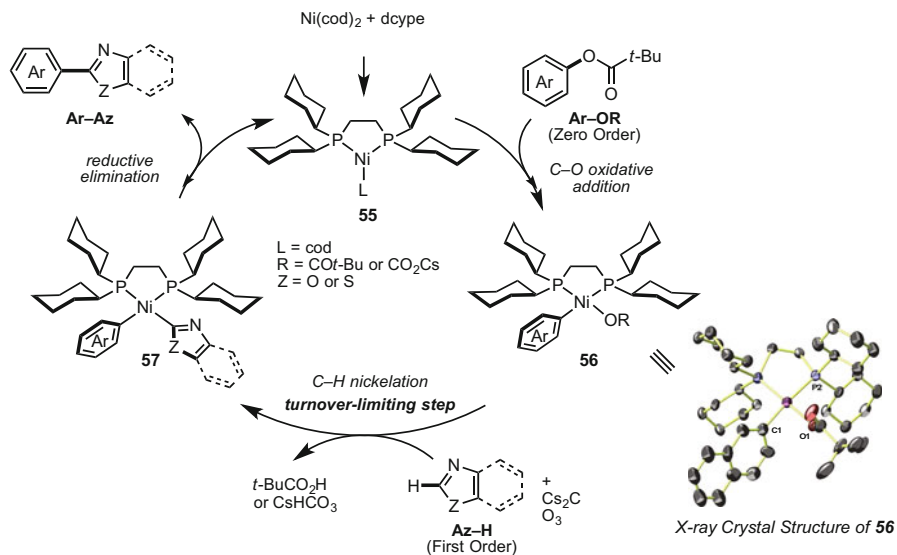
Qu, Guo (2012)

**Scheme 24** C–H alkylation of benzimidazoles with organomagnesium reagents**Scheme 25** C–H arylation of azoles with phenol derivatives

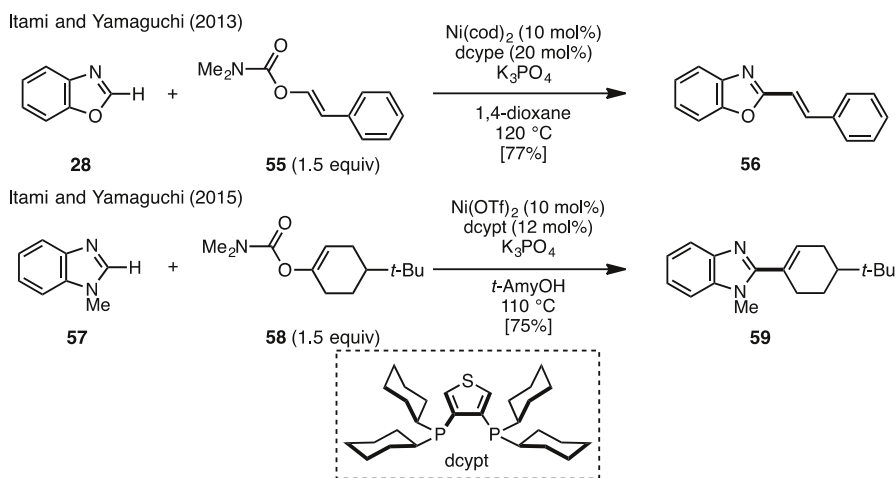
(carbamates) [14]. The catalyst can consist of Ni(II) such as  $\text{Ni(OTf)}_2$ , which is a less expensive complex compared to  $\text{Ni(cod)}_2$ .

**Scheme 26** depicts a plausible mechanism based on a Ni(0)/Ni(II) redox catalytic cycle, occurring via (1) oxidative addition of the aromatic C–O bond of Ar–OR to Ni(0) species **55**, (2) C–H nickelation of an azole (Az–H) with Ar–Ni(II)–OR species **56**, and (3) reductive elimination from **57** of the heterobiaryl product (Ar–Az) to regenerate the Ni(0) species. Extensive studies involving the isolation of intermediate **56** and kinetic studies have been reported by Itami, Yamaguchi, and Lei [47]. The isolation of key intermediate **56** resulting from C–O oxidative addition revealed this plausible Ni(0)/Ni(II) redox catalytic cycle. Additionally, kinetic studies and kinetic isotope effect investigations showed that the C–H nickelation is the turnover-limiting step in the catalytic cycle. Furthermore, theoretical calculations were performed to gain further insight regarding the effect of base, especially in the C–H nickelation step [48]. Through these combined experimental and computational studies, a detailed catalytic cycle and the dramatic dcype ligand effect on this reaction were unveiled.

In 2013, Itami and Yamaguchi found that Ni/dcype also catalyzes C–H/C–O alkenylation using enol derivatives (**Scheme 27**) [14, 49]. Benzoxazole (**28**) was coupled with enol derivative **55** under the nickel catalytic system using the dcype ligand to form alkenyl oxazole **56** in 77 % yield by C–H alkenylation at the C2 position of oxazoles. For the C–H alkenylation of imidazole derivatives, it was



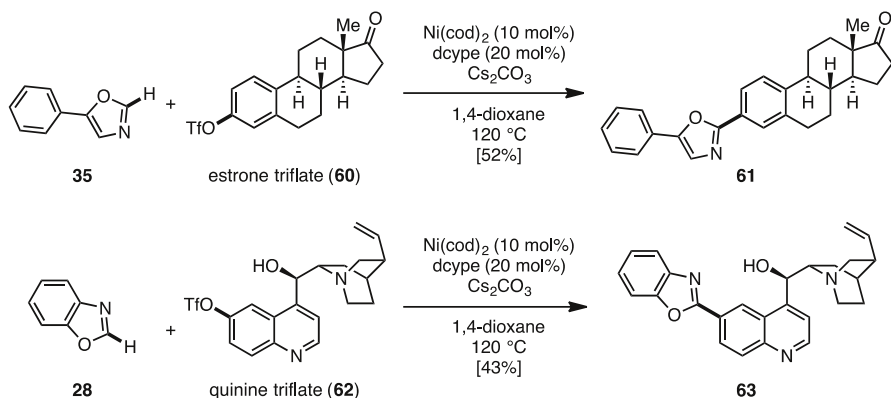
**Scheme 26** Plausible catalytic cycle of nickel-catalyzed C-H arylation with phenol derivatives



**Scheme 27** C-H alkenylation of azoles with phenol derivatives

found that 3,4-bis(dicyclohexylphosphino)thiophene (dcyp) is an effective ligand, and the coupling reaction of benzimidazole and enol derivative **58** in *t*-AmyOH as a solvent successfully afforded the corresponding coupling product **59** in 75 % yield.

To demonstrate the applicability of this approach, a Ni-catalyzed C-H/C-O coupling to functionalize estrone and quinine was attempted (**Scheme 28**). The coupling of estrone triflate (**60**) with **35** proceeded smoothly under the standard conditions to afford heteroarylated estrone **61** in 52 % yield. The C-H/C-O coupling of quinine triflate (**62**) with **28** also occurred, giving the quinine-



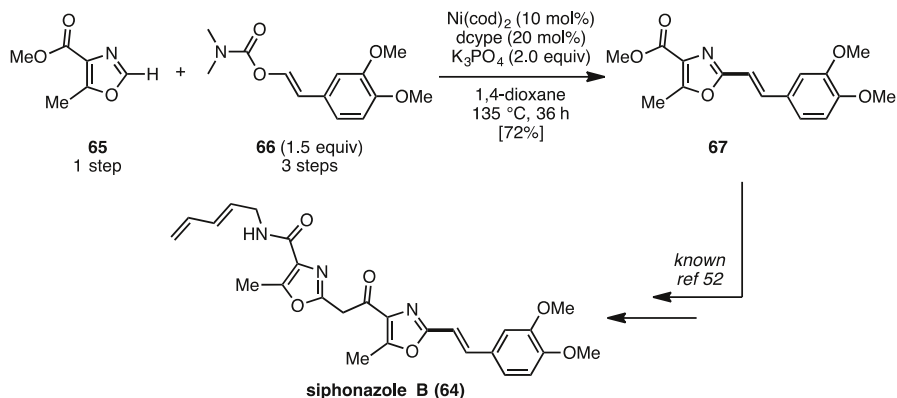
**Scheme 28** Late-stage C–O bond heteroarylation of naturally occurring biomolecules by nickel catalysis

benzoxazole hybrid molecule **63**, albeit with somewhat lower efficiency. Notably, the hydroxyl, amine, and olefin functionalities were tolerated under the coupling conditions. This successful application to the functionalization of the quinine structure, which is known to be sensitive under acidic, basic, and redox conditions, highlights the potential of the present nickel catalysis for further development and applications.

To showcase the utility of this new azole alkenylation method, this reaction was applied to the synthesis of siphonazole B (**64**), a natural product isolated from a metabolite from *Herpetosiphon* sp. (Scheme 29) [50]. Although **64** had already been synthesized by Moody and coworkers [51, 52] as well as Zhang and Ciufolini [53], their syntheses took an excessive number of steps because of a parallel repetition of linear synthetic sequences. To tackle this problem, a convergent synthesis of **64** through nickel-catalyzed C–H alkenylation was designed. Although **67** was a useful intermediate in the previous synthesis, this had required seven linear steps. Thus, this was retrosynthetically divided into oxazole **65** and alkenyl enol **66**. The C–H/C–O alkenylation of **65** and **66** delivered **67** in good yield over four linear steps, thus accomplishing the formal synthesis of siphonazole B (**64**).

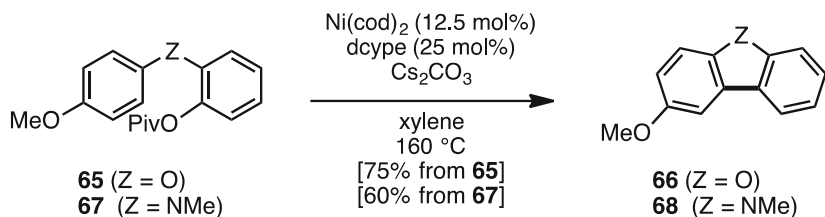
Meanwhile, an intramolecular C–H/C–O coupling with the same nickel catalyst was also reported in 2013 by the Kalyani group (Scheme 30) [54]. For example, pivalate **65** was subjected to reaction conditions similar to Itami's group, but in xylene instead of dioxane, to give benzofuran **66** in 75 % yield. This benzofuran synthesis could be expanded to the synthesis of carbazoles (Z = NMe, 60 % yield). This result is the first example of nickel-catalyzed C–H arylation of simple arenes using C–O electrophiles.

Recently, Han and coworkers reported the nickel-catalyzed C–H alkylations of azoles/pentafluorobenzene with benzylic alcohol derivatives (Scheme 31) [55]. Using a Ni(cod)<sub>2</sub>/dppb catalytic system and NaOt-Bu as a base, 1,3-azoles and pentafluorobenzene could be alkylated with pivalates at the benzyl position to give the corresponding products in good to excellent yields. Although these reactions seem to proceed via nucleophilic substitution, they did not proceed without nickel catalyst.



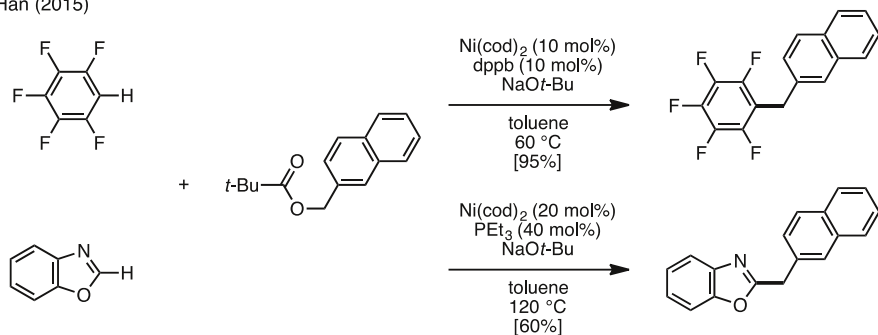
Scheme 29 Synthesis of siphonazole B

Kalyani (2013)



Scheme 30 Dibenzofuran and carbazole synthesis through intramolecular C-H/C-O coupling

Han (2015)

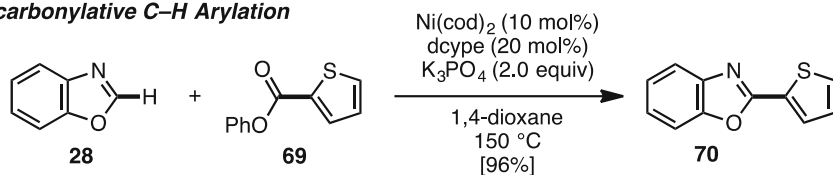
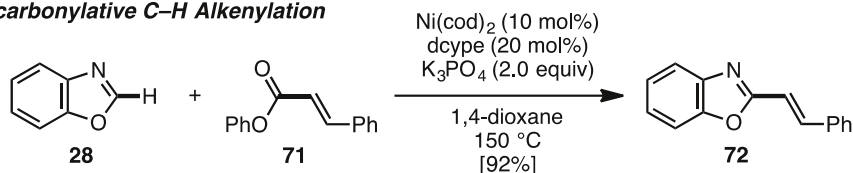


Scheme 31 C-H alkylation of fluorobenzenes and azoles with benzyl alcohol derivatives

## 4.2 Esters and Carboxylic Acids

In 2012, the group of Itami discovered the first nickel-catalyzed decarbonylative C-H biaryl coupling of azoles and aryl esters (Scheme 32) [56]. Under a catalytic system similar to the aforementioned nickel-catalyzed Ar-H/Ar-O coupling (see Scheme 24), decarbonylative C-H coupling of benzoxazole (28) and phenyl



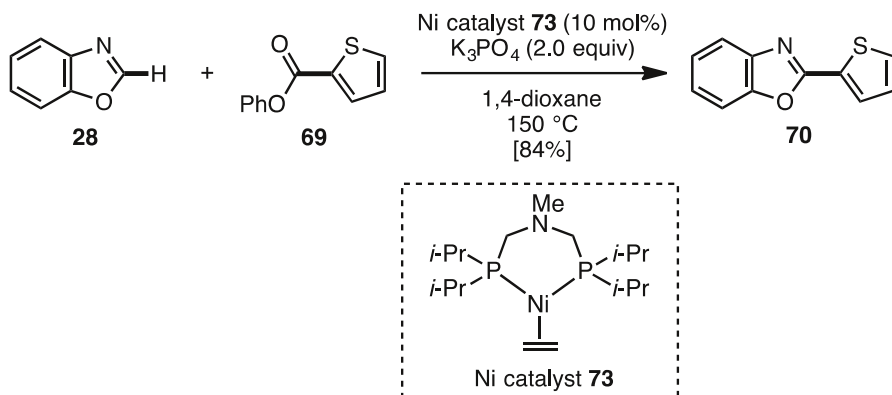
**Decarbonylative C–H Arylation****Decarbonylative C–H Alkenylation****Scheme 32** Decarbonylative C–H arylation and alkenylation of azoles

thiophenecarboxylate (**69**) proceeds smoothly to furnish the corresponding coupling product **70** in 96 % yield. Various esters, particularly heteroaromatic esters such as furans, thiophenes, thiazoles, pyridines, and quinolines, can be used in this reaction to give the corresponding coupling products. Additionally, these reaction conditions can be applied to the decarbonylative C–H alkenylation of azoles and  $\alpha,\beta$ -unsaturated phenyl esters such as **71** [49].

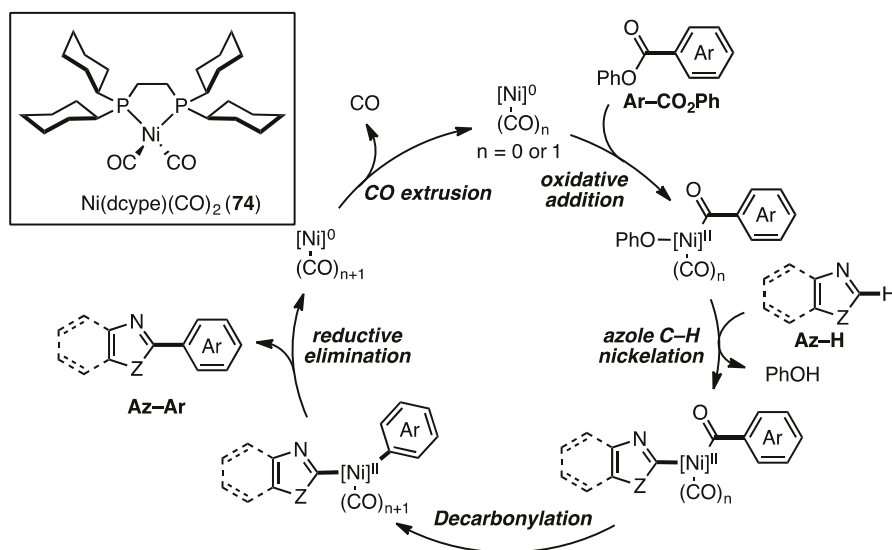
Thereafter, Gade and coworkers also demonstrated the same reaction using a unique nickel catalyst (**Scheme 33**) [57]. They prepared nickel complex **73** from  $[\text{NiCl}_2\text{Py}_4]$  and bis(diisopropylphosphinomethyl)amine, and coupling of **28** and **69** was conducted in the presence of 10 mol% **73** to afford the coupling product **70** in 84 % yield.

A plausible reaction mechanism of the decarbonylative C–H functionalization is shown in **Scheme 34**. The reaction might proceed through  $\text{Ni}^0/\text{Ni}^{\text{II}}$  redox catalysis involving (1) oxidative addition of the phenyl ester C–O bond onto  $\text{Ni}^0$ ; (2) C–H nickelation of azole (Het–H) with  $\text{Ar–Ni}^{\text{II}}(\text{CO})_n\text{–OPh}$  to generate  $\text{Ar–Ni}^{\text{II}}(\text{CO})_n\text{–Het}$ ; (3) CO migration (decarbonylation) onto the nickel center to produce an  $\text{Ar–Ni}^{\text{II}}(\text{CO})_{n+1}\text{–Het}$  species ( $n = 0$  or  $1$ ) [58]; and (4) reductive elimination to release the coupling product (Het–Ar) and to generate a  $\text{Ni}^0(\text{CO})_{n+1}$  species. Although a seemingly inactive nickel dicarbonyl complex **74** would be produced after two turnovers, the active  $\text{Ni}^0$  catalyst could be regenerated by thermal extrusion of CO from **74**. After Itami's and Gade's reports, the group of Houk [59] and Lu [60] independently reported the mechanistic studies of this decarbonylative coupling as well as Ar–H/Ar–O coupling (see **Scheme 26**) by density functional theory (DFT) calculations.

This newly developed decarbonylative C–H functionalization is useful in complex natural product synthesis. For example, Itami and Yamaguchi achieved the synthesis of muscoride A (**74**), a natural product with antibacterial activity (**Scheme 35**) [56, 61]. Two azole esters, **75** and (–)-**76**, were coupled under Ni/dcype catalysis to furnish the corresponding coupling product (–)-**77** in 39 % yield. As the conversion of (–)-**77** into (–)-**74** had been previously described [62], a formal synthesis of (–)-muscoride A (**74**) was completed. If the synthesis was planned and executed with



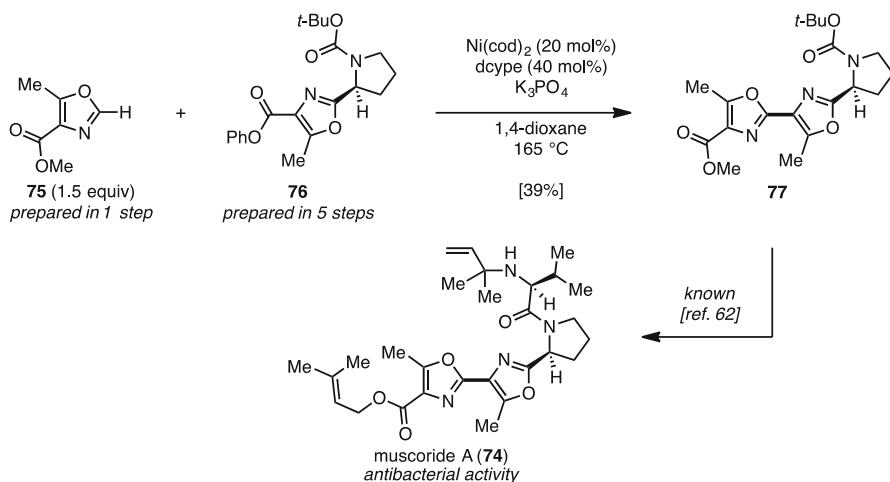
**Scheme 33** Decarbonylative C–H arylation by an alternative nickel catalyst



**Scheme 34** Plausible reaction mechanism of decarbonylative C–H functionalization

typical cross-coupling substrates (aryl halides and organometallic reagents) instead, it would have become much less efficient, with many added steps.

Very recently, Yamaguchi and Itami also applied their decarbonylative C–H arylation to the formal synthesis of thiopeptide antibiotics GE2270s (**Scheme 36**) [63]. Two azole esters **78** and **79**, which were prepared in five steps and three steps respectively from commercially available compounds, were coupled under modified conditions to afford the corresponding coupling product **80** in 49 % yield. Next, coupling product **80** was reacted with thiazolyl acrylic acid **81** in *o*-dichlorobenzene at  $180\text{ }^\circ\text{C}$  via a decarboxylative Diels–Alder reaction to afford the corresponding

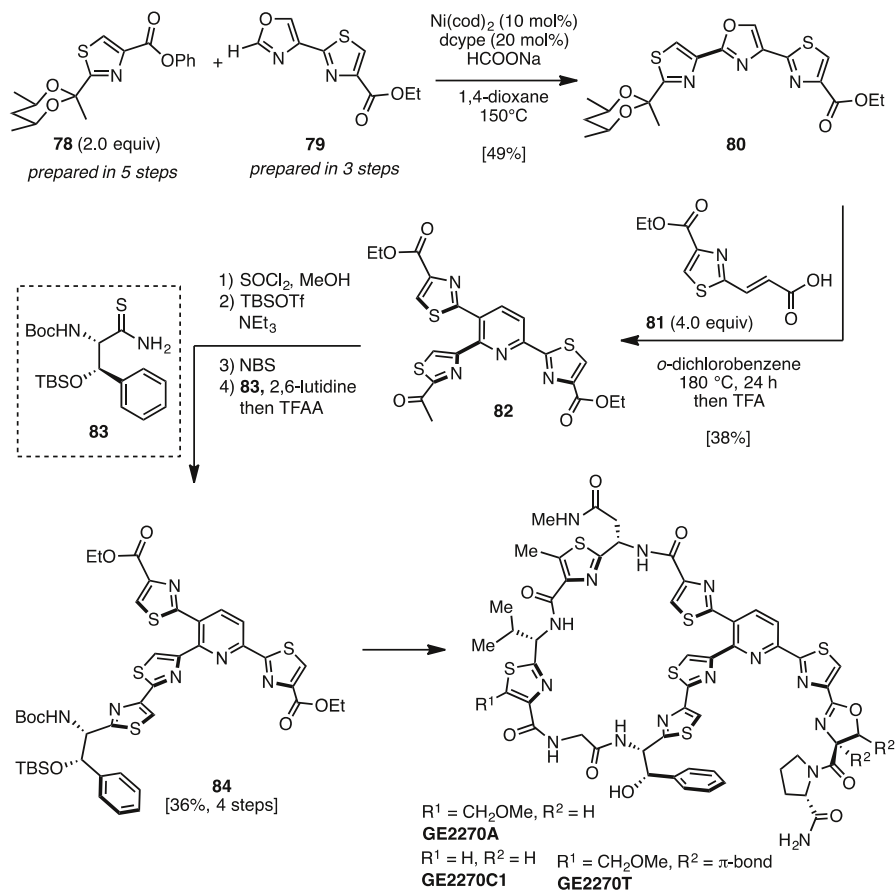


**Scheme 35** Synthesis of muscoride A via decarbonylative C–H arylation

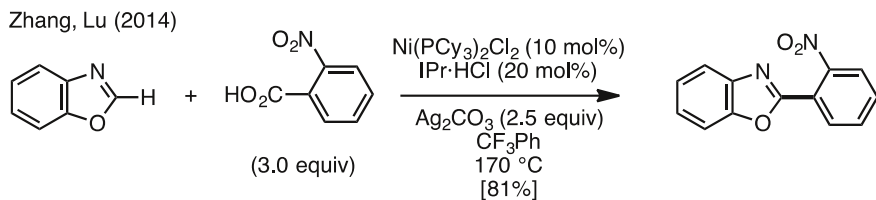
trithiazolopyridine. Subsequently, removal of the acetal group by trifluoroacetic acid (TFA) afforded **82** in 38 % yield over two steps. The key trithiazolopyridine **82** can be converted to thiopeptide antibiotic precursors. Compound **82** was treated with *tert*-butyldimethylsilyl trifluoromethanesulfonate (TBSOTf) and NEt<sub>3</sub> followed by bromination with *N*-bromosuccinimide (NBS) to afford brominated products. These products were treated with thioamide **83** followed by trifluoroacetic anhydride (TFAA) to afford **84** in 36 % yield (four steps). Since the conversion of **84** to GE2270s had been described previously by Nicolaou and coworkers [64, 65], the formal syntheses of GE2270s were accomplished through intermediate **82**.

Zhang and coworkers reported a nickel-catalyzed decarboxylative coupling of 1,3-azoles and carboxylic acid derivatives (Scheme 37) [66]. The catalyst Ni(PCy<sub>3</sub>)<sub>2</sub>Cl<sub>2</sub> in conjunction with IPr·HCl was effective in increasing yields. Although this catalytic transformation was already reported with other metals such as palladium, copper, iron, rhodium, and ruthenium, they were the first to investigate this type of reaction using nickel catalyst. Although electron-deficient substituents such as nitro or fluoro groups were required at the *ortho* position of arenecarboxylic acids, 2-arylazoles can be obtained from arenecarboxylic acids as the coupling partner.

Ge and coworkers also reported a nickel-catalyzed decarboxylative coupling using  $\alpha$ -oxoglyoxylic acids as coupling partners (Scheme 38) [67]. Although a similar palladium-catalyzed C–H acylation using  $\alpha$ -oxoglyoxylic acids had already been reported, it was the first time in which C–H acylation proceeded by nickel catalysis. For example, benzoxazole (**28**) and phenyloxoglyoxylic acid (**85**) were heated with a catalytic amount of Ni(ClO<sub>4</sub>)<sub>2</sub>·6H<sub>2</sub>O and stoichiometric Ag<sub>2</sub>CO<sub>3</sub> in benzene to afford acylation product **86** in 85 % yield.



Scheme 36 Formal syntheses of GE2270s

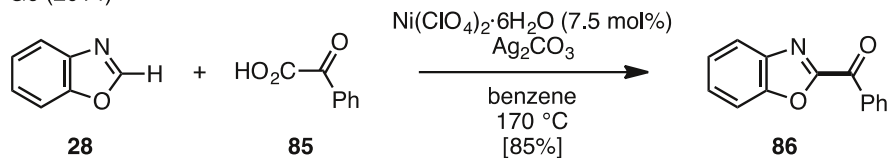
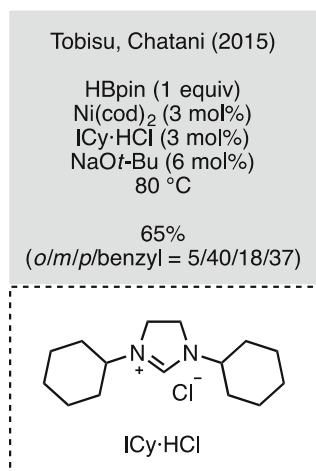
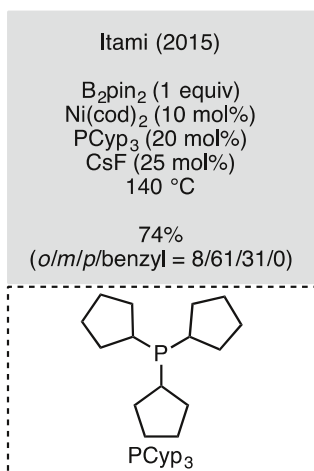
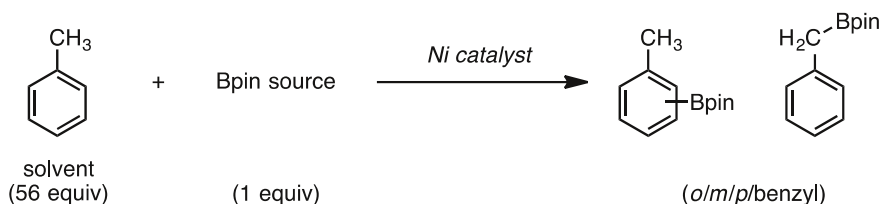


Scheme 37 Decarbonylative coupling of 1,3-azoles and arenecarboxylic acids

## 5 Introduction of Heteroatoms at Aromatic C–H Bonds

Examples of introducing heteroatoms at aromatic C–H bonds by nickel catalysts are still rare, and only several studies have been reported for aromatic C–H borylation and thiolation. In 2015, the Itami group and the Tobisu–Chatani group

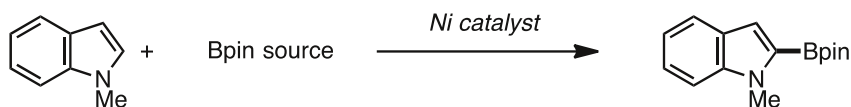
Ge (2014)

**Scheme 38** Decarboxylative C–H acylation of 1,3-azoles and  $\alpha$ -oxoglyoxylic acids**Scheme 39** C–H borylation of arenes

independently reported the C–H borylation of (hetero)aromatic rings by nickel catalysis (**Scheme 39**) [68, 69]. The Itami group used a  $\text{Ni}(\text{cod})_2$ /tricyclopropylphosphine ( $\text{PCyp}_3$ )/ $\text{CsF}$  catalytic system and bis(pinacolato)diboron ( $\text{B}_2\text{pin}_2$ ) as the borylation agent, whereas Tobisu and Chatani used a  $\text{Ni}(\text{cod})_2$ / $\text{ICy} \cdot \text{HCl}$ / $\text{NaOt-Bu}$  catalytic system and pinacolborane ( $\text{HBpin}$ ) as the borylation agent. Under both conditions, toluene was preferentially borylated at the *meta* position, along with a mixture of *ortho*, *para*, and benzylic borylation products.

These reaction conditions were not only applicable when using excess amounts of simple arenes but also when using stoichiometric amounts of heteroaromatics such as indoles (**Scheme 40**) [68, 69].

In contrast, the groups of Lu, Shi, and Kambe independently reported a nickel-catalyzed C–H thiolation of benzamide derivatives containing a chelation-assisted



(1 equiv)

Itami (2015)

$\text{B}_2\text{pin}_2$  (1.5 equiv)  
 $\text{Ni}(\text{cod})_2$  (10 mol%)  
 $\text{PCyp}_3$  (20 mol%)  
 $\text{CsF}$  (25 mol%)  
 THF  
 80 °C

61%

Tobisu, Chatani (2015)

HBpin (2.0 equiv)  
 $\text{Ni}(\text{OAc})_2$  (3 mol%)  
 $\text{ICy}\cdot\text{HCl}$  (3 mol%)  
 $\text{NaOt-Bu}$  (6 mol%)  
 methylcyclohexane  
 80 °C

quant  
(gram scale)

**Scheme 40** C–H borylation of indoles

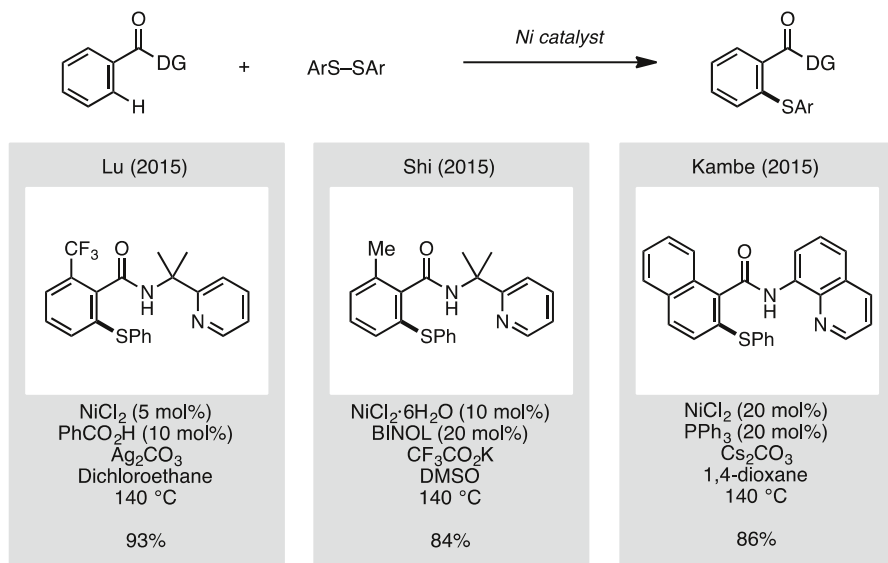
group in 2015 (Scheme 41) [70–72]. Although the chelation-assisted group differed (2-pyridyldimethylamine by Lu and Shi, and 8-aminoquinoline by Kambe), they all used disulfides for the thiolating reagent.

## 6 Hydroarylation-Type C–H Functionalization

The addition of a (hetero)arene C–H bond onto alkynes or alkenes under transition metal catalysis to generate alkenyl or alkyl arenes can be classified as a hydroarylation-type C–H functionalization (Scheme 42). Although hydroarylations using other metal catalysts have been reported, this section focuses on nickel-catalyzed hydroarylation-type C–H functionalization. Mechanistically, these reactions typically start with the coordination of an alkyne/alkene to a Ni(0) species. The complex is reacted with a (hetero)aromatic C–H bond via oxidative addition, followed by hydronickelation forming an Ar–Ni(II)–alkenyl (alkyl) intermediate, which then undergoes reductive elimination to afford hydro(hetero)arylation products. Since an excellent review of this reaction type by nickel catalysis has already been reported by Nakao [6], details are omitted and only reaction types are classified here.

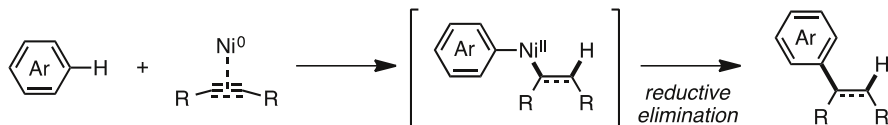
### 6.1 Hydroarylation of Alkynes

In 2006, Nakao, Hiyama, and coworkers reported a nickel-catalyzed hydroarylation of alkynes with heteroarenes (Scheme 43) [73]. Various heteroarenes such as indoles, benzofurans, benzimidazoles, and benzoxazoles reacted with alkynes in the presence of  $\text{Ni}(\text{cod})_2/\text{PCyp}_3$  in toluene under mild conditions to give the



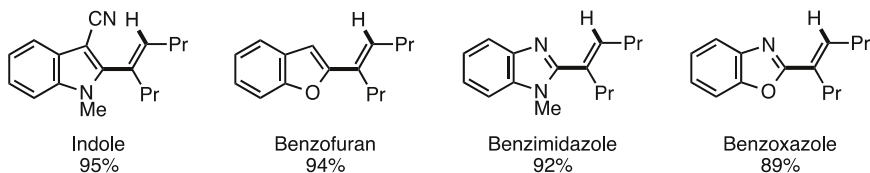
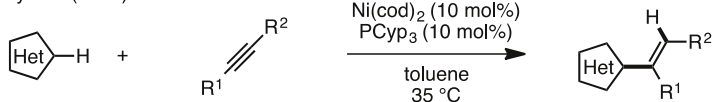
**Scheme 41** C–H thiolation of benzamides

*Hydroarylation-type C–H functionalization*

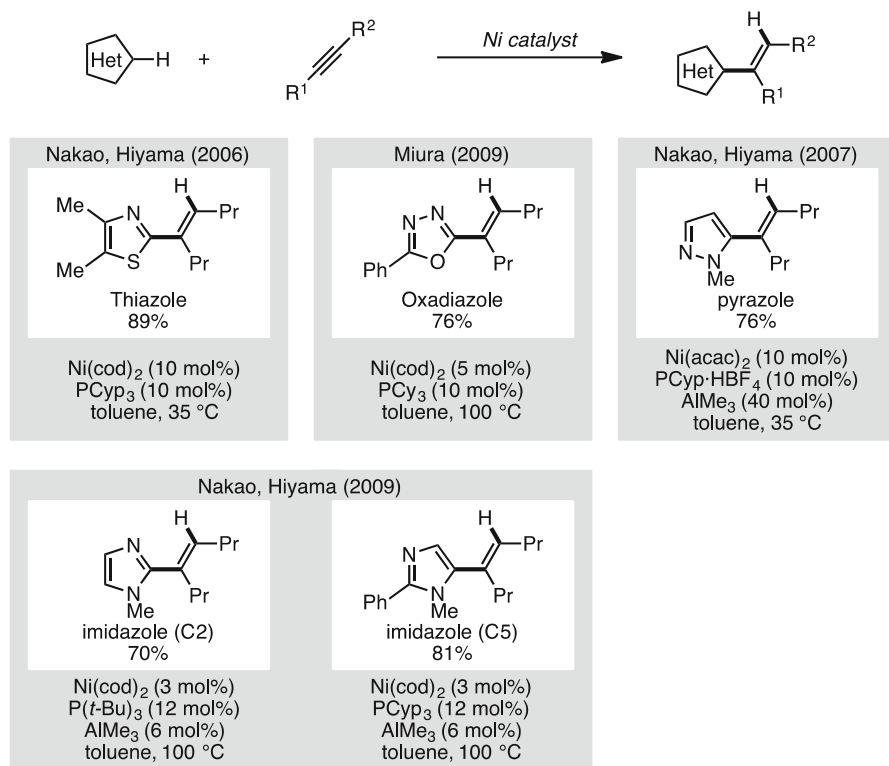


**Scheme 42** Hydroarylation-type C–H functionalization

Nakao, Hiyama (2006)



**Scheme 43** Hydroarylation of alkynes using heteroarenes



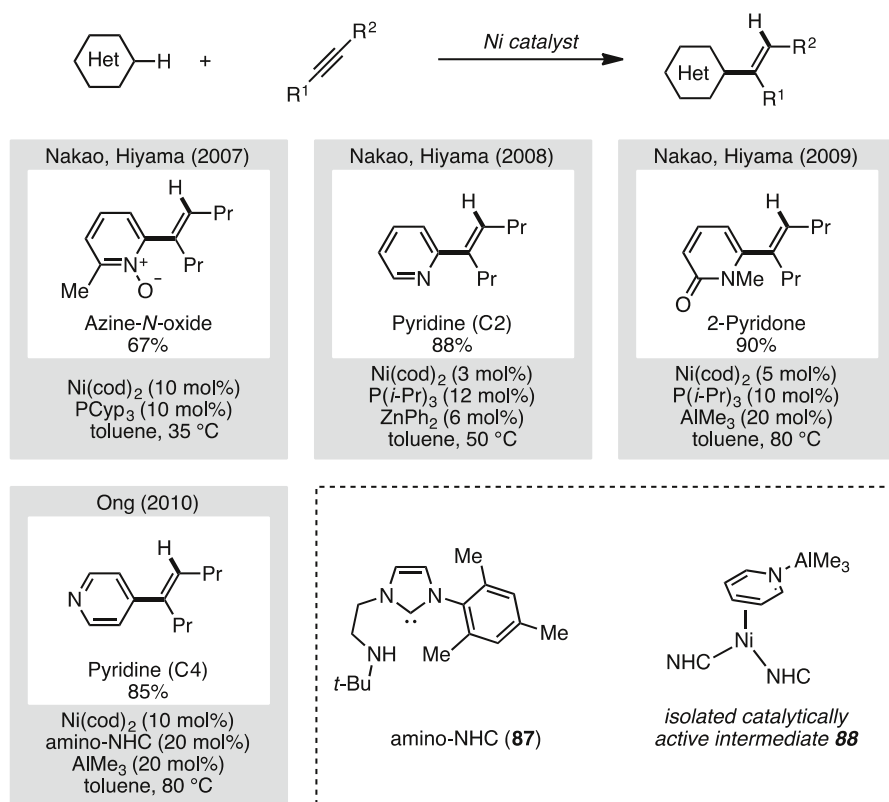
**Scheme 44** Hydroarylation of alkynes with 5-membered heteroarenes

corresponding heteroaryl-substituted ethenes with high chemo-, stereo-, and regioselectivity.

This nickel-catalyzed hydroarylation is applicable not only for benzoheteroarenes, but also for five-membered heteroarenes (Scheme 44). For example, Nakao and Hiyama demonstrated the hydroarylation of thiazoles using the same nickel catalyst [73], and the Miura group reported the hydroarylation of oxadiazoles by using a Ni(cod)<sub>2</sub>/PCyp<sub>3</sub> catalytic system [74]. Additionally, Nakao and Hiyama discovered that AlMe<sub>3</sub> is an effective additive for pyrazoles and imidazoles [75, 76]. These reactions typically proceeded selectively at the C2 position on heteroarenes. However, when imidazoles bearing a C2 substituent were used, hydroarylation proceeded at the C5 position of imidazoles. When using dialkylethyne, the reaction proceeded with *syn* addition, whereas diarylethyne led to *anti*-addition products.

The first example of nickel-catalyzed hydroarylation of electron-deficient heteroaromatics was reported by Nakao and Hiyama in 2007 (Scheme 45) [77]. Alkynes were reacted with azine *N*-oxides under nickel catalysis to afford alkenyl products in good yields. In 2008, they discovered that the addition of Lewis acids such as ZnMe<sub>2</sub> or ZnPh<sub>2</sub> instead of using *N*-oxides is effective, affording the corresponding hydroarylation products regioselectively at the C2 position on





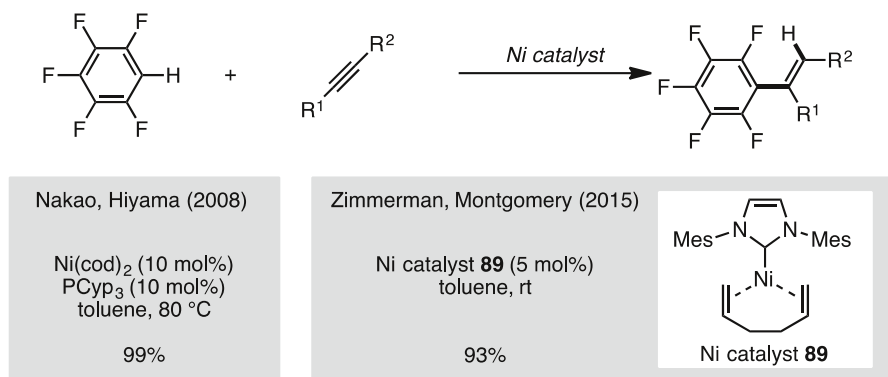
**Scheme 45** Hydroarylation of alkynes with electron-deficient heteroarencs

pyridines [78]. In 2009, they also applied modified catalytic conditions to the alkenylation of pyridone derivatives [79]. In contrast, Ong and coworkers reported a nickel-catalyzed hydroarylation of alkynes and pyridines at the C4 position [80]. They assumed that the complexation of amino-NHC (**87**) and AlMe<sub>3</sub> such as **88** activated a C–H bond on pyridine at the C4 position.

This nickel catalysis enables the hydroarylation of alkynes with fluoroarenes (Scheme 46). In 2008, Nakao and Hiyama demonstrated that pentafluorobenzene can react with alkynes using a Ni(cod)<sub>2</sub>/PCyp<sub>3</sub> catalyst [81]. Recently, Zimmerman and Montgomery found that 1,5-cyclooctadiene (cod) plays an inhibitory role in nickel-catalyzed reactions, and therefore they used precatalyst **89** involving 1,5-hexadiene instead of cod [82]. With this modification, the hydroarylation of alkynes with fluoroarenes smoothly proceeded at room temperature to afford the corresponding alkenylated products in good yields.

## 6.2 Hydroarylation of Alkenes

Hydroarylation is applicable not only for alkynes but also for alkenes (Scheme 47). In 2010, Nakao and Hiyama reported a nickel-catalyzed hydroheteroarylation of



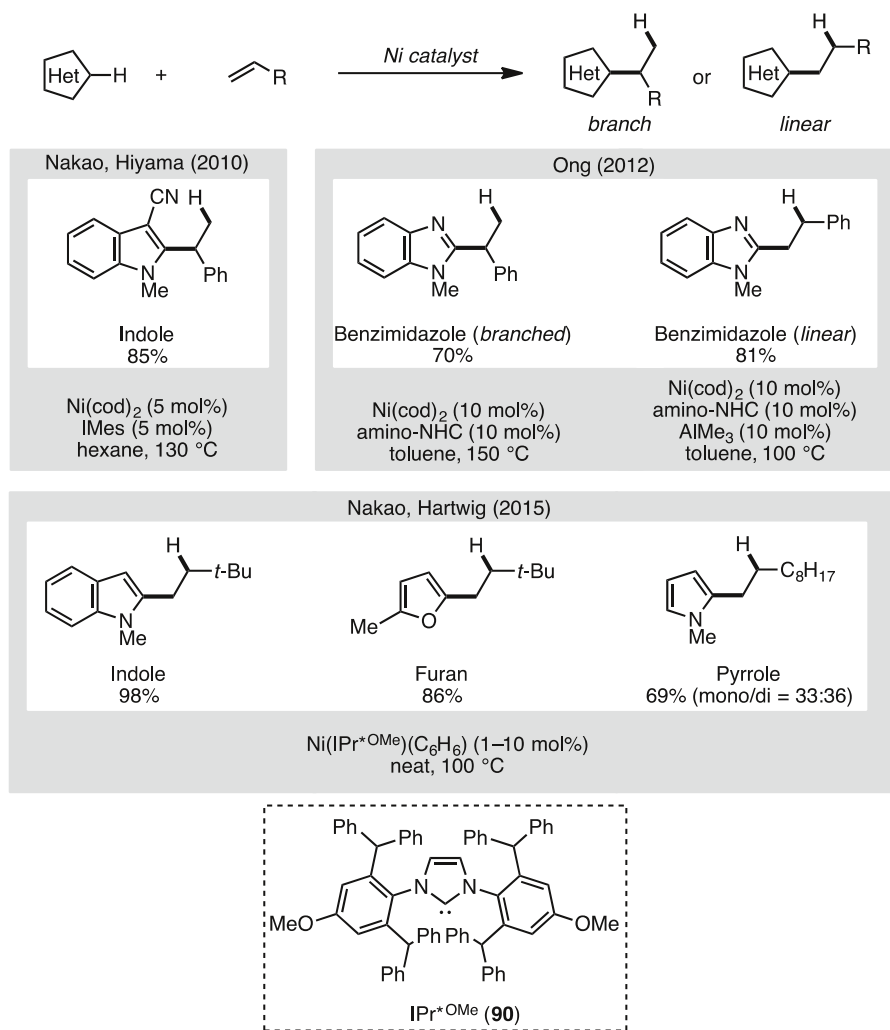
**Scheme 46** Hydroarylation of alkynes with pentafluorobenzenes

alkenes with benzo-annulated heteroarenes such as indoles using a Ni(cod)<sub>2</sub>/IMes catalytic system [83]. Ong and coworkers reported a similar reaction using Ni(cod)<sub>2</sub> and an amino-NHC ligand (**87**) [84, 85]. In their investigation, it was found that the regioselectivity switches when using AlMe<sub>3</sub> as the additive. The hydroarylation normally affords branched products, whereas linear adducts (anti-Markovnikov products) are obtained when using AlMe<sub>3</sub>. Recently, collaborative research by the groups of Nakao and Hartwig also demonstrated an anti-Markovnikov hydroheteroarylation of alkenes catalyzed by a hindered nickel NHC (**90**) system [86]. This reaction proceeded with high anti-Markovnikov selectivity and showed broad substrate scope, as it was applicable for unactivated alkenes, internal alkenes, and cyclic alkenes as the alkene component and indoles, pyrroles, benzofurans, and furans as the heteroarene component.

For the hydroarylation of alkenes with electron-deficient heteroarenes such as pyridines, Nakao and Hiyama achieved regioselective hydroarylation when using a bulky Lewis acid additive, methylaluminum bis(2,6-di-*tert*-butyl-4-methylphenoxide) (MAD) (Scheme 48) [87]. In this reaction, alkenes bearing aromatics afforded branched products, whereas alkenes bearing alkyl chains gave linear products.

In 2014, the Hartwig group also demonstrated a nickel-catalyzed hydroarylation of electron-deficient aromatics (Scheme 49) [88]. Although only 1,3-bis(trifluoromethyl)benzene worked well, catalytic Ni(IPr)<sub>2</sub>/NaOt-Bu gave alkylated benzene derivatives in good to moderate yields.

Typically, the hydroarylation of alkynes and alkenes is applicable only for heteroarenes and specific arenes (see Sect. 6). In the case of simple arenes such as benzoic acid derivatives and anilines, utilization of chelation-assisted groups is required for enhanced reactivity. In 2011, Chatani and coworkers attempted a nickel-catalyzed hydroarylation of alkynes with benzamides containing a 2-pyridylaminomethane moiety and obtained isoquinoline derivatives via oxidative cyclization (annulation) (Scheme 50) [89]. Although similar types of reactions have already been reported using noble metals such as ruthenium and rhodium, this was the first example of nickel-catalyzed *ortho* C–H bond activation and hydroarylation of alkynes with simple arenes. Ackermann and coworkers also

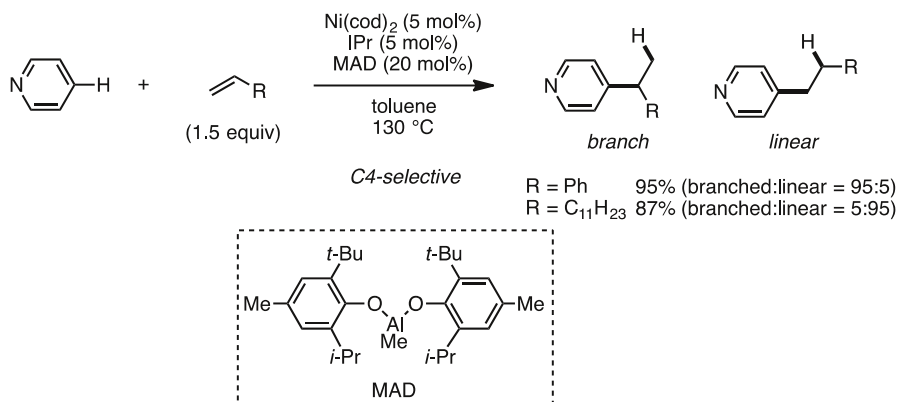


**Scheme 47** Hydroarylation of alkenes with electron-rich heteroaremetics

reported a similar type of reaction involving a nickel-catalyzed annulation of anilines and alkynes to form substituted indoles [90].

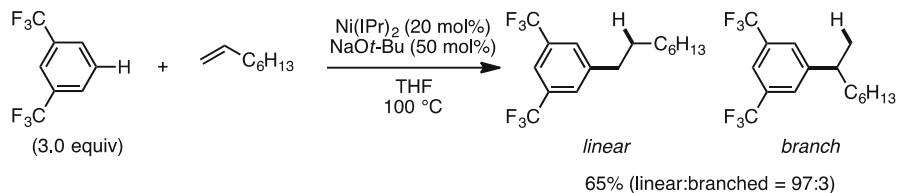
## 7 Summary

The field of nickel-catalyzed aromatic C–H functionalization has evolved significantly in the past decade. Such reactions are not only advantageous because of the low cost associated with nickel catalysts but they also enable unique transformations on aromatic starting materials for conversion into new organic materials, natural



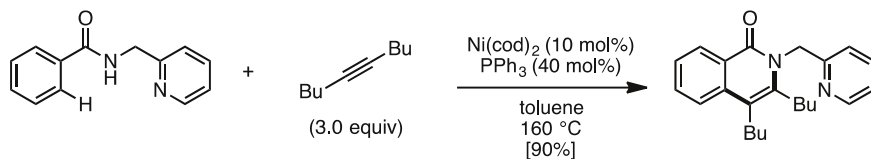
**Scheme 48** Hydroarylation of alkenes with pyridines

Hartwig (2014)

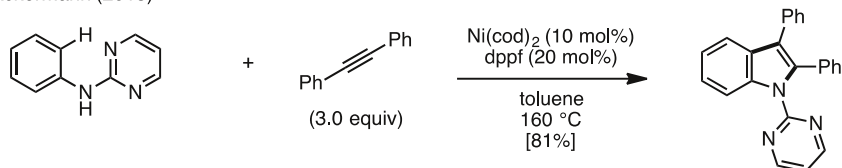


**Scheme 49** Hydroarylation of alkenes with electron-deficient arenes

Chatani (2011)



Ackermann (2013)



**Scheme 50** Alkyne annulation via *ortho* C–H bond activation

products, and pharmaceuticals. Additionally, while this review focused on aromatic C–H functionalization, nickel-catalyzed  $sp^3$  C–H functionalization with haloarenes [91–97], oxidative coupling [98–102], heteroatom formation [103–107],

hydrocarboxylation and hydroalkylation of alkynes and alkenes [108–111], and annulation [112] also appeared recently. With continued development of novel catalysts [113–117], nickel-catalyzed C–H functionalization is becoming a broadly applicable and reliable synthetic method for next-generation organic synthesis.

## References

1. Tasker SZ, Standley EA, Jamison TF (2014) *Nature* 509:299–309
2. Yamaguchi J, Muto K, Itami K (2013) *Eur J Org Chem* 19–30
3. Cai X-H, Xie B (2015) *ARKIVOC* 184–211
4. Hyster TK (2015) *Catal Lett* 145:458–467
5. Khan MS, Haque A, Al-Suti MK, Raithby PR (2015) *J Organomet Chem* 793:114–133
6. Nakao Y (2011) *Chem Rec* 11:242–251
7. Castro LCM, Chatani N (2015) *Chem Lett* 44:410–421
8. Klelman JP, Dubeck M (1963) *J Am Chem Soc* 85:1544–1545
9. Liang L-C, Cheng P-S, Huang Y-L (2006) *J Am Chem Soc* 128:15562–15563
10. Canivet J, Yamaguchi J, Ban I, Itami K (2009) *Org Lett* 11:1733–1736
11. Hachiya H, Hirano K, Satoh T, Miura M (2009) *Org Lett* 11:1737–1740
12. Yamamoto T, Muto K, Komiyama M, Canivet J, Yamaguchi J, Itami K (2011) *Chem Eur J* 17:10113–10122
13. Iaroshenko V, Ali I, Mkrtychyan S, Semeniuchenko V, Ostrovskiy D, Langer P (2012) *Synlett* 23:2603–2608
14. Muto K, Hatakeyama T, Yamaguchi J, Itami K (2015) *Chem Sci* 6:6792–6798
15. Watanabe K, Tanaka T, Kondo S (1994) *Jpn Kokai Tokkyo Koho* 329647
16. Razavi H, Palaninathan SK, Powers ET, Wiseman RL, Purkey HE, Mohamedmohaideen NN, Deechongkit S, Chiang KP, Dendle MTA, Sacchetti JC, Kelly JW (2003) *Angew Chem Int Ed* 42:2758–2761
17. Domínguez XA, de La Fuente G, Gonzal ez AG, Rein M, Timon I (1998) *Heterocycles* 27:35–38
18. Kobayashi O, Uraguchi D, Yamakawa T (2009) *Org Lett* 11:2679–2682
19. Yokota A, Aihara Y, Chatani N (2014) *J Org Chem* 79:11922–11932
20. Matsuyama N, Hirano K, Satoh T, Miura M (2009) *Org Lett* 11:4156–4159
21. Liu YJ, Liu YH, Yan SY, Shi BF (2015) *Chem Commun* 51:6388–6391
22. Yi J, Yang L, Xia C, Li F (2015) *J Org Chem* 80:6213–6221
23. Landge VG, Shewale CH, Jaiswal G, Sahoo MK, Midya SP, Balaraman E (2016) *Catal Sci Technol* 6:1946–1951
24. Cho H, Iwama Y, Okano K, Tokuyama H (2014) *Chem Pharm Bull* 62:354–363
25. Vechorkin O, Proust V, Hu X (2010) *Angew Chem Int Ed* 49:3061–3064
26. Yao T, Hirano K, Satoh T, Miura M (2010) *Chem Eur J* 16:12307–12311
27. Yao T, Hirano K, Satoh T, Miura M (2012) *Angew Chem Int Ed* 51:775–779
28. Liu C, Liu D, Zhang W, Zhou L, Lei A (2013) *Org Lett* 15:6166–6169
29. Aihara Y, Chatani N (2013) *J Am Chem Soc* 135:5308–5311
30. Aihara Y, Wuelbern J, Chatani N (2015) *Bull Chem Soc Jpn* 88:438–446
31. Uemura T, Yamaguchi M, Chatani N (2016) *Angew Chem Int Ed* 55:3162–3165
32. Barsu N, Kalsi D, Sundararaju B (2015) *Chem Eur J* 21:9364–9368
33. Cong X, Li Y, Wei Y, Zeng X (2014) *Org Lett* 16:3926–3929
34. Song W, Lackner S, Ackermann L (2014) *Angew Chem Int Ed* 53:2477–2480
35. Ruan Z, Lackner S, Ackermann L (2016) *Angew Chem Int Ed* 55:3153–3157
36. Wu X, Zhao Y, Ge H (2015) *J Am Chem Soc* 137:4924–4927
37. Hachiya H, Hirano K, Satoh T, Miura M (2010) *Angew Chem Int Ed* 49:2202–2205
38. Hachiya H, Hirano K, Satoh T, Miura M (2010) *Chem Cat Chem* 2:1403–1406
39. Qu G-R, Xin P-Y, Niu H-Y, Wang D-C, Ding R-F, Guo H-M (2011) *Chem Commun* 47:11140–11142
40. Tobisu M, Hyodo I, Chatani N (2009) *J Am Chem Soc* 131:12070–12071

41. Hyodo I, Tobisu M, Chatani N (2012) *Chem Asian J* 7:1357–1365
42. Hyodo I, Tobisu M, Chatani N (2012) *Chem Commun* 48:308–310
43. Matsuyama N, Kitahara M, Hirano K, Satoh T, Miura M (2010) *Org Lett* 12:2358–2361
44. Liu Y-H, Liu Y-J, Yan S-Y, Shi B-F (2015) *Chem Commun* 51:11650–11653
45. Xin P-Y, Niu H-Y, Qu G-R, Ding R-F, Guo H-M (2012) *Chem Commun* 48:6717–6719
46. Muto K, Yamaguchi J, Itami K (2012) *J Am Chem Soc* 134:169–172
47. Muto K, Yamaguchi J, Lei A, Itami K (2013) *J Am Chem Soc* 135:16384–16387
48. Xu H, Muto K, Yamaguchi J, Zhao C, Itami K, Musaev DG (2014) *J Am Chem Soc* 136:14834–14844
49. Meng L, Kamada Y, Muto K, Yamaguchi J, Itami K (2013) *Angew Chem Int Ed* 52:10048–10051
50. Nett M, Erol Ö, Kehraus S, Köck M, Krick A, Eguereva E, Neu E, König GM (2006) *Angew Chem Int Ed* 45:3863–3867
51. Linder JR, Moody CJ (2007) *Chem Commun* 1508–1509
52. Linder JR, Blake AJ, Moody CJ (2008) *Org Biomol Chem* 6:3908–3916
53. Zhang J, Ciufolini MA (2009) *Org Lett* 11:2389–2392
54. Wang J, Ferguson DM, Kalyani D (2013) *Tetrahedron* 69:5780–5790
55. Xiao J, Chen T, Han L-B (2015) *Org Lett* 17:812–815
56. Amaike K, Muto K, Yamaguchi J, Itami K (2012) *J Am Chem Soc* 134:13573–13576
57. Kruckenberg A, Wadepohl H, Gade LH (2013) *Organometallics* 32:5153–5170
58. Yamamoto T, Ishizu J, Kohara T, Komiya S, Yamamoto A (1980) *J Am Chem Soc* 102:3758–3764
59. Hong X, Liang Y, Houk KN (2014) *J Am Chem Soc* 136:2017–2025
60. Lu Q, Yu H, Fu Y (2014) *J Am Chem Soc* 136:8252–8260
61. Nagatsu A, Kajitani H, Sakakibara J (1995) *Tetrahedron Lett* 36:4097–4100
62. Wipf P, Venkatraman S (1996) *J Org Chem* 61:6517–6522
63. Amaike K, Itami K, Yamaguchi J (2016) *Chem Eur J* 22:4384–4388
64. Nicolaou KC, Zou B, Dethe DH, Li DB, Chen DY-K (2006) *Angew Chem Int Ed* 45:7786–7792
65. Nicolaou KC, Dethe DH, Leung GY, Zou B, Chen DY-K (2008) *Chem Asian J* 3:413–429
66. Yang K, Wang P, Zhang C, Kadi AA, Fun H-K, Zhang Y, Lu H (2014) *Eur J Org Chem* 7586–7589
67. Yang K, Zhang C, Wang P, Zhang Y, Ge H (2014) *Chem Eur J* 20:7241–7244
68. Zhang H, Hagihara S, Itami K (2015) *Chem Lett* 44:779–781
69. Furukawa T, Tobisu M, Chatani N (2015) *Chem Commun* 51:6508–6511
70. Yang K, Wang Y, Chen X, Kadi AA, Fun H-K, Sun H, Zhang Y, Lu H (2015) *Chem Commun* 51:3582–3585
71. Yan S-Y, Liu Y-J, Liu B, Liu Y-H, Shi B-F (2015) *Chem Commun* 51:4069–4072
72. Reddy VP, Qiu R, Iwasaki T, Kambe N (2015) *Org Biomol Chem* 13:6803–6813
73. Nakao Y, Kanyiva KS, Oda S, Hiyama T (2006) *J Am Chem Soc* 128:8146–8147
74. Mukai T, Hirano K, Satoh T, Miura M (2009) *J Org Chem* 74:6410–6413
75. Kanyiva KS, Nakao Y, Hiyama T (2007) *Heterocycles* 72:677–680
76. Kanyiva KS, Löbermann F, Nakao Y, Hiyama T (2009) *Tetrahedron Lett* 50:3463–3466
77. Kanyiva KS, Nakao Y, Hiyama T (2007) *Angew Chem Int Ed* 46:8872–8874
78. Nakao Y, Kanyiva KS, Hiyama T (2008) *J Am Chem Soc* 130:2448–2449
79. Nakao Y, Idei H, Kanyiva KS, Hiyama T (2009) *J Am Chem Soc* 131:15996–15997
80. Tsai CC, Shih WC, Fang CH, Li CY, Ong TG, Yap GPA (2010) *J Am Chem Soc* 132:11887–11889
81. Nakao Y, Kashihara N, Kanyiva KS, Hiyama T (2008) *J Am Chem Soc* 130:16170–16171
82. Nett AJ, Zhao W, Zimmerman PM, Montgomery J (2015) *J Am Chem Soc* 137:7636–7639
83. Nakao Y, Kashihara N, Kanyiva KS, Hiyama T (2010) *Angew Chem Int Ed* 49:4451–4454
84. Shih WC, Chen WC, Lai YC, Yu MS, Ho JJ, Yap GPA, Ong TG (2012) *Org Lett* 14:2046–2049
85. Lee WC, Shih WC, Wang TH, Liu Y, Yap GPA, Ong TG (2015) *Tetrahedron* 71:4460–4464
86. Schramm Y, Takeuchi M, Semba K, Nakao Y, Hartwig JF (2015) *J Am Chem Soc* 137:12215–12218
87. Nakao Y, Yamada Y, Kashihara N, Hiyama T (2010) *J Am Chem Soc* 132:13666–13668
88. Bair JS, Schramm Y, Sergeev AG, Clot E, Eisenstein O, Hartwig JF (2014) *J Am Chem Soc* 136:13098–13101
89. Shiota H, Ano Y, Aihara Y, Fukumoto Y, Chatani N (2011) *J Am Chem Soc* 133:14952–14955
90. Song W, Ackermann L (2013) *Chem Commun* 49:6638–6640
91. Fernández-Salas JA, Marelli E, Nolan SP (2015) *Chem Sci* 6:4973–4977
92. Aihara Y, Chatani N (2014) *J Am Chem Soc* 136:898–901
93. Li M, Dong J, Huang X, Li K, Wu Q, Song F, You J (2014) *Chem Commun* 50:3944–3946

94. Iyanaga M, Aihara Y, Chatani N (2014) *J Org Chem* 79:11933–11939
95. Wang X, Zhu L, Chen S, Xu X, Au C-T, Qiu R (2015) *Org Lett* 17:5228–5231
96. Liu Y-J, Zhang Z-Z, Yan S-Y, Liu Y-H, Shi B-F (2015) *Chem Commun* 51:7899–7902
97. Wu X, Zhao Y, Ge H (2014) *J Am Chem Soc* 136:1789–1792
98. Li K, Wu Q, Lan J, You J (2015) *Nat Commun* 6:8404
99. Liu D, Liu C, Li H, Lei A (2013) *Angew Chem Int Ed* 52:4453–4456
100. Gartia Y, Ramidi P, Jones DE, Pulla S, Ghosh A (2014) *Catal Lett* 144:507–515
101. Cao W, Liu X, Peng R, He P, Lin L, Feng X (2013) *Chem Commun* 49:3470–3472
102. Wu X, Zhao Y, Ge H (2015) *J Am Chem Soc* 137:4924–4927
103. Yan S-Y, Liu Y-J, Bin L, Liu Y-H, Zhang Z-Z, Shi B-F (2015) *Chem Commun* 51:7341–7344
104. Lin C, Yu W, Yao J, Wang B, Liu Z, Zhang Y (2015) *Org Lett* 17:1340–1343
105. Wang X, Qiu R, Yan C, Reddy VP, Zhu L, Xu X, Yin S-F (2015) *Org Lett* 17:1970–1973
106. Ye X, Petersen JL, Shi X (2015) *Chem Commun* 51:7863–7866
107. Wu X, Zhao Y, Ge H (2014) *Chem Eur J* 20:9530–9533
108. Nakao Y, Idei H, Kanyiva KS, Hiyama T (2009) *J Am Chem Soc* 131:5070–5071
109. Li M, Yang Y, Zhou D, Wan D, You J (2015) *Org Lett* 17:2546–2549
110. Maity S, Agasti S, Earsad AM, Hazra A, Maiti D (2015) *Chem Eur J* 21:11320–11324
111. Miyazaki Y, Yamada Y, Nakao Y, Hiyama T (2012) *Chem Lett* 41:298–300
112. Nakao Y, Morita E, Idei H, Hiyama T (2011) *J Am Chem Soc* 133:3264–3267
113. Ruan Z, Lackner S, Ackermann L (2016) *ACS Catal* 6:4690–4693
114. Zheng X-X, Du C, Zhao X-M, Zhu X, Suo J-F, Hao X-Q, Niu J-L, Song M-P (2016) *J Org Chem* 81:4002–4011
115. Zhan B-B, Liu Y-H, Hu F, Shi B-F (2016) *Chem Commun* 52:4934–4937
116. Aihara Y, Chatani N (2016) *ACS Catal* 6:4323–4329
117. Yan Q, Chen Z, Yu W, Yin H, Liu Z, Zhang Y (2015) *Org Lett* 17:2482–2485

# Iron-Catalyzed C–H Functionalization Processes

Gianpiero Cera<sup>1</sup> · Lutz Ackermann<sup>1</sup> 

Received: 17 May 2016 / Accepted: 23 July 2016  
© Springer International Publishing Switzerland 2016

**Abstract** Iron-catalyzed C–H activation has recently emerged as an increasingly powerful tool for the step-economical transformation of unreactive C–H bonds. Particularly, the recent development of low-valent iron catalysis has set the stage for novel C–H activation strategies via chelation assistance. The low-cost, natural abundance, and low toxicity of iron prompted its very recent application in organometallic C–H activation catalysis. An overview of the use of iron catalysis in C–H activation processes is summarized herein up to May 2016.

**Keywords** Iron · C–H activation · Chelation assistance · Arylation · Alkylation · Alkenylation · Amination

## Abbreviations

|       |   |
|-------|---|
| AQ    | Aminoquinoline                            |
| Ar    | Aryl                                      |
| BHT   | 2,6-Bis(1,1-dimethylethyl)-4-methylphenol |
| Bu    | Butyl                                     |
| Bn    | Benzyl                                    |
| DABCO | 1,4-Diazabicyclo[2.2.2]octane             |
| DCIB  | 1,2-Dichloroisobutane                     |
| DCP   | 1,2-Dichloropropane                       |
| DG    | Directing group                           |

This article is part of the Topical Collection “Ni- and Fe-Based Cross-Coupling Reactions”; edited by Arkaitz Correa.

✉ Lutz Ackermann  
[lutz.ackermann@chemie.uni-goettingen.de](mailto:lutz.ackermann@chemie.uni-goettingen.de)

<sup>1</sup> Institut für Organische und Biomolekulare Chemie, Georg-August-Universität Göttingen, Tammannstr. 2, 37077 Göttingen, Germany

Published online: 06 August 2016

Reprinted from the journal

191

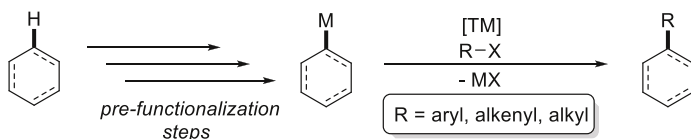


|          |  |
|----------|--|
| dppb     | 1,4-Bis(diphenylphosphino)butane                         |
| dppe     | 1,2-Bis(diphenylphosphino)ethane                         |
| dppen    | <i>cis</i> -1,2-Bis(diphenylphosphino)ethylene           |
| dtbpy    | 4,4'-Di- <i>tert</i> -butyl-2,2'-dipyridyl               |
| E        | Electrophile   |
| EDG      | Electron-donating group                                  |
| equiv    | Equivalent   |
| EWG      | Electron-withdrawing group                               |
| FG       | Functional group   |
| Hal      | Halogen  |
| Het      | Heteroatom   |
| Me       | Methyl   |
| Mes      | Mesityl  |
| PA       | Picolinic acid   |
| Ph       | Phenyl   |
| Ph-dppen | ( <i>Z</i> )-1-Phenyl-1,2-bis(diphenylphosphino)ethylene |
| Pin      | Pinacol  |
| PMP      | <i>p</i> -Methoxyphenyl                                  |
| Pr       | Propyl   |
| Q        | 8-Aminoquinoline   |
| SET      | Single electron transfer                                 |
| TAM      | Triazolylaminomethyl                                     |
| TEMPO    | (2,2,6,6-Tetramethylpiperidin-1-yl)oxidanyl              |
| TM       | Transition metal   |

## 1 Introduction

Transition metal-catalyzed cross-coupling reactions are valuable tools for the formation of C–C bonds in organic chemistry [1–8]. However, the preparation of the prerequisite organometallic reagents R–M requires a number of synthetic operations, during which undesired waste is generated (Scheme 1).

In recent years, the direct functionalization of C–H bonds has emerged as an environmentally benign and economically attractive strategy for achieving unprecedented C–C and C–X bond forming reactions, which avoid the synthesis and use of prefunctionalized substrates [9–13]. Specifically, the utilization of inexpensive, naturally abundant 3d transition metals [14–18] has gained considerable attention as an alternative to precious second- and third-row transition metal



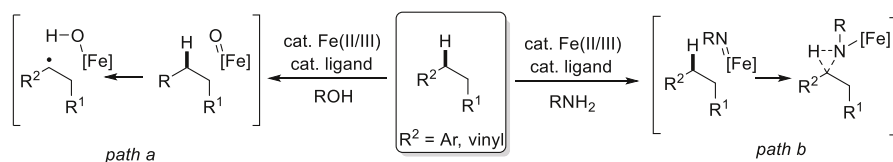
**Scheme 1** Metal-catalyzed cross-coupling reactions with prefunctionalized substrates

complexes [19–23]. In this context, iron catalysis constitutes an effective platform not only as a Lewis acid or in oxidation and hydrogenation reactions [24–28] but also in the field of C–H functionalizations. Indeed, iron is the most abundant metal in the earth’s crust after aluminium [29]. Moreover, various iron compounds are present in biological systems and are an essential part of important metabolic processes, such as in cytochrome P450. As a result, iron’s low toxicity allows for its application in pharmaceutical and agricultural industries or in the synthesis of cosmetics, among others [30, 31]. As for other transition metal-catalyzed C–H functionalizations [32–37], the reactivity of iron catalysts can be categorized into two distinct reaction manifolds. First, catalysis that involves an outer-sphere activation mode [38, 39], and, second, catalysts that operate by an inner sphere, that is organometallic, mechanism [13, 40]. In the first case, the C–H functionalization step does not proceed through the formation of an organometallic species with a C–Fe bond, but is rather induced by the ligand on the metal center. In these transformations, iron is normally found in its higher oxidation states, typically featuring oxo or imido ligands (Scheme 2). These C–H functionalizations were predominantly suggested to proceed through radical pathways via hydrogen abstraction (Scheme 2a), [41–44] or operating by C–H insertions with iron-oxo or iron-imido species as the key intermediates (Scheme 2b) [45, 46].

These outer-sphere reactions usually occur at the weakest C–H bonds, that is mostly benzylic, allylic, or tertiary alkyl C–H bonds.

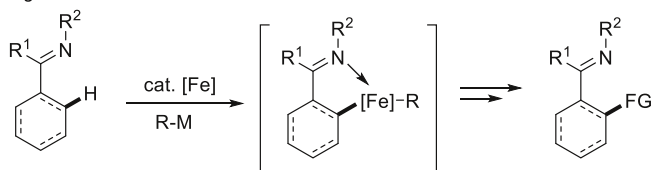
In the second scenario, reducing reaction conditions gives access to iron species in their lower oxidation states, largely ranging from –II to +I [47, 48], and thereby generating nucleophilic iron species that are able to promote several unique organic transformations, such as nucleophilic substitutions, cycloisomerizations, conventional cross-couplings, and hydrosilylation reactions [49, 50]. Inspired by early reports from Kochi on iron-catalyzed cross-coupling reactions [51, 52], the scientific community only recently started to appreciate the use of easily accessible iron complexes for C–H activation strategies. In this review, we focus on iron-catalyzed C–H activation processes for cross-couplings, in which the use of organometallic iron intermediates proved to be the key to success. The low-valent iron species have proven instrumental for the activation of thermodynamically stable aryl and alkenyl C(sp<sup>2</sup>)–H bonds and likewise proved applicable to C(sp<sup>3</sup>)–H functionalizations (Scheme 3).

From a historical perspective, it is noteworthy that an early example of stoichiometric organometallic C–H activation was reported by Miyake in 1968 [53].

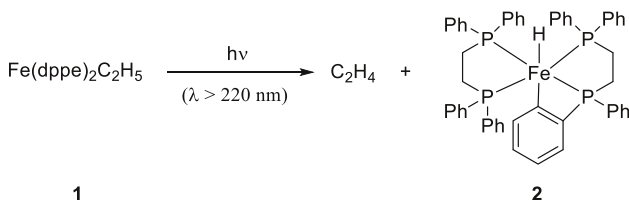


**Scheme 2** Iron-catalyzed outer-sphere C–H functionalization pathways: **a** hydrogen abstraction, **b** C–H insertion with high-valent imido species

## organometallic C–H activation



**Scheme 3** Organometallic iron-catalyzed C–H functionalization via chelation assistance



**Scheme 4** Synthesis of cyclometallated complex **2** via activation of a C(sp<sup>2</sup>)–H bond

The synthesis of complex **2** was achieved by irradiating the iron complex **1** with UV-light (**Scheme 4**).

Subsequent contributions demonstrated the feasibility of iron complexes to promote the stoichiometric activation of C–H bonds [54–56]. For instance, Klein and coworkers demonstrated that low-valent iron complexes, such as the well-defined complex Fe(PMe<sub>3</sub>)<sub>4</sub> (**4**), were suitable for the stoichiometric *ortho*-selective metalation of ketimines **3** (**Scheme 5**) [57].

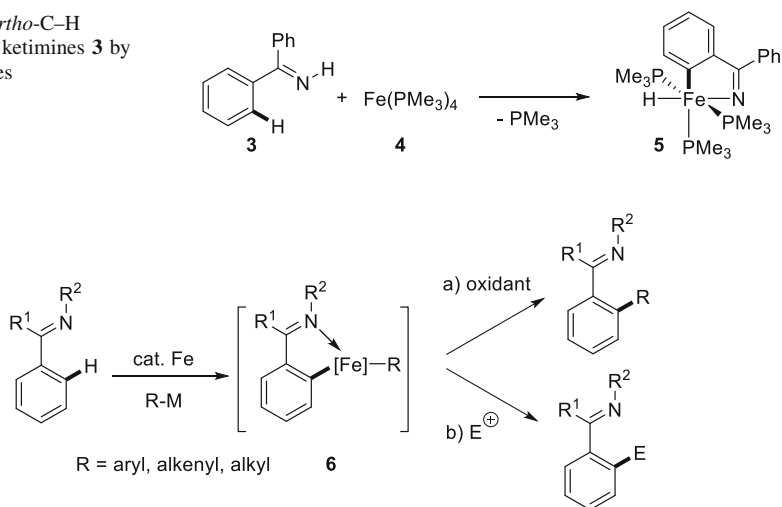
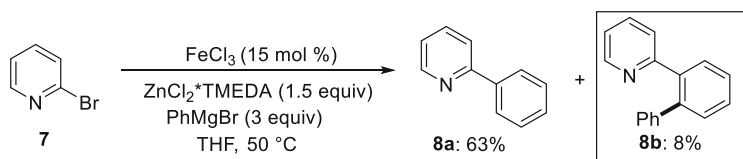
With respect to implementing the stoichiometric C–H metalation into catalytic C–H functionalizations, two possible reaction manifolds can be envisioned. First, C–H transformations can occur with organometallic reagents, along with an external oxidant, thereby facilitating an oxidation-induced reductive elimination (**Scheme 6a**). Second, the C–H functionalizations can proceed by means of organic electrophiles reacting with the nucleophilic intermediate **6** (**Scheme 6b**).

While recent computational studies on low-valent iron-catalyzed C–H arylations invoke a catalytic cycle, in which the oxidation state evolves in the sequence Fe(II)/Fe(III)/Fe(I) [58], a detailed mechanistic rationale is often not at hand. Thus, herein the catalytic transformations are summarized according to (i) oxidative transformations with organometallic reagents as well as (ii) reaction with organic electrophiles until May 2016.

## 2 Iron-Catalyzed C–H Activation with Organometallic Reagents

### 2.1 Iron-Catalyzed C–H Arylations with Organozinc Reagents

Inspired by early studies on iron-catalyzed cross-coupling reactions [51, 52], Nakamura, Yoshikai, and coworkers discovered an unusual C–H activation within

**Scheme 5** *Ortho*-C–H metalation of ketimines **3** by iron complexes**Scheme 6** Organometallic iron-catalyzed C–H functionalization manifolds**Scheme 7** Iron-catalyzed cross-coupling of 2-bromopyridine (**7**) with C–H arylation of 2-phenylpyridine (**8a**)

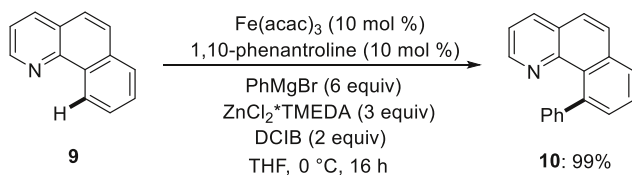
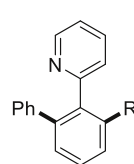
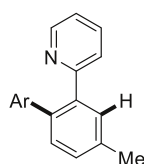
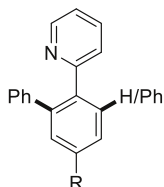
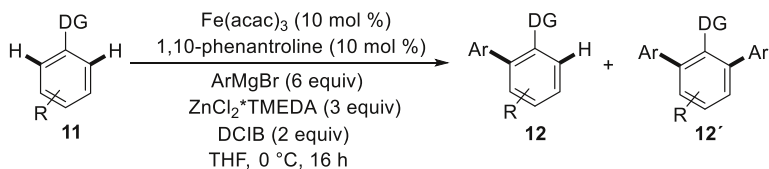
an attempted cross-coupling of 2-bromopyridine (**7**) with an in situ generated diphenylzinc reagent. Thus, product **8b** was also observed, which was suggested to be formed by an iron-catalyzed C–H arylation of the initially formed 2-phenylpyridine (**8a**) (Scheme 7) [59].

This observation and the subsequent detailed optimization studies of the key reaction parameters led to the development of an efficient low-valent iron-catalyzed C–H arylation (Scheme 8).

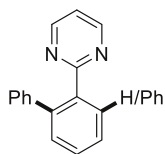
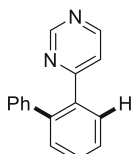
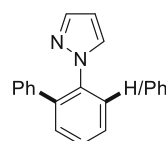
Particularly,  $\text{Ph}_2\text{Zn}$  generated in situ from  $\text{PhMgBr}$  and  $\text{ZnCl}_2\cdot\text{TMEDA}$  was found to be crucial to guarantee the C–H transformation, while other organometallic reagents, such as  $\text{Ph}_2\text{Zn}$  or  $\text{PhZnBr}$ , were completely ineffective under otherwise identical reaction conditions. Dichloroisobutane (DCIB) proved to be essential, which was rationalized by its role as an oxidant in analogy to *vic*-dihaloalkanes previously being used in iron-catalyzed cross-coupling reactions [60, 61].

The optimized catalytic system was applied to the direct arylation of various 2-arylpyridines **11** (Scheme 9) [59].

The iron catalyst featured a broad scope and a high functional group tolerance allowing for the chemo-selective synthesis of arylated pyridines **12** even in the presence of an ester moiety. Interestingly, additional nitrogen-containing

**Scheme 8** Iron-catalyzed C–H arylation of  $\alpha$ -benzoquinoline (**9**)R = H (**12a**): 81%/ (**12a'**): 12%

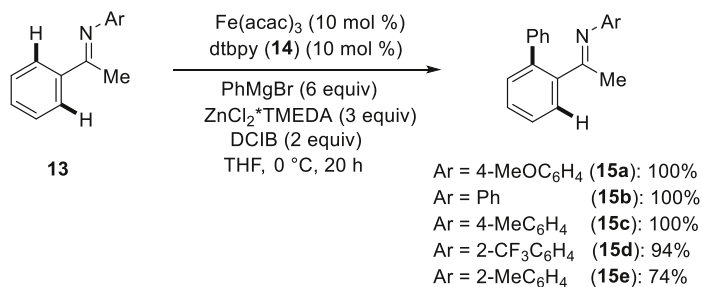
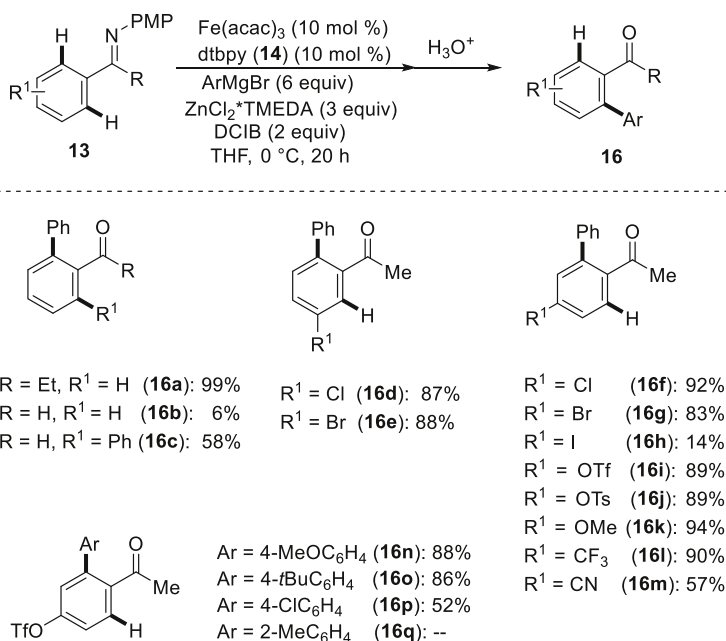
Ar = Ph

(**12e**): 89%R = Me (**12k**): 17%R = OMe (**12b**): 65%/ (**12b'**): 21%Ar = 3-FC<sub>6</sub>H<sub>4</sub>(**12f**): 82%R = Ph (**12l**): 60%R = F (**12c**): 80%/ (**12c'**): 20%Ar = 4-FC<sub>6</sub>H<sub>4</sub>(**12g**): 78%R = CO<sub>2</sub>Et (**12d**): 77%/ (**12d'**): 13%Ar = 4-tBuC<sub>6</sub>H<sub>4</sub>(**12h**): 82%Ar = 4-MeOC<sub>6</sub>H<sub>4</sub>(**12i**): 76%Ar = 2-MeC<sub>6</sub>H<sub>4</sub>(**12j**): --**12m**: 81%/ **12m'**: 9%**12n**: 18%**12o**: 59%/ **12o'**: 10%**Scheme 9** Iron-catalyzed arylation of 2-arylpyridines **11**

heterocycles, such as pyrimidine **11m** and pyrazole **11o**, were found to be competent directing groups in the C–H arylation manifold.

Significant subsequent advances were constituted by the development of a protocol for the direct arylation of synthetically useful ketimines **13** (Scheme 10) [62].

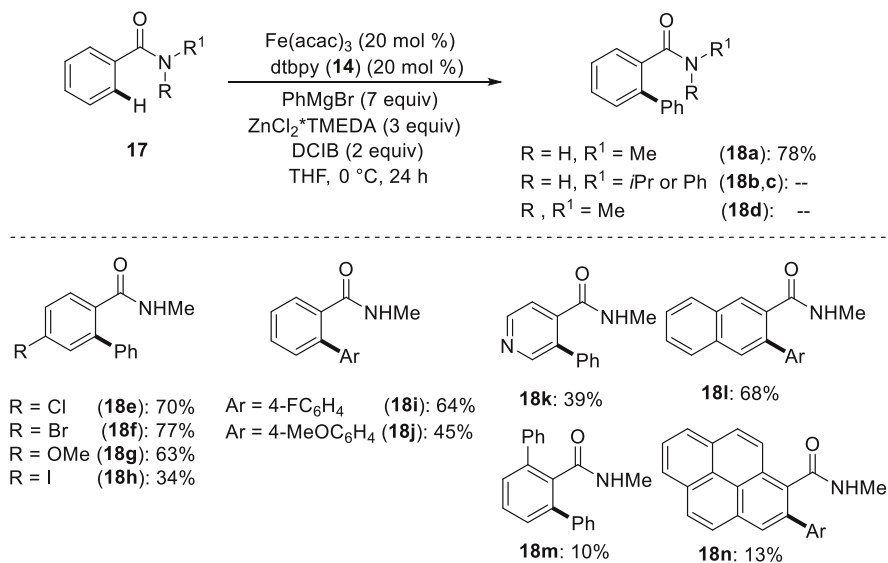
The use of the bipyridine dtbpy **14** as the ligand, along with DCIB as the oxidant, led to complete conversion of the starting materials **13** into acetophenone derivatives **16** upon subsequent hydrolysis under rather mild reaction conditions (Scheme 11).

**Scheme 10** Iron-catalyzed C–H arylation of aryl imines **13****Scheme 11** Scope of the iron-catalyzed C–H arylation of ketimines **13**

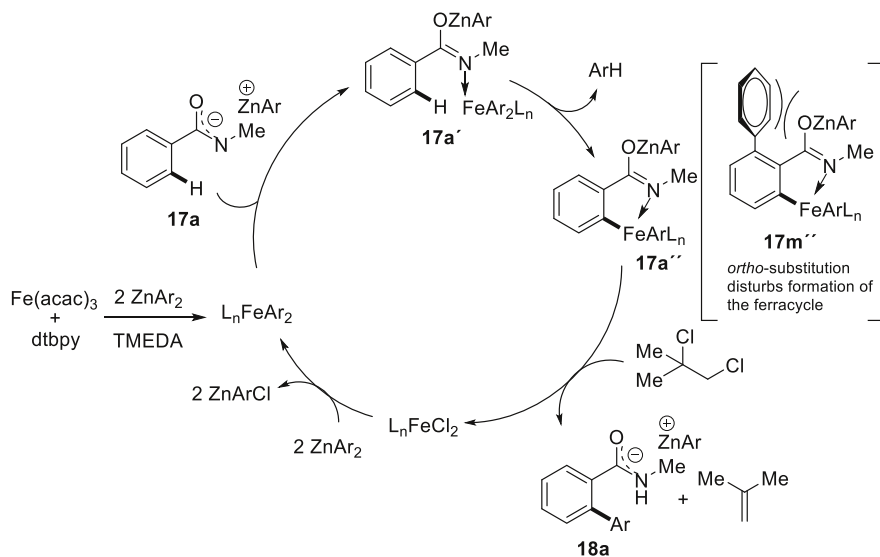
The protocol displayed high functional group tolerance and ample scope, hence enabling the synthesis of functionalized acetophenone derivatives **16** after aqueous work-up. Interestingly, the reaction showed high chemo-selectivity in that aryl triflates and tosylates were fully tolerated, without any cross-coupling products being formed.

Likewise, benzamides **17** were identified as suitable substrates for the iron-catalyzed C–H arylation under the optimized reaction conditions (Scheme 12) [63].

Notably, *N*-isopropyl and *N*-phenyl amides **17b–c** (Scheme 12) could not be converted, indicating the repulsive nature of steric interactions. Furthermore, tertiary *N,N*-dimethyl benzamide **17d** failed to undergo the C–H arylation, suggesting that the N–H acidic motif is essential. Thus, under the optimized



**Scheme 12** Iron-catalyzed *ortho*-monoarylation of benzamides **17**



**Scheme 13** Proposed catalytic cycle and rationale for the selective monoarylation

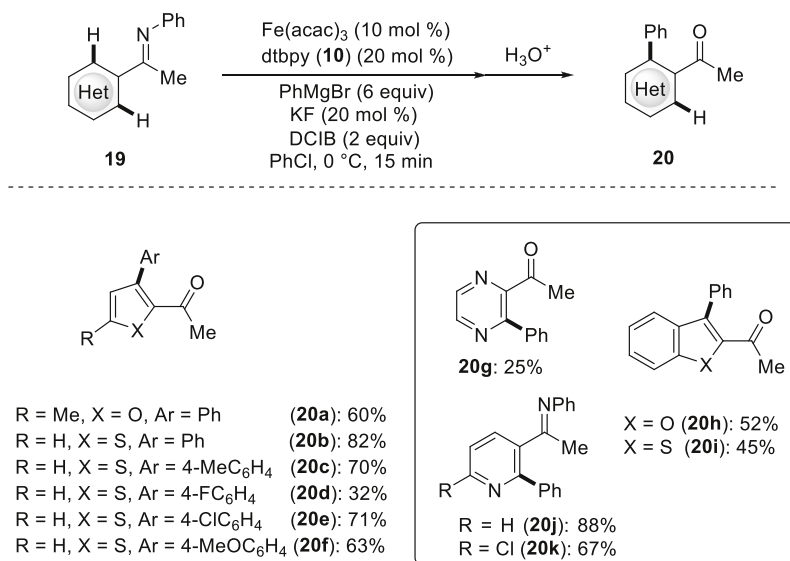
reaction conditions, various *N*-methyl benzamides **17** were efficiently transformed into the corresponding arylated products **18** with moderate yields and good functional group tolerance, while *ortho*-substituted benzamide **17m** and electron-deficient heteroarenes gave less satisfactory results.

A plausible catalytic cycle was put forward, which is depicted in [Scheme 13](#).

Hence, a low-valent iron species that is in situ generated by reduction with the organometallic reagents is coordinated by the deprotonated benzamide generating the ferracycle **17a'**. Subsequently, the C–H activation is suggested to take place, inducing the metalation of the *ortho*-C–H bond. The low reactivity of *ortho*-substituted benzamides **17** may be accounted for by sterics that prevent the formation of the key ferracycle **17 m''**. In a key elementary step of the catalytic cycle, the low-valent iron intermediate is oxidized by DCIB, which induces the final reductive elimination. Thereby, the arylated benzamide **18** is obtained, and the catalytically active iron species is regenerated after transmetalation with the organozinc reagent.

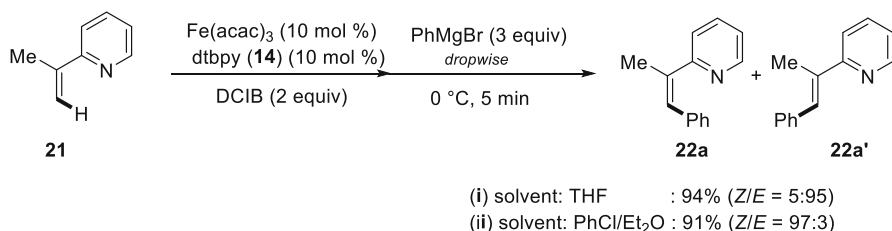
The iron-catalyzed arylations proved also applicable to a set of N-, S-, and O-containing heterocycles **19** with excellent levels of chemo and positional selectivity ([Scheme 14](#)) [64].

A careful control of the reaction conditions allowed for the efficient catalytic transformation of ketimines **19** in a remarkably short reaction time of only 15 min. The dropwise addition of the Grignard reagent and a large surface area of the reaction vessel were found to impact the yields of desired products **20**. Moreover, the presence of catalytic amounts of KF [65] suppressed the formation of biphenyl as undesired byproduct, leading to an improved performance of the iron catalyst [64]. Among a variety of heterocycles, thiophene derivatives furnished the best results. The corresponding heteroaromatic ketones were generally obtained upon acidic work-up, while the pyridine derivatives **20j–k** could be directly isolated in high yields as the ketimines.

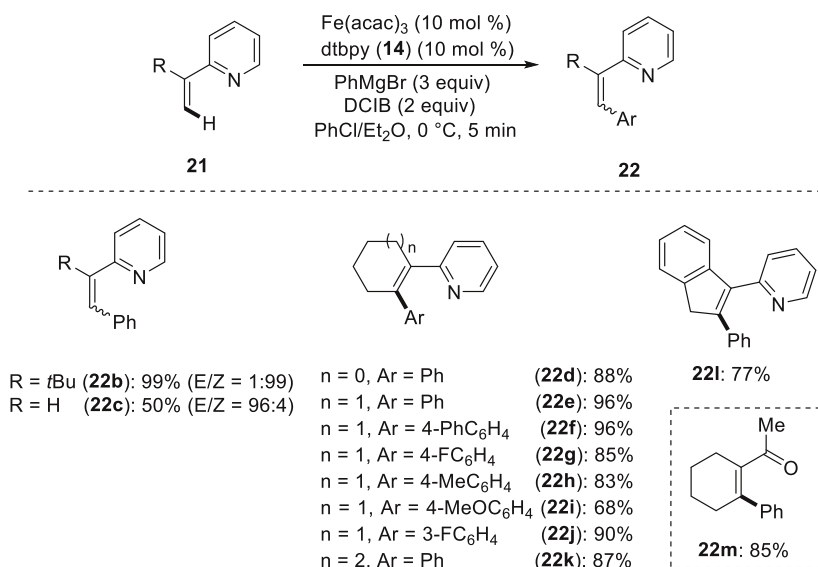


**Scheme 14** Iron-catalyzed *ortho*-arylation of heteroaromatic ketimines **19**





**Scheme 15** Iron-catalyzed diastereoselective C–H arylation of olefins



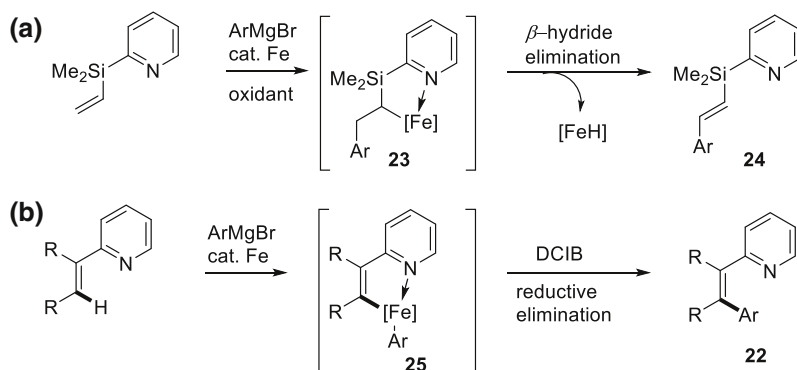
**Scheme 16** Scope of the iron-catalyzed C–H arylation of olefinic substrates **21**

The robust nature of the iron catalyst allowed for the selective C–H arylation of alkenes **21**, as reported by Nakamura and coworkers [66]. Indeed, the dropwise addition of the Grignard reagents proved beneficial for the stereospecific arylation of the olefinic C–H bonds (Scheme 15).

It is particularly noteworthy that the reaction medium played a crucial role in controlling the diastereo-selectivity of the C–H arylation reaction. Hence, mechanistic studies suggested that a *Z/E* isomerization was promoted by a low-valent iron species when using THF as the solvent (Scheme 15, i). In contrast, an aromatic solvent, such as chlorobenzene [67, 68], was proposed to act as a ligand for the active iron species, thereby inhibiting the *Z/E* isomerization (Scheme 15, ii) [66].

With the optimized protocol in hand, a variety of cyclic and acyclic olefins **21** featuring a pyridyl directing group were converted into the corresponding products **22** with high *Z*-diastereo-selectivity (Scheme 16) [66].

In stark contrast, 2-vinylpyridine **21c** delivered the *E*-diastereomer (Scheme 16, entry **22c**). Careful monitoring of the reaction progress after 1, 3, and 5 min upon



**Scheme 17** Potential reaction manifolds: **a** carbometalation followed by  $\beta$ -hydride elimination, **b** C–H cleavage followed by reductive elimination

the addition of the Grignard reagent led to the observation of an effective isomerization process ( $E/Z = 35:65$ ,  $65:35$ ,  $96:4$ , respectively). Notably, ketimine **21m** was smoothly arylated to the corresponding unsaturated ketone **22m** upon aqueous hydrolysis.

As to the catalysts working mode, a dichotomy caused by an iron-catalyzed Mizoroki–Heck reaction was initially put forward (Scheme 17a) [69].

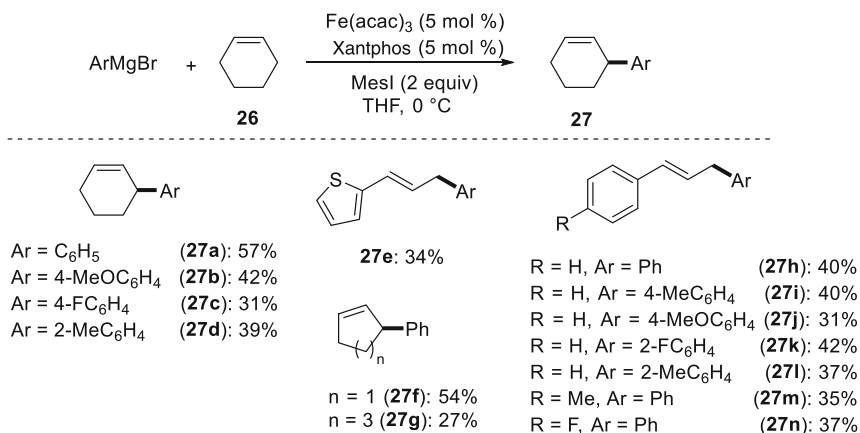
However, if a Mizoroki–Heck-type mechanism was operative (path a), the five-membered metalacycle **23** would need to undergo a  $\beta$ -hydride elimination in order to afford product **24** as the *E*-isomer. Thereby, a highly reactive iron hydrido species would be generated, which are known to affect the reduction of the substrate **21** or the arylated product **22** to the corresponding alkanes [69]. Since alkane products were not detected during the C–H arylation process, a different mode of action was proposed to be operative. Particularly, the formation of metalacycle **25** is more likely, which then undergoes an oxidation-induced reductive elimination in the presence of DCIB (path b).

## 2.2 Iron-Catalyzed Arylations of Allylic C–H Bonds

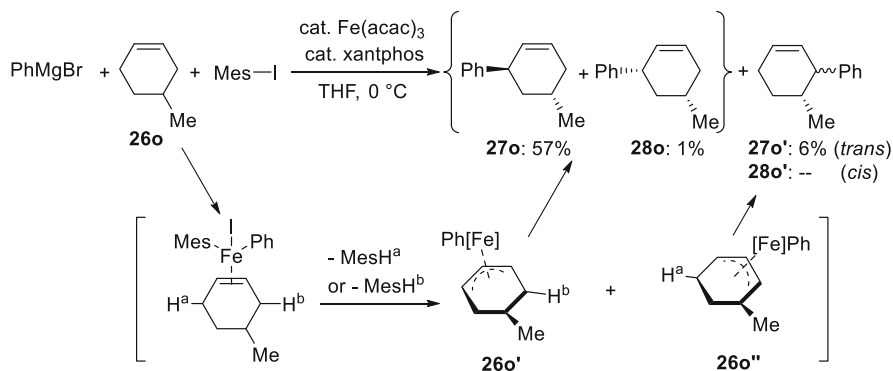
An early example of allylic diversification was reported by Tsuji by means of a  $\pi$ -allylpalladium complex [70]. In contrast, recently, Nakamura and coworkers reported the coupling of an aryl Grignard reagent with an alkene under iron catalysis [71]. The reaction proceeded through the functionalization of an allylic C–H bond of cyclohexene **26** with a relatively high catalyst turnover number (TON) of up to 240 (Scheme 18).

The reaction highlighted a fair functional group tolerance with respect to the aryl Grignard reagents, featuring both electron-donating and electron-withdrawing substituents. Moreover, several cyclic alkenes **26f–g** underwent a selective arylation of the allylic  $\text{C}(\text{sp}^3)\text{–H}$  bond.

To gain insight into the reaction mechanism, (*rac*)-4-methylcyclohexene (**26o**) was submitted to the optimized reaction conditions, as depicted in Scheme 19.



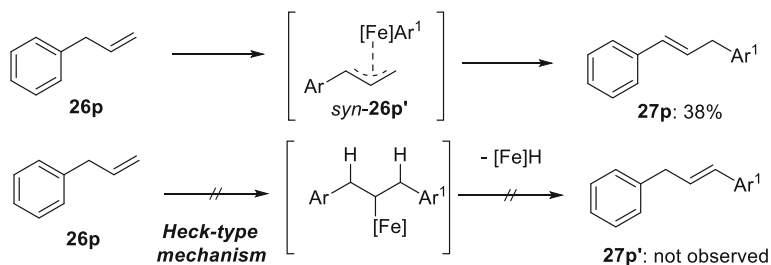
**Scheme 18** Iron-catalyzed allylic arylation of olefins via C(sp<sup>3</sup>)-H activation



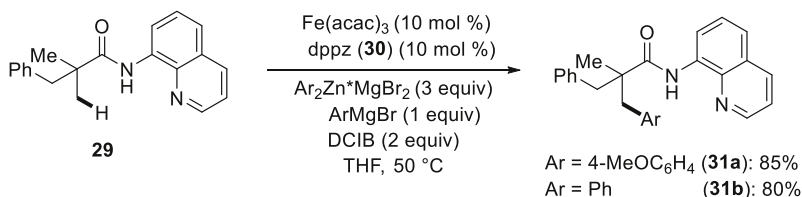
**Scheme 19** Proposed mechanism for the phenylation of (*rac*)-4-methylcyclohexene (**26o**)

Thus, the reaction of (*rac*)-4-methylcyclohexene (**26o**) delivered *trans*-5-methyl-3-phenyl-cyclohexene (**27o**) as the major product. This compound was formed through the coordination of the iron catalyst by the alkene, followed by an intramolecular abstraction of the axial H<sup>a</sup> to give the allyl iron intermediate **26o'**. The abstraction of the H<sup>b</sup> to produce intermediate **26o''** was less favored due to repulsive steric interactions. The *cis*-isomer products **28o-o'** were obtained only in trace amounts, likely because of the elementary step of reductive elimination being sensitive to steric congestion.

Notably, the product selectivity in the case of allylbenzene **26p** further supported the formation of a π-allyl-iron intermediate, rendering a Mizoroki–Heck-type mechanism less likely to be of relevance here (Scheme 20) [72].



**Scheme 20** Experimental evidence disfavoring a Mizoroki–Heck-type mechanism



**Scheme 21**  $\beta$ -Arylation of amides **29** via iron-catalyzed C(sp<sup>3</sup>)–H activation

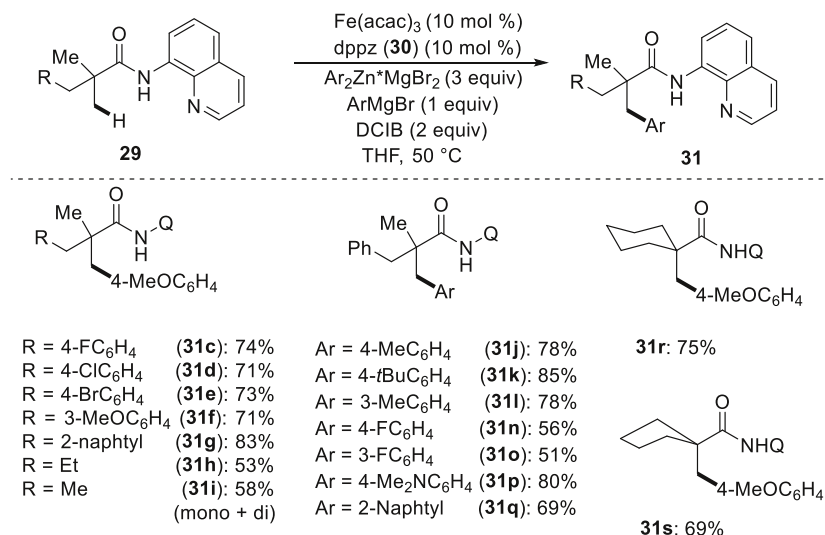
### 2.3 Iron-Catalyzed C–H Functionalizations by Bidentate Assistance

Major recent progress in the area of iron-catalyzed C–H activations has been achieved by developing protocols for the challenging functionalization of unactivated C(sp<sup>3</sup>)–H [73–75] bonds by chelation assistance. The use of 8-aminoquinoline (Q) as a powerful directing group was originally established by Daugulis for palladium-catalyzed functionalizations of unactivated C(sp<sup>3</sup>)–H bonds [76]. In contrast, Nakamura reported on user-friendly, air and moisture-stable iron catalysts in combination with the diphosphine ligand dppz (**30**) for the arylation of unactivated C(sp<sup>3</sup>)–H bonds by Q-assistance (**Scheme 21**) [77].

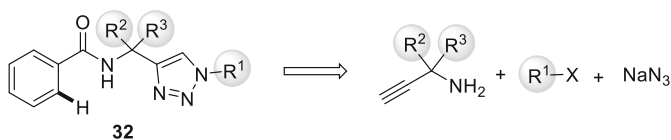
A bidentate-chelated low-valent organoiron intermediate was proposed as the key intermediate in the arylation of C(sp<sup>3</sup>)–H bonds. The functionalization of the  $\beta$ -methyl position of a 2,2-disubstituted propionamide bearing the Q as directing group proceeded with high yields and good functional group tolerance. The organometallic character of the iron catalysis was, among others, reflected by the preference of the methyl group over the more reactive benzylic position as well as by the strong influence of the phosphine ligand.

The optimized iron catalyst displayed a broad substrate scope and functional group tolerance as illustrated in **Scheme 22**.

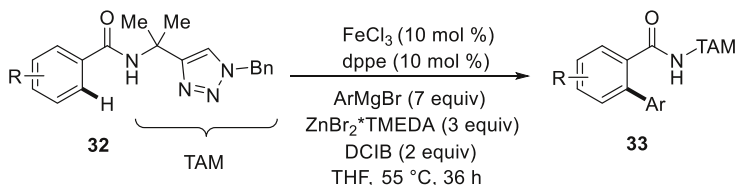
The Q auxiliary is difficult to access in a modular fashion, and its removal usually requires harsh reaction conditions, such as concentrated HCl at 130 °C. Thus, a major advance in iron-catalyzed C–H activation was accomplished by introducing a modular family of easily accessible triazole-based TAM groups, in an area thus far being dominated by the Q directing group (**Scheme 23**) [78–81]. In this context it is



**Scheme 22** Iron-catalyzed C(sp<sup>3</sup>)-H arylation of Q-amides **29**



**Scheme 23** Retrosynthetic analysis for the TAM directing group



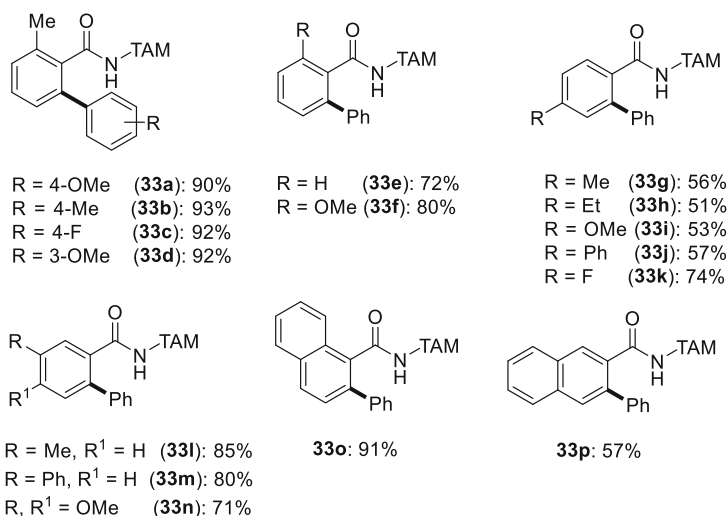
**Scheme 24** Iron-catalyzed C(sp<sup>2</sup>)-H arylation of TAM-carboxamides **32**

noteworthy that the TAM group is prepared by the copper-catalyzed click 1,3-dipolar cycloaddition in a highly modular manner [79, 80, 82].

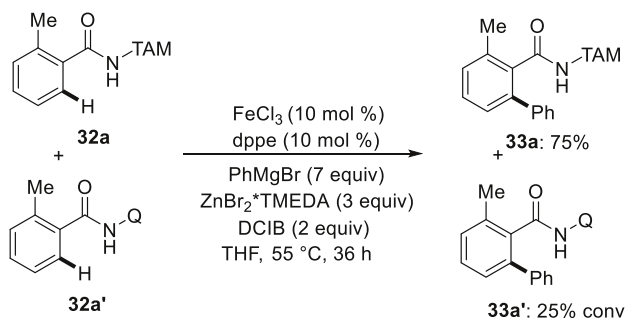
In 2014, Ackermann and coworkers identified the easily accessible 1,2,3-triazole as an enabling motif in bidentate directing groups for the iron-catalyzed C(sp<sup>2</sup>)-H and C(sp<sup>3</sup>)-H arylations (Scheme 24) [82].

Thereby, a wealth of TAM-derived benzamides **32** was efficiently converted with ample scope and high catalytic efficacy to the corresponding arylated amides **33** (Scheme 25).

Interestingly, an intermolecular competition experiment between the TAM-amide **32a** and the corresponding Q-amide **32a'** derived from 8-aminoquinoline,



**Scheme 25** Scope of the iron-catalyzed C(sp<sup>2</sup>)-H arylation by TAM-assistance



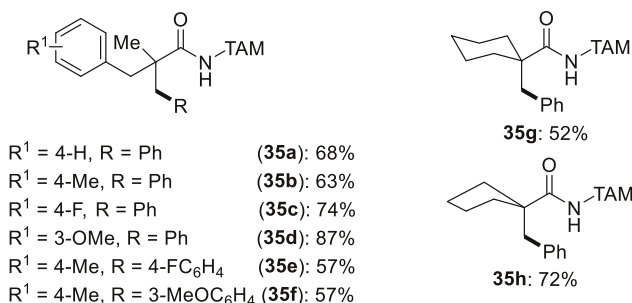
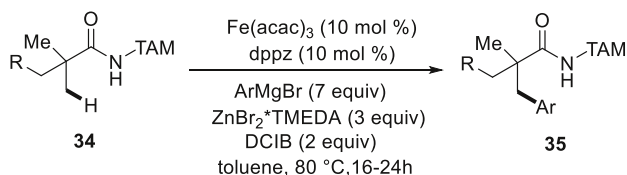
**Scheme 26** Competition experiment: directing group ability

clearly revealed the TAM group to display an improved directing group power (Scheme 26).

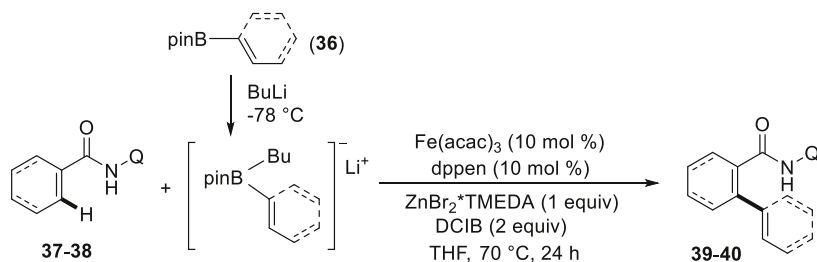
The judicious choice of the phosphine ligand and the solvent even allowed for the challenging iron-catalyzed C(sp<sup>3</sup>)-H arylation with good yields and complete mono-selectivity by TAM-assistance (Scheme 27).

## 2.4 Iron-Catalyzed Arylation and Alkenylation with Boronates

Metal-catalyzed C-H functionalizations with shelf-stable organoboron compounds are of particular topical interest in organic synthesis, with considerable advances being achieved by the aid of precious 4d and 5d transition metals [83–86]. While this strategy proved to be powerful, it displayed significant limitations, particularly with respect to the stereo-selective formation of alkenyl-aryl and alkenyl-alkenyl linkages. This observation was partly attributed to the strong interactions of the 4d



**Scheme 27** Iron-catalyzed  $\text{C}(\text{sp}^3)\text{-H}$  arylation by triazole assistance



**Scheme 28** Iron-catalyzed  $\text{C}(\text{sp}^2)\text{-H}$  functionalization with organoboron compounds **36**

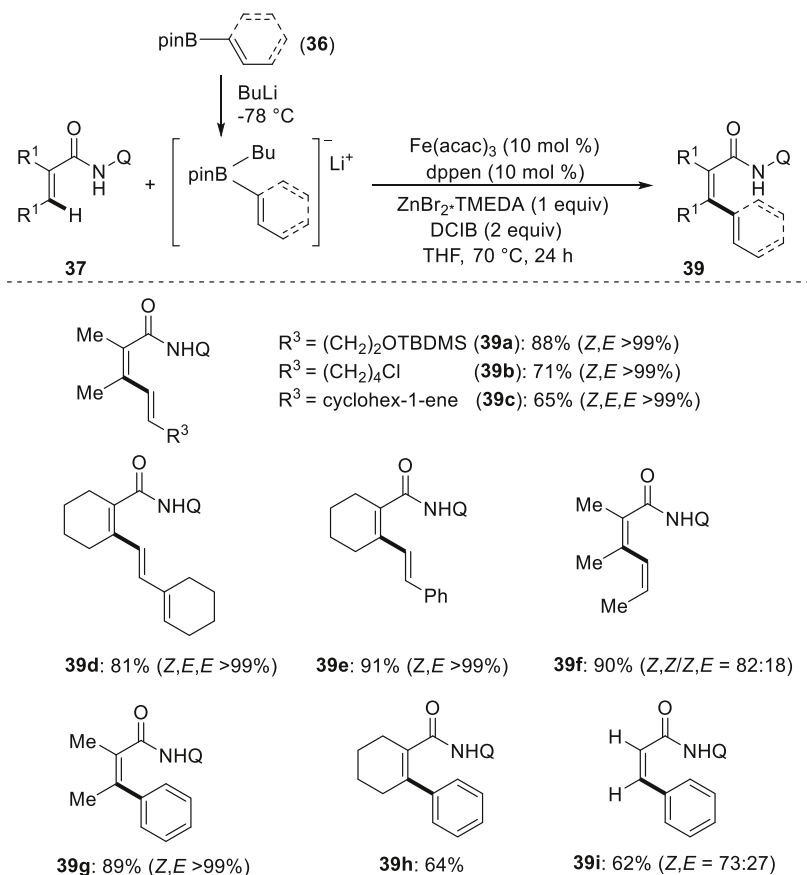
and 5d orbitals with the  $\pi$ -bonds of the alkene, which likely leads to undesired alkene isomerization [87–89]. To overcome these limitations, Nakamura developed a protocol for the  $\text{C}\text{-H}$  arylation and alkenylation using organoboron compounds **36**, employing iron catalysts that feature only a minor  $\pi$ -back-donation (Scheme 28) [90].

The use of *n*-butyllithium allowed for the generation of boronate salts. However, it is noteworthy that zinc additives proved to be mandatory here for the  $\text{C}\text{-H}$  functionalization process to occur [91, 92].

Furthermore, the use of the boronic acid ester precursors **36** set the stage for the synthesis of olefins **39** with excellent *Z*-diastereo-selectivity (Scheme 29).

Here, a good functional group tolerance was reflected by fully accepting the silylether, chloride, diene, and triene motifs (**39a–e**). The stereochemistry of *E*-boronates **39a–e** was fully retained, while in the case of a *Z*-boronate **39f** a slight decrease (*Z,Z/Z,E* = 82:18) was noted.

The same iron catalyst proved applicable for alkenylations and arylations of aromatic *Q*-benzamides **38** as well (Scheme 30) [90].



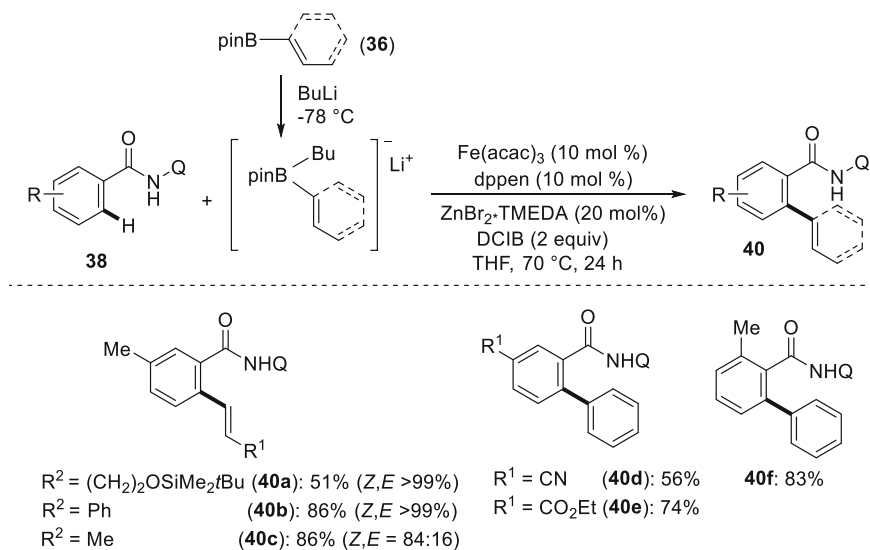
**Scheme 29** Alkenylation and arylation with organoboron compounds **36**

The oxidative functionalization approach with organometallic reagents was not limited to arylations and alkenylations. Indeed, direct alkylations were accomplished as well [93]. The use of in situ generated alkylzinc reagents thus allowed for the *ortho*-selective alkylation [94] via bidentate chelation assistance with the AQ auxiliary (Scheme 31) [93].

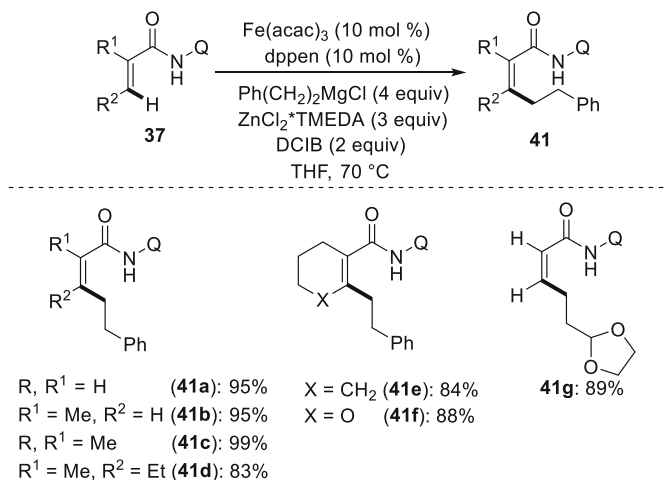
Notably, the homo-coupling and  $\beta$ -hydride elimination of the in situ generated alkylzinc reagents were largely suppressed, delivering the desired alkylated amides **42** in good yields and high *Z*-stereoselectivity. Likewise, the protocol proved amenable to the alkylation of aromatic benzamides **38** with primary and secondary alkylzinc reagents (Scheme 32) [93].

The methyl group represents a key structural motif of various bioactive compounds, and the introduction of a single methyl substituent can significantly impact the biological activities and physical properties of pharmacologically relevant drug molecules. Hence, a methyl group increases the hydrophobic character of a given molecule and thereby its affinity to bind to biomolecules. This so-called magic methyl effect can induce a hundred-fold boost in potency, resulting in a





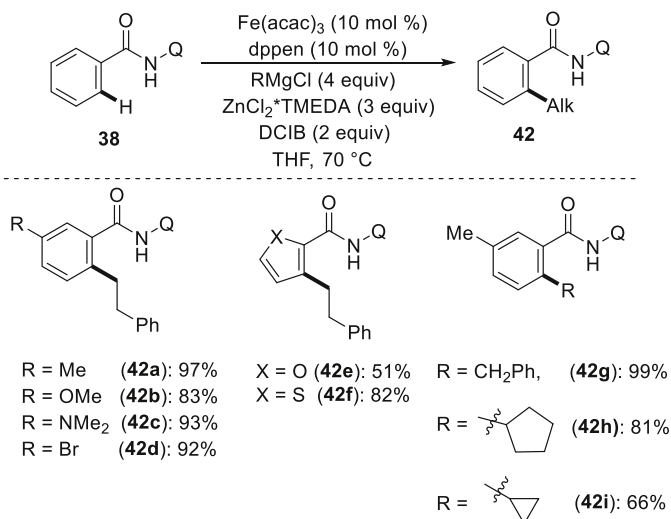
**Scheme 30** Alkenylation and arylation of aromatic benzamides **38**



**Scheme 31** Iron-catalyzed C–H alkylation of olefins **37**

considerable improvement of its  $\text{IC}_{50}$  value [95]. The direct introduction of a methyl group has until recently been predominantly achieved with 4d transition metal catalysts based on palladium and rhodium catalysts [95–98]. In contrast, Ackermann introduced a widely applicable iron-catalyzed methylation protocol for  $\text{C}(\text{sp}^2)\text{--H}$  and  $\text{C}(\text{sp}^3)\text{--H}$  bonds by TAM-assistance (Scheme 33) [99].

The method proved not only amenable for the C–H methylation of arenes and heteroarenes, but also for the ethylation with  $\beta$ -hydrogen containing  $\text{EtMgBr}$  as the alkylating reagent (**43m–o**, Scheme 33) [99].



**Scheme 32** C–H alkylation of aromatic benzamides **38**

It is noteworthy that the exact same protocol was also found suitable for challenging  $\text{C}(\text{sp}^3)\text{--H}$  methylations, as depicted in [Scheme 34](#) [99]. The C–H functionalization was shown to operate by an organometallic mode of action and to occur as the “turnover-limiting” step of the catalytic reaction [100], as was indicated by the strong phosphine ligand effect as well as by a kinetic isotopic effect (KIE) of 1.8 as determined from two parallel reactions.

Another approach for the positional selective iron-catalyzed C–H methylation was established with trimethylaluminum or its air-stable derivative DABCO- $2\text{AlMe}_3$ . The iron catalyst was found to be effective even at a low catalyst loading of only 1.0 mol%. The protocol was applicable to several picolinamide (PA) derivatives **45**, notably in the absence of zinc additives ([Scheme 35](#)) [101].

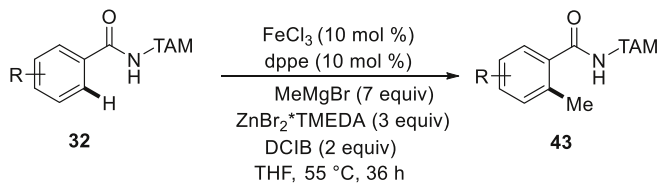
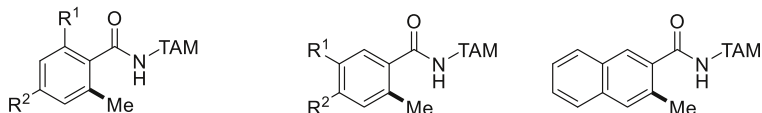
The substrate scope included amides **38** bearing different functional groups, while the catalyst was not restricted to picolinamide derivatives **45**. Indeed, also C–H methylations of benzamides **38** derived from the 8-AQ bidentate auxiliary were accomplished ([Scheme 36](#)).

The catalytic system also proved competent for the selective functionalization of  $\text{C}(\text{sp}^3)\text{--H}$  bonds, again occurring in the absence of zinc additives ([Scheme 37](#)).

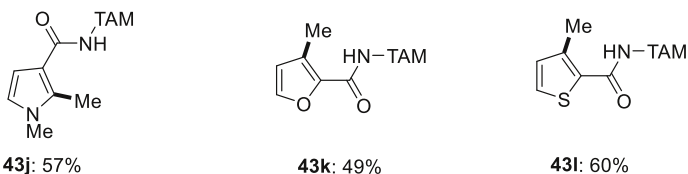
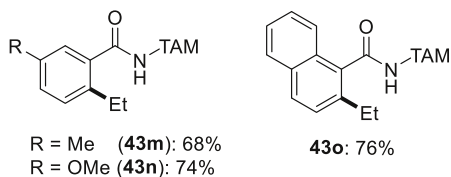
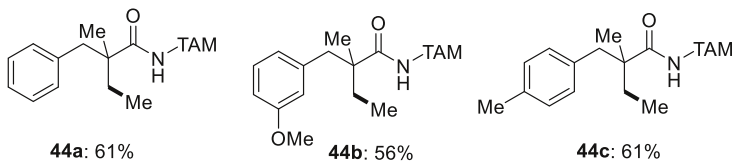
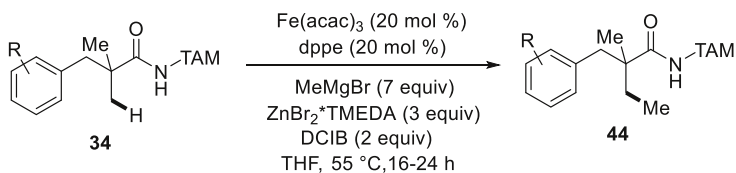
### 3 Iron-Catalyzed C–H Activation with Organic Electrophiles

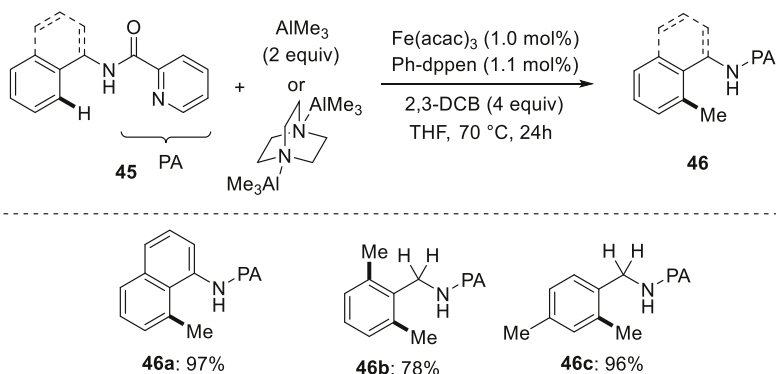
#### 3.1 Iron-Catalyzed C–H Alkylations

The oxidative iron-catalyzed C–H functionalizations generally proceeded through the formation of a putative alkyl or aryl-substituted low-valent iron intermediate **49** (vide supra) that was proposed to directly couple with a nucleophile by the action of an external oxidant ([Scheme 38a](#)).

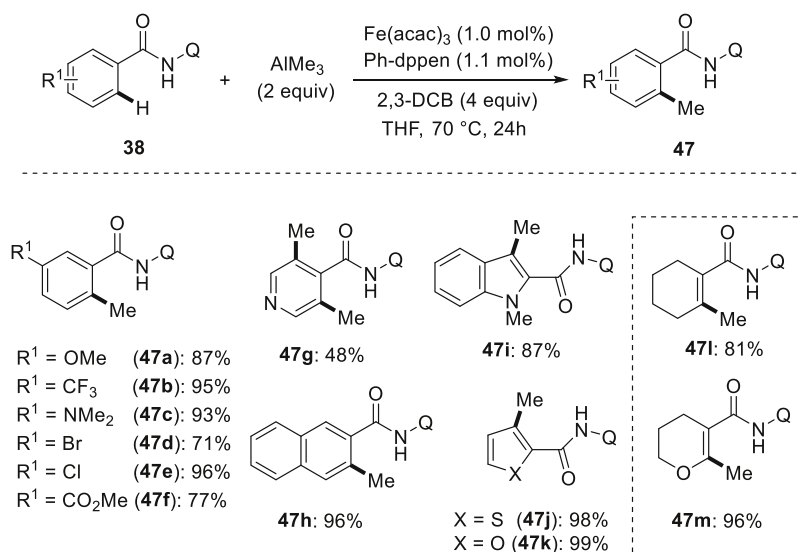
*C-H methylation of arenes*

$\text{R}^1 = \text{Me}$ ,  $\text{R}^2 = \text{Ph}$  (**43b**): 96%     $\text{R}^1 = \text{Me}$ ,  $\text{R}^2 = \text{H}$  (**43f**): 80%    **43i**: 95%  
 $\text{R}^1 = \text{Me}$ ,  $\text{R}^2 = \text{F}$  (**43c**): 76%     $\text{R}^1 = \text{Cl}$ ,  $\text{R}^2 = \text{H}$  (**43g**): 81%  
 $\text{R}^1 = \text{Me}$ ,  $\text{R}^2 = \text{CF}_3$  (**43d**): 87%     $\text{R}^1, \text{R}^2 = \text{OMe}$  (**43h**): 74%  
 $\text{R}^1 = \text{OMe}$ ,  $\text{R}^2 = \text{H}$  (**43e**): 80%

*C-H methylation of heteroarenes***43j**: 57%**43k**: 49%**43l**: 60%*C-H ethylation of arenes***Scheme 33** Iron-catalyzed C–H methylations by TAM-assistance**Scheme 34** Iron-catalyzed C(sp<sup>3</sup>)–H methylations by triazole assistance



**Scheme 35** Iron-catalyzed C–H methylation with organoaluminium reagents



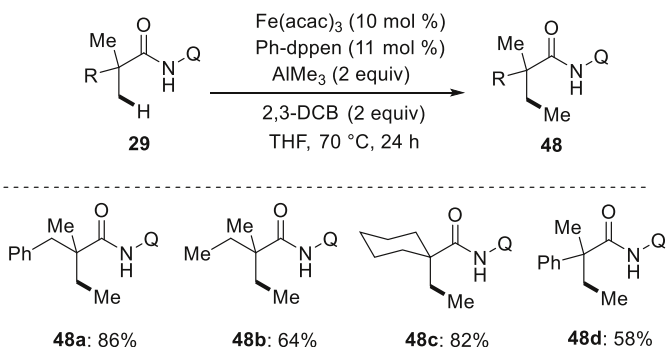
**Scheme 36** Scope of iron-catalyzed benzamide C(sp<sup>2</sup>)-H methylations

Very recently, a major advance in iron-catalyzed C–H activation was represented by unraveling that the low-valent iron species **49** could directly be reacted with various organic electrophiles (Scheme 38b).

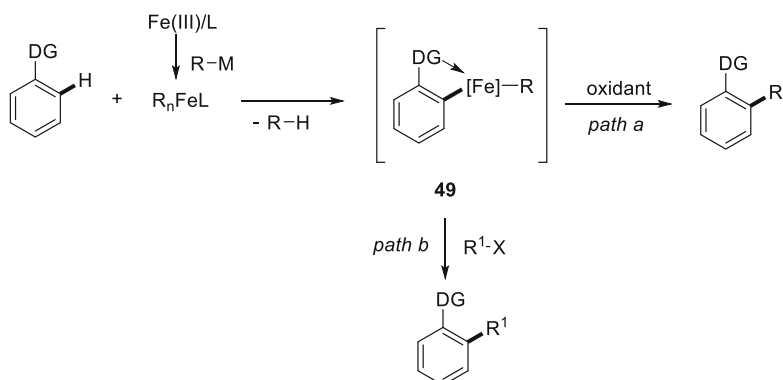
Hence, Nakamura reported an early example of iron-catalyzed C–H allylation using allyl ether **50** as the electrophile. The method was widely applicable and displayed a high functional group tolerance (Scheme 39) [102, 103].

The use of the organometallic base was crucial, since C–H methylation and arylations were observed in the presence of simple organozinc reagents, such as Me<sub>2</sub>Zn or Ph<sub>2</sub>Zn, respectively.

To gain information on the catalysts mode of action, a C–H allylation was performed in the presence of (1,1-dideuterio-allyloxy)benzene ([D]<sub>2</sub>-**50**), selectively



**Scheme 37** Iron-catalyzed C(sp<sup>3</sup>)-H methylations of aliphatic amides **29**



**Scheme 38** Possible pathways for iron-catalyzed C-H transformations

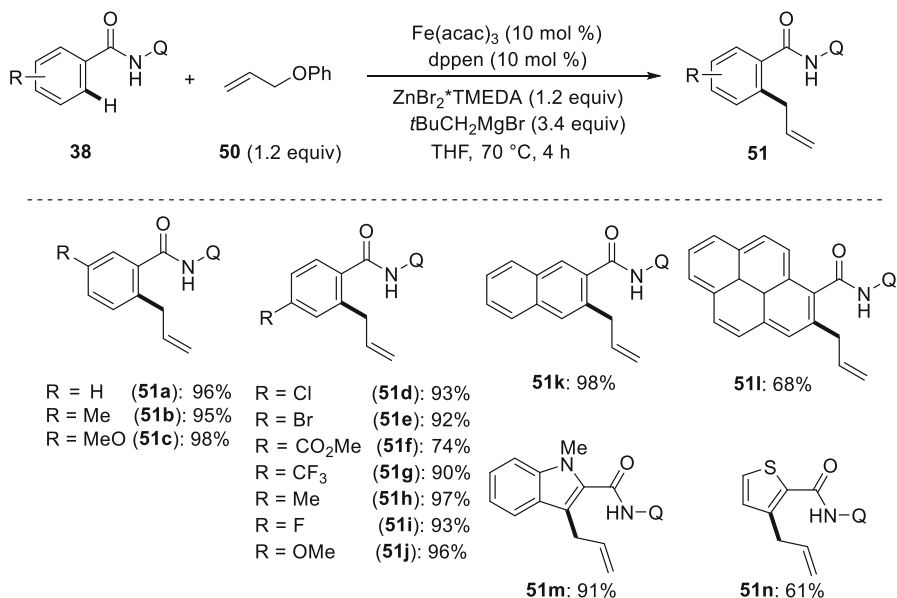
affording the  $\gamma,\gamma$ -deuterated-product [D]<sub>2</sub>-**51**. This finding provided strong support for a S<sub>N</sub>2'-type reaction manifold (Scheme 40).

The concept was extended to the direct alkylation of alkenyl amides **37** with primary and secondary tosylates **52** (Scheme 41) [104]. The use of alkyl tosylates **52** is particularly noteworthy, since such alkylations were thus far mostly accomplished with alkyl halides [105].

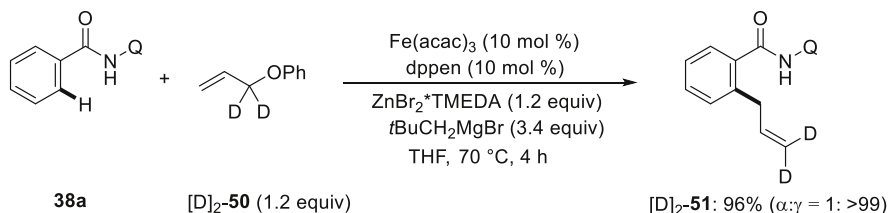
The use of an excess of NaI is crucial in order to suppress the C-H arylation, although the occurrence of an in situ Finkelstein reaction between the tosylates and excess iodide could not be ruled out [106]. As for the reaction scope, several amides **37** were alkylated with primary and secondary alkyl tosylates **52** [104]. Interestingly, the stereochemical information was partially sacrificed when using stereochemically well-defined *trans*-4-*tert*-butylcyclohexyl tosylate **52j**. This observation can be rationalized in terms of a radical-based C-O cleavage [107].

Likewise, the C-H transformation smoothly proceeded for the alkylation of aromatic benzamides **62** with a wide range of alkyl tosylates **52** (Scheme 42).

Several mechanistic findings are noteworthy. First, the regiochemical integrity of the secondary tosylates indicates that a potential  $\beta$ -elimination/hydroarylation sequence is not operative here. Second, the use of the radical scavenger TEMPO



**Scheme 39** Iron-catalyzed C–H allylation with allyl ether **50**



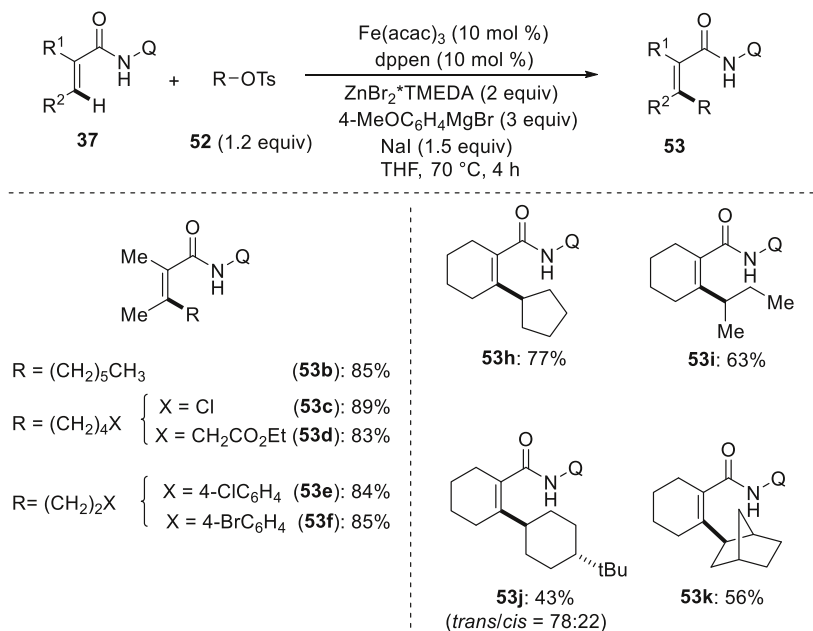
**Scheme 40** Evidence for a  $\text{S}_{\text{N}}2'$ -type mechanism in C–H allylations

completely inhibited the catalytic efficacy, highlighting the radical character of the C–X cleavage process.

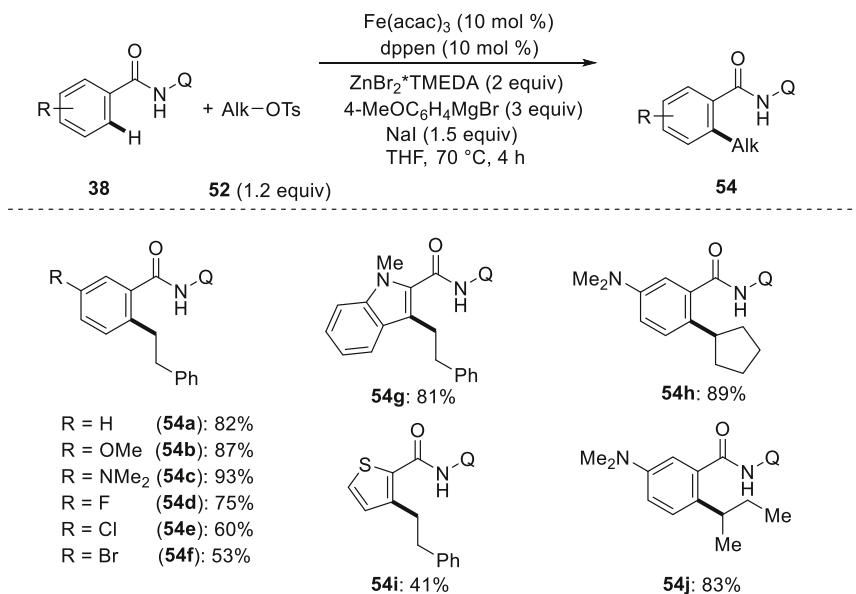
Another approach to the alkylation of C–H bonds was independently disclosed by Cook, reporting a strategy for the iron-catalyzed *ortho*-benzylation (Scheme 43) [108].

The slow addition of the Grignard reagents proved to be beneficial in order to achieve optimal efficacy of the iron catalyst. Furthermore, it was found that the reaction is best performed within a short reaction time, while the use of zinc additives was interestingly found to be detrimental. The selective monoalkylation protocol was widely applicable to different aromatic amides **38**. For instance, thioether, amino and halogen substituents were fully tolerated, thereby affording the corresponding benzylated products **55**.

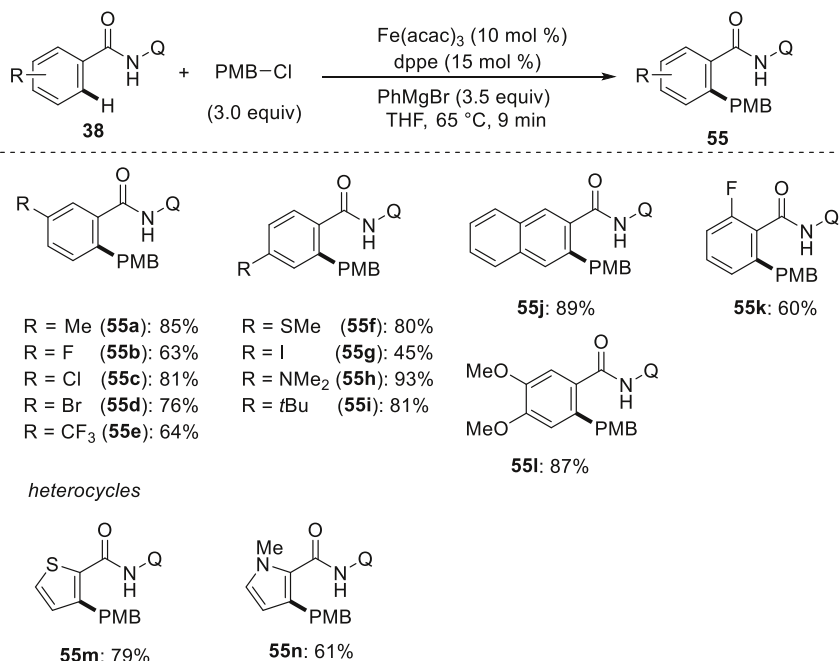
The optimized protocol also proved to be viable for the alkylation with secondary alkyl bromides **56**. Here, the radical inhibitor BHT was employed in order to avoid the formation of transient secondary alkyl radicals (Scheme 44).



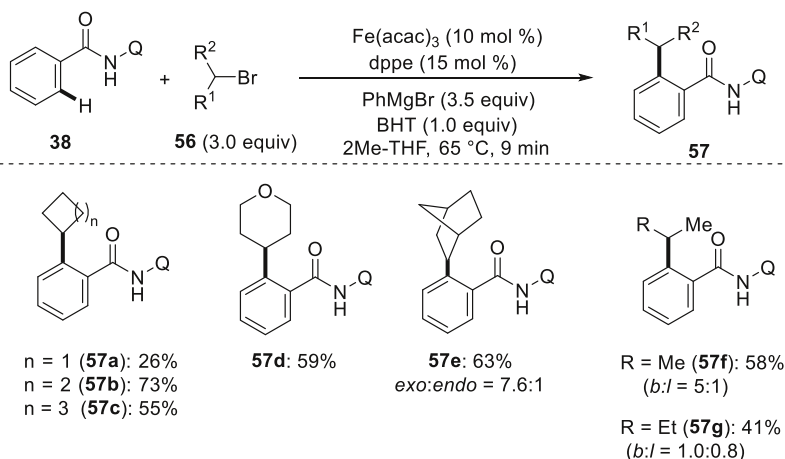
**Scheme 41** Iron-catalyzed C(sp<sup>2</sup>)-H alkylation with primary and secondary alkyl tosylates **52**



**Scheme 42** Iron-catalyzed direct C-H alkylation of aromatic amides **38**



**Scheme 43** Iron-catalyzed Q-assisted C(sp<sup>2</sup>)-H benzylation

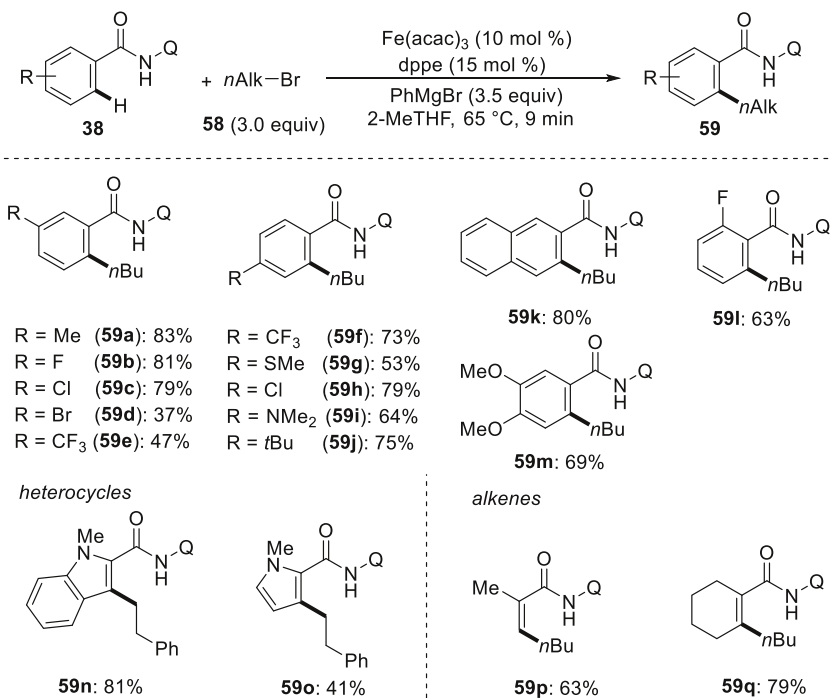


**Scheme 44** Iron-catalyzed C(sp<sup>2</sup>)-H alkylations with secondary alkyl bromides **56**

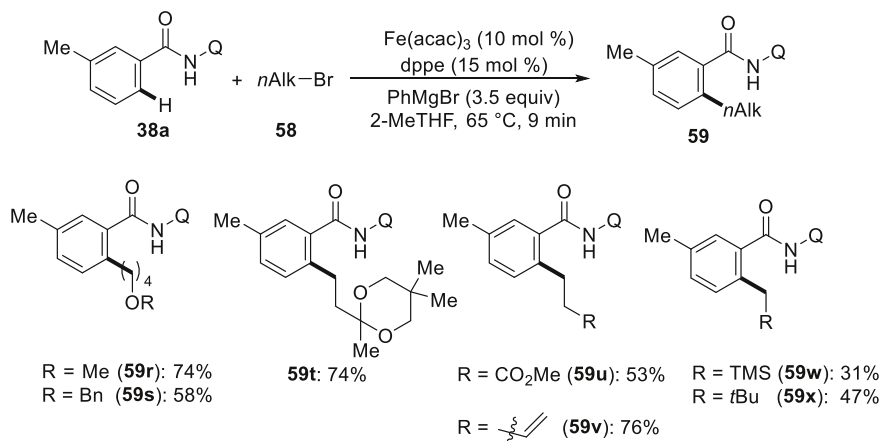
In addition, Cook observed that C-H alkylations with primary alkyl bromides **58** proved to be viable under otherwise identical reaction conditions (Scheme 45) [109].

A good functional group tolerance was noted with respect to the viable substitution patterns of the alkyl bromides **58**. Namely, substrates bearing ether,





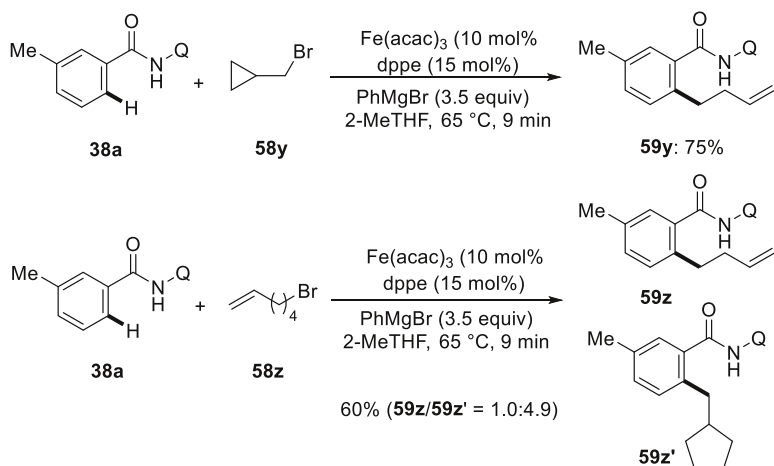
**Scheme 45** Iron-catalyzed C(sp<sup>2</sup>)-H alkylations with primary alkyl bromides **58**



**Scheme 46** Iron-catalyzed alkylation with primary alkyl bromides **58**

silyl ether, and ester groups yielded the corresponding alkylated benzamides (Scheme 46).

Experiments were carried out in order to shed light on the reaction mechanism. To this end, the reaction with cyclopropylmethyl bromide (**58y**) provided the



**Scheme 47** Evidence for radical intermediates

homoallylated product **59y** as the sole product (**Scheme 47**). Moreover, 6-bromo-1-hexene (**58z**) furnished product **59z'** with a 5:1 ratio along with the linear product **59z**, being suggestive of a single-electron-transfer (SET)-type C–Br cleavage [110, 111].

In independent studies, Ackermann devised a widely applicable method for the C–H alkylations, employing the user-friendly TAM entity (**Scheme 48**) [112].

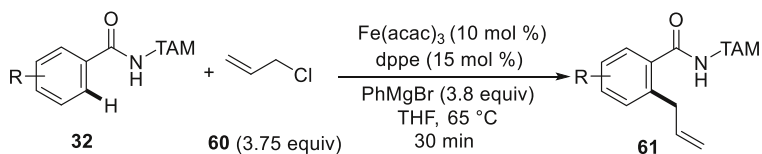
The protocol proved to be generally applicable for various aromatic and heteroaromatic benzamides **32**. Interestingly, differently substituted allyl chlorides **62a–b** furnished the same allylated product **63g–h** with comparable levels of regioselectivity (**Scheme 48c**) [112]. These findings provided strong support for the formation of a  $\eta^3$ -allyl-iron intermediate [113, 114].

Notably, allyl chlorides **60** also turned out to be excellent substrates for the unprecedented alkenyl C–H allylation of amides **64**. The triazole-assisted alkene C–H functionalizations were characterized by remarkably short reaction times and excellent diastereo-selectivities (**Scheme 49**).

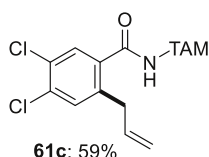
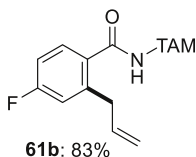
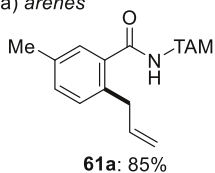
Under otherwise identical reaction conditions, the most generally applicable protocol also allowed for the C–H benzylation, methylation and alkylation employing benzyl, methyl and primary or secondary alkyl bromides **66**, respectively (**Scheme 50**). Furthermore, the versatile iron catalyst enabled the C–H alkylation with alkyl iodides, bromides, and even chlorides as the electrophiles.

The working mode of the versatile iron catalyst was studied in great detail (**Scheme 51**) and the results were consistent with a SET-type C–Hal cleavage.

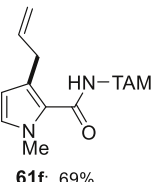
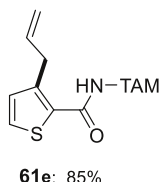
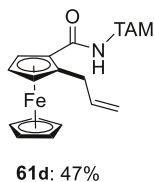
Importantly, a novel protocol for the facile removal of the TAM auxiliary was devised. Thus, NOBF<sub>4</sub>-promoted the cleavage of the triazole directing group under exceedingly mild reaction conditions [112], overcoming an important limitation of the Q-directing groups in C–H activation methodologies (**Scheme 52**) [115, 116].



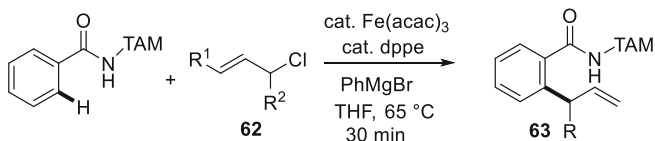
## a) arenes



## b) ferrocene and heteroarenes



## c) substituted allyl chlorides



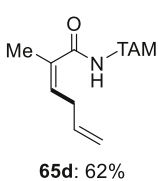
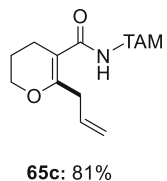
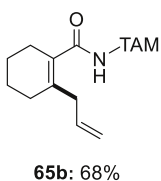
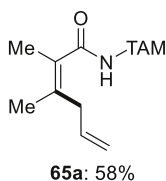
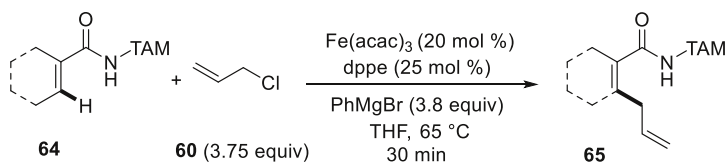
$\text{R}^1 = \text{Me}, \text{R}^2 = \text{H}$  (**62a**)

$\text{R}^1 = \text{H}, \text{R}^2 = \text{Me}$  (**62b**)

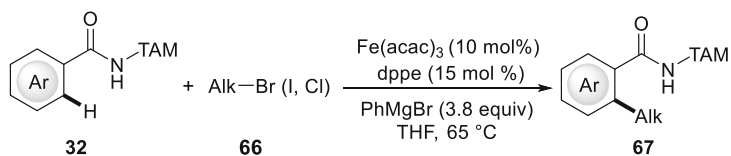
$\text{R} = \text{Me}$  (**63g**): 80% (b:l = 4.2:1)

$\text{R} = \text{Me}$  (**63h**): 75% (b:l = 2.5:1)

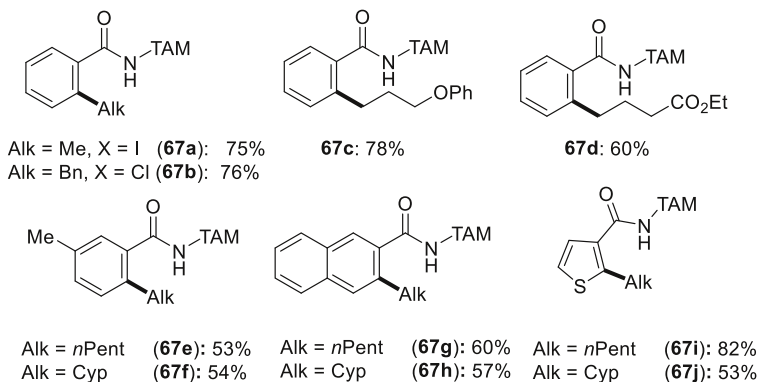
**Scheme 48** Iron-catalyzed  $\text{C}(\text{sp}^2)\text{-H}$  allylation by TAM-assistance



**Scheme 49** Iron-catalyzed  $\text{C}(\text{sp}^2)\text{-H}$  allylation of alkenes **64**

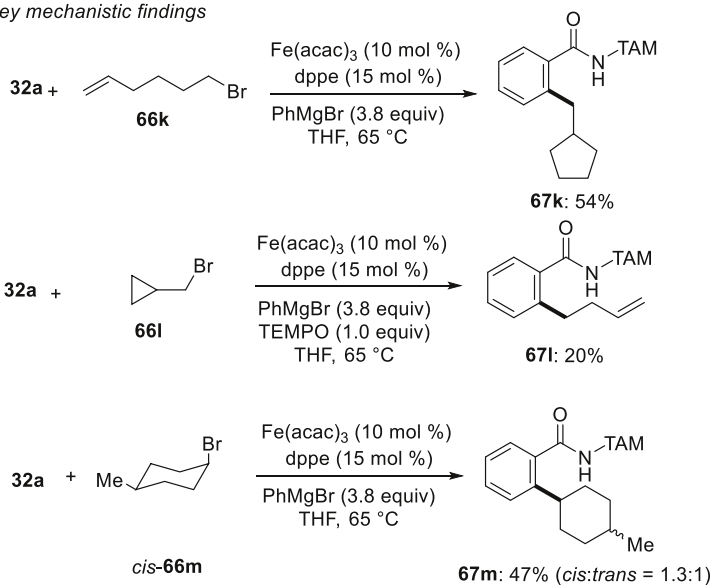


*C-H benzylations and alkylation with alkyl halides*



**Scheme 50** Iron-catalyzed C(sp<sup>2</sup>)-H benzylations, methylations, and alkylations by TAM-assistance

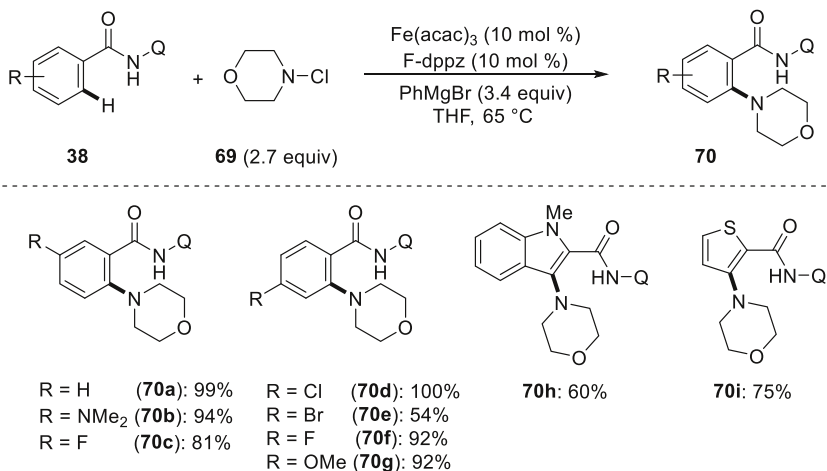
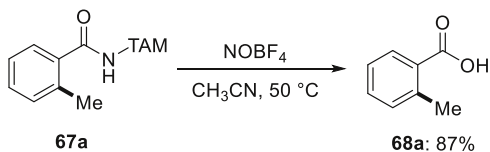
*Key mechanistic findings*



**Scheme 51** Key mechanistic findings for the iron-catalyzed C-H alkylations

### 3.2 Iron-Catalyzed C-H Aminations

The direct catalytic conversion of C-H bonds into C-N bonds constitutes an important challenge in organic synthesis due to the practical relevance of amines in

**Scheme 52** Mild removal of the TAM directing group**Scheme 53** Iron-catalyzed C–H aminations of benzamides **38**

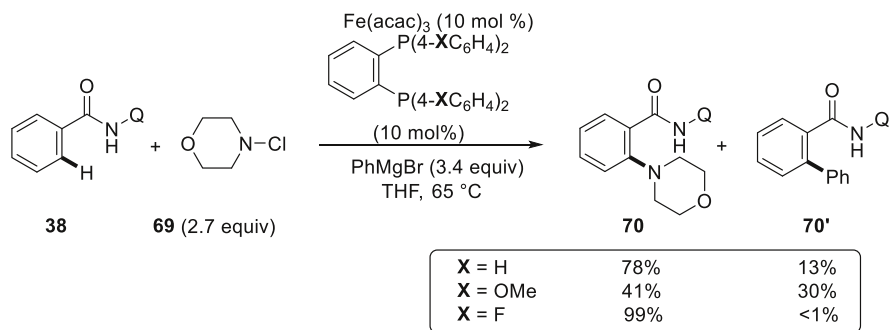
pharmaceutical and chemical industries, medicinal chemistry, and material sciences [117, 118]. In a research area being dominated by the use of precious transition metal catalysts, Nakamura reported on an iron-catalyzed C–H amination using *N*-chloroamines **69** as the electrophilic aminating reagents (Scheme 53) [119].

A simultaneous dropwise addition of the Grignard reagents and the *N*-chloroamine **69** led to complete conversion of the starting materials under bidentate assistance of 8-AQ to give anthranlyic acid derivatives **70**. Interestingly, the ligand displayed a key role in controlling the chemo-selectivity of the C–H nitrogenation process. Particularly, electron-deficient bidentate phosphine ligands performed best, highlighting the importance of electronic effects (Scheme 54).

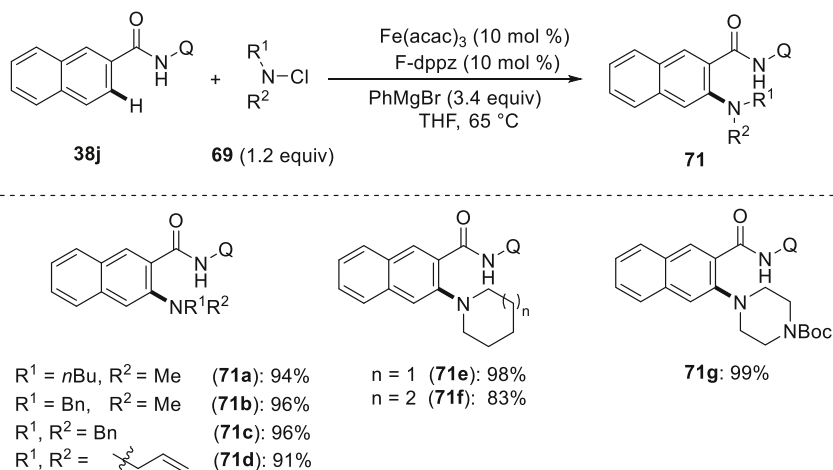
The optimized catalytic system proved tolerant of functional groups and allowed for the transformation of various substituted benzamides **38** (Scheme 53). The amination was viable with different *N*-chloroamines **69** as well, as shown in Scheme 55.

## 4 Conclusions

During recent years, C–H functionalization has emerged as an increasingly viable alternative to traditional cross-coupling reactions. Particularly, iron complexes have received considerable recent attention as inexpensive, non-toxic, and environmentally benign catalysts for C–H activations. These approaches largely avoid the synthesis and use of prefunctionalized substrates that are required for classical



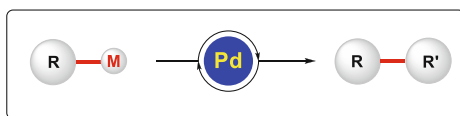
**Scheme 54** Ligand effect on C–H aminations



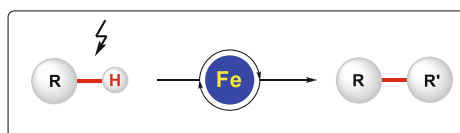
**Scheme 55** Scope of iron-catalyzed C–H aminations with *N*-chloroamines **69**

**Scheme 56** Palladium-catalyzed cross-coupling versus iron-catalyzed C–H functionalization

i) traditional cross-coupling reactions



ii) iron-catalyzed C–H functionalization approach



cross-coupling reactions. Thereby, a minimization of undesired waste is accomplished, which renders the C–H activation strategy a most user-friendly platform for academia and the practitioner in industries (Scheme 56).

Particular success has been achieved in oxidative C–H activations as well as C–H transformations with organic electrophiles, with major contributions by *inter alia* Nakamura, Ackermann and Cook. Thus, oxidative arylations, alkenylations, and alkylations of C(sp<sup>2</sup>)–H bonds were achieved under rather mild reaction conditions using monodentate directing groups or bidentate auxiliaries. Particularly, the bidentate binding motif has proven to be instrumental for the challenging functionalization of unactivated C(sp<sup>3</sup>)–H bonds. The robustness of the iron catalysts was further reflected by the recent development of iron-catalyzed C–H hydroarylation reactions by an organometallic mode of action (for miscellaneous reactions involving low-valent iron species, see [120, 121]). In contrast, organic electrophiles were only recently identified as suitable substrates for novel C–H alkylation and nitrogeneration reactions. Thus, significant advances have been accomplished by bidentate chelation assistance ensured by the 8-aminoquinoline or modular 1,2,3-triazoles. Particularly, the triazole-assisted C–H arylations, benzylation, and primary or secondary alkylations were characterized by ample substrate scope, good functional tolerance, and the facile removal of the bidentate auxiliary in a traceless fashion. Considering the sustainable nature of C–H functionalization technologies, along with the cost-effective nature of iron catalysis, further exciting developments are expected in this rapidly evolving research area, which should address enantioselective transformations and the effective reuse of heterogeneous [122] iron catalysts, among others. These studies should be guided by detailed experimental and computational mechanistic studies to fully delineate the key role of the metal additives and ligands in organometallic iron-catalyzed C–H activation processes.

## References

1. Ackermann L (2009) Modern arylation methods. Wiley, Weinheim
2. Johansson Seechurn CC, Kitching MO, Colacot TJ, Snieckus V (2012) *Angew Chem Int Ed* 51:5062
3. Jana R, Pathak TP, Sigman M (2011) *Chem Rev* 111:1417
4. Cahiez G, Moyeux A (2010) *Chem Rev* 110:1435
5. Hartwig JF (2009) *Organotransition metal chemistry: from bonding to catalysis*. University Science Books, Sausalito
6. Ilies L, Nakamura E (2014) *Iron-catalyzed cross-coupling reactions: in the chemistry of organoiron compounds*. Wiley, Chichester
7. Czaplik WM, Mayer M, Cvengros J, Von Wangelin AJ (2009) *Chem Sus Chem* 2:396
8. Sherry BD, Fuerstner A (2008) *Acc Chem Res* 41:1500
9. Tani S, Uehara TN, Yamaguchi J, Itami K (2014) *Chem Sci* 5:123
10. Borie C, Ackermann L, Nechab M (2016) *Chem Soc Rev* 45:1368
11. Rouquet G, Chatani N (2013) *Angew Chem Int Ed* 52:11726
12. Chen X, Engle KM, Wang DH, Yu JQ (2009) *Angew Chem Int Ed* 48:5094
13. Bergman RG (2007) *Nature* 446:391
14. Moselage M, Li J, Ackermann L (2016) *ACS Catal* 6:498

15. Liu W, Ackermann L (2016) *ACS Catal* 6:3743
16. Su B, Cao ZC, Shi ZJ (2015) *Acc Chem Res* 48:886
17. Ackermann L (2014) *J Org Chem* 79:8948
18. Nakao Y (2011) *Chem Rev* 11:242
19. Ye B, Cramer N (2015) *Acc Chem Res* 48:1308
20. Ackermann L, Li J (2015) *Nat Chem* 7:686
21. Ackermann L (2014) *Acc Chem Res* 47:281
22. Kuhl N, Hopkinson MN, Wencel-Delord J, Glorius F (2012) *Angew Chem Int Ed* 51:10236
23. Neufeldt SR, Sanford MS (2012) *Acc Chem Res* 45:936
24. Bauer I, Knolker HJ (2015) *Chem Rev* 115:3170
25. Morris H (2009) *Chem Soc Rev* 38:282
26. Czaplik WM, Mayer M, Cvengros V, von Wangelin AJ (2009) *Chem Sus Chem* 2:396
27. Enthaler S, Junge K, Beller M (2008) *Angew Chem Int Ed* 47:3317
28. Bolm C, Legros J, Le Paih J, Zani L (2004) *Chem Rev* 104:6217
29. Enghag P (2004) *Encyclopedia of elements*. Wiley, Weinheim
30. Plietker B (2008) *Iron catalysis in organic chemistry*. Wiley, Weinheim
31. Toxicity data of the FDA. <http://www.inchem.org/documents/jecfa/jecmono/v18je18.htm>. Accessed 15 May 2016
32. Dyker G (2005) *Handbook of C–H transformation. Application in organic synthesis*. Wiley, Weinheim
33. Poli R (2004) *J Organomet Chem* 689:4291
34. Ackermann L (2007) *Top Organomet Chem* 24:35
35. Dyker G (1999) *Angew Chem Int Ed* 38:1698
36. Dick AR, Sanford MS (2006) *Tetrahedron* 62:2439
37. Ackermann L, Vicente R, Kapdi AR (2009) *Angew Chem Int Ed* 48:9792
38. Sun CL, Li BJ, Shi ZJ (2011) *Chem Rev* 111:1293
39. Sun X, Huang X, Sun C (2012) *Curr Inorg Chem* 2:64
40. Yoshikai N, Nakamura E (2010) *J Org Chem* 75:6061
41. De Montellano PRO (2010) *Chem Rev* 110:932
42. MacFaul PA, Wayner DDM, Ingold K (1998) *Acc Chem Res* 31:159
43. Chen MS, White MC (2010) *Science* 327:566
44. Chen MS, White MC (2007) *Science* 318:783
45. Paradine SM, White MC (2012) *J Am Chem Soc* 134:2036
46. Wang Z, Zhang Y, Fu H, Jiang Y, Zhao Y (2008) *Org Lett* 10:1863
47. Fuerstner A (2009) *Angew Chem Int Ed* 48:1364
48. Fuerstner A, Leitner A, Mendez M, Krause H (2002) *J Am Chem Soc* 124:13856
49. McNeil E, Ritter T (2015) *Acc Chem Res* 48:2330
50. Fuerstner A, Martin R, Majima K (2005) *J Am Chem Soc* 127:12236
51. Tamura M, Kochi JK (1971) *J Am Chem Soc* 93:1487
52. Neumann SM, Kochi JK (1975) *J Org Chem* 40:599
53. Hata G, Kondo H, Miyake A (1968) *J Am Chem Soc* 90:2278
54. Barton DHR, Doller D (1992) *Acc Chem Res* 25:504
55. Rahtke JW, Muetterties EL (1975) *J Am Chem Soc* 97:3272
56. Baker MV, Field LD (1987) *J Am Chem Soc* 109:2825
57. Camadanli S, Beck R, Floerke U, Klein HF (2009) *Organometallics* 28:2300
58. Sun Y, Tang H, Chen K, Hu L, Yao J, Shaik S, Chen H (2016) *J Am Chem Soc* 138:3715
59. Norinder J, Matsumoto A, Yoshikai N, Nakamura E (2008) *J Am Chem Soc* 130:5858
60. Nakano T, Hayashi T (2005) *Org Lett* 7:491
61. Cahiez G, Chaboche C, Mamuteau-Betzer F, Ahr M (2005) *Org Lett* 7:1943
62. Yoshikai N, Matsumoto A, Norinder J, Nakamura E (2009) *Angew Chem Int Ed* 48:2925
63. Ilies L, Konno E, Chen Q, Nakamura E (2012) *Asian J Org Chem* 1:142
64. Sirois JJ, Davis R, DeBoef B (2014) *Org Lett* 16:868
65. Agrawal T, Cook SP (2013) *Org Lett* 15:96
66. Ilies L, Asako S, Nakamura E (2011) *J Am Chem Soc* 133:7672
67. Bart SC, Hawrelak EJ, Lobkovsky E, Chirik PJ (2005) *Organometallics* 24:5518
68. Radonovich LJ, Eyring MW, Groshens TJ, Klabund KJ (1982) *J Am Chem Soc* 104:2816
69. Ilies L, Okabe J, Yoshikai N, Nakamura E (2010) *Org Lett* 12:2838
70. Tsuji J, Takahashi H, Morikawa M (1965) *Tetrahedron Lett* 49:4387



71. Sekine M, Ilies L, Nakamura E (2013) *Org Lett* 15:714
72. Larock RC, Baker BE (1988) *Tetrahedron Lett* 29:905
73. Daugulis O, Roane J, Tran LD (2015) *Acc Chem Res* 48:1053
74. Baudoin O (2011) *Chem Soc Rev* 40:4902
75. Tobisu M, Chatani N (2006) *Angew Chem Int Ed* 118:1713
76. Zaitsev VG, Shabashov D, Daugulis O (2005) *J Am Chem Soc* 127:13154
77. Shang R, Ilies L, Matsumoto A, Nakamura E (2013) *J Am Chem Soc* 135:6030
78. Irastorza A, Airzpurua JM, Correa A (2016) *Org Lett* 18:1080
79. Al Mamari HH, Diers E, Ackermann L (2014) *Chem Eur J* 20:9739
80. Cera G, Ackermann L (2016) *Chem Eur J* 22:8475
81. Ye X, He Z, Weise K, Akhmedov NG, Petersen J, Shi X (2013) *Chem Sci* 4:3712
82. Qu Q, Al Mamari HH, Graczyk K, Diers E, Ackermann L (2014) *Angew Chem Int Ed* 53:3868
83. Thuy-Boun PS, Villa G, Dang D, Richardson P, Su S, Yu JQ (2013) *J Am Chem Soc* 135:17508
84. Karthikeyan J, Haridharan R, Cheng CH (2012) *Angew Chem Int Ed* 51:12343
85. Tredwell MJ, Gulias M, Bremeyer NG, Johansson CCC, Collins BSL, Gaunt MJ (2011) *Angew Chem Int Ed* 50:1076
86. Nishikata T, Abela AT, Huang S, Lipshutz BH (2010) *J Am Chem Soc* 132:4978
87. Ueno S, Chatani N, Kakiuchi F (2007) *J Org Chem* 72:3600
88. Wasa M, Chan KSL, Yu JQ (2011) *Chem Lett* 40:1004
89. Waterman R (2013) *Organometallics* 32:7249
90. Shang R, Ilies L, Asako S, Nakamura E (2014) *J Am Chem Soc* 136:14349
91. Bedford RB, Brenner PB, Carter E, Clifton J, Cogswell PM, Gower NJ, Haddow MF, Harvey JN, Kehl JA, Murphy DM, Neeve EC, Neidig ML, Nunn J, Snyder BER, Taylor J (2014) *Organometallics* 33:5767
92. Jia Z, Liu Q, Peng XS, Wong HNC (2016) *Nat Commun* 7:10614
93. Ilies L, Ichikawa S, Asako S, Matsubara T, Nakamura E (2014) *Adv Synth Catal* 357:2175
94. Ackermann L (2010) *Chem Commun* 46:4866
95. Schönherr H, Cernak T (2013) *Angew Chem Int Ed* 52:12256
96. Pan F, Lei ZQ, Wang H, Li H, Sun J, Shi ZJ (2013) *Angew Chem Int Ed* 52:2063
97. Neufeldt SR, Seigerman CK, Sanford MS (2013) *Org Lett* 15:2302
98. Dai HX, Stepan AF, Plummer MS, Zhang YH, Yu JQ (2011) *J Am Chem Soc* 133:7222
99. Graczyk K, Haven T, Ackermann L (2015) *Chem Eur J* 21:8812
100. Simmons EM, Hartwig JF (2012) *Angew Chem Int Ed* 51:3066
101. Shang R, Ilies L, Nakamura E (2015) *J Am Chem Soc* 137:7660
102. Asako S, Ilies L, Nakamura E (2013) *J Am Chem Soc* 135:17755
103. Asako S, Norinder J, Ilies L, Yoshikai N, Nakamura E (2014) *Adv Synth Catal* 356:1481
104. Ilies L, Matsubara T, Ichikawa A, Asako S, Nakamura E (2014) *J Am Chem Soc* 136:13126
105. Chatani N, Aihara Y (2013) *J Am Chem Soc* 135:5308
106. Finkelstein H (1910) *Ber Dtsch Chem Ges* 43:1528
107. Ito S, Fujiwara YI, Nakamura M, Nakamura E (2009) *Org Lett* 11:4306
108. Fruchey ER, Monks B, Cook SP (2014) *J Am Chem Soc* 136:13130
109. Monks B, Fruchey ER, Cook SP (2014) *Angew Chem Int Ed* 53:11605
110. Noda D, Sunada Y, Hatakeyama, Nakamura M, Nagashima H (2009) *J Am Chem Soc* 131:6078
111. Fuerstner A, Majima K, Martin R, Krause H, Kattnig E, Goddard R, Lehmann CW (2008) *J Am Chem Soc* 130:1992
112. Cera G, Haven T, Ackermann L (2016) *Angew Chem Int Ed* 55:1484
113. Plietker B, Dieskau A, Moews K, Jatsch K (2007) *Angew Chem Int Ed* 47:198
114. Plietker B (2006) *Angew Chem Int Ed* 45:1469
115. Olah GA, Olah JA (1965) *J Org Chem* 30:2386
116. Ye X, Xu C, Wojtas L, Akhmedov NG, Chen H, Shi X (2016) *Org Lett* 18:2970
117. Jiao J, Murakami K, Itami K (2016) *ACS Catal* 6:610
118. Thirunavukkarasu VS, Kozhushkov SI, Ackermann L (2014) *Chem Commun* 50:29
119. Matsubara T, Asako S, Ilies L, Nakamura E (2014) *J Am Chem Soc* 136:646
120. Wong MY, Yamakawa T, Yoshikai N (2015) *Org Lett* 17:442
121. Matsubara T, Ilies L, Nakamura E (2016) *Chem Asian J* 11:380
122. Santoro S, Kozhushkov S, Ackermann L, Vaccaro L (2016) *Green Chem.* doi:10.1039/C6GG00385K

# Fe-Catalyzed Cross-Dehydrogenative Coupling Reactions

Leiyang Lv<sup>1</sup> · Zhiping Li<sup>1</sup>

Received: 1 April 2016 / Accepted: 19 May 2016 / Published online: 8 June 2016  
© Springer International Publishing Switzerland 2016

**Abstract** Cross-dehydrogenative coupling (CDC), which enables the formation of carbon–carbon (C–C) and C–heteroatom bonds from the direct coupling of two C–H bonds or C–H/X–H bonds, represents a new state of the art in the field of organic chemistry. Iron, a prominent metal, has already shown its versatile application in chemical synthesis. This review attempts to provide a comprehensive understanding of the evolution of cross-dehydrogenative coupling via iron catalysis, as well as its application in synthetic chemistry.

**Keywords** Cross-dehydrogenative coupling (CDC) · Iron catalysis · C–H bond · C–C bond · C–X bond

## 1 Introduction

The development of selective, efficient, sustainable, and environmentally benign synthetic methodologies for the formation of carbon–carbon (C–C) and C–heteroatom bonds is an area of great interest to chemists, and one that is being actively pursued. Carbon–hydrogen (C–H) bonds exist broadly in a variety of organic molecules. Catalytic functionalization of C–H bonds has evolved as a powerful tool for organic synthesis, which not only provides an atom-economic alternative method, but also opens new routes to the target molecules. This trend is evidenced by reports of the ever-increasing utilization of C–H bonds as substrates for cross-coupling reactions [1–6]. Among reported methods, *cross-*

---

This article is part of the Topical Collection “Ni- and Fe-Based Cross-Coupling Reactions”, edited by Arkaitz Correa.

---

✉ Zhiping Li  
[zhipingli@ruc.edu.cn](mailto:zhipingli@ruc.edu.cn)

<sup>1</sup> Department of Chemistry, Renmin University of China, Beijing 100872, China

*dehydrogenative coupling* (CDC), which enables C–C and C–heteroatom bond formation from the direct coupling of two C–H bonds or C–H/X–H bonds, has emerged as the most attractive—and also the most challenging [7–10]. It is worth noting that in most cases, hydrogen gas ( $H_2$ ) is not produced in CDC transformation, and an appropriate sacrificial oxidant is generally needed. The obvious benefit of this strategy is that there is no need for preparation and isolation of activated reagents, or for pre-functionalization of easily available chemicals, thus improving atom and step economy. However, the conundrum that chemists must confront is how to overcome the low reactivity of C–H bonds and achieve site-selective functionalization of one C–H bond in the presence of all others. Li et al. have pioneered work addressing this challenge, and have made significant contributions in developing a series of synthetic methodologies in this field [11–16].

Iron, as one of the most abundant metals, is particularly attractive given its low cost, non-toxicity, and environmentally benign character. Various iron complexes have been incorporated into biological systems, with resulting low toxicity that is critical in the pharmaceutical and food industries. In addition, versatile iron-catalyzed organic transformations have been achieved over the past few decades. Several instructive and significant reviews have been published on this fascinating chemistry from various perspectives [17–22].

The current review focuses mainly on the evolution of iron-catalyzed CDC through C–H bond oxidation. Advances in other metal-mediated and metal-free CDC reactions have already been well documented and are beyond the scope of this work. In general, iron-catalyzed CDC results mainly in the formation of C–C, C–N, and C–O bonds. This review is structured around the hybridization of both of the C–H coupling partners. We hope that this paper provides a comprehensive overview of this topic, sheds light on new perspectives, and inspires chemists to work towards further improving and expanding the application of CDC.

## 2 Coupling of $C(sp^3)$ –H with $X(sp^3)$ –H

Iron-catalyzed direct C–H oxidation for the construction of C–C and C–X bonds ( $X=O, S, N, P, \text{etc.}$ ), with its remarkable potential for step efficiency, atom economy, and environmental sustainability, has emerged as one of the most significant tools in synthetic organic chemistry. Oxidative  $C(sp)$ –H and  $C(sp^2)$ –H cross-coupling for the formation of C–C bonds has garnered much attention and has seen great progress over the past decade. However, oxidative couplings involving  $C(sp^3)$ –H bonds remain challenging, given their low reactivity and lack of suitable coordination site for the iron catalyst. The following section will focus on advances in iron-catalyzed CDC reactions involving  $C(sp^3)$ –H bonds. These transformations are classified by the type of C–H bonds, including benzylic C–H bonds and C–H bonds adjacent to heteroatoms (Fig. 1).

The general reaction pathway of iron-catalyzed CDC is depicted in Fig. 2. The reaction with benzylic substrates proceeds as follows (Eq. 1): the initial hydrogen abstraction of the substrate by the oxidant generates the carbon radical **I**. Then **I** is further oxidized by the Fe catalyst through single-electron transfer (SET) to give the



**Fig. 1** General substrate types of C(sp<sup>3</sup>)-H bonds in CDC

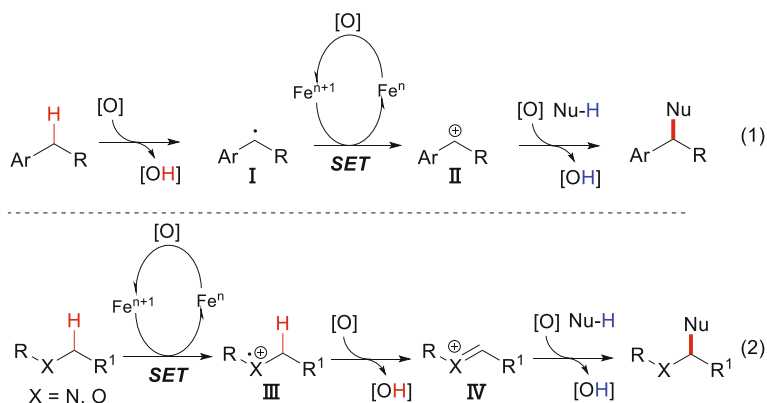


**Fig. 2** General reaction pathways of iron-catalyzed CDCs

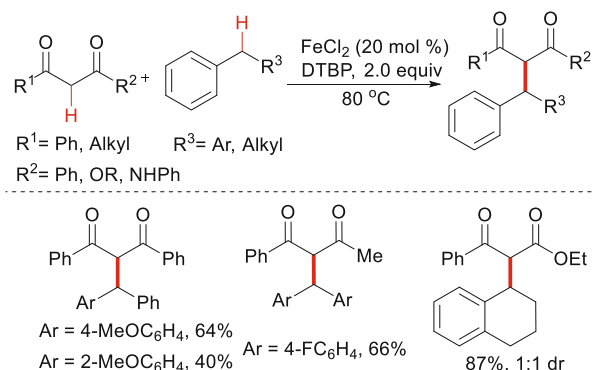
radical cation **II**, which is trapped by a nucleophile to give the final product. The process involving C(sp<sup>3</sup>)-H bonds adjacent to heteroatoms is also shown (Eq. 2). The Fe catalyst first oxidizes the substrate through SET to give the radical cation **III**. Then **III** is readily  $\alpha$ -deprotonated by the oxidant to generate a carbenium ion **IV**, which is trapped by a nucleophile to give the final product. In both cases, the deprotonation of Nu-H occurs either before or after being trapped, depending on the acidity of the Nu-H proton.

## 2.1 C-C Bond Formation

The formation of C-C bonds is an important area of research in modern organic synthesis, and a variety of critical contributions have been made over the past several decades [23–26]. Among the methods reported thus far, the direct oxidative coupling of C(sp<sup>3</sup>)-H bonds and other C-H bonds to construct C-C bond architecture is the most convenient.

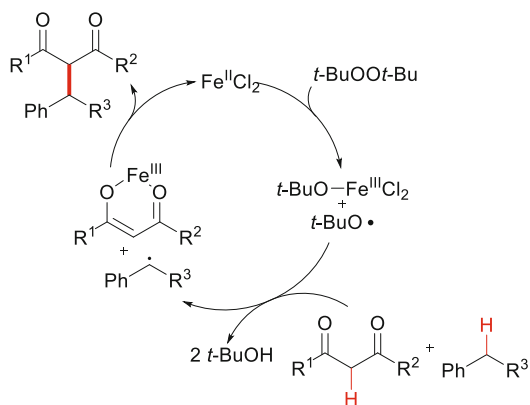
### 2.1.1 Benzylic C(sp<sup>3</sup>)-H Bond

In 2007, Li et al. reported the first instance of an iron-catalyzed CDC of a benzylic C-H bond with an active dicarbonyl methylene to form a new C(sp<sup>3</sup>)-C(sp<sup>3</sup>) bond (Scheme 1) [27]. Among various iron salts, FeCl<sub>2</sub> exhibited the highest efficacy, giving the desired products in good yields. Other transition-metal salts such as CuBr and CoCl<sub>2</sub> were far less efficient. The use of di-*tert*-butyl peroxide (DTBP) as an oxidant in place of *tert*-butyl hydroperoxide (TBHP) further increased the yield.



**Scheme 1**  $\text{FeCl}_2$ -catalyzed benzylic alkylation with dicarbonyl methylene

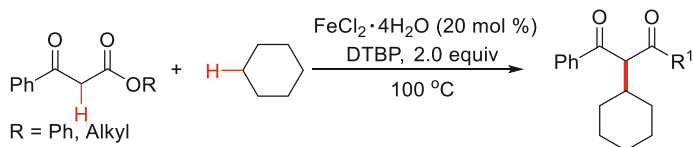
**Scheme 2** Proposed mechanism for  $\text{FeCl}_2$ -catalyzed benzylic alkylation



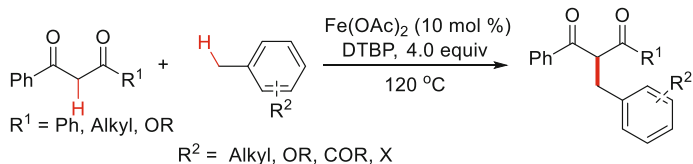
This transformation was applicable to both cyclic and acyclic benzylic compounds, and the electronic properties of substituents showed little influence on the reaction outcome.

The reaction mechanism is depicted in [Scheme 2](#). The homolytic cleavage of the peroxide bond of DTBP generates a *tert*-butoxyl radical, which abstracts one hydrogen atom from the benzyl substrate to form a benzylic radical. The iron(III) catalyst reacts with 1,3-dicarbonyls, leading to a chelate Fe-enolate complex, which then reacts with the benzylic radical to give the final product and regenerate the Fe(II). The reaction was also found to proceed efficiently at room temperature, and the coupling product was isolated in 80 % yield when the reaction time was extended.

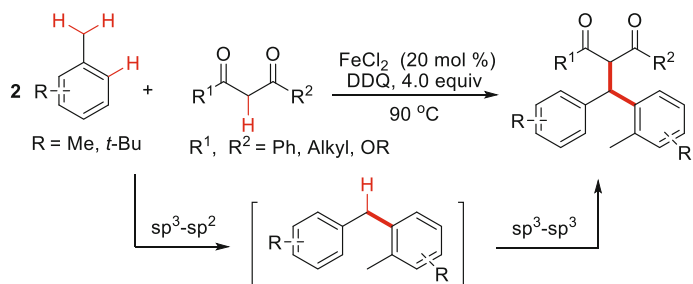
Li and Zhang further demonstrated an iron-catalyzed alkylation of activated 1,3-diketones with inactive cycloalkanes in the presence of DTBP ([Scheme 3](#)) [28]. In contrast to classical Fenton-type initiation, the active catalyst was considered as the chelate Fe-enolate complex formed from the  $\text{FeCl}_2$  and dicarbonyl compound.



**Scheme 3**  $\text{FeCl}_2 \cdot 4\text{H}_2\text{O}$ -catalyzed alkylation of activated 1,3-diketones with simple cycloalkanes



**Scheme 4**  $\text{Fe(OAc)}_2$ -catalyzed alkylation of toluene derivatives with 1,3-dicarbonyl compounds

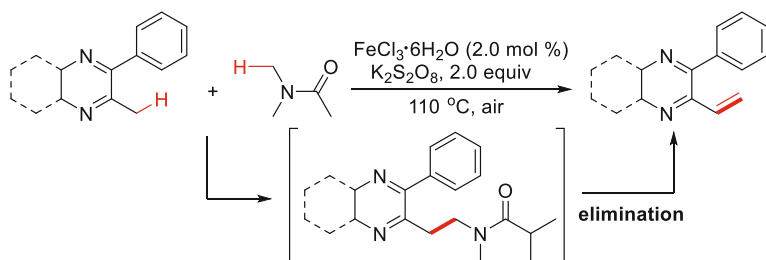


**Scheme 5**  $\text{FeCl}_2$ -catalyzed tandem CDC of toluene derivatives with 1,3-dicarbonyls

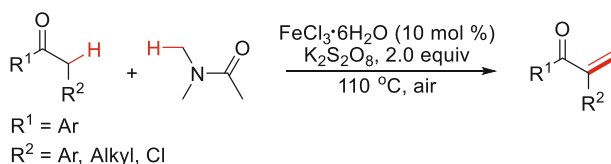
In 2012, Li et al. applied toluene derivatives to oxidative coupling reactions with 1,3-dicarbonyl compounds.  $\text{Fe(OAc)}_2$  was selected as the best catalyst and DTBP as the ideal oxidant (Scheme 4) [29]. Various toluene derivatives were efficiently coupled with 1,3-dicarbonyl compounds under optimized conditions. The mechanistic study suggested that the benzylic radical addition to the benzoyl methano-iron species may occur in the CDCs.

In 2014, Song et al. reported an iron-catalyzed tandem cross-dehydrogenative arylation of toluene derivatives with 1,3-dicarbonyl compounds using 2,3-Dichloro-5,6-dicyano-1,4-benzoquinone (DDQ) as oxidant (Scheme 5) [30]. This transformation afforded one new  $\text{C(sp}^3\text{)-C(sp}^2\text{)}$  bond and one new  $\text{C(sp}^3\text{)-C(sp}^3\text{)}$  bond in a one-pot protocol. The mechanistic study suggested that the process was initiated by homo-coupling of two aryl methane molecules to produce diaryl methylene intermediates, followed by CDC with 1,3-dicarbonyl compounds to give the final products.

In 2012, Xu et al. reported a novel iron-catalyzed vinylation of benzylic  $\text{C(sp}^3\text{)-H}$  bonds with *N,N*-dimethyl amides (Scheme 6) [31]. This reaction efficiently transferred one carbon atom in the *N*-methyl moiety of *N,N*-dimethylacetamide to



**Scheme 6**  $\text{FeCl}_3 \cdot 6\text{H}_2\text{O}$ -catalyzed vinylation of benzylic C–H bonds



**Scheme 7**  $\text{FeCl}_3 \cdot 6\text{H}_2\text{O}$ -catalyzed  $\alpha$ -methylenation of ketones

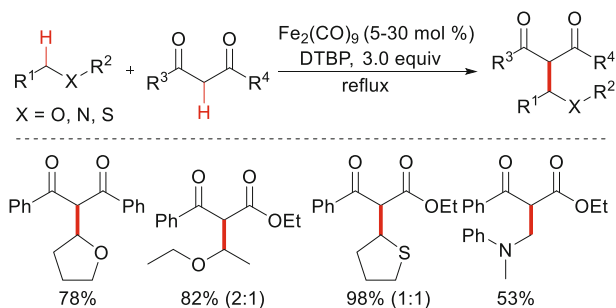
2-methyl aza-arenes. Mechanistic investigations indicated that the CDC between 2-methyl aza-arenes and *N,N*-dimethyl amides occurred preferentially, followed by elimination to generate vinylarenes. Independently, Wang et al. reported a similar Fe-catalyzed vinylation of 2-methylquinoline with *N,N*-dimethyl formamide in the presence of TBHP [32].

Li et al. also recently reported an iron-catalyzed  $\alpha$ -methylenation of ketones using *N,N*-dimethylacetamide as the one-carbon source (Scheme 7) [33]. Various ketones including aryl and alkyl ketones, enones, and dicarbonyl compounds were well tolerated and gave the corresponding  $\alpha,\beta$ -unsaturated carbonyls in moderate to excellent yields.

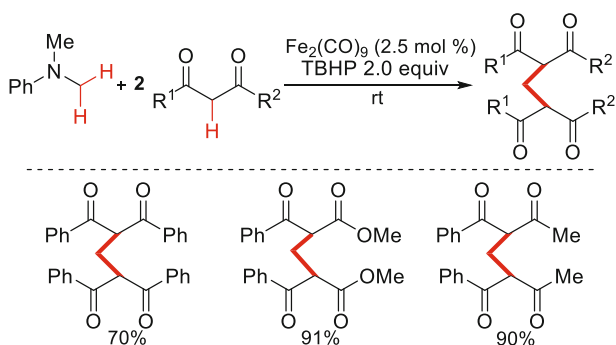
### 2.1.2 $C(\text{sp}^3)\text{--H}$ Bond Adjacent to Heteroatom

Direct functionalization of  $C(\text{sp}^3)\text{--H}$  bonds adjacent to heteroatoms is a highly desirable method for the derivation of heteroatom-containing compounds in organic synthesis. Inspired by the success of iron-catalyzed CDC with biphenyl-methane derivatives, Li et al. reported a general iron-catalyzed C–C bond formed by direct oxidation of  $\alpha\text{--C--H}$  bonds of ethers with 1,3-dicarbonyls (Scheme 8) [34]. Catalyst screening showed that  $\text{Fe}(\text{OAc})_2$ ,  $\text{FeCl}_2$ ,  $\text{FeBr}_2$ , and  $\text{Fe}_2(\text{CO})_9$  displayed almost identical catalytic efficiency, indicating the excellent redox capability of iron catalysis in this radical transformation. Under optimized conditions, both cyclic and linear ether derivatives reacted smoothly with 1,3-dicarbonyls to give the desired products in good yields. Sulfide and amine groups were also found to be suitable substrates in this iron-catalyzed C–H bond oxidative transformation.

Li et al. subsequently extended their work, using *N,N*-dimethylaniline as a substrate, and reported a novel dialkylation of the methylene group with 1,3-



**Scheme 8** Iron-catalyzed oxidative coupling of C–H bonds adjacent to heteroatoms with 1,3-dicarbonyls



**Scheme 9**  $Fe_2(CO)_9$ -catalyzed dialkylation of the methylene group with 1,3-dicarbonyls

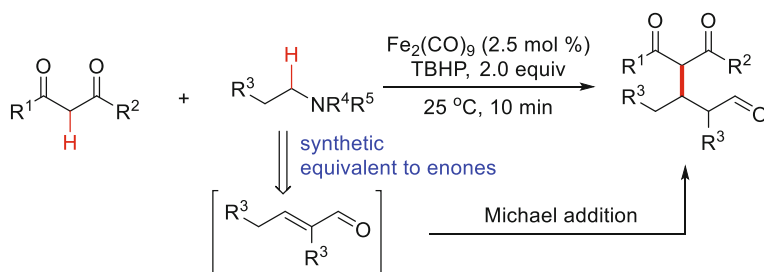
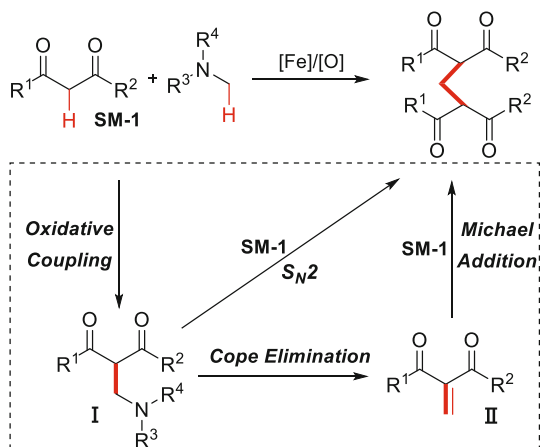
dicarbonyls (Scheme 9) [35]. In this transformation, *N,N*-dimethylaniline was used for the first time as the methylenic source, and a variety of methylene-bridged bis-1,3-dicarbonyls were constructed selectively and efficiently.

There are several possible pathways to account for this dialkylation reaction, as depicted in Scheme 10. Initially, the intermediate **I** was formed via the oxidative coupling of the substrates in the  $Fe_2(CO)_9/TBHP$  system. One possibility is that **I** undergoes a Cope elimination to give the intermediate **II**, followed by Michael addition with a second molecule of 1,3-dicarbonyl to generate the methylene-bridged bis-1,3-dicarbonyl product. Another possibility is that **I** undergoes an  $S_N2$  substitution by the second molecule of 1,3-dicarbonyl to afford the desired product. It is also possible that the reaction of 1,3-dicarbonyl with formaldehyde, which is generated in situ via iron-catalyzed oxidative *N*-demethylation, leads to the final product.

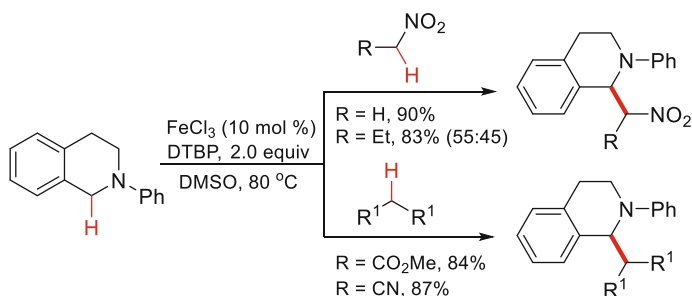
In addition to *N,N*-dimethylaniline acting as methylenic source, *N*-alkyl tertiary amines can be used as a synthetic equivalent of enones. In 2011, Li et al. reported an iron-catalyzed oxidative reaction between two molecules of *N*-alkyl tertiary amines and 1,3-dicarbonyls in a  $Fe_2(CO)_9/TBHP$  system (Scheme 11) [36]. The reaction was completed within 10 min at room temperature, and gave various  $\beta$ -1,3-dicarbonyl aldehydes in moderate to good yields. The authors proposed that two



**Scheme 10** Proposed pathways for  $\text{Fe}_2(\text{CO})_9$ -catalyzed dialkylation of the methylenes



**Scheme 11**  $\text{Fe}_2(\text{CO})_9$ -catalyzed oxidation of *N*-alkyl tertiary amines



**Scheme 12**  $\text{FeCl}_3$ -catalyzed coupling of tetrahydroisoquinolines with nitroalkanes and activated methylenes

molecules of tertiary amines are first condensed in the presence of TBHP, and the in situ-generated key intermediates  $\alpha,\beta$ -unsaturated aldehydes then undergoes Michael addition to give the final products.

Coupling of tetrahydroisoquinolines with nitroalkanes in the presence of  $\text{FeCl}_3/\text{DTBP}$  was reported by Hayashi and Shirakawa in 2011 (Scheme 12) [37]. This

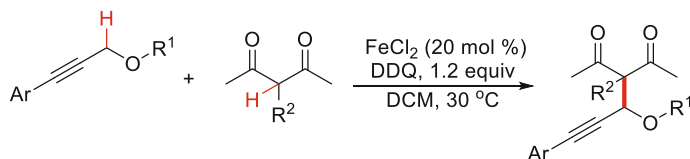
direct oxidative coupling provided various 1-nitroalkyl-substituted tetrahydroisoquinolines in high yields. In addition, activated methylene compounds were successfully utilized as nucleophiles.

A similar transformation was reported by Li et al. using magnetic  $\text{Fe}_3\text{O}_4$  or  $\text{CuFe}_2\text{O}_4$  nanoparticles as catalysts. Notably, the catalysts were easily recovered and reused for at least nine runs, with no loss of activity [38, 39]. In addition, in the work of Mancheño and Richter, the coupling of isochroman with 1,3-dicarbonyls was realized in the presence of catalytic amounts of iron(II) triflate and oxammonium salt of TEMPO as oxidant [40]. Zhang et al. reported an oxidative coupling of propargylic ethers with 1,3-dicarbonyls in the presence of  $\text{FeCl}_2/\text{DDQ}$ , affording various propargylated  $\beta$ -dicarbonyl compounds in moderate yields (Scheme 13) [41].

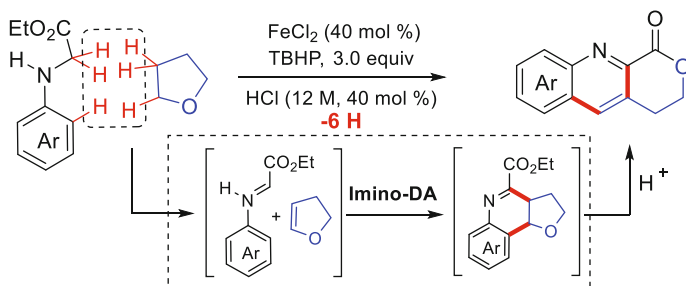
In 2015, Huo et al. reported a novel iron-catalyzed dual-oxidative dehydrogenative tandem annulation of glycine derivatives with tetrahydrofuran (THF) (Scheme 14) [42]. This transformation was performed under mild reaction conditions and afforded various quinoline-fused lactones in moderate yields. The authors proposed a possible reaction mechanism. Initially, glycine ester and THF are converted to aryl imine and DHF in the presence of  $\text{FeCl}_2/\text{TBHP}$ . An oxidative imino Diels–Alder reaction then occurs, generating the tetrahydro-quinazoline intermediate, which is isomerized to give the final product under acidic conditions.

## 2.2 C–N Bond Formation

Transition metal-catalyzed C–N bond formation has emerged as a powerful and efficient protocol for the synthesis of *N*-containing compounds. Tremendous



**Scheme 13**  $\text{FeCl}_2$ -catalyzed oxidative coupling of propargylic ethers with 1,3-dicarbonyls



**Scheme 14**  $\text{FeCl}_2$ -catalyzed dual-oxidative dehydrogenative tandem annulation of glycine derivatives with THF

contributions have been made in this field over the past few decades [43–45]—for example, Buchwald–Hartwig cross-coupling [46, 47], the Ullmann condensation [48, 49], and *N*-arylation of amide [50, 51]. However, because the pre-functionalization of starting materials is required, direct C–H bond amination is highly desirable and of great significance. For now, however, direct C–H bond amination via hetero-CDC remains challenging.

### 2.2.1 Benzylic C(sp<sup>3</sup>)–H Bond

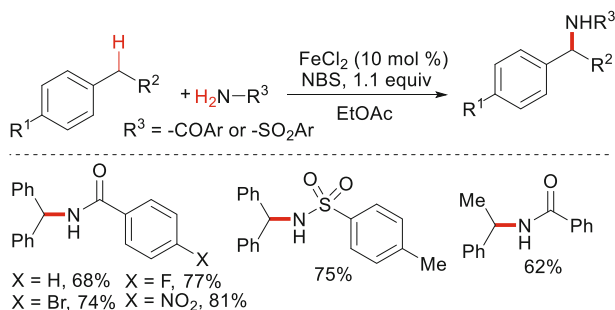
In 2008, Fu et al. reported the first instance of iron-catalyzed amidation of benzylic C(sp<sup>3</sup>)–H bonds by means of CDC (Scheme 15) [52]. This reaction was carried out in an efficient, cheap, and air-stable FeCl<sub>2</sub>/NBS catalyst/oxidant system. Carboxamides and sulfonamides were reacted with a series of benzylic reagents, respectively, under optimized conditions, and gave the corresponding products in moderate to good yields.

The amidation mechanism of FeCl<sub>2</sub>-catalyzed benzylic C(sp<sup>3</sup>)–H bonds is depicted in Scheme 16. The bromination of sulfonamide with NBS produces *N*-bromosulfonamide **I**, which then reacts with iron salt to give intermediate **II**. Subsequently, **II** is transferred into iron-nitrene complex **III**. The reaction of **III** with benzylic C–H bonds forms intermediate **IV**. Finally, removal of the iron salt provides the target product.

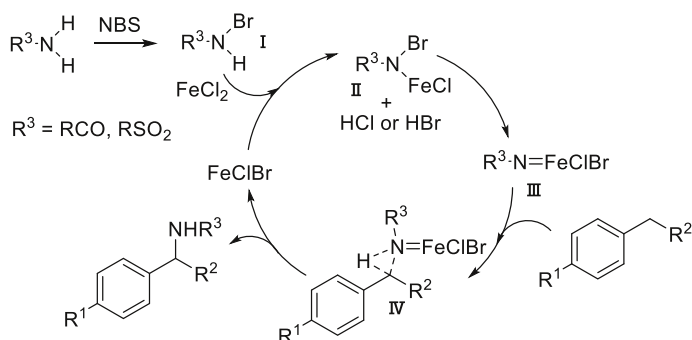
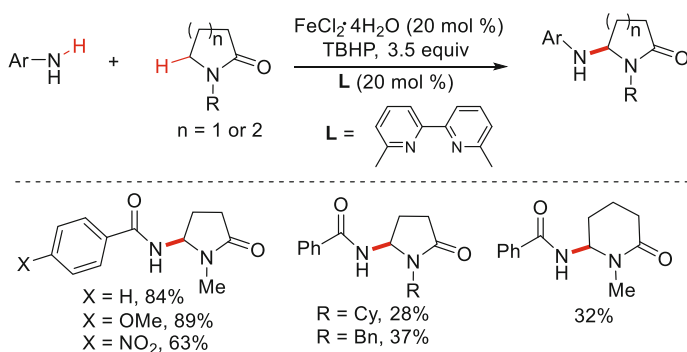
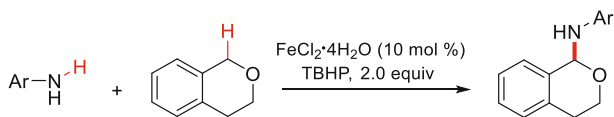
### 2.2.2 C(sp<sup>3</sup>)–H Bond Adjacent to Heteroatom

In 2012, Zhu et al. reported the direct amination of aryl amides with *N*-substituted pyrrolidin-2-ones in a Fe(II) complex/TBHP system (Scheme 17) [53]. The transformation was highly regioselective, and only the methylenic sp<sup>3</sup>C–H bond adjacent to the nitrogen was aminated. This facile method provided rapid access to the amination reaction of *N*-substituted pyrrolidin-2-ones in moderate to excellent yields. In 2014, Bao et al. reported a similar reaction under FeCl<sub>3</sub>/TBHP without a ligand [54].

In 2013, Yang et al. reported an iron-catalyzed direct C-1 amination of isochroman derivatives with anilines (Scheme 18) [55]. A variety of cyclic

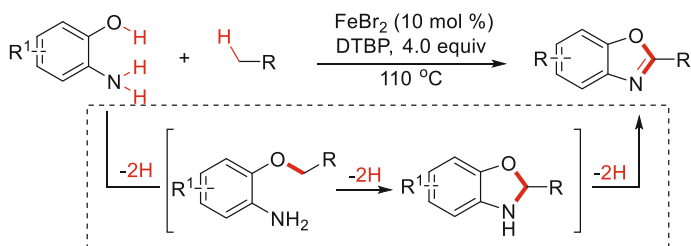


**Scheme 15** FeCl<sub>2</sub>-catalyzed benzylic C(sp<sup>3</sup>)–H bond amidation

**Scheme 16**  $FeCl_2$ -catalyzed benzylic  $C(sp^3)$ -H bond amidation**Scheme 17**  $FeCl_2 \cdot 4H_2O$ -catalyzed amination of *N*-substituted pyrrolidin-2-ones**Scheme 18**  $FeCl_2 \cdot 4H_2O$ -catalyzed amination of isochroman derivatives

hemiaminals were selectively obtained in good to excellent yields under mild conditions. The authors posited that the C-1 position is oxidized to the carbenium oxonium ion, which is subsequently trapped by the *N*-nucleophile.

Gu et al. further developed iron-catalyzed tandem oxidative cyclization of simple toluene derivatives with 2-aminophenols (**Scheme 19**) [56]. The reaction was carried out in a  $FeCl_2$ /DTBP system, and afforded a series of substituted benzoxazoles in a selective and efficient manner. In this transformation, the oxidative  $C(sp^3)$ -H/O-H coupling of 2-aminophenols with toluene occurred first, followed by an oxidative  $C(sp^3)$ -H/N-H cyclization and aromatization. Six protons were removed in a one-pot procedure.



**Scheme 19** FeBr<sub>2</sub>-catalyzed tandem oxidative cyclization

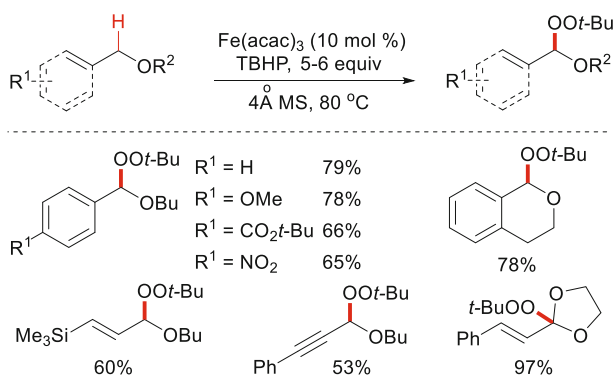
## 2.3 C–O Bond Formation

The direct esterification and etherification of C–H has attracted much attention over the past few years. The process involves the oxidative coupling of commercial starting materials, and offers high step efficiency and atom economy. Several transition-metal catalysts, including palladium, rhodium, platinum, and copper, have been developed for this C–H oxidative functionalization [57–59].

### 2.3.1 Benzylic C(sp<sup>3</sup>)–H Bond

In 2012, Urabe et al. reported an iron-catalyzed C–H bond oxygenation for the synthesis of *tert*-butyl peroxyacetals (Scheme 20) [60]. With this method, a series of olefinic and acetylenic *tert*-butyl peroxyacetals, and also unsaturated peroxy orthoesters were synthesized in good to excellent yields.

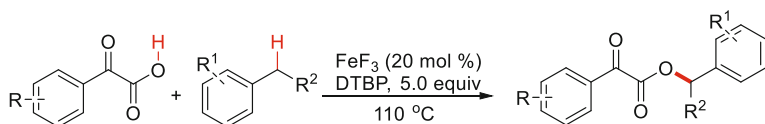
A pathway was proposed for the formation of *tert*-butyl peroxyacetals (Scheme 21) as follows: The hydrogen abstraction from ether forms the benzyl radical, which is transmitted to benzyl cation stabilized by an oxygen atom under iron catalysis. The subsequent nucleophilic attack by *t*-BuOOH generates the final product.



**Scheme 20** Fe(acac)<sub>3</sub>-catalyzed synthesis of *tert*-butyl peroxyacetals



**Scheme 21** Proposed mechanism for the formation of *tert*-butyl peroxyacetals



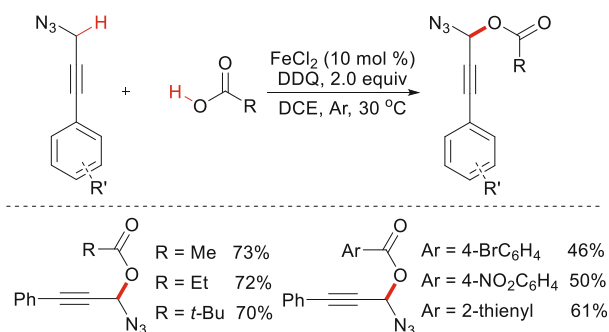
**Scheme 22** FeF<sub>3</sub>-catalyzed esterification of a benzylic C–H bond

A benzyl cation generated by the oxidation of a benzyl C–H bond was trapped by carboxylic acid to give an ester (**Scheme 22**) [61]. This transformation was carried out using benzyl derivatives and benzoylformic acids as the substrates in a FeF<sub>3</sub>/DTBP system, thus providing straightforward access to various  $\alpha$ -keto benzyl esters. Mechanistically, the nucleophilic attack of benzoylformic acid on the benzyl cation accounts for the generation of the desired ester.

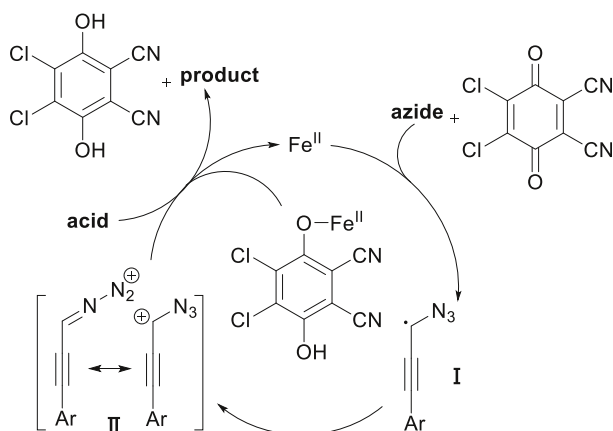
### 2.3.2 Propargylic C(sp<sup>3</sup>)–H Bond

In 2012, Jiao et al. reported an oxidative dehydrogenative coupling of aryl propargyl azides with carboxylic acids in a FeCl<sub>2</sub>/DDQ system (**Scheme 23**) [62]. The azides were prepared in situ from NaN<sub>3</sub> and the corresponding chlorides. The authors found that although the homologous chloride had a structure similar to azide, it lacked an azido group, and did not afford the desired C–O coupling product. This result suggests that the azido group acted as an assisting group to facilitate this C(sp<sup>3</sup>)–H functionalization. The obtained acyloxylated propargyl azides were further transformed to 4,5-disubstituted-1,2,3-triazoles, 3-alkoxyenals, and benzotriazoles.

The tentative reaction mechanism is proposed in **Scheme 24**. Initially, azide undergoes hydrogen abstraction through an iron-facilitated single-electron oxidation with DDQ to form the radical species **I**, which may be stabilized by the azido group.

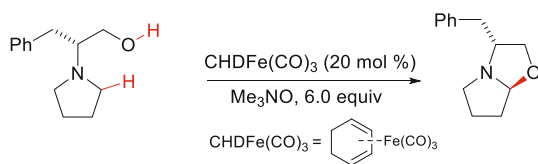


**Scheme 23** FeCl<sub>2</sub>-catalyzed CDC of aryl propargyl azides with carboxylic acids



**Scheme 24** Proposed mechanism of  $\text{FeCl}_2$ -catalyzed oxidative dehydrogenative C–O bond formation

**Scheme 25**  $\text{CHDFe}(\text{CO})_3$ -catalyzed stereoselective oxidation of chiral 2-pyrrolidino-1-ethanols



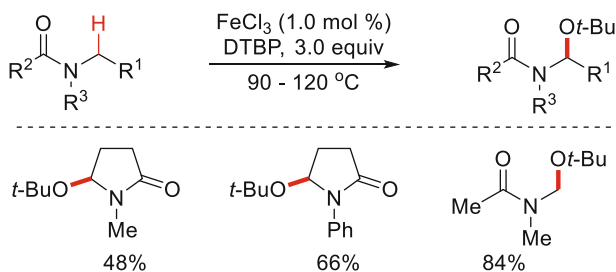
Subsequently, the radical species **I** is further oxidized to give the aryl propargyl cation **II**. The nucleophilic attack of cation **II** by carboxylic acid then gives the desired product with regeneration of the catalyst.

### 2.3.3 $C(\text{sp}^3)\text{--H}$ Bond Adjacent to Heteroatom

In 2005, Pearson and Kwak reported an iron-catalyzed stereoselective oxidation of chiral 2-pyrrolidino-1-ethanol derivatives to oxazopyrrolidines (**Scheme 25**) [63]. This transformation employed tricarbonyl(cyclohexadiene)iron complex as catalyst and trimethylamine *N*-oxide ( $\text{Me}_3\text{NO}$ ) as oxidant. It was believed that  $\text{Me}_3\text{NO}$  could be used for the removal of CO ligands from metal carbonyls and the demetallation of diene– $\text{Fe}(\text{CO})_3$  complexes. Although the detailed mechanism of this process is unclear, it was assumed that the actual oxidant coordinates to the –OH group, and the amine oxidation reaction occurs intramolecularly. The –OH group reacts with the iminium intermediate to form the oxazolidine ring.

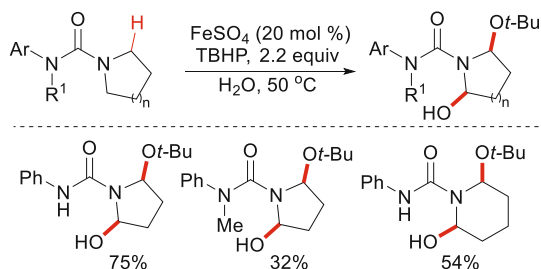
In 2011, Hiyashi et al. reported an  $\text{FeCl}_3$ -catalyzed oxidation of alkylamides to  $\alpha$ -(*tert*-butoxy) alkylamides with DTBP [64]. The authors proposed that the acyliminium salt, which is generated under a  $\text{FeCl}_3/\text{DTBP}$  system, reacts with *t*-BuOH to give the desired  $\alpha$ -(*tert*-butoxy) alkylamide (**Scheme 26**).

Around the same time, Liang et al. reported a similar C–O bond formation by iron(II)-catalyzed oxidation of  $C(\text{sp}^3)\text{--H}$  bonds adjacent to a nitrogen atom of unprotected arylureas with TBHP in water (**Scheme 27**) [65]. This method enabled



**Scheme 26** FeCl<sub>3</sub>-catalyzed oxidation of alkylamides to  $\alpha$ -(*tert*-butoxy) alkylamides

**Scheme 27** FeSO<sub>4</sub>-catalyzed oxygenation of C(sp<sup>3</sup>)-H bonds in aryl ureas



the efficient simultaneous dioxygenation of both  $\alpha$ -positions to the nitrogen atom, providing various *tert*-butoxylated and hydroxylated arylureas in good yields.

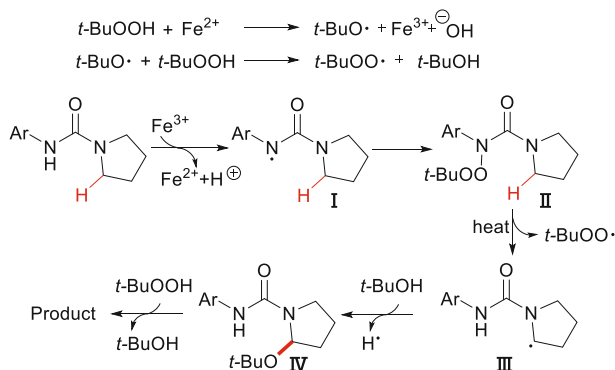
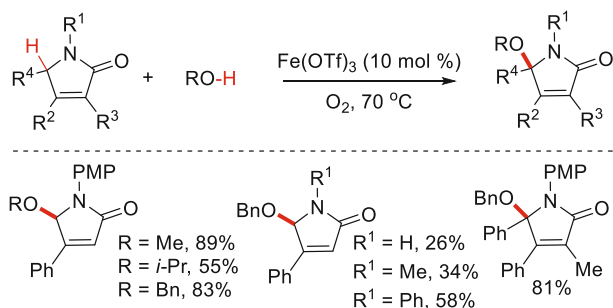
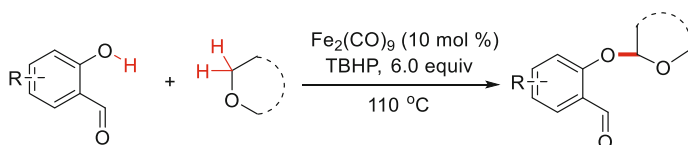
A possible mechanism is proposed in [Scheme 28](#). Initially, TBHP decomposes into a *tert*-butoxyl radical in the presence of FeSO<sub>4</sub>, which further gives a *tert*-butyl peroxy radical. The resulting peroxy radical reacts with aminyl radical **I** derived from the oxidation of the arylurea to form the unstable *N*-(*tert*-butylperoxy)urea **II**. The elimination of the *tert*-butylperoxy radical then generates a new carbon radical **III** via 1,4-hydrogen radical transfer, which is trapped by *tert*-butanol to give a  $\alpha$ -*tert*-butoxylated urea **IV** and regenerates TBHP. Finally, a hydroxyl group is introduced to the other  $\alpha$ -position of **IV** via hydrogen abstraction by TBHP, releasing the final product.

Tang et al. recently reported an efficient and practical method of iron catalysis for the functionalization of pyrrolones with alcohols ([Scheme 29](#)) [66]. This transformation was carried out under mild conditions using Fe(OTf)<sub>3</sub> as the catalyst and O<sub>2</sub> as the oxidant. The authors proposed that the aerobic oxidation of pyrrolones catalyzed by Fe(OTf)<sub>3</sub> forms the reactive *N*-acyliminium ion intermediates, which undergo nucleophilic additions with alcohols to give the corresponding products.

In 2014, Chang and Wang reported an iron-catalyzed oxidative coupling of salicyl-aldehydes with cyclic ethers through the direct  $\alpha$ -C-H functionalization of ethers. This transformation produced the corresponding acetals in moderate to excellent yields in the presence of a labile aldehyde group ([Scheme 30](#)) [67].

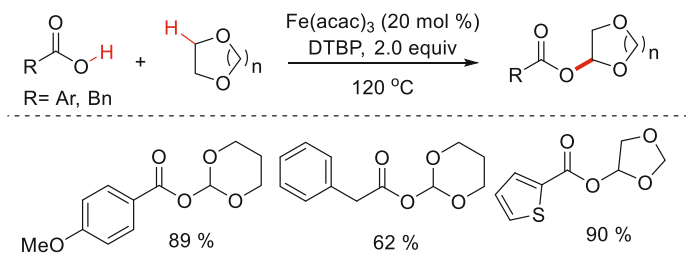
In 2014, Han et al. reported an iron-catalyzed oxidative CDC esterification of C-H bonds in cyclic ethers with carboxylic acids ([Scheme 31](#)) [68]. In this transformation, aromatic acid and phenylacetic acid were identified as



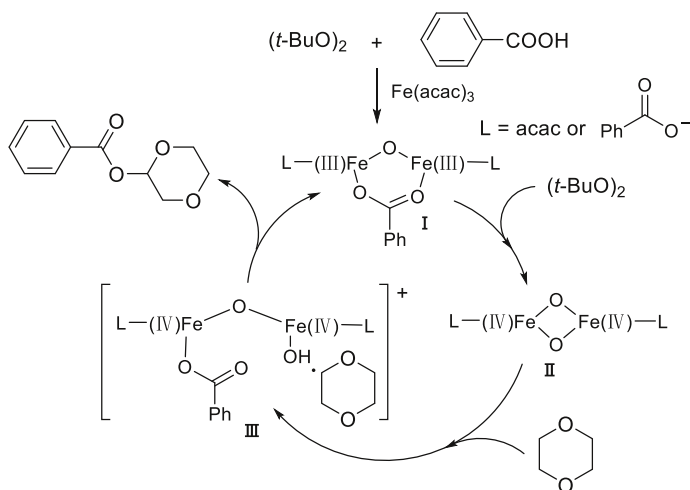
**Scheme 28** Proposed mechanism**Scheme 29**  $\text{Fe}(\text{OTf})_3$ -catalyzed oxidative coupling of pyrrolones with alcohols**Scheme 30**  $\text{Fe}_2(\text{CO})_9$ -catalyzed oxidative coupling of salicyl-aldehydes with cyclic ethers

suitable substrates and reacted with various cyclic ethers to give the desired  $\alpha$ -acyloxy ethers. This oxidative esterification exhibited excellent regioselectivity. When non-equivalent ether such as 1,3-dioxolane was tested, only the methylenic C–H bond adjacent to one oxygen atom was selectively esterified. However, the decarboxylative alkenylation of cyclic ether occurred when cinnamic acid was used as the substrate under the same conditions.

The proposed mechanism is depicted in [Scheme 32](#). A  $\mu$ -oxo,  $\mu$ -carboxylate diiron(III) intermediate **I** is initially generated upon the reaction of the iron catalyst, carboxylic acid, and the oxidant, which is further oxidized to give the Fe(IV)



**Scheme 31** Fe(acac)<sub>3</sub>-catalyzed direct C–O bond formation



**Scheme 32** Proposed mechanism

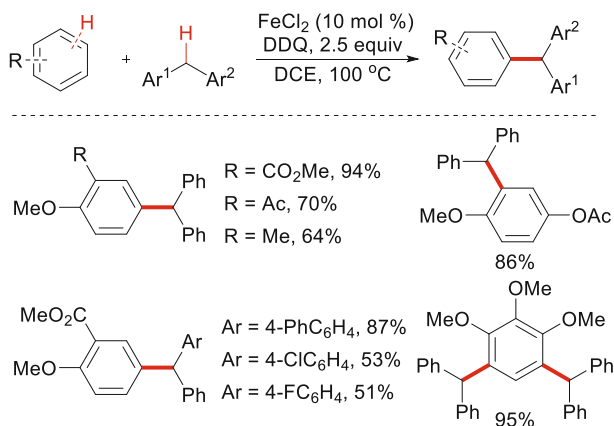
intermediate **II**. Intermediate **II** then reacts with a cyclic ether to generate intermediate **III**, which undergoes a cross-coupling process to give the desired product and active catalyst Fe(III) intermediate **I**. Additional intermolecular competing kinetic isotope effect (KIE) experiments were carried out and indicated that C(sp<sup>3</sup>)–H bond cleavage may be involved in the rate-determining step.

### 3 Coupling of C(sp<sup>3</sup>)–H with X(sp<sup>2</sup>)–H

#### 3.1 C–C Bond Formation

##### 3.1.1 Benzylic C(sp<sup>3</sup>)–H Bond

In 2009, Shi et al. reported for the first time the cross-dehydrogenative arylation (CDA) of benzylic C–H bonds with electron-rich arenes in a FeCl<sub>2</sub>/DDQ system (**Scheme 33**) [69]. A variety of electron-rich arenes and various diarylmethanes



**Scheme 33**  $\text{FeCl}_2$ -catalyzed CDA of aryl C–H bonds with benzylic C–H bonds

were found to be suitable substrates for this transformation, giving the desired products in good yields with excellent regioselectivity. Notably, increasing the electron density of the arenes was shown to improve yields, which is consistent with their nucleophilicity, thus suggesting a Friedel–Crafts-type reaction feature. With the more electron-rich arenes such as 1,2,3-trimethoxybenzene, a double-CDA product was obtained with high efficiency.

Mechanistically, this reaction is initiated by the iron-assisted SET oxidation to generate the benzyl radical, which may be further oxidized to the benzyl cation. Subsequent Friedel–Crafts-type alkylation, followed by abstraction of the proton by the reduced hydroquinone, delivers the desired product and regenerates the catalyst (Scheme 34). A large intramolecular kinetic isotopic effect ( $k_{\text{H}}/k_{\text{D}} = 6.0$ ) is also observed, indicating that the cleavage of the benzylic C–H bond is involved in the rate-determining step.

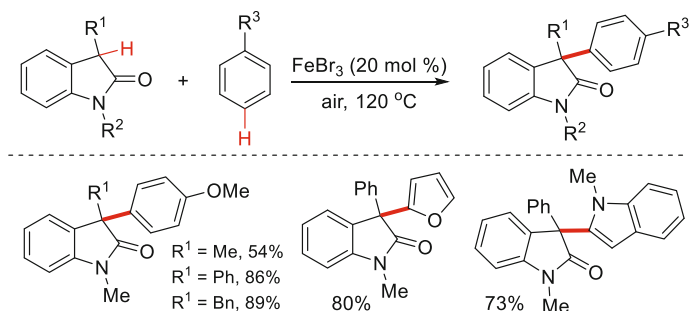
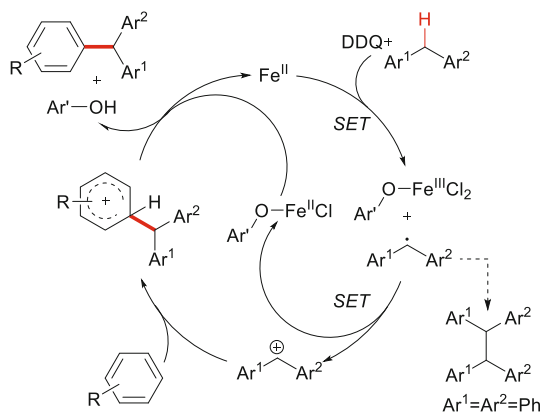
In 2015, Li et al. reported a similar  $\text{FeBr}_3$ -catalyzed CDA of 3-substituted oxindoles with electron-rich aromatic and heteroaromatic compounds (Scheme 35) [70]. This transformation was carried out under an air atmosphere and gave various 3,3'-disubstituted oxindoles in moderate to good yields.

### 3.1.2 $\text{C}(\text{sp}^3)\text{-H}$ Bond Adjacent to Heteroatom

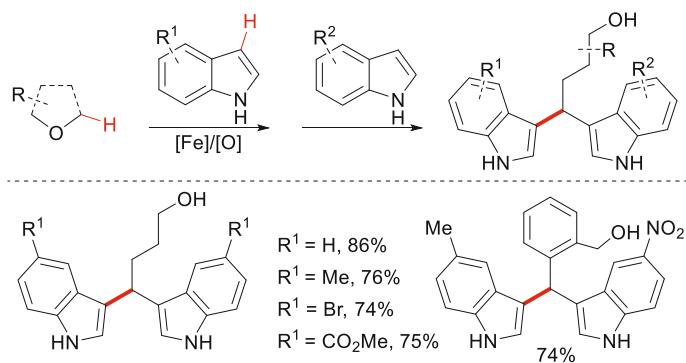
In 2009, Li et al. reported a CDC reaction of C–H bonds adjacent to an oxygen atom with indole derivatives in a  $\text{FeCl}_2/\text{DTBP}$  system. The reaction proceeded via tandem C–H bond oxidative coupling and C–O bond cleavage (Scheme 36) [71].

Mechanistically (Scheme 37), the indole-ether adduct, which is generated in situ via C–H oxidation, reacts efficiently with another molecule of electron-rich indole to deliver 1,1-biaryl products via Friedel–Crafts alkylation. Notably, when electron-poor 4-nitroindole was applied to react with isochroman, the mono-indolation product was selectively obtained. The results indicated that the first indolation step was easy and was less influenced by the electronic properties of indoles, while the

**Scheme 34** Proposed mechanism of FeCl<sub>2</sub>-catalyzed CDA



**Scheme 35** FeBr<sub>3</sub>-catalyzed CDA of 3-substituted oxindoles with arenes

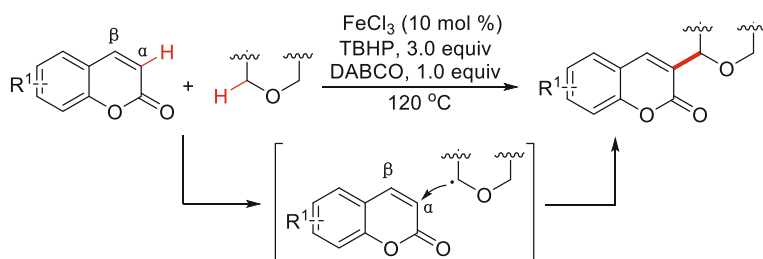
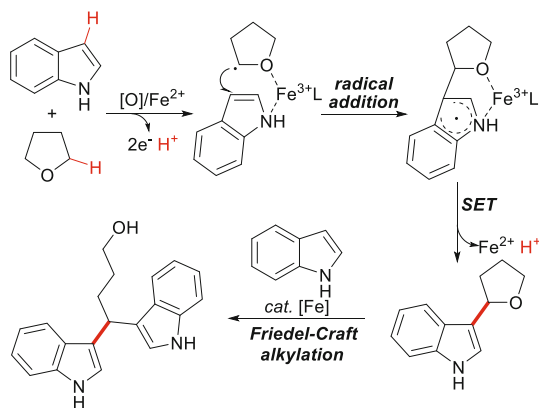


**Scheme 36** FeCl<sub>2</sub>-catalyzed tandem C-H bond oxidative coupling and C-O bond cleavage

second indolation step was the rate-determining step, and proceeded efficiently only with electron-rich indoles, which agrees with Friedel-Crafts aromatic alkylation.

Coumarins are valuable natural product classes in drug discovery, with carbonyl-conjugated olefin functions in their structures. In 2015, Ge and Zhou reported an

**Scheme 37** Proposed mechanism of FeCl<sub>2</sub>-catalyzed synthesis of 1,1-bis-indolylmethanes

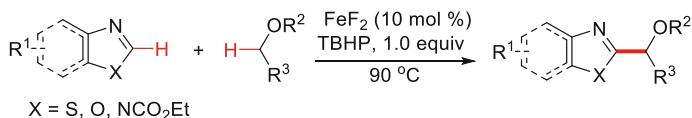
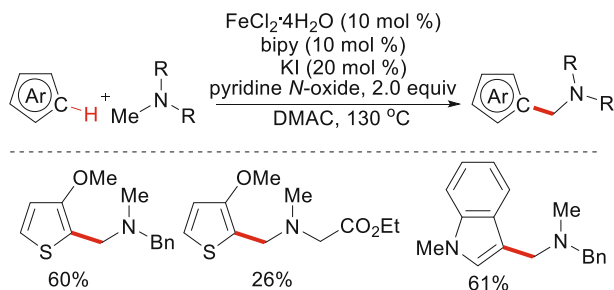
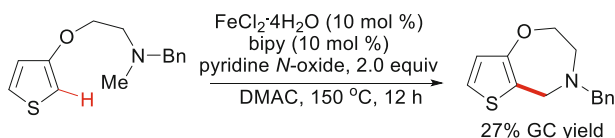


**Scheme 38** FeCl<sub>3</sub>-catalyzed CDC of coumarins with ethers

iron-catalyzed CDC of coumarins with ethers via C(sp<sup>3</sup>)-H oxidation (**Scheme 38**) [72]. This reaction was highly regioselective, and the ether substrates were bound to the more electron-rich  $\alpha$ -position of the coumarin esters. The authors posited that the nucleophilic ether radical attacks the  $\alpha$ -position of coumarin's olefin moiety to generate a more stable radical intermediate, and thus the  $\alpha$ -ether-substituted coumarin derivatives are obtained in a regioselective manner.

In 2015, Correa et al. reported an iron-catalyzed  $\alpha$ -arylation of ethers with azoles (**Scheme 39**) [73]. This practical oxidative method allowed the efficient C<sub>2</sub>-alkylation of a variety of (benzo)azoles, which constituted straightforward access to heterocycles of the utmost medicinal significance. The experiments and DFT calculations revealed that FeF<sub>2</sub> plays a key redox role in assisting both the heterolytic cleavage of the oxidant and the oxidation of the carbon radical to the oxonium ion.

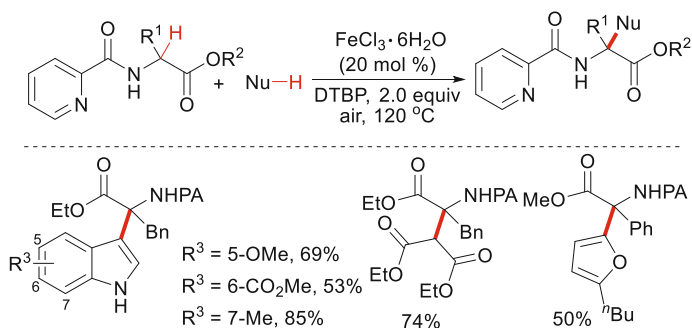
As amines are known to undergo oxidation to form iminium ion intermediates, this process can be utilized in oxidative coupling reactions. In 2009, Itami and Wünsh reported an iron-catalyzed oxidative coupling of heteroarenes with *N*-methyl amines in a FeCl<sub>2</sub>·4H<sub>2</sub>O/pyridine *N*-oxide system (**Scheme 40**) [74]. The oxidative coupling reaction was successfully applied to the intermolecular coupling of thiophenes, furans, and indoles with methylamines. Notably, this reaction took place

**Scheme 39** FeF<sub>2</sub>-catalyzed direct  $\alpha$ -arylation of ethers with azoles**Scheme 40** FeCl<sub>2</sub>·4H<sub>2</sub>O-catalyzed oxidative coupling of heteroarenes with *N*-methyl amines**Scheme 41** Intramolecular oxidative coupling for constructing benzazepine-like bicyclic nitrogen heterocycle

predominantly at *N*-methyl C–H bonds though other reactive bonds, including the more acidic benzylic C–H and the C–H bond to the carbonyl group.

The authors also applied this protocol to intramolecular oxidative coupling, and a benzazepine-like bicyclic nitrogen heterocycle was formed, albeit in 27 % GC yield (Scheme 41). The low efficiency may arise from the general difficulty in achieving cyclization of a seven-membered ring. The obtained product showed good binding affinity and selectivity towards the  $\sigma$ 1,  $\sigma$ 2, and NMDA receptors.

In 2013, You et al. reported an efficient iron-catalyzed oxidative coupling of *N*-(pyridin-2-ylcarbonyl)-substituted  $\alpha$ -amino acid derivatives with indoles (Scheme 42) [75]. The high efficiency and ready elimination made 2-pyridinecarbonyl an ideal candidate for the *N*-protecting group. Other activating substituents at the amino group, such as imidazol-2-ylcarbonyl, 2-quinolin-2-ylcarbonyl, isoquinoline-1-ylcarbonyl, and pyrimidin-2-ylcarbonyl groups, were found to be less efficient, and non-nitrogen-containing substituents were inactive. This C–H/C–H cross-coupling was highly tolerant of various synthetically valuable functional groups on both  $\alpha$ -amino acids and nucleophiles, and delivered a series of  $\alpha$ -quaternary  $\alpha$ -amino acid derivatives in good yields.

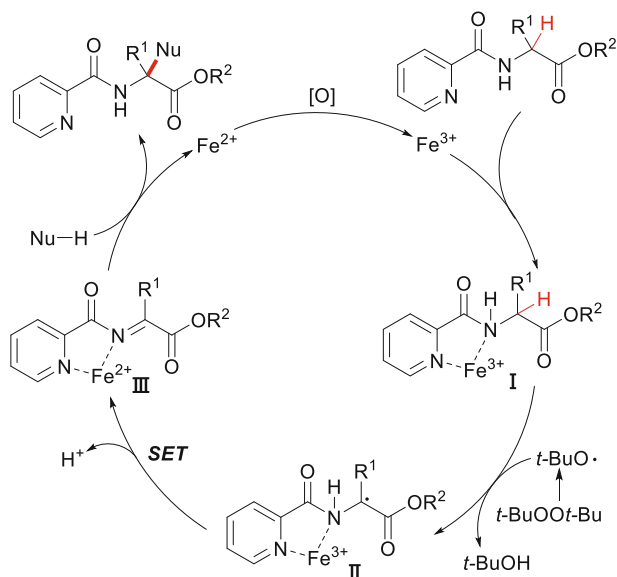


**Scheme 42**  $\text{FeCl}_3 \cdot 6\text{H}_2\text{O}$ -catalyzed oxidative coupling of  $\alpha\text{-C}(\text{sp}^3)\text{-H}$  bonds of  $\alpha$ -tertiary  $\alpha$ -amino acid esters

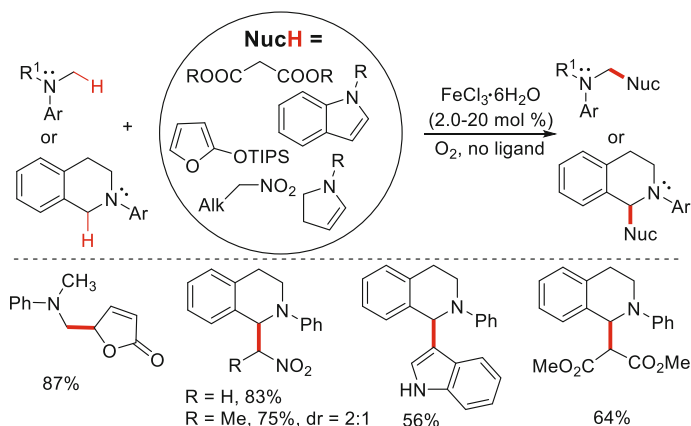
Mechanistically (Scheme 43), the 2-picolinamido  $\alpha$ -tertiary amino acid ester coordinates with  $\text{Fe}^{\text{III}}$  to yield the intermediate **I**. The *tert*-butoxyl radical (*t*-BuO $\cdot$ ) generated from DTBP then abstracts the  $\alpha$ -hydrogen atom of **I** to form the radical intermediate **II**. Subsequently, the radical species **II** undergoes an intramolecular single-electron transfer (SET) to give the  $\alpha$ -ketimine intermediate **III**. The coordination of the picolin-amido group with  $\text{Fe}^{3+}$  species activates the  $\alpha$ -ketimine and facilitates the addition of the nucleophile to give the desired  $\alpha$ -quaternary  $\alpha$ -amino acid ester product. The model reaction was performed under an  $\text{N}_2$  atmosphere, and the desired product was obtained in only 39 % yield. This suggests that the released  $\text{Fe}^{2+}$  is reoxidized to  $\text{Fe}^{3+}$  by air as well as DTBP to fulfil the catalytic cycle.

In 2013, Doyle et al. reported an iron-catalyzed aerobic C–H functionalization of tertiary anilines with tetrahydroisoquinolines (Scheme 44) [76]. The oxidative protocol allowed facile functionalization of an aliphatic C–H bond in *N,N*-dialkylanilines with siloxyfuran, nitroalkanes, and other nucleophiles using a cheap  $\text{FeCl}_3$  catalyst and a green  $\text{O}_2$  oxidant. Interestingly, when nitroalkane was utilized as the coupling partner, the addition of 1.0 equiv of weak acid such as 1,1,1,3,3,3-hexafluoro-2-propanol (HFIP) strongly promoted the oxidative aza-Henry reaction. The authors proposed that the oxidation of tertiary anilines under a  $\text{Fe}(\text{III})/\text{O}_2$  system forms reactive iminium ion intermediates, which undergo Mannich reactions with various nucleophiles to give the corresponding products.

The detailed mechanism for this oxidative Mannich reaction is depicted in Scheme 45. The initial step is the electron transfer between ferric chloride and amine to produce radical cation and iron(II) chloride. This process is compatible with the potentials of the  $\text{Fe}(\text{III})/\text{Fe}(\text{II})$  (+0.77 V vs NHE) and amine/radical cation redox pairs (+0.79 V/+1.08 V vs NHE). One hydrogen atom abstraction from the radical cation then produces the iminium ion through iron(II)-bound dioxygen. The resulting peroxo species then enters Haber–Weiss or Fenton-like chemistry to complete the process. The requirement of weak acid in the aza-Henry reaction is proposed to inhibit the coordination of iron(III) with the amine reactant or to activate the nitroalkane.



**Scheme 43** Possible mechanism of the  $\alpha$ -C( $sp^3$ )-H bond oxidation of  $\alpha$ -substituted  $\alpha$ -amino acid esters



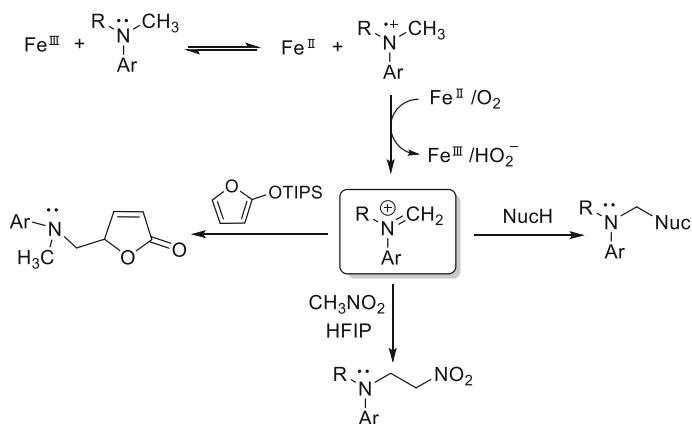
**Scheme 44**  $FeCl_3$ -catalyzed aerobic C-H functionalization of tertiary anilines with tetrahydroisoquinolines

## 3.2 C-N Bond Formation

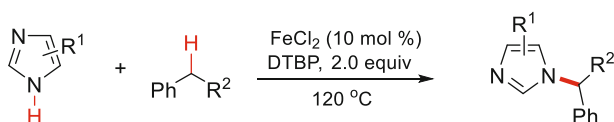
### 3.2.1 Benzylic C( $sp^3$ )-H Bond

In 2011, Chen and Qiu reported an iron-catalyzed C-N bond formation between imidazoles and benzylic hydrocarbons (**Scheme 46**) [77]. The direct amidation of the benzylic C( $sp^3$ )-H bonds is an important method for the synthesis of valuable





**Scheme 45** Possible reaction mechanism



**Scheme 46**  $\text{FeCl}_2$ -catalyzed direct C-N coupling of imidazoles and benzylic compounds

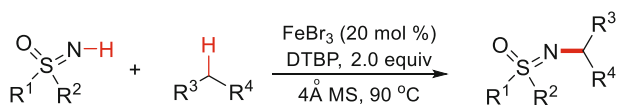
nitrogen-containing compounds without the need for a pre-functionalized starting material. The nucleophilic addition reaction of imidazole with benzyl cation delivered the desired product. In 2012, Chen et al. reported a similar transformation [78].

In 2014, Bolm et al. reported an efficient iron-catalyzed C-N bond formation by hetero-CDC between sulfoximines and diarylmethanes. This transformation provided a new strategy for the synthesis of *N*-alkylated sulfoximines with  $\alpha$ -branched substituents (Scheme 47) [79].

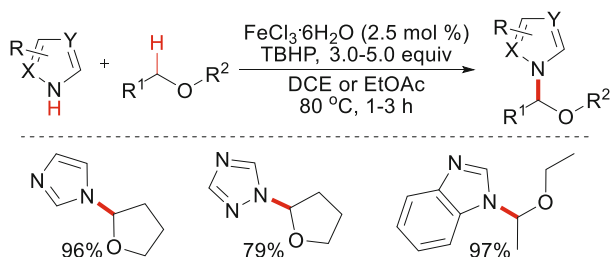
### 3.2.2 $C(\text{sp}^3)$ -H Bond Adjacent to Heteroatom

In 2010, Li et al. reported an iron-catalyzed *N*-alkylation of azoles via oxidation of a  $C(\text{sp}^3)$ -H bond adjacent to an oxygen atom under neutral conditions (Scheme 48) [80]. A wide variety of azoles and ethers were selectively transformed into the corresponding oxidative coupling products in good to excellent yields. In 2015, Wang and He reported a similar transformation using aryl tetrazoles as the coupling partner [81].

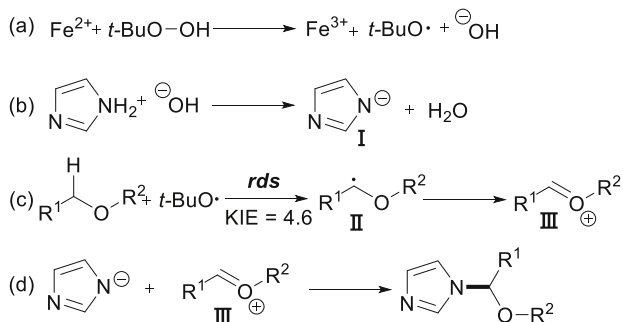
The proposed mechanism is shown in Scheme 49. Initially, TBHP decomposes into a *tert*-butoxyl radical and hydroxyl anion in the presence of the iron catalyst (step a). Deprotonation of the azole gives the anion species **I** (step b). Meanwhile, a hydrogen abstraction from the C-H bond adjacent to an oxygen atom affords **II**, which can be trapped by TEMPO, followed by ferric oxidation to generate oxonium



**Scheme 47** FeBr<sub>3</sub>-catalyzed hetero-CDC between sulfoximines and diarylmethanes



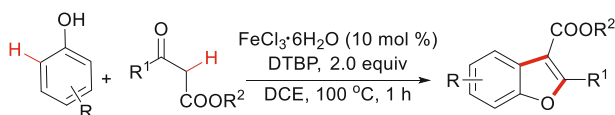
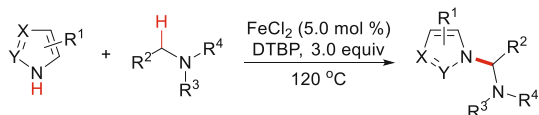
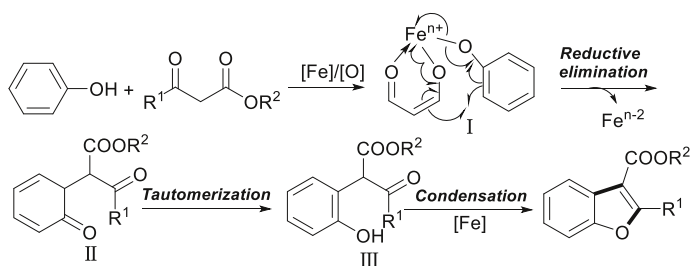
**Scheme 48** FeCl<sub>3</sub>·6H<sub>2</sub>O-catalyzed *N*-alkylation of azoles



**Scheme 49** Plausible pathway for FeCl<sub>3</sub>·6H<sub>2</sub>O-catalyzed *N*-alkylation of azoles

ion **III** (step c). Finally, the nucleophilic addition of **I** to **III** provides the desired coupling product (step d). A competition experiment was carried out to investigate the electronic properties of azoles in this reaction. The results indicated that the reactivity of azoles is related to the nucleophilicity of the conjugate bases of azoles rather than their acidity, which agrees with the nucleophilic reaction. Moreover, a large isotopic effect ( $k_{\text{H}}/k_{\text{D}} = 4.0 \pm 0.1$ ) indicates that the cleavage of the  $\alpha$ -C–H bond of ether is involved in the rate-determining step.

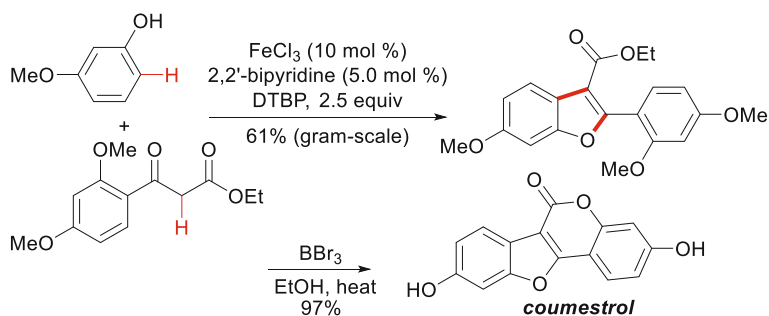
In 2012, Chen et al. reported the *N*-alkylation of azoles via oxidative cleavage of a C(sp<sup>3</sup>)–H bond adjacent to the *N*-atom of amides and sulfonamides (Scheme 50) [82]. This method efficiently and selectively provided a variety of azole derivatives, which are fundamental structural motifs in *N*-heterocyclic carbenes (NHC) and ionic liquids. A similar transformation was reported by Reddy et al. in 2015 [83].

**Scheme 50** FeCl<sub>2</sub>-catalyzed *N*-alkylation of azoles**Scheme 51** FeCl<sub>3</sub>·6H<sub>2</sub>O-catalyzed tandem oxidative coupling and annulation between phenols and  $\beta$ -keto esters**Scheme 52** Tentative mechanism of FeCl<sub>3</sub>·6H<sub>2</sub>O-catalyzed oxidative reaction of phenols and  $\beta$ -keto esters

### 3.3 C–O Bond Formation

In 2009, Li et al. reported a breakthrough in the construction of polysubstituted benzofurans via iron-catalyzed tandem oxidative coupling and annulation between phenols and  $\beta$ -keto esters (Scheme 51) [84]. Various iron salts were tested, with little observed effect on efficiency. Notably, the water in iron catalysts had a dramatic effect on promotion of the reaction. For example, the desired products were obtained in high yields in the presence of FeCl<sub>3</sub>·6H<sub>2</sub>O, while adding a 4Å molecular sieve completely inhibited the transformation. The authors postulated that water may assist the proton transfer process involved in the reaction. Other proton sources, such as methanol, ethanol, acetic acid, benzoic acid, and *tert*-butanol, were examined and were found to promote this transformation. In addition, the kinetic isotopic effect ( $k_H/k_D = 1.0 \pm 0.1$ ) indicates that aromatic C–H bond cleavage is not involved in the rate-determining step.

The proposed reaction mechanism is depicted in Scheme 52. An intermediate Fe<sup>n+</sup>-chelated species **I** is formed in situ, followed by reductive elimination to produce the adduct **II**. The tautomerization of **II** then gives phenol **III**, which undergoes intramolecular condensation in the presence of the iron catalyst to afford the desired benzofuran. Notably, the iron catalyst displays dichotomous catalytic behavior, acting as transition-metal catalyst in the oxidative coupling step and a Lewis acid in the condensation step.

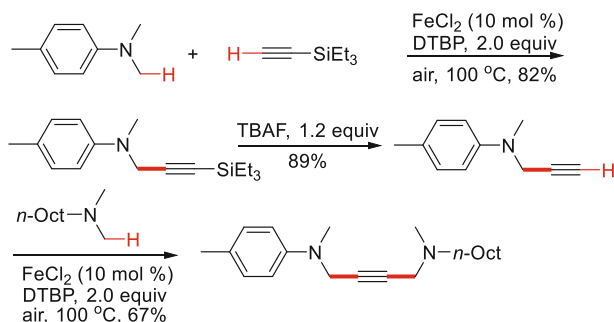


**Scheme 53** Total synthesis of coumestrol via iron-catalyzed CDC reaction

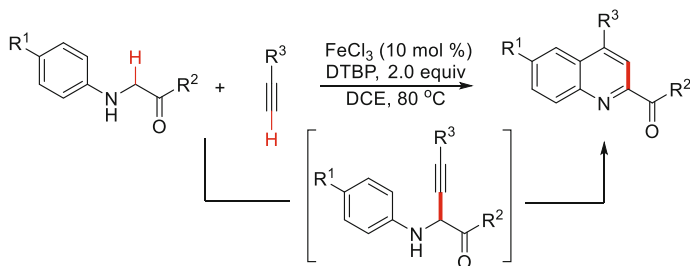
In 2013, Pappo et al. successfully applied this methodology to the total synthesis of coumestrol (Scheme 53) [85]. The first stage of the two-step synthesis of coumestrol involved a modified aerobic oxidative cross-coupling between ethyl 2-(2,4-dimethoxybenzoyl)acetate and 3-methoxyphenol, with  $\text{FeCl}_3$  (10 mol %) as the catalyst. The benzofuran coupling product was then subjected to a sequential deprotection and lactonization protocol, affording the natural product in 59 % overall yield.

#### 4 Coupling of $\text{C}(\text{sp}^3)\text{-H}$ with $\text{C}(\text{sp})\text{-H}$

In 2009, Vogel et al. reported a chemoselective oxidative  $\text{C}\text{-C}$  cross-coupling of tertiary amines with terminal alkynes into propargylamines (Scheme 54) [86]. This reaction was applied to a large variety of aromatic and aliphatic amines with alkynes in a  $\text{FeCl}_2/\text{DTBP}$  system. The reaction was highly chemoselective due to steric hindrance, and thus the methyl amino group reacted much more rapidly than other alkyl amino groups. In addition, the silyl group was successfully applied for protection of the other side of the terminal alkyne, providing an efficient method for constructing asymmetric 1,4-propargylic diamine via double-CDC processes. Mechanistically, it was proposed that the iron-catalyzed SET oxidation generates



**Scheme 54** Chemoselective  $\text{FeCl}_2$ -catalyzed oxidative coupling with two different tertiary amines



**Scheme 55** An efficient route for formation of quinolines by  $\text{FeCl}_3$ -catalyzed oxidative coupling of *N*-arylglycine derivatives with alkynes

an iminium intermediate, which is quenched by an alkynyl carbon anion to give the desired product.

In 2009, Hu et al. reported an iron-catalyzed oxidative coupling of *N*-arylglycine derivatives with alkynes. This facile method provided a series of substituted quinolines in good yields. Mechanistically, the prior  $\text{C}(\text{sp}^3)\text{-H}/\text{C}(\text{sp})\text{-H}$  coupling and subsequent intramolecular Friedel–Crafts reaction was responsible for the formation of quinolines (Scheme 55) [87].

## 5 Coupling of $\text{C}(\text{sp}^2)\text{-H}$ with $\text{X}(\text{sp}^3)\text{-H}$

In 2013, Bao et al. reported a novel iron-catalyzed intramolecular C–H amination, with  $\text{O}_2$  as the oxidant (Scheme 56) [88]. With this method, a series of polysubstituted 1*H*-indazoles and 1*H*-pyrazoles were obtained in good yields.

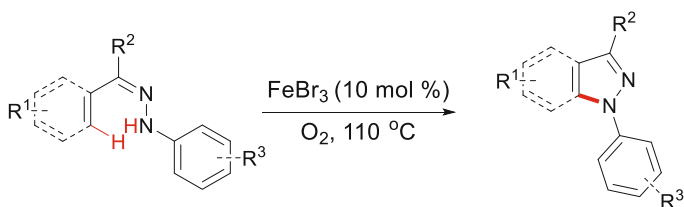
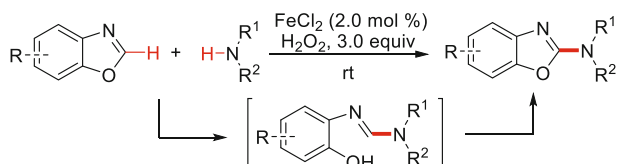
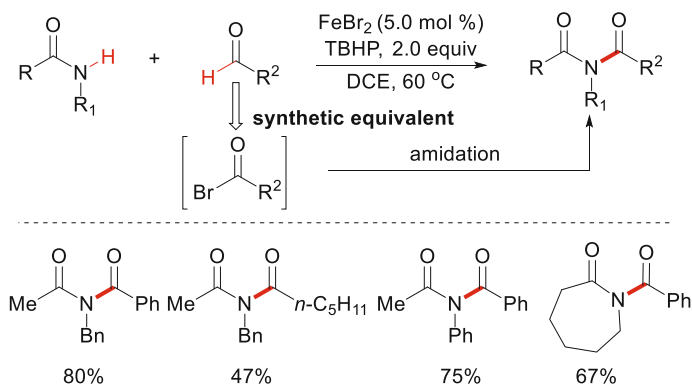
That same year, Sun et al. developed an environmentally friendly method for the amination of benzoxazoles with  $\text{H}_2\text{O}_2$  as a green oxidant (Scheme 57) [89]. This transformation comprised two steps, and was conducted using a one-pot procedure: ring opening to form an amidine intermediate, and iron-catalyzed oxidative intramolecular cyclization.

In 2014, Lei et al. reported an iron-catalyzed oxidative coupling of amides with aldehydes (Scheme 58) [90]. The authors tested the suitability of a variety of amides and aldehydes for use as substrates in a  $\text{FeBr}_2/\text{TBHP}$  system for the direct, efficient construction of imides. Mechanistic studies revealed that an acyl bromide intermediate is generated in situ from aldehyde and  $\text{FeBr}_2$  in the presence of TBHP, which reacts with the respective amide to give the desired imide.

## 6 Coupling of $\text{C}(\text{sp}^2)\text{-H}$ with $\text{X}(\text{sp}^2)\text{-H}$

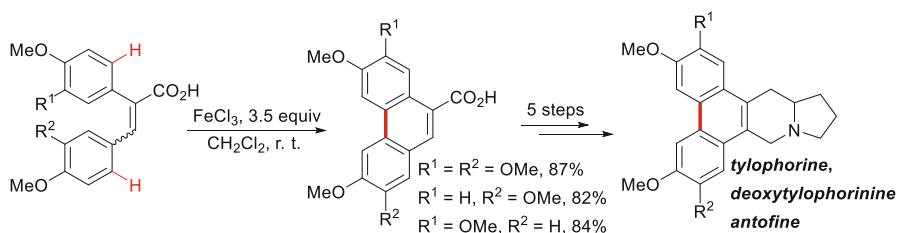
### 6.1 $\text{C}(\text{sp}^2)\text{-H}$ Bond of Arenes

Biaryl coupling, discovered more than a century ago, is now among the most important tools in organic synthesis. The macro-arenes are widely present in various

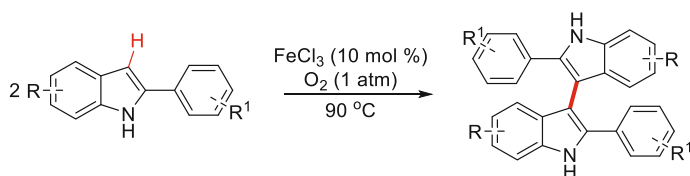
**Scheme 56** FeBr<sub>3</sub>-catalyzed intramolecular C–H amination**Scheme 57** FeCl<sub>2</sub>-catalyzed amination of benzoxazoles with H<sub>2</sub>O<sub>2</sub>**Scheme 58** FeBr<sub>2</sub>-catalyzed oxidative coupling of amides with aldehydes

biologically active molecules and functional materials. In 2008, Wang et al. reported an iron-catalyzed intramolecular oxidative biaryl coupling reaction (Scheme 59) [91], in which phenanthrene-9-carboxylic acids were efficiently constructed from *E*- and *Z*-2,3-diphenylacrylic acid using iron(III) chloride, in excellent yields. The coupling products were further manipulated for the synthesis of naturally occurring alkaloids such as tylophorine, deoxytylophorinine, and antofine.

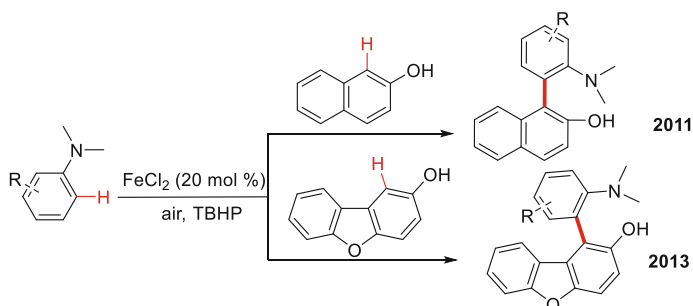
In 2010, Zhang et al. reported an iron-catalyzed intermolecular oxidative homo-coupling of indoles towards 3,3'-biindolyis (Scheme 60) [92]. In addition, Zheng et al. recently reported a Fe(OTf)<sub>3</sub>-catalyzed intermolecular homo-coupling reaction to synthesize fused porphyrin dimers [93].



**Scheme 59**  $\text{FeCl}_3$ -catalyzed intramolecular biaryl coupling



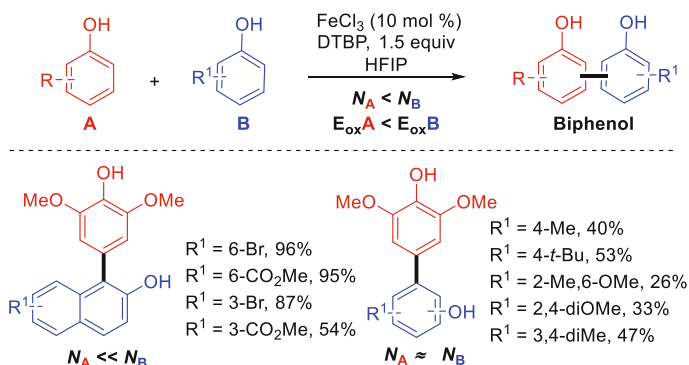
**Scheme 60**  $\text{FeCl}_3$ -catalyzed intermolecular oxidative homo-coupling of indoles



**Scheme 61**  $\text{FeCl}_2$ -catalyzed direct biaryl couplings

As we all know, homo-couplings are generally inevitable when different coupling partners are involved. Over the past few decades, various efforts have been made to resolve this frustrating obstacle in biaryl coupling, wherein one of two coupling partners is pre-activated, while the second is subjected to direct coupling. Selective CDC is still a challenge in the construction of an aryl–aryl bond without the use of pre-functionalized substrates.

In 2011, Chandrasekharam et al. reported an efficient iron-catalyzed CDC of two aromatic compounds using DTBP as oxidant (Scheme 61) [94]. This direct biaryl coupling reaction was highly regioselective, and the C–C bond was created at the *ortho* position relative to the functional group of the substrate. Importantly, no homo-coupled products were observed under optimized conditions. Moreover, this cross-coupling reaction was not sensitive to moisture or air, and produced a variety



**Scheme 62**  $\text{FeCl}_3$ -catalyzed selectively oxidative unsymmetrical biphenol coupling

of dialkyl amino- and hydroxy-substituted biaryls. The authors proposed that a sufficient difference in oxidation potential between the two coupling partners (difference of 440 mV) favored the selective formation of cross-coupled products. In 2013, Chandrasekharam et al. applied this methodology to the synthesis of various anilino-dibenzo furanols, which showed moderate to good anti-mycobacterial activity [95].

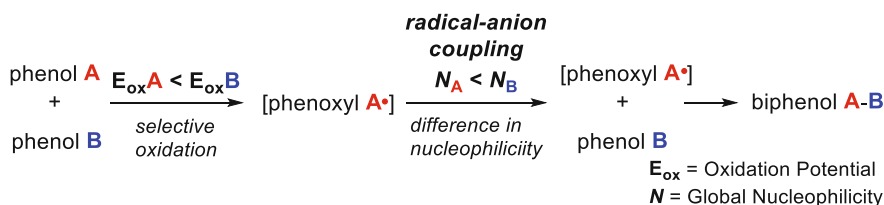
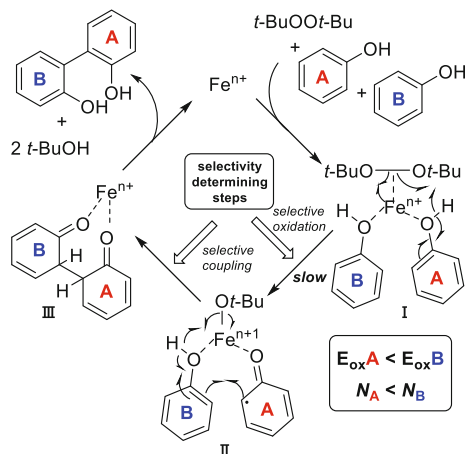
Pappo et al. recently reported an iron-catalyzed selectively oxidative unsymmetrical biphenol coupling with 1,1,1,3,3,3-hexafluoropropan-2-ol (HFIP) as the solvent (Scheme 62) [96]. The kinetic studies support a chelated radical–anion coupling mechanism in which both phenolic components are attached to the catalyst during the C–C-forming step.

The detailed reaction mechanism is depicted in Scheme 63. The initial step is the reversible binding of the phenolic components **A** and **B** and the peroxide to the iron salt (complex I). The peroxide bond is then cleaved by the metal, which is likely involved in the rate-determining step, followed by a SET process to form a bound phenoxyl **A**• radical (complex II). The latter electrophile reacts with the chelated phenol(ate) **B** (complex III) or with a second chelated phenol(ate) **A** in a homocoupling process. The catalytic cycle is terminated by a ligand exchange process that gives both the biphenol and *tert*-butyl alcohol. The phenol oxidation and coupling steps determine the chemoselectivity of the reaction.

In addition, based on mechanistic studies, the authors proposed a general model (Scheme 64) for predicting the feasibility of cross-coupling for a given pair of phenols, as well as electrochemical methods and density functional theory calculations. Specifically, the authors proposed that (1) phenol **A** undergoes selective oxidation to a phenoxyl **A**• radical in the presence of phenol **B** ( $E_{\text{ox}A} < E_{\text{ox}B}$ ); (2) the coupling takes place via a radical–anion coupling mechanism; and (3) phenol **B** is a stronger nucleophile than phenol **A** ( $N_B > N_A$ ), where  $N$  is the theoretical global nucleophilicity.



**Scheme 63** Mechanism of chelated radical-anion oxidative coupling



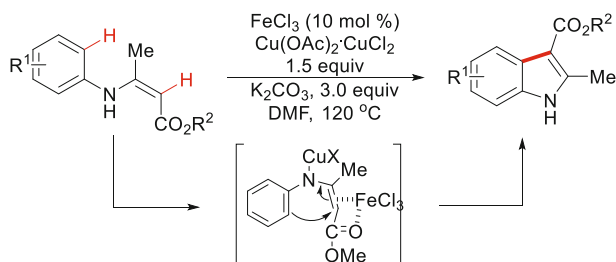
**Scheme 64** General principles for the cross-coupling of phenols

## 6.2 C(sp<sup>2</sup>)-H Bond of Alkenes

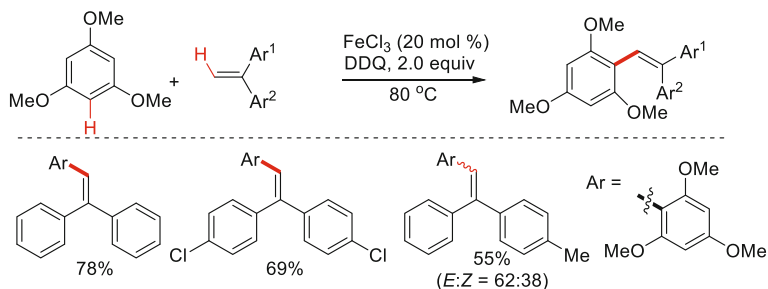
In 2010, Liang et al. reported the preparation of indoles via iron-catalyzed intramolecular oxidative coupling (**Scheme 65**) [97]. The iron catalyst combined with quantitative oxidant  $\text{Cu}(\text{OAc})_2\text{-CuCl}_2$  to facilitate this C-H oxidation reaction. The authors posited that, mechanistically, a copper and iron bimetallic chelate complex may be formed by the coordination of the nitrogen and the double bond, which significantly enhances the reaction activity of the enolates.

In 2015, Lei et al. reported a novel iron-catalyzed oxidative C-H/C-H cross-coupling reaction between electron-rich arenes and diaryl-ethylenes, with DDQ as the oxidant (**Scheme 66**) [98]. Mechanistic studies indicated that this reaction proceeded via a radical pathway, and that DDQ played a key role in the formation of the aryl radical. Experiments utilizing X-ray absorption fine structure (XAFS) revealed that the oxidation state of the iron catalyst did not change during the reaction, suggesting that  $\text{FeCl}_3$  might serve as a Lewis acid.

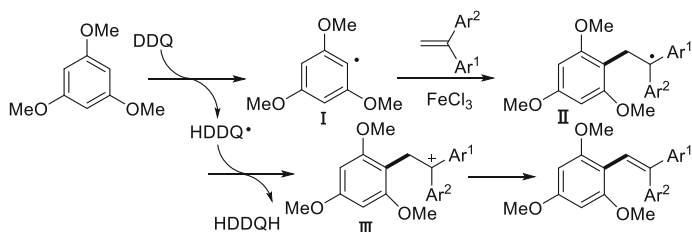
The detailed reaction mechanism is depicted in **scheme 67**. The electron-rich arene is oxidized by DDQ to produce the aryl radical **I**, which is trapped by C-C bonds to yield the radical intermediate **II**. **II** is subsequently oxidized to afford the cationic intermediate **III**, which loses one proton to give the desired triaryl-ethylene.



**Scheme 65** FeCl<sub>3</sub>-catalyzed direct oxidative coupling for the preparation of indoles



**Scheme 66** FeCl<sub>3</sub>-catalyzed oxidative cross-coupling between electron-rich arenes and diaryl-ethylenes

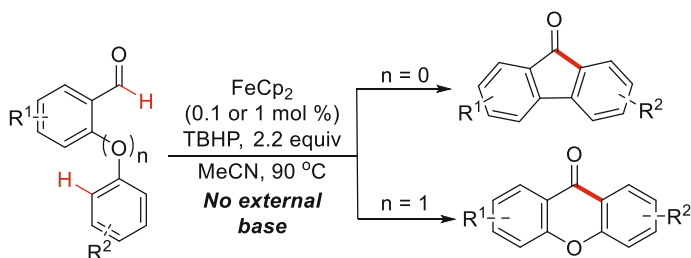


**Scheme 67** Proposed reaction mechanism

### 6.3 C(sp<sup>2</sup>)-H Bond of Carbonyls

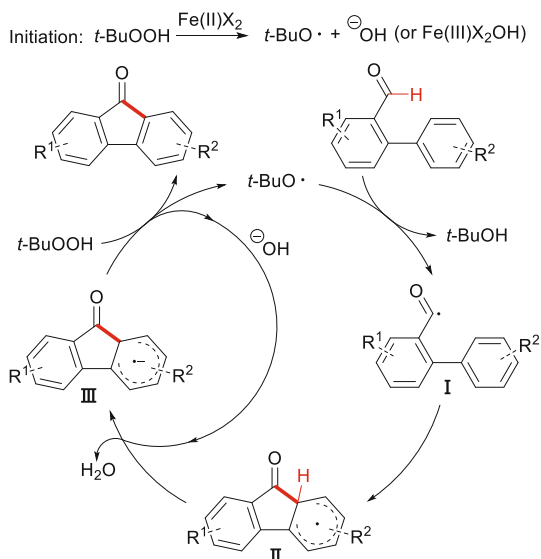
In 2013, Studer et al. reported an iron-catalyzed CDC via base-promoted homolytic aromatic substitution (BHAS) (Scheme 68) [99]. With this method, fluorenones and xanthenes were efficiently prepared via readily available *ortho*-formyl biphenyls and *ortho*-formyl biphenyl ethers, respectively. In contrast to the more commonly known BHAS reaction, this transformation does not require a halide as a radical leaving group or an external strong base, thereby improving the step efficiency and atom economy of the overall process.

The BHAS reaction pathway is depicted in Scheme 69. The combination of TBHP and Fe(II) produces a *t*-BuO<sup>•</sup> radical and Fe(III) complex. Hydrogen abstraction of aldehyde by the *t*-BuO<sup>•</sup> radical gives the acyl radical I, which then



**Scheme 68** FeCp<sub>2</sub>-catalyzed CDC via base-promoted homolytic aromatic substitution (BHAS)

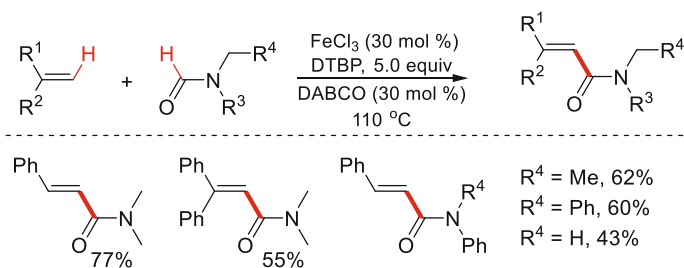
**Scheme 69** Proposed mechanism for BHAS reaction



attacks the arene to form the cyclohexadienyl radical **II**. Deprotonation by basic OH<sup>−</sup> forms the biaryl radical anion **III**, which then reacts with TBHP to deliver the desired product and *tert*-butoxyl radical. Because the basic OH<sup>−</sup> is generated in situ in this transformation, no external base is needed.

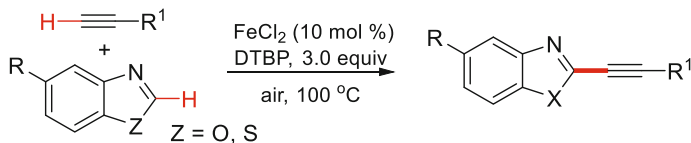
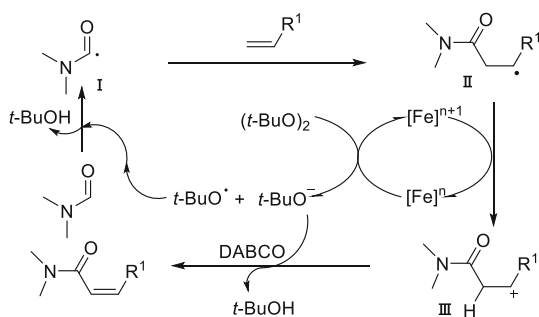
In 2015, Li et al. reported a direct oxidative coupling of alkenes with the C(sp<sup>2</sup>)–H bonds of formamide (**Scheme 70**) [100]. This new method provided  $\alpha,\beta$ -unsaturated amides with excellent chemo- and regioselectivity. Just as the authors predicted, the presence of FeCl<sub>3</sub> lowered the capacity of alkenes to react with the C(sp<sup>3</sup>)–H bonds of amides, as the ·OH radical was consumed to form the Fe<sup>n+</sup>(OH) species, thus suppressing the generation of the *t*-BuO· radical.

Mechanistically (**Scheme 71**), the hydrogen abstraction from *N,N*-dimethylformamide (DMF) by *t*-BuO· radical delivers carbonyl radical **I**, and then **I** is added across alkenes to afford alkyl radical **II**, which is oxidized by Fe<sup>n+1</sup> to give alkyl cation **III**. Finally,  $\beta$ -H elimination of **III** with *t*-BuO· using the DABCO base gives the desired product.



**Scheme 70**  $\text{FeCl}_3$ -catalyzed direct oxidative coupling of alkenes with formamide

**Scheme 71** Proposed reaction mechanism



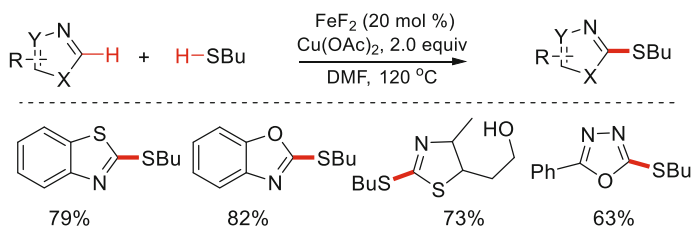
**Scheme 72**  $\text{FeCl}_2$ -catalyzed oxidative alkylation of azoles with terminal alkynes

## 7 Coupling of $\text{C}(\text{sp}^2)\text{-H}$ with $\text{C}(\text{sp})\text{-H}$

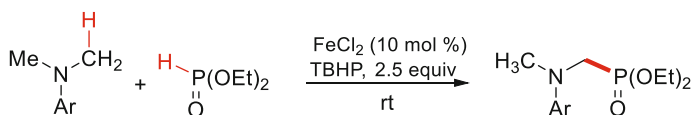
In 2011, Bobade et al. reported an iron-catalyzed oxidative alkylation of azoles with terminal alkynes under ligand- and solvent-free conditions (Scheme 72) [101]. With this method, a series of 2-alkynylated benzoxazoles and benzothiazoles were obtained in high yields.

## 8 Miscellaneous

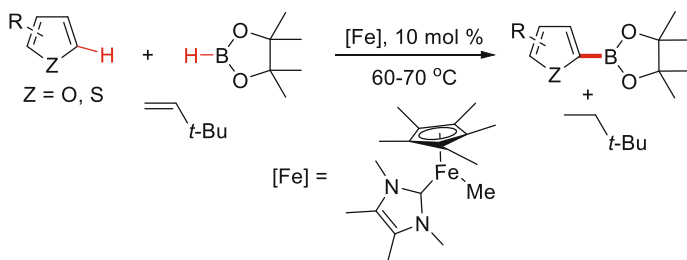
Heteroaryl sulfide structural motifs are found in many pharmaceutically active compounds and advanced materials. The synthesis of heteroaryl thioethers by direct thiolation of heteroarene C–H bonds with thiols is a highly desirable method. In 2012, Gao and Yu reported a Lewis acid-catalyzed, copper(II)-mediated thiolation



**Scheme 73** FeF<sub>2</sub>-catalyzed thiolation of heteroarene C–H bonds



**Scheme 74** FeCl<sub>2</sub>-catalyzed  $\alpha$ -phosphonation of tertiary amines



**Scheme 75** [Fe]NHC-catalyzed dehydrogenative borylation

reaction for the synthesis of heteroaryl thioethers (Scheme 73) [102]. In this transformation, FeF<sub>2</sub> was used as Lewis acid, which was able to activate heteroarenes and coupling with thiols in the presence of copper(II).

Organophosphorus compounds exist in a wide range of nucleotides, pharmaceuticals, and phosphine-containing ligands. They also play an important role in cell metabolism and growth, cell division, and genetic processes. In 2009, Ofial et al. reported an iron-catalyzed oxidative  $\alpha$ -phosphonation of *N,N*-dimethylanilines with dialkyl H-phosphonates. This method allowed the formation of new C–P bonds with non-functionalized starting materials (Scheme 74) [103, 104].

In 2010, Tatsumi and Ohki reported a dehydrogenative borylation of furans and thiophenes with pinacolborane, using a coordinatively unsaturated NHC iron complex as catalyst (Scheme 75) [105]. The evolved hydrogen equivalent was trapped by *tert*-butylethylene. The reaction proceeded regioselectively in the 2(5)-position, providing borylation of heterocycles in good yields.

## 9 Conclusion and Outlook

Research efforts exploring green and sustainable chemistry in the field of organic synthesis have seen the emergence of a new concept, that of cross-dehydrogenative coupling reactions. Various carbon–carbon (C–C) and C–heteroatom bonds have been formed directly from C–H and C–H bonds under oxidative conditions. This concept continues to evolve, with reports of many fascinating examples. For example, Wu et al. reported a visible light-promoted cross-coupling hydrogen evolution reaction without the use of any sacrificial oxidants [106]. By combining eosin Y and graphene-supported RuO<sub>2</sub> nanocomposite (G-RuO<sub>2</sub>) as photosensitizer and catalyst, the desired cross-coupling products and H<sub>2</sub> were achieved in quantitative yields. Li and Mi recently reported the successful photo-induced conversion of naturally abundant methane into benzene over GaN nanowires [107, 108]. This non-oxidative dehydroaromatization of light alkanes represents a green method for the fabrication of aromatics without the use of petroleum cracking or steam reforming. These reactions provide a foundation for the next generation of chemical synthesis, guided by the principles of green chemistry.

The need for practical approaches to C–H bond oxidation using more environmentally friendly reagents, such as oxygen, electricity, and visible light, will be a key consideration in future research efforts. In terms of asymmetric catalysis, the enantioselective cross-dehydrogenative coupling reaction is still in its infancy. Ultimately, the application of CDC in the total synthesis of structurally complex and biologically relevant molecules will demonstrate its true utility.

**Acknowledgments** Financial support was provided by the National Science Foundation of China, State Key Laboratory of Heavy Oil Processing, the Fundamental Research Funds for the Central Universities, Research Funds of Renmin University of China, and Beijing National Laboratory for Molecular Sciences.

## References

1. Moselage M, Li J (2016) Ackermann L ACS Catal 6:498
2. Su B, Cao ZC, Shi ZJ (2015) Acc Chem Res 48:886
3. Delord WJ, Dröge T, Liu F, Glorius F (2011) Chem Soc Rev 40:4740
4. Chen X, Engle KM, Wang DH (2009) Yu JQ Angew Chem Int Ed 48:5094
5. Daugulis O (2009) Top Curr Chem 292:57
6. Labinger JA, Bercaw JE (2002) Nature 417:507
7. Shang X, Liu ZQ (2013) Chem Soc Rev 42:3253
8. Kozhushkov SI, Ackermann L (2013) Chem Sci 4:886
9. Yeung CS, Dong VM (2011) Chem Rev 111:1215
10. Scheuermann CJ (2010) Chem Asian J 5:436
11. Li Z, Bohle DS, Li CJ (2006) Proc Natl Acad Sci USA 103:8928
12. Li CJ, Li Z (2006) Pure Appl Chem 78:935
13. Girard SA, Knauber T, Li CJ (2014) Angew Chem Int Ed 53:74
14. Li CJ (2014) From C–H to C–C bonds cross-dehydrogenative-coupling RSC London
15. Yoo WJ, Li CJ (2009) Top Curr Chem 292:281
16. Li CJ (2009) Acc Chem Res 42:335
17. Bauer I, Knölker HJ (2015) Chem Rev 115:3170
18. Jia F, Li Z (2014) Org Chem Front 1:194
19. Sun CL, Li BJ, Shi ZJ (2011) Chem Rev 111:1293
20. Correa A, García MO, Bolm C (2008) Chem Soc Rev 37:1108

21. Bolm C, Legros J, Le Paih J, Zani L (2004) *Chem Rev* 104:6217
22. For a book on iron-catalyzed organic reactions, see: Plietker B (2008) *Iron catalysis in organic chemistry: reactions and applications* Wiley-VCH Weinheim Germany
23. Huang K, Sun CL, Shi ZJ (2011) *Chem Soc Rev* 40:2435
24. Johansson CCC, Colacot TJ (2010) *Angew Chem Int Ed* 49:676
25. Rodríguez N, Gossen LJ (2011) *Chem Soc Rev* 40:5030
26. Ritleng V, Sirlin C, Pfeffer M (2002) *Chem Rev* 102:1731
27. Li Z, Cao L, Li CJ (2007) *Angew Chem Int Ed* 46:6505
28. Zhang Y, Li CJ (2007) *Eur J Org Chem* 4654
29. Pan S, Liu J, Li Y, Li Z (2012) *Chin Sci Bull* 57:2382
30. Yang K, Song Q (2015) *Org Lett* 17:548
31. Lou SJ, Xu DQ, Shen DF, Wang YF, Liu YK, Xu ZY (2012) *Chem Commun* 48:11993
32. Li Y, Guo F, Zha Z, Wang Z (2013) *Chem Asian J* 8:534
33. Li YM, Lou SJ, Zhou QH, Zhu LW, Zhu LF, Li L (2015) *Eur J Org Chem* 3044
34. Li Z, Yu R, Li H (2008) *Angew Chem Int Ed* 47:7497
35. Li H, He Z, Guo X, Li W, Zhao X, Li Z (2009) *Org Lett* 11:4176
36. Liu W, Liu J, Ogawa D, Nishihara Y, Guo X, Li Z (2011) *Org Lett* 13:6272
37. Shirakawa E, Yoneda T, Moriya K, Ota K, Uchiyama N, Nishikawa R, Hayashi T (2011) *Chem Lett* 40:1041
38. Zeng T, Song G, Moores A, Li CJ (2010) *Synlett* 13:2002
39. Hudson R, Ishikawa S, Li CJ, Moores A (2013) *Synlett* 24:1637
40. Richter H, Mancheño OG (2010) *Eur J Org Chem* 4460
41. Xie Y, Yu M, Zhang Y (2011) *Synthesis* 17:2803
42. Huo C, Chen F, Yuan Y, Xie H, Wang Y (2015) *Org Lett* 17:5028
43. Louillat ML, Patureau FW (2014) *Chem Soc Rev* 43:901
44. Bariwal J, Eycken EV (2013) *Chem Soc Rev* 42:9283
45. Shin K, Lim H, Chang S (2015) *Acc Chem Res* 48:1040
46. Surry DS, Buchwald SL (2008) *Angew Chem Int Ed* 47:6338
47. Hartwig JF (2008) *Acc Chem Res* 41:1534
48. Hassan J, Sevingnon M, Gozzi C, Shulz E (2002) *Lemaire M Chem Rev* 102:1359
49. Ley SV, Thomas AW (2003) *Angew Chem Int Ed* 42:5400
50. Klapars A, Huang X, Buchwald SL (2001) *J Am Chem Soc* 123:7727
51. Klapars A, Antila JC, Huang X, Buchwald SL (2002) *J Am Chem Soc* 124:7421
52. Wang Z, Zhang Y, Fu H, Jiang Y, Zhao Y (2008) *Org Lett* 10:1863
53. Mao X, Wu Y, Jiang X, Liu X, Cheng Y, Zhu C (2012) *RSC Advances* 2:6733
54. Sun M, Zhang T, Bao W (2014) *Tetrahedron Lett* 55:893
55. Chen D, Pan F, Gao J, Yang J (2013) *Synlett* 24:2085
56. Gu L, Wang W, Xiong Y, Huang X, Li G (2014) *Eur J Org Chem* 319
57. Song G, Wang F, Li X (2012) *Chem Soc Rev* 41:3651
58. Muci AR, Buchwald SL (2002) *Top Curr Chem* 219:131
59. Lee C, Matunas R (2007) In *comprehensive organometallic chemistry III*. Eds Elsevier Boston 10:649
60. Iwata S, Hata T, Urabe H (2012) *Adv Synth Catal* 354:3480
61. He Y, Mao J, Rong G, Yan H, Zhang G (2015) *Adv Synth Catal* 357:2125
62. Wang T, Zhou W, Yin H, Ma JA, Jiao N (2012) *Angew Chem Int Ed* 51:10823
63. Pearson AJ, Kwak Y (2005) *Tetrahedron Lett* 46:3407
64. Shirakawa E, Uchiyama N, Hayashi T (2011) *J Org Chem* 76:25
65. Wei Y, Ding H, Lin S, Liang F (2011) *Org Lett* 13:1674
66. Liu LW, Wang ZZ, Zhang HH, Wang WS, Zhang JZ, Tang Y (2015) *Chem Commun* 51:9531
67. Barve BD, Wu YC, El-Shazly M, Korinek M, Cheng YB, Wang JJ, Chang FR (2014) *Org Lett* 16:1912
68. Zhao J, Fang H, Zhou W, Han J, Pan Y (2014) *J Org Chem* 79:3847
69. Li YZ, Li BJ, Lu XY, Lin S, Shi ZJ (2009) *Angew Chem Int Ed* 48:3817
70. Wu HR, Huang HY, Ren CL, Liu L, Wang D, Li CJ (2015) *Chem Eur J* 21:16744
71. Guo X, Pan S, Liu J, Li Z (2009) *J Org Chem* 74:8848
72. Niu B, Zhao W, Ding Y, Bian Z, Pittman CU, Zhou A, Ge H (2015) *J Org Chem* 80:7251
73. Correa A, Fiser B, Gómez BE (2015) *Chem Commun* 51:13365
74. Ohta M, Quick MP, Yamaguchi J, Wunsch B, Itami K (2009) *Chem Asian J* 4:1416

75. Li K, Tan G, Huang J, Song F, You J (2013) *Angew Chem Int Ed* 52:12942
76. Ratnikov MO, Xu X, Doyle MP (2013) *J Am Chem Soc* 135:9475
77. Xia Q, Chen W, Qiu H (2011) *J Org Chem* 76:7577
78. Liu X, Chen Y, Li K, Wang D, Chen B (2012) *Chin J Chem* 30:2285
79. Cheng Y, Dong W, Wang L, Parthasarathy K, Bolm C (2014) *Org Lett* 16:2000
80. Pan S, Liu J, Li H, Wang Z, Guo X, Li Z (2010) *Org Lett* 12:1932
81. Zhu KQ, Wang L, Chen Q, He MY (2015) *Tetrahedron Lett* 56:4943
82. Xia Q, Chen W (2012) *J Org Chem* 77:9366
83. Saidulu G, Kumar RA, Reddy KR (2015) *Tetrahedron Lett* 56:4200
84. Guo X, Yu R, Li H, Li Z (2009) *J Am Chem Soc* 131:17387
85. Kshirsagar UA, Parnes R, Goldshtein H, Ofir R, Zarivach R, Pappo D (2013) *Chem Eur J* 19:13575
86. Volla CMR, Vogel P (2009) *Org Lett* 11:1701
87. Liu P, Wang Z, Lin J, Hu X (2012) *Eur J Org Chem* 1583
88. Zhang T, Bao W (2013) *J Org Chem* 78:1317
89. Xu D, Wang W, Miao C, Zhang Q, Xia C, Sun W (2013) *Green Chem* 15:2975
90. Wang J, Liu C, Yuan J, Lei A (2014) *Chem Commun* 50:4736
91. Wang KL, Lv MY, Wang QM, Huang RQ (2008) *Tetrahedron* 64:7504
92. Niu T, Zhang Y (2010) *Tetrahedron Lett* 51:6847
93. Feng CM, Zhu YZ, Zhang SC, Zang Y, Zheng JY (2015) *Org Biomol Chem* 13:2566
94. Chandrasekharam M, Chiranjeevi B, Gupta KSV, Sridhar B (2011) *J Org Chem* 76:10229
95. Chiranjeevi B, Koyyada G, Prabusreenivasan S, Kumar V, Sujitha P, Kumar CG, Sridhar B, Shaik S, Chandrasekharam M (2013) *RSC Advances* 3:16475
96. Libman A, Shalit H, Vainer Y, Narute S, Kozuch S, Pappo D (2015) *J Am Chem Soc* 137:11453
97. Guan ZH, Yan ZY, Ren ZH, Liu XY, Liang YM (2010) *Chem Commun* 46:2823
98. Ma Y, Zhang D, Yan Z, Wang M, Bian C, Gao X, Bunel EE, Lei A (2015) *Org Lett* 17:2174
99. Wertz S, Leifert D, Studer A (2013) *Org Lett* 15:928
100. Yang XH, Wei WT, Li HB, Song RJ, Li JH (2014) *Chem Commun* 50:12867
101. Patil SS, Jadhav RP, Patil SV, Bobade VD (2011) *Tetrahedron Lett* 52:5617
102. Dai C, Xu Z, Huang F, Yu Z, Gao YF (2012) *J Org Chem* 77:4414
103. Han W, Ofial AR (2009) *Chem Commun* 6023
104. Han W, Mayer P, Ofial AR (2010) *Adv Synth Catal* 352:1667
105. Hatanaka T, Ohki Y, Tatsumi K (2010) *Chem Asian J* 5:1657
106. Meng QY, Zhong JJ, Liu Q, Gao XW, Zhang HH, Lei T, Li ZJ, Feng K, Chen B, Tung CH, Wu LZ (2013) *J Am Chem Soc* 135:19052
107. Li L, Fan S, Mu X, Mi Z, Li CJ (2014) *J Am Chem Soc* 136:7793
108. Li L, Mu X, Liu W, Kong X, Fan S, Mi Z, Li CJ (2014) *Angew Chem Int Ed* 53:14106



# Iron-Catalyzed C–C Cross-Couplings Using Organometallics

Amandine Guérinot<sup>1</sup>  · Janine Cossy<sup>1</sup>

Received: 7 April 2016 / Accepted: 20 June 2016 / Published online: 20 July 2016  
© Springer International Publishing Switzerland 2016

**Abstract** Over the last decades, iron-catalyzed cross-couplings have emerged as an important tool for the formation of C–C bonds. A wide variety of alkenyl, aryl, and alkyl (pseudo)halides have been coupled to organometallic reagents, the most currently used being Grignard reagents. Particular attention has been devoted to the development of iron catalysts for the functionalization of alkyl halides that are generally challenging substrates in classical cross-couplings. The high functional group tolerance of iron-catalyzed cross-couplings has encouraged organic chemists to use them in the synthesis of bioactive compounds. Even if some points remain obscure, numerous studies have been carried out to investigate the mechanism of iron-catalyzed cross-coupling and several hypotheses have been proposed.

**Keywords** Iron · Cross-coupling · C–C bond formation · Organometallics

## Abbreviations

|      |                          |
|------|--------------------------|
| acac | Acetylacetonate          |
| CPME | Cyclopentyl methyl ether |
| dbm  | Dibenzoylmethide         |
| Dipp | 2,6-Diisopropylphenyl    |

---

This article is part of the Topical Collection “Ni- and Fe-Based Cross-Coupling Reactions”; edited by “Arkaitz Correa”.

---

✉ Amandine Guérinot  
[amandine.guerinot@espci.fr](mailto:amandine.guerinot@espci.fr)

✉ Janine Cossy

<sup>1</sup> Laboratoire de Chimie Organique, Institute of Chemistry, Biology and Innovation (CBI)-UMR 8231, ESPCI Paris/CNRS/PSL\* Research Institute, 10 rue Vauquelin, 75231 Paris Cedex 05, France

|        |   |
|--------|---|
| dpm    | Dipivaloylmethide   |
| dppbz  | 1,2-Bis(diphenylphosphino)benzene   |
| dppe   | 1,2-Bis(diphenylphosphino)ethane  |
| dppp   | 1,2-Bis(diphenylphosphino)propane   |
| HMTA   | Hexamethylenetetramine  |
| IMes   | 1,3-Bis(2,4,6-trimethylphenyl)-1,3-dihydro-2 <i>H</i> -imidazol-2-ylidene |
| IPr    | 1,3-Bis(2,6-diisopropylphenyl)-1,3-dihydro-2 <i>H</i> -imidazol-2-ylidene |
| NMI    | <i>N</i> -Methylimidazole   |
| NMP    | <i>N</i> -Methylpyrrolidinone   |
| OA     | Oxidative addition  |
| PEG    | Polyethylene glycol   |
| RE     | Reductive elimination   |
| SciOPP | Spin-control-intended <i>o</i> -phenylene bis-phosphine                   |
| SIPr   | 1,3-Bis(2,6-di- <i>i</i> -propylphenyl)imidazolidin-2-ylidene             |
| TC     | Thiophene carboxylate   |
| THF    | Tetrahydrofuran   |
| TM     | Transmetalation   |
| TMCD   | Tetramethylcyclohexan-1,2-diamine   |
| TMEDA  | Tetramethylethanediamine  |
| TMP    | Tetramethylpiperidine   |

## 1 Introduction

Nowadays, metal-catalyzed cross-coupling plays a key role in the chemical toolbox for the formation of C–C bonds. In this field, palladium and nickel catalysis are still predominant. However, due to economical and environmental issues, there is a growing need for cheap and low-toxic catalysts. Despite the seminal works of Kharash et al. in 1941 and Kochi et al. in the 1970s, iron-catalyzed cross-coupling has been an under-explored field for a long period of time. In 1998, Cahiez et al. had a significant breakthrough by highlighting the high synthetic potential of iron-catalyzed cross-couplings. Since then, the development of iron-catalyzed cross-couplings has become an expanding area of research as attested by the impressive number of publications and reviews reported (for a selection of books and reviews, see [1–12]). In this chapter, we would like to give an overview of the evolution of iron-catalyzed cross-couplings from Kharash's and Kochi's early work to the very last developments. We will focus on the formation of C–C bonds by cross-couplings of halides or (pseudo)halides with organometallic reagents. The iron-catalyzed CH-activation will not be presented herein as it is the topic of another chapter of this book. The review will be divided into sections depending on the nature of the coupling partners. A section dedicated to the mechanistic studies and hypotheses will be presented at the end of the chapter.

## 2 Alkenyl (pseudo)halides

### 2.1 Coupling with Alkyl Organometallics (Csp<sup>2</sup>-Csp<sup>3</sup>)

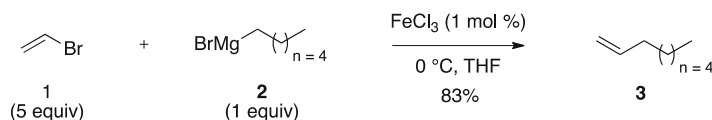
#### 2.1.1 Alkenyl Halides

**2.1.1.1 With Alkyl Grignard Reagents** The first example of an iron-catalyzed cross-coupling between alkenyl halides and alkyl Grignard reagents was reported by Kochi et al. in the early 1970s [13–15]. A low catalytic loading in FeCl<sub>3</sub> (1 mol%) was sufficient to perform the alkenylation of various alkyl Grignard reagents and the coupling products were isolated in good yields. Interestingly, the geometry of the double bond was maintained during the process. The main drawback of the method was the excess alkenyl halide required (5 equiv) that can be a limit to its application for synthetic purposes (Scheme 1).

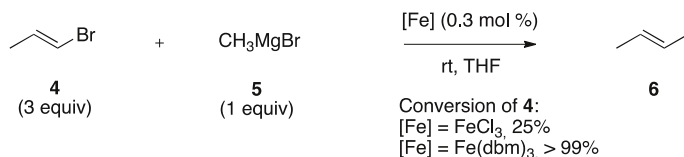
Iron(III) catalysts possessing diketone ligands such as Fe(dbm)<sub>3</sub> (dbm = dibenzoylmethide) showed higher performances than iron trichloride and a decreased amount of alkenyl bromide from 5 equiv to 3 equiv was possible (Scheme 2) [16].

During the next 20 years, only few developments of iron-catalyzed cross-coupling were reported in the literature. In 1986, Naso et al. studied the metal-catalyzed cross-coupling between bromo-alkenyl sulphides and secondary alkyl Grignard reagents. Among the screened palladium, nickel and iron salts, Fe(dpm)<sub>3</sub> (dpm = dipivaloylmethide) was the most effective catalyst allowing the chemoselective formation of the coupling product. Worthy of note, a complete retention of the geometry of the double bond was observed during the reaction (Scheme 3) [17].

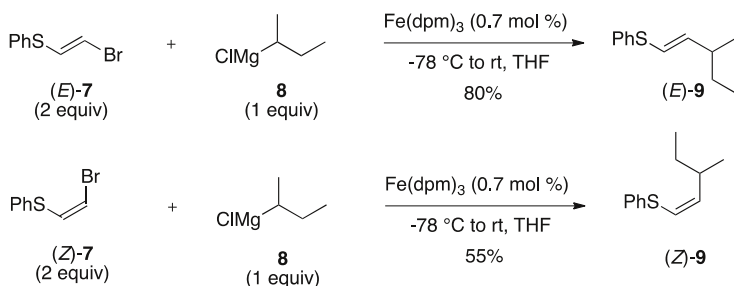
In 1998, Cahiez et al. made a significant breakthrough in the area of iron-catalyzed cross-coupling by demonstrating the positive role played by a co-solvent added to THF. When the Fe(acac)<sub>3</sub>-catalyzed coupling between 1-bromoprop-1-ene and octylmagnesium chloride was performed in pure THF a moderate yield of 40 % in **11** was obtained. In contrast, when 2 equiv of *N*-methylpyrrolidinone (NMP) were added, the yield jumped to 87 % (Scheme 4, eq 1). Among the co-solvent tested, DMPU, DMF, and DMA also showed good results. The nature of the



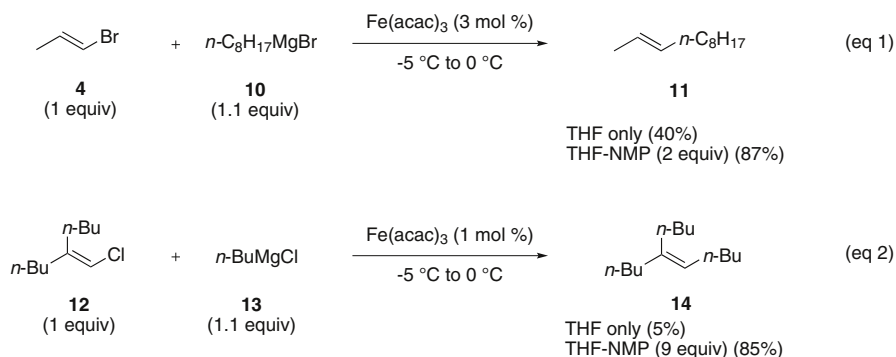
**Scheme 1** Early example from Kochi et al.



**Scheme 2** Fe(dbm)<sub>3</sub>-catalyzed coupling of alkenyl halides



**Scheme 3** Coupling involving bromo-alkenyl sulphides



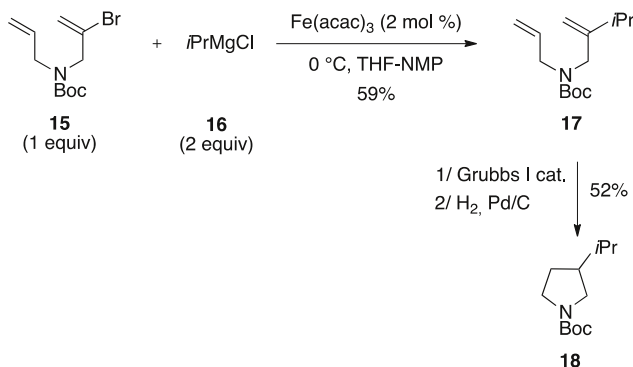
**Scheme 4** Crucial role of the NMP

iron(III) catalyst had a low impact on the outcome of the coupling as similar results were obtained with  $\text{Fe}(\text{acac})_3$ ,  $\text{Fe}(\text{dbm})_3$ ,  $\text{Fe}(\text{dpm})_3$ , or  $\text{FeCl}_3$ . The geometry of the double bond was retained during the cross-coupling. The presence of NMP even allowed the use of poorly reactive alkenyl halides such as alkenyl chlorides (Scheme 4, eq 2) [18].

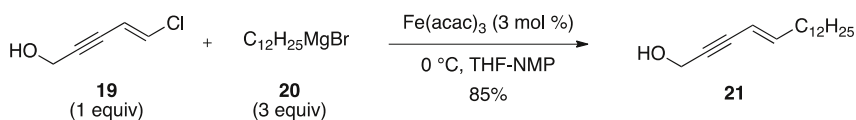
This method was successfully applied to the alkylation of a pyrrolidine precursor, **15**, and the coupling product could be engaged directly in a ring-closing metathesis without purification to produce the substituted pyrrolidine **18** (Scheme 5) [19].

The possibility of using alkenyl chlorides was exploited by Alami et al. for the functionalization of chloroenynes. The coupling products were obtained with good yields (61–88 %) with complete retention of the geometry of the double bond. Interestingly, free alcohols were tolerated under the reaction conditions even if an excess of Grignard reagent was required (Scheme 6) [20].

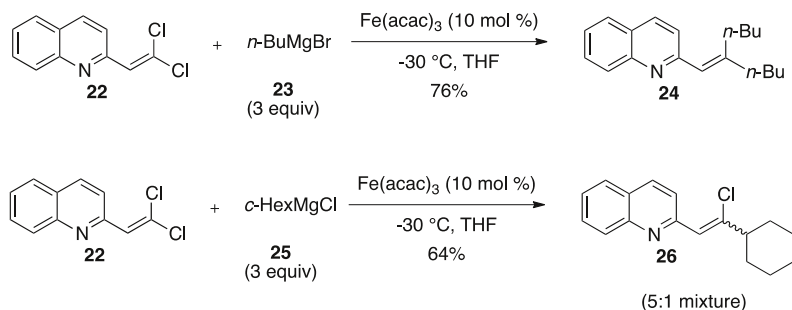
The same authors also studied the alkylation of 1,1-dichloro-1-alkenes. Surprisingly, in this case, the presence of NMP proved detrimental to the reaction and good yields could be obtained in THF at  $-30$  °C. When primary alkyl Grignard reagents were involved, the bis-alkylated product was the only isolated compound. In contrast, in the presence of cyclohexylmagnesium bromide, the mono-alkylated product was formed in 64 % yield as a 5:1 mixture of undetermined *E/Z* isomers (Scheme 7) [21].



**Scheme 5** Synthesis of pyrrolidine **18**



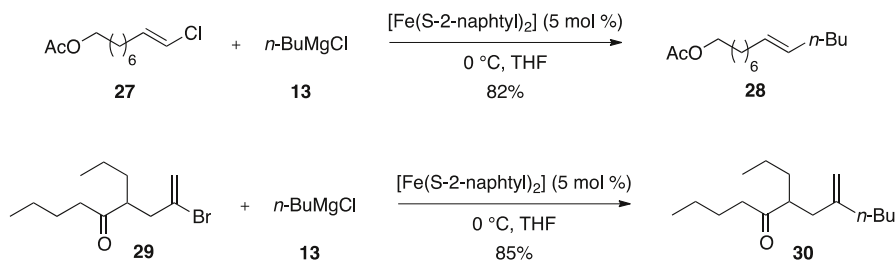
**Scheme 6** Functionalization of chloroenynes



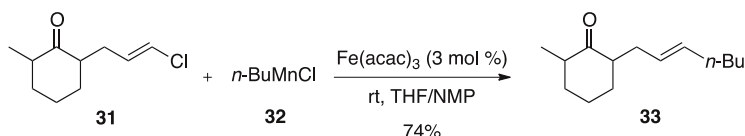
**Scheme 7** Cross-coupling involving 1,1-dichloro-1-alkenes

Recently, NMP was identified as a reprotoxin and thus could be considered as a limit in the use of iron-catalyzed cross-coupling in industrial applications. Cahiez and coworkers showed that iron(II) thiolates prepared from  $\text{FeCl}_2$  or  $\text{FeCl}_3$  and  $\text{ArSMgCl}$  were effective precatalysts for the coupling of alkenyl halides with alkyl Grignard reagents. Alkenyl bromides as well as alkenyl chlorides were suitable partners and a broad range of functional groups such as ester, ketone, or acetal were well tolerated (**Scheme 8**) (see also [22–26]).

**2.1.1.2 With Alkyl Organomanganese Reagents** As an alternative to alkyl Grignard reagents, Cahiez et al. demonstrated that organomanganese chlorides could be efficiently coupled to alkenyl chlorides, bromides, and iodides. The



**Scheme 8** Iron thiolates as catalysts



**Scheme 9** Coupling involving an organomanganese reagent

reaction proceeded with complete retention of the geometry of the double bond and tolerated the presence of sensitive functional groups such as ketones, which could be problematic in the presence of more nucleophilic Grignard reagents (Scheme 9) [27, 28].

### 2.1.2 Enol Triflates

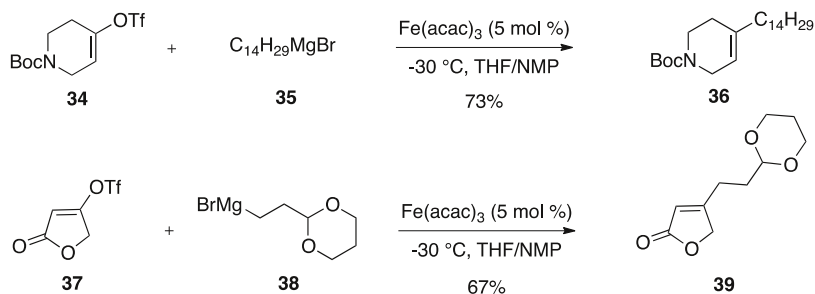
Enol triflates can be considered as attractive partners in cross-couplings due to their easy preparation from the corresponding ketones. In 2004, Fürstner et al. studied the iron-catalyzed cross-coupling between alkenyl triflates and alkyl Grignard reagents. A broad range of functional groups were tolerated and moderate to good yields were generally obtained in favor of the coupling product (Scheme 10) [29].

The iron-catalyzed cross-coupling between enol triflate **40** and the alkyl Grignard reagent **41** was performed to synthesize latrunculin A, B, C, M, S, and their analogues (Scheme 11) [30–33].

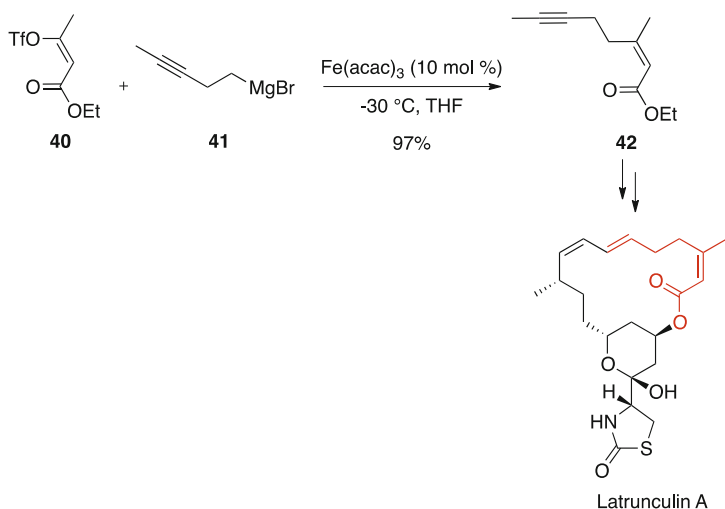
To achieve the cross-coupling of bicyclic alkenyl triflates with an alkyl Grignard reagent, a mixture of THF and NMP (1:3) was again identified as the optimal solvent even if the use of DMPU could also give good results (Scheme 12) [34, 35] (for other applications of iron-catalyzed cross-coupling between enol triflates and alkyl Grignard reagents, see [36–40]).

### 2.1.3 Enol Phosphates

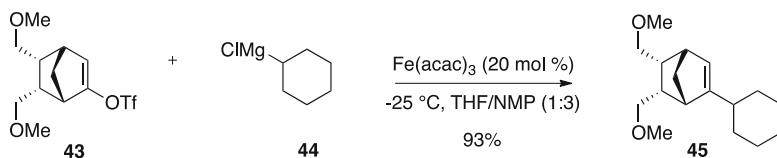
Similarly to enol triflates, enol phosphates are easily accessible from the corresponding ketones. In addition, compared to enol triflates, they are less expensive, more stable and thus easier to handle. Cahiez et al. were the first to realize an iron-catalyzed cross-coupling involving an enol phosphate. This latter



**Scheme 10** Enol triflates as coupling partners



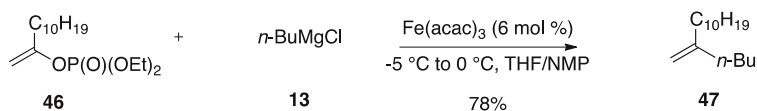
**Scheme 11** Application to the synthesis of latrunculin A



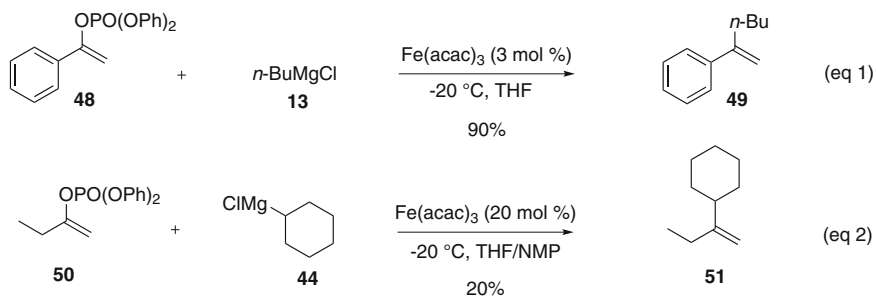
**Scheme 12** Functionalization of bicyclic alkenyl triflates

was less reactive compared to its halide counterpart and, consequently a higher catalytic loading in  $\text{Fe(acac)}_3$  (6 vs. 1 mol%) as well as a larger amount of Grignard reagent (2 equiv vs. 1.1 equiv) were necessary to reach complete conversion. In these conditions, the coupling product was isolated with a good yield of 78 % (Scheme 13) [18].

In 2008, the same authors generalized the reaction to various enol phosphates and a deeper study of such cross-coupling was achieved [41]. Interestingly, NMP should



**Scheme 13** Enol phosphates as electrophilic partners



**Scheme 14** Cross-couplings involving enol phosphates

be omitted and good yields in favor of the cross-coupling products were obtained in pure THF (Scheme 14, eq 1). The authors hypothesized that the enol phosphate itself may play the role of a ligand, stabilizing the iron intermediates. The cross-coupling could be performed on both acyclic and cyclic enol phosphates but the reaction was limited to primary alkyl Grignard reagents as poor yields were obtained with secondary alkyl Grignard reagents (Scheme 14, eq 2).

Worthy of note, as the (*E*)-enol phosphate reacted faster than the (*Z*)-isomer, the (*E*)- and (*Z*)- isomers could be differentiated during the reaction (Scheme 15).

Enol phosphate **54** derived from 4-piperidone was efficiently coupled to *n*-butylmagnesium chloride using  $\text{Fe}(\text{acac})_3$  as the catalyst (Scheme 16) [42].

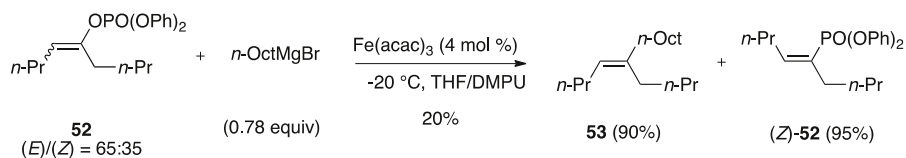
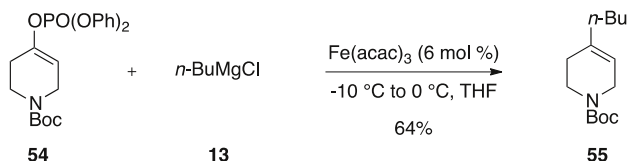
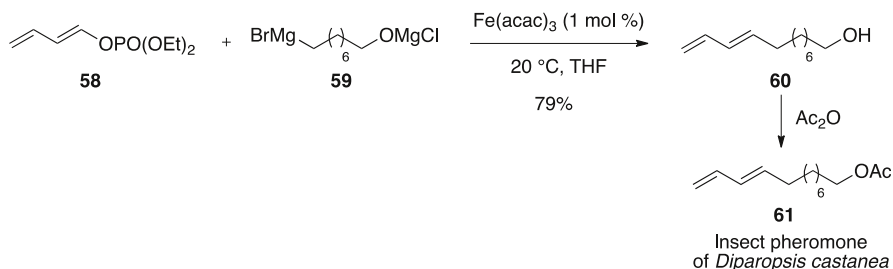
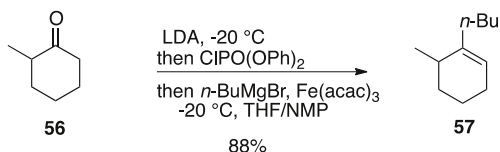
A one-pot procedure including the preparation of the enol phosphate starting from the ketone and the cross-coupling was developed delivering the expected product in good yield (88 %) (Scheme 17).

The reaction was successfully applied to dienol and trienol phosphates allowing the synthesis of an insect pheromone of *Diparopsis castanea* (Scheme 18) [43] (for another synthetic application, see [44]).

#### 2.1.4 Alkenyl Pivalates, Acetates, and Tosylates

In 2009, Shi et al. explored the feasibility of an iron-catalyzed cross-coupling between alkenyl carboxylates and Grignard reagents. Alkenyl pivalates were selected, and among the catalytic systems tested for the coupling with an alkyl Grignard reagent,  $\text{FeCl}_2$  associated to an NHC ligand ( $\text{H}_2\text{IMes}$ ) were the most effective. Surprisingly, the cross-coupling worked well with the hexylmagnesium chloride but failed with the hexylmagnesium bromide. This absence of reactivity could be solved by adding an excess of  $\text{LiCl}$  (6 equiv) and, under these conditions, the NHC ligand was no more required (Scheme 19). Several functional

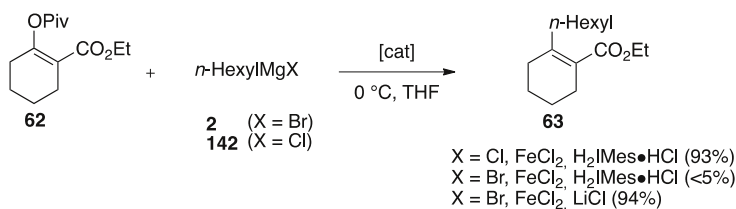


**Scheme 15** (E)/(Z) differentiation**Scheme 16** Functionalization of a piperidine**Scheme 17** One-pot procedure**Scheme 18** Synthesis of an insect pheromone

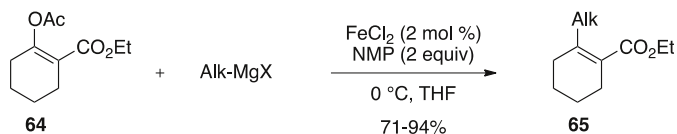
groups were tolerated under the reaction conditions including acetals, esters and ketones [45, 46].

In the previous example, the steric hindrance of the pivaloyl group disfavored the direct nucleophilic attack of the Grignard reagents on the ester moiety. However, the use of easily accessible and cheap alkenyl acetates could be attractive, notably from an atom economy point of view. Consequently, a cross-coupling between alkenyl acetates and alkyl Grignard reagents was examined. FeCl<sub>2</sub> was selected as the catalyst and the use of an additive was essential. Among the amines, NHC and ethers tested, *N*-methyl-2-pyrrolidinone gave the best results. A range of alkenyl acetates were efficiently coupled with Grignard reagents<sup>1</sup> affording the desired product in good yields (Scheme 20) [47].

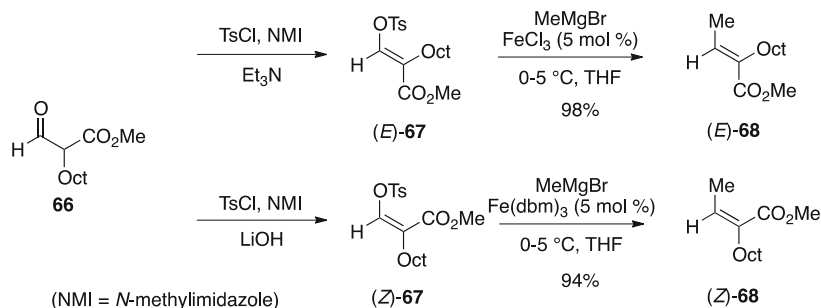
<sup>1</sup> Some aryl Grignard reagents were also coupled.



**Scheme 19** Cross-coupling of an alkenyl pivalate with an alkyl Grignard reagent



**Scheme 20** Cross-coupling involving an alkenyl acetate



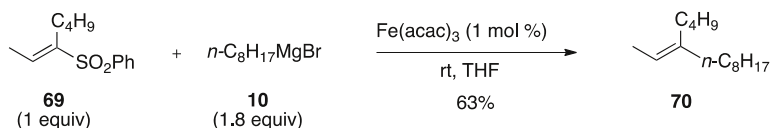
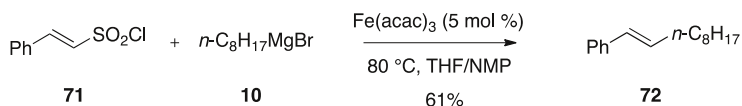
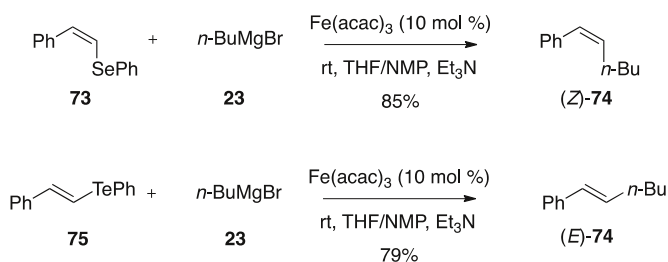
**Scheme 21** Cross-coupling involving alkenyl tosylates

Depending on the conditions, (*E*)- or (*Z*)-enol tosylates could be accessed from  $\beta$ -keto esters. Both enols were involved in iron-catalyzed cross-coupling delivering the product in good yields.  $\text{FeCl}_3$  was preferred for the cross-coupling of (*E*)-enol tosylates whereas  $\text{Fe}(\text{dbm})_3$  was more effective than  $\text{FeCl}_3$  for (*Z*)-enol tosylates (Scheme 21). In some cases, a slight (*Z*)/(*E*) isomerization was observed [48].

### 2.1.5 Alkenyl Sulphur Derivatives and Alkenyl Chalcogenides

Alkenyl sulphones could be used as the coupling partner instead of alkenyl halides. Iron(III) acetylacetonate was used as the catalyst and, once again, a perfect retention of the stereochemistry of the double bond was obtained during the cross-coupling (Scheme 22) [49]. A similar reaction using  $\text{FeCl}_3$  as the catalyst was applied to the synthesis of a sexual pheromone of yellow scale [50, 51].

An iron-catalyzed desulfinylative cross-coupling using sulfonyl chloride was reported by Vogel et al. in 2008. For example, (*E*)-styrenesulfonyl chloride was

**Scheme 22** Alkenyl sulphones as electrophilic partners**Scheme 23** Desulfinylative cross-coupling**Scheme 24** Coupling involving alkenyl selenides and tellurides

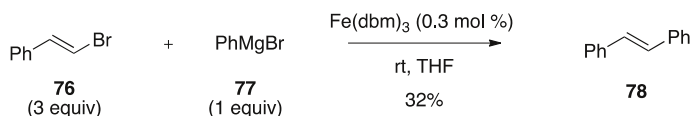
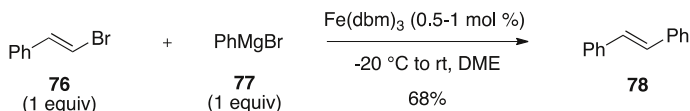
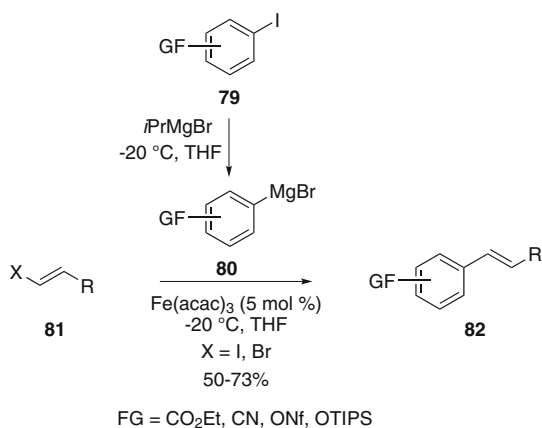
reacted with *n*-octylmagnesium bromide to give the coupling product in 61 % yield and with a perfect retention of the geometry of the double bond (Scheme 23). From a mechanistic point of view, the authors proposed an oxidative addition of the iron into the S-Cl bond followed by a SO<sub>2</sub> release (for more details about the mechanism of iron-catalyzed cross-coupling, see Sect. 7) [52].

Alkenyl selenides as well as alkenyl tellurides were successfully involved in an iron-catalyzed cross-coupling with alkyl Grignard reagents. The coupling was completely stereoselective regarding the geometry of the double bond of the starting material. The reaction was performed in a THF/NMP mixture and a positive role of Et<sub>3</sub>N was noticed (Scheme 24) [53].

## 2.2 Coupling with Aryl Organometallics (Csp<sup>2</sup>-Csp<sup>2</sup>)

### 2.2.1 Alkenyl Halides

In their seminal work, Kochi et al. described the first iron-catalyzed cross-coupling of phenylmagnesium bromide with an alkenyl halide. However, 3 equiv of the halide partner were necessary and the cross-coupling product was obtained with a low yield of 32 % (Scheme 25) [3].

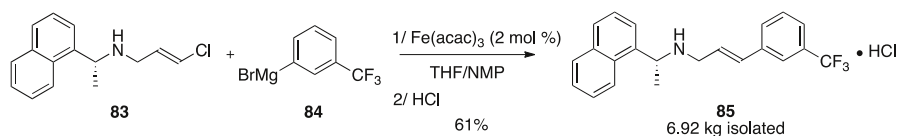
**Scheme 25** Low-efficient alkenyl/aryl cross-coupling**Scheme 26** Cross-coupling between an alkenyl bromide and phenylmagnesium bromide**Scheme 27** Functionalized aryl Grignard reagents in cross-coupling

A few years later, Molander et al. carried out an optimization of the reaction conditions and they demonstrated that the use of DME as the solvent instead of THF, associated to a decrease of the temperature, led to a significant improvement in the yield of the coupling product (68 % versus 32 %) (Scheme 26) [54].

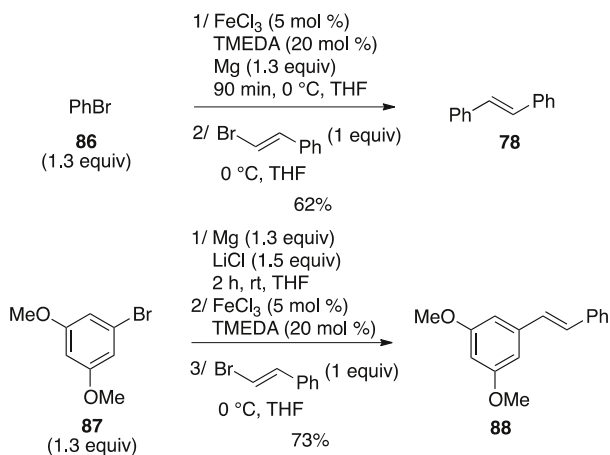
In 2001, the reaction was generalized to functionalized aryl magnesium bromides, prepared by a halide/metal exchange from the corresponding iodides using isopropyl magnesium bromide. Alkenyl iodides as well as alkenyl bromides were suitable partners in the cross-coupling which tolerates a wide range of functional groups including esters, cyanides, nonaflates, and silyl ethers (Scheme 27) [55].

The cross-coupling between alkenyl halides and aryl Grignard reagent was applied to an efficient synthesis of the calcium receptor binder cinacalcet and, worthy of note, the reaction could be performed on kilogram scale (Scheme 28) [56] (for another synthetic application, see [57]).

A one-pot procedure including the in situ formation of the aryl Grignard reagent and the subsequent iron-catalyzed cross-coupling with an alkenyl bromide was developed. The aryl bromide was first treated with FeCl<sub>3</sub> (5 mol%) and tetramethylethylenediamine (TMEDA) (20 mol%) in the presence of a stoichiometric



**Scheme 28** Kilogram-scale synthesis of **85**



**Scheme 29** One-pot procedure including Grignard formation

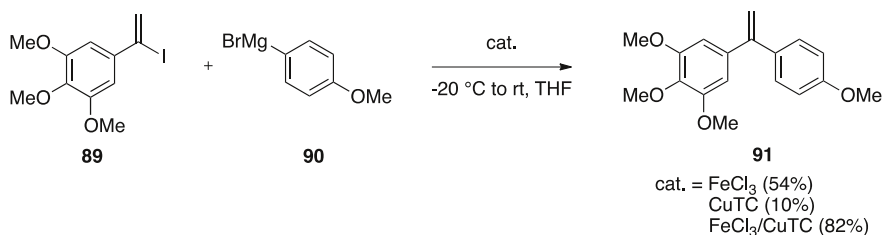
amount of magnesium to induce the formation of the Grignard reagent and then the alkenyl halide was added to give the coupling product. The scope of this domino process was rather limited and, when electron-rich aryl bromides or heteroaryl bromides were used, a tandem process including an iron-free pre-formation of the Grignard reagent followed by the addition of the alkenyl halide was preferred to suppress biarylic by-products (Scheme 29) [58].

A cross-coupling involving 1-arylvinyhalides and aryl Grignard reagent was developed to access 1,1-diarylethylene motifs, which are present in numerous bioactive products. Interestingly, an iron/copper co-catalysis was used to promote the cross-coupling. Both FeCl<sub>3</sub> and CuTC play an important role as lower yields in the coupling product were obtained when only one of the two salts was used. However, the exact role of each metal salt in the coupling has not been investigated (Scheme 30) [59].

## 2.2.2 Enol Triflates

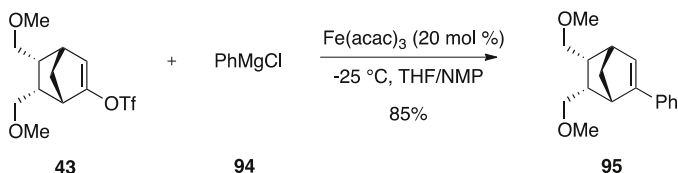
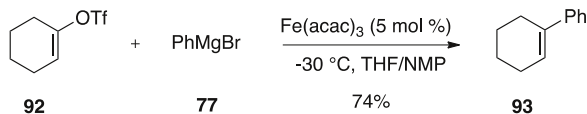
### 2.2.2.1 With Aryl Grignard Reagents

Enol triflates can be considered as an attractive alternative to alkenyl halides. The cross-coupling between alkenyl triflates and aryl Grignard reagents was first reported in 2004 using Fe(acac)<sub>3</sub> as a catalyst and a mixture of THF and NMP (Scheme 31) [29].



**Scheme 30** Synthesis of 1,1-diarylethylene motif

**Scheme 31** Enol triflates as electrophilic partners



**Scheme 32** Arylation of a bicyclic alkenyl triflate

This method was applied to the arylation of bicyclic alkenyl triflates ([Scheme 32](#)) [34].

**2.2.2.2 With Aryl Organocopper Reagents** Interestingly, functionalized aryl copper reagents could be efficiently coupled to alkenyl triflates or nonaflates. A range of functional groups on the aryl copper reagent are tolerated and the reaction is only slightly sensitive to steric hindrance ([Scheme 33](#)) [60].

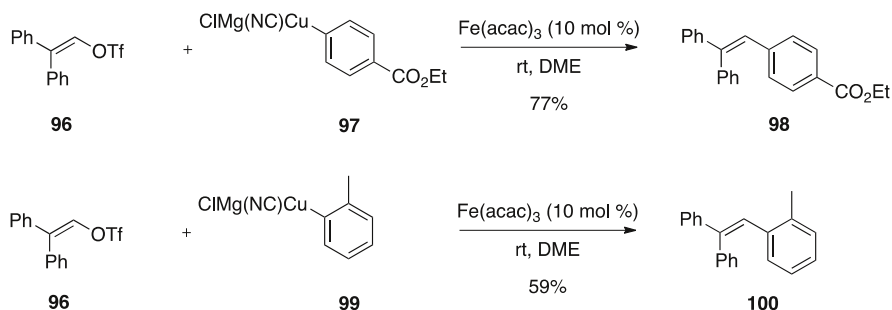
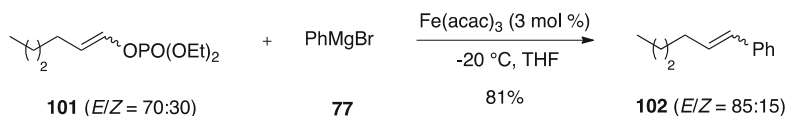
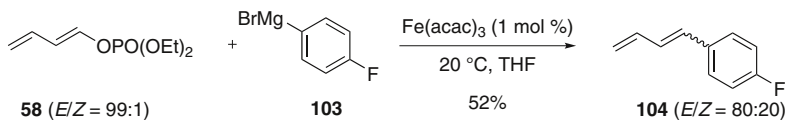
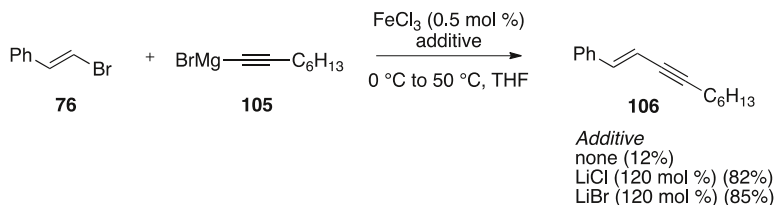
### 2.2.3 Enol Phosphates

The stable and low expensive enol phosphates have also been used as coupling partners with aryl Grignard reagents. The phosphate could play the role of the ligand of the iron catalyst and thus, additives could be omitted. The reaction between enol phosphate **101** and phenyl magnesium bromide occurred with partial isomerization of the double bond ([Scheme 34](#)) [41].

This reaction was successfully applied to the arylation of dienol phosphates even if a partial isomerization of the double bond was observed ([Scheme 35](#)) [43].

## 2.3 Coupling with alkynyl Grignard reagent (Csp<sup>2</sup>-Csp)

A cross-coupling between alkenyl halides and alkynyl Grignard reagents was developed to afford the corresponding enynes. The reaction was sluggish in the

**Scheme 33** Coupling involving enol triflates and organocopper reagents**Scheme 34** Arylation of an enol phosphate**Scheme 35** Arylation of a dienol phosphate**Scheme 36** Alkynylation of an alkenyl bromide

absence of any additives but the addition of a stoichiometric amount of lithium salt considerably improved the yield in the coupling product (**Scheme 36**). The authors hypothesized that the presence of the lithium salt induced the formation of a magnesium ate complex that could be a better reducing agent toward the iron catalyst than the Grignard reagent [61].

### 3 Aryl (pseudo)halides

#### 3.1 Coupling with Alkyl Organometallics (Csp<sup>2</sup>-Csp<sup>3</sup>)

##### 3.1.1 Aryl Halides

**3.1.1.1 With Alkyl Grignard Reagents** The first example of iron-catalyzed cross-coupling involving an aryl chloride was reported in 1989 by Pridgen and coworkers. *o*-Chloro arylimine **107** was coupled to alkyl Grignard reagents using Fe(acac)<sub>3</sub> as a catalyst (Scheme 37). In this case, the iron catalyst proved superior to Ni(acac)<sub>2</sub> as, with nickel catalyst, a reduction of the imine was observed [62].

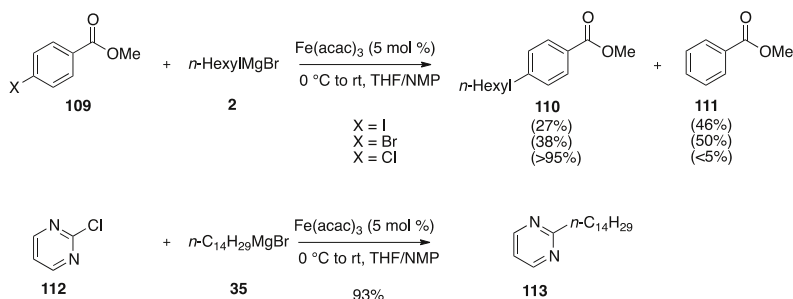
A large variety of couplings between (hetero)aryl chlorides and alkyl Grignard reagents were reported in 2002 using Fe(acac)<sub>3</sub> as a catalyst. Interestingly, the use of aryl iodides and bromides instead of chlorides led to lower yields in the coupling product that can be explained by the formation of a significant amount of dehalogenated compound (Scheme 38) [63, 64] (for an extension of this method to chloro styrenyl derivatives, see [65]) (for an application to the functionalization of corannulenes, see [66]) (for an iron-catalyzed cross-coupling involving 2-bromofuran, see [67]).

The method was applied to the functionalization of heteroaryl chlorides and especially to dichloropurines and pyrimidines, which are intermediates in the synthesis of nucleosides. Worthy of note, the iron-catalyzed cross-coupling was selective towards the most reactive chlorine atom and could be followed by a subsequent Suzuki cross-coupling to afford bis-functionalized *N*-heterocycles (Scheme 39) [68–70] (for other iron-catalyzed cross-couplings involving heteroaryl chlorides, see [71–79]).

Most of the coupling reactions between (hetero)aryl chlorides and alkyl Grignard reagents involved the supposed reprototoxic NMP as a co-solvent. To avoid the use of

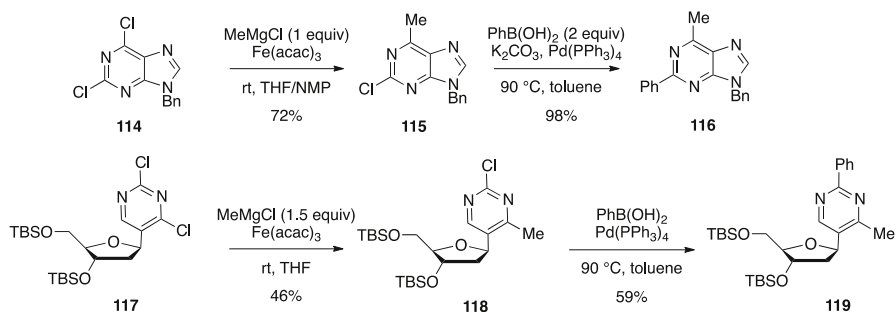
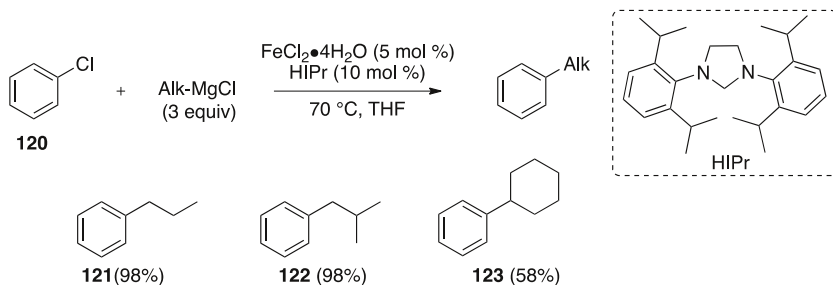
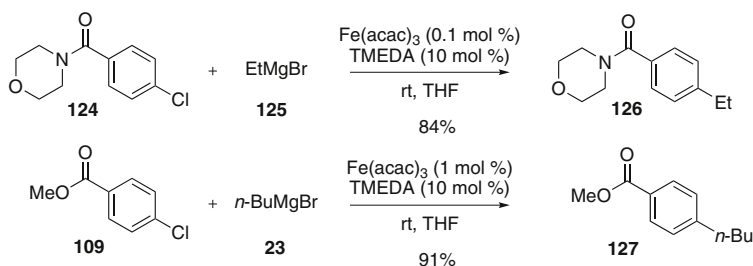


**Scheme 37** Cross-coupling involving a *o*-chloro arylimine



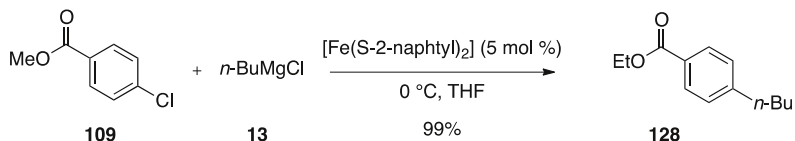
**Scheme 38** Cross-coupling involving (hetero)aryl chlorides



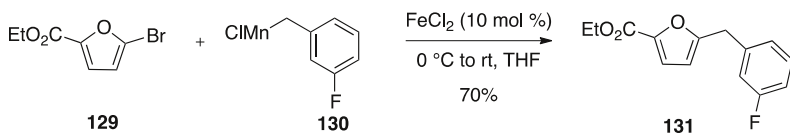
**Scheme 39** Functionalization of dichloropurines and pyrimidines**Scheme 40** NMP-free coupling of chlorobenzene**Scheme 41** Alkylation of aryl chlorides

this additive, several catalytic systems have been developed. In the presence of an NHC ligand (HIPr) and  $\text{FeCl}_2 \cdot 4\text{H}_2\text{O}$ , aryl chlorides were coupled to primary and secondary alkyl Grignard reagents in THF (Scheme 40) [80].

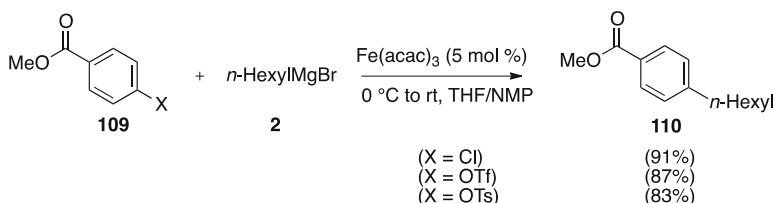
Using a catalytic amount of TMEDA allowed the cross-coupling between aryl chlorides and alkyl Grignard reagents at room temperature with a low catalytic loading of the iron catalyst (0.1–1 mol%). The reaction conditions were tolerant toward the presence of an ester or an amide moiety on the aromatic ring (Scheme 41) [81].



**Scheme 42** Iron thiolate-catalyzed alkylation of an aryl chloride



**Scheme 43** Cross-coupling involving a benzylic organomanganese reagent



**Scheme 44** Coupling involving aryl sulfonates

Cahiez et al. showed that the iron thiolate complex was able to catalyze the reaction between aryl chlorides and *n*-butylmagnesium chloride. The coupling was carried out at 0 °C and delivered the expecting products in high yields (Scheme 42) [22].

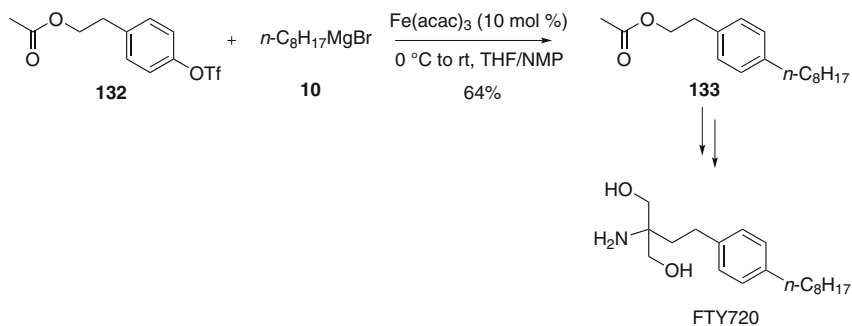
**3.1.1.2 With alkyl organomanganese reagents** Recently, an iron-catalyzed benzylation of (hetero)aryl halides was reported using benzylic manganese chlorides (Scheme 43) [82].

### 3.1.2 Aryl Sulfonates

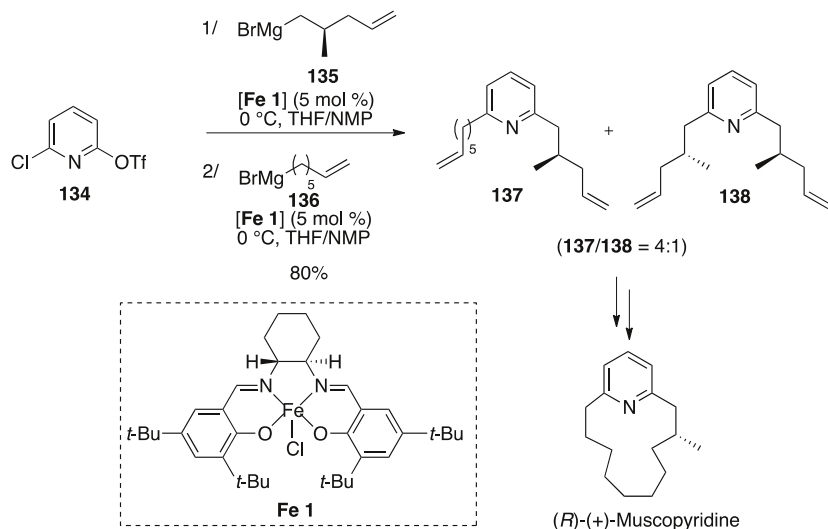
As an alternative to aryl chlorides, aryl triflates and tosylates can be involved in iron-catalyzed cross-coupling with alkyl Grignard reagents and the resulting product was isolated in similar yields (Scheme 44) [63, 64] (for another examples of cross-coupling involving an (hetero)aryl tosylates, see [83, 84]).

The reaction was applied to a scalable synthesis of the immunosuppressive agent FTY720 and 23 mmol (ca. 7 g) of the aryl triflate **132** were transformed into **133** (Scheme 45) [85, 86].

Aryl triflates are more reactive than aryl chlorides under iron-catalyzed cross-coupling conditions and Fürstner et al. took advantage of this difference of reactivity to perform two consecutive cross-couplings on the chloro-sulfonate pyridine **134**. The obtained 2,6-alkyl pyridine was then transformed into muscopyridine, an odoriferous alkaloid (Scheme 46) [87].



Scheme 45 Synthesis of FTY720



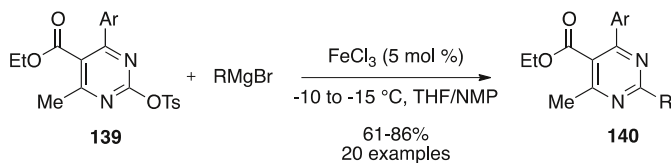
Scheme 46 Key steps in the synthesis of muscopyridine

Recently, a cross-coupling involving heteroaromatic tosylates and alkyl Grignard reagents<sup>2</sup> was studied and a library of tetrasubstituted pyrimidines was prepared (Scheme 47) [88].

### 3.1.3 Other Aryl Derivatives (Sulfamates, Carbamates, and Phosphates)

In 2012, Garg and coworkers developed an iron-catalyzed alkylation of aryl sulfamates and carbamates. Among the catalytic systems tested, the use of  $\text{FeCl}_2$  in the presence of a NHC ligand gave the best result for the coupling. Surprisingly, the addition of substoichiometric amount of  $\text{CH}_2\text{Cl}_2$  was crucial to get the coupling products with good yields but the authors have no explanation concerning its putative role in the process. The reaction was not sensitive to steric hindrance on the aryl sulfamate or carbamate and tolerated the presence of *N*-heteroaromatics. In

<sup>2</sup> Some examples of coupling with aryl Grignard reagents are also reported albeit with moderate yields.



**Scheme 47** Cross-coupling involving an heteroaromatic tosylate

most cases, sulfamates and carbamates exhibited similar reactivity (Scheme 48) [89, 90].

Aryl sulfamates could also be coupled to primary and secondary alkyl Grignard reagents using  $\text{FeF}_3 \cdot 3\text{H}_2\text{O}$  as a catalyst and IPr as a ligand. It is worth mentioning that the use of this iron salt limits the formation of undesired linear product when a secondary Grignard reagent, such as isopropylmagnesium chloride, is involved in the coupling (Scheme 49) (for another example of cross-coupling involving an (hetero)aryl tosylates, see [83, 84]).

Heteroaryl phosphates are also good partners in iron-catalyzed cross-coupling with alkyl Grignard reagents (Scheme 50) [83].

### 3.1.4 Aryl Trimethylammonium Triflates

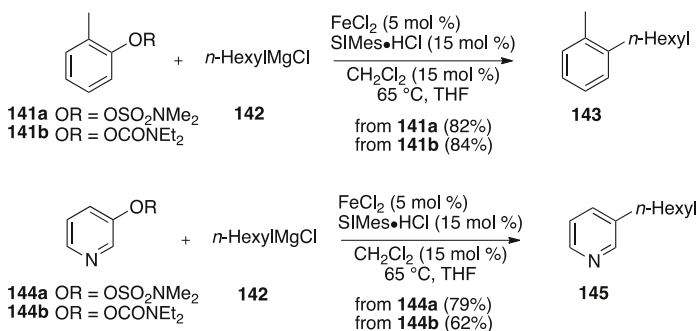
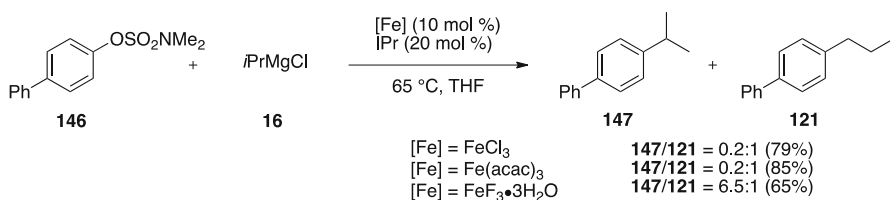
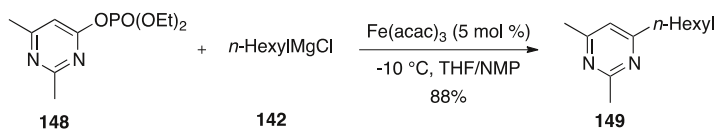
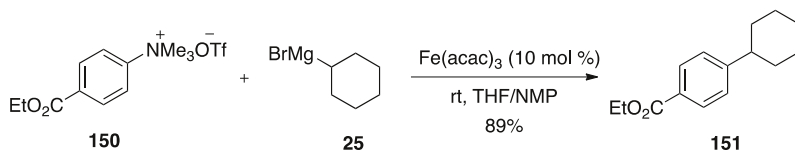
In 2013, an iron-catalyzed cross-coupling between aryl trimethylammonium triflates and alkyl Grignard reagents was reported.  $\text{Fe}(\text{acac})_3$  was selected as the catalyst and the addition of NMP proved beneficial to the reaction, which proceeded smoothly at room temperature (Scheme 51) [91].

## 3.2 Coupling with Aryl Organometallics ( $\text{Csp}^2\text{-Csp}^2$ )

### 3.2.1 With aryl Grignard Reagents

Unsymmetrical biaryl compounds constitute an important class of compounds that find a broad variety of applications not only in the pharmaceutical industry but also in organic materials (see for example [92, 93]) and liquid crystals [94]. Thus, the development of efficient, scalable, and sustainable methods allowing the formation of this motif is highly desirable. In that context, several examples of iron-catalyzed cross-coupling between aryl halides or (pseudo)halides and aromatic organometallics have been developed, the main difficulty being the suppression of the undesired homocoupling side-reaction. Indeed, in the early reports from Kharasch et al., iron salts were shown to induce the homocoupling of Grignard reagents in the presence of aryl halides that played the role of oxidizing agents [95]. In the reported aryl–aryl cross-coupling, (hetero)aryl chlorides are generally preferred over bromides as they are less reactive towards halogen-magnesium exchange.

The first iron-catalyzed aryl–aryl cross-coupling was reported by Fürstner et al. in 2002 using  $\text{Fe}(\text{acac})_3$  in a THF/NMP mixture. Disappointingly, when phenylmagnesium bromide was added to aryl chloride **109**, a low yield of 28 % was

**Scheme 48** Couplings involving aryl sulfamates and carbamates**Scheme 49** Alkylation of aryl sulfamates**Scheme 50** Heteroaryl phosphates as electrophilic partners**Scheme 51** Coupling involving an aryl trimethylammonium triflate

obtained in favor of the coupling product. The major formation of the biphenyl homocoupling product was responsible for the low yield in **152**. In contrast, when the coupling reaction was carried out on 2-chloropyridine, the desired coupling product was isolated with a good yield of 73 % (**Scheme 52**). This difference of behavior between aryl chlorides and heteroaryl chlorides could be explained by a lower oxidizing potential of heteroaryl chlorides that are not able to induce the homocoupling of the Grignard reagent. The reaction was extended to a wide range of heteroaryl chlorides including pyrimidines, pyrazines, or isoquinolines [63, 64]

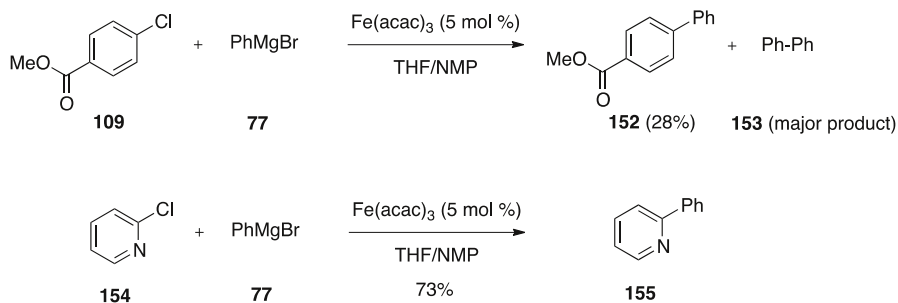
(for other examples of iron-catalyzed cross-coupling between heteroaryl chlorides and aryl Grignard reagents, see [96, 97]) (for an example of iron-catalyzed cross-coupling between heteroaryl sulfamates and aryl Grignard reagent, see Ref. [61]).

In 2012, Knochel et al. reexamined the reaction and found that the use of  $\text{FeBr}_3$  in a mixture of *t*-BuOMe and THF gave good yield in the coupling of 2-chloropyridine with phenylmagnesium bromide. The low-toxic ethereal co-solvent *t*-BuOMe is a good substitute of NMP, particularly for industrial perspectives. The reaction was extended to a variety of functionalized Grignard reagents prepared by LiCl-mediated Mg insertion from the corresponding bromides (Scheme 53) [98] (for the preparation of the functionalized Grignard reagents, see [99]).

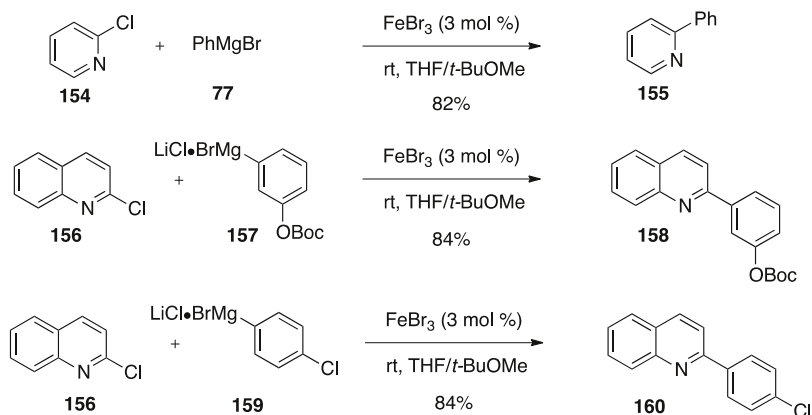
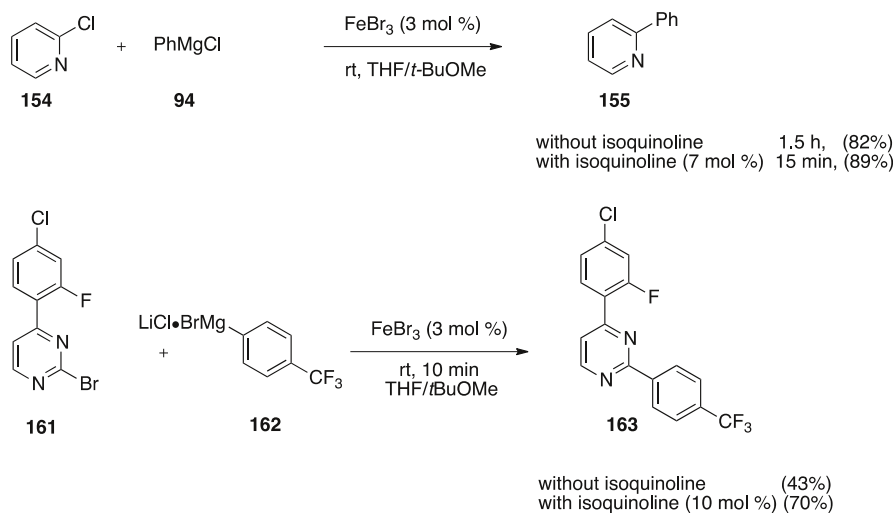
One year later, the same group showed that the addition of a catalytic amount of isoquinoline allowed to increase the reaction rate and improved the yield of coupling that were reluctant under the ligand-free conditions (Scheme 54). The conditions were applied to heteroaryl chlorides and bromides. It could be hypothesized that isoquinoline helps the stabilization of low-valent iron species [100, 101].

An iron-catalyzed cross-coupling between aryl Grignard reagents and chloro-styrene derivatives was reported. The reaction proceeded using  $\text{Fe}(\text{acac})_3$  as a catalyst in a mixture of THF and NMP. However, it was strictly restricted to styrenyl derivatives as in the absence of the double bond, no reaction occurred. The authors hypothesized an olefin coordination of the iron catalyst followed by haptotropic migration along the  $\pi$ -system (Scheme 55) [102].

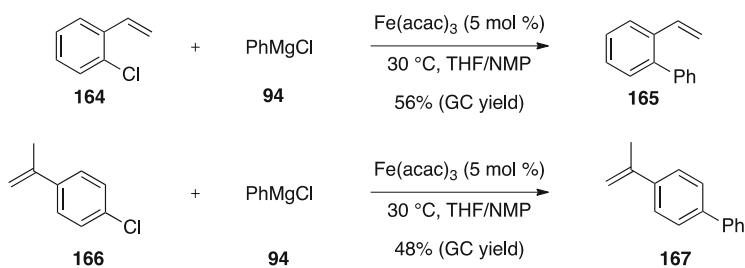
The first general iron-catalyzed aryl–aryl coupling was developed by Nakamura et al. in 2007. They demonstrated that using  $\text{FeF}_3 \cdot 3\text{H}_2\text{O}$  in association with a NHC ligand allowed the suppression of the homocoupling product. The reaction was quite general and delivered the coupling product in good-to-excellent yields. To explain the difference of reactivity between  $\text{FeCl}_3$  and  $\text{FeF}_3$ , the authors suggested that the presence of the strongly coordinated fluoride atoms could prevent the formation of ferrate complex of type  $[\text{Ar}_3\text{Fe}]$ , which could be at the origin of the homocoupling product. The bulky electron-donor NHC ligand not only accelerates the oxidative addition but also could prevent the undesired “over”-transmetalation that delivers  $[\text{Ar}_3\text{M}]$  (Scheme 56) [103, 104].



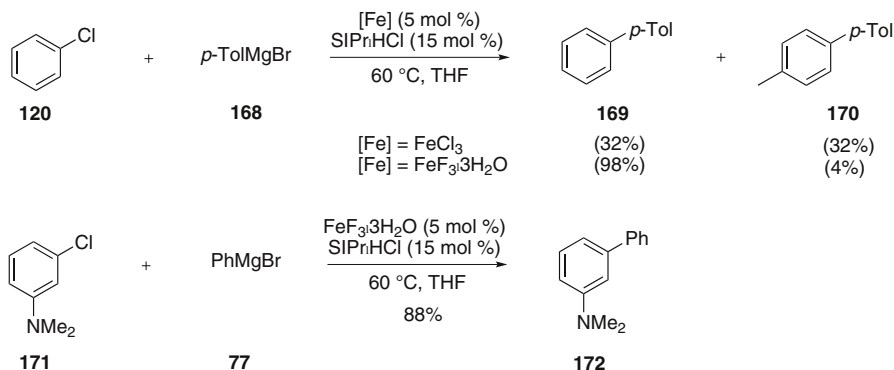
**Scheme 52** First iron-catalyzed aryl–aryl coupling

Scheme 53 FeBr<sub>3</sub>-catalyzed aryl–aryl coupling

Scheme 54 Positive role of catalytic isoquinoline



Scheme 55 Cross-couplings involving chloro-styrenes



**Scheme 56**  $\text{FeF}_3$ -catalyzed aryl–aryl cross-coupling

Cook and coworkers further extended this reaction to the coupling of aryl tosylates and sulfamates with aryl Grignard reagents. Once again, among the iron salt tested,  $\text{FeF}_3 \cdot 3\text{H}_2\text{O}$  gave the best conversion of the starting material in favor of the heterocoupling product (**Scheme 57**) [105].

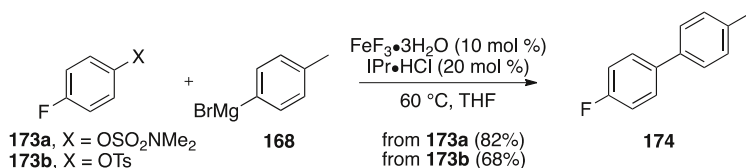
An iron alkoxide should be used instead of  $\text{FeF}_3$  to suppress the formation of the homocoupling product. The presence of the NHC ligand SIPr was crucial and an addition of a catalytic amount of *t*-BuONa proved beneficial. Under these conditions, various aryl and heteroaryl chlorides were efficiently coupled to aryl Grignard reagents (**Scheme 58**) [106].

Due to its reluctance in catalyzing the homocoupling reaction,  $\text{Fe}(\text{OTf})_2$  was identified as a good catalyst in the cross-coupling of aryl chlorides and tosylates with aryl Grignard reagents. As previously, the use of the NHC precursor SIPr·HCl together with a base allowed a good selectivity in favor of the coupling product over homocoupling by-products. An impressive numbers of biaryl motifs were constructed using this efficient method (**Scheme 59**) [107] (for an example of cross-coupling between heteroaromatic tosylates and aryl Grignard reagents, see also Ref. [87]).

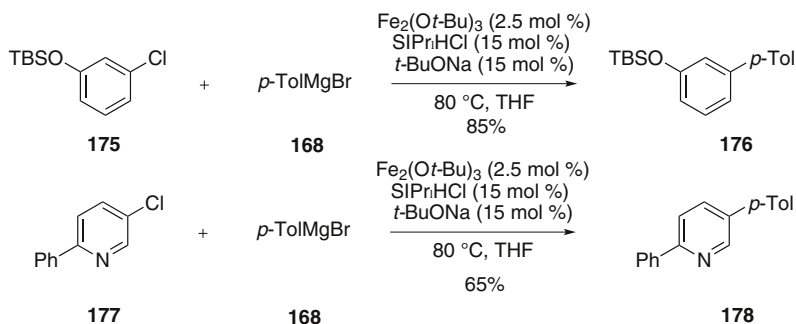
### 3.2.2 With aryl copper reagents

The cross-coupling of non-heteroaromatic aryl chlorides revealed more difficult because of their propensity to induce the homocoupling of the Grignard reagent. To address this issue, less reactive aryl copper reagents were prepared by transmetalation of the corresponding Grignard reagents and involved in an iron-catalyzed cross-coupling with aryl halides. In the presence of  $\text{Fe}(\text{acac})_3$  catalyst, aryl iodides, bromides, and chlorides were converted to the biaryl with a decreasing reactivity. The reaction tolerated a wide range of functional groups including ketones, esters, or nitriles on both partners (**Scheme 60**). The main drawback of this coupling was the required preparation of the aryl copper reagents that needed a stoichiometric amount of copper salt [108, 109].

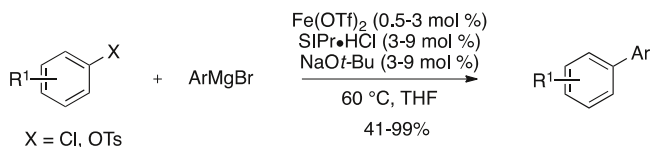
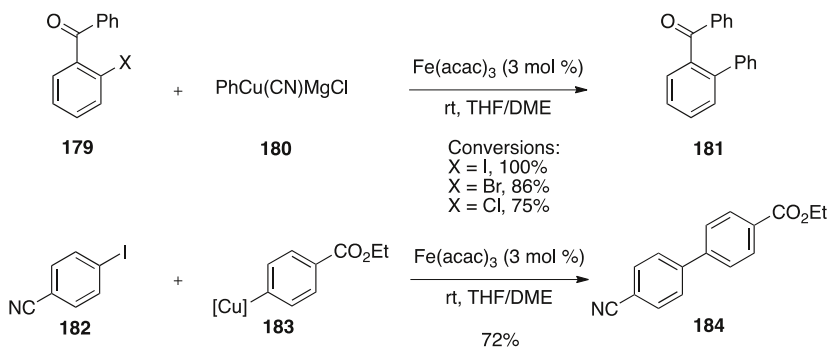




Scheme 57 Arylation of aryl tosylates



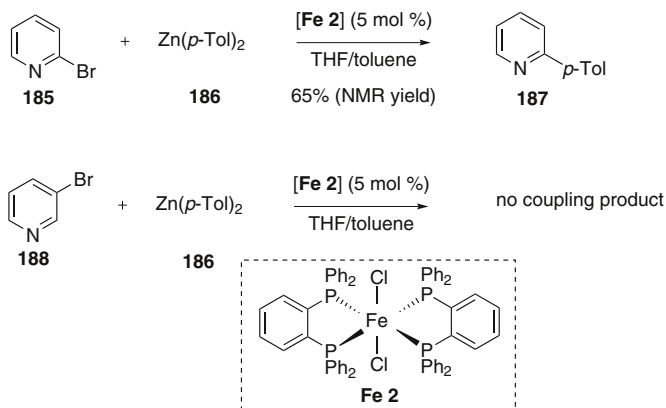
Scheme 58 Use of an iron alkoxide catalyst for aryl-aryl cross-coupling

Scheme 59 Fe(OTf)<sub>2</sub> catalyzed aryl-aryl coupling

Scheme 60 Arylation using aryl copper reagents

### 3.2.3 With arylzinc reagents

A Negishi-type cross-coupling between *N*-heteroaryl halides and diarylzinc reagents was developed using an iron catalyst bearing two bisphosphine ligands, catalyst **Fe**



**Scheme 61** Negishi-type aryl–aryl cross-coupling

2. However, the reaction was limited to 2-halogeno pyridines or pyrimidines and moderate yields in coupling products were obtained (Scheme 61) [110].

### 3.2.4 With tetraarylborates

The same catalyst **Fe 2** was also used in a Suzuki type cross-coupling between 2-bromo pyridines and sodium tetraphenylborate. A diarylzinc reagent was required as an additive in order to form the “true” catalyst of the reaction (Scheme 62) [110] (for another example of iron-catalyzed Ar-Ar Suzuki-type cross-coupling, see [111]).

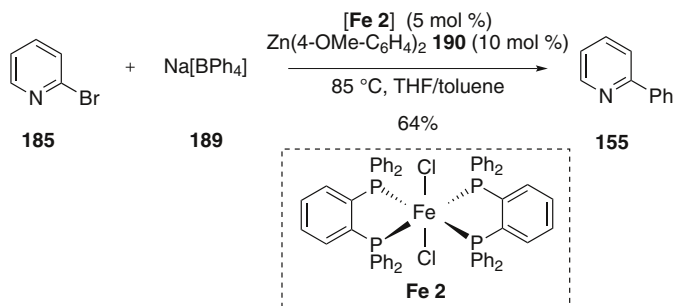
## 4 Alkynyl Halides

### 4.1 With Aryl Organocuprate Reagents (Csp-Csp<sup>2</sup>)

To the best of our knowledge, only one example of iron-catalyzed cross-coupling between an alkynyl halide and an organometallic has been described in the literature. Castagnolo et al. reported that 1-bromoalkynes could be coupled to organocuprate reagents under iron catalysis. The organocuprates were formed in situ by addition of the corresponding Grignard reagents on copper chloride (Scheme 63) [112].

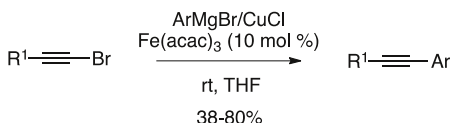
## 5 Activated Alkyl (pseudo)halides

Alkyl electrophiles bearing β-hydrogen atoms have been considered for a long time as unsuitable substrates in metal-catalyzed reactions. Several reasons may explain their reluctance to undergo metal-catalyzed cross-coupling. At first, the C(sp<sup>3</sup>)-X bond is more electron-rich than the C(sp<sup>2</sup>)-X bond rendering the oxidative addition



**Scheme 62** Suzuki-type aryl–aryl cross-coupling

**Scheme 63** Arylation of alkynyl bromides



to a metal center more difficult. In addition, the absence of  $\pi$ -electrons able to stabilize the resulting alkyl metal by interaction with the empty d orbitals species favors side reactions such as  $\beta$ -elimination or hydrodehalogenation. Despite these difficulties, metal-catalyzed cross-couplings involving alkyl halides have known tremendous developments over the past decades, particularly using nickel, cobalt, and iron salts.

## 5.1 Propargylic Derivatives

### 5.1.1 With Alkyl Grignard Reagents ( $Csp^3$ - $Csp^3$ )

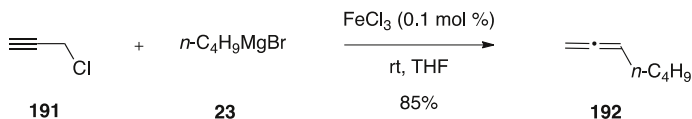
The first examples of iron-catalyzed cross-coupling involving alkyl (pseudo)halides were developed with activated alkyl (pseudo)halides such as propargylic, allylic, or benzylic derivatives.

In the 1970s, a cross-coupling between propargylic chloride and an alkyl Grignard reagent delivering an allene product was described (Scheme 64). A mechanism including an oxidative addition, a transmetalation, a rearrangement toward the allene tautomer and a final reductive elimination was proposed to explain the formation of the observed product [113, 114] (for another example of coupling on propargylic halides, see [115]).

## 5.2 Allylic Derivatives

### 5.2.1 With Alkyl and Aryl Grignard reagents ( $Csp^3$ - $Csp^3$ and $Csp^3$ - $Csp^2$ )

Most of the reported iron-catalyzed cross-couplings involving allylic derivatives are performed on allyl (pseudo)halides such as allyl acetates, allyl phosphates or allyl sulfonyl chlorides. In the presence of  $\text{Fe(acac)}_3$ , primary allylic phosphates were



**Scheme 64** Alkylation of propargyl chloride

efficiently coupled to alkyl and aryl Grignard reagents producing a  $S_N2$  type product with high selectivity (Scheme 65) [116, 117].

The allylation of aryl Grignard reagents using allyl acetate in the presence of a catalytic amount of  $\text{Fe}(\text{acac})_3$  was reported in 2010 [118]. Interestingly, in the presence of the iron salt, the acetate group acts as a leaving group, whereas in the absence of any catalyst, a bis-addition of the Grignard reagent on the carbonyl moiety was observed (Scheme 66).

A desulfonylative cross-coupling involving allylic sulfonyl chlorides was developed to perform the allylation of various Grignard reagents. The reaction proceeded at room temperature delivering the coupling products in good yields. Starting from a mixture of (*E*)- and (*Z*)-**203** resulted in a mixture of the linear and branched product in a 90:10 ratio in favor of the linear compound (Scheme 67) [119].

### 5.3 Benzylic Derivatives

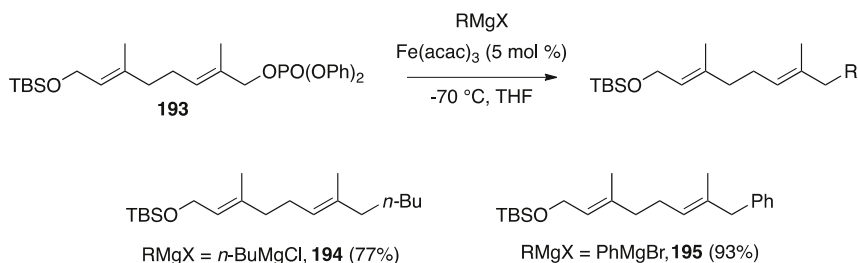
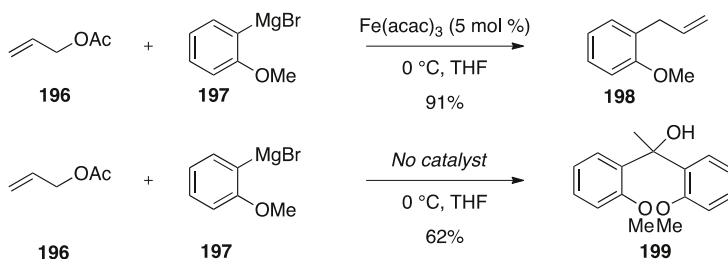
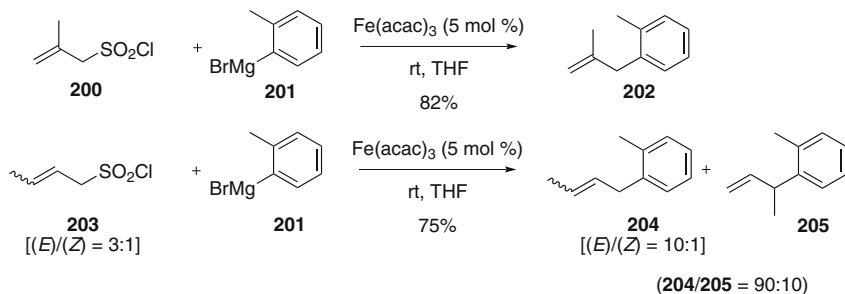
#### 5.3.1 With Aryl Grignard Reagents ( $Csp^3-Csp^2$ )

The coupling of benzylic electrophiles remains problematic because of the competing homocoupling of the halide partner. When a cross-coupling between benzyl chloride and *p*-methoxymagnesium bromide was carried out in the presence of a catalytic amount of  $\text{FeCl}_2$  without any additional ligand, the desired diarylmethane was isolated in a low yield of 31 % while the homocoupling product was the major product (64 %). To circumvent this difficulty, Nakamura et al. screened a panel of iron catalysts bearing different bisphosphine ligands and **Fe 3** was identified as the most efficient one, delivering the coupling product in 71 % yield. However, the formation of the homocoupling product was not completely inhibited and the reaction was sensitive to steric hindrance of the benzyl chloride (Scheme 68) [120].

The iron(III) amine-bis(phenolate) complex **Fe 4** was developed for the cross-coupling between benzylic halides and aryl Grignard reagents resulting in the expected product in variable yields (0–94 %) (Scheme 69) [121].

#### 5.3.2 With Arylzinc Reagents

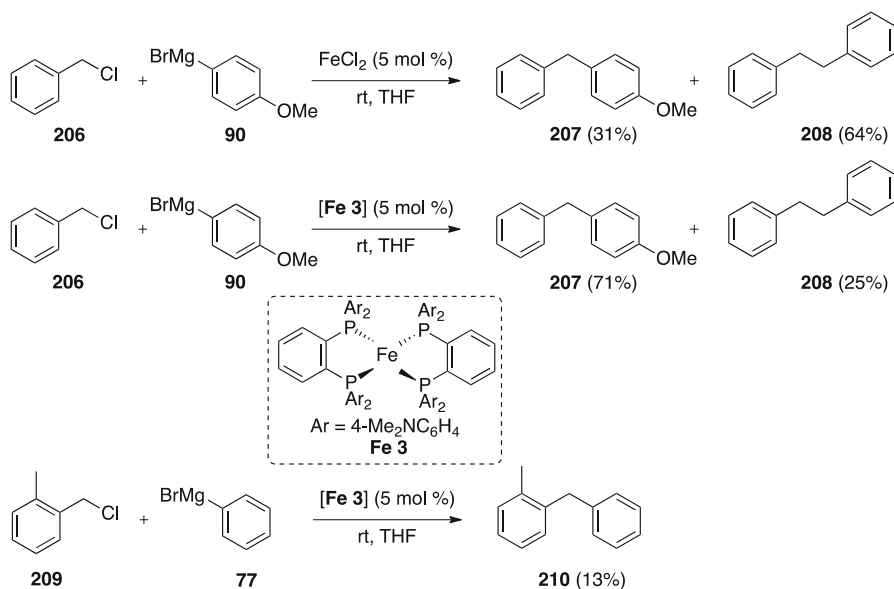
Bedford et al. developed an iron-catalyzed Negishi-type cross-coupling between benzylic halides and diarylzinc reagents. The use of these softer nucleophiles compared to the Grignard reagents allowed to reduce the amount of the undesired homocoupling products. The bis(dpbz) iron(II) complex **Fe 2** exhibited the best

**Scheme 65** Cross-couplings involving allylic phosphates**Scheme 66** Allyl acetate in cross-coupling**Scheme 67** Desulfinylation cross-coupling involving allylic sulfonyl chlorides

performances toward the formation of the coupling product (**Scheme 70**) [122] (for a mechanistic study of this Negishi-type cross-coupling, see [123]) (for a screening of diphosphine ligands in the Negishi-type cross-coupling between benzylic halides and diarylzinc reagents, see [124]).

The main drawback of these reactions is the cost of the bis-phosphine ligand which reduces the attractiveness of the iron complex from an economical point of view. With this idea in mind, the authors developed a less-expensive iron catalyst incorporating two (diphenylphosphino)ethane ligands. This iron complex was able to catalyze a Negishi-type cross-coupling with benzylic halides (**Scheme 71**) [125].

An even simpler monophosphine **214** could be used in a similar Negishi-type cross-coupling involving benzyl bromides and diphenylzinc reagent (**Scheme 72**) [126].



**Scheme 68** Arylation of benzyl chlorides

### 5.3.3 With Tetraarylborates ( $\text{Csp}^3\text{-Csp}^2$ )

The iron catalyst **Fe 2** was used in a Suzuki-type cross-coupling involving benzylic halides and sodium tetraphenylborate in the presence of a catalytic amount of diarylzinc reagent as reducing agent of the iron complex (**Scheme 73**) [110] (for an extension to the coupling of benzyl halides with aryltrialkylborates, tetraaryl aluminates, and tetraarylidates, see [127]).

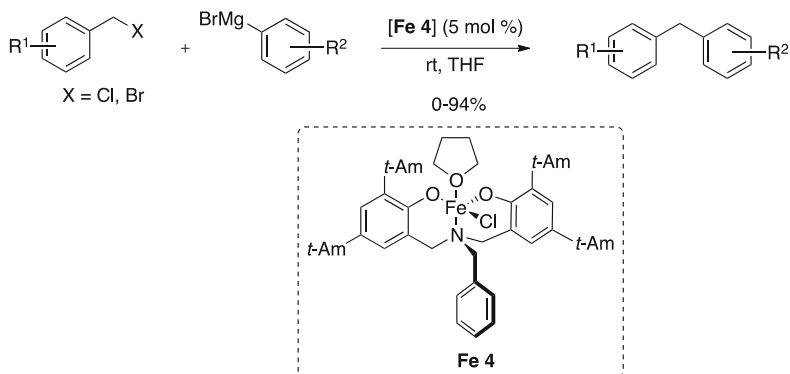
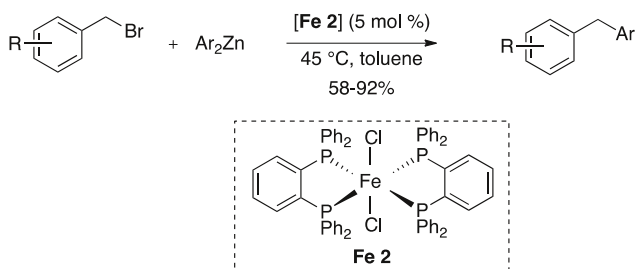
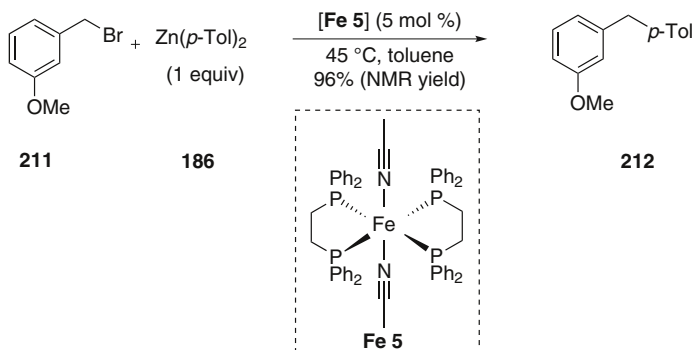
## 6 Non-Activated Alkyl (pseudo)halides

### 6.1 Coupling with Aryl Organometallics ( $\text{Csp}^3\text{-Csp}^2$ )

#### 6.1.1 Alkyl Halides

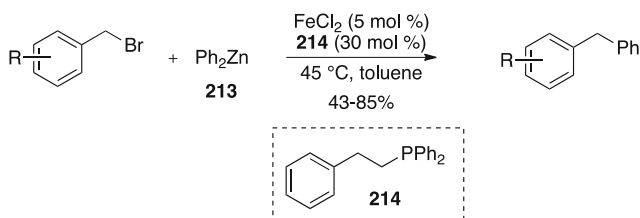
**6.1.1.1 With Aryl Grignard Reagents In the Presence of an External Ligand** The pioneering work for the coupling of non-activated alkyl halides with aryl Grignard reagents was achieved by Nakamura et al. in 2004. By using  $\text{FeCl}_3$  and TMEDA, an efficient arylation of primary and secondary alkyl iodides, bromides, and chlorides was performed (**Scheme 74**) [128] (for an application to the coupling of alkyl halides with biphenyl Grignard reagents, see [129]) ( $\text{Et}_3\text{N}$  and DABCO could also be used as ligands in similar cross-couplings, see [130]).

To reduce the amount of TMEDA, the iron complex  $[(\text{FeCl}_3)_2(\text{TMEDA})_3]$  could be prepared, isolated and stored. It was used successfully in the arylation of primary

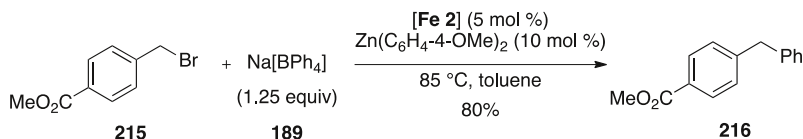
**Scheme 69** Fe 4-catalyzed arylation of benzyl halides**Scheme 70** Fe 2-catalyzed Negishi-type cross-coupling involving benzylic bromides**Scheme 71** Fe 5-catalyzed Negishi-type cross-coupling involving benzylic bromides

and secondary alkyl bromides. Alternatively, the addition of hexamethylenetetramine (HMTA) to the reaction mixture allowed working with a catalytic amount of TMEDA and HMTA (Scheme 75) [131].

As an alternative to diamine ligands, phosphines, and phosphites can be associated to simple iron salt such as  $\text{FeCl}_3$  to induce cross-couplings between alkyl halides and aryl Grignard reagents, however with less efficiency (Scheme 76) [132].



**Scheme 72** Negishi-type cross-coupling of benzylic bromides in the presence of ligand **214**



**Scheme 73** Suzuki-type cross-coupling involving a benzylic bromide

In 2011, Knochel et al. studied the diastereoselective cross-coupling of TBS-protected iodohydrine with aryl magnesium halides. Several catalytic systems were screened and the best results in term of yield and diastereoselectivity were obtained with  $\text{FeCl}_2 \cdot 2\text{LiCl}$  and 4-fluorostyrene. The latter has been already used in nickel-catalyzed cross-coupling and was known to facilitate the reductive elimination. Under these conditions, the *trans*-2-arylated cyclic products were efficiently prepared. It should be noted that a large amount of the iron salt was used (0.85 equiv) (Scheme 77) [133].

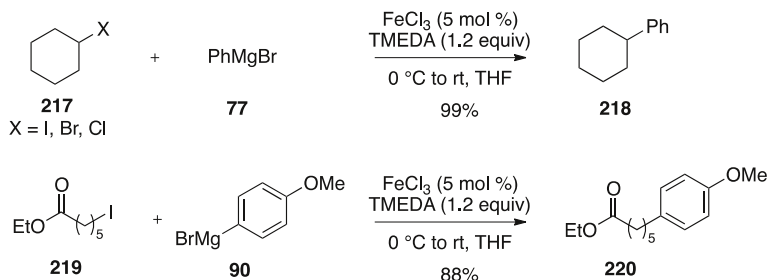
An efficient iron-catalyzed arylation of iodo-azetidines was developed using tetramethylcyclohexane-1,2-diamine (TMCD) as the ligand (Scheme 78, eq 1). When 2,3-disubstituted azetidines were engaged in the coupling a good diastereoselectivity in favor of the *trans*-compound was observed (Scheme 78, eq 2). A few months later, a similar coupling on iodo-azetidines was reported using  $\text{Fe}(\text{acac})_3$  and TMEDA (Scheme 78, eq 3) [134, 135].

In 2010, Daugulis et al. showed that the Grignard reagents could be accessed by selective deprotonation using  $\text{TMPMgCl} \cdot \text{LiCl}$  (TMP = tetramethylpiperidine) as a base. Using this method, heteroaromatic Grignard reagents could be efficiently coupled to alkyl halides in the presence of  $\text{FeCl}_3$  and the *trans*-*N,N'*-1,2-dimethylcyclohexane-1,2-diamine ligand (Scheme 79) [136].

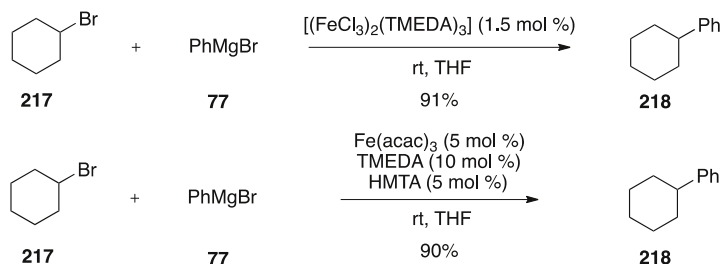
Very recently, Nakamura et al. were the first to develop a chemoselective and enantioselective iron-catalyzed cross-coupling. The reaction was performed between chloroesters and aryl Grignard reagents using  $\text{Fe}(\text{acac})_3$  and an optically active bisphosphine ligand. The reaction was enantioconvergent and the enantiomeric ratio (er) varied from 74:26 to 91:9 (Scheme 80) [137].

The main problem encountered in the absence of any ligand is the precipitation of the low-valent iron species. Bedford et al. proposed that iron nanoparticles could be formed during the reduction of iron by the Grignard reagent and would aggregate in the absence of a stabilizer. To test their hypothesis, polyethylene glycol (PEG), a

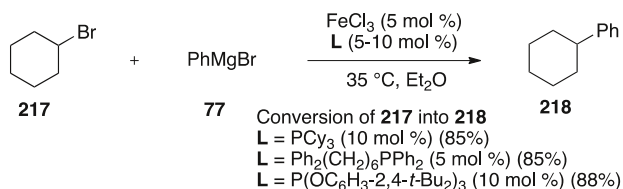




**Scheme 74** First arylation of non-activated alkyl halides



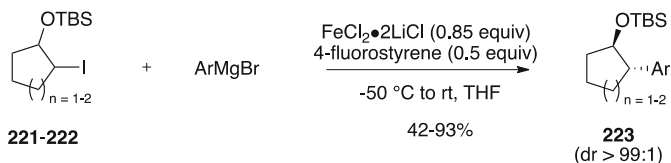
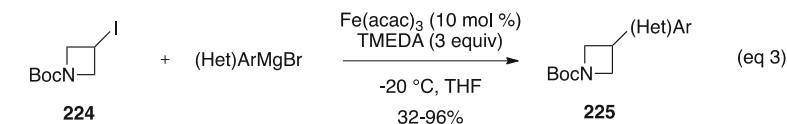
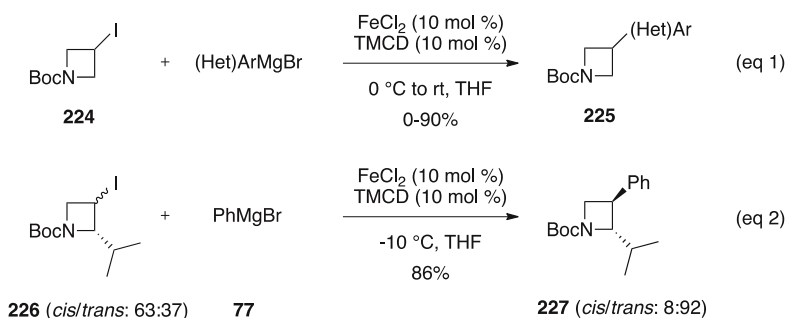
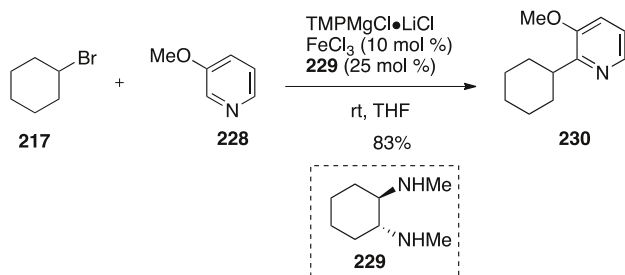
**Scheme 75** Arylation of non-activated alkyl halides using a catalytic amount of ligands



**Scheme 76** Phosphines and phosphites ligands for the arylation of alkyl halides

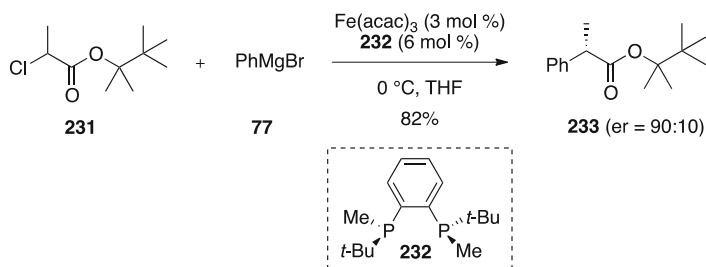
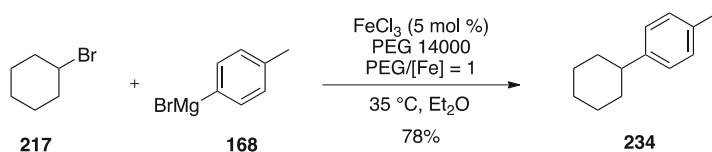
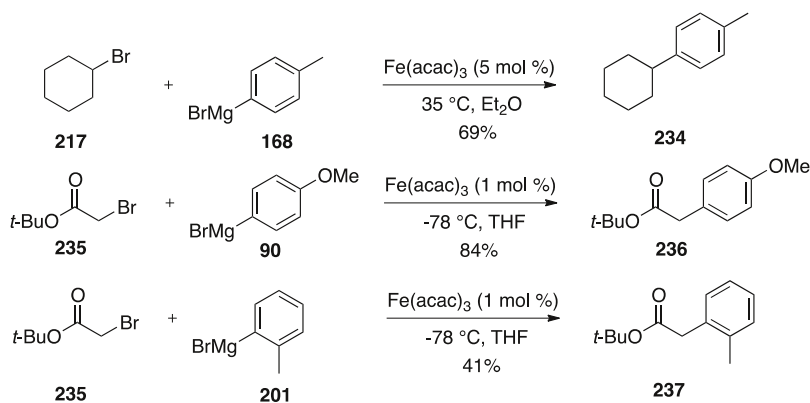
known stabilizing agent of nanoparticles was added to  $\text{FeCl}_3$  prior to the Grignard reagent and alkyl halide. This system was able to catalyze the coupling between alkyl bromides and aryl Grignard reagents (Scheme 81). The observation of samples of the cross-coupling reaction using TEM revealed the presence of iron nanoparticles with size ranging from 7 to 13 nm [138].

*Without any External Ligands* Only few ligandless conditions were developed for the coupling between arylmagnesium bromides and alkyl halides using commercially available iron sources. The use of a catalytic amount of  $\text{Fe}(\text{acac})_3$  in refluxing ether gave the best results and the expected products were delivered in moderate yields. In contrast, when  $\alpha$ -bromo esters were involved as coupling partners, the reaction was carried out in THF at  $-78^\circ\text{C}$  to avoid non-catalyzed addition of the Grignard reagents on the ester moiety. Among the bromo-esters tested, only *t*-butyl

**Scheme 77** Diastereoselective cross-coupling of TBS-protected iodohydrines**Scheme 78** Arylation of iodoazetidines**Scheme 79** Cross-coupling of alkyl halides with in situ prepared Grignard reagents

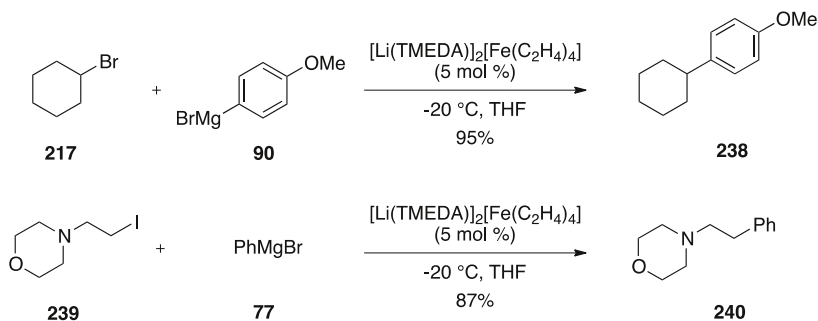
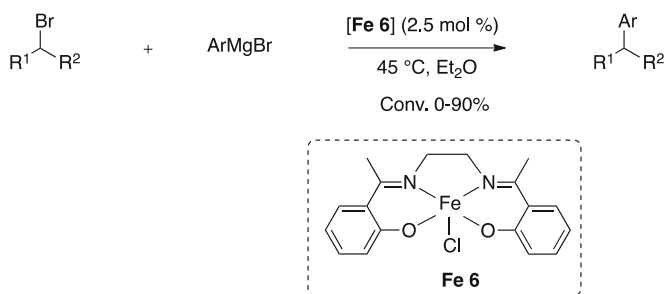
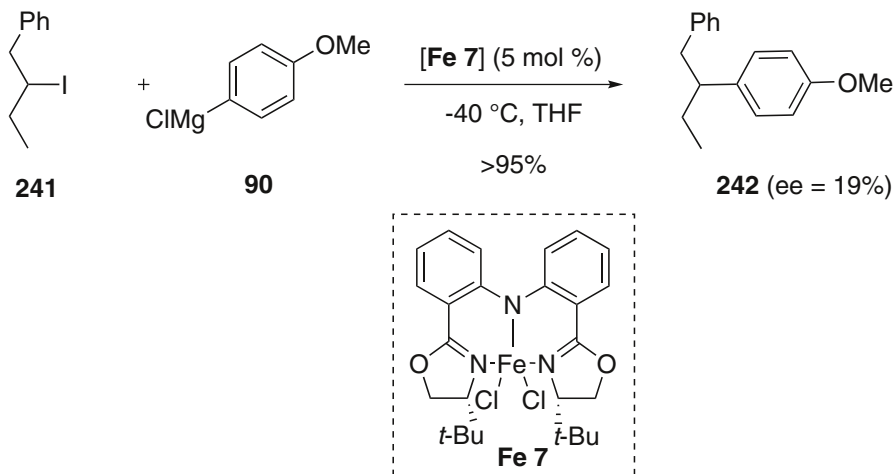
bromo-acetate was suitable and the reaction was sensitive to the steric hindrance of the Grignard reagent (Scheme 82) [139, 140].

During mechanistic investigations concerning iron-catalyzed cross-coupling, Fürstner et al. suspected the involvement of low-valent iron species (see Sect. 7 for more details about the mechanism of iron-catalyzed cross-couplings). To confirm this hypothesis, they evaluated the ferrate complex  $[\text{Li}(\text{TMEDA})]_2[\text{Fe}(\text{C}_2\text{H}_4)_4]$  containing a Fe(-II) iron center in the cross-coupling of a variety of alkyl halides

**Scheme 80** First enantioselective iron-catalyzed cross-coupling**Scheme 81** Iron nanoparticles-catalyzed cross-coupling**Scheme 82** Ligandless conditions for the arylation of alkyl bromides

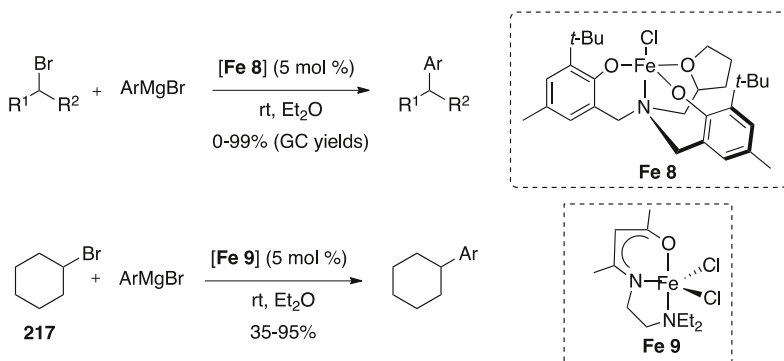
with aryl Grignard reagents. The reaction proceeded at  $-20\text{ }^\circ\text{C}$  delivering the coupling products in good to excellent yields (**Scheme 83**). Based on these positive results, the authors hypothesized that Fe(-II) low-valent iron species could be involved in the mechanism of cross-coupling when Fe(II) or Fe(III) salts are used as precatalysts [141].

Iron (III)-salen complexes have been evaluated in the cross-coupling of alkyl halides with aryl Grignard reagents and, among the iron complexes tested, **Fe 6** showed the best performance (**Scheme 84**). The iron complex **Fe 6** was easily prepared from  $\text{FeCl}_3$  and a Schiff base ligand. Its low hygroscopy makes it easy to handle [142].

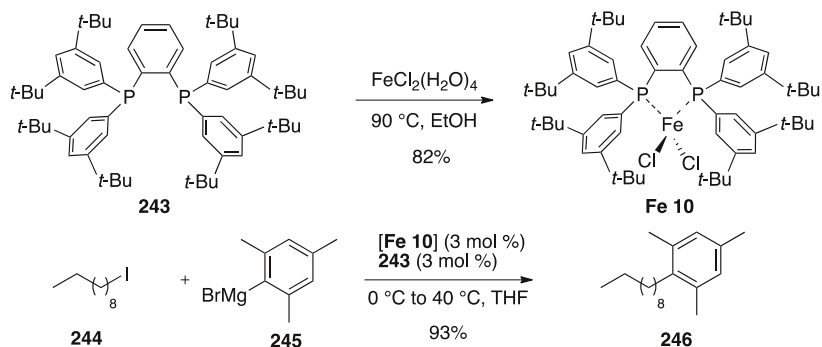
**Scheme 83** [Li(TMEDA)]<sub>2</sub>[Fe(C<sub>2</sub>H<sub>4</sub>)<sub>4</sub>]-catalyzed arylation of alkyl halides**Scheme 84** Fe 6-catalyzed arylation of alkyl bromides**Scheme 85** Fe 7-catalyzed arylation of an alkyl iodide

A chiral iron pincer complex was used in the cross-coupling of alkyl halides with phenylmagnesium chloride. The coupling products were isolated in good yields albeit with low enantioselectivity (**Scheme 85**) [143, 144].

The iron(III) amine-bis(phenolate) complex **Fe 8** as well as an iron(III) complex **Fe 9** possessing a tridentate-aminoketonato ligand were developed for the cross-



**Scheme 86** Fe **8**- and Fe **9**-catalyzed arylation of alkyl bromides



**Scheme 87** Arylation of an alkyl iodide using a sterically hindered Grignard reagent

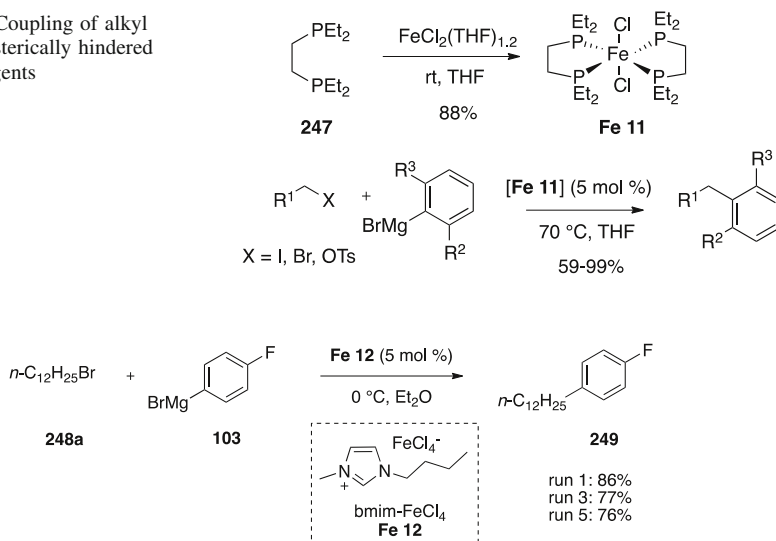
coupling of alkyl halides with aryl Grignard reagents. In both cases, no additional ligand was required and the reactions could be carried out at room temperature furnishing the expected products in modest to good yields (Scheme 86) [145, 146] (an iron-phenolate complex was also used for the activation of the C-Cl bond of  $\text{CH}_2\text{Cl}_2$ , see [147]).

Nakamura et al. synthesized an iron-bisphosphine complex by reaction of  $\text{FeCl}_2(\text{H}_2\text{O})_4$  with 1,2-bis{bis[3,5-di(*t*-butyl)phenyl]phosphine}-benzene (3,5-*t*-Bu<sub>2</sub>-SciOPP) and demonstrated that this iron complex was efficient to catalyze the cross-coupling between alkyl halides and aryl Grignard reagents. Interestingly, it allowed the use of challenging *ortho*-substituted aryl Grignard reagents such as mesitylmagnesium bromide (Scheme 87) [148].

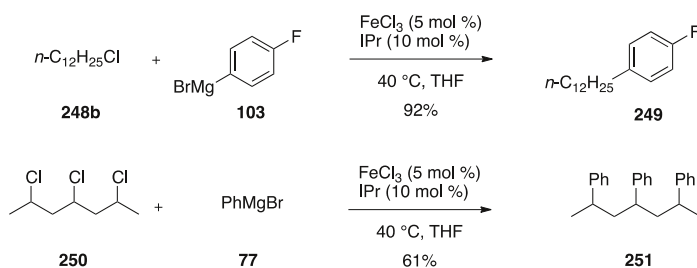
Fürstner et al. developed a more convenient procedure for the coupling of alkyl halides with such sterically hindered Grignard reagents, using the bis(diethylphosphino)ethane iron(II) complex **Fe 11** (Scheme 88) [149].

With the aim of developing a recyclable catalyst, iron-containing ionic liquid were examined as catalyst for the cross-coupling between alkyl halides and aryl Grignard reagents. The ionic liquid butylmethylimidazolium tetrachloroferrate was identified as a promising catalyst for the coupling of a variety of alkyl halides with

**Scheme 88** Coupling of alkyl halides with sterically hindered Grignard reagents



**Scheme 89** Cross-coupling in an iron-containing ionic liquid



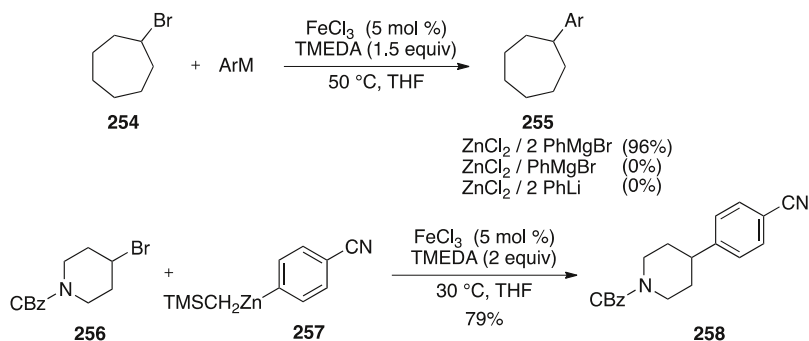
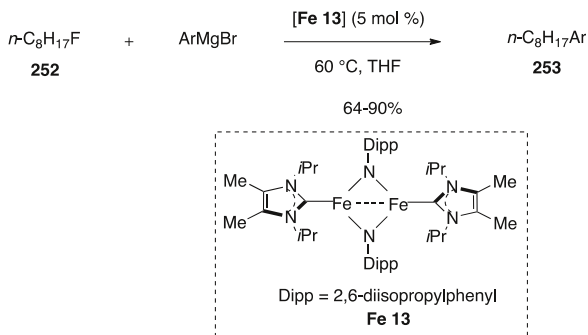
**Scheme 90** Arylation of chloro-derivatives

aryl Grignard reagents. Worthy of note, the catalyst could be recycled and reused without a significant decrease of activity (**Scheme 89**) [150] (for other examples of recyclable ionic iron catalysts in cross-coupling, see [151, 152]).

Most of the examples described above involve the use of alkyl bromides and alkyl iodides whereas alkyl chlorides are known to be less reactive. The use of  $\text{FeCl}_3$  in association with the NHC ligand IPr efficiently catalyzed the arylation of mono- as well as poly-chloroalkanes (**Scheme 90**) [153].

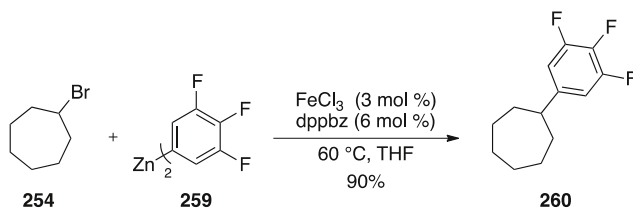
A dinuclear iron complex bearing NHC ligands was identified as a powerful catalyst for the arylation of alkyl fluorides. To the best of our knowledge, it is the first example of iron-catalyzed functionalization of  $\text{C}(\text{sp}^3)\text{-F}$  bond (**Scheme 91**) [154] (for other examples of iron-NHC complexes in cross-coupling, see [155, 156]).

**6.1.1.2 With Arylzinc Reagents** Due to their high reactivity, the access to functionalized Grignard reagents incorporating sensitive electrophilic groups is

**Scheme 91** Arylation of an alkyl fluoride**Scheme 92** Arylation of alkyl bromides using arylzinc reagents

difficult thus limiting the scope of the cross-coupling. To circumvent this difficulty, Nakamura et al. examined the iron cross-coupling of the softer nucleophiles (di)arylzinc reagents with alkyl halides. A diarylzinc reagent (prepared from 1 equiv of ZnCl<sub>2</sub> and 2 equiv of PhMgBr), in the presence of FeCl<sub>3</sub> and TMEDA, reacted smoothly with bromocycloheptane to give the expected coupling product. Using phenylzinc halide prepared from 1 equiv of ZnCl<sub>2</sub> and 1 equiv of PhMgBr, no reaction occurred demonstrating the importance of diarylzinc reagents. Interestingly, the presence of a magnesium salt was crucial as a diphenylzinc prepared from phenyllithium (2 equiv) and zinc dichloride (1 equiv) was totally unreactive. It is worth noting that to avoid the loss of an aryl group, a non-transferable group could be introduced on the zinc atom (Scheme 92) [157].

The coupling of polyfluorinated diarylzinc reagents with alkyl halides was then examined. However, with these nucleophiles, the catalytic system composed of FeCl<sub>3</sub> and TMEDA proved ineffective. The authors suspected a catalyst poisoning caused by fluoride anions generated in situ by a side reaction between the iron complex and the fluoroaromatic groups. Among the screened ligand, 1,2-bis(diphenylphosphino)benzene (dppbz) was the most efficient and selective toward the formation of the coupling product. Using this catalytic system, mono-, di-, and tri-fluoro arylzinc reagents were efficiently coupled to a variety of alkyl halides (Scheme 93) [158].



**Scheme 93** Coupling of a polyfluorinated diarylzinc reagent with bromocycloheptane

A cross-coupling involving diarylzinc reagents and alkyl halides bearing  $\beta$ -fluorines was performed under iron catalysis. The main by-product observed was **263**, which resulted of a deiododefluorination and, using a mixture of TMEDA<sup>3</sup> and diphenylphosphinopropane (dppp) together with FeCl<sub>2</sub>, gave the best selectivity in favor of the coupling product **262** (Scheme 94) [159].

**6.1.1.3 With lithium Arylborates** Nakamura et al. developed an iron-catalyzed Suzuki-type cross-coupling between alkyl halides and lithium arylborates prepared from arylboronic acid pinacol ester and alkyllithium reagents. An iron complex bearing two bulky phosphine ligands was identified as the best catalyst in this reaction and the addition of MgBr<sub>2</sub> was necessary. The coupling was applied to a range of primary and secondary alkyl halides possessing sensitive groups such as esters, nitriles, and ketones (Scheme 95) [160].

A few years later, Bedford et al. demonstrated that the catalytic system could be simplified by using either Fe(acac)<sub>3</sub> or FeCl<sub>2</sub>(dppp), thus avoiding the bulky and expensive diphosphine ligand (Scheme 96) [161].

**6.1.1.4 With Tetraarylaluminates** The same authors also examined briefly the cross-coupling between alkyl halides and arylaluminates using the iron complex **Fe 5** as the catalyst. The coupling products were obtained in good yields but only one out of the four aryl groups was transferred (Scheme 97) [125] (for a cross-coupling between triarylaluminium reagents and alkyl halides using FeCl<sub>2</sub>(dppbz)<sub>2</sub> as catalyst, see [162]).

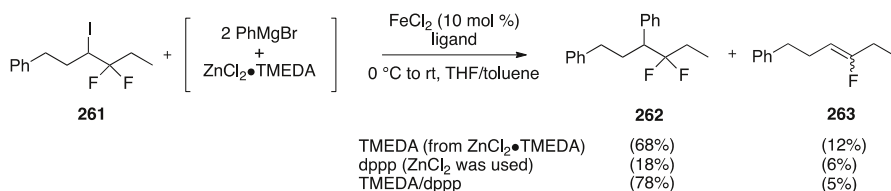
Tetraarylaluminates prepared by transmetalation from the corresponding Grignard reagent and AlCl<sub>3</sub> were efficiently coupled to a variety of halohydrins using the iron catalyst **Fe 14**. A good diastereoselectivity in favor of the *trans*-isomer was generally obtained (Scheme 98) [163].

## 6.1.2 Alkyl pseudohalides

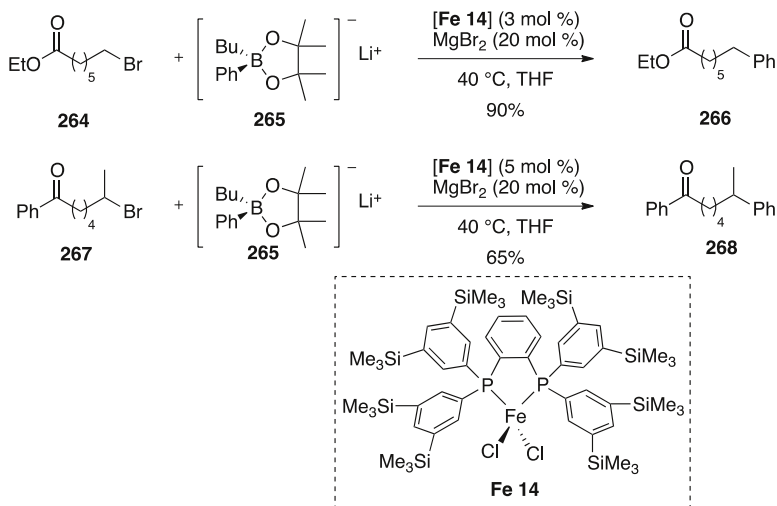
**6.1.2.1 With Aryl Grignard Reagents** Alkyl pseudohalides and particularly sulfonyl chlorides, sulfur and sulfone derivatives could be involved in a desulfinylative iron-catalyzed cross-coupling with aryl Grignard reagents. The desulfinylative arylation of alkyl sulfonyl chlorides was performed using a catalytic

<sup>3</sup> ZnCl<sub>2</sub>-TMEDA was used as a source of TMEDA.

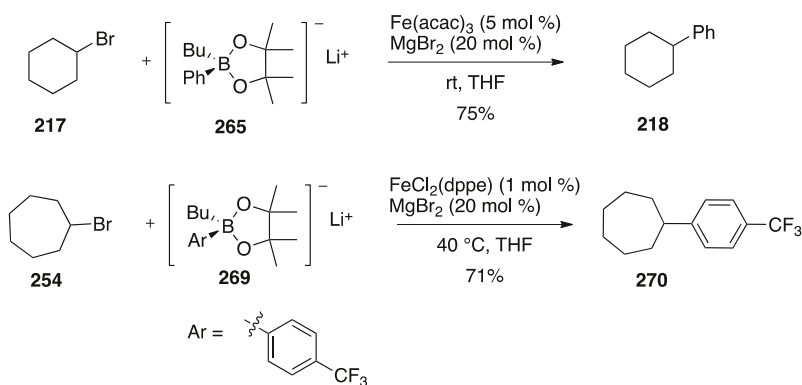




**Scheme 94** Coupling of a diarylzinc reagent with **261** bearing  $\beta$ -fluorines

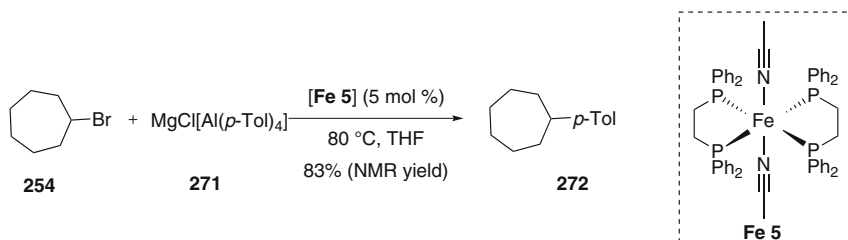


**Scheme 95** Arylation of alkyl bromides using lithium arylborates

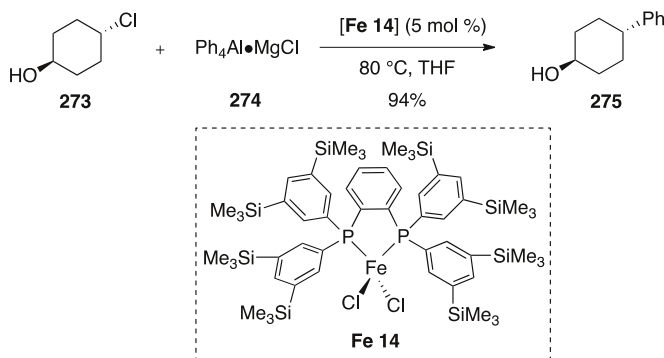


**Scheme 96** Suzuki-type cross-coupling between alkyl halides and lithium arylborates

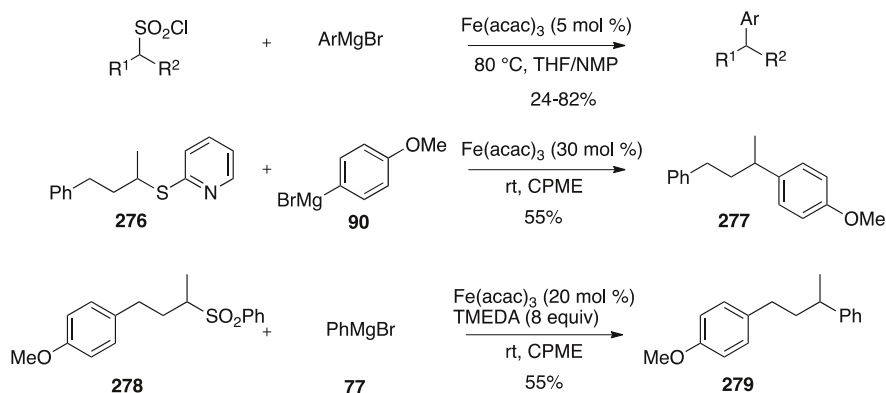
amount of  $\text{Fe}(\text{acac})_3$  in a THF/NMP mixture delivering the products in moderate yields. In 2013, Denmark et al. studied the cross-coupling involving alkyl aryl thioethers or aryl alkylsulfones as the electrophilic partner. Using  $\text{Fe}(\text{acac})_3$  as the



**Scheme 97** Arylation of bromocycloheptane with an organoaluminum reagent

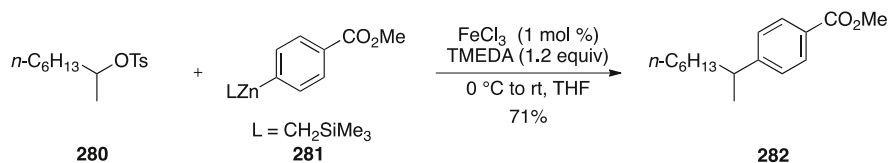


**Scheme 98** Coupling between halohydrins and tetraarylaluminates



**Scheme 99** Desulfinylative iron-catalyzed cross-coupling with aryl Grignard reagents

catalyst, cyclopentyl methyl ether (CPME) was selected as the solvent and no additional ligand was required for the coupling of thio ethers. In contrast, the addition of an excess of TMEDA was necessary to reach satisfactory yields when sulfones were used as starting materials ([Scheme 99](#)) (see Refs. [43] and [164]).



**Scheme 100** Coupling between alkyl tosylates and arylzinc reagents

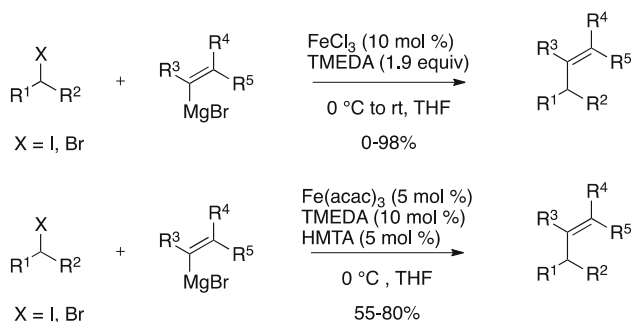
**6.1.2.2 With Arylzinc Reagents** A cross-coupling between alkyl tosylates and arylzinc reagents was developed using  $\text{FeCl}_3$  and TMEDA as the catalytic system (Scheme 100) [165].

## 6.2 Coupling with Alkenyl Organometallics ( $\text{Csp}^3\text{-Csp}^2$ )

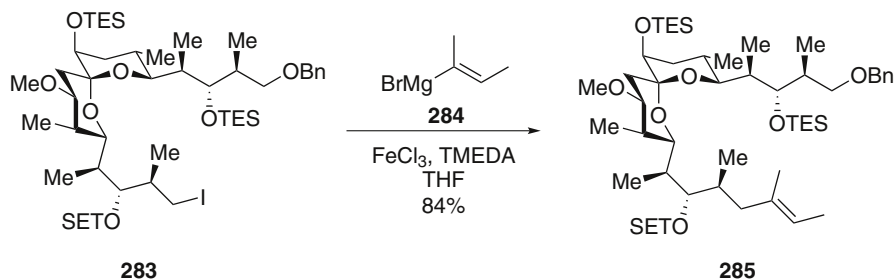
### 6.2.1 With alkenyl Grignard Reagents

The reported examples of iron-catalyzed alkenylation of alkyl halides remain rare in the literature (for a seminal example, see [166]). In 2007, Cossy et al. and Cahiez et al. reported in independent work the cross-coupling between alkyl halides and alkenyl Grignard reagents [167, 168]. In the first article, iron trichloride associated to an excess of TMEDA efficiently promoted the alkenylation of a range of primary and secondary alkyl iodides and bromides. [118a] In the second report, it was demonstrated that the amount of ligand could be lowered by addition of HMTA to the reaction mixture. [118b] The less hygroscopic  $\text{Fe}(\text{acac})_3$  was preferred over  $\text{FeCl}_3$  and both TMEDA and HMTA were introduced in a catalytic amount. This ternary system efficiently catalyzed the cross-coupling between alkyl halides and various alkenyl Grignard reagents (Scheme 101).

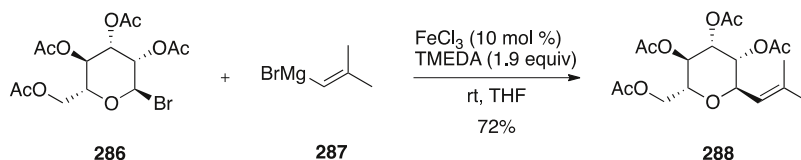
This iron-catalyzed alkenylation was applied in the synthesis of natural products notably in synthetic studies towards the cytotoxic metabolite, spirangien A. In 2013, Rizzacasa et al. performed an iron-catalyzed cross-coupling on a highly functionalized alkyl iodide to introduce the trisubstituted double bond present in spirangien A. The high yield obtained in the coupling product illustrated the high functional group tolerance of the reaction (Scheme 102) [169, 170] (for other examples of applications in the synthesis of natural products, see [171, 172]).



**Scheme 101** Alkenylation of alkyl halides



**Scheme 102** Application to the synthesis of a precursor of spirangien A



**Scheme 103** Alkenylation of a C-bromo mannopyranose

The same catalytic system was applied to the alkenylation of C-bromo mannopyranose within the synthesis of a fragment of amphidinol 3 (**Scheme 103**). A slow addition of a mixture of the Grignard reagent and TMEDA ( $200 \text{ mmol}\cdot\text{h}^{-1}$ ) was essential to get high yield in the coupling product [173].

### 6.2.2 With Alkenylzinc Reagents

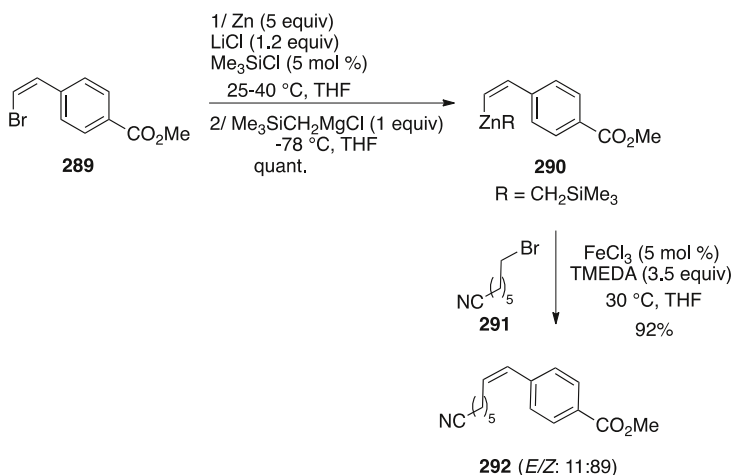
In order to use more functionalized alkenyl organometallics in the cross-coupling with alkyl halides, Nakamura et al. turned their attention towards alkenylzinc reagents. The use of diorganozinc reagents was required and the addition of an excess of TMEDA was crucial to get high yield in the coupling product. A non-transferable alkyl group could be introduced on the zinc atom to prevent the loss of one alkenyl moiety (**Scheme 104**) [174].

### 6.2.3 With Alkenyl Borates

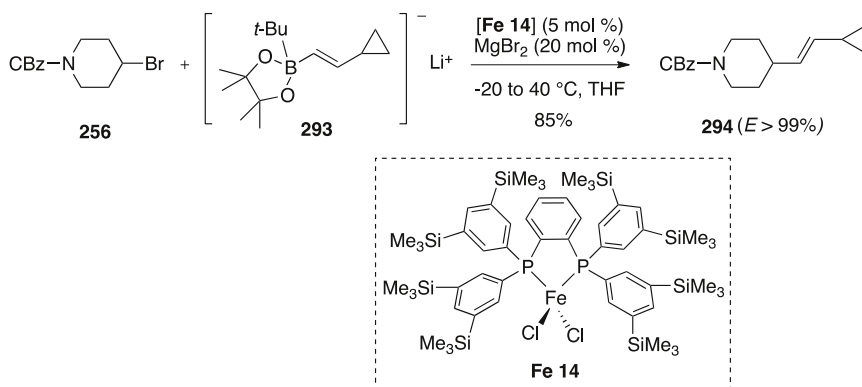
A Suzuki-type cross-coupling involving an alkenyl lithium borate and alkyl halides was reported in 2012. The reaction was catalyzed by the bulky iron complex **Fe 14** and the addition of  $\text{MgBr}_2$  was essential. High yield in favor of the cross-coupling product was obtained and a complete retention of the geometry of the double bond was observed (**Scheme 105**) [175].

## 6.3 Coupling with Alkynyl Organometallics ( $\text{Csp}^3\text{-Csp}$ )

In 2011, Nakamura et al. developed an iron-catalyzed alkylation of non-activated alkyl halides using an iron catalyst possessing a bulky bisphosphine ligand. This “Sonogashira-type” coupling was performed on a range of primary and secondary



**Scheme 104** Alkenylation using alkenylzinc reagents



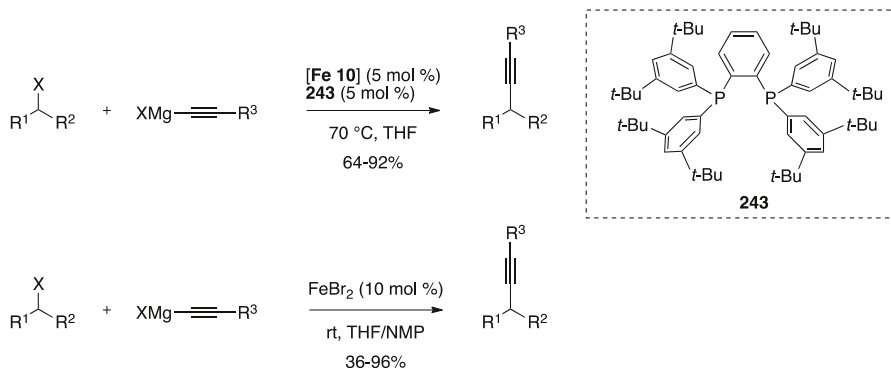
**Scheme 105** Suzuki-type coupling between an alkenyl lithium borate and an alkyl halide

alkyl halides delivering the alkynes in good yields. Few years later, the reaction conditions were simplified by Xu et al. who demonstrated that the cross-coupling could be performed using FeBr<sub>2</sub> in the absence of any ligand in a THF/NMP mixture (Scheme 106) [176, 177].

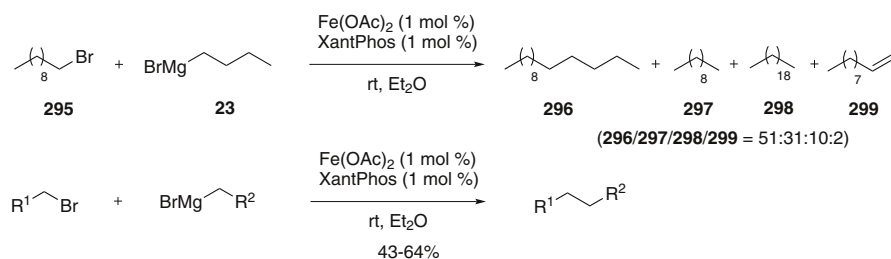
## 6.4 Coupling with Alkyl Organometallics (Csp<sup>3</sup>-Csp<sup>3</sup>)

### 6.4.1 With Alkyl Grignard Reagents

The alkyl-alkyl cross-coupling is particularly difficult because of competitive side reactions such as homocoupling, disproportionation, dehalogenation, or  $\beta$ -elimination. As a consequence, only few examples of iron-catalyzed alkyl-alkyl cross-



**Scheme 106** Alkynylation of alkyl halides

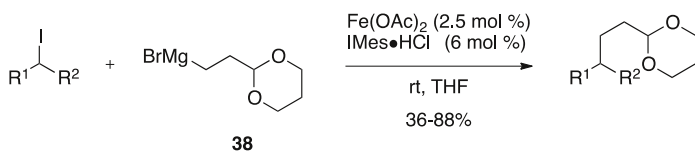


**Scheme 107** Alkyl-alkyl cross-coupling

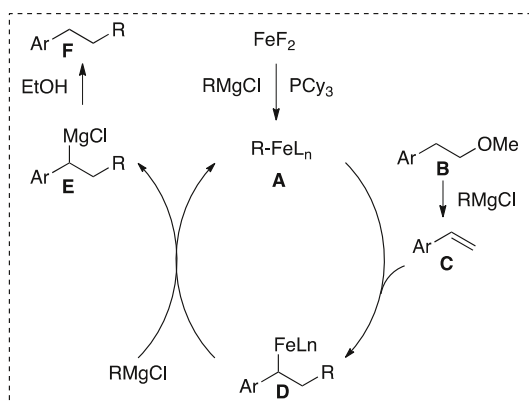
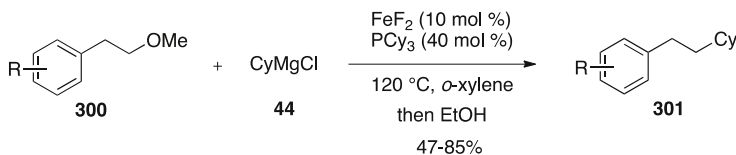
couplings are reported in the literature and further developments and optimization are still needed. The first study concerning the iron-catalyzed ( $\text{sp}^3$ )-( $\text{sp}^3$ ) coupling was reported in 2007 by Chai et al. A panel of ligands was tested for the coupling of bromododecane with *n*-butylmagnesium bromide in the presence of a catalytic amount of  $\text{Fe(OAc)}_2$ . Among the amines, phosphites, and phosphines tested, XantPhos gave the best result toward the formation of the coupling product. However, the formation of the dehalogenated product as well as the homocoupling product could not be totally suppressed. In addition, the reaction is limited to primary alkyl bromides (modest yields of ca. 40 % were obtained starting from secondary alkyl bromides) and only non-functionalized compounds were involved (Scheme 107) [178].

The precedent reaction was improved by replacing the phosphine by a NHC ligand. Variable yields ranging from 36 % to 88 % were obtained in the coupling products and the scope was broadened as functional groups such as acetals, esters, or carbamates on the alkyl iodide as well as on the Grignard reagent were tolerated (Scheme 108) [179].

The cross-coupling between homobenzylic methyl ethers and alkyl Grignard reagents was reported using  $\text{FeF}_2$  and  $\text{PCy}_3$ . To explain the formation of the coupling product, the authors hypothesized an elimination of the methoxy group



**Scheme 108** Alkyl-alkyl cross-coupling in the presence of a NHC ligand

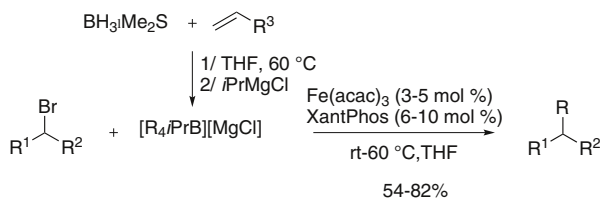


**Scheme 109** Cross-coupling involving a homobenzylic methyl ether

using the Grignard reagent as a base followed by a carbometalation of the resulting alkene **C** with an alkyl-Fe species **A**. A transmetalation of intermediate **D** with the Grignard reagent furnished **E** that could provide the coupling product by quenching the reaction with ethanol (**Scheme 109**) [180] (for an example of an iron-catalyzed cross-coupling of  $\text{CH}_2\text{Cl}_2$ ,  $\text{CHCl}_3$ , and  $\text{CCl}_4$  with alkyl organometallics, see [181]).

#### 6.4.2 With Tetraalkylborates

A catalytic system composed of  $\text{Fe}(\text{acac})_3$  and XantPhos was efficient to promote a Suzuki type cross-coupling between alkyl halides and tetraalkyl borates. The latter were obtained by hydroboration of an olefin using  $\text{BH}_3 \cdot \text{Me}_2\text{S}$  followed by addition of isopropyl magnesium chloride to form the ate complex. Under these conditions, moderate-to-good yields were obtained in favor of the alkyl-alkyl coupling products (**Scheme 110**) [182].



**Scheme 110** Coupling between alkyl bromides and tetraalkylborates

## 7 Acyl Electrophiles

### 7.1 Acyl Chlorides and Acyl Cyanides

#### 7.1.1 With Grignard Reagents

In the absence of any catalyst, the reaction between an acyl chloride and a Grignard reagent generally provides a mixture of ketone and tertiary alcohol resulting from a bis-addition of the Grignard reagent. In 1953, Cook et al. were the first to perform an iron-catalyzed cross-coupling between an acyl chloride and an alkyl Grignard reagent. The addition of a catalytic amount of  $\text{FeCl}_3$  allowed reaching selectively the ketone product (**Scheme 111**) [183].

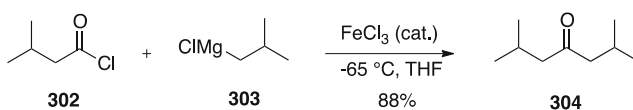
Marchese et al. generalized the reaction to a variety of acyl chlorides and Grignard reagents delivering the ketone product in high yields (**Scheme 112**) [184, 185]. The method was applied to the synthesis of 2,4,6-cycloheptatrienyl ketones [186].

The reaction was further extended to acyl chlorides and Grignard reagents bearing sensitive functional groups such as esters and acetals. Interestingly, a complete selectivity was observed toward the coupling of the acyl chloride with the Grignard reagent when an aryl bromide was present on the substrate (**Scheme 113**) [29] (for a supported catalysis, see [187]).

The reaction was applied to the synthesis of the musk odorant (3*R*)-(Z)-5-muscenone (**Scheme 114**) [188].

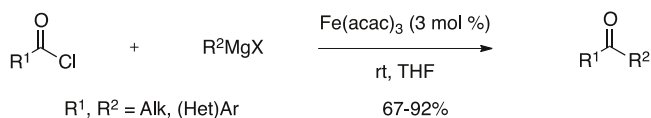
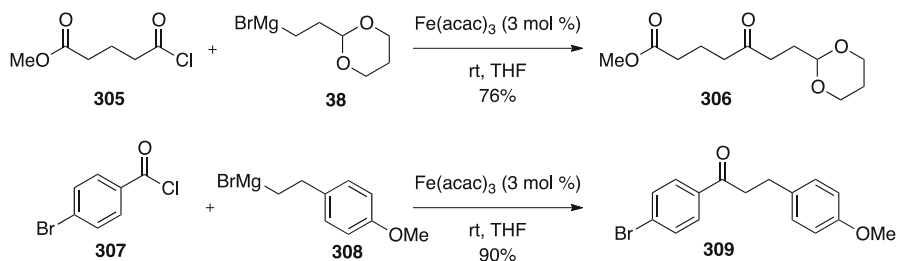
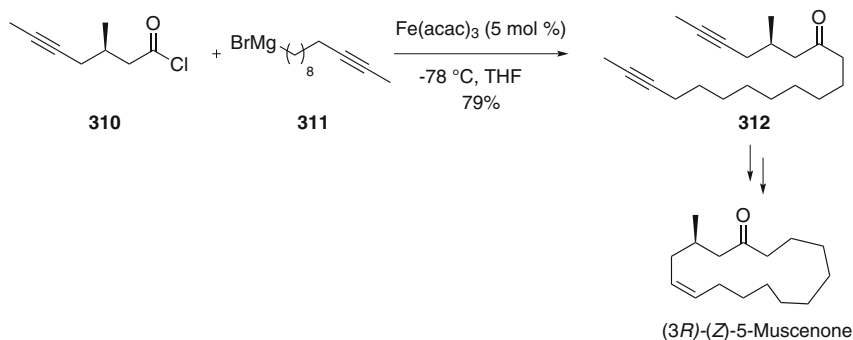
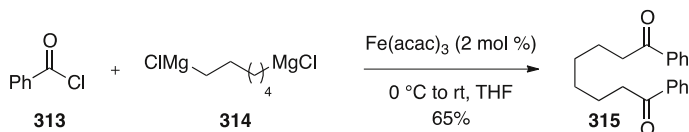
The use of a di-Grignard reagent in a cross-coupling with an acyl chloride furnished the symmetrical diketone (**Scheme 115**) [189].

As an alternative to acyl chlorides, acyl cyanides could be used as partners in iron-catalyzed cross-coupling with Grignard reagents. The use of acyl cyanides instead of acyl chlorides could be advantageous for the preparation of diaryl ketones as the coupling between aryl acyl chlorides and aryl Grignard reagents generally proceeds with moderate yields (**Scheme 116**) [190, 191].



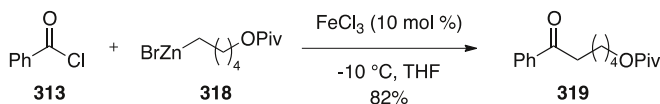
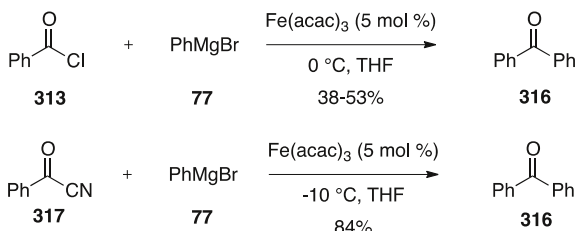
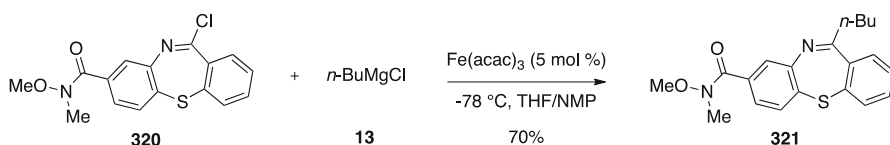
**Scheme 111** Alkylation of an acyl chloride



**Scheme 112** Functionalization of acyl chlorides**Scheme 113** Cross-coupling involving functionalized acyl chlorides**Scheme 114** Application to the synthesis of muscenone**Scheme 115** Coupling of a di-Grignard reagent with an acyl chloride

### 7.1.2 With Alkylzinc Reagents

The iron-catalyzed acylation of organozinc reagents using acyl chlorides has been reported in 1996 (Scheme 117) [192].

**Scheme 116** Arylation of acyl chlorides and cyanides**Scheme 117** Alkylation of an acyl chloride using an organozinc reagent**Scheme 118** Alkylation of an imidoyl chloride

## 7.2 Imidoyl Chlorides

Iron-catalyzed cross-coupling involving imidoyl chlorides and Grignard reagents have been developed. The cross-coupling was carried out in a THF/NMP mixture in the presence of a catalytic amount of  $\text{Fe(acac)}_3$  and tolerated several functional groups including esters and Weinreb amides (Scheme 118) [193].

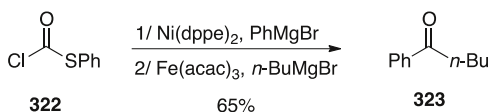
## 7.3 Thioesters

Thioesters were also identified as good partners in iron-catalyzed cross-coupling reaction with alkyl and aryl Grignard reagents. Particularly, *S*-phenyl carbonochloridothioate could be involved in two successive selective cross-couplings involving a nickel salt and then an iron salt as catalysts (Scheme 119) [194, 195].

## 8 Mechanism Investigations

Since the pioneering work of Kochi [13–16], the mechanism of iron-catalyzed cross-coupling has been thoroughly investigated. Several points have been debated such as the oxidation state of the active catalyst, the nature and the order of the elementary steps, the presence of radical intermediates, or the role of the ligand. Depending on the nature of the two partners, different pathways could be involved.

**Scheme 119** Successive cross-couplings involving a chloro-thioester



In addition, the study and identification of the active in situ generated catalysts is rendered difficult by their high sensitivity and short lifetime. In this section, a brief overview of the works that have been done to address these different questions is given. For the sake of clarity, we tried to divide this section into four main parts even if some results could be interconnected.

## 8.1 Oxidation State of the Active Catalyst in Kumada-Type Cross-Coupling [196]

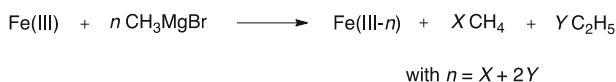
### 8.1.1 Iron-Catalyzed $Csp^2$ - $Csp^3$ Cross-Couplings

The first question that arises when considering iron-catalyzed cross-coupling is the nature of the active catalyst. Indeed, Fe(III) or Fe(II) salts are generally employed as commercially available and bench stable pre-catalysts but it is well accepted that a preliminary reduction of these iron salts induced by the Grignard reagent is required to initiate the catalytic cycle. The nature of the resulting low-valent iron complex, whose oxidation state should be inferior or equal to one, has been the object of several debates.

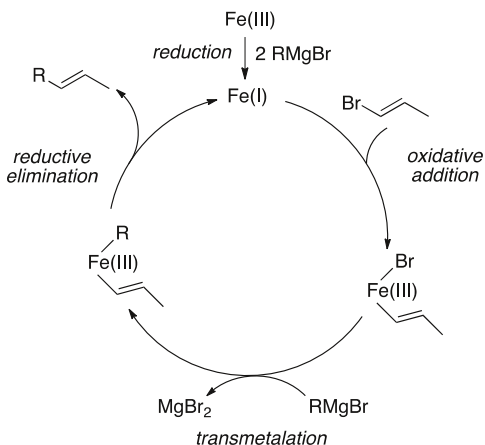
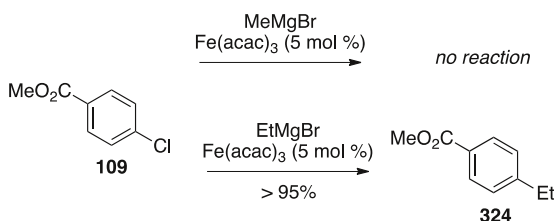
In the 1970s, Kochi et al. were the first to examine the mechanism of iron-catalyzed cross-coupling between alkenyl halides and alkyl Grignard reagents [16]. To determine the oxidation state of the active catalyst, they studied the reaction between Fe(III) salts and methylmagnesium bromide that should proceed according to the equation presented in [Scheme 120](#). By using GC analysis, they measured the amount of methane and ethane formed and deduced the  $n$  number. This experimental investigation led them to postulate the formation of a Fe(I) species ( $n = 2$ ). However, the possible formation of a Fe(0) was not completely excluded.

Inspired by the mechanism proposed for nickel-catalyzed Kumada cross-coupling, they hypothesized the pathway depicted in [Scheme 121](#) that included an oxidative addition of the alkenyl halide to the reduced iron center followed by a transmetalation and a reductive elimination. However, they clearly precised that this mechanism was a basis for discussion and that deeper investigations were needed [16, 197–199].

In the cross-coupling between aryl chlorides and Grignard reagents, Fürstner et al. observed a marked difference of reactivity between methylmagnesium bromide and ethylmagnesium bromide. When methylmagnesium bromide was used,



**Scheme 120** Reduction of Fe(III) by  $\text{CH}_3\text{MgBr}$

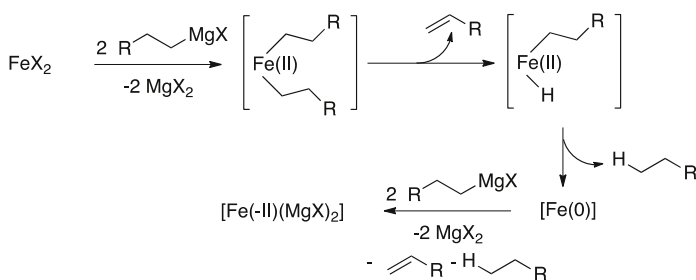
**Scheme 121** Hypothesized mechanism by Kochi et al.**Scheme 122** Difference of reactivity between MeMgBr and EtMgBr

no reaction occurred whereas the coupling product was delivered in quantitative yield in the presence of ethylmagnesium bromide (Scheme 122) [200].

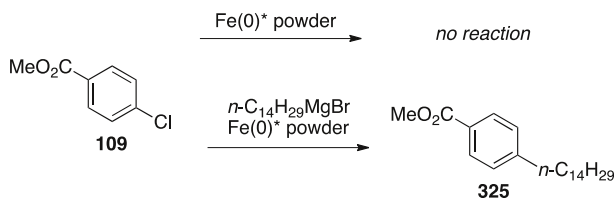
This difference was attributed to the absence of  $\beta$ -hydrogens on methylmagnesium bromide and two pathways were proposed according to the nature of the Grignard reagents. According to a previous work concerning the formation of “inorganic Grignard reagents”, [201, 202] four equivalents of ethylmagnesium bromide could react with a Fe(II) salt to give the new iron species  $[\text{Fe}(\text{MgX})_2]$ . In this species, iron centers are connected to the magnesium centers via fairly covalent interactions to form small clusters and the iron center possesses the formal oxidation state (-II) (Scheme 123). Owing to its high nucleophilic character, this non-stabilized Fe(-II) species is able to oxidatively add to aryl halides [203] and the authors hypothesized that Fe(-II) could be the active catalyst of the cross-coupling [38, 143].

To support the involvement of this Fe(-II) species, a reaction between aryl chloride **109** and a highly activated Fe(0) powder was tested. No insertion was observed whereas when an excess of an alkyl Grignard reagent was added to the Fe(0) powder, the coupling product was formed (the yield in **325** was not mentioned) (Scheme 124) [63, 64, 200].

To bring an additional experimental evidence, the Fe(-II) ferrate complex  $[\text{Li}(\text{TMEDA})_2][\text{Fe}(\text{C}_2\text{H}_4)_4]$  (**Fe 15**) was prepared as a mimic of  $[\text{Fe}(\text{MgX})_2]$ . It was successfully used as a catalyst for the coupling between aryl halides and alkyl



**Scheme 123** Formation of a Fe(-II) species



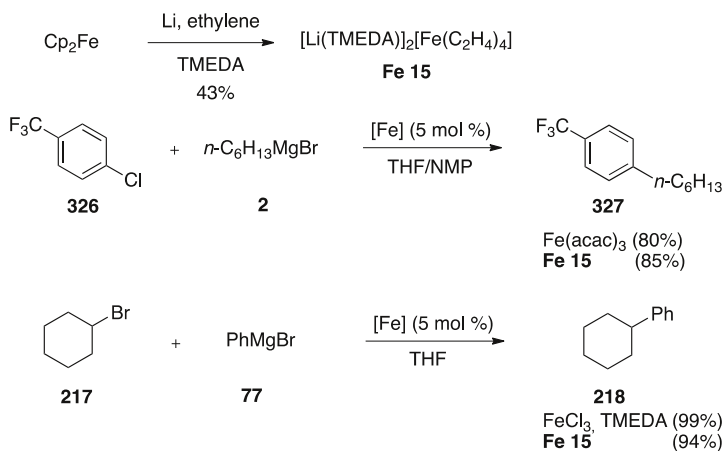
**Scheme 124** Cross-coupling using Fe(0)\* powder as the catalyst

Grignard reagents and for the arylation of alkyl halides with aryl Grignard reagents demonstrating that this Fe(-II) species can be able to enter into the catalytic cycle (Scheme 125) [141, 200].

The mechanism depicted in Scheme 126 including an oxidative addition, an alkylation and a reductive elimination was proposed.

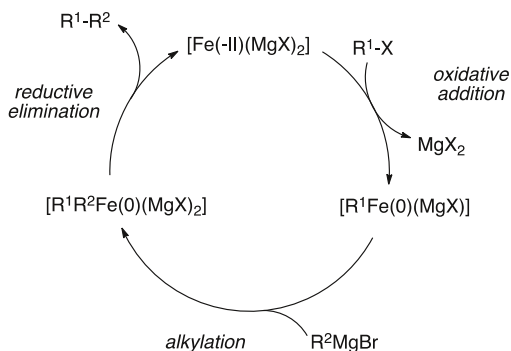
When using Grignard reagents that do not possess  $\beta$ -hydrogens such as MeMgBr or PhMgBr, an organoferrate complex is supposed to be formed [143].

With the objective to reconcile the two different scenarios proposed by Kochi et al. [13–16] and by Fürstner et al. [141, 200] Norrby and coworkers re-examined the iron-catalyzed cross-coupling between aryl chlorides or triflates and alkyl Grignard reagents [204]. At first, they studied the reaction between an aryl chloride and an increasing amount of  $C_8H_{17}MgBr$  in the presence of an iron salt by titrating the starting material, the coupling product and octane. This plot allowed them to highlight the existence of three phases: an initiation phase corresponding to the reduction of the iron salt, a linear phase when the coupling occurred and a deactivation phase. They next proceeded to a Hammett study using several substituted aryl triflates as electrophilic partners. They showed that electron-withdrawing groups on the aryl triflate strongly accelerated the reaction and a Hammett constant of  $\rho = +3.8$  was determined. This strongly positive  $\rho$  value indicated that a negative charge is created on the aromatic ring during the transition state of the oxidative addition. Two catalytic cycles were envisaged (Scheme 127): the first one (pathway a) was the one proposed by Kochi et al., including an oxidative addition followed by a transmetalation and a final reductive elimination.



**Scheme 125** [Li(TMEDA)<sub>2</sub>][Fe(C<sub>2</sub>H<sub>4</sub>)<sub>4</sub>]-catalyzed cross-coupling

**Scheme 126** Hypothesized mechanism by Fürstner et al.



**Scheme 127** Two possible pathways for iron-catalyzed cross-coupling

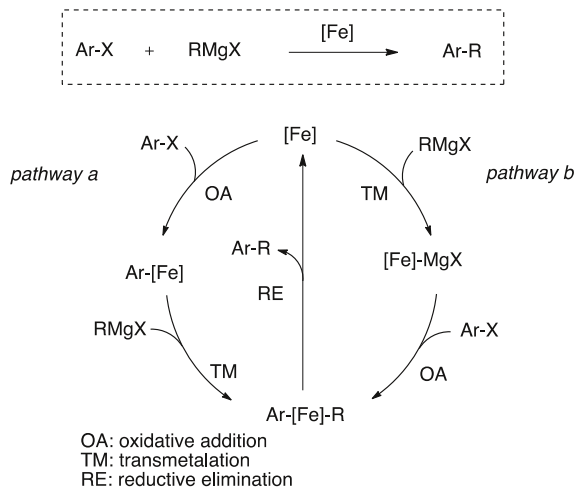


**Table 1** Free energies of the reductive elimination step

| PhCl + EtMgBr $\xrightarrow{[\text{Fe}]}$ Ph-Et |                        |                     |                              |
|---|------------------------|---------------------|------------------------------|
| [Fe]  | Ox. state <sup>a</sup> | $\Delta G$ (kJ/mol) | $\Delta G^\ddagger$ (kJ/mol) |
| FeMg  | (-II)                  | 195                 | –                            |
| FeMgCl  | (-I)                   | 94                  | –                            |
| Fe  | (0)                    | 30                  | 191                          |
| FeCl  | (+1)                   | –181                | 10                           |

<sup>a</sup> Oxidation state of Fe after reductive elimination

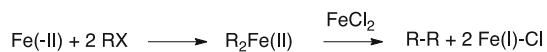
In the second one (pathway b), the transmetalation occurred first, followed by oxidative addition and reductive elimination.

Finally, Norrby et al. have performed computational studies to determine the oxidation state of the active iron catalyst. Four active catalysts were postulated whose oxidation ranged from Fe(-II) to Fe(I) and a model reaction between phenyl chloride and ethyl magnesium chloride was selected. To determine the oxidation state of the active catalyst, the authors focused on the free energies of the reductive elimination, which is the common step to the two possible catalytic cycles proposed. In the presence of Fe(-II) and Fe(-I) catalysts, the reductive elimination revealed to be very endergonic making these oxidation states thermodynamically unfavorable. To differentiate the Fe(II)/Fe(0) cycle from a Fe(III)/Fe(I) cycle, the activation barrier for the reductive elimination was calculated and a very low  $\Delta G^\ddagger$  was obtained for the Fe(III)/Fe(I) couple validating the initial hypothesis of Kochi et al. (Table 1) [205].

To explain the successful results of the Fe(-II) pre-catalyst in the cross-coupling described by Fürstner et al., the authors proposed that a double oxidative addition of the halide to the Fe(-II) center could occur giving a  $\text{R}_2\text{Fe(II)}$  species that could combine with another Fe(II) salt to release a Fe(I) species (Scheme 128).

In contrast, it was not possible to decide between the “oxidative addition first” and the “transmetalation first” pathways using calculations as very tiny differences of free energy were obtained. The authors hypothesized that the two modes could be operating depending on the concentration of the different partners. In both scenarios, the oxidative addition would be the rate-limiting step.

In a subsequent article, the same group performed a competitive Hammett study for the cross-coupling between cyclohexyl bromides and *p*-substituted aryl Grignard reagents [206]. A moderate correlation was found between the relative rate ( $\log(k_{\text{rel}})$ ) and the  $\sigma$  value and an estimated  $\rho$  value of -0.5 was calculated. This negative value showed that Grignard reagents bearing electron-donating substituents were more reactive in the cross-coupling. As previously, two different pathways (“oxidative addition first” or “transmetalation first”) could be operative and the authors hypothesized that the mechanism may differ according to the

**Scheme 128** Hypothetic role of the Fe(-II) species in cross-coupling

nucleophilicity of the Grignard reagents justifying the difficulties encountered during the Hammett plot.

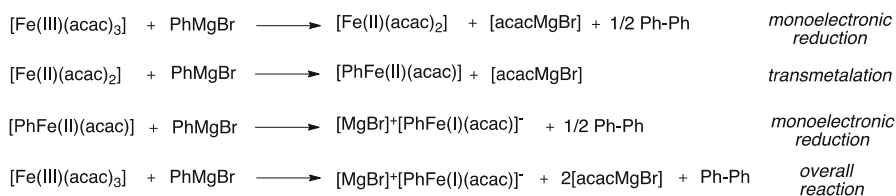
Based on DFT calculations, the same group suggested that an atomic transfer process could be lower in energy compared to a classical oxidative addition. However, their calculations were performed on a specific iron alkoxide catalyst and the energy levels strongly depend on the number of solvent molecules coordinated to the iron center [207].

The paramagnetic character of the iron species formed during the cross-couplings made difficult the collection of experimental evidences notably using spectroscopic methods. Bauer et al. used X-ray absorption spectroscopy to determine the nature of the active catalyst [208]. XANES (X-ray absorption near edge structure) experiments performed on  $\text{Fe}(\text{acac})_3$  in the presence of an increasing amount of  $\text{PhMgCl}$  (0–4 equiv) led to the hypothesis of a Fe(I) center. In addition, they demonstrated that only 3 equiv of the Grignard reagent were necessary to access the active catalytic species. This result was confirmed by a quantitative analysis (GC) of the biphenyl product resulting from the reduction of iron by the Grignard reagent. EXAFS (extended X-ray absorption fine structure) were also carried out to get some insights concerning the structure of the active iron species. The formation of Fe(I) clusters was suggested and the existence of a  $[\text{Fe}(\text{I})\text{-Ph}]_n$  active species was proposed rather than the usual  $[\text{Fe}(\text{I})\text{-X}]$  complex. Finally, a classical catalytic cycle including an oxidative addition, a transmetalation and a reductive elimination was suggested (A Fe(II)/Fe(0) scenario was also proposed elsewhere, see ref. [131]) [209].

### 8.1.2 Iron-Catalyzed $\text{Csp}^2\text{-Csp}^2$ Cross-Coupling

Jutand et al. combined NMR spectroscopy, EPR spectroscopy and cyclic voltammetry to investigate the mechanism of iron-catalyzed aryl–aryl cross-coupling [210]. Based on these three techniques, they showed that phenylmagnesium bromide was able to reduce  $\text{Fe}(\text{acac})_3$  to the Fe(I) complex  $[\text{MgBr}]^+[\text{PhFe}(\text{I})(\text{acac})]^-$  by the mean of a first monoelectronic reduction followed by a transmetalation and a second monoelectronic reduction (Scheme 129). The oxidation step of the final Fe(I) complex was confirmed by EPR spectroscopy.

The Fe(I) complex revealed rather unstable and could undergo a dismutation to give a Fe(II) complex and undefined Fe(0) species, which appeared as black precipitate in the reaction mixture (Scheme 130).



**Scheme 129** Hypothetic Fe(I) active catalyst by Jutand et al.



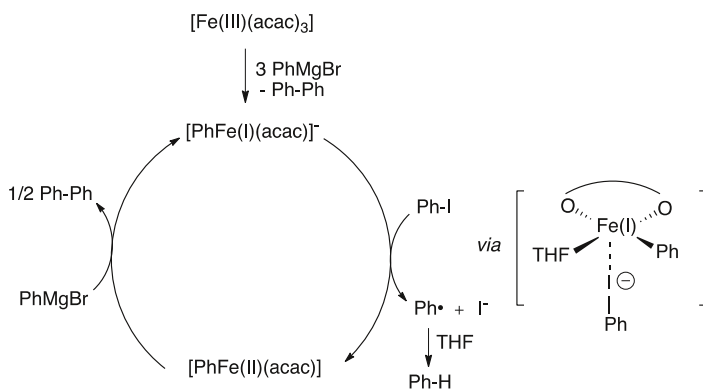
**Scheme 130** Dismutation of the Fe(I) species

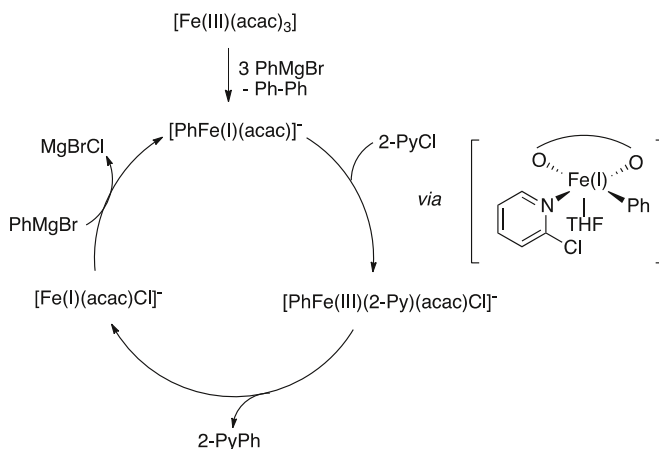
The authors next compared the reactivity of  $[\text{PhFe(I)(acac)}]^-$  toward phenyl iodide and 2-chloropyridine and significant differences were observed. The iron complex  $[\text{PhFe(I)(acac)}]^-$  reduced PhI to give  $[\text{PhFe(II)(acac)}]$  and a phenyl radical that could abstract a hydrogen from THF to deliver benzene. DFT calculations showed that this monoelectronic reduction was facilitated by an interaction between the iron center and the iodide and proceeds according to an inner-sphere mechanism. The resulting Fe(II) complex was unable to react with PhI and could be reduced by the Grignard reagent in excess to regenerate the Fe(I) species (Scheme 131). Under these conditions, no coupling product was formed.

In stark contrast, no halogen-bonding was operating between the Fe(I) center and the chlorine of 2-chloropyridine. DFT calculations highlighted an  $\text{S}_{\text{N}}\text{Ar}$ -type oxidative addition of the chloropyridine to the metal center providing a 2-Py-Fe(III) complex. A reductive elimination delivered the coupling product and the Fe(I) complex  $[\text{Fe(I)(acac)Cl}]^-$ , which after transmetalation led to the initial Fe(I) catalyst (Scheme 132).

This study explained why the aryl-aryl cross-coupling is much easier when electron-poor heteroaryl halides are used instead of aryl halides and why in the latter case, the homocoupling of the Grignard reagent is the major product.

Nakamura et al. demonstrated that iron fluoride showed excellent performance in aryl-aryl cross-coupling [62]. In combination with a NHC ligand, the coupling product was formed and few amounts of the homocoupling product were detected. These observations were in contrast with the results obtained with  $\text{FeCl}_2$  or  $\text{FeCl}_3$ . The authors hypothesized that upon treatment of iron chloride with the Grignard reagent, a ferrate complex of type  $[\text{Ph}_4\text{Fe}][\text{MgX}]_2^+$  could be formed and delivered the homocoupling product after reductive elimination. In contrast, the presence of strongly coordinated fluorides on the iron center could prevent the formation of such

**Scheme 131** Reaction of  $[\text{PhFe(I)(acac)}]^-$  with PhI



**Scheme 132** Reaction of  $[\text{PhFe(I)(acac)}]^-$  with 2-chloropyridine

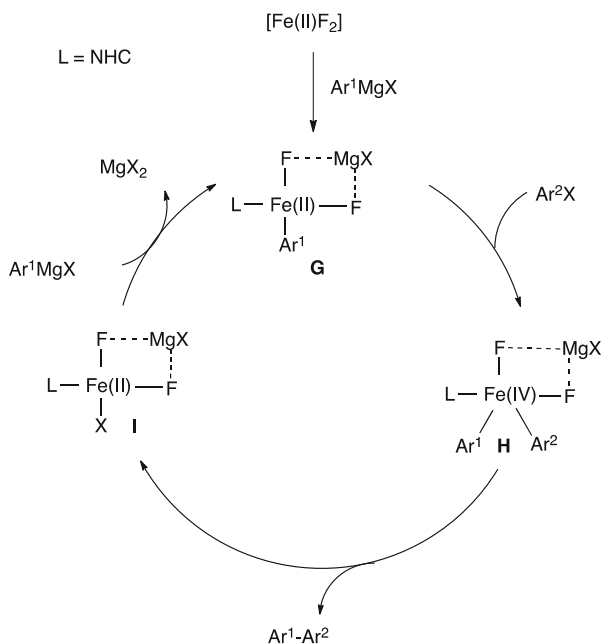
metalate complexes thus decreasing the homocoupling side reaction. The mechanism depicted on [Scheme 133](#) was proposed. An addition of the aryl Grignard reagent on the  $\text{FeF}_2$  complex led to the metalate **G**. An oxidative addition gave the unstable high-valent  $\text{Fe(IV)}$  species **H**, which underwent a fast reductive elimination providing the coupling product and the  $\text{Fe(II)}$  complex **I**. Upon transmetalation with the Grignard reagent, the initial metalate **G** was regenerated ([Scheme 133](#)). The fast reductive elimination should prevent the formation of ate complexes which could be at the origin of the homocoupling products.

### 8.1.3 Iron-Catalyzed $\text{Csp}^3\text{-Csp}^3$ Cross-Coupling

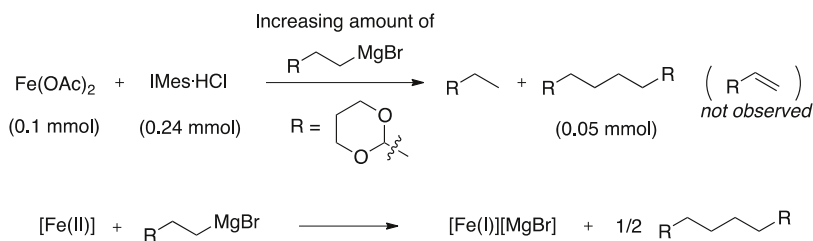
Cárdenas et al. studied the catalytic system composed of  $\text{Fe(OAc)}_2$  and  $\text{IMes}\cdot\text{HCl}$ , which is active in alkyl–alkyl cross-coupling. An increasing amount of the alkyl Grignard reagent was added to a mixture of  $\text{Fe(OAc)}_2/\text{IMes}\cdot\text{HCl}$  and the homocoupling product was titrated using GC analysis. An increase of the quantity of the homocoupling product upon addition of the Grignard was first observed and stabilization to a value of 0.5 mmol per 1 mmol of Fe was then observed. According to the equation depicted in [Scheme 134](#), this value was in favor of a monoreduction of the iron(II) species into an iron(I) complex. The presence of a  $\text{Fe(I)}$  was confirmed by EPR spectroscopy [179].

## 8.2 Formation of Radical Intermediates

Several experimental evidences are in favor of the formation of radical intermediates during iron-catalyzed cross-coupling involving alkyl halides. In 2004, Nakamura et al. showed that the cross-couplings between 1-bromo-4-*t*-butylcyclohexane and an aryl magnesium bromide gave the same diastereomer (*trans/cis* = 96:4) irrespective to the relative configuration of the starting bromide



**Scheme 133** Hypothetic mechanism for the aryl–aryl cross-coupling by Nakamura et al.



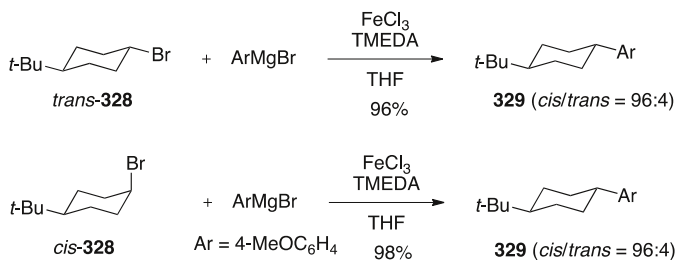
**Scheme 134** Mechanistic hypotheses for alkyl–alkyl cross-coupling

(**Scheme 135**). This stereoconvergence suggests the presence of a radical intermediate [128].

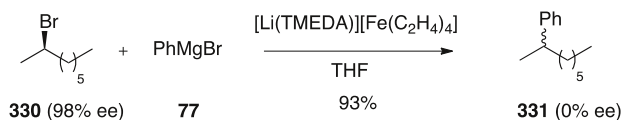
When a cross-coupling was performed on an optically active bromo-alkane, a complete loss of the enantiomeric purity was observed indicating the possible formation of a radical species (**Scheme 136**) [141].

To confirm the formation of radical intermediates, several cross-couplings have been performed on radical-clocks i.e., alkyl halides bearing a pendant olefin moiety or a cyclopropylmethyl halide. In most cases, a cyclization/ring-opening prior to the cross-coupling was observed. Selected examples are presented on **Scheme 137** [141, 148, 167].

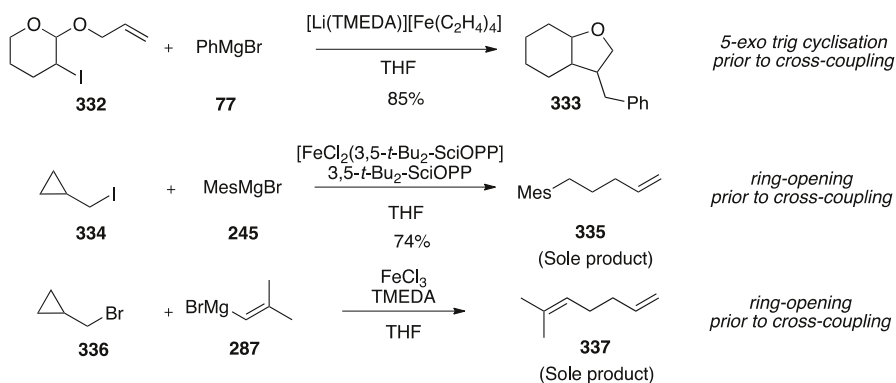
To explain the intervention of radical intermediates, one of the most currently accepted hypothesis is the splitting of the oxidative addition into two consecutive



**Scheme 135** Stereoconvergence in the cross-coupling of 1-bromo-4-*t*-butylcyclohexane



**Scheme 136** Loss of enantiomeric purity during an iron-catalyzed cross-coupling



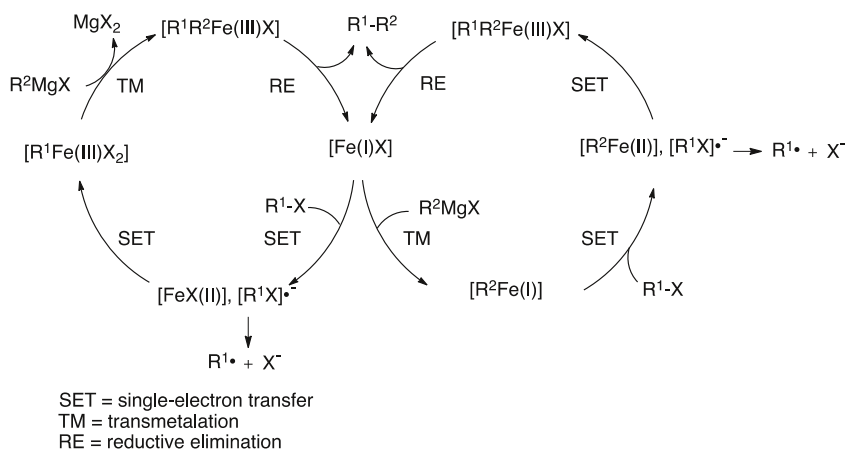
**Scheme 137** Radical clocks in iron-catalyzed cross-coupling

single electron transfer. An example of an hypothetical mechanism is proposed on [Scheme 138](#). However, the order of the elementary steps (“SET first” or “transmetalation first”) still remained uncertain [180].

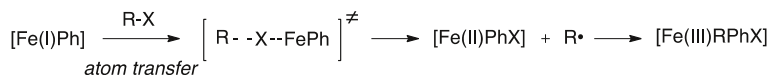
Recently, Norrby and coworkers investigated the nature of the oxidative addition using Hammett studies and proposed that an atom transfer initiated by a coordination of the iron center to the halide could be more probable than a SET mechanism [211]. The radical could then recombine with the Fe(II) species to give a Fe(III) and complete the formal oxidative addition ([Scheme 139](#)).

### 8.3 Role of the Ligands

The precise effect of the ligand on iron-catalyzed reactions has not been fully elucidated. Particularly, the fact that the nature of the preferred ligand varies with



**Scheme 138** Proposed mechanism with radical intermediates

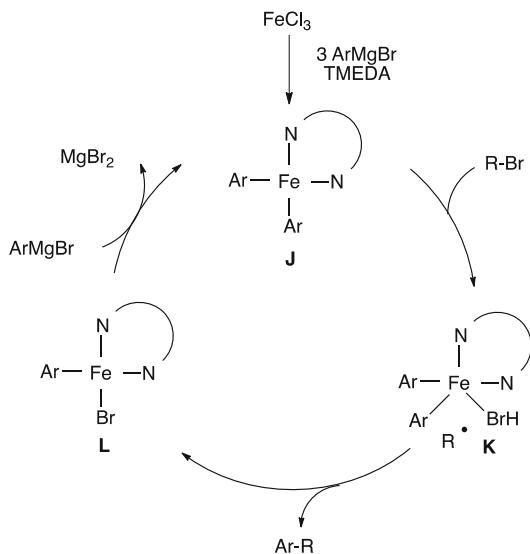


**Scheme 139** Hypothesis of an atom transfer mechanism

the nature of the cross-coupling ( $\text{Csp}^3\text{-Csp}^2$ ,  $\text{Csp}^2\text{-Csp}^2$ ,  $\text{Csp}^3\text{-Csp}^3$ ) still remains unclear and further studies are needed. However, some research groups have tried to investigate the role of the ligands on iron-catalyzed cross-couplings and their results are summarized in this section.

### 8.3.1 Diamine Ligands

In 2009, Nakamura et al. studied the role of the TMEDA in the iron-catalyzed cross-coupling between alkyl halides and aryl Grignard reagents [212]. The authors chose the reaction between 1-bromooctane and mesitylmagnesium bromide and conducted it in the presence of  $\text{FeCl}_3$  and TMEDA in a THF/ $\text{C}_6\text{D}_6$  mixture. In the absence of 1-bromooctane, the iron complex  $(\text{TMEDA})\text{Fe}(\text{Mes})_2$  **J** could be isolated and characterized by NMR, X-ray and elemental analysis ( $\text{FeCl}_3$ ,  $\text{MesMgBr}$  and TMEDA were introduced in a 1:3:8 ratio). Addition of 1-bromooctane to **J** triggered the formation of  $(\text{TMEDA})\text{Fe}(\text{mes})\text{Br}$  **L** together with the coupling product. Based on experiments with radical clocks, the authors proposed the existence of a short-lived radical **K** and postulated the following mechanism: TMEDA coordinates to the iron center and this coordination initiates the catalytic cycle. In addition, a Fe(II)/Fe(III) couple is suggested (Scheme 140). However, we should keep in mind that the bulky mesitylmagnesium bromide may be a particular case and that the isolation of complexes is not an absolute evidence of their involvement in the catalytic cycle. Besides, **J** was formed under specific conditions (only 3 equivalents

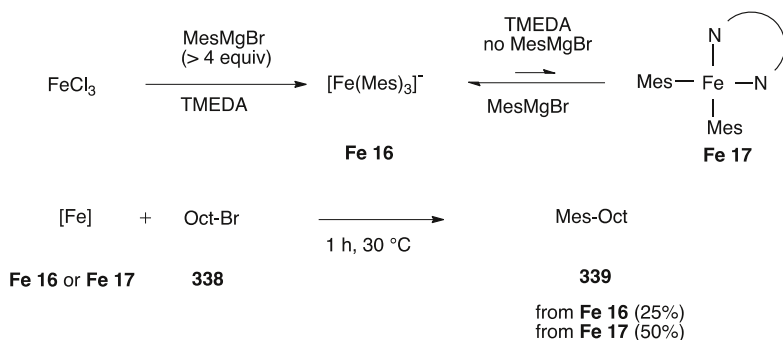
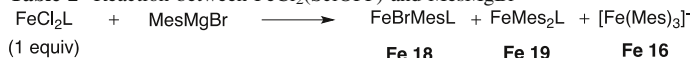
**Scheme 140** Proposed role of the TMEDA as ligand

of Grignard calculated based the iron salt) that differ from the classical cross-coupling conditions.

To complete this work, Bedford and coworkers studied a reaction between  $\text{FeCl}_3$ , TMEDA, and mesitylmagnesium bromide in the presence of an excess of Grignard reagent to mimic the usual catalytic conditions [213]. They were not able to detect  $(\text{TMEDA})\text{Fe}(\text{Mes})_2$  **Fe 17** using  $^1\text{H}$  NMR but instead observed the formation of the Fe(II) ate complex  $[\text{Fe}(\text{Mes})_3]^-$ . The reaction between 1-bromooctane and  $[\text{Fe}(\text{Mes})_3]^-$  was significantly faster than the one involving **Fe 17** (Scheme 141). In addition, when the cross-coupling reaction was carried out in the absence of TMEDA, the formation of side-products such as octane and octene increased. From these results, the authors deduced that TMEDA does not coordinate to the iron center in the catalytically relevant species but instead traps off-cycle intermediates that otherwise may conduct to undesired by-products. The Fe(II) complex may be stabilized by the bulky mesityl ligands, which prevent the reductive elimination, thus explaining why in this special case, Fe(I) species does not seem to be involved in the catalytic cycle. However, the authors suggested that with less bulky aryl Grignard reagents the formation of iron complex with an oxidation state inferior to Fe(II), i.e., Fe(I) or Fe(0) was more probable.

### 8.3.2 Bisphosphine Ligands

Bisphosphine ligands proved useful in a range of iron-catalyzed cross-coupling including Kumada-type, Negishi-type and Suzuki-type cross-couplings. To identify the catalytic species formed during the coupling between primary alkyl halides and mesitylmagnesium bromide in the presence of  $\text{FeCl}_2(\text{SciOPP})$ , Neidig et al. used a combination of  $^{57}\text{Fe}$  Mössbauer spectroscopy, Magnetic Circular Dichroism (MCD)

**Scheme 141** Mechanism of coupling with MesMgBr**Table 2** Reaction between  $\text{FeCl}_2(\text{SciOPP})$  and MesMgBr

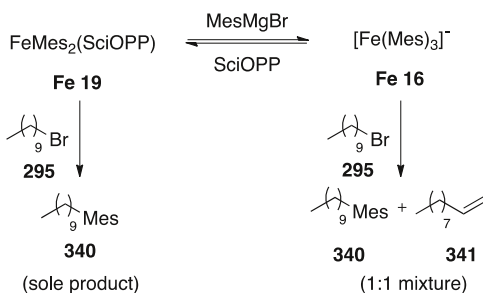
L = SciOPP

| Entry | MesMgBr (equiv) | <b>Fe 18</b> (equiv) | <b>Fe 19</b> (equiv) | <b>Fe 16</b> (equiv) |
|-------|-----------------|----------------------|----------------------|----------------------|
| 1     | 1               | 1                    | 0                    | 0                    |
| 2     | 2               | 0.03                 | 0.90                 | 0.07                 |
| 3     | 20              | 0                    | 0.38                 | 0.62                 |
| 4     | 100             | 0                    | 0.02                 | 0.98                 |

and DFT calculations [214]. They first synthesized the well-defined iron complexes  $\text{Fe}(\text{Mes})\text{Br}(\text{SciOPP})$  and  $\text{Fe}(\text{Mes})_2(\text{SciOPP})$  upon addition of MesMgBr on  $\text{FeCl}_2(\text{SciOPP})$ . These two complexes were fully characterized using Mössbauer spectroscopy and MCD. The authors next studied the reaction between  $\text{FeCl}_2(\text{SciOPP})$  and increasing amounts of MesMgBr to identify the in situ formed species by comparison with their previously synthesized well-defined iron complexes. In the presence of 1 equiv of MesMgBr, the only iron complex that could be detected was  $\text{Fe}(\text{Mes})\text{Br}(\text{SciOPP})$  (Table 2, entry 1) but when 2 equiv of MesMgBr were added, a mixture of  $\text{Fe}(\text{Mes})\text{Br}(\text{SciOPP})$ ,  $\text{Fe}(\text{Mes})_2(\text{SciOPP})$  and  $[\text{Fe}(\text{mes})_3]^-$  was observed (Table 2, entry 2). Interestingly, in conditions that are closer to those of the cross-coupling (20 equiv or more of the Grignard reagent), the ate complex  $[\text{Fe}(\text{Mes})_3]^-$  was formed together with  $\text{Fe}(\text{Mes})_2(\text{SciOPP})$  (Table 2, entries 3–4).

These two complexes are in equilibrium that can be displaced by addition of MesMgBr or free SciOPP. The reactivity of the in situ generated  $[\text{Fe}(\text{Mes})_3]^-$  and  $\text{Fe}(\text{Mes})_2(\text{SciOPP})$  towards alkyl halides proved significantly different.  $\text{Fe}(\text{Mes})_2(\text{SciOPP})$  reacted cleanly with 1-iododecane to form  $\text{Fe}(\text{Mes})\text{I}(\text{SciOPP})$  and mesityldecane whereas the reaction involving  $[\text{Fe}(\text{Mes})_3]^-$  and 1-iododecane led to an equimolar mixture of mesityldecane and decene (Scheme 142). Both reactions occurred with similar kinetic rates demonstrating that the formation of  $[\text{Fe}(\text{Mes})_3]^-$  could dramatically reduce the selectivity of the cross-coupling.

**Scheme 142** Difference of reactivity between **Fe 19** and **Fe 16**



Notably, when MesMgBr was added slowly to a mixture containing FeCl<sub>2</sub>(-SciOPP), the alkyl halide and free SciOPP no [Fe(Mes)<sub>3</sub>]<sup>-</sup> could be detected. This observation shows that the “slow addition protocol” combined with the presence of the bisphosphine ligand protect the iron from the formation of undesired [Fe(Mes)<sub>3</sub>]<sup>-</sup> that would lead to undesired side-reaction. During the cross-coupling, EPR spectroscopy indicated that no Fe(I) was formed, confirming the hypothesis of a Fe(II)/Fe(III) couple. However, the authors pointed out that this situation could be restricted to the particular case of this bulky Grignard reagent. This study is in accordance with a mechanism proposed by Nakamura et al. for Suzuki-type cross-coupling in the presence of FeCl<sub>2</sub>(SciOPP) (Scheme 143) [160].

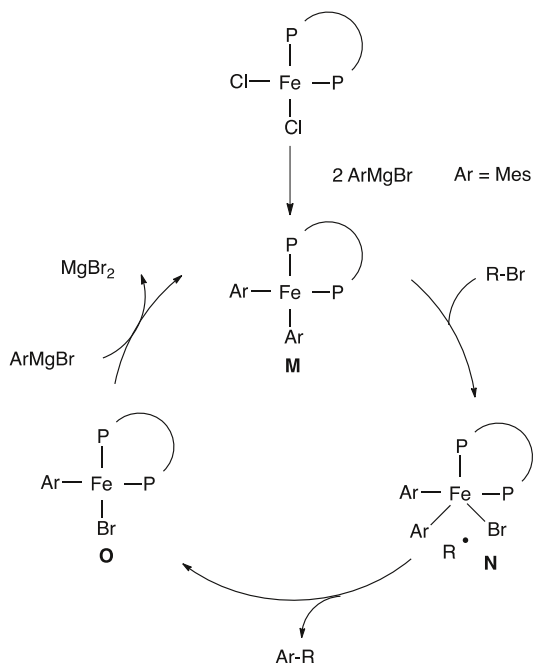
The same group then extended the study to the less bulky aryl Grignard reagent phenylmagnesium bromide using a similar experimental approach [215]. Upon addition of 2.2 equiv of PhMgBr on FeCl<sub>2</sub>(SciOPP), the formation of the Fe(0) complex [Fe(η<sup>6</sup>-biphenyl)(SciOPP)], resulting from a bis-addition of the Grignard followed by a reductive elimination, was observed. However, this complex reacted sluggishly with chloro-cycloheptane and thus, did not seem to be kinetically relevant. Consequently, the authors focused on iron species that could be formed prior to the reductive elimination leading to the Fe(0) inactive complex and they showed that [Fe(Ph)X(SciOPP)] as well as [Fe(Ph)<sub>2</sub>(SciOPP)] could be formed during the reaction. The former reacted smoothly with bromocycloheptane delivering phenylcycloheptane (84–92 %) and cycloheptene (9–14 %) whereas the latter gave a 1:1 mixture of phenylcycloheptane and cycloheptene. Taking together, these data suggest that [Fe(Ph)X(SciOPP)] could be the active catalytic species during the cross-coupling between aryl Grignard reagents and alkyl halides (Scheme 144) [216].

### 8.3.3 NHC Ligands

With the objective of investigating the mechanism of cross-coupling mediated by an iron NHC complex, (IPr<sub>2</sub>Me<sub>2</sub>)<sub>2</sub>FePh<sub>2</sub> was prepared from FeCl<sub>2</sub>, IPr<sub>2</sub>Me<sub>2</sub>, and phenylmagnesium bromide and characterized using X-ray diffraction, <sup>1</sup>H NMR and Mössbauer spectroscopy. Its reactivity with a stoichiometric amount of alkyl halide was then studied and excellent yields for the formation of the coupling product were obtained. In addition, when cyclopropylmethyl bromide was used a ring-opening prior to the cross-coupling was observed suggesting the formation of radical



**Scheme 143** Proposed mechanism for the coupling between alkyl halides and MesMgBr



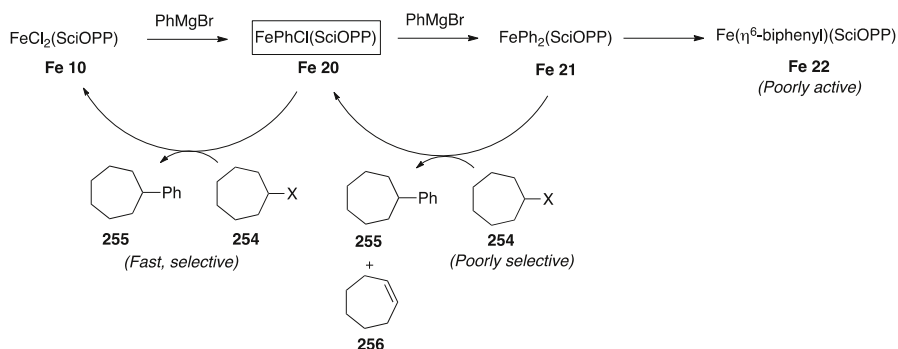
intermediates. During this reaction, the main iron-containing product was  $(\text{IPr}_2\text{Me}_2)_2\text{FePhX}$  (Scheme 145).

Two possible mechanisms for this stoichiometric reaction between  $(\text{IPr}_2\text{Me}_2)_2\text{FePh}_2$  and alkyl halides were proposed. After a single-electron transfer from the Fe(II) complex to the alkyl halide, the resulting radical may either react with the formed Fe(III) complex (Scheme 146, eq 1') or with another molecule of the initial Fe(II) complex (Scheme 146, eq 2').

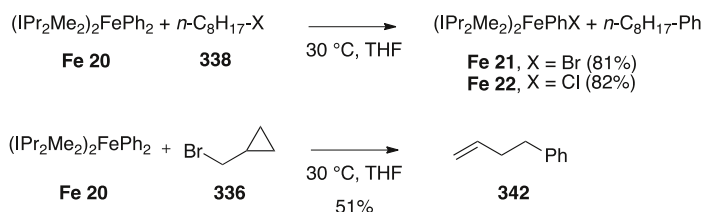
The performance of  $(\text{IPr}_2\text{Me}_2)_2\text{FePh}_2$  was lower under catalytic conditions as alkene and alkane side products derived from the alkyl halide were formed in significant amount. The authors suggested that in the presence of an excess of the Grignard reagent, anionic species such as  $[(\text{IPr}_2\text{Me}_2)_2\text{FeAr}_3]^-$  or  $[\text{FeAr}_4]^-$  could be formed and would lead to the formation of by-products (Scheme 147) [217].

Tonzetich et al. studied the catalytic performances of  $[\text{Fe}(\text{IPr})\text{Cl}_2]_2$  in a variety of cross-couplings of alkyl and aryl halides with aryl and alkyl Grignard reagents [218]. The best results were obtained for the coupling involving alkyl halides and aryl Grignard reagents (Scheme 148).

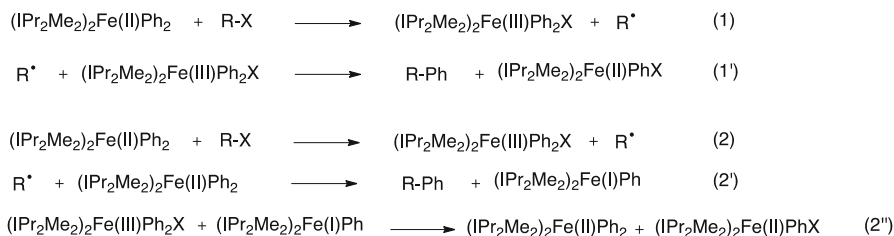
The formation of radical intermediates was highlighted by the use of a radical trap, BHT (2,6-di-*tert*-butyl-4-methylphenol) which completely inhibited the coupling between cyclohexyl bromide and phenylmagnesium bromide. In addition, when 1-bromo-5-hexene was used as a substrate, a mixture of the linear product **347** and the cyclic compound **348** was formed. The amount of the linear product increased with higher catalytic loadings in the iron complex suggesting the dissociation of the radical from the solvent cage of the catalyst (Scheme 149).



**Scheme 144** Reaction between  $\text{FeCl}_2(\text{SciOPP})$  and phenylmagnesium bromide



**Scheme 145** Couplings in the presence of NHC ligands

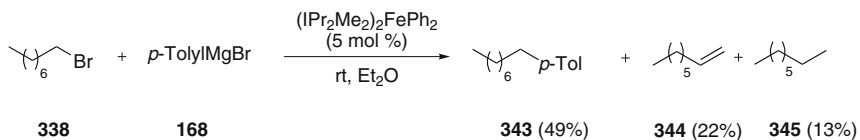


**Scheme 146** Proposed mechanisms for the reaction between  $[(\text{IPr}_2\text{Me}_2)_2\text{FePh}_2]$  and alkyl halides

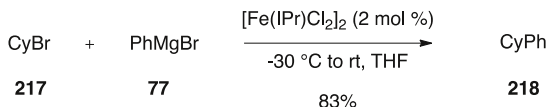
Based on these results, the following mechanism was proposed. The (NHC)Fe(II) precursor would undergo a transmetalation to give **P** that could perform a halogen atom abstraction on the alkyl halide. The resulting radical would dissociate from the metal solvent cage and would react with an aryl group present on the Fe(III) complex to deliver the coupling product and a Fe(II) complex. A transmetalation performed on the latter would regenerate the catalyst **P** (Scheme 150).

## 8.4 Mechanistic Investigation on Negishi and Suzuki-type Cross-Couplings

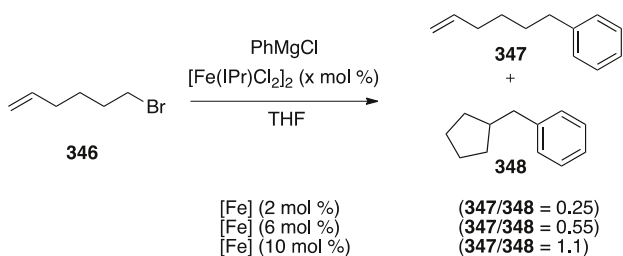
To investigate the mechanism of Negishi-type iron-catalyzed cross-coupling, Bedford et al. chose the reaction between benzyl bromide **211** and ditolylzinc **186** in



**Scheme 147** Performance of  $(\text{IPr}_2\text{Me}_2)_2\text{FePh}_2$  under catalytic conditions

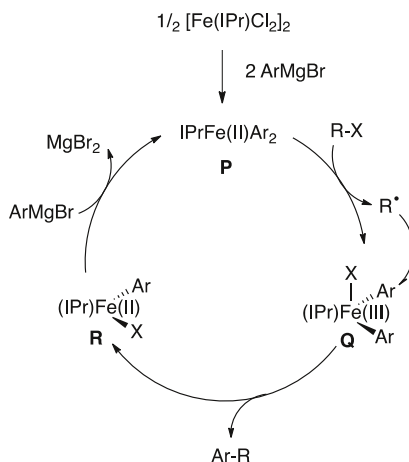


**Scheme 148**  $[\text{Fe}(\text{IPr})\text{Cl}_2]_2$ -catalyzed arylation of cyclohexyl bromide

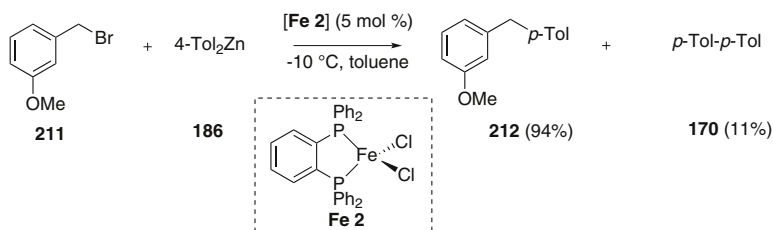


**Scheme 149** Use of a radical clock in  $[\text{Fe}(\text{IPr})\text{Cl}_2]_2$ -catalyzed cross-coupling

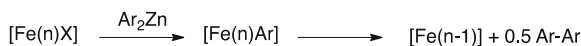
**Scheme 150** Proposed mechanism for  $[\text{Fe}(\text{IPr})\text{Cl}_2]_2$ -catalyzed cross-coupling



the presence of the iron catalyst **Fe 2**.<sup>80</sup> The reaction proceeded smoothly at  $-10^\circ\text{C}$  delivering, after 30 min, the coupling product in high yield (94 %) together with the biaryl product (11 %) which was essentially formed at the beginning of the coupling (Scheme 151).



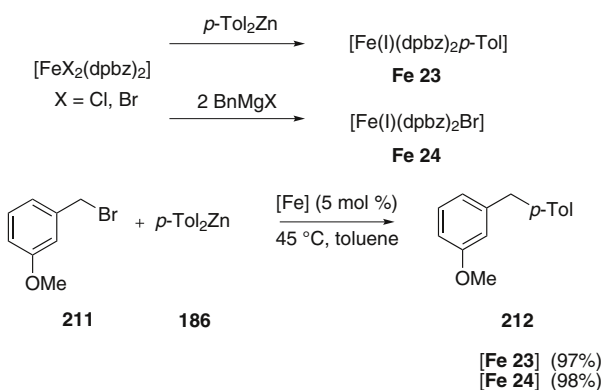
**Scheme 151** Negishi-type arylation of benzylic bromide **211**



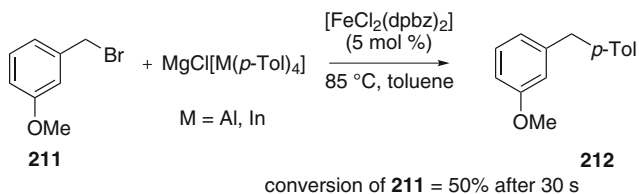
**Scheme 152** Reaction between the iron complex and the arylzinc reagent

To determine the oxidation state of the true iron catalyst, the reaction between the diarylzinc and the iron complex was studied in the absence of an electrophile. The authors argued that, under these conditions, the oxidation state of the iron catalyst generated in situ could be directly deduced from the amount of the biaryl product resulting from the reduction of the iron center (**Scheme 152**).

The titration of the biaryl product formed during the time let the authors to postulate the formation of a Fe(I) complex. Even if the iron catalyst possessing an oxidation state inferior to Fe(I) could be accessed by reaction with the diarylzinc reagent, their formation was too slow regarding to the timescale of the cross-coupling. The two Fe(I) complexes **Fe 23** and **Fe 24** were then synthesized and characterized using X-ray diffraction and EPR. Both were able to catalyze the reaction between the benzyl bromide and the diarylzinc reagent but the reaction with **Fe 24** was faster and its reaction rate was comparable to those of the classical cross-coupling (**Scheme 153**). Consequently, the authors proposed that **Fe 24** could be the active catalytic species formed by reaction between the precatalyst and the diarylzinc while complex **Fe 23** could be an off-cycle species.

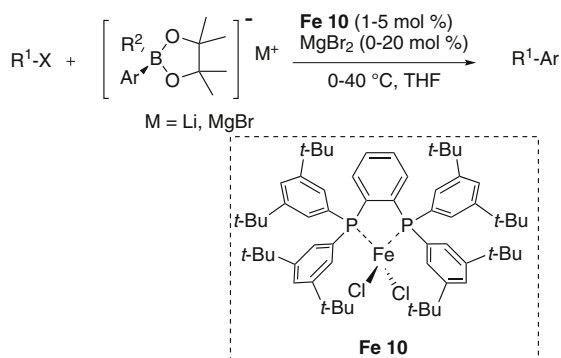


**Scheme 153** Hypothesis of an iron(I) catalyst

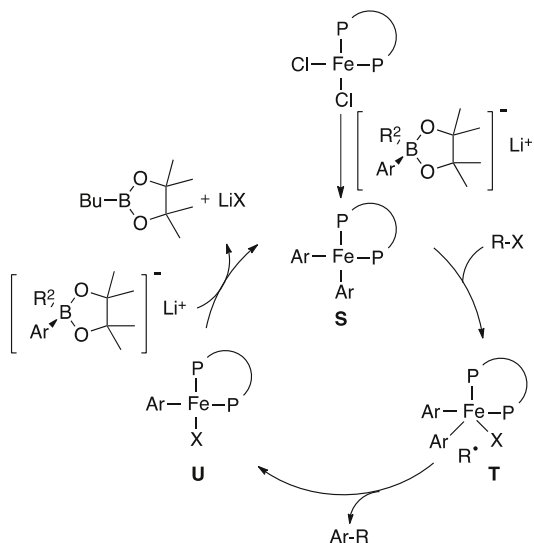


**Scheme 154** Coupling of **211** with organoaluminum or organoindate reagents

**Scheme 155** Suzuki-type coupling of alkyl halides with aryl lithium borates



**Scheme 156** Proposed mechanism for the Suzuki-type coupling



A similar study based on the titration of the biaryl product was carried out for the cross-coupling between benzyl bromide and aluminates or indates [84]. In the presence of the precatalyst **Fe 2**, the reaction between **211** and  $\text{MgCl}[\text{M}(4\text{-Tol})_4]$  ( $\text{M} = \text{Al}, \text{In}$ ) reached 50 % completion after only 30 s (**Scheme 154**). In the absence of the benzyl bromide, the titration of the biaryl by-product indicated that, after 30 s, a  $\text{Fe}(\text{I})$  complex was formed.

Based on their previous studies concerning iron-catalyzed cross-couplings,[155] Nakamura et al. proposed a mechanism for the Suzuki-type coupling between alkyl halides and aryl borates (Scheme 155) [160].

As no biaryl product was observed during the reaction, the authors hypothesized that no reduction of the Fe(II) complex occurred. After formation of complex S upon reaction between the borate and the precatalyst, a homolytic cleavage of the R-X bond afforded a Fe(III) species together with an alkyl radical (Scheme 156). The latter reacted with an aryl group present on the iron center to give the coupling product and a Fe(II) complex. After transmetalation, the active complex S was regenerated. The authors hypothesized that the steric bulk induced by the phosphine ligand may prevent the undesired formation of ferrate complexes. A similar mechanism was proposed for the alkyl-alkyl Suzuki-type cross-coupling [182].

## References

- Bolm C, Legros J, Le Paih J, Zani L (2004) *Chem Rev* 104:6217–6254
- Bauer EB (2008) *Curr Org Chem* 12:1341–1369
- Sherry BD, Fürstner A (2008) *Acc Chem Res* 41:1500–1511
- Nakamura E, Yoshikai N (2010) *J Org Chem* 75:6061–6067
- Jana R, Pathak TP, Sigman MS (2011) *Chem Rev* 111:1417–1492
- Jegelka M, Plietker B (2011) *Top Organomet Chem* 33:177–213
- Nakamura E, Hatakeyama T, Ito S, Ishizuka K, Ilies L, Nakamura M (2014) *Org React* 83:1–209
- Bauer I, Knölker HJ (2015) *Chem Rev* 115:3170–3387
- Legros J, Figadère B (2015) *Nat Prod Rep* 32:1541–1555
- Bedford RB, Brenner PB (2015) *Top Organomet Chem* 50:19–46
- Legros J, Figadère B (2016) In: Cossy J, De Gruyter (ed) *Grignard reagents and transition metal catalysts*
- Mako TL, Byers JA (2016) *Inorg Chem*. doi:10.1039/c5qi00295h
- Tamura M, Kochi J (1971) *J Am Chem Soc* 93:1487–1489
- Tamura M, Kochi J (1971) *Synthesis* 303–305
- Tamura M, Kochi JK (1971) *Bull Chem Soc Jpn* 44:3063–3073
- Neumann SM, Kochi JK (1975) *J Org Chem* 40:599–606
- Fiandanese V, Miccoli G, Naso F, Ronzini L (1986) *J Organomet Chem* 312:343–348
- Cahiez G, Avedissian H (1998) *Synthesis* 1199–1205
- Østergaard N, Pedersen BT, Skjærbaek N, Vedsø P, Begtrup M (2002) *Synlett* 2002:1889–1891
- Seck M, Franck X, Hocquemiller R, Figadère B, Peyrat JF, Provot O, Brion JD, Alami M (2004) *Tetrahedron Lett* 45:1881–1884
- Dos Santos M, Franck X, Hocquemiller R, Figadère B, Peyrat JF, Provot O, Brion JD, Alami M (2004) *Synlett* 2697–2700
- Cahiez G, Gager O, Buendia J, Patinote C (2012) *Chem Eur J* 18:5860–5863
- Shakhmaev RN, Sunagatullina AS, Zorin VV (2013) *Russ J Gen Chem* 83:2018
- Shakhmaev RN, Sunagatullina AS, Zorin VV (2013) *Russ J Org Chem* 49:669
- Shakhmaev RN, Sunagatullina AS, Zorin VV (2014) *Russ J Org Chem* 50:322
- Operamolla A, Omar OH, Babudri F, Vitulli M, Farinola GM (2009) *Lett Org Chem* 6:573
- Cahiez G, Marquis S (1996) *Tetrahedron Lett* 37:1773–1776
- Cahiez G, Marquis S (1996) *Pure Appl Chem* 68:53–60
- Scheiper B, Bonnekessel M, Krause H, Fürstner A (2004) *J Org Chem* 69:3943–3949
- Fürstner A, De Souza D, Parra-Rapado L, Jensen JT (2003) *Angew Chem Int Ed* 42:5358–5360
- Fürstner A, Turet L (2005) *Angew Chem Int Ed* 44:3462–3466
- Fürstner A, de Souza D, Turet L, Fenster MDB, Parra-Rapado L, Wirtz C, Mynott R, Lehmann CW (2007) *Chem Eur J* 13:115–134

33. Fürstner A, Kirk D, Fenster MDB, Aissa C, De Souza D, Nevado C, Tuttle T, Thiel W, Müller O (2007) *Chem Eur J* 13:135–149
34. Le Marquand P, Tsui GC, Whitney JCC, Tam W (2008) *J Org Chem* 73:7829–7832
35. Abele S, Inauen R, Spielvogel D, Moessner C (2012) *J Org Chem* 77:4765–4773
36. Fürstner A, Hannen P (2006) *Chem Eur J* 12:3006–3019
37. Fürstner A, Schlecker A (2008) *Chem Eur J* 14:9181–9191
38. Hamajima A, Isobe M (2006) *Org Lett* 8:1205–1208
39. Boukouvalas J, Albert V, Loach RP, Lafleur-Lambert R (2012) *Tetrahedron* 68:9592–9597
40. Berthon-Gelloz G, Hayashi T (2006) *J Org Chem* 71:8957–8960
41. Cahiez G, Gager O, Habiak V (2008) *Synthesis* 2636–2644
42. Larsen US, Martiny L, Begtrup M (2005) *Tetrahedron Lett* 46:4261–4263
43. Cahiez G, Habiak V, Gager O (2008) *Org Lett* 10:2389–2392
44. Scheerer JR, Lawrence JF, Wang GC, Evans DA (2007) *J Am Chem Soc* 129:8968–8969
45. Li BJ, Xu L, Wu ZH, Guan BT, Sun CL, Wang BQ, Shi ZS (2009) *J Am Chem Soc* 131:14656–14657
46. Li BJ, Zhang XS, Shi ZJ (2014) *Org Synth* 91:83–92
47. Gärtner D, Stein AL, Grupe S, Arp J, von Wangelin AJ (2015) *Angew Chem Int Ed* 54:10545–10549
48. Nishikado H, Nakatsuji H, Ueno K, Nagase R, Tanabe Y (2010) *Synlett* 2087–2092
49. Fabre JL, Julia M, Verpeaux JN (1982) *Tetrahedron Lett* 23:2469–2472
50. Alvarez E, Cuvigny T, du Penhoat H, Julia M (1988) *Tetrahedron* 44:111–118
51. Alvarez E, Cuvigny T, du Penhoat H, Julia M (1988) *Tetrahedron* 44:119–126
52. Rao Volla CM, Vogel P (2008) *Angew Chem Int Ed* 47:1305–1307
53. Silveira CC, Mendes SR, Wolf L (2010) *J Braz Chem Soc* 21:2138–2145
54. Molander GA, Rahn BJ, Shubert DC, Bonde SE (1983) *Tetrahedron Lett* 24:5449–5452
55. Dohle W, Kopp F, Cahiez G, Knochel P (2001) *Synlett* 1901–1904
56. Tewari N, Maheshwari N, Medhane R, Nizar H, Prasad M (2012) *Org Process Res Dev* 16:1566–1568
57. Camacho-Dávila AA (2008) *Synth Commun* 38:3823–3833
58. Czaplík WM, Mayer M, von Wangelin AJ (2011) *ChemCatChem* 3:135–138
59. Hamze A, Brion JD, Alami M (2012) *Org Lett* 14:2782–2785
60. Dunet G, Knochel P (2006) *Synlett* 407–410
61. Hatakeyama T, Yoshimoto Y, Gabriel T, Nakamura M (2008) *Org Lett* 10:5341–5344
62. Pridgen LN, Snyder L, Prol J (1989) *J Org Chem* 54:1523–1526
63. Fürstner A, Leitner A (2002) *Angew Chem Int Ed* 41:609–612
64. Fürstner A, Leitner A, Méndez M, Krause H (2002) *J Am Chem Soc* 124:13856–13863
65. Gülak S, Gieshoff TN, von Wangelin AJ (2013) *Adv Synth Catal* 355:2197–2202
66. Mattarella M, Siegel JS (2012) *Org Biomol Chem* 10:5799–5802
67. Haner J, Jack K, Nagireddy J, Raheem MA, Durham R, Tam W (2011) *Synthesis* 731–738
68. Hocek M, Dvořáková H (2003) *J Org Chem* 68:5773–5776
69. Fürstner A, Leitner A, Seidel G (2005) *Org Synth* 81:33–41
70. Kubelka T, Slavětinská L, Klepetářová B, Hocek M (2010) *Eur J Org Chem* 2666–2669
71. Hocek M, Hocková D, Dvořáková H (2004) *Synthesis* 889–894
72. Hocek M, Pohl R (2004) *Synthesis* 2869–2876
73. Hocek M, Pohl R, Císařová I (2005) *Eur J Org. Chem* 3026–3030
74. Bartocchini F, Piersanti G, Armaroli S, Cerri A, Cabri W (2014) *Tetrahedron Lett* 55:1376–1378
75. Dickschat JS, Reichenbach H, Wagner-Döbler I, Schulz S (2005) *Eur J Org Chem* 4141–4153
76. Colacino E, Benakki H, Guenoun F, Martínez J, Lamaty F (2009) *Synth Commun* 39:1583–1591
77. Scheiper B, Bonnekessel M, Krause H, Fürstner A (2004) *J Org Chem* 69:3943–3949
78. Malhotra S, Seng PS, Koenig SG, Deese AJ, Ford KA (2013) *Org Lett* 15:3698–3701
79. Scheiper B, Glorius F, Leitner A, Fürstner A (2004) *Proc Natl Acad Sci USA* 101:11960–11965
80. Perry MC, Gillet AN, Law TC (2012) *Tetrahedron Lett* 53:4436–4439
81. Rushworth PJ, Hulcoop DG, Fox DJ (2013) *J Org Chem* 78:9517–9521
82. Benischke AD, Breuillac AJA, Moyeux A, Cahiez G, Knochel P (2016) *Synlett* 471–476
83. Gögsig TM, Lindhardt AT, Skrydstrup T (2009) *Org Lett* 11:4886–4888
84. Agrawal T, Cook SP (2013) *Org Lett* 15:96–99
85. Seidel G, Laurich D, Fürstner A (2004) *J Org Chem* 69:3950–3952
86. Feng X, Mei Y, Lu W (2012) *Monatsh Chem* 143:161–164

87. Fürstner A, Leitner A (2003) *Angew Chem Int Ed* 42:308–311
88. Chen X, Quan ZJ, Wang XC (2015) *Appl Organometal Chem* 29:296–300
89. Silberstein AL, Ramgren SD, Garg NK (2012) *Org Lett* 14:3796–3799
90. Mesganaw T, Garg NK (2013) *Org Process Res Dev* 17:29–39
91. Guo WJ, Wang ZX (2013) *Tetrahedron* 69:9580–9585
92. Holder E, Langeveldt BMW, Schubert US (2005) *Adv Mater* 17:1109–1121
93. Shih HT, Lin CH, Shih HH, Cheng CH (2002) *Adv Mater* 14:1409–1412
94. Demus D, Goodby JW, Gray GW, Spiess HW, Vill V (1998) *Handbook of liquid crystals*. Wiley-VCH, Weinheim
95. Kharasch MS, Fields EK (1941) *J Am Chem Soc* 63:2316–2320
96. Quintin J, Franck X, Hocquemiller R, Figadère B (2002) *Tetrahedron Lett* 43:3547–3549
97. Bouilly L, Turck A, Plé N, Darabantu M (2005) *J Heterocycl Chem* 42:1423–1428
98. Kuzmina OM, Steib AK, Flubacher D, Knochel P (2012) *Org Lett* 14:4818–4821
99. Piller FM, Metzger A, Schade MA, Haag BA, Gavryushin A, Knochel P (2009) *Chem Eur J* 15:7192–7202
100. Kuzmina OM, Steib AK, Markiewicz JT, Flubacher D, Knochel P (2013) *Angew Chem Int Ed* 52:4945–4949
101. Kuzmina OM, Steib AK, Fernandez S, Boudot W, Markiewicz JT, Knochel P (2015) *Chem Eur J* 21:8242–8249
102. Güllak S, von Wangelin AJ (2012) *Angew Chem Int Ed* 51:1357–1361
103. Hatakeyama T, Nakamura M (2007) *J Am Chem Soc* 129:9844–9845
104. Hatakeyama T, Hashimoto S, Ishizuka K, Nakamura M (2009) *J Am Chem Soc* 131:11949–11963
105. Agrawal T, Cook SP (2014) *Org Lett* 16:5080–5083
106. Chua YY, Duong HA (2014) *Chem Commun* 50:8424–8427
107. Chua YY, Duong HA (2016) *Chem Commun* 52:1466–1469
108. Sapountzis I, Lin W, Kofink CC, Despotopoulou C, Knochel P (2005) *Angew Chem Int Ed* 44:1654–1657
109. Kofink CC, Blank B, Pagano S, Götz N, Knochel P (2007) *Chem Commun* 1954–1956
110. Bedford RB, Hall MA, Hodges GR, Huwe M, Wilkinson MC (2009) *Chem Commun* 6430–6432
111. Guo Y, Young DJ, Hor TSA (2008) *Tetrahedron Lett* 49:5620–5621
112. Castagnolo D, Botta M (2010) *Eur J Org Chem* 3224–3228
113. Pasto DJ, Hennion GF, Shults RH, Waterhouse A, Chou SK (1976) *J Org Chem* 41:3496
114. Pasto DJ, Chou SK, Waterhouse A, Shults RH, Hennion GF (1978) *J Org Chem* 43:1385–1388
115. Hashmi ASK, Szeimies G (1994) *Chem Ber* 127:1075–1089
116. Yanagisawa A, Nomura N, Yamamoto H (1991) *Synlett* 513–514
117. Yanagisawa A, Nomura N, Yamamoto H (1994) *Tetrahedron* 50:6017–6028
118. Mayer M, Czaplik WM, von Wangelin AJ (2010) *Adv Synth Catal* 352:2147–2152
119. Volla CMR, Marković D, Reddy Dubbaka S, Vogel P (2009) *Eur J Org Chem* 6281–6288
120. Kawamura S, Nakamura M (2013) *Chem Lett* 42:183–185
121. Chard EF, Dawe LN, Kozak CM (2013) *J Organomet Chem* 737:32–39
122. Bedford RB, Huwe M, Wilkinson MC (2009) *Chem Commun* 600–602
123. Adams CJ, Bedford RB, Carter E, Gower NJ, Haddow MF, Harvey JN, Huwe M, Cartes MA, Mansell SM, Mendoza C, Murphy DM, Neeve EC, Nunn J (2012) *J Am Chem Soc* 134:10333–10336
124. Clifton J, Habraken ERM, Pringle PG, Manners I (2015) *Catal Sci Technol* 5:4350–4353
125. Bedford RB, Carter E, Cogswell PM, Gower NJ, Haddow MF, Harvey JN, Murphy DM, Neeve EC, Nunn J (2013) *Angew Chem Int Ed* 52:1285–1288
126. Brown CA, Nile TA, Mahon MF, Webster RL (2015) *Dalton Trans* 44:12189–12195
127. Bedford RB, Brenner PB, Carter E, Clifton J, Cogswell PM, Gower NJ, Haddow MF, Harvey JN, Kehl JA, Murphy DM, Neeve EC, Neidig ML, Nunn J, Snyder BER, Taylor J (2014) *Organometallics* 33:5767–5780
128. Nakamura M, Matsuo K, Ito S, Nakamura E (2004) *J Am Chem Soc* 126:3686–3687
129. Dai ZQ, Liu KQ, Zhang ZY, Wei BM, Guan JT (2013) *Asian J Chem* 2013(25):6303–6305
130. Bedford RB, Bruce DW, Frost RM, Hird M (2005) *Chem Commun* 4161–4163
131. Cahiez G, Habiak V, Duplais C, Moyeux A (2007) *Angew Chem Int Ed* 46:4364–4366
132. Bedford RB, Betham M, Bruce DW, Danopoulos AA, Frost RM, Hird M (2006) *J Org Chem* 71:1104–1110
133. Steib AK, Thaler T, Komeyama K, Mayer P, Knochel P (2011) *Angew Chem Int Ed* 50:3303–3307



134. Barré B, Gonnard L, Campagne R, Reymond S, Marin J, Ciapetti P, Brellier M, Guérinot A, Cossy J (2014) *Org Lett* 16:6160–6163
135. Parmar D, Henkel L, Dib J, Rueping M (2015) *Chem Commun* 51:2111–2113
136. Tran LD, Daugulis O (2010) *Org Lett* 12:4277–4279
137. Jin M, Adak L, Nakamura M (2015) *J Am Chem Soc* 137:7128–7134
138. Bedford RB, Betham M, Bruce DW, Davis SA, Frost RM, Hird M (2006) *Chem Commun* 1398–1400
139. Nagano T, Hayashi T (2004) *Org Lett* 6:1297–1299
140. Jin M, Nakamura M (2011) *Chem Lett* 40:1012–1014
141. Martin R, Fürstner A (2004) *Angew Chem Int Ed* 43:3955–3957
142. Bedford RB, Bruce DW, Frost RM, Goodby JW, Hird M (2004) *Chem Commun* 2822–2823
143. Kuzmina OM, Steib AK, Moyeux A, Cahier G, Knochel P (2015) *Synthesis* 47:1696–1705
144. Bauer G, Wodrich MD, Scopelliti R, Hu X (2015) *Organometallics* 34:289–298
145. Chowdhury RR, Crane AK, Fowler C, Kwong P, Kozak CM (2008) *Chem Commun* 94–96
146. Yamagushi Y, Ando H, Nagaya M, Hinago H, Ito T, Asami M (2011) *Chem Lett* 40:983–985
147. Qian X, Kozak CM (2011) *Synlett* 852–856
148. Hatakeyama T, Fujiwara Y, Okada Y, Itoh T, Hashimoto T, Kawamura S, Ogata K, Takaya H, Nakamura M (2011) *Chem Lett* 40:1030–1032
149. Sun CL, Krause H, Fürstner A (2014) *Adv Synth Catal* 356:1281–1291
150. Bica K, Gaertner P (2006) *Org Lett* 8:733–735
151. Xia CL, Xie CF, Wu YF, Sun HM, Shen Q, Zhang Y (2013) *Org Biomol Chem* 11:8135–8144
152. Xia Y, Yan CH, Li Z, Gao HH, Sun HM, Shen Q, Zhang Y (2013) *Chin Sci Bull* 58:493
153. Ghorai SK, Jin M, Hatakeyama T, Nakamura M (2012) *Org Lett* 14:1066–1069
154. Mo Z, Zhang Q, Deng L (2012) *Organometallics* 31:6518–6521
155. Gao HH, Yan CH, Tao XP, Xia Y, Sun HM, Shen Q, Zhang Y (2010) *Organometallics* 29:4189–4192
156. Meyer S, Orben CM, Demeshko S, Dechert S, Meyer F (2011) *Organometallics* 30:6692–6702
157. Nakamura M, Ito S, Matsuo K, Nakamura E (2005) *Synlett* 1794–1798
158. Hatakeyama T, Kondo Y, Fujiwara Y, Takaya H, Ito S, Nakamura E, Nakamura M (2009) *Chem Commun* 1216–1218
159. Lin X, Zheng F, Qing FL (2012) *Organometallics* 31:1578–1582
160. Hatakeyama T, Hashimoto T, Kondo Y, Fujiwara Y, Seike H, Takaya H, Tamada Y, Ono T, Nakamura M (2010) *J Am Chem Soc* 132:10674–10676
161. Bedford RB, Brenner PB, Carter E, Carvell TW, Cogswell PM, Gallagher T, Harvey JN, Murphy DM, Neeve EC, Nunn J, Pye DR (2014) *Chem Eur J* 20:7935–7938
162. Kawamura S, Ishizuka K, Takaya H, Nakamura M (2010) *Chem Commun* 46:6054–6056
163. Kawamura S, Kawabata T, Ishizuka K, Nakamura M (2012) *Chem Commun* 48:9376–9378
164. Denmark SE, Cresswell AJ (2013) *J Org Chem* 78:12593–12628
165. Ito S, Fujiwara Y, Nakamura E, Nakamura M (2009) *Org Lett* 11:4306–4309
166. Brinker UH, König L (1983) *Chem Ber* 116:882–893
167. Guérinot A, Reymond S, Cossy J (2007) *Angew Chem Int Ed* 46:6521–6524
168. Cahiez G, Duplais C, Moyeux A (2007) *Org Lett* 9:3253–3254
169. Guérinot A, Lepesqueux G, Sablé S, Reymond S, Cossy J (2010) *J Org Chem* 75:5151–5163
170. Gregg C, Gunawan C, Ng AWY, Wimala S, Wickremasinghe S, Rizzacasa MA (2013) *Org Lett* 15:516–519
171. Yamada K, Sato T, Hosoi M, Yamamoto Y, Tomioka K (2010) *Chem Pharm Bull* 58:1511–1516
172. Neelam UK, Gangula S, Reddy VP, Bandichhor R (2013) *Chem Biol Interface* 3:14–17
173. Bensoussan C, Rival N, Hanquet G, Colobert F, Reymond S, Cossy J (2013) *Tetrahedron* 69:7759–7770
174. Hatakeyama T, Nakagawa N, Nakamura M (2009) *Org Lett* 11:4496–4499
175. Hashimoto T, Hatakeyama T, Nakamura M (2012) *J Org Chem* 77:1168–1173
176. Hatakeyama T, Okada Y, Yoshimoto Y, Nakamura M (2011) *Angew Chem Int Ed* 50:10973–10976
177. Cheung CW, Ren P, Hu X (2014) *Org Lett* 16:2566–2569
178. Dongol KG, Koh H, Sau M, Chai CLL (2007) *Adv Synth Catal* 349:1015–1018
179. Guisán-Ceinos M, Tato F, Buñuel E, Calle P, Cárdenas DJ (2013) *Chem Sci* 4:1098–1104
180. Luo S, Yu DG, Zhu RY, Wang X, Wang L, Shi ZJ (2013) *Chem Commun* 49:7794–7796
181. Gartia Y, Pulla S, Ramidi P et al (2012) *Catal Lett* 142:1397

182. Hatakeyama T, Hashimoto T, Kathirarachchi KKADS, Zenmyo T, Seike H, Nakamura M (2012) *Angew Chem Int Ed* 51:8834–8837
183. Percival WC, Wagner RB, Cook NC (1953) *J Am Chem Soc* 75:3731–3734
184. Fiandanese V, Marchese G, Martina V, Ronzini L (1984) *Tetrahedron Lett* 25:4805–4808
185. Cardellicchio C, Fiandanese V, Marchese G, Ronzini L (1987) *Tetrahedron Lett* 28:2053–2056
186. Ritter K, Hanack M (1985) *Tetrahedron Lett* 26:1285–1288
187. Dell'Anna MM, Mastroianni P, Nobile CF, Marchese G, Taurino MR (2000) *J Mol Catal A* 161:239–243
188. Lehr K, Fürstner A (2012) *Tetrahedron* 68:7695–7700
189. Babudri F, D'Ettore A, Fiandanese V, Marchese G, Naso F (1991) *J Organomet Chem* 405:53–58
190. Duplais C, Bures F, Sapountzis I, Korn TJ, Cahiez G, Knochel P (2004) *Angew Chem Int Ed* 43:2968–2970
191. Choi HH, Son YH, Jung MS, Kang EJ (2011) *Tetrahedron Lett* 52:2312–2315
192. Reddy CK, Knochel P (1996) *Angew Chem Int Ed* 35:1700–1701
193. Ottesen LK, Ek F, Olsson R (2006) *Org Lett* 8:1771–1773
194. Cardellicchio C, Fiandanese V, Marchese G, Ronzini L (1985) *Tetrahedron Lett* 26:3595–3598
195. Fiandanese V, Marchese G, Naso F (1988) *Tetrahedron Lett* 29:3587–3590
196. Bedford RB (2015) *Acc Chem Res* 48:1485–1493
197. Smith RS, Kochi JK (1976) *J Org Chem* 41(502–509):502
198. Kochi JK (2002) *J Organomet Chem* 653:11–19
199. Kochi JK (1974) *Acc Chem Res* 7:351–360
200. Fürstner A, Martin R, Krause H, Seidel G, Goddard R, Lehmann GW (2008) *J Am Chem Soc* 130:8773–8787
201. Aleandri LE, Bogdanović B, Bons P, Duerr C, Gaidies A, Hartwig T, Hockett SC, Lagarden M, Wilszok U, Brand RA (1995) *Chem Mater* 7:1153–1170
202. Bogdanović B, Schwickardi M (2000) *Angew Chem Int Ed* 39:4610–4612
203. Siedlaczek G, Schwickardi M, Kolb U, Bogdanovic B, Blackmond DG (1998) *Catal Lett* 55:67–72
204. Kleimark J, Hedström A, Larsson PF, Johansson C, Norrby PO (2009) *ChemCatChem* 1:152–161
205. Hedström A, Lindstedt E, Norrby P-O (2013) *J Organomet Chem* 748:51–55
206. Hedström A, Bollmann U, Bravidor J, Norrby PO (2011) *Chem Eur J* 17:11991–11993
207. Bekhradnia A, Norrby PO (2015) *Dalton Trans* 44:3959–3962
208. Schoch R, Desens W, Werner T, Bauer M (2013) *Chem Eur J* 19:15816–15821
209. Kleimark J, Larsson PF, Emamy P, Hedström A, Norrby PO (2012) *Adv Synth Catal* 354:448–456
210. Lefèvre G, Jutand A (2014) *Chem Eur J* 20:4796–4805
211. Hedström A, Izakian Z, Vreto I, Wallentin CJ, Norrby PO (2015) *Chem Eur J* 21:5946–5953
212. Noda D, Sunada Y, Hatakeyama T, Nakamura M, Nagashima H (2009) *J Am Chem Soc* 131:6078–6079
213. Bedford RB, Brenner PB, Carter E, Cogswell PM, Haddow MF, Harvey JN, Murphy DM, Nunn J, Woodall CH (2014) *Angew Chem Int Ed* 53:1804–1808
214. Daifuku SL, Al-Afyouni MH, Snyder BER, Kneebone JL, Neidig ML (2014) *J Am Chem Soc* 136:9132–9143
215. Daifuku SL, Kneebone JL, Snyder BER, Neidig ML (2015) *J Am Chem Soc* 137:11432–11444
216. Kneebone JL, Fleischauer VE, Daifuku SL, Shaps AA, Bailey JM, Iannuzzi TE, Neidig ML (2016) *Inorg Chem* 55:272–282
217. Liu Y, Xiao J, Wang L, Song Y, Deng L (2015) *Organometallics* 34:599–605
218. Przyojski JA, Veggeberg KP, Arman HD, Tonzetich ZJ (2015) *ACS Catal* 5:5938–5946